SEDIMENTOLOGY AND DEPOSITIONAL HISTORY OF THE CHAPEL ISLAND FORMATION (LATE PRECAMBRIAN TO EARLY CAMBRIAN), SOUTHEAST NEWFOUNDLAND

PAUL MICHAEL MYROW

NOTICE

The quality of this microform is heavily dependent upon the quality of the original thesis submitted for microfilming. Every effort has been made to ensure the highest quality of reproduction possible.

If pages are missing, contact the university which granted the degree.

Some pages may have indistinct print especially if the original pages were typed with a poor typewriter ribbon or if the university sent us an inferior photocopy.

Previously copyrighted materials (journal articles, published tests, etc.) are not filmed.

Reproduction in full or in part of this microform is governed by the Canadian Copyright Act, R.S.C. 1970, c. C-30.

AVIS

La qualité de cette microforme dépend grandement de la qualité de la thèse soumise au microfilmage. Nous avons tout fait pour assurer une qualité supérieure de reproduction.

S'il manque des pages, veuillez communiquer avec l'université qui a conféré le grade.

La qualité d'impression de certaines pages peut laisser à désirer, surtout si les pages originales ont été dactylographiées à l'aide d'un ruban usé ou si l'université nous a fait parvenir une photocopie de qualité inférieure.

Les documents qui font déjà l'objet d'un droit d'auteur (articles de revue, tests publiés, etc.) ne sont pas microfilmés.

La reproduction, même partielle, de cette microforme est soumise à la Loi canadienne sur le droit d'auteur, SRC 1970, c. C-30.

SEDIMENTOLOGY AND DEPOSITIONAL HISTORY OF THE CHAPEL ISLAND FORMATION [LATE PRECAMBRIAN TO EARLY CAMBRIAN], SOUTHEAST NEWFOUNDLAND

by

© Paul Michael Myrow, M.Sc.

A thesis submitted to the School of Graduate Studies in partial fulfillment of the requirements for the degree of Doctor of Philosophy

Department of Earth Sciences
Memorial University of Newfoundland

May 1987

St. John's Newfoundland

ISBN 0-315-39475-7

ABSTRACT

The Chapel Island Formation, a 1000 m thick shelf sequence of late Precambrian — Early Cambrian age, is receiving considerable attention as a leading candidate for the boundary stratotype for the Precambrian — Cambrian boundary. The formation, composed of five informally defined members, has been divided into six facies associations (1-6).

Facies Association 1 consists of red and green sandstones and shales (Facies 1.1/1.2), and grey to black, thinly laminated shales and silty shales (Facies 1.3), deposited in tidally-influenced peritidal and semi-restricted shoreline environments, respectively.

Facies Association 2 consists of very thin to medium bedded sandstones and siltstones (Facies 2.1/2.2) with subordinate green and red laminated silstones (Facies 2.3/2.4), deposited within a muddy deltaic system. Storm-generated sandstones (tempestites), and other storm-related features (e.g., gutter and pot casts), dominate Facies 2.1 and 2.2. These facies are also characterized by abundant and diverse slide and gravity-flow features (debrites, turbidites, and liquefied flow deposits) formed under conditions of high sediment supply in a delta front/upper prodelta setting. Thin bedded and laminated siltstones of Facies 2.3/2.4 form excellent marker horizons and represent delta abandonment facies.

Laminated green siltstones of Facies Association 3 are considered outer shelf deposits. Sandstone laminae are interpreted as distal tempestites deposited by waning flows below storm wave base.

Facies Association 4 consists of red, green and gray mudstones of inner shelf origin and thin fossiliferous algal limestones deposited in peritidal environments. Deposition took place on a low energy, oxygen-stratified muddy shelf, with the limestone beds forming during low stands of sea level.

Facies Associations 5 and 6 were deposited on a storm- and wave-dominated shelf below and above the influence of storm waves, respectively. The thin to medium bedded sandstones and siltstones of Facies Association 5 represent distal tempestites. The planar laminated and hummocky/swaly cross-stratified sandstones of Facies Association 6 represent inner shelf and shoreface environments.

The depositional history of the Chapel Island Formation records a shift from tectonically-active fault-bounded basins (underlying Rencontre Formation) to a tectonically-stable platform (overlying Random Formation). Three distinct phases of sedimentation have been delineated. Phase 1, corresponding to the lower part of the formation (members 1-3), is a period of relative sea level rise recording a shift from marginal marine environments to delta front/prodelta settings to the outer shelf. Phase 2 , represented by members 3 and 4 , is interpreted as a time of dropping relative sea level and low sediment input. Small scale relative sea level changes are recorded by variations in color, sedimentary and biogenic structures, diagenetic features and the deposition of thin peritidal limestone beds. Phase 3 (member 5) is a period of rapid deepening followed by shallowing with the progradation of a storm- and wave-dominated shelf. This phase, recording high sediment influx and strong storm and wave influence, is associated with major uplift and re-orientation of the shoreline from the southwest to the northeast.

ACKNOWLEDGMENTS

Thesis advisor R. Hiscott suggested this project, provided the necessary funding, and made numerous and detailed critical reviews of the thesis. I gratefully acknowledge his contributions. Thesis committee members N. James and C. Barnes provided advice and encouragement throughout.

Special thanks are extended to M. Anderson for his considerable help, and for familiarizing me with the Precambrian — Cambrian stratigraphy of the Burin Peninsula. His review of Chapters 1 and 9 are greatly appreciated.

I would like to also thank G. Narbonne for the identification of trace fossils and his great effort with the boundary stratotype proposal, and E. Landing for his keen field observations and many thoughtful discussions.

I am particularly indebted to J. Southard for helping me to recognize and evaluate a wide variety of wave and combined-flow features, and for numerous illuminating discussions. His critical review of the thesis greatly enhanced the work.

This project was financed by Natural Sciences and Engineering Research Council grants to R.N. Hiscott. Helicopter scholarships were provided by Sealand Helicopter Company. An academic scholarship and bursary were supplied by the Graduate School of Memorial University.

I gratefully acknowledge the help given by the following people: E. Cummins for his assistance during the summer of 1984 and for sharing the trials and tribulations of navigating a leaky boat in Fortune Bay; Margaret and Robert Murphy, Tony Rockel and Anita Best for their hospitality, friendship and use of their homes; D. Furey for taking in two stranded boatmen; C. Mehrtens for reviewing Chpt. 6 and for continued friendship and support; M. Coniglio for critical reviews of my thesis proposal and Chapter 6; A. King, R. Hyde and S. Solomon for many thoughtful discussions on unusual sedimentary structures;

A. Nottvedt and R. Kreisa for supplying a preprint of their paper on HCS; F. Thornhill, L. Warford, G. Ford, and R. Soper for making thin sections and providing access to equipment and supplies; Wilf Marsh for variety of photographic services and advice; Larry Nowlan for drafting the long Fortune Dump section; S. Loupe for photographic printing; R. Hopkins for use of his laser printer; P. Tauvers for help in the acquisition of computer goods.

Thanks to J. Botsford, N. Caplow, M. Coniglio, D. Furey, N. Chow, S. Gardiner, F. Mengel, D. Mosher, S. Pohler, L. Quinn, S. Schillereff, S. Solomon; S. Stenzel, and many others for consultation, support and friendship. I would also like to thank my various cross-country teamates, and others in the local running community, for their friendship and for sharing the hard training. Special thanks to T. Lane for providing sanity (insanity?) and late night companionship throughout this ordeal.

This project would not have been possible without the love and support of family. I am particularly grateful to my parents for their financial support and their unflagging love and dedication.

TABLE OF CONTENTS

Chapter 4: FACIES ASSOCIATION 2

LIST OF FIGURES

LIST OF TABLES

LIST OF PLATES

Chapter 1

INTRODUCTION

1.1 INTRODUCTORY REMARKS

Interest in shelf sedimentation has increased dramatically during the past two decades. This is particularly true for storm deposition, for which interest seems to have been sparked by early studies of the effects of hurricanes in the Gulf Coast region (e.g., Hayes, 1967). These were later followed by numerous studies of ancient storm deposits, with particular emphasis on hummocky cross-stratification (HCS). The shelf environment is one of the most complex because of the complicated interaction of tides, waves, storms, a variety of shelf currents, and additional factors such as the Coriolis effect and biogenic activity. This complexity makes it difficult to study modern shelf environments, particularly during storm events. Much of the stratification formed on shelves seems to be produced by omnidirectional oscillatory currents or combined-flow currents, the latter having oscillatory and unidirectional components, either or both of which may vary in intensity and orientation with time. Present understanding of stratification styles such as hummocky cross-stratification or combined-flow ripples is still in a formative stage and requires flume experiments of greater sophistication (complex flows) and more detailed observations on modern shelf processes and deposits as well as ancient shelf deposits.

Facies models for storm deposition along fine-grained shorelines have received little attention in comparison to their sandy counterparts. Areas in front of, and flanking, major river systems are characterized by high sedimentation rates and metastable sediment accumulations that are sites for a spectrum of mass movements. Storms can be a major factor in triggering these movements. Slides and other mass movements are well documented from modern deltaic settings but are poorly known from the rock record, especially those formed in siltstones and mudstones. Poor preservation of attributes of fine-grained flows is due to their fissile nature and their susceptibility to cleavage development.

The Chapel Island Formation (CIF), of late Precambrian to Early Cambrian age, is a relatively undeformed sequence of sandstones, siltstones, mudstones and minor limestones exposed on the Burin Peninsula and throughout Fortune Bay, Eastern Newfoundland (Figure 1.1). Excellent coastal exposures are available for study, especially along the southwestern part of the Burin Peninsula, where this study is primarily focused. The CIF consists of siliceous volcaniclastic sediments like many other units in the Newfoundland Avalon Zone (Hughes, 1976). The siliceous nature renders these rocks nonfissile and less susceptible to cleavage development, providing a rare opportunity for the detailed study of sedimentary structures in fine-grained rocks, particularly gravity-flow deposits.

The CIF contains a wide variety of shelf deposits including fine-grained deltaic deposits with well preserved storm-generated sandstones and a wide variety of marine slides and gravity-flow deposits. The CIF strata provide an excellent opportunity for the construction of depositional models for fine-grained shorelines and the detailed process interpretation of storm-generated features and shelf sediment failures.

Figure 1.1: Outcrop distribution of Chapel Island Formation (shown in black). The formation occurs within the Newfoundland Avalon Zone (index map)

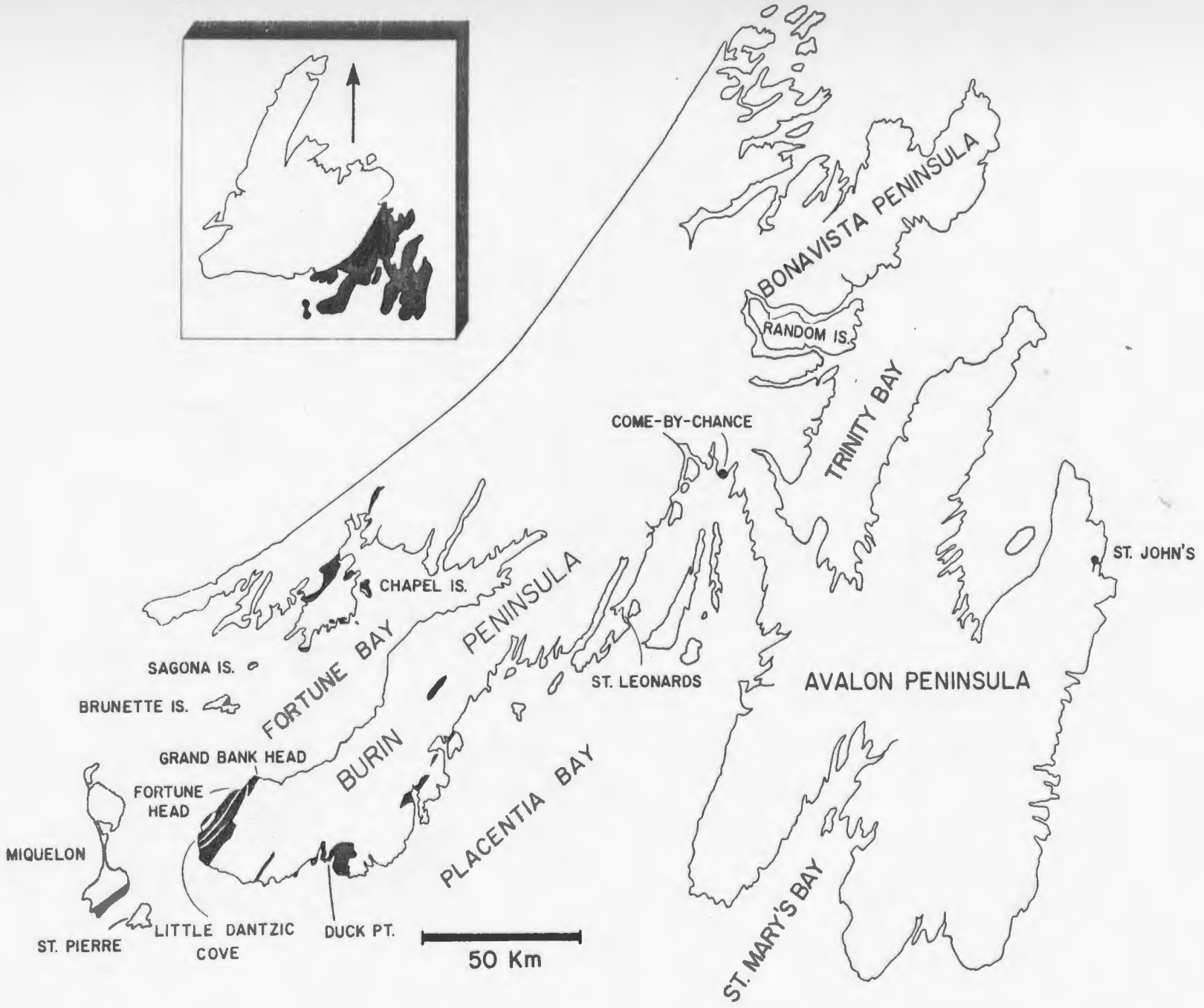
BONAVISTA PENINSULA
RANDOM IS.
TRINITY BAY
COME-BY-CHANCE
ST. JOHN'S
CHAPEL IS.
FORTUNE BAY
BURIN PENINSULA
SAGONA IS.
BRUNETTE IS.
ST. LEONARDS
AVALON PENINSULA
GRAND BANK HEAD
FORTUNE HEAD
MIQUELON
PLACENTIA BAY
ST. MARY'S BAY
ST. PIERRE
LITTLE DANTZIC COVE
DUCK PT.
50 Km

1.2 PURPOSE OF STUDY

The aim of this thesis is a sedimentological study of the Chapel Island Formation, including facies analyses and detailed process interpretations of sedimentary structures. The development or modification of models for particular facies or sedimentary structures is a fundamental aspect of this work. One aim of this work is to present, through careful measurement and correlation of outcrops, a revised lithostratigraphy which can then serve as a framework for the tabulation of accurate range charts of biostratigraphic data, especially of trace fossils and shelly fossils. This is particularly important because exposures of the CIF on the Burin Peninsula are presently considered one of three potential candidates for the Precambrian—Cambrian boundary stratotype.

This study attempts to fill a gap in our understanding of the Late Precambrian — Early Cambrian Avalonian sedimentary history of this area, outlined by Hiscott (1982) and Smith and Hiscott (1983), but based mainly on the formations that stratigraphically bound the CIF: the Rencontre below and the Random above. A sedimentary history of the CIF, including the construction of a relative-sea-level curve, is attempted following measurement of stratigraphic sections and collection of paleocurrent data from outcrops throughout the Fortune Bay area.

1.3 REGIONAL GEOLOGY

1.3.1 Introduction

The Chapel Island Formation lies within the Avalon Zone, a tectonostratigraphic subdivision of the Appalachian Orogen (Williams, 1979; Williams and Hatcher, 1983). The

rocks of this zone in Newfoundland are correlated with rocks in Nova Scotia, New Brunswick, Massachusetts, the Carolinas, the British Caledonides, the Hercynides of France and Iberia and along the northern and eastern margins of the west African Shield.

The Dover - Hermitage Bay Fault Zone defines the western limit of the Avalon Zone in Newfoundland (O'Brien et al.,1983). To the east the zone extends offshore to the present continental margin or beyond (Lilly, 1966; Haworth and Lefort, 1979).

1.3.2 Stratigraphy

The geology of the Newfoundland part of the Avalon Zone (Figure 1.2) has been discussed by numerous authors (e.g., Williams et al., 1974; Rast et al.,1976; Strong, 1979; Strong et al., 1978b, 1980; King, 1980; O'Brien et al.,1983). The rocks of this zone can conveniently be divided into three major assemblages (Bruckner in King et al.,1974). The lower and middle assemblages are of late Precambrian age. The lower assemblage is a thick succession of terrestrial and marine, acidic to basic volcanic rocks (Harbour Main and Love Cove Groups), and marine fine-grained volcaniclastic flysch (Conception and Connecting Point Groups). The middle assemblage consists of marine black shales (St. John's Group) and a thick overlying sequence of coarse deltaic and alluvial deposits (Signal Hill Group). The upper assemblage is of Paleozoic age, earliest Cambrian to Lower Ordovician, and it includes quartzites, sandstones, limestones and shales.

The geology of the southern Burin Peninsula (Strong, 1979; Strong et al., 1978a; Strong et al., 1980) — the area that contains the rocks described in this thesis — differs in some respects from the above scheme. The sequence on the Burin Peninsula begins with the Burin Group, a series of mafic pillow lavas, volcanigenic sediments, shales and limestones (some containing large, as yet unidentified, stromatolites) (Strong et al., 1978a). Even though this is an oceanic sequence - alkalic at its base, but dominated by oceanic tholeiite - it does not resemble a typical ophiolite sequence in that it conspicuously

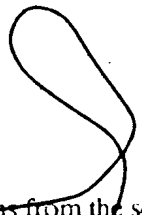

Figure 1.2: Correlation chart of stratigraphic sections from the southern Burin Peninsula, Bonavista Bay — west Placentia Bay, and eastern Avalon Peninsula regions. The Gaskiers Formation is a submarine debris flow formed during a late Precambrian glacial period. the Precambrian—Cambrian boundary, shown in a heavy line, is found within the Chapel Island Formation. This figure is modified from Smith and Hiscott (1983; Fig. 1). Correlations are essentially those of O'Brien and Taylor (1983). No age relationships are implied for the older units in this diagram.

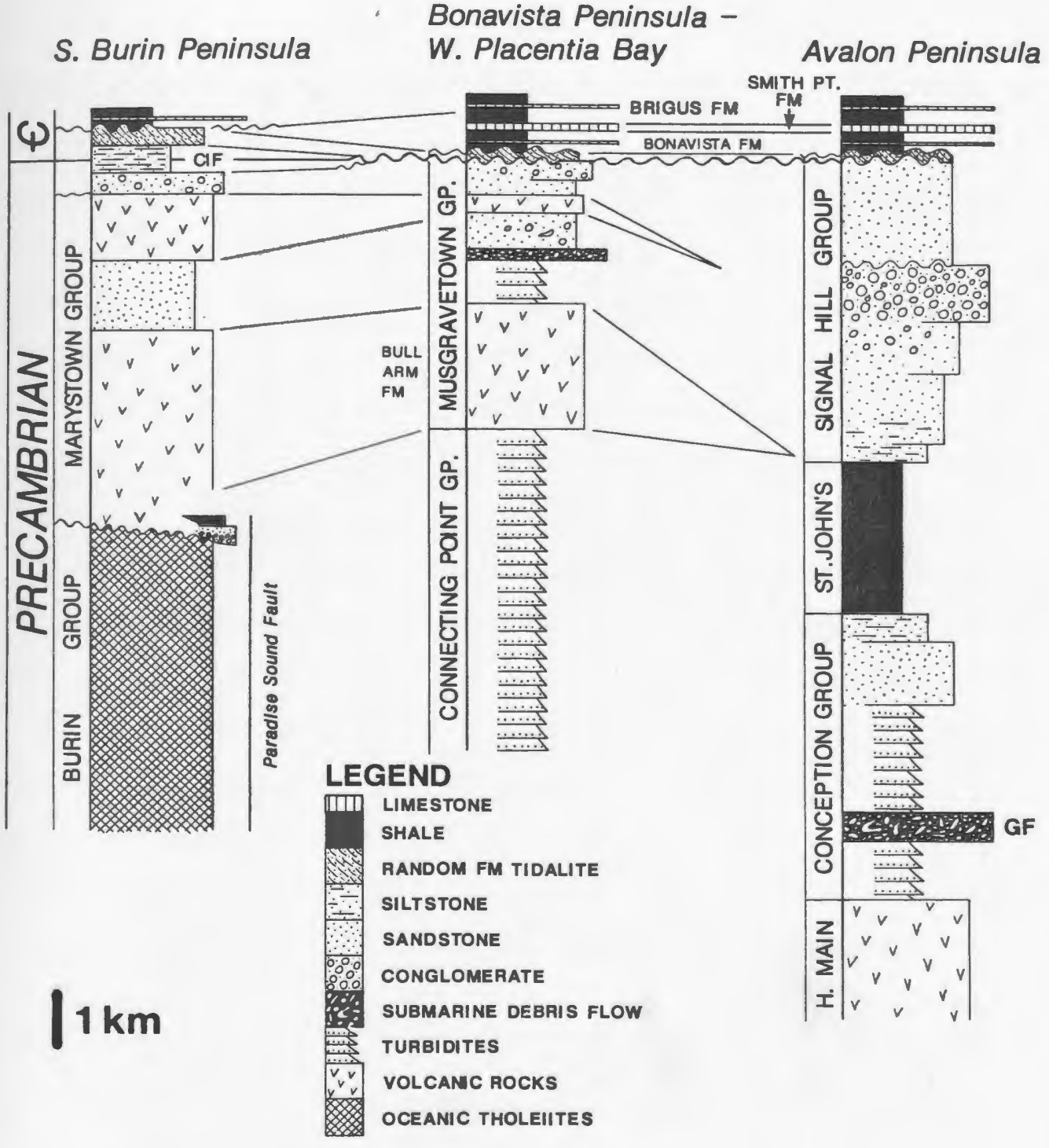
S. Burin Peninsula
Bonavista Peninsula –
W. Placentia Bay
Avalon Peninsula
SMITH PT. FM
BRIGUS FM
BONAVISTA FM
CIF
PRECAMBRIAN
MARYSTOWN GROUP
BURIN GROUP
BULL ARM FM
MUSGRAVETOWN GP.
CONNECTING POINT GP.
SIGNAL HILL GROUP
ST.JOHN'S
CONCEPTION GROUP
H. MAIN
GF
Paradise Sound Fault
1 km
LEGEND
LIMESTONE
SHALE
RANDOM FM TIDALITE
SILTSTONE
SANDSTONE
CONGLOMERATE
SUBMARINE DEBRIS FLOW
TURBIDITES
VOLCANIC ROCKS
OCEANIC THOLEIITES

lacks the lower ophiolite layers (i.e., ultramafics and sheeted dikes) (Strong, 1979). A 1500 m-thick sill intruding the Burin Group , the Wandsworth Gabbro, had been dated at 763 ± 2 Ma (Krogh et al., 1983).

The Burin Group was subjected to greenschist metamorphism and mild tectonism (tilting and faulting) prior to deposition of the overlying Marystown Group. The Marystown Group is a thick succession of bimodal (basalt-rhyolite) volcanics (mostly acidic pyroclastics) and subordinate volcaniclastic sediments, which formed in a subaerial environment (Strong et al., 1978a; O'Brien and Taylor, 1983). Equivalent rocks in the northern part of the peninsula have been dated at 608 ± 25 Ma (U-Pb in zircons: Dallmeyer, 1980). The lower part of the Marystown Group is stratigraphically roughly equivalent to, or somewhat younger than, Conception Group strata on the Avalon Peninsula (O'Brien and Taylor, 1983) that contain late Precambrian soft-bodied megafossils (Anderson and Misra, 1968; Misra 1969; Anderson, 1978; Anderson and Conway Morris, 1982).

The Marystown Group is overlain disconformably by a continuous sequence of siliciclastic rocks that spans the Precambrian-Cambrian boundary: in ascending order, the Rencontre, Chapel Island and Random formations. The redbed conglomerates, sandstones and shales of the Rencontre Formation were deposited in a variety of fluvial and marginal marine settings (Smith and Hiscott, 1984). The sandstones, siltstones and minor limestones of the Chapel Island Formation were deposited in nearshore and shelf environments (Crimes and Anderson, 1985; Myrow, 1985; and this study). The sandstones, shales and quartzites of the Random Formation were deposited in tidally dominated nearshore and shoreline environments (Anderson, 1981; Hiscott, 1982; Smith and Hiscott, 1984).

While the pre-Random volcanic and sedimentary sequences described above were forming in the Fortune Bay region, a separate sequence was forming on the Avalon Peninsula, presumably in an isolated and distinct basin from the Fortune basin. The strata in this region include the Conception, St. John's, and Signal Hill groups, which record

shoaling from deep-sea fan environments through to a prograding delta front and a broad alluvial plain (King, 1980). Paleocurrents and lateral lithofacies distributions imply multiple source areas within the basin. The Random Formation is stratigraphically the first regionally correlatable unit in the Newfoundland Avalon Zone.

In the Fortune Bay area the Random Formation is in conformable contact with the underlying Chapel Island Formation, whereas elsewhere, to the northeast and east, its base is unconformable (Hutchinson, 1953; McCartney, 1967; Fletcher, 1972; Anderson, 1981). Where the base is unconformable, the underlying strata provide evidence for gentle folding and, in places, deep erosion prior to the deposition of the Random Formation. Thus 1800 m of Precambrian sediments were eroded from an area southeast of Trinity Bay (McCartney, 1967), and over 450 m of Precambrian sediments were removed from the southeastern part of the Cape St. Mary's Peninsula (Fletcher, 1972). The Random Formation was deposited during a marine transgression, with the marine basin opening toward the southwest, and depositional onlap toward the north and northeast (Anderson, 1981; Hiscott, 1982).

In the Trinity Bay area, the Random Formation is disconformably overlain by fossiliferous Cambrian mudstones and carbonates: in ascending order, the Lower Cambrian Bonavista, Smith Point, and Brigus formations and Middle Cambrian Chamberlain's Brook Formation (Jenness, 1963). Deposition of the Cambrian sediments took place during marine transgression in a northeast-southwest-oriented trough whose axis extended from the northern end of the Bonavista Peninsula through Random Island and the isthmus of Avalon into Placentia Bay (Hutchinson, 1962). The advance of the sea was from the northeast, implying a 180 degree shift in shoreline orientation from that associated with the underlying Random Formation. As transgression proceeded, it resulted in a gradual widening of the elongate basin and the progressive onlap of younger and younger sediments outward from the basin axis. Hence, on the west side of the Burin Peninsula (e.g., Dantzic Cove) the Random Formation is overlain by the lower part of the Early

Cambrian Brigus Formation, and still further west, north of Fortune Bay, the Random Formation is overlain by the Youngs Cove Group, the base of which is equivalent to the upper part of the Middle Cambrian Chamberlains Brook Formation (Hutchinson, 1962; Anderson, 1981).

The Bonavista Formation consists of red, green and purple mudstones, calcareous nodules and bedded limestones. Deposition was in peritidal (Benus and Landing, 1984) and subtidal settings.

The Smith Point Formation (0-16 m) is a stromatolitic limestone containing mud mounds, oncolites, tepee and sheet crack structures, and numerous hardground surfaces, which formed during a period of shoaling and emergence (Landing and Benus, 1984). Paleoenvironments range regionally from peritidal to normal marine. In the Avalon Zone of Newfoundland Callavia broeggeri and other trilobites make their first appearance close to the top of the Smith Point Formation (Walcott, 1900; Hutchinson, 1962; Fletcher, 1972).

The overlying Brigus Formation (10-210 m) consists of red and green mudstone and minor limestones that are of medial to late Early Cambrian age. On the east side of Conception Bay the formation overlies granitic rocks (Holyrood Granite) and Harbour Main volcanics.

1.3.3 Tectonism, Structure and Metamorphism

Three periods of deformation have been identified in the Avalon Zone of Newfoundland, the first two of which were major events. The first period of deformation was the late Precambrian "Avalonian" Orogeny. Evidence for this orogeny includes the "H.D. Lilly Unconformity" (Anderson et al., 1975), in which sediments of the Signal Hill Group shed from a major uplift north of the Bonavista and Avalon peninsulas overlie an erosion surface in folded Conception Group shales (King, 1980); also, at Bacon Cove, flat-lying Lower Cambrian sediments of the Bonavista Formation overlie folded and

cleaved siltstones of the lower part of the Conception Group (King, et al., 1974; King and Anderson, 1982). The effects of this orogeny included block faulting, granitoid emplacement (Holyrood granite), and gentle folding, but no extensive metamorphism or penetrative fabric development (O'Brien et al., 1983).

The second and most widespread orogeny to affect the Avalon Zone was the Late Devonian Acadian Orogeny (Dallmeyer et al., 1983). The effects of the Acadian Orogeny are strongest in the western part of the Avalon Zone "...where the Paleozoic and older sequences of the Burin Peninsula are asymmetrically folded and thrust towards the southeast..." (Strong, 1979). Metamorphism in this part of the Avalon Zone occurred under prehnite-pumpellyite to mid-greenschist facies conditions (King and O'Brien, in press).

The third deformational event is the poorly defined Late Carboniferous (Hercynian) deformation represented by granitoid plutonism and very localized folding and faulting (King and O'Brien, in press).

1.3.4 Tectonic Models

The tectonic history of the Avalon Zone is distinct from that of much of the Appalachian Orogen. "The Cambrian strata of the Avalon Zone indicate that it acted as a stable platform during Early Paleozoic time, when the Iapetus cycle was most in evidence in the west" (Williams, 1979, p. 793). The Avalon Zone is considered by some authors to be a Pan-African terrane. "The term Pan-African (Kennedy, 1964) is currently used to denote the late Precambrian to early Paleozoic period of orogenesis, basin rejuvenation, granitoid emplacement, and thermal overprinting recognized throughout much of the African continent" (O'Brien et al., 1983, p. 211). This time period is loosely considered to range from 1000 Ma to 500 Ma.

The "docking" of the Avalon Zone with the adjacent Gander Zone (these "Zones" being "Terranes" in recent analyses; e.g., Williams and Hatcher, 1983) took place prior to intrusion of the Ackley Granite (Dallmeyer, 1980), a pluton that straddles the two tectonostratigraphic zones. Dallmeyer et al. (1983) place the age of the intrusion at 352-356 Ma, using $^{40}Ar/^{39}Ar$ dating techniques. They conclude that the deformation and metamorphism in the western Avalon Zone occurred simultaneously with the tectonic "docking" of the Avalon Zone during the Acadian Orogeny.

Hughes (1972) correlated the rocks of the Avalon Zone with those of Morocco. Schenk (1971) provides a review and correlation of Maritime geology with African geology, and provides plate reconstructions for various time periods. More recently, O'Brien et al. (1983) and King and O'Brien (in press) have proposed more detailed correlations between eastern Canada and northern Africa and have offered tectonic models for the Avalon Zone.

Two contrasting tectonic models have been suggested for the Avalon Zone. The first involves a rift setting (e.g. Papezik, 1970; Strong et al., 1978b; Strong, 1979), and the second a consuming plate margin or ensialic island arc (e.g. Rast et al., 1976; Hughes, 1970). According to Strong et al. (1980), the Avalon "...succession indicates a Proterozoic tectonic history of prolonged continental extension and local rupturing, with eventual stabilization during the Paleozoic." Schenk (1971) called for extended rifting of an Avalonian microcontinent from the North American craton. More specifically, Strong (1979) envisioned a "long-lived tensional environment with local rifting and oceanic crust formation..., ...possibly indicating rifting of a West Africa-North America-Baltic supercontinent at this time." These views are opposed by workers like Hughes (1970), who proposed that the Avalonian volcanics evolved as part of an island arc, despite the disturbing lack of compressional tectonic features. Rast et al. (1976) envision an island arc underlain by continental basement. They note a limited extent of metamorphism in the

Avalonian rocks of the British Isles (Anglesey), and explain it by collision between an island arc and a continent, as opposed to a continent-continent collision.

By comparing the geology of the Avalon Zone with parts of other Pan-African terranes, notably in Morocco, O'Brien et al. (1983) have raised some very important points concerning the variablility of tectonic settings along the length of a single orogen. Their review of the Pan-African of Morocco indicates that both extensional (rifting) and compressional (folding, thrusting, ophiolite obduction, etc.) tectonics took place simultaneously, in different regions along the length of the orogen. Coupled with temporal tectonic changes, these observations place serious limitations on the development of unified models for the Avalon Zone of Newfoundland.

Working within these constraints, O'Brien et al. (1983) present a model for the tectonic history of the Avalon Zone. Their model is an elaboration of the model of Strong (1979), especially of the later stages. The model begins with initial attempts at rifting (ensialic flysch-basin deposits of the Green Head Group of New Brunswick, and flyschlike parts of Burin Group). The second phase is further rifting to produce the Burin Group. The third phase calls for closure of local ocean basins, the collision resulting in crustal melting to yield late Proterozoic volcanics. The next phase consists of marine to terrestrial sedimentation (King, 1980). This is followed by peneplanation and transgression of the Cambrian sea.

1.4 PREVIOUS WORK

Dale (1927) examined a number of outcrops in the Fortune Bay region. During a traverse along the coast from Point May to Dantzic Cove he found trilobite fragments (Paradoxides bennetti Salter and Paradoxides eteminicus Matthew) in a gray shale, and Callavia broeggeri (Walcott), Coleoloides, Micrometra labradorica, and hyolithids in nodular limestone and mudstone units. Dale considered the rocks along this part of the coast to be entirely of Lower and Middle Cambrian age. He noted a similarity between the Cambrian faunas of Newfoundland and those of America and Europe, particularly Europe. In comparing the faunas with those in England he stated that "many of them [species] are identical — which seems to indicate that the Cambrian areas of England and Newfoundland consisted of a single life province, made up largely of shallow-water forms which migrated back and forth over the shortest route between these two regions" (Dale, 1927; p. 429).

White (1939) mapped in the Rencontre East area of Fortune Bay. He proposed the name Young's Cove Group for a 610 m (2000 feet) thick sequence of siltstones, sandstones and shales, that conformably overlie the red beds of the Doten Cove Formation (also named by White). White considered the Young's Cove Group to be early Middle Cambrian to Late Cambrian or Early Ordovician in age. White was mistaken about the age relationships and correlation of some of the units in this region. These errors were not rectified until the early 1970's (see Williams, 1971, p. 13-14). White believed that the Young's Cove Group is overlain by a thick sequence of silicic to mafic volcanic rocks and associated sedimentary rocks that he called the Long Harbour Series. The contact between them was later interpreted by Williams (1971) as a thrust fault. The Long Harbour Series is overlain by the same red beds that underlie the Young's Cove Group. White, believing the red beds above the Long Harbour Series to be a separate, younger sequence, named it the Rencontre Formation. Thus White unknowingly erected two discrete formations, Doten Cove and Rencontre, for the same set of red beds, and assigned different ages to them,

Early Cambrian and Silurian, respectively. Both names have been used in the literature since that time, but the name 'Rencontre' is now preferred (Williams et al., 1985). The Long Harbour Series (changed to the Long Harbour Group by Williams, 1971) and the Rencontre Formation are of late Precambrian age. However, prior to 1971, they were considered to be of Lower Paleozoic age (Ordovician — Silurian).

The geology of the Hermitage Bay area (including the west side of Fortune Bay and Chapel Island) was studied by Widmer (1950). He proposed the formation names Chapel Island and Blue Pinion for, respectively, a sequence of green and red siltstones overlying the Doten Cove Formation, and a sequence of white quartzitic sandstones overlying the Chapel Island rocks; both sequences crop out on Chapel Island and at other localities around Hermitage and Fortune Bays. The rocks of these 'new' formations had been included by White (1939) in the Lower part of his Young's Cove Series. Widmer therefore found it necessary to redefine that series as "...those shales above the white sandstones [Blue Pinion Formation] that contain Medial Cambrian fossils and the related rocks of definitely Medial Cambrian age (1950; p. 198). He considered the 'new' formations and the Doten Cove Formation (conformable above with the Chapel Island Formation) to be Lower Cambrian.

Hutchinson (1962) reduced the status of the Middle Cambrian Young's Cove Group to that of a formation. He was apparently the first to recognize that the rocks of the Chapel Island and Doten Cove (Rencontre) Formations underlying the Blue Pinion Formation north of Fortune Bay are the same as those beneath the Blue Pinion Formation in the southwest part of the Burin Peninsula. The rocks of that part of the peninsula were mapped and described by Potter (1949) before Widmer completed his studies in the Hermitage Bay region, and therefore he gave different names to the rock units he distinguished in the local succession (which correspond closely to those recognized elsewhere in Fortune Bay), namely: Admiral Cove= Doten Cove (Rencontre), Point May= Chapel Island, and Point Crew= Blue Pinion. Potter's work received little recognition from

later workers in the area, including Green and Williams (1974), and Hutchinson (1962) appears to have been unaware of it.

Potter (1949) was, in fact, the first person to give a detailed account of the Chapel Island Formation (his Point May Formation). He distinguished three facies in a stratigraphic section measured at Grand Bank Head. Facies 1 consists of red and green thin-bedded sandstones, siltstones, and mudstones (estimated at 400 m; 1300 feet) that are found in transition with the underlying redbeds of the Rencontre Formation (his Admiral Cove Formation). The base of the Chapel Island Formation was arbitrarily placed at the oldest green bed. Potter considered Facies 1 to be a shallow-water deposit - based on the presence of mud cracks, raindrop prints, and ripple marks - that was laid down during "the early stages of a transgressive sea which reached its greatest extent during the deposition of the second facies" (p. 28).

The second facies of Potter (1949) is made up predominantly of thin-bedded gray and green silty argillites and siltstones (185 m; 600 feet) commonly containing carbonate nodules. Included in the upper part of this facies are intercalations of red and brown mudstones and, marking its top, a thick bed of limestone. Potter noted algal structures in this limestone, that he attributed to the genus Collenia. The third facies consists of 275+ m [900+ feet] of green-gray sandstones and silty sandstones. Red sandstones at the top of this sequence were placed by Potter in a separate formation called the Dantzic Formation. Walthier (1948) considered these sandstones as a separate member (Fortune Head Member) within the Chapel Island Formation.

De La Rue (1951) described the succession of sediments underlying the French island of Langlade in Fortune Bay. The Rencontre, Chapel Island and Random formations, as well as trilobite-bearing Middle Cambrian shales, are all represented there. However, De La Rue (1951) placed all these units (distinguished by lithology and unnamed at that time) in the Cambrian, as he considered the trilobite-bearing shales to be the oldest beds in the succession. The order of deposition of the lithological units recognized by De La Rue was

reinterpreted by Anderson (1975). Recent mapping by Green (personal communication) has revealed much structural complexity that is not evident on De La Rue's map.

Hutchinson (1962) disagreed with the inclusion by White (1939) and Widmer (1950) of the Chapel Island and Rencontre Formations in the Lower Cambrian. He noted that even though these rocks underlie Middle Cambrian rocks, there is no fossil evidence to suggest that these rocks are Lower Cambrian, and so he placed them, and the overlying Blue Pinion Formation, in the latest Precambrian.

The work of Williams (1971) was instrumental in establishing the correct stratigraphic order for the volcanic and sedimentary rocks in the Fortune Bay region. However, Williams erred in restoring the Chapel Island and Blue Pinion formations to the Young's Cove Group, so that they do not appear as separate units on his map. This change was made despite the fact that Williams believed the Chapel Island Formation, at least in the Chapel Island area, to probably be of late Precambrian age.

Greene and Williams (1974) discovered fossils in the Chapel Island Formation near Little Dantzic Cove thereby establishing that, at least at the southern end of the Burin Peninsula, the overlying Blue Pinion Formation is of Early Cambrian age. They also established that the Blue Pinion Formation of the Fortune Bay region is a lateral equivalent of the Random Formation of other parts of eastern Newfoundland. The name 'Blue Pinion' therefore became redundant. Green and Williams also presented stratigraphic sections of the Random Formation and adjacent units for a number of localities in Fortune and Placentia Bays to show the position of the base of the Cambrian in those parts of southeastern Newfoundland. Most importantly though, it was their fossil discovery that attracted the interest of paleontologists, who were concerned with finding a suitable stratotype candidate for the Precambrian-Cambrian boundary.

The Harbour Breton area (northern side of Fortune Bay) and, north of it, the adjoining Gaultois area were mapped, respectively, by Greene (1975) and Greene and O'Driscoll (1975). Their maps show the most westerly known exposures of the Rencontre,

Chapel Island and Random Formations; the last named is, however, unrepresented in the Gaultois area.

The first detailed geologic maps of the entire southern portion of the Burin Peninsula (Grand Bank, Lamaline, and Marystown-St. Lawrence map areas) were prepared by O'Brien et al. (1976, 1977) and Strong et al. (1978a). At that time, the relationship of the succession of late Precambrian — Cambrian sedimentary rocks exposed on the east side of the Burin Peninsula to successions of comparable age in the Fortune Bay area (including the southwestern part of the Burin Peninsula) and elsewhere in the Avalon Zone was uncertain. O'Brien et al. (1977, p. 7) stated that "It is possible that the sedimentary sequence west of the Fortune Mountain Fault System was formed in a depositional basin which was separated from the eastern basin by a volcanic highland in late Hadrynian times". However, Green and Williams (1974) had earlier correlated units found at localities on the eastern side of the Burin Peninsula (Duck Point, St. Leonards, Come By Chance) with the Random and Chapel Island Formations of Fortune Bay. Strong (1976) also used these formation names in his study of the Lawn Area (including Duck Point). Nevertheless, O'Brien et al. (1976) gave the name Inlet Group to all the late Precambrian and Lower Cambrian sedimentary rocks at these east side of the Burin Peninsula south of Marystown. Formation names were subsequently given by Taylor (1976) to the four numbered but unnamed units of the Inlet Group distinguished earlier by O'Brien et al (1976), namely, in ascending order, the Bay View, Salt Pond, Burnt Island, and Pleasant View Farm formations. These names were also used by Strong et al. (1978a) in their description of the geology of the Marystown and St. Lawrence map areas.

The Bay View Formation is a sequence of grey-green siltstones and red micaceous silty sandstones. According to Strong et al. (1978a) this formation unconformably overlies the Burin Group and underlies fossiliferous mudstones of the Salt Pond Formation (approximately equivalent to the Bonavista Formation, the oldest Lower Cambrian formation recognized at that time in southeastern Newfoundland). In the upper part of the

Bay View Formation there are several beds of quartzite that were correlated by Taylor (1976) and Strong et al. (1978a) with the Random Formation. The underlying part of the formation was therefore considered equivalent to the Chapel Island Formation, plus, possibly, the uppermost part of the Rencontre Formation. The quartzites in the Bay View Formation, attributed to the Random Formation by Taylor, are presently considered to be interbeds in the Chapel Island Formation. The formations in the Inlet Group were poorly defined, and the use of local names for formations lithologically indistinguishable from already named formations elsewhere was confusing and unnecessary. Hence the formations proposed by Taylor (1976) and later by Strong et al. (1978) were not adopted by later workers.

In a report on silica recources in Newfoundland, Butler and Greene (1976) devoted a significant part to a comprehensive review of the Random Formation that included an isopach map, a facies distribution map, and numerous measured stratigraphic sections. In addition, they reproduced a modified and updated version of Walthier's (1948) geological map of the southwestern tip of the Burin Peninsula.

In a discussion aimed at establishing the age and relationship of the Random to bounding formations, Anderson (1981) showed that (1) the Random Formation (previously believed to range in age from early Lower Cambrian to early Middle Cambrian) is of early Cambrian (Tommotian) age throughout southeastern Newfoundland, (2) the base of the Random is only slightly diachronous (a little older west of the Burin Peninsula than elsewhere in the Avalon Zone), and (3) the underlying Chapel Island Formation is, with the exception of its lowermost part, also of Early Cambrian (Tommotian) age. Anderson also noted the presence of a wide variety of trace fossils in the Chapel Island Formation and their absence in the underlying Rencontre Formation. He attributed the sudden appearance of the trace fossils in these strata to a change from fluvial to marine paleoenvironments.

Bengtson and Fletcher (1983) provided information on the Lower Cambrian biostratigraphy, including a discussion of the small shelly fossils present in the Chapel Island Formation. These authors divided the formation into five members (not formally named — see Section 1.5 below). They collected shelly fossils from the limestones toward the top of the Chapel Island Formation (member 4) and from the Bonavista Formation at localities on the southern part of the Burin Peninsula. The skeletal fossils from these units comprise what Bengtson and Fletcher (1983) call an Aldanella attleborensis assemblage, a fauna that suggests correlation with the Tommotian Stage of the Lower Cambrian of the Siberian Platform. Bengtson and Fletcher (1983) were the first to recognize the changes in trace fossil assemblages in the lower part of the Chapel Island Formation. They reported Precambrian trace fossils in their member 1, and an assemblage of well preserved diagnostic Paleozoic trace fossils that first appear in member 2.

A detailed analysis of the trace fossils present in the Chapel Island and Random formations was undertaken by Crimes and Anderson (1985). They described the different forms, and the associations of such forms (assemblages), present within each member of the Chapel Island Formation (as defined by Bengtson and Fletcher (1983)) and in the Random Formation. Generalizations concerning the depositional environments of these units were also given.

Hiscott (1982) provided a sedimentological analysis of the Random Formation, which he interpreted as macrotidal, shoreline and nearshore deposits. He provided a description and interpretation for the red sandstones that are present in the Random Formation and the upper portion of the Chapel Island Formation (member 5). His discussion of other facies and structures in the Random Formation are also pertinent to the analysis of the Chapel Island sequence.

The red shales, sandstones and conglomerates of the underlying Rencontre Formation were recently studied by Smith and Hiscott (1984). Their description of these

terrestrial to shallow-marine deposits included a general discussion of the latest Precambrian to Early Cambrian basin evolution of the Fortune Bay region. The focus of this work was on the tectonic and depositional history of the Rencontre Formation, but the discussion also included younger units such as the Chapel Island Formation. Smith and Hiscott (1984) concluded that the Rencontre Formation was deposited during periods of active tectonism, possibly strike-slip in character. They attributed the change in the character of sedimentation from the Rencontre Formation into the overlying Chapel Island and Random formations to a general waning in tectonic activity accompanied by a gradual global rise in sea level.

1.5 LITHOSTRATIGRAPHY OF THE CHAPEL ISLAND FORMATION

The thickness of the Chapel Island Formation in northern Fortune Bay was estimated by Widmer (1950) as 520 m [1,700 feet] minimum. There are several estimates for the thickness of the sequence in the Grand Bank area. Potter (1949) estimated 855 m [2,800 feet] for the Point May Formation (= most of Chapel Island Formation), and 70 m [220 feet] for the Dantzic Formation (= red sandstones at top of Chapel Island Formation), which means an overall thickness for the Chapel Island Formation of 920 m [3020 feet]. Walthier (1948) gave a thickness of 1100 m [3600 feet] for the same sequence. O'Brien et al. (1977) reported a thickness of 740 meters. The author considers a measurement of this accuracy impossible given the problems of structure and lack of exposure in certain localities, and agrees with Bengtson and Fletcher (1983) that the thickness is "over 900 m"; in fact over 1000 m.

The most useful published scheme for the stratigraphic subdivision of the Chapel Island Formation is that of Bengtson and Fletcher (1983), in which the formation is divided into five informal members, numbered 1-5, based on the outcrops at Grand Bank (lower

members) and Little Dantzic Cove (upper members). This same scheme was also used without modification by Crimes and Anderson (1985), who studied the same outcrops. These informal members are easily recognizable in the field and are used in this study (Figure 1.3).

Previous studies of the CIF have not included measured sections, and the boundaries between some members have not been clearly defined. During the course of this study it became evident that facies changes within the formation are more complex than previously thought and that both the thickness of members (which in cases had to be radically altered) and the member boundaries needed to be better defined. Figure 1.4 shows the location of outcrops measured during this study. Correlations between outcrops, including the positions of member boundaries, are given in Figures 1.5 and 1.6.

The base of the CIF, most easily defined at Grand Bank Head, is arbitrarily taken as the first green interval greater than 1 m thick in the transition from the underlying redbeds of the Rencontre Formation, following Potter's (1949) suggestion. Member 1 consists of ~180 m of red and green, thin to medium bedded sandstones, siltstones and shales with intervals of laminated black shales and gray shaly siltstones in the upper half.

The contact between member 1 and member 2, best exposed at Fortune Dump, is herein placed at the first stratigraphic occurrence of the very diagnostic and easily recognizable gray-green siltstone and sandstone beds that characterize most of member 2. Packages of red and green sandstones and shales, similar in character to those in member 1, are present above this base but are included in member 2. It is unclear where the boundary between member 1 and 2 was placed by earlier workers, but the estimate of 400 m for member 1 by Bengtson and Fletcher (1983) suggests either a large error, or that the higher redbeds were used as an upper boundary for member 1.

The contact between members 2 and 3 was placed by Bengtson and Fletcher (1983) and Crimes and Anderson (1985) at the base of a red siltstone unit (Facies 2.3 of this study) at Grand Bank Head. At this locality, the red siltstone is succeeded by several

Figure 1.3: Generalized stratigraphic column of Chapel Island Formation, its subdivision into members, and the distribution of facies described in this study. Note that certain member boundaries have been redefined; see text for details. Scale is in meters.

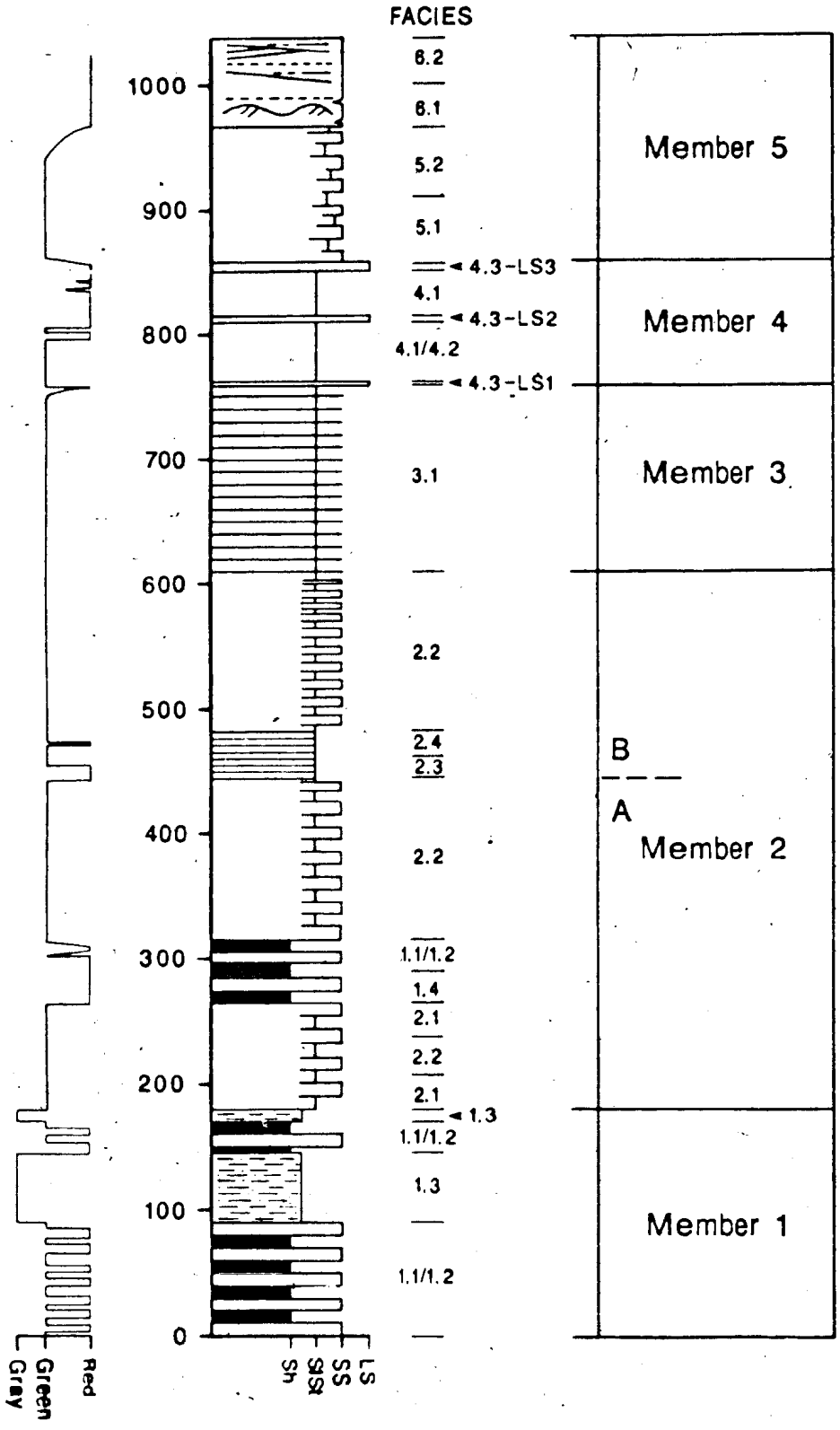
FACIES
1000
900
800
700
600
500
400
300
200
100
0
6.2
6.1
5.2
5.1
4.3-LS3
4.1
4.3-LS2
4.1/4.2
4.3-LS1
3.1
2.2
2.4
2.3
2.2
1.1/1.2
1.4
2.1
2.2
2.1
1.3
1.1/1.2
1.3
1.1/1.2
Member 5
Member 4
Member 3
B
A
Member 2
Member 1
Red
Green
Gray
Sh
SltSt
SS
LS

Figure 1.4: Fortune Bay area with the locations of measured stratigraphic sections. Locality abbreviations are as follows: Brunette Island (BI); Chapel Island (CI); Dantzic Cove (DC); Grand Bank (GB); Fortune Dump (FD); Fortune North (FN); Lewin's Cove (LC); Point May (PM); Radio Station (RS); Sagona Island (SI).

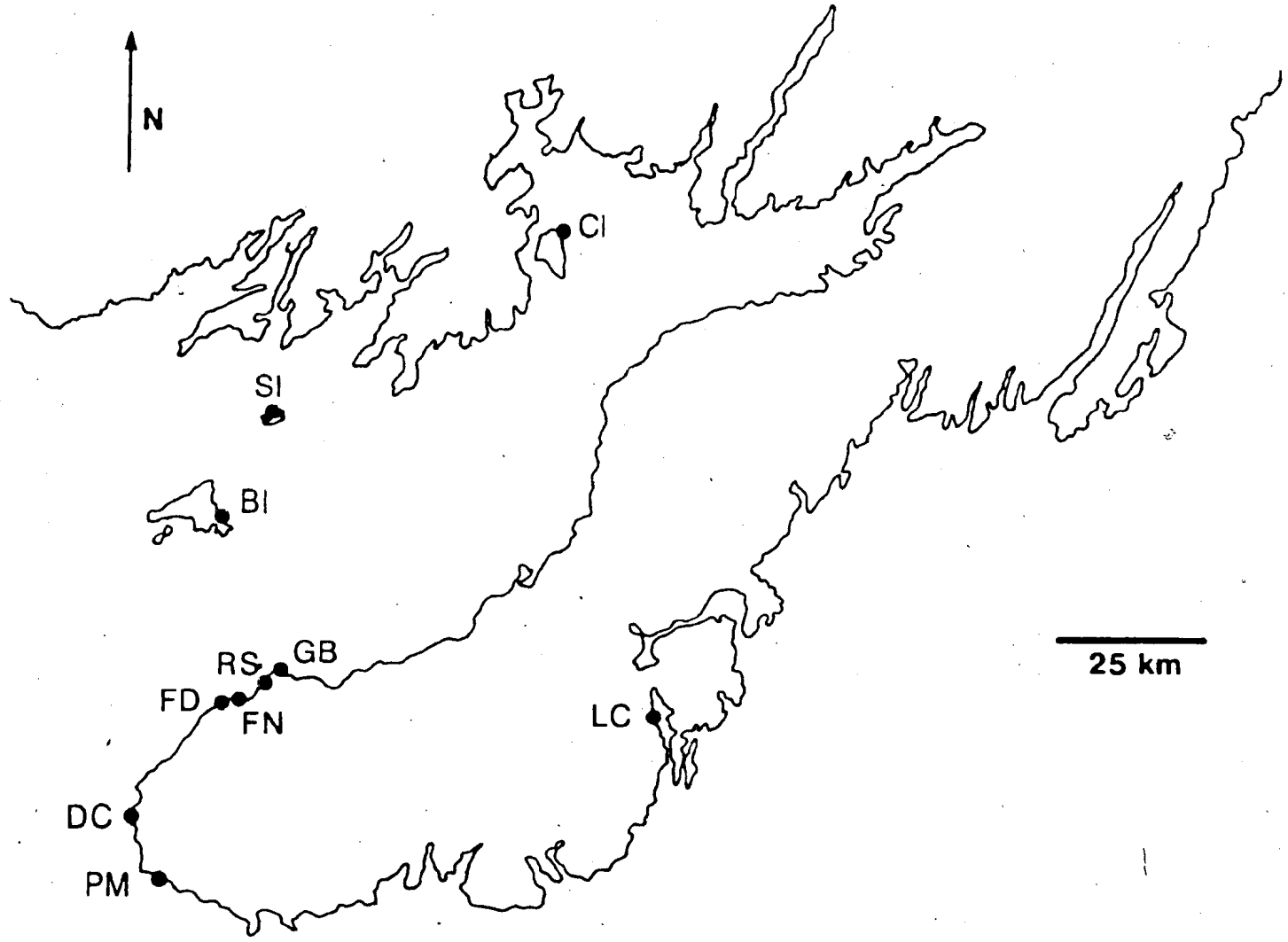
N
CI
SI
BI
RS
GB
FD
FN
LC
DC
PM
25 km

Figure 1.5: Correlation of outcrops for the lower Chapel Island Formation. The section at Duck Point is tectonically disrupted and was therefore not measured; its presentation is schematic. Symbols used in this diagram are the same as those used for measured sections; see Figure 2.4.

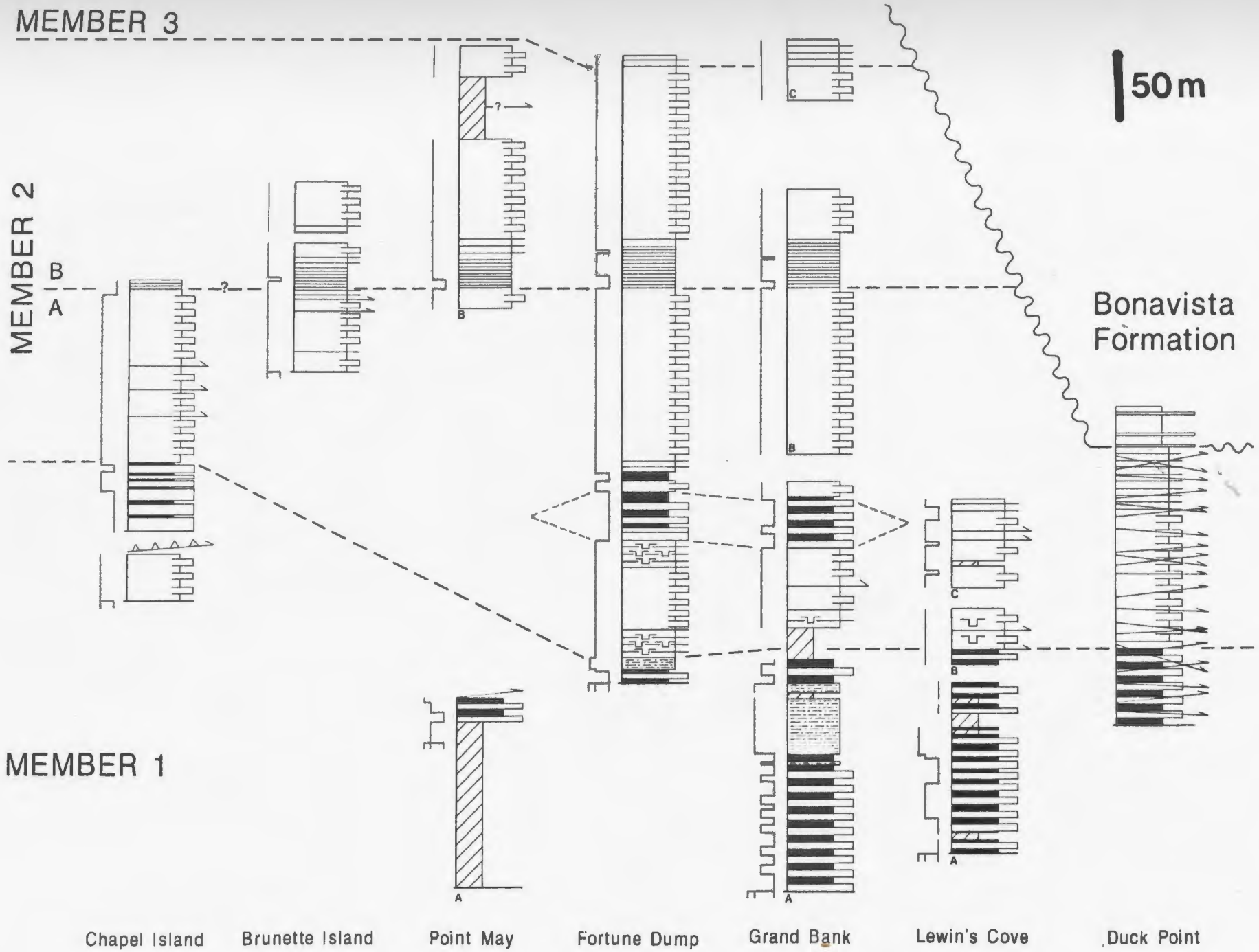
MEMBER 3
MEMBER 2
B
A
MEMBER 1
50m
Bonavista Formation
Chapel Island
Brunette Island
Point May
Fortune Dump
Grand Bank
Lewin's Cove
Duck Point

Figure 1.6: Correlation of outcrops for the upper Chapel Island Formation. Symbols used in this this diagram are the same as those used for measured sections; see Figure 2.4.

RANDOM FORMATION

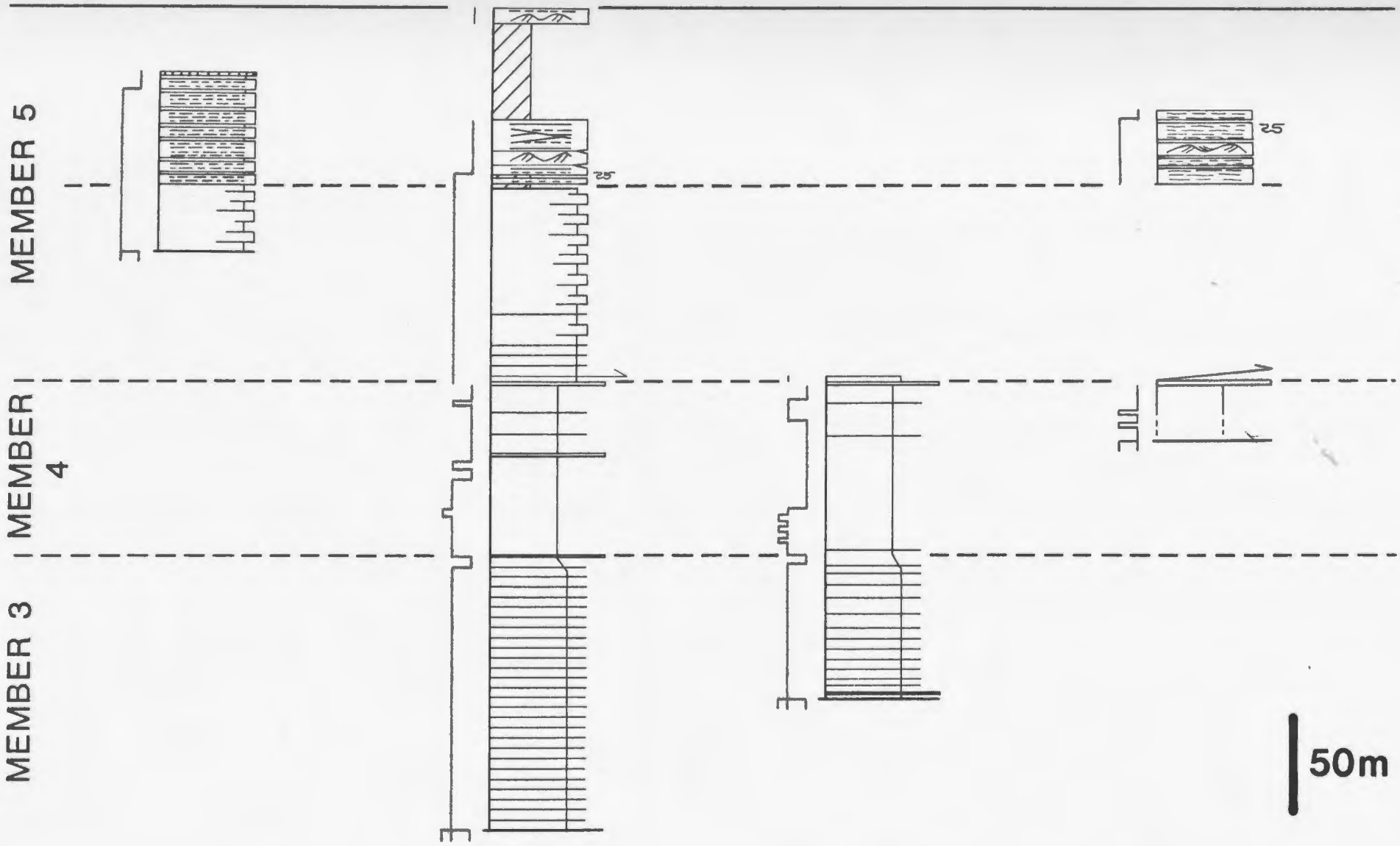

meters of green laminated siltstone (Facies 2.4 of this study), at which point the outcrop becomes highly faulted. These previous workers equated these laminated siltstones with member 3, which is lithologically similar and is found (with its base not exposed) at Dantzic Cove. At Fortune Dump, however, these red and green siltstones (formerly part of member 3) are succeeded by green sandstones and siltstones of the same facies as that of member 2; this can also be demonstrated at Grand Bank Head by carefully tracing beds across numerous faults. The lower boundary of member 3 has therefore been moved upward from its former position to a point higher in the formation where the sandstones and siltstones grade into the laminated siltstones of member 3. The old boundary between member 2 and member 3, which now lies within member 2, is used to separate the member into two parts, 2A and 2B. This is done because of the usefulness of the red siltstone horizon as a marker unit (traceable from Point May to Grand Bank), and also to retain a reference to the old member boundary so that other workers can compare the results of this and future work with that of earlier workers. The early estimate of 50 m for member 2 has been revised in this study to ~430 m, with 265 m for 2A and ~165 m for 2B.

The change from member 2 to the carbonate-concretion-bearing laminated siltstones of member 3 is gradational, and records a decrease in sandstone bed thickness and a concomitant reduction in percentage of sandstone. No outcrop of the CIF contains a full transition from member 2 to member 4, and a lack of marker beds leaves the exact thickness of member 3 in question. The most complete stratigraphic section of member 3 is found at Dantzic Cove, where the 135 m of strata serve as a minimum thickness. Facies characteristics indicate that the thickness of member 3 is not significantly greater than the estimate of 150 m given by Bengtson and Fletcher (1983).

Member 4 consists of red and green bioturbated mudstones, gray pyritiferous mudstones, and thin, micritic and stromatolitic limestones. The contact between member 3 and member 4 is defined as the base of the first limestone bed at Dantzic Cove (LS 1). The few meters of red mudstone that underlie this first limestone can be traced to Fortune

North, where the top of these red mudstones defines the top of member 3 in the absence of LS 1. Using these boundaries, separate measurements of the thickness of member 4 at the two localities are 85 m (the two measurements differed by only 20 cm!). The estimate of 165 m given by Bengtson and Fletcher (1983) was based on an incorrect correlation between a limestone bed (coalesced carbonate concretions) within member 3 at Fortune North and the lowest limestone bed (LS 1) at Dantzic Cove (Fletcher, pers. comm., 1985).

Member 5 consists, at the base, of green, thin to medium bedded sandstones and sandy siltstones that show an upward increase in bed thickness and sandstone percentage. This trend continues into the upper part of member 5, which consists of medium to thick bedded, red, micaceous sandstones. The thickness of member 5, with its base at the top of the third limestone bed at Dantzic Cove (LS 3), and its top at the first quartzitic sandstone bed of the Random Formation, is 178 m (previous estimate was ca. 150 m).

The thickness of the members of the CIF may be different in separate areas; the figures quoted above are drawn entirely from the Grand Bank Head, Fortune Dump and Dantzic Cove exposures. It should be emphasized that these members are informal, and that the focus of this study is primarily sedimentological, not stratigraphic, so that formal members are not proposed in this thesis.

1.6 BIOSTRATIGRAPHY OF THE CHAPEL ISLAND FORMATION AND THE PRECAMBRIAN-CAMBRIAN BOUNDARY

Ever since the discovery of small shelly fossils in the CIF at Dantzic Cove by Green and Williams (1974), there has been increasing interest in defining the Precambrian-Cambrian boundary within these strata. The International Precambrian-Cambrian Boundary Working Group, established in 1972 by the International Commission on Stratigraphy to examine potential boundary stratotypes around the world, concluded at a 1983 meeting in

Bristol, England, that the Burin Peninsula was one of three serious candidates to receive more in-depth analysis (Cowie, 1985). The other two sections, located in the Ulakhan-Sulugar region, Siberia, U.S.S.R. and the Meishucun region of southern China, are dominated by carbonate rocks and are therefore more fossiliferous than the Burin section, which is dominantly siliciclastic. The Burin section does, however, have the most abundant and diverse assemblage of trace fossils of this time period. These trace fossils show a distinct shift from simple 'Precambrian' forms to complex 'Paleozoic-type' trace fossils (Bengtson and Fletcher, 1973; Crimes and Anderson, 1985; Narbonne et al., 1987). It has been suggested that trace fossils should be used to define the Precambrian-Cambrian Boundary in the Burin section and for correlation of the boundary around the world (Narbonne et al., 1987). Part of the appeal of the Burin section as a boundary stratotype is its great thickness of sub-trilobitic Cambrian strata — greater than 1000 m as compared to less than 100 m for the other leading candidates.

Prior to this study, a major drawback to the Burin section has been the lack of a detailed measured stratigraphic section through the CIF. Because of this, faunal occurrences have been considered on a member-by-member or formational scale. The lack of measured sections led to poorly defined member boundaries, erroneous member thicknesses and miscorrelation of local outcrops. During the course of this study these problems were rectified and a significant body of new biostratigraphic data documented. Although the aims of this thesis are primarily sedimentological the author also carefully noted the position of numerous trace fossils. Several new forms were found, and the ranges of some extremely important traces (e.g., arthropod resting traces) were extended to far lower stratigraphic positions. These findings prompted the author to engage the help of trace-fossil specialists G.M. Narbonne and M.M. Anderson, and shelly-fossil expert E. Landing. Collaborative studies with these workers during the last two years have led to revision of the biostratigraphy of the CIF and formal proposal of a boundary stratotype (Narbonne et al., 1987). This group is organizing a meeting of the Precambrian-Cambrian

Boundary Working Group during August, 1987 in St. John's. A post-meeting field trip will visit three of the major outcrops on which this thesis has been based: Dantzic Cove, Fortune Dump and Grand Bank Point.

1.7 ORGANIZATION

This thesis is subdivided into ten Chapters. Chapter 1 is an introduction to the thesis aims, the general stratigraphic and geologic history of the field area, previous work and the lithostratigraphy and biostratigraphy of the Chapel Island Formation.

Chapter 2 outlines the approach to the study, including the techniques and methods employed, and includes a section on terminology and definitions in which abbreviations and sedimentologic terms used within the thesis are defined. The organization of lithofacies into facies associations is also discussed.

Chapters 3-8 include a thorough description and process interpretation for each of the lithofacies from each facies association. For each facies association, a summary of the lithofacies distributions, descriptions of individual outcrop localities, and a paleoenvironmental analysis are provided. Facies characteristics like color, texture, grain size, bed thickness and overall geometry, organic structures, and sedimentary structures are used to interpret the processes of sedimentation including: role of tides, waves, various currents and variable sediment input; timing and relative intensity of erosion and deposition; support mechanisms in gravity flows; relative water depths; approximations of current strengths; paleo-oxygen conditions during deposition and early diagenesis; and biogenic influence on sedimentation.

Chapter 9 contains a synthesis of the sedimentary history of the Chapel Island Formation within the overall context of known Avalonian geology. Chapter 10 presents a summary of the salient points of the thesis.

Chapter 2

INTRODUCTION TO LITHOFACIES DESCRIPTION AND INTERPRETATION

2.1 APPROACH TO STUDY

This study is field-based, with particular emphasis on detailed description and interpretation of lithofacies from outcrop and slabbed samples. Field work was carried out over the course of four summers from 1983 to 1986. Stratigraphic sections were measured at outcrops around the perimeter of the southern Burin Penisula and throughout northern Fortune Bay (Figure 1.4). Emphasis has been given to those outcrops on the southwestern Burin Peninsula, in particular those at Dantzic Cove, Fortune Dump and Grand Bank Head, where long, relatively continuous exposures of the entire formation are readily accessible.

Stratigraphic sections were measured with a metric tape and Jacob staff. Over 2160 m of strata were measured and drafted at a scale of 1 inch = 5 m; 528 m of this, and an additional 156 m section, were measured in more detail and plotted at a scale of 1 inch = 1 m. Several hundred hand samples were collected and slabbed. Many were then polished and sprayed with a clear laquer finish. 681 paleocurrent measurements were obtained from a wide variety of different sedimentary structures and plotted on equal-area rose diagrams. Paleocurrent measurements taken from dipping strata were rotated to correct for tilt directly

in the field using a wooden board with a built in level. Where necessary, correction for plunge of folds was done with the use of a stereonet. 120 standard thin sections of siliciclastic samples were examined. In addition, 40 standard and 35 3X2 inch thin sections of limestones were polished, stained with Alizarin Red S and potassium ferricyanide and then coated with a spray-on cover. Wet chemical analysis for P_2O_5 was performed on 5 samples of phosphatic shale.

2.2 TERMINOLOGY AND DEFINITIONS

The following section is a guide to the description of lithofacies that follows. Terminology and abbreviations used in the thesis are explained.

2.2.1 Descriptive Hierarchy of Stratification and Grain Size

Unless otherwise stated, stratification is described using the scheme of Ingram (1954). The use of this scheme has some drawbacks, and attempts are made, whenever possible, to provide specific unit thicknesses. Figure 2.1 summarizes the terminology used for the subdivision of beds and the grouping of beds into facies and facies associations. Facies and facies associations are referred to by number in the order in which they appear in the text. The abbreviation FA is used for individual facies associations, followed by the appropriate number; e.g., FA 2. Facies are given numbers according to the facies association from which they are described. The first number refers to the number of the facies association and the second number is the facies number: e.g., Facies 2.2 is the second facies described from Facies Association 2.

Grain size and roundness were determined in the field by comparison with a commercial sand gauge (McCollough, 1984). The size grade scale used in this study is the

Figure 2.1: Terms for field descriptions of beds, their subdivision and their arrangement into larger sedimentary units. Modified from Blatt et al. (1980; Fig. 5-1). Beds are layers of sedimentary rock that are distinguishable from layers above and below based on rock type, sedimentary structures, or texture. Beds do not have distinct discontinuities but are composed of divisions with their own suite of sedimentary structures. Amalgamated beds are composite or multiple beds deposited from more than one event; the separate portions of these beds are called layers. Beds are grouped into facies according to lithologic, structural or organic aspects detectable in the field. Facies which are stratigraphically interrelated are grouped into facies associations.

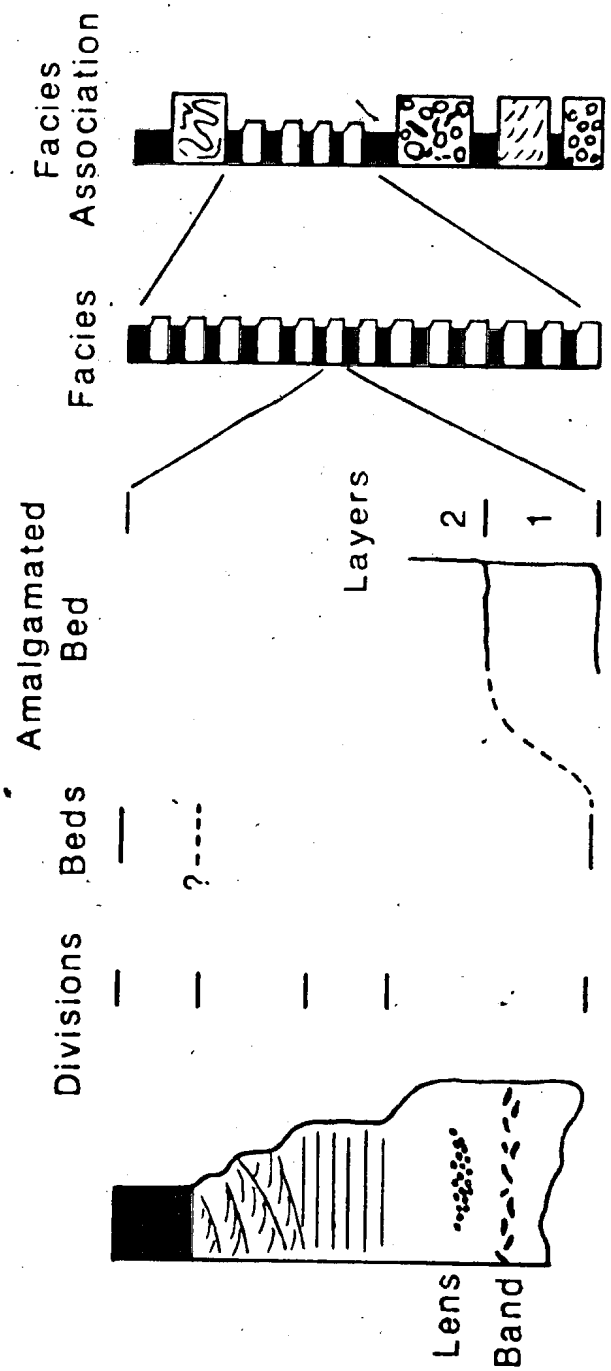
Facies Association
Facies
Amalgamated Bed
Layers
2
1
Beds
?----
Divisions
Lens
Band

Udden-Wentworth scale (see Blatt et al., 1980, Table 3-3). Field names for texture follow Figure 2.2 (ternary diagram). The terms 'siltstone' and 'mudstone' are used in field determinations, but for description of cut slabs the siltstone and mudstone fields have been subdivided (see Figure 2.2).

2.2.2 Outcrop Localities and Stratigraphic Position of Beds

Abbreviations for outcrop localities are given in Table 2.1. Specific beds or intervals from particular stratigraphic sections will be referred to during the course of the thesis. In order to locate these more easily on the drafted sections provided, the bed or horizon will be referred to using the abbreviation for the outcrop followed by the stratigraphic position above the base of the section. For example, a bed with base located 240.5 meters stratigraphically above the base of the measured section at Dantzic Cove is referred to as DC-240.5. The three localities most commonly referred to in this way are: (1) Grand Bank Head, GB; (2) Fortune Dump, FD; (3) Dantzic Cove, DC. Some outcrops, including the Grand Bank Head section, were divided into several subsections labelled A, B, and C, each of which is numbered individually starting with 0 m at the base. This was done where the outcrop had a covered or inaccessible interval of unknown stratigraphic thickness. In these cases reference to stratigraphic position is similar to that described above, but the stratigraphic position is followed by a letter referring to the subsection at that locality, e.g., GB-122.8A. In addition to outcrop abbreviations, the abbreviation used throughout this thesis for the Chapel Island Formation is CIF.

2.2.3 Sedimentological Terminology and Definitions

The terminology used to describe climbing-ripple cross-laminae comes from Harms et al. (1982). Examples that record only lee-side preservation will be referred to as

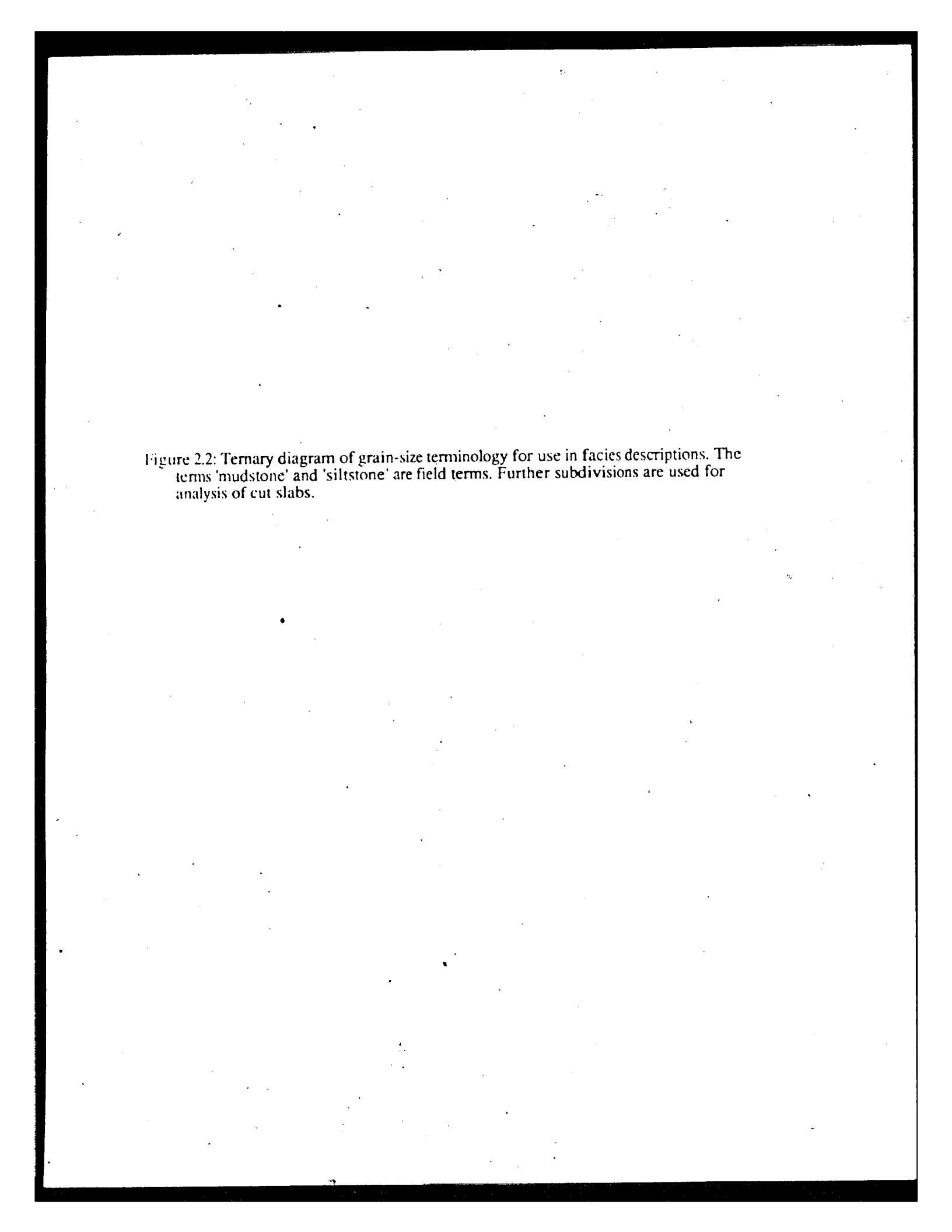

Figure 2.2: Ternary diagram of grain-size terminology for use in facies descriptions. The terms 'mudstone' and 'siltstone' are field terms. Further subdivisions are used for analysis of cut slabs.

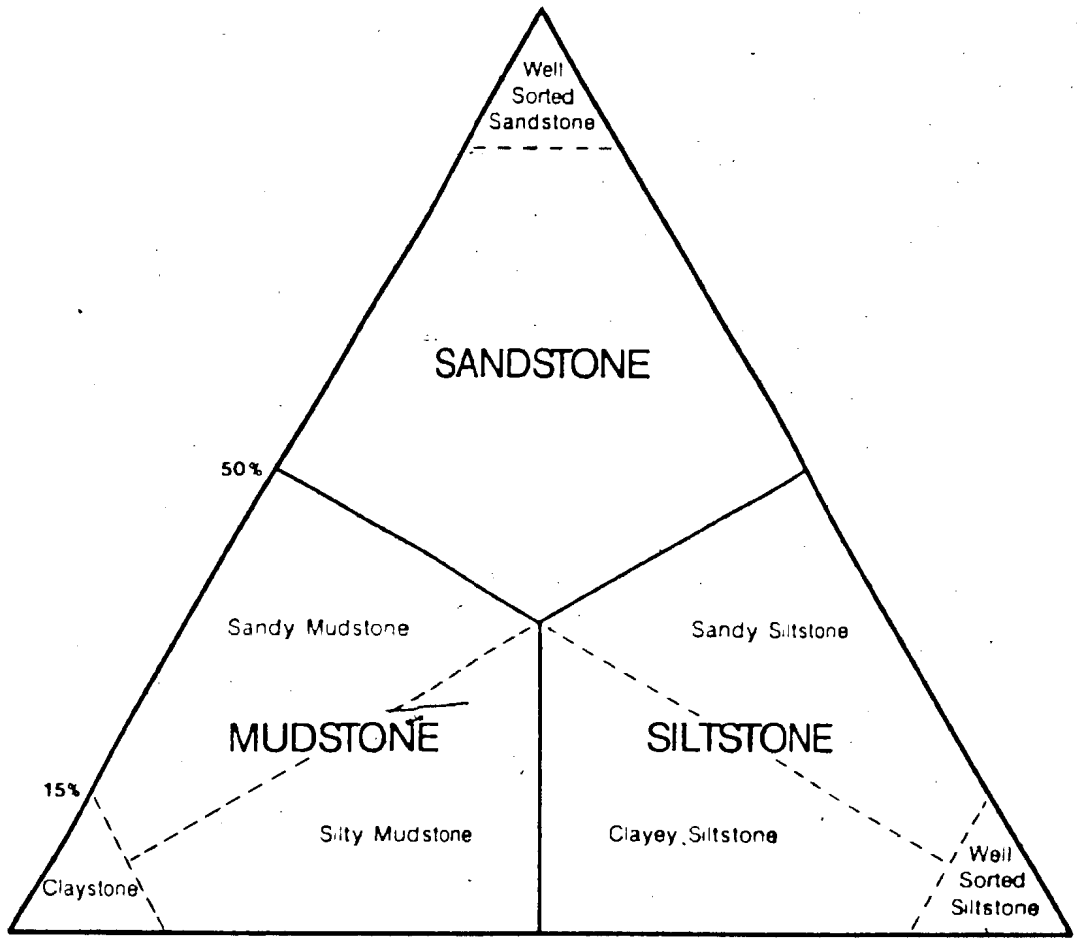
Well
Sorted
Sandstone
SANDSTONE
50%
Sandy Mudstone
Sandy Siltstone
MUDSTONE
SILTSTONE
15%
Silty Mudstone
Clayey Siltstone
Claystone
Well
Sorted
Siltstone

TABLE 2.1: OUTCROP LOCALITIES

Dantzic Cove	DC
Fortune Dump	FD
Grand Bank Point	GB
Fortune North	FN
Radio Station	RS
Lewins Cove	LC
Sagona Island	SI
Brunette Island	BI
Chapel Island	CI
Point May	PM
Boxey Point	BP

"erosional-stoss" cross-laminae, while those in which the stoss side of the ripple form has been preserved will be referred to as "depositional-stoss" cross-laminae. The former were designated 'Type A' by Jopling and Walker (1968) and 'Type 2' by Reineck and Singh (1980); the latter were called 'Type B' and 'Type 1' by the same authors, respectively.

'Oscillatory' and 'bidirectional' currents are alluded to in this thesis. These terms are used as follows: the term 'oscillatory' is used in reference to short-period reversing flows beneath wind-generated waves, and the term 'bidirectional' is used in reference to long-period reversing currents such as tidal currents.

2.2.4 Mass-movement and Gravity-Flow Deposits

Mass-transport processes and deposits are discussed in detail in Chapter 4. The term 'slide' will refer to essentially rigid masses that move along discrete shear surfaces. 'Slumps' are considered a subset of slides in which rotational movement occurs along a curved shear surface (Nardin et al., 1979). Sediment gravity flows are classified according to the dominant sediment-support mechanisms (Middleton and Hampton, 1973). In turbidity currents, grain support comes from the upward component of fluid turbulence. Grain flows are those in which grains are supported by direct grain-to-grain interactions (collisions and near collisions). Debris flows are sediment gravity flows in which grains are dispersed in a slurry of water and fine sediments and grains are supported by the inherent strength of this slurry. In liquefied flows, grains are suspended by water that is upwardly displaced (by settling of grains) during readjustment of loosely packed sediment to a more stable packing (Lowe, 1976a). These gravity flows will be discussed in more detail later in the thesis.

2.3 FACIES ASSOCIATIONS

The grouping of facies into facies association is subjective, based on intimate association of sets of facies. The facies associations tend not to range over more than one member, one exception being the presence of Facies 1.1, 1.2 and 1.4 within member 2 (Figure 1.3), and no facies are found in more than one facies association. This reflects the progressive evolution of fundamentally distinct depositional systems through time (i.e., large-scale, nonrepetitive change). The correspondence between facies associations and members results from members being fundamentally distinct lithologic groupings. Those facies association numbers that do not correspond directly with member numbers are: (a) the inclusion of units of facies from FA 1 within member 2, and (b) the division of member 5 into two facies associations (FA 5 and 6) (Figure 1.3).

A section on paleoenvironmental analysis immediately follows the description and process interpretation of each of the six facies associations. This approach is adopted due to the considerable length of the sections on description and process interpretation. The interpretation of paleoenvironment rests in part on the stratigraphic relationships between facies associations, so the lithologies, sedimentary structures, and environmental interpretations for each facies association have been summarized for reference in Figure 2.3.

Measured stratigraphic sections from the principal localities of Fortune Dump, Grand Bank, and Dantzic Cove are given at this point in the thesis (Figures 2.5-2.7; a legend is provided in Figure 2.4). The location of measured sections at these and all other outcrops is given in Appendix A. The remaining stratigraphic sections (CI, LC, BI, PM, RS and SI localities) are given in Appendix B. Detailed sections are given in Appendices C (FD locality) and D (DC and FN localities). Reference to Appendix C is strongly urged for discussion of member 2.

Figure 2.3: Generalized stratigraphic column and vertical facies distributions of the Chapel Island Formation and list of lithologies, sedimentary structures and paleoenvironmental interpretations.

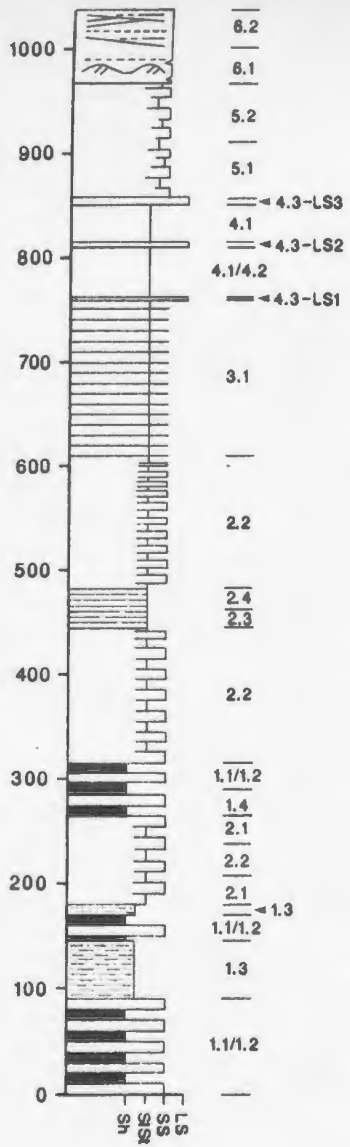

FACIES	LITHOLOGY	SEDIMENTARY STRUCTURES	ENVIRONMENTAL INTERPRETATION
FACIES 6.1a/b	Red micaceous sandstone; minor siltstone and conglomerate	Parallel lamination; hummocky and swaly cross-stratification; wave ripples	Prograding storm-dominated shelf (nearshore)
FACIES 5.1/5.2	Interbedded green sandstone and sandy siltstone	Graded sandstones,; parallel lamination; current ripples; rare convolute bedding	Prograding storm-dominated shelf (offshore)
FACIES 4.3	Red to white micritic and stromatolitic limestone	Fossiliferous; desiccation cracks; tepee and sheetcrack structures; mud mounds; planar/columnar stromatolites; oncolites	Peritidal; low energy
FACIES 4.2	Gray mudstone	Burrowed; pyrite nodules; pyritic steinkerns	Low energy dysaerobic shelf
FACIES 4.1	Red and green mudstone	Bioturbated; abundant carbonate concretions	Low energy oxygenated inner shelf
FACIES 3.1	Green laminated siltstone	Parallel lamination; current ripples; carbonate concretions; current/parting lineations	Outer shelf (sub wave-base)
FACIES 2.3/2.4	Red and green laminated siltstone	Red: parallel lamination, wave-ripple lamination Green: carbonate nodules, pyrite nodules	Low energy subtidal shelf; Delta abandonment facies
FACIES 2.2	Thin to medium bedded gray-green sandstone and siltstone	Grading; wave and combined-flow ripples; pebble lags; parallel lamination; mass movement deposits; HCS; graded rhythmites	Storm-influenced subtidal Lower delta front/prodelta
FACIES 2.1	Very thin to thin bedded gray-green sandstone and siltstone	Abundant gutter and pot casts; pinch-and-swell and lenticular bedding; unifite siltstone beds	Storm-influenced shallow subtidal Upper shoreface/delta front
FACIES 1.4	Medium bedded red sandstone and shale	Channel sandstones; parallel lamination; shale rip-up clasts; synaeresis/desiccation cracks	Peritidal, high energy,tidal influence
FACIES 1.3	Gray to black laminated sandstone and shale	Contorted bedding; synaeresis cracks; pyrite and phosphate nodules; channel sandstones	Semi-restricted low-energy
FACIES 1.1/1.2	Red and green sandstone and shale	Flaser, wavy and lenticular bedding; scour and channel sandstones; synaeresis/desiccation cracks; parallel and ripple cross-lamination	Peritidal, tidally-influenced

Figure 2.4: Legend for stratigraphic columns for FD, GB, DC (Figures 2.5-2.7) and CI, LC, RS, PM, BI, SI (Figures B1-B6: Appendix B).

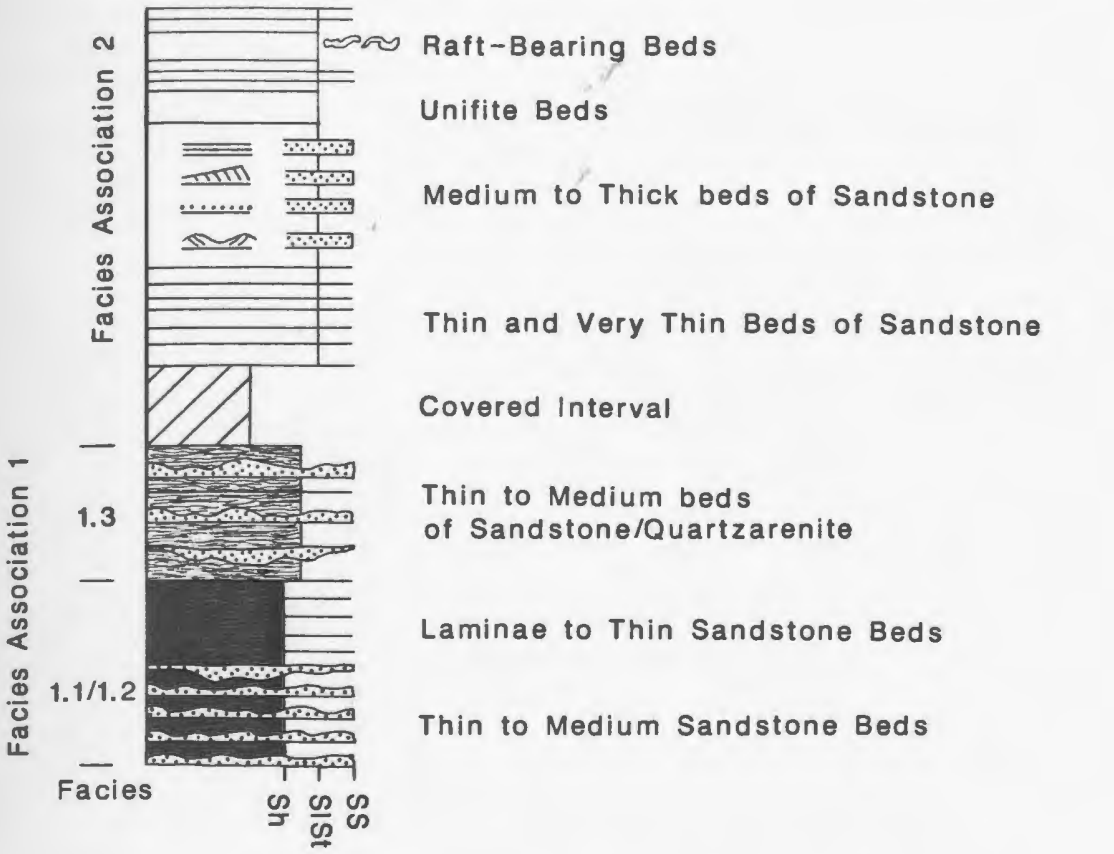

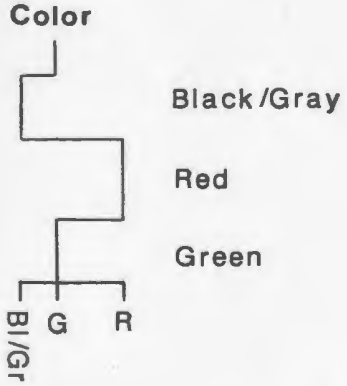

Paleocurrent Information

- Groove Marks
- Current/Parting Lineations
- Flute Marks

KEY

- Parallel Laminations
- Ripple Cross-Laminations
- Graded Bedding
- HCS
- Current Ripples
- Wave Ripples
- Gutter Casts
- Slump Fold
- Rafts
- Q — Quartzarenite Beds
- Shrinkage Cracks
- Mudstone Intraclasts
- Phosphate Nodules
- Pyrite Nodules
- Ball and Pillow
- Raindrop Prints
- Bioturbation
- Arthropod Scratches

Figure 2.5: Stratigraphic section from the Fortune Dump locality. Detailed section of this locality is given in Appendix C.

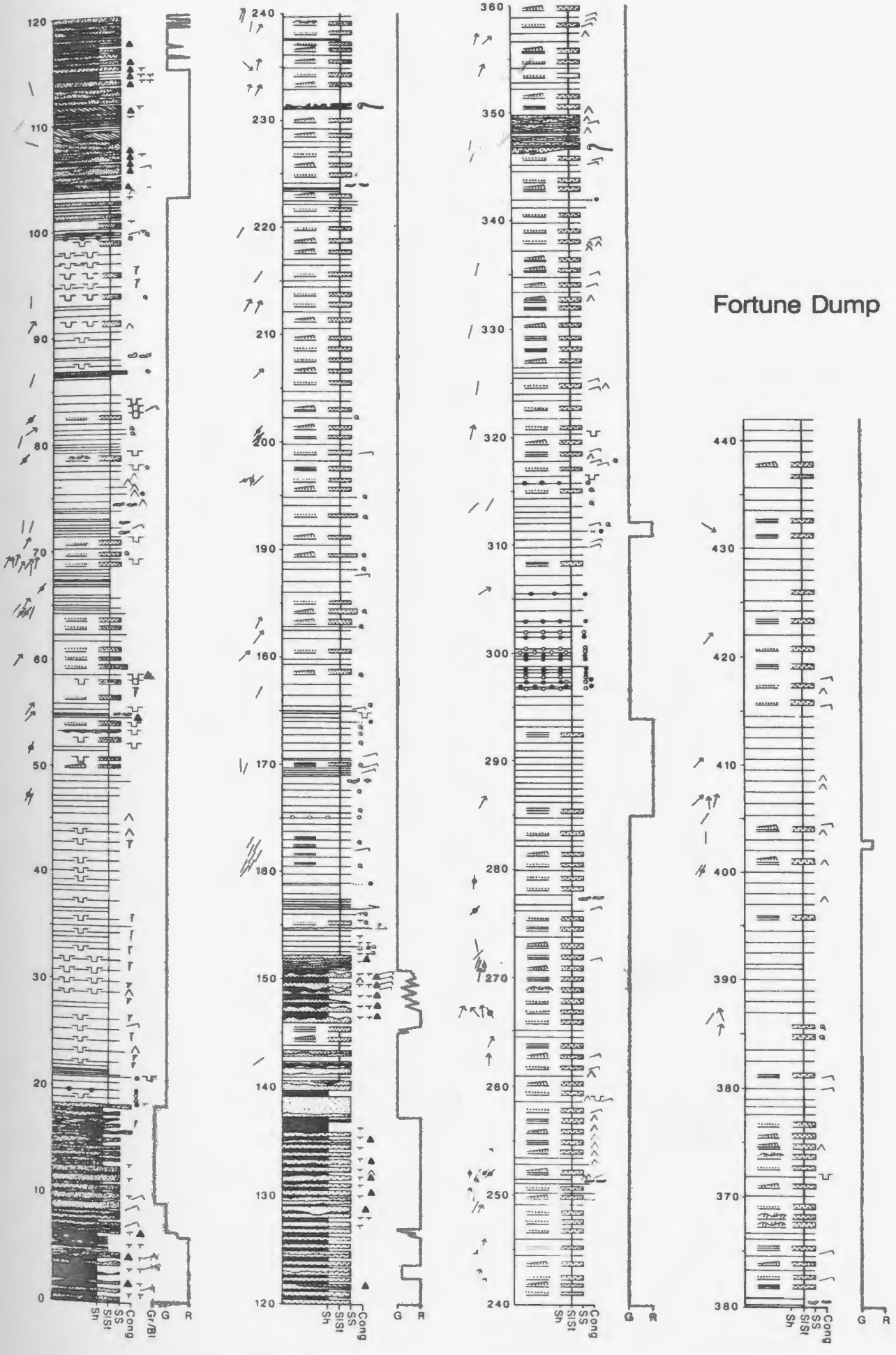
Fortune Dump
Sh
SlSt
SS
Cong
Gr/Bl
G
R

Figure 2.6: Stratigraphic section from the Grand Bank locality. Portions of this section are accessible only by boat.

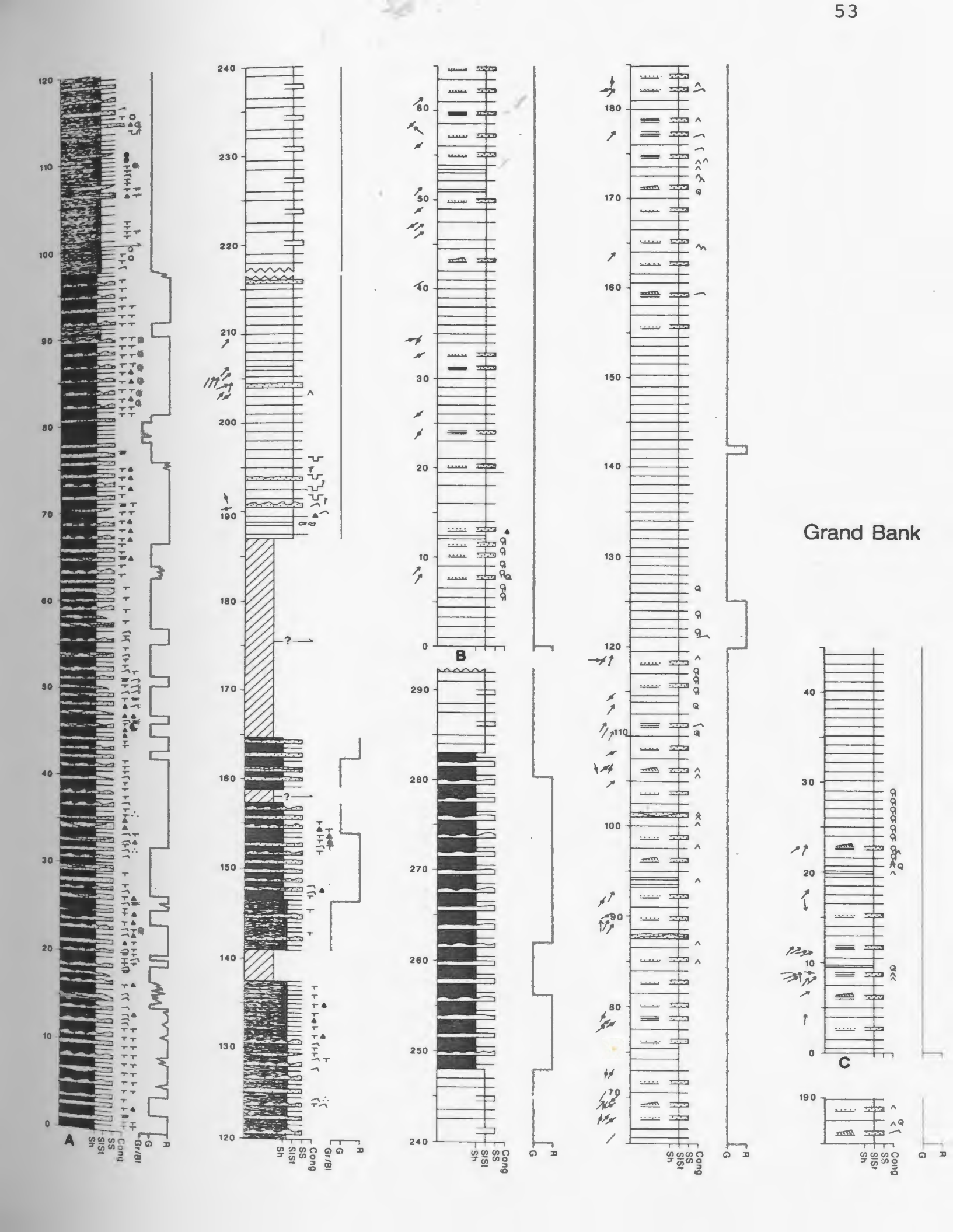
Grand Bank
A
B
C
Sh
SlSt
SS
Cong
Gr/Bl
G
R

Figure 2.7: Stratigraphic section from the Dantzic Cove locality. Detailed section of members 3 and 4 at this locality is given in Appendix D.

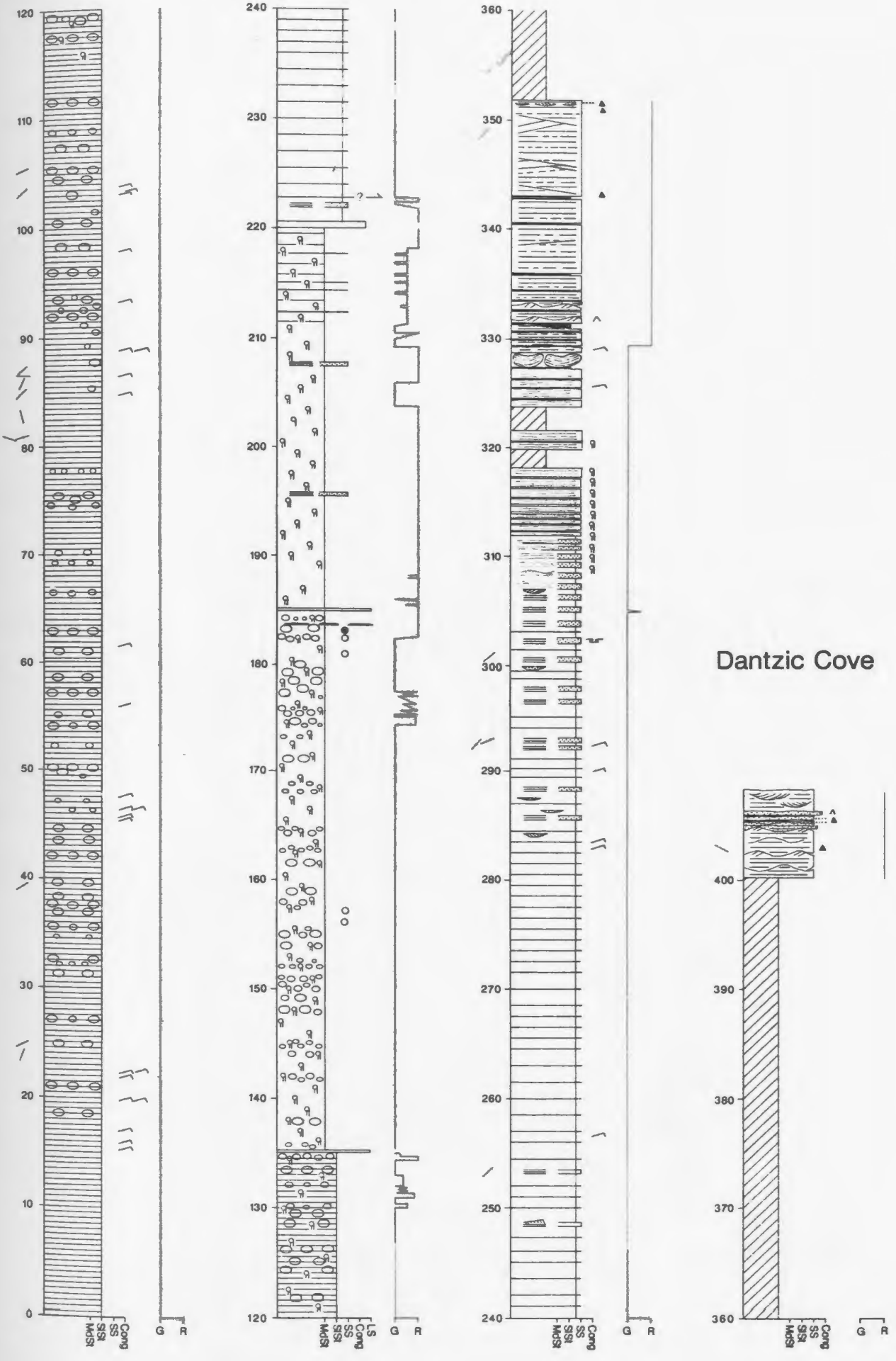
Dantzic Cove
MdSt
SlSt
SS
Cong
LS
G
R

Chapter 3

FACIES ASSOCIATION 1

3.1 INTRODUCTION

Facies Association 1 has been divided into four lithofacies, each of which is described below. Facies 1.1 and 1.2 are intergradational, and in places, interlayered on a small scale. The four facies described below constitute all of Member 1 and a small part of Member 2 (Figure 1.3). A discussion of the vertical and lateral lithofacies distribution is given in Section 3.5.

3.2 RED AND GREEN THIN/MEDIUM BEDDED SANDSTONE/SHALE FACIES (1.1)

Facies 1.1 is composed of red and green, thin to medium bedded, fine to medium grained beds of sandstones, interbedded with thinner beds of siltstone and shale (Plate 1a). The sandstone component makes up roughly 50-80% of this lithofacies. Only a handful of examples were noted in which maximum grain size exceeds sand grade. In these, small pebbles are present at the base of sandstone beds.

Red and green strata alternate stratigraphically on a meter scale, with a very minor percentage of strata color banded on a centimeter or decimeter scale. Such mixed units always exhibit green sandstone and red or pink siltstone and shale beds. Individual

PLATE 1: RED AND GREEN SANDSTONES AND SHALES (FA 1)

a: Typical exposure of Facies 1.1 strata at GB illustrating the style of interbedding and the irregularity and lenticularity of sandstone beds. Stratigraphic top is to the left. Scale is 9 cm long.

b: View of steeply dipping strata at GB looking stratigraphically upsection. These well-exposed soles show synaeresis and desiccation cracks and the imprints of current ripples. Cliff is approximately 15 m high.

c: Polygonal cracks on the base of a bed at GB-21.2A. These are interpreted as desiccation features. Scale is 15 cm long.

d: This close-up of green Facies 1.2 strata shows the scale and style of these wavy and lenticular bedded sandstones and shales. Starved ripples and shrinkage cracks (mostly ptygmatically folded synaeresis cracks) are especially abundant. Stratigraphic top is up. Scale is 9 cm long.

e: Discontinuous, spindle-like shrinkage cracks at the base of GB-24.1A. These are interpreted as synaeresis cracks. Scale is 9 cm long.

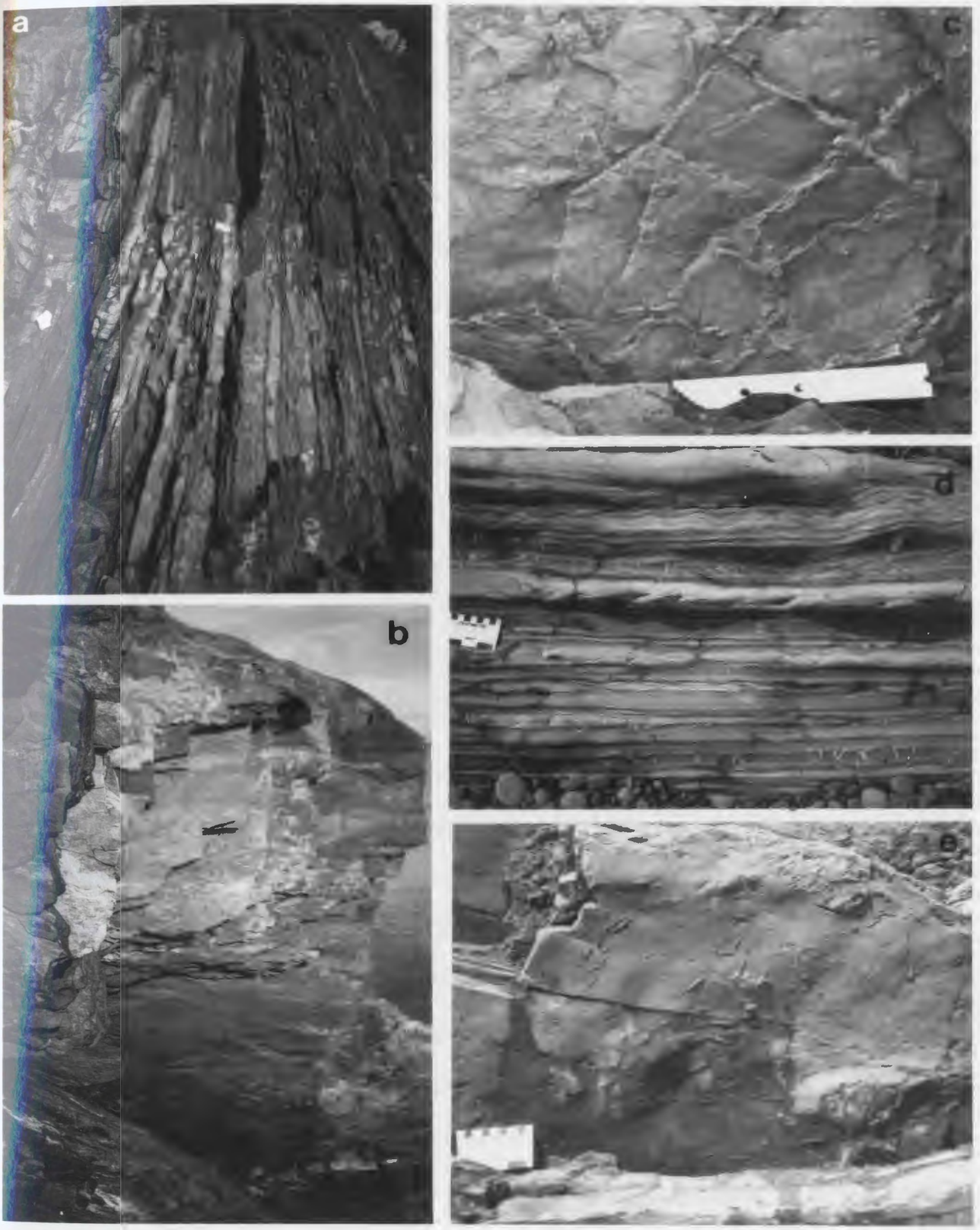
a
b
c
d
e

packages of red or green strata vary considerably in thickness from 50 cm to 10 m. At least 70-80% of these packages are between 1 and 5 m thick. Differences exist in the overall character of green versus red parts of this lithofacies; these differences are generalized, not rigid, and will be discussed in more detail below. The green units usually contain thicker and more abundant sandstone beds.

Flaser, wavy and lenticular bedding are characteric features of this lithofacies. Lower bedding surfaces are sharp, and may be planar or irregular. Upper surfaces are also sharp, and are either flat, rippled, or very irregular, with truncation of underlying laminae (Plate 1a). Sandstone beds less than 3 cm thick may be structureless, parallel laminated, or ripple cross-laminated, and are often discontinuous, defining lenticular bedding. Form sets of asymmetrical ripples are abundant, and provide abundant paleocurrent data. These thinner sandstone beds also include starved ripples, with asymmetric profiles and unidirectional cross-laminae.

Thin to medium beds of sandstone are more diverse internally and often contain amalgamation surfaces. A common motif in these beds consists of: (1) a lower division of structureless sandstone with abundant angular shale clasts, overlain by (2) parallel-laminated sandstone with or without minor quantities of shale clasts, capped by (3) unidirectionally cross-laminated, asymmetric ripples. Shale clasts in the lower division of these 'motif-beds' show grading in terms of abundance, and to a lesser degree in terms of size. Many beds are composed of both top-cut-out motifs (Divisions 1 and 2 only) and base-cut-out motifs (Divisions 2 and 3 only). The bases of these beds are usually quite irregular, truncating laminae in the beds below.

Some beds display complexly cross-stratified sandstone in which cosets of cross-strata are separated by curved lower surfaces that show multiple orders of truncation and are found at various angles to bedding. These beds, and other less complicated cross-stratified beds, may display depositional-stoss and erosional-stoss climbing-ripple cross-laminae (Jopling and Walker, 1968; terminology of Harms et al., 1982).

Sandstone beds are characteristically discontinuous. This is due, in part, to the abundant erosional surfaces that characterize this lithofacies. There are two types of erosional surfaces in this lithofacies. The first type consists of irregular, extensive surfaces that pass laterally into amalgamation surfaces. These surfaces may be overlain by fine-grained rocks (shales or laminated shales) or by sandstone.

A second type of erosional surface defines — with an overlying sedimentary package — isolated, lenticular, concave-up beds. Geometrical data for some of these beds are given in Table 3.1, and include (a) the product of width x thickness, a rough measure of cross-sectional area, and (b) the ratio of width/thickness, called the 'scour-and-fill index' (Nagtegaal, 1966). The beds above these scour surfaces vary lithologically from 100% sandstone to sandstone interlaminated or interbedded with shale, and include structureless, parallel-laminated and ripple-laminated sandstone beds. In all cases, layering abuts sharply against the margins of the scours (Figure 3.1). Sandstone beds may show a single set of cross-lamination (Figure 3.2a,c), like that illustrated by Potter (1963, Figure 22). In some cases, a complex series of sandstone-filled erosional surfaces is preserved, with clear cross-cutting relationships (Figure 3.2c).

Sedimentary structures on upper bedding plane surfaces include straight, sinuous, and interference ripples, and rare raindrop prints. It is not unusual to find two separate ripple sets preserved on one bedding surface, one ripple set superimposed on the other. Many lower bedding surfaces have ball-and-pillow structures. In places, load balls of sandstone are found 'floating' in shale (Figure 3.2b).

Sandstone-filled shrinkage cracks are conspicuous features on both upper and lower bedding surfaces. In cross section these features are found projecting down as much as several centimeters from the bases of sandstone beds into underlying shale layers. They may cut through as much as 5 cm or more of shale, or interbedded sandstone and shale. Though irregularly bent and commonly ptygmatically folded, most crack fillings are tapered

TABLE 3.1: LENTICULAR SANDSTONE BEDS: FACIES 1.1/1.2

Width (cm)	Thickness (cm)	Width X Thickness (cm^2)	Width/Thickness
80	14	1120	5.7
50	5.5	275	9.1
55	9	495	6.1
260	11.5	2990	22.6
460	16	7360	28.8
240	11	2640	21.8

Figure 3.1: Sketch of outcrop of Facies 1.1 at GB-16.3A. Features include discontinuous and lenticular bedding; erosional upper and lower surfaces; unidirectional ripple cross-lamination with bidirectional pattern; transitions from parallel lamination to ripple cross-lamination; lenticular beds of both sandstone and thin beds of siltstone, shale and sandstone.

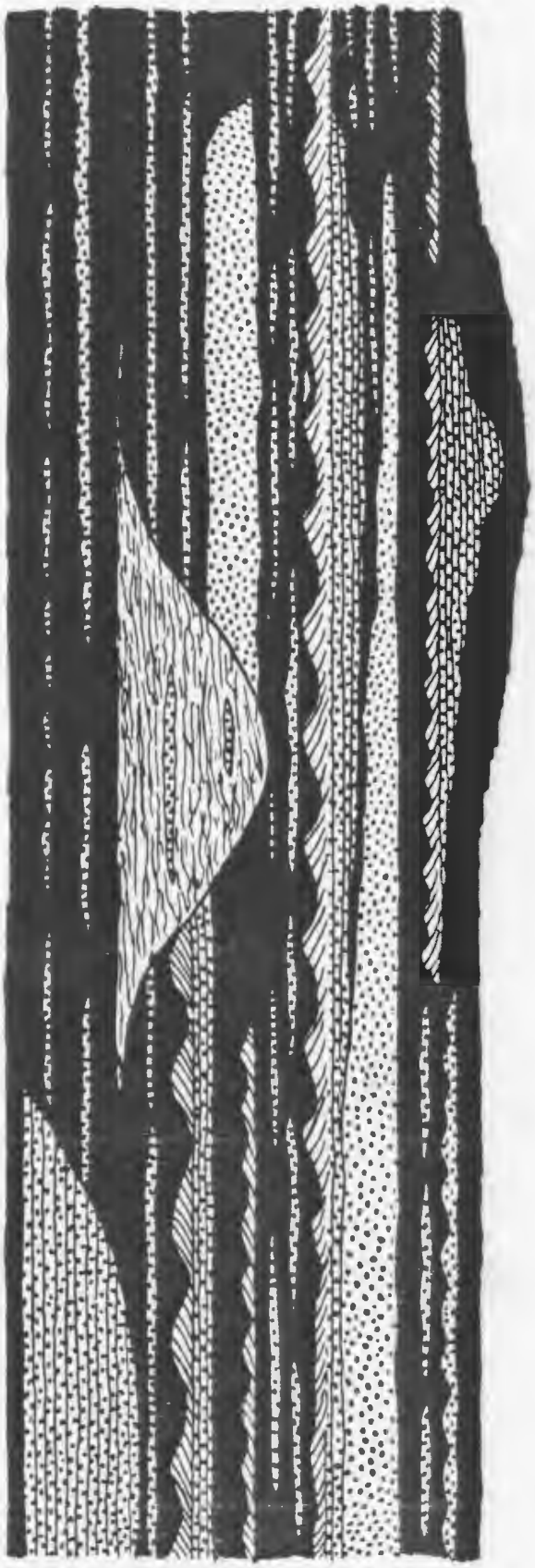

50 cm

20 cm

Figure 3.2: Sketches of outcrop of Facies 1.1/1.2.

(A) GB-70.0A. Note lenticular bedding, abundant shrinkage cracks, and thick lenticular sandstone bed with a single set of cross-laminae.

(B) GB-3.8A. Note discontinuity of bedding, erosional upper surfaces, bidirectional orientation of ripple cross-lamination, transition from parallel lamination to ripple cross-lamination, shale chips, and load-ball horizon.

(C) GB-44.5A. Note erosional upper surfaces, graded beds, shale-chip conglomerate, transitions from structureless to parallel-laminated divisions and a discontinuous rippled bed. Note lenticular sandstone beds with cross-lamination and evidence for multiple periods of downcutting.

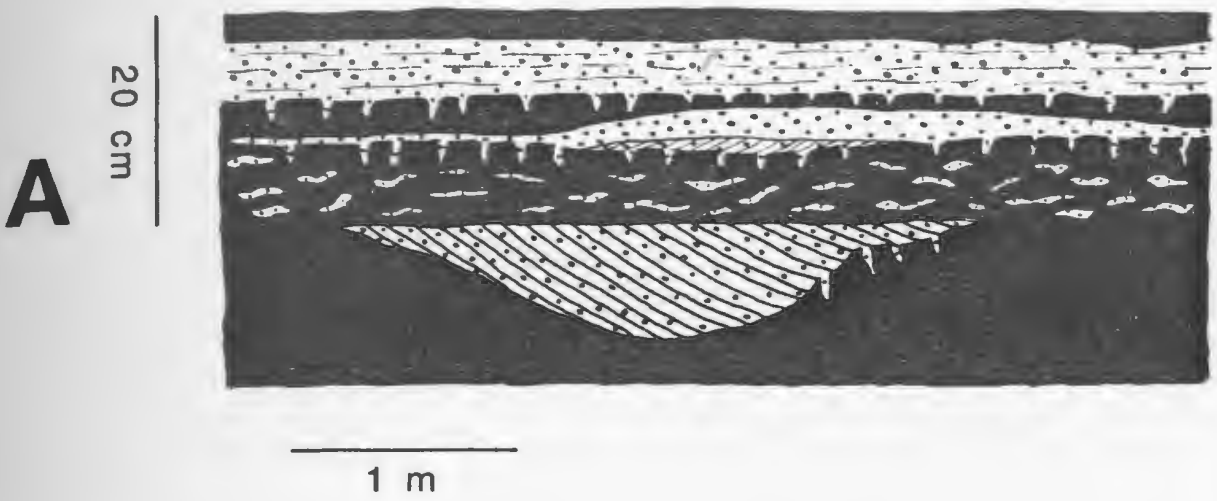
A
20 cm
1 m

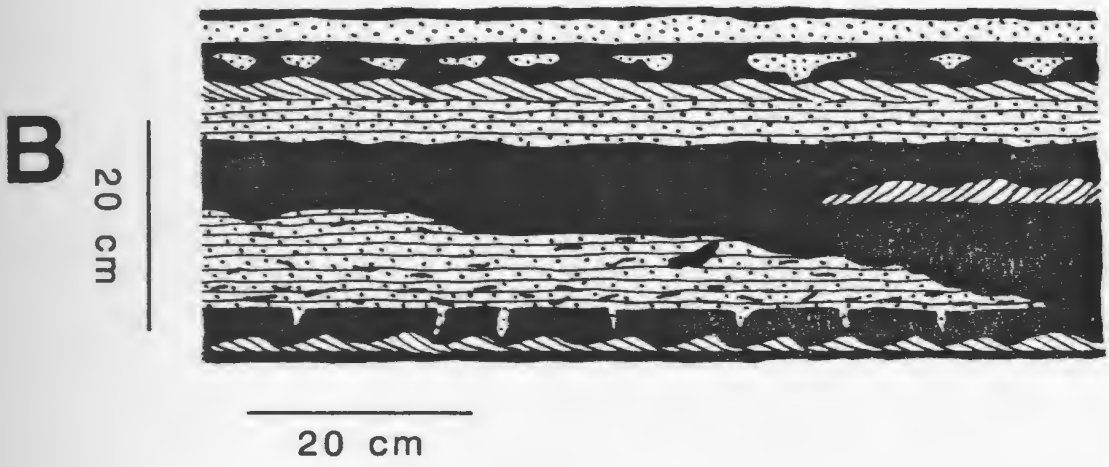
B
20 cm
20 cm

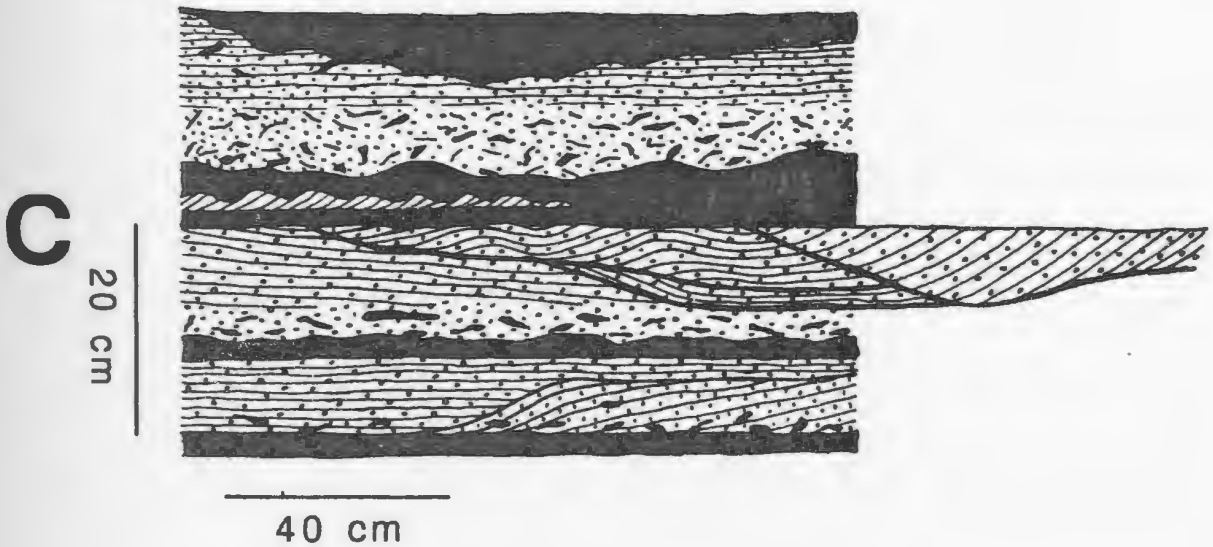
C
20 cm
40 cm

downward. A few examples have a nontapered rectangular shape with unusual sharp, flat bottoms. Cross-sectional irregularities include downward variation in thickness and downward bifurcation or merging of adjacent cracks (Plate 1d).

In plan view these shrinkage cracks weather as sandstone ridges that show the following morphotypes: (1) polygons several centimeters across (Plate 1c), (2) three-armed star shapes, and (3) linearly oriented, straight to slightly irregular spindles (Plate 1e). In the last, the ridges may bifurcate, with the two forks remaining essentially parallel to the overall preferred direction. The linear examples extend along the bedding plane anywhere from 1-2 cm to tens of centimeters. Their width may vary from a few millimeters to greater than 1 cm. Polygonal patterns are only slightly less common than the other types. These generally have a polygon width of several centimeters, but larger examples tens of centimeters across were noted at several localities.

In general, green units in this lithofacies have: (1) a greater total percentage of sandstone, (2) greater average bed thickness, and (3) lower abundance of shrinkage cracks and starved ripples than red units.

The paleocurrent data gathered for Facies 1.1 and 1.2 (Figure 3.3) are grouped together because of the difficulty in distinguishing, in all cases, these two transitional lithofacies in the field. Greater than 90% of the data are derived from rocks that certainly can be defined as Facies 1.1. Very few measurements were taken from strata decidedly of Facies 1.2 because of the smooth weathering pattern of these rocks.

3.2.1 Process Interpretation

Flaser, wavy, and lenticular bedding styles are formed by alternations of (i) current-induced bed-load transport and deposition of sand and (ii) slack-water deposition of muds from suspension (Reineck and Wunderlich, 1968). The fine-grained fraction of this lithofacies contains little or no disseminated sand-sized grains, ruling out a winnowing

Figure 3.3: Paleocurrent rose diagrams from Grand Bank Point (GBP-A) of Facies 1.1/1.2. "A" shows data on ripple paleocurrent (n=58) and "B" shows data on ripple crest-trend (n=19); see text for discussion.

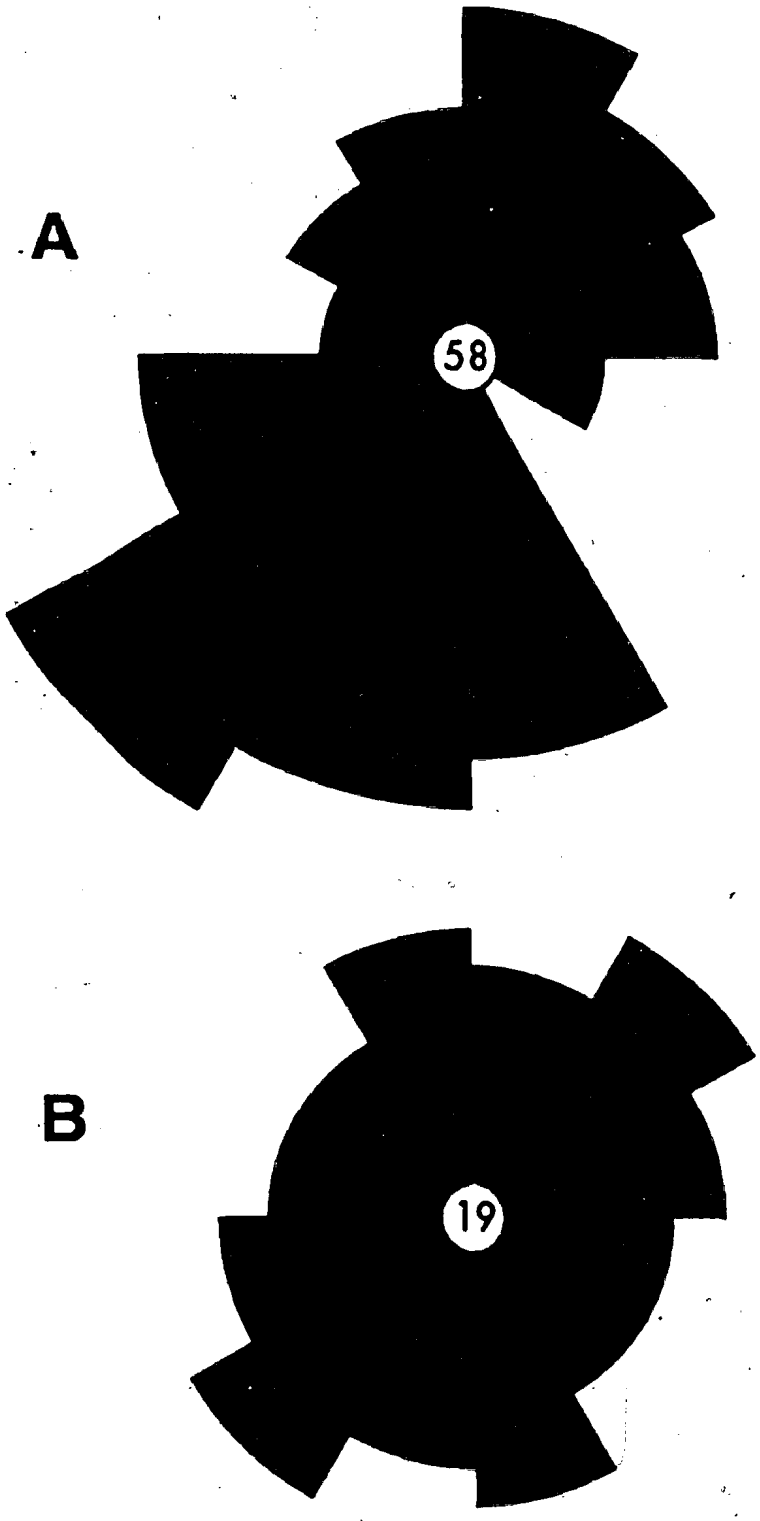
A
58
B
19

origin for the sandstone beds. Most of the sandstone beds have tractional sedimentary structures such as ripples and parallel lamination. Only a small proportion of sandstone beds, and divisions of sandstone beds, are nonlaminated and therefore may have been deposited directly from suspension.

Flaser bedding resulted from (a) partial erosion of, and sand deposition over, clay-draped sand beds, and (b) sand deposition into partially clay-draped scours. Lenticular bedding was formed under depositional conditions in which the supply of sandy sediment was insufficient to allow the full development of a rippled bed surface, resulting in sand lenses and starved ripples.

The motifs that are common in the thin and medium bedded sandstones represent deposition by decelerating currents. The lower, mudstone-clast-bearing division of the motif represents the highest energy conditions, and was itself deposited by decelerating flow, as indicated by the grading of shale clasts. This division is either massive, indicating deposition from suspension with possible short-lived, postdepositional liquefaction, as suggested for the Bouma 'a' division of turbidites (Middleton, 1967; Middleton and Hampton, 1973), or it contains discontinuous flat-lying laminae, indicating that some traction transport occurred before deposition. The similarity of the mudstone clasts to the surrounding mudstone layers, the angularity of the clasts, and the erosional bases of these beds indicate that strong currents scoured the sediment surface, eroding semilithified mudstone layers, just prior to or during deposition of this basal layer. Desiccation and cracking of shale layers (discussed below) may have aided in the formation of these shale chips.

The parallel-laminated division of the motifs represents traction transport and deposition in upper-plane-bed conditions, and the rippled upper division indicates traction transport and deposition in the lower flow regime. Base-cut-out motifs were formed by currents that were of insufficient strength to strongly erode the underlying substrate. The

top-cut-out motifs were likely formed by currents that decelerated from upper-plane-bed conditions to no movement too rapidly to allow the development of ripples.

The ripples in this lithofacies were formed by unidirectional currents, as indicated by their: (1) asymmetrical profile, (2) lack of bifurcating crests, (3) lack of draping laminae, (4) form-concordance, and (5) unimodal foreset orientation within individual ripple trains.

Shrinkage cracks form during volume decrease of fine-grained sediments. Laboratory experiments indicate that these may form subaqueously, from changes in salinity or from sediment compaction and dewatering. In the former case this occurs at the sediment-water interface, and in the latter the process occurs substratally (Donovan and Foster, 1972; Plummer and Gostin, 1981; J.R.L. Allen, 1984). These subaqueous features are called synaeresis cracks. Shrinkage cracks that form at the surface due to subaerial evaporative water loss are termed desiccation cracks. These involve tensile stresses orders of magnitude larger than than those associated with synaeresis (JR.L. Allen, 1984; p. 550).

Early workers postulated, from examples in the rock record, that some shrinkage cracks formed subaqueously (Pettijohn, 1949; Rich, 1951). Later, synaeresis cracks were formed in the laboratory (Burst, 1965; Jungst, 1934; White, 1961). Picard and High (1969) describe modern subaqueous shrinkage cracks from a fluvial environment. The distinction of these two types of shrinkage crack in the rock record has been discussed by Donovan and Foster (1972), Plummer and Gostin (1981), and others. Based on these references the shrinkage cracks in this lithofacies are interpreted as both desiccation and synaeresis types. The star-shaped and oriented spindle patterns are generally considered characteristic of synaeresis cracking, while the polygonal shapes are generally attributed to desiccation, although it must be noted that "...overlap in crack morphology exists between the two groups (Plummer and Gostin, 1981, p. 1153). Many examples of polygonal cracks in the CIF display overprinting of several generations of cracks, a feature very strongly diagnostic of desiccation cracking (Plummer and Gostin,1981).

The arguments used by Hiscott (1982) to suggest a shallow-water origin for synaeresis cracks in his Facies 1 of the Random Formation hold for this lithofacies; i.e., (1) synaeresis is favored by high salinities and is therefore most probable in shallow-water settings, and (2) association of synaeresis cracks with flaser, wavy, and lenticular bedding, interference ripple marks, and abundant mudstone rip-up clasts is strong evidence for shallow-water conditions, perhaps with periodic exposure. The formation of synaeresis-style cracks may have been aided, in part, by short-term exposure. Such an interpretation is supported by the close stratigraphic proximity to beds with polygonal cracks and rare examples of raindrop prints.

The abundance of truncation surfaces and scour-fill sandstones indicate that local erosion was very common during deposition of this lithofacies. The data in Table 3.1 indicate that scour depth does not increase with scour width. The degree of lithification and consolidation (especially for the muds) may have been a prime factor in controlling the depth of scour. Rapid consolidation of the sediment with depth might have inhibited deep erosion, and enhanced lateral erosion, resulting in wider, rather than deeper, scours with prolonged erosion.

The paleocurrent data (Figure 3.3), >90% of which is from this lithofacies, consists of measurements of current-ripple migration and ripple-crest trends. Data on ripple-crest trends were taken from those ripples for which it was not possible to acquire paleocurrent information directly due to poor weathering or exposure. The ripple-migration readings (n=58) indicate bimodal-bipolar flow conditions, with the stronger mode towards the southwest. The ripple-crest trends (n=19) are more or less uniformly distributed, with a very weak preferred northeast-southwest orientation. These latter data indicate that a small percentage of ripples were oriented at all angles to the strong bipolar pattern. The weak northeast-southwest orientation to this data is somewhat puzzling, but may be partly

attributable to preservational bias, by which, due to the strike and dip of bedding, it would have been more difficult to gather paleocurrent data from these ripples.

The difference in the bedding characteristics and abundance of sedimentary structures in the green versus red units of this lithofacies indicates that the green units were formed under higher-energy conditions. Observations indicate that the abundance of shrinkage cracks in the red units cannot be attributed entirely to a greater percentage and thickness of shale layers in the red units. It is therefore likely that these sediments suffered one or more of the following: (1) a greater degree of subaerial exposure, (2) higher salinities, or (3) more intense compaction and water expulsion.

The strong red coloration of the terrestrial and marginal marine Rencontre Formation (Smith and Hiscott, 1984) and parts of Facies Association 1, with features indicating very-shallow-marine conditions with periodic subaerial exposure, indicates a strong environmental control on the development of color. With few (but important) exceptions, it is a recurring aspect of the CIF and the underlying Rencontre Formation that shallow-water or subaerially exposed sediments are red and that deeper-marine deposits are darker colored. The following discussion on the origin of color in these deposits has been included so that associations of color and other aspects of the rocks such as sedimentary structures can be used to refine or support process interpretations and later paleoenvironmental interpretations.

3.2.1.1 Color

The question of how sedimentary rocks acquire their color has been a long-standing question in geology. Much of the work has centered around explaining the red coloring of red-bed sequences. The consensus is that color is almost always an early diagenetic phenomenon (Tomlinson, 1916; Downing and Squirrel, 1965; Walker, 1967; Thompson, 1970; Van Houton, 1973; McBride, 1974; Hubert and Reed, 1978; McPherson, 1980;

Potter et al., 1980).The early work of Tomlinson (1916) demonstrated that the controlling factor in the development of color in shales is the Fe^{+3}/Fe^{+2} ratio and not the total percent of iron. McBride (1974) postulated that as the Fe^{+3}/Fe^{+2} ratio in a rock decreased, the resulting color change would be from red to purple to gray. Potter et al. (1980) further suggest that organic content determines a second color sequence from greenish gray to black that is independent of the oxidation state of iron (Figure 3.4). Figure 3.4 suggests that the sediments of this lithofacies contained very little organic matter, less than ~0.1 percent. Although color is a function of the final Fe^{+3}/Fe^{+2} ratio, an important primary control is the organic content of the sediment, because the quantity of organic matter controls the Fe^{+3}/Fe^{+2} ratio by oxidation-reduction reactions (Potter et al., 1980; McPherson, 1980). The quantity of organics in a sediment is controlled by many factors, most importantly: (1) rate of supply of organics, (2) rate of accumulation and (3) rate of decay of organics in the upper few centimeters of the sediment column (in turn a function of oxygen levels) (Potter et al., 1980).

Red color is imparted to sediments under oxidizing conditions by the early-postdepositional alteration of iron-bearing minerals, including: (1) dehydration reactions in which the limonite stain on detrital particles is altered to hematite, (2) dissolution of iron silicates and precipitation of the released iron and (3) direct oxidation of magnetite and ilmenite grains (Hubert and Reed, 1978). Red sediments can later be converted to green by reduction of the iron (Hubert and Reed, 1978; Potter, et al., 1980), which is then carried away in solution (Picard, 1965; Friend, 1966; McPherson, 1980) or reprecipitated as iron-rich clays such as chlorite (Thompson, 1970).

McBride (1974) noted that the strength of the color, red or green, in a sediment or rock, is a function of grain size: fine-grained rocks have higher iron content and therefore more intense color. According to McPherson (1980), the precurser to hematite in red sediments is an amorphous or poorly crystalline iron oxide that attaches itself to clays. The diagenetic change from red to green, occurring as sediments are buried below the water

Figure 3.4: Graph relating color of rock (Y axis), which from empirical data is shown to be a function of organic content and oxidation state of iron, to Eh and Time (X axis). "Time" refers to the length of time that pore fluids interact with the sediment prior to lithification. Sedimentation rate is inversely related to time because it controls the length of time that sediment undergoes reactions with shallow surface waters. The development of dark colors, olive gray to black, are primarily determined by organic content, and for a given unit of sediment the trend through time is toward lighter color with the oxidation of organic matter; this change is irreversible. The lighter colors, green-gray to red, are controlled by the mole fraction representing the proportion of iron in the +2 state (each unit in fraction represents the number of moles of iron per gram of rock) - color changes are reversible through time depending on Eh. Assuming that there is dissolved oxygen available in the sediment, the trend through time will be toward lighter color, first through the oxidation of organic carbon and later through the oxidation of reduced iron. For instance, if one starts with a black sediment rich in organics and a pore water of moderate Eh, at T_1 the sediment will be gray, at T_2 it will be green, and at T_4 it will be red. The left side of this graph is modified from Potter et al. (1980, Fig. 1.25).

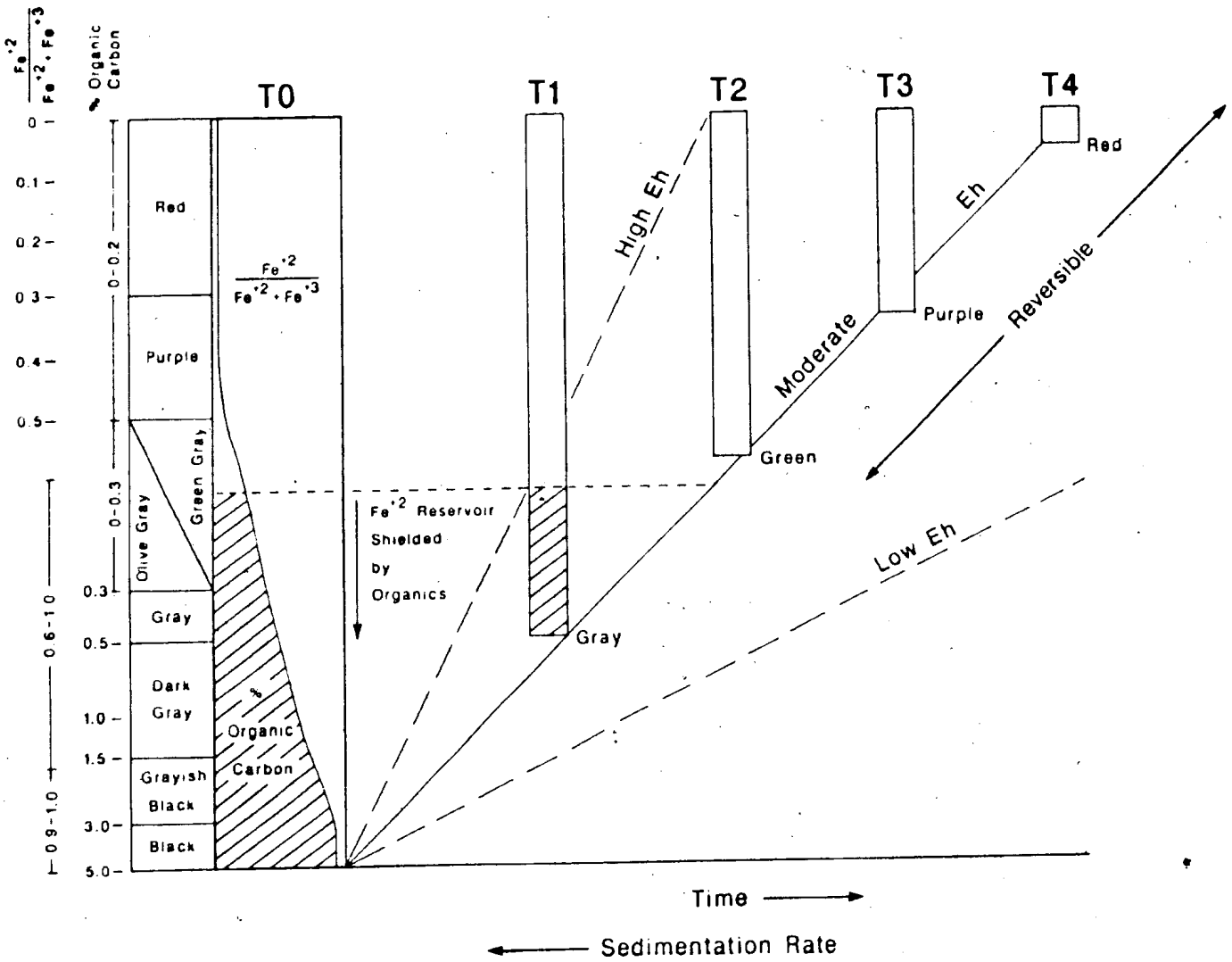
T0
T1
T2
T3
T4
Red
Purple
Green Gray
Olive Gray
Gray
Dark Gray
Grayish Black
Black
Green
Gray
High Eh
Moderate
Low Eh
Eh
Reversible
Fe+2 Reservoir Shielded by Organics
% Organic Carbon
Time
Sedimentation Rate

table, results from interaction with reducing fluids. It is therefore likely that the relationship between grain size and color is controlled by permeability: relatively high permeability for sands, low for muds.

The factors controlling color in the rocks of Facies 1.1 are varied. The general difference in the lithology and sedimentary structures between green and red units indicates that they may have been deposited in slightly different settings and experienced different diagenetic geochemical conditions. The sedimentology of the green units indicates slightly deeper-water conditions in which exposure was less likely. Under these conditions one might expect incomplete oxidation of organics and therefore a lesser intensity of oxidation and dehydration reactions involving iron-bearing phases. The coarser, more permeable nature of the green units would have enhanced penetration by reducing fluids during later burial. The sedimentology of the muddier, red parts indicates shallower-water conditions, with higher likelihood of exposure. Under these conditions the sediment would have experienced a greater degree of oxidation prior to burial, and therefore early decay of any organic fraction. The early decay of organics allowed thorough oxidation of the iron, and the low permeability of the sediment stifled any flow of reducing fluids from adjacent sediments.

3.2.2 Summary: Facies 1.1

In summary, the alternation of traction and suspension deposition, availability of sand, and overall energy conditions during deposition were important factors in determining bedding styles in Facies 1.1. Deposition took place under reversing currents. Erosion was a very important process, creating bedding discontinuities and scour-and-fill structures. Finally, shrinkage of shale layers (desiccation and/or synaeresis) produced sand-filled cracks and aided in the formation of shale clasts. Some of these cracks were formed under subaerial conditions. Finally, the red units in this lithofacies were: (1)

deposited under slightly lower energy conditions, (2) subaerially exposed more frequently and (3) subjected to stronger oxidizing conditions and were more impermeable to reducing fluids during deposition and early diagenesis, than the green units.

3.3 SHALY FACIES (1.2)

This lithofacies is similar in most respects to Facies 1.1 but is distinguished by a lower sandstone/shale ratio and different proportions of primary sedimentary structures. The shale content of this lithofacies varies from 50 to 85 percent. The sandstone fraction is dominantly very thin beds and laminae, while thin and medium beds of sandstone make up a small percentage (< 10%) of this lithofacies. Bedding planes are not well exposed. The abundance of starved ripples and shrinkage cracks is higher than in Facies 1.1. Also, the association of shrinkage cracks with color of strata is more pronounced: red units normally have very abundant shrinkage cracks, while green units are more variable with some having a moderate number of shrinkage cracks, and others having few, if any.

Wavy and lenticular bedding dominates this lithofacies; flaser bedding is absent. Unlike Facies 1.1, there are fewer parallel-laminated beds, shale-clast conglomerates and fining-up motifs. This lithofacies also contains fewer erosional surfaces. As a result, bedding planes are more extensive. Lenticular erosional-based sandstone beds are present but are generally not as thick or abundant as in Facies 1.1. Also found in this lithofacies, but not present in Facies 1.1, are rare carbonate concretions within which original depositional structures and thicknesses are delicately preserved.

3.3.1 Process Interpretation: Shaly Facies (1.2)

The wavy and lenticular bedding is attributed to alternation between traction transport and deposition and suspension deposition, the latter being the dominant process. The higher shale/sandstone ratio and lower average sandstone bed thickness indicates lower-energy conditions than for Facies 1.1. The paucity of large-relief erosional surfaces and the reduction in abundance and scale of small scours and channels means that current energy was mostly below that sufficient to erode semilithified mud. The difference in average bed thickness and the abundance of shale indicate generally lower-energy conditions. The abundance of starved ripples indicates low sediment supply.

The plan-view geometry of shrinkage cracks is in most cases unknown because of poor exposure of bedding planes, but shrinkage cracks of both desiccation and synaeresis type were observed. The increase in abundance of cracks (seen in cross section) in comparison to Facies 1.1 indicates that the sediment was more often subjected to shrinkage, and therefore was more often under one or more of the environmental conditions that form these cracks (desiccation, elevated salinities, dewatering and compaction). It is therefore also likely that the sediments of this lithofacies were also more often exposed subaerially.

3.4 BLACK THINLY LAMINATED SHALE/SILTY SHALE FACIES (1.3)

The Black Thinly Laminated Shale/Silty Shale Facies occurs within the middle and upper parts of Member 1 (Figure 1.3). It varies from very thinly laminated (pin-striped), dark gray to black shale, containing 40-60% very fine and fine grained, white, quartzose sandstone laminae (Plate 3c), to a complex interbedding of dark shale, silver-grey siltstone,

and thin to medium-bedded quartzites and sandstones (Plate 2a, 3a). The quartz arenites and sandstone beds are very irregular in thickness, and are often lenticular in geometry. These range from very thin beds of starved ripples to medium beds with channel-like geometries (Plate 2c) to those with relatively flat bases and tops that show evidence of considerable erosion (Plate 2a). The thicker quatzite and sandstone beds may contain large mudstone flat pebbles. The gray siltstone is interbedded with the shale on a lamina-by-lamina scale or on a larger scale in which centimeter-scale siltstone beds alternate with centimeter to decimeter-thick beds of pin-striped shale. Appreciable thicknesses of strata (decimeters to meters) may contain little or no siltstone.

In the pin-striped shale, individual white-weathering sandstone laminae rarely exceed 2 mm in thickness. Mini-loads (0.5-1 mm wide) may be present, projecting up to 0.5 mm off the base of these laminae (Plate 3c). The laminae are grouped into sandy packages up to 1.5 cm in thickness, and shaly packages of subequal thickness. These packages are less clearly defined when observed close-up, where one can see their complex and transitional nature. The sandy packages contain slightly thicker sand laminae, with closer spacing, than those in the shaly packages. Thickness of the laminae is generally uniform, but thicker sand laminae display pinching and swelling, defining a blebby structure. Subtle, low-angle, undulose and planar laminae appear to form incipient ripples defined by very small cross-laminae. In most cases it can be demonstrated that these features are different views of laminae that drape very-low-angle erosional surfaces. Low-angle erosional surfaces, with relief of less than a few centimeters, are locally abundant (Plate 3a). In some cases these surfaces define the boundary between sandy and shaly packages.

One of the most dominant aspects of this lithofacies is the abundance of soft-sediment deformation structures. Much of the strata contain small-scale slides, convolutions and ball-and-pillow features. Some samples contain small (1-3 mm long) injection structures (clastic dikes) and small-scale synsedimentary faults (Plate 3c). The

PLATE 2: FACIES 1.2/1.3

a: Particularly sandy interval of Facies 1.3 at GB-~105-107A. Medium sandstone bed on the right has an erosional base and top, while bed in center of photo has an erosional top and is laterally truncated near base of photo. Stratigraphic top is to left. Scale is 15 cm long.

b: Load ball horizon in Facies 1.2 at GB-48.8A. Stratigraphic-up is to right. Scale is 15 cm long.

c: Lenticular, channel-fill sandstone in Facies 1.3 at GB-107.7A. Little or no internal structure is visible on the weathered surface. Stratigraphic top to right. Scale is 15 cm long.

d: Bedding plane view of Facies 1.3 at Member 1-2 boundary at FD-18.26. These rounded shale clasts are scattered across the surface and are concentrated in erosional irregular, partially-dendritic erosional scours. Note shrinkage (desiccation?) cracks. Scale is 15 cm long.

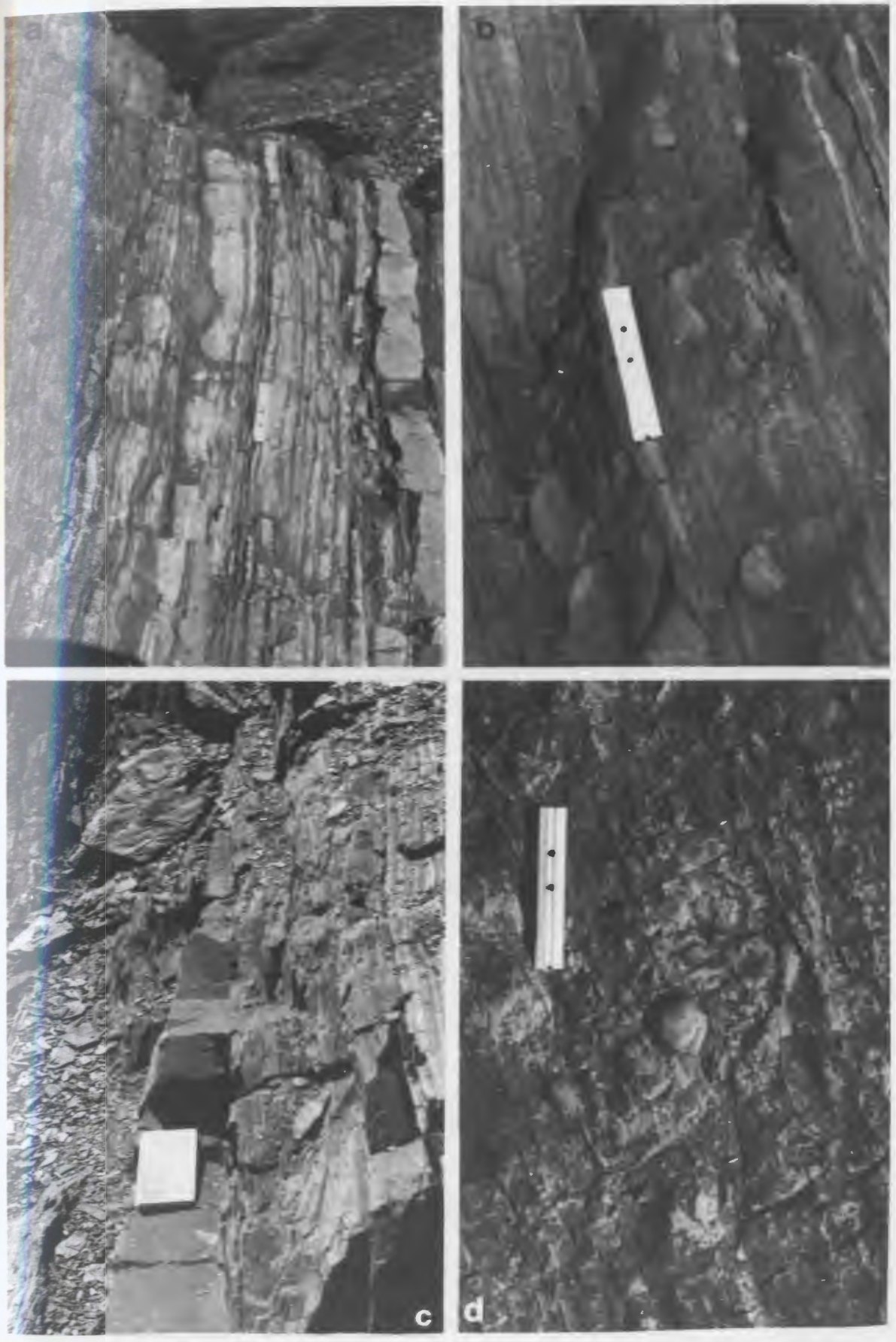
a
b
c
d

PLATE 3: GREY/BLACK SHALE FACIES (1.3)

a: Pin-stripe interlamination of shale and fine sandstone showing subtle multiple scour surfaces. Note shrinkage cracks in thick shale lamina. Stratigraphic top is up. Scale is 15 cm long.

b: Locally abundant synaeresis cracks. This is an oblique shot of bedding with stratigraphic top to upper left. Scale is 15 cm long.

c: Slabbed and polished surface of pin-striped black shale from Point May. Note synsedimentary faults, small injection structures and small load structures at the base of many laminae. A large, rounded, phosphatic shale clast (center) affected the overlying laminae during compaction. Stratigraphic top is up. Scale is 1 cm long.

d: Lenticular, bedding-parallel phosphate nodules (arrows) from GB-110A. These formed in situ as concretionary growths. Stratigraphic top is up. Scale is 15 cm long.

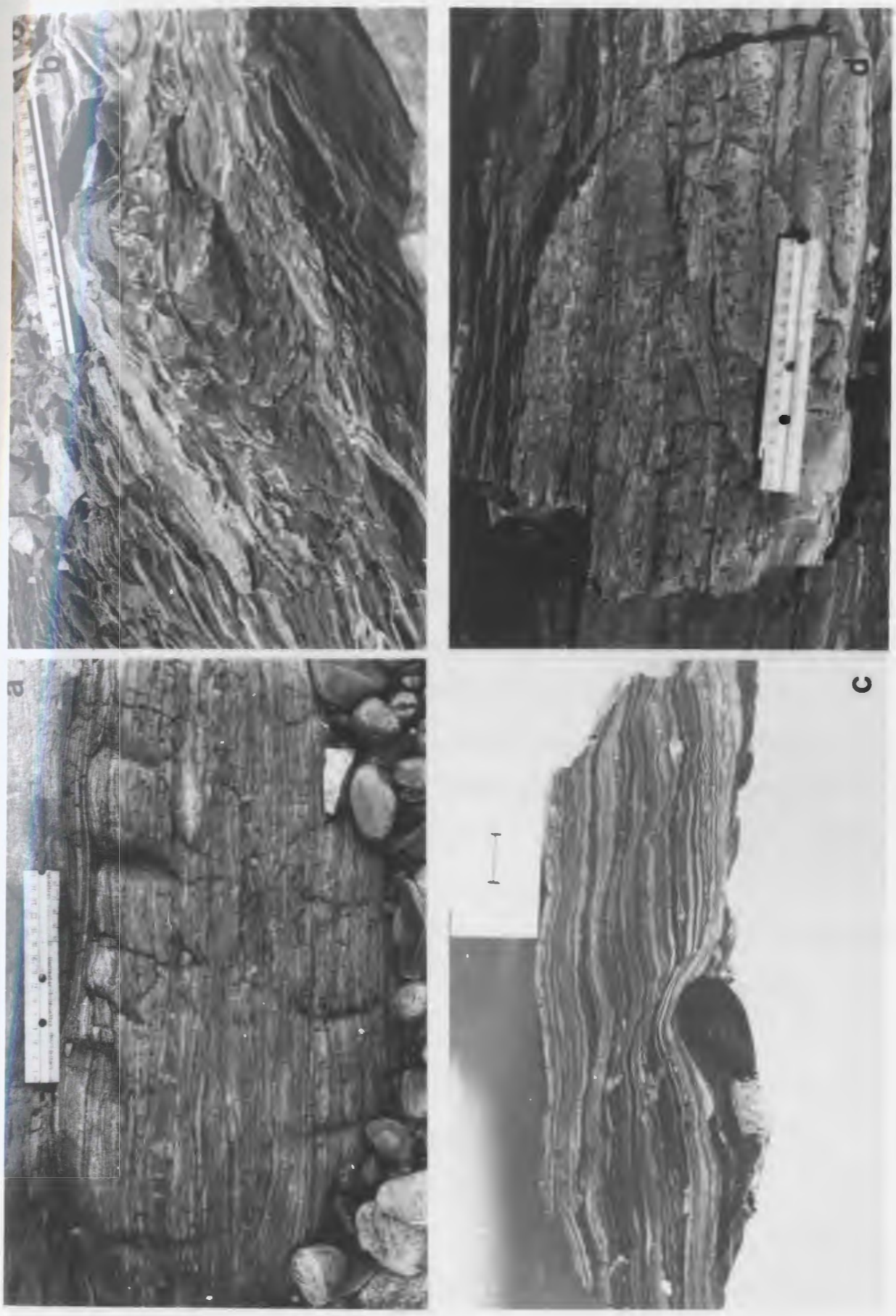
a
b
c
d

injection structures are often squashed or ptygmatically folded, imparting a blebby appearance to the rock where abundant. The synsedimentary faults record both brittle and plastic behavior at different points along their length. In some cases the faults flatten toward bedding and die out with depth, appearing listric in nature. A few soft-sediment dikes appear to follow these fault planes (Plate 3c).

Shrinkage cracks are locally abundant in this lithofacies (Plate 3b). They are conspicuously absent in this lithofacies at GB-77.9-80.2A, whereas only a few meters above and below this interval shrinkage cracks are abundant. At LC, shrinkage cracks are abundant throughout this lithofacies. At LC-87.4A, aligned linear shrinkage cracks are well exposed on a bedding plane.

Pyrite and phosphatic shale nodules are common in this lithofacies. Wet-chemical analysis for percent P_2O_5 was performed on several phosphate nodules from this lithofacies at various localities; the data are given in Table 3.2. Some of the phosphate nodules are found with their long axes at an angle to bedding, while others are parallel to bedding. The bedding-parallel examples show the following characteristics: (1) tapered, elongate geometry (Plate 3d), (2) curved, but continuous, underlying and overlying laminae, (3) incorporation of laminae within some nodules, and (4) indistinct, gradational contacts in some examples. Both bedding-concordant and bedding-discordant nodules (Plate 3c) were noted at PM-15.4A.

This facies contains a number of small and simple trace fossils. The concentration of trace fossils is not very high, nor is there evidence to suggest that the sediment was burrowed to a significant degree.

TABLE 3.2: PHOSPHATE NODULES: WET CHEMICAL ANALYSIS FOR P_2O_5

SAMPLE	% P_2O_5
FD-18.26	18.6
FD-18.26	14.6
FD-153.1	11.8
LC-9.1B	20.4
GD-10.0B	20.4

3.4.1 Process Interpretation

This lithofacies is similar to the "Finely Laminated Mudstones" of Hentz (1985). He describes calcitic lenticular, wavy, and planar laminae of similar scale and style that contain in situ phosphate nodules, phosphatic shale clasts, and synsedimentary faults.

The characteristics of this lithofacies indicate a low-energy setting periodically subjected to high-energy events. The deposition of sand beds up to several orders of magnitude thicker than the norm for the facies argues for deposition by high-energy events. The compositional maturity of many sandstone beds indicates transport from an adjacent, high-energy (micro)environment. Some of these beds may have formed as shallow channels that cut into a fine-grained substrate and generated mudstone fragments (flat pebbles).

The gray to black shale, with its lenticular/wavy bedding and incipient ripple cross-laminae, records suspension deposition of sand and mud with gentle, episodic current activity that formed microripples on a silty bottom. Extremely shallow, shale-draped scours mark occasional, minor, erosional events. The synsedimentary faults in these shales may have formed from hydraulic fracturing during the release of high pore pressures (Pickering, 1983). The association of soft-sediment micro-dikes, especially those along the fault traces, support this interpretation.

The abundance of soft-sediment deformational structures indicates conditions of high pore pressure. High sedimentation rates and the presence of liquefaction-susceptible silts probably contributed to the repeated sediment failures that characterize this lithofacies (full discussion of liquefaction, its causes and susceptibility, is given in Section 4.16.2.1). Based their morphology, the shrinkage cracks in this lithofacies are attributed to synaeresis.

The phosphate nodules in this lithofacies formed early enough, and at shallow enough depths, to allow for erosion and transport of some nodules by rare, strong

currents. Worldwide, phosphate is found as small nodules in gray and black shales (e.g., Kidder, 1985; Hentz, 1985) and carbonates of a wide variety of ages (Cook and McElhinney, 1979), especially at the Precambrian — Cambrian boundary (Cook and Shergold, 1984).

The analysis of phosphate concentrations and solubility in sea water is complex (Waples, 1982, p. 141); the reader is referred to reviews by Baturin (1982) and Froelich et al. (1982). Baturin (1982, p. 23) concludes that the available evidence from field and laboratory rules out "...the possibility of chemical precipitation of phosphate from ordinary sea and ocean waters under natural conditions". In a purely chemical sense, the precipitation of phosphorus is strongly controlled by pH and generally unaffected by Eh conditions in the same manner as is calcium carbonate (Krumbein and Garrels, 1952). The solubility curves of calcite and calcium phosphate are similar, with the latter having a lower absolute value, so that water saturated with respect to both minerals will only precipitate calcite. Krumbein and Garrels (1952) therefore conclude that the precipitation of calcium phosphate would occur in restricted basins with pH too low for calcite to form (pH 7.0-7.5).

Organics, and therefore indirectly Eh, play an important role in the deposition of phosphorus (Bushinski, 1964; Christie, 1978; Baturin, 1982; Waples, 1982; Kidder, 1985). Accumulation of organic matter is greatest in anoxic or near-anoxic conditions. Under low-oxygen but not completely stagnant conditions, the phosphate stored in organic matter is degraded by micro-organisms at, and immediately below, the sediment-water interface (Waples, 1982, p. 143). Under these conditions the released phosphorus is retained in the sediment, raising the concentration and allowing for precipitation (Baturin, 1982; Froelich et al., 1982; Waples, 1982). Restricted or semi-restricted conditions are very important in concentrating organic matter over a small region to produce anoxic bottom conditions (Heckel, 1977, p. 1055). In these settings the loss of phosphorus to the overlying water column is minimized (Waples, 1982; Hentz, 1985) by preventing the early

oxidation of organic matter (low Eh) and the loss of phosphorus by physical agitation of the sediment by waves (Zicker et al., 1956), or burrowing organisms.

In a pioneering study of phosphorite deposition, Kazakov (1937) drew attention to the importance of upwelling of cold, phosphate-rich ocean water for the precipitation of phosphate. Bromley (1967) recognized that the bathymetric distribution of phosphate-rich water in the oceans today is controlled by the loss of phosphorus from descending organic matter, most of which is released well above 1000 meters. He suggests that optimum conditions are shallow, warm waters, particularly between 30 and 300 meters water depth. The deposition of phosphorus is now thought to be concentrated within, and particularly at the boundaries of, the oxygen-minimum zone (Veeh et al., 1973; Heckel, 1977; Waples, 1982). According to Christie (1978), most phosphates form at "...water depths considerably less than 500 m — possibly between 50 and 150 m as off southwest Africa today" (p. 3). Bromley (1967) suggests 30-300 m, and Bushinski (1964), 30-200 m.

To review, the phosphate nodules indicate: (1) low-oxygen, anoxic or near anoxic, conditions, (2) a restricted, low-energy setting, (3) a lack of burrowing organisms and (4) warm, shallow marine waters.

The high concentrations of organic matter that favor the precipitation of phosphorus also favor growth of pyrite nodules. High sedimentation rates, inferred from the abundance of soft-sediment features, would also favor high organic content by shortening the time in which organic matter remained in the upper, oxidizing diagenetic zones. According to Potter et al. (1980), the dark gray to black color is characteristic of shales with high organic content: greater than 0.5% for dark gray shales and greater than 3 percent for black shales (see Figure 3.4). Whereas low oxygen conditions are indicated by the dark color and presence of phosphorus and pyrite concretions, dysaerobic rather than anaerobic conditions are favored because of the presence of a moderate abundance of trace fossils.

In summary, the characteristics of this lithofacies indicate: (1) restricted, low-energy conditions with periodic high-energy events, (2) high sedimentation rates and

locally high postdepositional pore pressures, (3) shallow-water conditions, probably with occasional elevated salinities, (4) high organic concentrations, (5) presence of a limited community of burrowing organisms, (6) nearly anoxic (dysaerobic) conditions.

3.5 RED MEDIUM-BEDDED SANDSTONE/SHALE FACIES (1.4)

The following description is based on exposure of this facies in the intervals FD-103.7--115. This lithofacies consists of red (and minor green), thin to thick, massive and laminated sandstones, siltstones and shales (Plate 4a). Well sorted fine sandstone beds, generally forming 80-90% of the facies, average 15-20 cm in thickness and reach a maximum of ~60 cm. Lower and upper bedding surfaces are mildly to very strongly erosional, and amalgamation surfaces are common (Plate 4c,d). Scour surfaces are overlain by medium and thick lenticular sandstone beds, with or without a thin intervening shale layer (Plate 4b,c). One large sandstone lens is 4 m long and 35 cm thick, in cross section. These lenticular sandstones are mostly parallel laminated; a few show cross-lamination.

Stratification in the sandstone beds is dominated by parallel lamination with minor trough cross-stratification. Sedimentary structures include abundant mud-chip conglomerate (Plate 4e), synaeresis and desiccation cracks, small current ripples, rare current lineation and convolute lamination (Plate 4b). Desiccation polygons reach large dimensions: in one example one arm of a polygon is 40 cm long.

3.5.1 Process Interpretation: Red Medium-Bedded Sandstone/Shale Facies (1.4)

Many of the conditions under which this lithofacies was deposited are similar to those of Facies 1.1, and to a lesser degree Facies 1.2. Sandstone bed thicknesses, and

PLATE 4: MEDIUM-BEDDED RED SANDSTONES AND SHALES

a: View of strata from FD-~105-115. Stratigraphic top to right.

b: Convolute laminae in sandstone bed at FD-108.5. Stratigraphic top is up. Scale is 15 cm long.

c: Erosional surface at FD-104 overlain by shale then sandstone with rippled top (on right). Stratigraphic top is up. Notebook is 18.5 cm long.

d: Shale-draped scour surface and lenticular sandstone beds from FD-104. Stratigraphic top is to right. Notebook is 18.5 cm long.

e: Mudstone intraclast conglomerate on upper bedding plane at FD-114.3. Scale is 15 cm long.

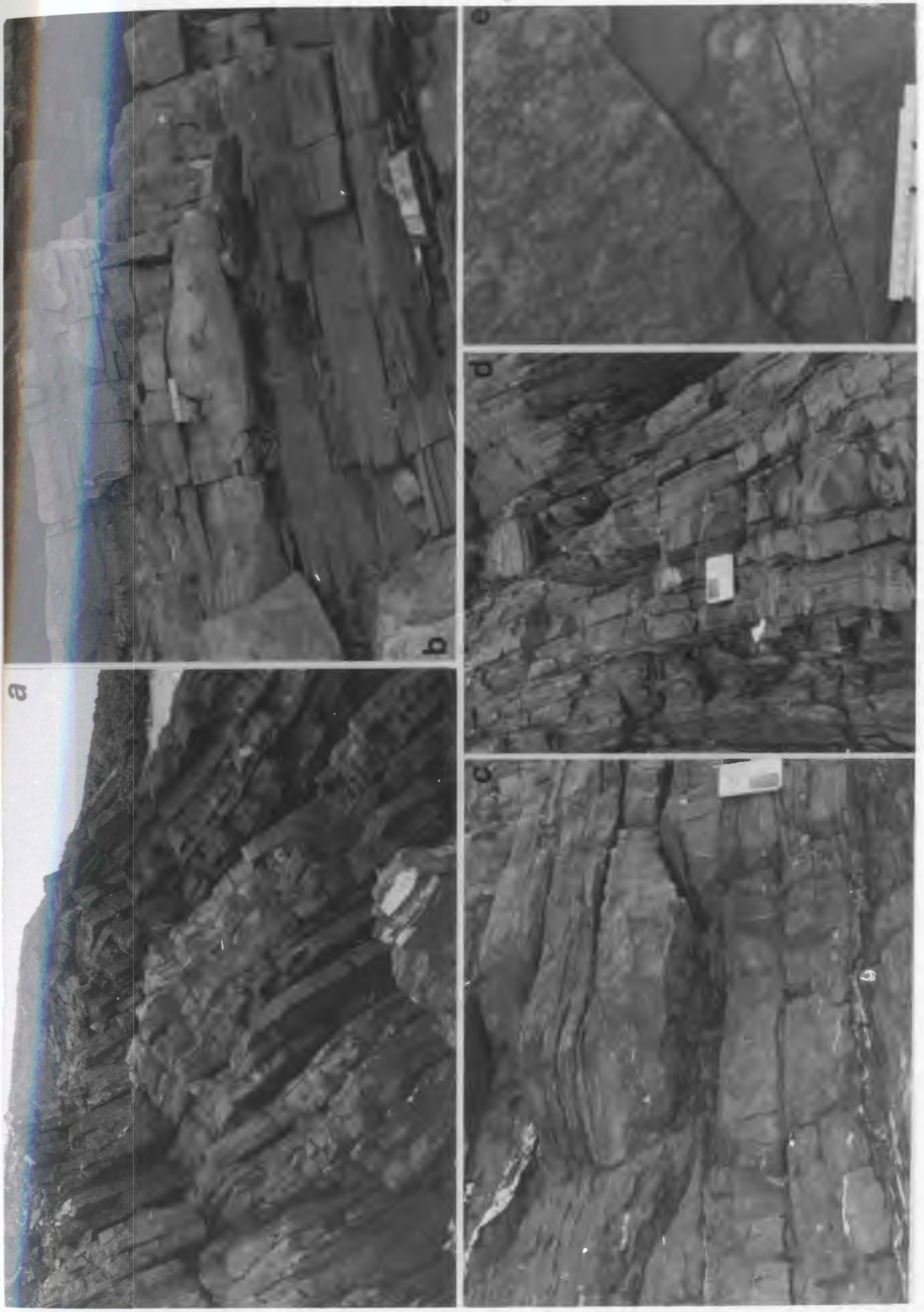
a
b
c
d
e

depths of erosion associated with scour surfaces, are much larger than that of Facies 1.1. implying generally higher-energy conditions. The red coloring and the presence of shrinkage cracks, particularly large polygonal desiccation cracks, indicate well oxygenated conditions with periodic exposure. Shale chips may have formed from the erosion of the curled-up edges of desiccation polygons.

Clay drapes on scour surfaces imply a time lag between the erosion and infilling of channels. Amalgamation surfaces evidence repeated episodes of erosion, passive accumulation of shale and later erosion of the shale drape and deposition of another sand bed. The lack of lag deposits and the well sorted nature of the sandstones implies a fairly homogeneous source of sand.

3.6 LITHOFACIES DISTRIBUTION: FA 1

Facies Association 1 is generally confined to member 1 of the CIF (Figure 1.3). The base of member 1 is composed of the red and green strata of Facies 1.1 and 1.2. The upper part of member 1 consists of the gray to black Facies 1.3, with thick intercalations of Facies 1.1 and 1.2. One thick package of Facies 1.1 and 1.2 is also present in member 2 (see Figure 1.3). FA 1 distributions: Facies 1.1=40%, 1.2=30%, 1.3=25% and 1.4=5%.

The lithofacies of this facies association are best exposed at Grand Bank Head. The section at this locality is cut by a series of northeast-trending faults. These cause only minor stratigraphic disruption (the throw on the faults is not large - usually several meters - and the fault planes are often nearly parallel to bedding), but result in high rugged cliffs and steep-walled coves, making access difficult. At Grand Bank Head, the transition from the upper part of the underlying Rencontre Formation to member 1 of the CIF is well exposed. This transition is also present on Brunette Island and Chapel Island and at Boxey Point. At these three latter localities the top of the underlying Rencontre and the lower transition zone into member 1 of the CIF is much thicker bedded, containing large channel fills and tabular cross-bed sets up to 1 m thick. At Grand Bank the bedding styles in the top of the Rencontre Formation are qualitatively similar to Facies 1.1 and 1.2 of FA 1, but the strata are entirely red, and less variable in terms of sedimentary structures.

Facies Association 1 is also exposed at FD. At the base of the section, only 20-25 m of strata from member 1 are accessible without a boat. Strata of Facies 1.1, 1.2 and 1.3 are found in this interval. Red and green sandstones, siltstones and shales of Facies 1.1, 1.2 and 1.4 are exposed between FD-103.7 and FD-~154 in two thinning- and fining-upward sequences. The medium-bedded red sandstones of Facies 1.4 are found at FD-103.7 in sharp contact with a highly cleaved 'transition zone' (Facies 2.1 is below), and extend to FD-~111.5, where they are stratigraphically transitional into alternations of Facies 1.1 and 1.2 that continue until FD-137.3. At FD-137.3, in sharp contact with several

meters of Facies 1.2 below, is a second fining- and thinning-upward package, the base of which is sharply defined at the base of a 1.8 m-thick sandstone bed. This sandstone bed and the immediately overlying strata, green siltstone and sandstones, are part of FA 2 and are discussed in Chapter 4. The upper part of this fining-upward package, however, also contains strata of Facies 1.1 and 1.2 (FD-145-150.8). The paleoenvironmental interpretation of this second fining- and thinning-upward sequence will be discussed in Section 4.23.4.

The stratigraphic equivalent of the strata described above (FD-103.7 and FD-~154) is exposed GB-248-283A, but is poorly accessible and obscured by weathering. The strata are predominantly red, as at FD, and are certainly similar in character — e.g., the lithology is the same and desiccation cracks, current ripples and other similar sedimentary structures were noted. There was no evidence at GB for the second fining-upward sequence seen at FD.

At Point May about 135 m of strata from this facies association are poorly exposed and generally accessible only at low tide. Approximately 125 m of this facies association are moderately well exposed at Lewins Cove in low-relief outcrop. Exposures of FA 1 at Brunette Island, Boxey Point and Chapel Island are thin and/or incomplete.

3.7 PALEOENVIRONMENTAL INTERPRETATION, FA 1: TIDE-INFLUENCED PERITIDAL AND SEMIRESTRICTED NEARSHORE

The red and green alternations that characterize FA 1 have been explained as a transition between the dominantly red fluvial rocks of the Rencontre Formation (Twenhofel, 1947; Smith and Hiscott, 1983) and the green 'marine' rocks of Member 2. Anderson (1981) describes the beds as alternations of fluvial and marine sediments. Potter (1949, p.34) says they are of a "littoral or completely subaerial nature". Crimes and

Anderson (1985) give a tentative interpretation for the lower part of Member 1 as fluvial to shallow marine, with tidal sands and mud flats.

Many of the features of the sandstones and shales of FA 1 are found in fluvial environments (e.g., rip-up clasts, desiccation cracks), but the full suite of sedimentary structures and overall organization of beds — there are no fining-up sequences — indicate marine conditions, as does the albeit limited suite of trace fossils. Many of the structures found in FA 1 are well known from modern and ancient shallow-water, tidally influenced facies (see Klein, 1977 a,b), although these structures are certainly not restricted to tidal settings. Thinly interlayered bedding (Reineck and Singh, 1973, 1980), prominent in FA 1, consists of alternations of sandstone and shale, and was initially named 'tidal bedding' by Reineck and Wunderlich (1967, 1968), who attributed this style of bedding to alternation of current or wave action (traction or suspension deposition) and slack-water suspension deposition, characteristic of tidal cycles. The styles of bedding range from flaser to wavy to lenticular. Thinly interlayered bedding is found in many ancient tidalite sequences (Singh, 1969; Wunderlich, 1970; DeRaaf and Boersma, 1971; Johnson, 1975; Vos and Eriksson, 1977; Driese et al., 1981).

The bimodal-bipolar paleocurrent distribution from Facies 1.1 and 1.2 is also typical of modern tidal systems (Reineck, 1963; Klein, 1967), and is common in ancient tidal sequences (Klein, 1970a; De Raaf and Boersma, 1971; Johnson, 1975; Rust, 1977; Vos and Eriksson, 1977; Mazzullo, 1978; Hiscott, 1982). Data from this facies association (Figure 3.3) and FA 2 (Chapter 4; Figure 4.2) indicate a northwest-southeast trending shoreline during deposition of the lower CIF. Flute marks in FA 2 indicate unequivocally that in Fortune Bay the shoreline was situated to the southwest, so that the data in Figure 3.3 signify a tidally influenced system characterized by flood-tidal asymmetry.

The ubiquitous mud-chip conglomerates of Facies 1.1 and 1.2 are also found, though not exclusively, in modern tidal settings (Van Straaten, 1954b; Reineck, 1967), and are a prominent feature of ancient tidalites (Johnson and Friedman, 1969; Klein, 1970a;

Von Brunn and Hobday, 1976; Eriksson, 1977; Rust, 1977; Tankard and Hobday, 1977; Vos and Eriksson, 1977; Driese et al., 1981). In modern environments, eroded mud chips can be transported for hundreds of meters or more (Wunderlich, 1970, p. 115). These often form by erosion of mud-cracked sediment, and a similar origin is envisioned for those of FA 1.

Modern tidal flats have received considerable study, beginning in earnest with the pioneering work of Van Straaten (e.g., 1950; 1953 a,b; 1954 a,b; 1959) on the tidal flats of the Dutch Wadden Sea. Numerous studies were undertaken in the following decade by Reineck (e.g., 1963, 1967) and others (e.g., Houbolt, 1968) on North Sea tidal flats. This work laid the foundation for recognizing and interpreting ancient tidalite sequences. The paper by Evans (1965) on the environments of the Wash, England, was particularly important, not just in providing a better understanding of modern tidal flats but also in proposing a vertical sequence of facies that would form during tidal-flat progradation. This formed the basis for later facies models that predicted small-scale fining-upward cycles in tidal-flat settings (e.g., De Jong, 1965; Eriksson, 1977; Tankard and Hobday, 1977; Klein, 1970b, 1971).

The differentiation of intertidal and subtidal deposits is difficult in ancient rocks (De Raaf and Boersma, 1971; Reineck and Singh, 1980). Tidal flats are often well zoned (see Evans, 1965); the general trend is to have the coarsest sediment at and below low tide mark and a steadily increasing quantity of mud toward high tide level (Van Straaten and Kuenen, 1958). The sandy sediment that forms flaser, wavy and lenticular bedding on tidal flats is derived from sand bars in the shallow subtidal, and is carried by tidal currents up onto tidal flats during the flood stage. As the flood stage progresses and higher levels of the flat are inundated, the current velocity decreases, resulting in: (1) lower-tidal-flat facies that are sand-rich and flaser bedded, (2) mid-flat facies that are thinner bedded with subequal quantities of mud and fine grained sand and (3) upper flat facies that are dominated by mud with lenticular bedding - often in the form of starved ripples (Klein, 1970a, 1977a).

The bedding style and associated structures of Facies 1.1 would be most typical of lower-tidal-flat to shallow-subtidal settings. Synaeresis-style cracks, abundant in Facies 1.1, are common in modern tidal settings (Van Straaten, 1954b). The numerous scours and erosion surfaces of Facies 1.1 are consistent with this setting as well. In tidal settings, "the main morphological features of subtidal zones are channels and sandbars" (Reineck, 1975, p. 6). In the shallow subtidal environments of the North Sea, the bathymetry may change by several meters within one day (Wunderlich, 1970, p. 124).

In contrast to Facies 1.1, the process interpretation for Facies 1.2 (Section 3.3.1) calls for lower-energy currents, less channelling, and more extreme and frequent desiccation. These requirements suggest, in the context of its close association with Facies 1.1, that Facies 1.2 was deposited in shallower water than Facies 1.1, probably in a middle to upper tidal flat setting. Middle to upper tidal flats are characterized by thinly interlayered bedding, abundant starved ripples and mudcracks (Klein, 1970a), features common in Facies 1.2.

The influence of storms during the deposition of FA 1 is difficult to assess. It is well known that a combination of storms and tides can move significant quantities of sediment: according to Wunderlich (1970, p. 124) as much as 100,000 m^3 of sand can be eroded and redeposited within a single tidal cycle during a storm. Johnson (1975) describes a tidal-flat facies containing sandstone beds with erosional bases, upper-flow-regime bedforms, and wide lateral extent, that he attributes to deposition by storms. Many of the FA 1 sandstone beds could be attributed to storm-enhanced tides. There is no direct evidence for storm deposition, but the common sandstone bed motifs of Facies 1.1 and 1.2, with mud chip conglomerate, parallel laminae and ripple cross-laminae, are indicative of strong current velocities capable of eroding mud and generating upper-flow-regime plane beds. These beds could have been deposited by storm-enhanced tidal currents.

The abundance of synaeresis cracks and the intimate large-scale interbedding with Facies 1.1 and 1.2 supports a shallow-water interpretation for Facies 1.3. Most of the strata of Facies 1.3 consist of a mixture of black shale and a distinctive silver-green siltstone that is a dominant lithology of FA 2 and 3. The siltstone was widespread on the shelf during member 2 (and 3) deposition. During the late stages of Member 1 deposition, silt that is believed to have come from the adjacent shelf (environments analogous to FA 2 and FA 3) was periodically introduced into the more restricted coastal area where the black shales accumulated.

Black shales, such as those that make up part of Facies 1.3, are generally attributed to anaerobic conditions, but not to any specific environment, although deep-water settings are most commonly reported (Pettijohn, 1975, p. 284; Heckel, 1977). Restricted, low-oxygen, nearshore settings might include lagoons, estuaries, tidal-flat ponds and interdistributary bays of deltas. A lagoonal environment would imply the presence of a barrier island, for which there is no direct evidence in FA 1. The thickness of Facies 1.3 alone (up to several tens of meters) precludes deposition in individual tidal ponds or abandoned tidal creeks, deposits of which are quite thin (i.e., tens of centimeters; see, for example, Goodwin and Anderson, 1974). More likely paleoenvironmental settings would be (a) a delta-plain environment such as an interdistributary bay or (b) a broad estuary. Although no features of FA 1 are diagnostic of deltaic sedimentation, such an interpretation is permitted by the data. De Raaf et al. (1965, Figure 9) illustrate deposits remarkably similar to Facies 1.3 which they interpret as 'subaqueous topset' deltaic deposits. Interdistributary bays can be very extensive and contain thick deposits, while maintaining generally shallow-water, restricted conditions. The medium quartz arenite and sandstone beds appear, from their geometry, and scale in relation to surrounding strata, to be high-energy event beds or channel deposits.

The medium to thick bedded red sandstones and shales of Facies 1.4, in its sole stratigraphic occurrence at FD-103.7-~111.5, form the base of a thinning- and fining-upward sequence, the upper sediments of which belong to Facies 1.1/1.2. The strata of Facies 1.4 are in striking contrast to the underlying thin-bedded green sandstones and siltstones of F.A. 2, which were deposited in a variety of subtidal deltaic environments (discussion to follow; Section 4.22 and 4.23). Channel sands are abundant at the base of the exposure and become less abundant above as this facies becomes transitional into Facies 1.1/1.2, which have already been interpreted in terms of a tidal-flat model.

The characteristics of Facies 1.4, and the vertical facies relationships, indicate that this facies was deposited in a periodically subaerially exposed, high-energy, shoreline environment or a near-shoreline fluvial setting. The abrupt stratigraphic appearance of this lithofacies suggests a shallowing event that represents an incursion of land-derived sediments. Possible environments include barrier beach, ebb-tidal delta, distributary channel, distributary mouth bar or estuary. There are no sedimentary structures strongly diagnostic of fluvial conditions (e.g., basal lags, fining-upward sequences), and there are no paleocurrent data to draw on. Despite vigorous searching no trace fossils were noted, but this does not rule out marine conditions for much or all of the facies, as very few traces are found in the red rocks of Facies 1.1/1.2, which are of certain marine origin. The presence of shale drapes covering erosional surfaces and a lack of a beach-style facies argues against a barrier beach origin. The presence of desiccation cracks within the first few meters of the fining-upward cycle indicates that these were not deposited at the base of a distributary channel or as distributary mouth bar sands, the latter of which would also tend to leave coarsening-up deposits. In light of (a) the presence of shale beds, (b) the transition into Facies 1.1/1.2, and (c) the constraint of deposition within a deltaic system (FA 2), a strong possibility is that this facies was deposited in a delta-front estuary just upstream from a distributary mouth. According to Elliot (1978, p. 112), in delta-top

settings influenced by tides "inner deltas comprising a maze of sand bars and mudflats occur at confluences between distributary channels, upstream from their outlet to the sea". Studies indicate that tidal processes are a major controlling factor in sediment distribution patterns and facies characteristics in modern estuaries (Postma, 1967; Boothroyd and Hubbard, 1975). The upward transition from the highly channelized deposits of Facies 1.4 into those of Facies 1.1/1.2 can be understood in terms of a shift in the position of the distributary channel(s) with the subsequent loss of direct fluvial input allowing for the establishment of tidal flats.

3.7.1 Tidal Range

Modern shorelines display a full spectrum of tide- and wave-influenced settings. Tidal range and tidal-current velocities are a function of shelf width (Redfield, 1958) and other factors. Tidal currents appear to have been an important influence in the deposition of FA 1, but the paleotidal range is not obvious. Macrotidal (> 4 m tidal range) deposits in the ancient record (Swett et al., 1971; Von Brunn and Hobday, 1976; Klein, 1977a; Rust, 1977; Tankard and Hobday, 1977; Hiscott, 1982) are dominated by compositionally and texturally supermature sandstones. This is particularly true for the lower Paleozoic, and for the late Precambrian — Lower Cambrian in particular. The deposits of FA 1 lack significant quantities of mineralogically supermature sandstone, and also lack important tide-diagnostic features like large herringbone cross-bed sets, reactivation surfaces in sand-wave deposits, and well defined fining-upward cycles. Apparently the tidal range was not macrotidal. Lack of evidence for sandstone beach deposits, so typical of microtidal shorelines and many mesotidal shorelines, indicates that the the tidal range was not extremely low either. A reasonable, but highly speculative, estimate of tidal range is 3-4 m.

The depositional environments outlined for FA 1 have not been placed in the framework of a larger depositional system. The data available solely from this FA 1

appears to be too limited. The stratigraphic relationships with FA 2 and the consequences of the inferred depositional environments of FA 2 are important factors for defining the depositional framework of the paleoenvironments of FA 1. Further discussion of FA 1 will be given in Chapter 9 following the description and interpretation of the remaining facies associations.

Chapter 4

FACIES ASSOCIATION 2

4.1 INTRODUCTION

Facies Association 2 consists dominantly of interbedded sandstones and siltstones. There is a wide variety of different bed types, with varying lithologies and sedimentary structures, that punctuate a volumetrically dominant 'background' of silver-green siltstone. These 'punctuating' beds include thin laminae to medium beds of sandstone, thin conglomerate laminae/beds, and a variety of 'disturbed' or resedimented beds.

The different bed types in this FA are given letter and number designations. Different portions of these bed types will be used to define lithofacies. Figure 4.1 is a detailed section (GB-153.6-158.6B) that shows the scale and style of interbedding of several of the volumetrically dominant bed types: S0, S1, S2, and S3. This same interval is shown in Plate 5a. In the following sections each bed type will have a separate description and process interpretation. Paleocurrent information from sole markings in this facies association (Bed-types S2-S4; see below) is plotted next to the stratigraphic columns for FD and GB in Figures 2.4 and 2.5. The most abundant and complete paleocurrent data, including sole markings, current lineations, and ripple data, is from FD, and the rose diagrams for this locality (Figure 4.2) will act as a representative suite for the following

Figure 4.1: Representative detailed stratigraphic section from F.A. 2 showing the scale and style of interbedding of S0-S3 beds. This is a 5 m section from the Grand Bank locality (GB-153.6-158.6B).

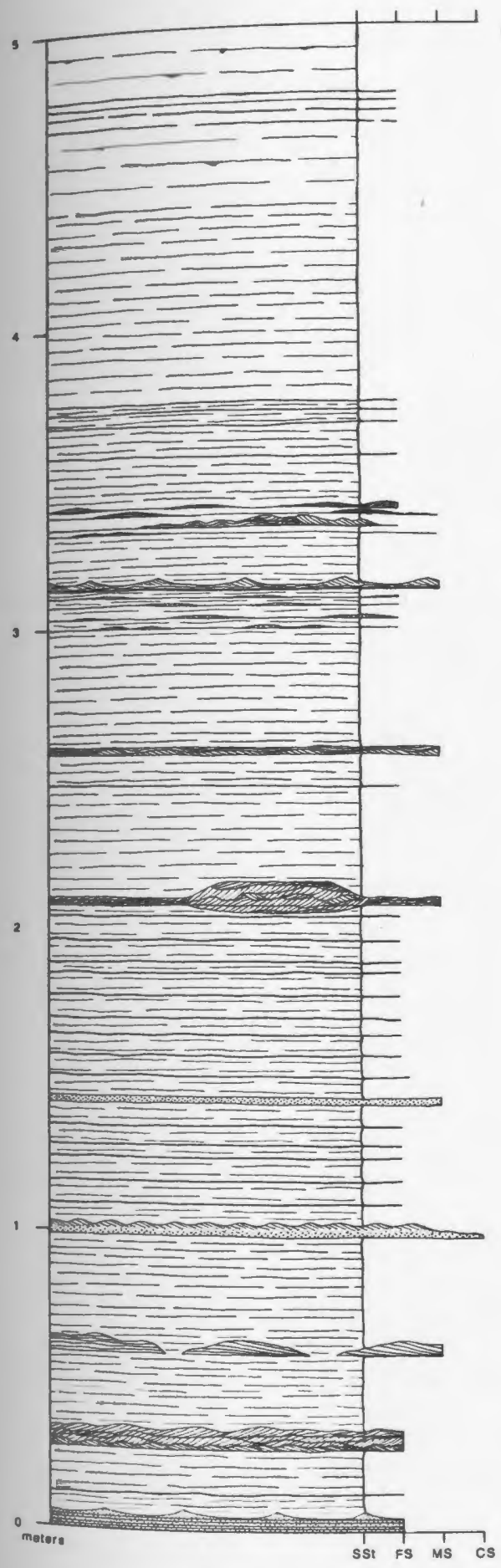

BED-TYPES

S1

S2 60cm- Widely spaced SlSt stringers, form small pods (burrows?); zone w/ 4 discontinuous FS lam's composed of closely-spaced 0.1-0.5mm thick lam's, grade laterally into 0.5-1.0cm lam's, traces on sole

S1

S1 (some S2)

65cm- SlSt w/ discontinuous stringers of VFS/FS (0.5mm ave)

S1/S2 35cm- SlSt w/ mm-thick VFS/FS lam's/streaks; widely spaced 1cm (ave) FS lam's

S2 8cm- FS/MS; ave-1-2cm, max-3.5cm; drastic changes in thickness, ripple x-lam's, draping lam's

S1/S2 18cm- SlSt w/ mm-thick lam's/streaks

S3 1.5-2.5- Undulatory lam's → ripples, Low R.I. with variable ave. ~12cm

S2 12cm- Four FS lam's, 5-10mm thick, pinch and swell, flutes and traces on sole

S1/S2 40cm- SlSt w/mm-thick VFS/FS lam's/streaks

S3 2cm- Ripple form-set at base, draping lam's over ripple flutes on sole (?)

S1/S2 48cm- SlSt w/ mm-thick VFS/FS lam's; 1 8mm FS lam

S3 1.5-2.5cm- MS/FS bed; Concreted thickness up to 7cm;
- Complex cross-lam's, form-discordant ripple x-lam's, climbing wave-ripple lam's, draping lam's

S1/S2 110cm- SlSt w/ mm-thick SS lam's and lenticular streaks; also 0.5-1.0cm lam's every 3-8 cm, show grading and ripple cross-lam's

S3 2cm- Graded bed MS→SlSt

S1/S2

S3 3-4cm- Graded bed: 2cm C/M SS → 1-2cm rippled FS

S1/S2 33cm- SlSt w/ mm-thick SS lam's

S3 8cm- Low-angle cross-lam's; discontinuous; 2-3m lateral extent

S1/S2 25 cm SlSt w/ mm thick SS lam's; A few 2-4mm thick

S3 8.5 - Complex cross-lamination and climbing wave-ripple lam's
- Concretioned bed; max. thickness = 10cm

S1/S2 22 cm - SlSt with mm thick SS streaks
- one 5-10 par. lam. FS lam.

S3 5 cm Parallel laminated → Wave ripples ~45 cm

PLATE 5: FA 2 OUTCROP, S0 AND S1 BEDS (FA 2)

a: A detailed drawing of this 5 m interval (covered by stretched tape) from GB-153.6-158.6B is given in Figure 4.1. This zone is particularly silty, and appears to be fining-upward in character. Stratigraphic top is to left. Scale is 1 m long.

b: Small, wiry traces within S0 siltstone. These are dominantly Planolites montanus traces. View looking roughly perpendicular to bedding. Scale is in 10 cm divisions.

c: S1 laminae and S0 siltstone from GB-~50B. Some of the S1 laminae form graded rhythmites (GR beds). Some S1/S2 interlaminae show evidence of bioturbation, while others are very delicately laminated. Stratigraphic top is up. Scale is 10 cm long.

d: Close-up of graded rhythmite (center) showing upward decrease in thickness of sandstone laminae. Note discontinuous S2 beds and S0 bed (directly above scale). Stratigraphic top is up. Scale is 10 cm long.

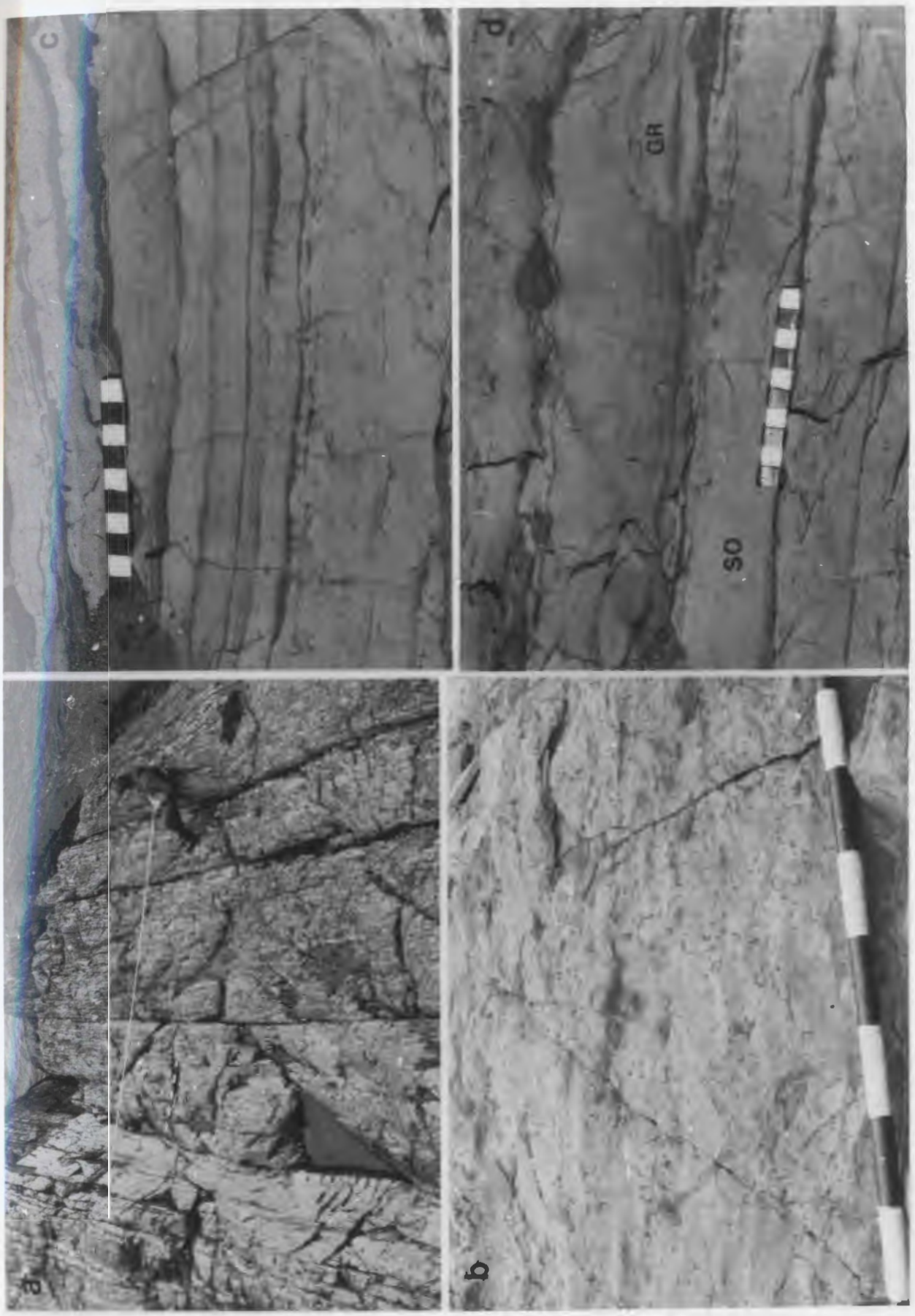
c
d
GR
SO
a
b

Figure 4.2: Paleocurrent information from Facies Association 2 (Facies 2.1/2.2) from Fortune Dump. 'A'= orientation of current lineations, 'B'= groove trends, 'C'= paleocurrent data from current/combined-flow ripples, 'D'= flute paleocurrents, 'E'= trends of wave ripple crests, and 'F'= ripple-crest trends (ripple type unknown).

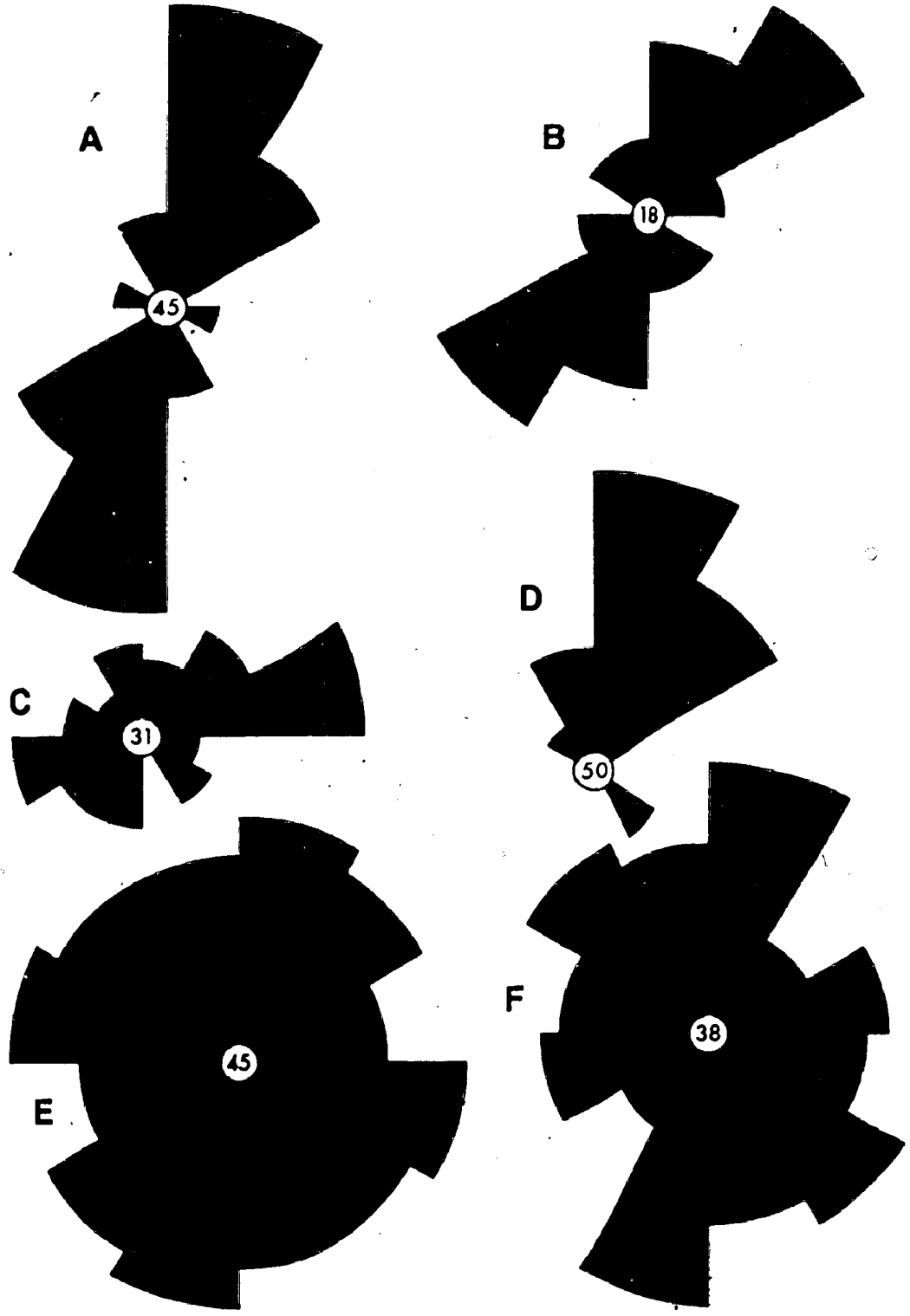
A
45
B
18
C
31
D
50
E
45
F
38

discussion. A full range of paleocurrent data from localities throughout the field area is summarized on rose diagrams in Figure 4.3.

A brief review of oscillatory bedforms and internal structures is given below as background to the description and process interpretations of many of the bed types that will follow, particularly S2, S3 and S4 beds.

4.1.1 Review of Bedforms and Internal Structures Produced by Oscillatory Flow

The sizes and shapes of various types of wave ripples have recently received considerable attention as a tool in reconstructing ancient sea conditions (e.g., Harms et al., 1982; P. Allen, 1981a, 1981b, 1984; Clifton and Dingler, 1984). The terminology for wave ripples, however, is complex. One classification scheme concerns the relationship between ripple spacing and orbital diameter. According to Inman (1957), and later Dingler (1974), the spacing of ripple crests is directly proportional to orbital diameter up to a critical diameter, above which the spacing at first decreases and then levels off at a fixed value. The ripples at the three stages of this relationship are defined as 'orbital', 'suborbital' and 'anorbital', respectively (cf. Clifton and Dingler, 1984, Fig. 5). A second scheme is concerned with the relationship between orbital diameter and the wavelength-to-height ratio. Bagnold (1946) coined the name 'rolling-grain ripples' for the low-amplitude ripples that form under small orbital diameters at the onset of grain motion, and 'vortex ripples' for those forms with low wavelength-to-height ratios in which sediment is carried in a vortex over the crests during each flow oscillation. At high flow velocities and large orbital diameters, before the transition into sheet flow, sand is eroded from rippled crests during each oscillation, resulting in low amplitude 'post-vortex' ripples (Dingler, 1974; Dingler and Inman, 1977), and at long oscillation periods 'reversing-crest' ripples (Harms et al., 1982). Confusion arises because some workers use the term 'rolling-grain ripple' for all wave ripples with high wavelength-to-height ratios (Sleath, 1976, Allen, 1979), which

Figure 4.3: Paleocurrent information from Facies Association 2 (Facies 2.1/2.2) from localities throughout field area. 'CL'= orientations of current lineations, 'GT'= groove trends, 'FP'= flute paleocurrents, 'RP'= ripple paleocurrents, 'WR'= wave-ripple-crest trends, 'RC'= ripple-crest trends (ripple type unknown).

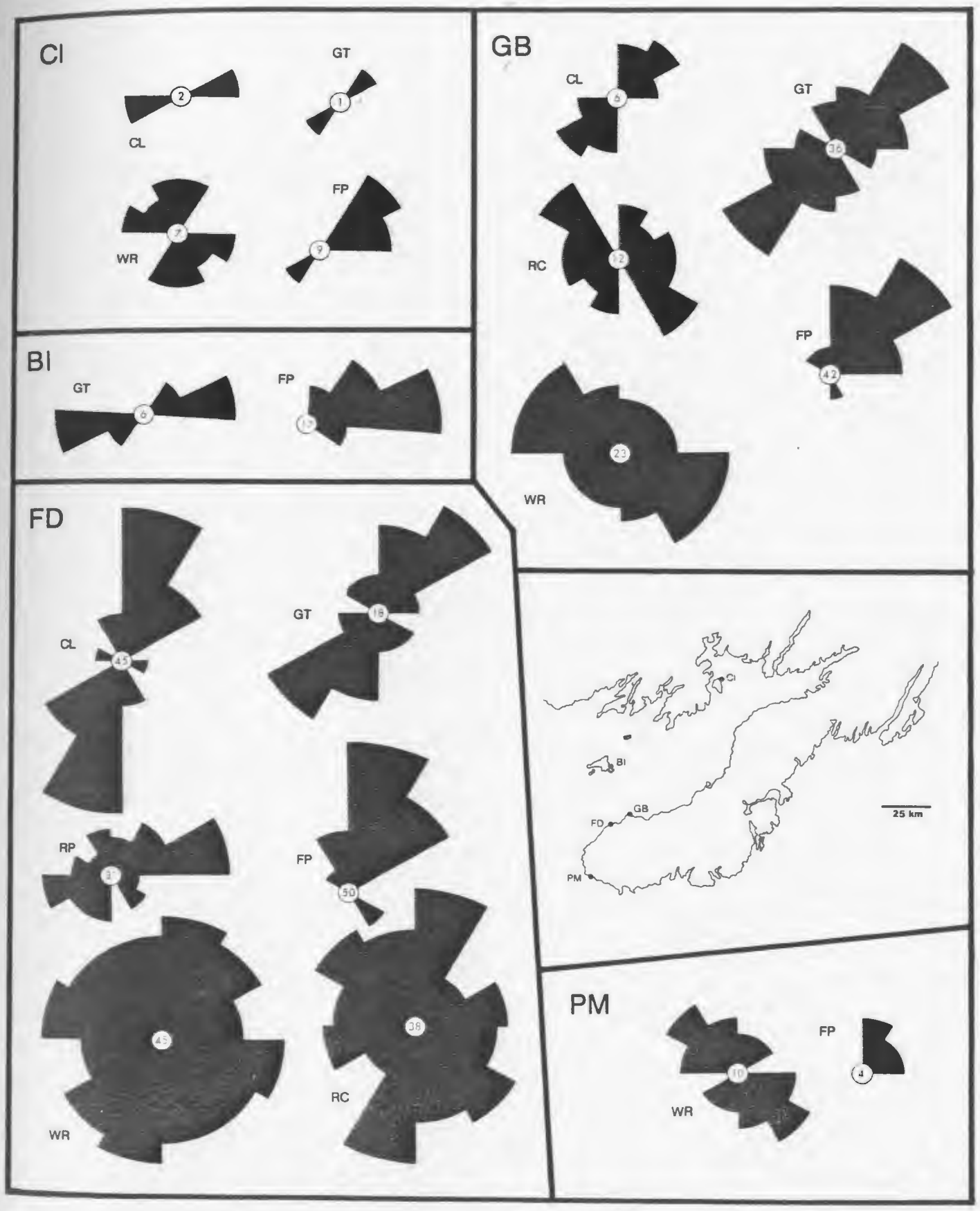
CI
GT
CL
FP
WR
GB
CL
GT
RC
FP
WR
BI
GT
FP
FD
CL
GT
RP
FP
WR
RC
BI
GB
FD
PM
25 km
PM
FP
WR

would include these 'post-vortex' and 'reversing-crest' ripples. The general consensus is that rolling-grain ripples, which form just above threshold velocities, are metastable and quickly convert to vortex ripples (Harms et al., 1982; Clifton and Dingler, 1984). These forms are apparently stable only on artificial oscillating beds in flumes (Miller and Komar, 1980). There is little or no information concerning the internal structures of post-vortex ripples.

According to Clifton and Dingler (1984), the two ripple classification schemes are not entirely correlative, although they strongly overlap. Postvortex and reversing-crest ripples (Harms et al., 1982) are considered anorbital ripples, but some orbital ripples are not vortex ripples, even though many workers have equated the two (Clifton and Dingler, 1984, p. 182).

The previous discussion has been concerned with the characteristics of oscillatory bedforms under simple oscillatory motion. Many of the oscillatory bedforms found in ancient marine strata may have formed under complex wave motions. The lack of empirical data on bedforms under nonsimple oscillations is a major gap in the understanding of oscillation ripples.

Wave-formed ripples have historically received little attention from geologists, especially in comparison to current-formed ripples. Until the mid-1960's the standard dogma was that the internal structure of wave ripples consisted of simple chevron-style lamination (Newton, 1968). McKee (1965) and Newton (1968) demonstrated that wave ripples often do not contain these chevron-style laminae, and that both wave and current ripples could exhibit similar characteristics. Boersma (1970) thoroughly described and summarized a whole suite of features diagnostic of waves. According to J.R.L. Allen (1984; pt. A, p. 428), these form when "...ripple marks become reformed under conditions of changeable waves and a low sediment net deposition rate". P. Allen (1981a) analysed some of these features in terms of various wave parameters. The features diagnostic of waves, as outlined by Boersma (1970) and De Raaf et al. (1977), are given in Figure 4.4.

Figure 4.4: General wave-diagnostic features of cross-lamination. Modified from Boersma (1970).

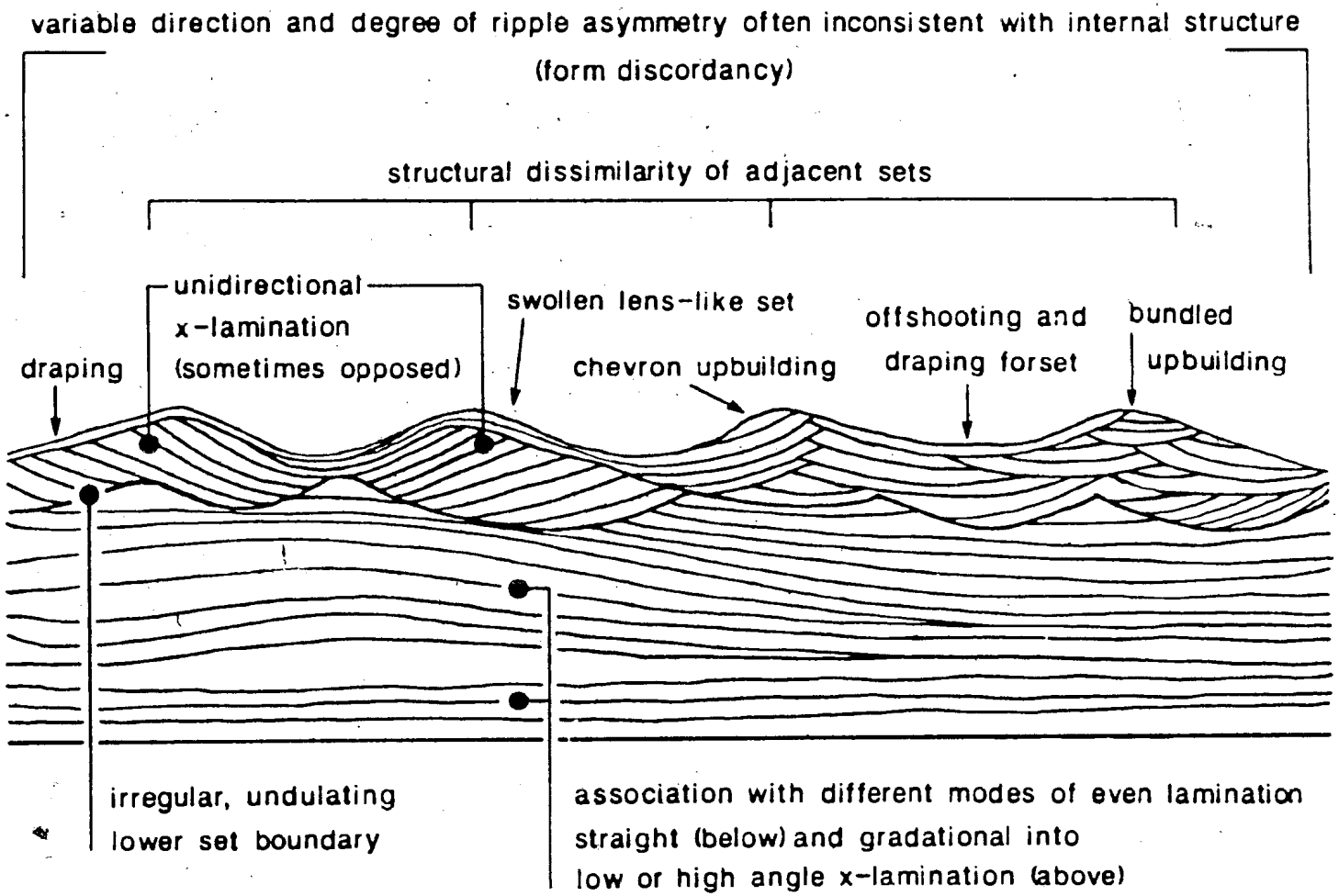
variable direction and degree of ripple asymmetry often inconsistent with internal structure
(form discordancy)
structural dissimilarity of adjacent sets
unidirectional
x-lamination
(sometimes opposed)
swollen lens-like set
offshooting and
draping forset
bundled
upbuilding
draping
chevron upbuilding
irregular, undulating
lower set boundary
association with different modes of even lamination
straight (below) and gradational into
low or high angle x-lamination (above)

4.2 SILVER-GREEN SILTSTONE: S0

These beds consist of homogeneous silver-green to grey-green muddy siltstone (Plate 5d). This siltstone is the background sediment for all other beds. These beds vary in thickness from a millimeters to tens of centimeters. This siltstone ranges from undisturbed to strongly bioturbated, as deduced from the preservation or disruption of interbedded delicate sand laminae (S1 and S2 — described below). Distinct traces are locally present in large numbers (Plate 5b). The traces in this siltstone are primarily simple forms (e.g., various species of Planolites).

One characteristic of this siltstone, especially prominent when interlaminae of sandstone are widely spaced, is the presence of extremely small fragments of shale a few millimeters long and less than 0.5 mm thick. These are noticeable on the weathered surface because of orange stains (halos) that surround the clasts.

4.2.1 Process Interpretation

The homogeneity of grain size and lack of lamination indicates uniform deposition from suspension. All or most of this siltstone could be attributed to slow fallout from the ambient waters. Some of this siltstone might be attributable to late-stage fall-out associated with deposition of interbedded sandstone beds. Distinction between these processes would be somewhat analogous to the distinction between T_f and T_e units in turbidites (Van der Lingen, 1969; Hesse, 1975; specifically the ungraded E_3 division of Piper, 1978, or the T_7 division of Stow and Shanmugam, 1980).

It is likely that the density and shape of the shale chips in this siltstone was such that they were roughly hydrodynamically equivalent to the surrounding silt, or at least close

enough to have been easily transported in suspension. The orange halos around these chips are iron-oxide staining, a weathering feature.

4.3 SILTSTONE/SANDSTONE THIN LAMINAE: S1

Thin S1 laminae consist of coarse siltstone to fine sandstone that are less than 0.5 mm thick and, in most cases, are remarkably persistent laterally (Plate 5c,d). The thickest of these laminae may weather positively, standing out from the surrounding fine siltstone by a fraction of a millimeter. These laminae may be closely spaced (millimeter scale) or more widely spaced (0.5-5 cm apart). These S1 laminae may show a vertical increase in spacing within clearly defined beds, described below as graded rhythmites (Section 4.7).

4.3.1 Process Interpretation

Several aspects of these S1 laminae indicate deposition from suspension: (1) extreme thinness, (2) lack of visible internal structure, (3) lateral persistence, (4) uniform thickness and (5) lack of evidence for erosional lower contacts.

Where these fraction-of-a-mm-thick laminae are separated by several centimeters of homogeneous siltstone, the laminae may be related to variation in the size of the sediment being supplied, or to variation in flow velocity. If oscillatory currents were involved, they were weak, as S1 laminae display no features diagnostic of waves. The sandstone laminae can be seen to be coarser than the coarsest grains in the muddy siltstone, ruling out in situ winnowing as a mechanism for generating the thin sandstone laminae.

In stratigraphic intervals where the very fine sandstone laminae are most abundant and thickest, the lithology (interbedding of S1 and S0) begins to resemble thinly interlayered bedding or 'rhythmites' (see Reineck and Singh, 1980; p. 123-130).

4.4 SANDSTONE LAMINAE S2

S2 laminae consist of discontinuous, grey- to brown-weathering sandstone. These sandstone laminae generally range from 1 to 10 mm in thickness (average ~5 mm), but pinch and swell (Plate 6a,e), locally reaching a maximum thickness of 1.5-2 cm. Radical changes in thickness and pinch-outs are diagnostic of S2 beds. These variations in thickness are most often associated with erosion at both the upper and lower surfaces. In some cases neither surface appears erosional, and changes in thickness are associated with small-scale incipient or fully developed ripple cross-lamination. S2 Laminae are locally disrupted by burrows (Plate 6c,d).

Most of the sandstone laminae appear internally massive. Where these laminae locally swell to 1 cm or greater in thickness, they exhibit grading, parallel lamination and ripple cross-lamination. Parallel laminae may pass laterally into unidirectional ripple cross-laminae. Upper bedding surfaces locally show sharp-crested symmetrical ripples with large spacing-to-height ratios; some of these ripples are starved and have crest heights less than 5 mm (Plate 6b). Cut slabs display form-discordant ripples with bundled lenses and irregular lower set boundaries and climbing wave-ripple laminae. Only a few examples of simple form-concordant ripples were noted.

Very few sole marks are exposed due to the thin and discontinuous nature of these beds (Plate 6a,c,d). Those that are exposed show small trace fossils (e.g., Planolites) and sole markings such as flute, groove and prod marks.

4.4.1 Process Interpretation

Where S2 laminae are interlaminated with S0 laminae/beds, the bedding style resembles 'thinly interlayered bedding' (Reineck and Singh, 1980). This term was

PLATE 6: S2 BEDS (FA 2)

a: The discontinuous character of S2 beds is illustrated in this photo from GB-~50B. A small part of the soles of a few of these beds are exposed here. Stratigraphic top is up. Scale is 10 cm long.

b: Partially-starved wave ripples at FD-364.5. Note tuning-fork junction. Stratigraphic top is up. Scale is 10 cm long.

c: Close-up of burrowed S1 and S2 beds. Note limited exposure of soles. Stratigraphic top is up. Scale is in 10 cm divisions.

d: Burrowed S1 and S2 beds as seen at GB-B. View is slightly oblique to bedding and stratigraphic top is up. Scale is in 10 cm divisions.

e: Discontinuous S2 laminae at FD-~22. Many of these laminae have flat bases and rounded tops while others have concave-down bases and flat tops. Note clastic dikes (arrow). Stratigraphic top is up. Scale is 10 cm long.

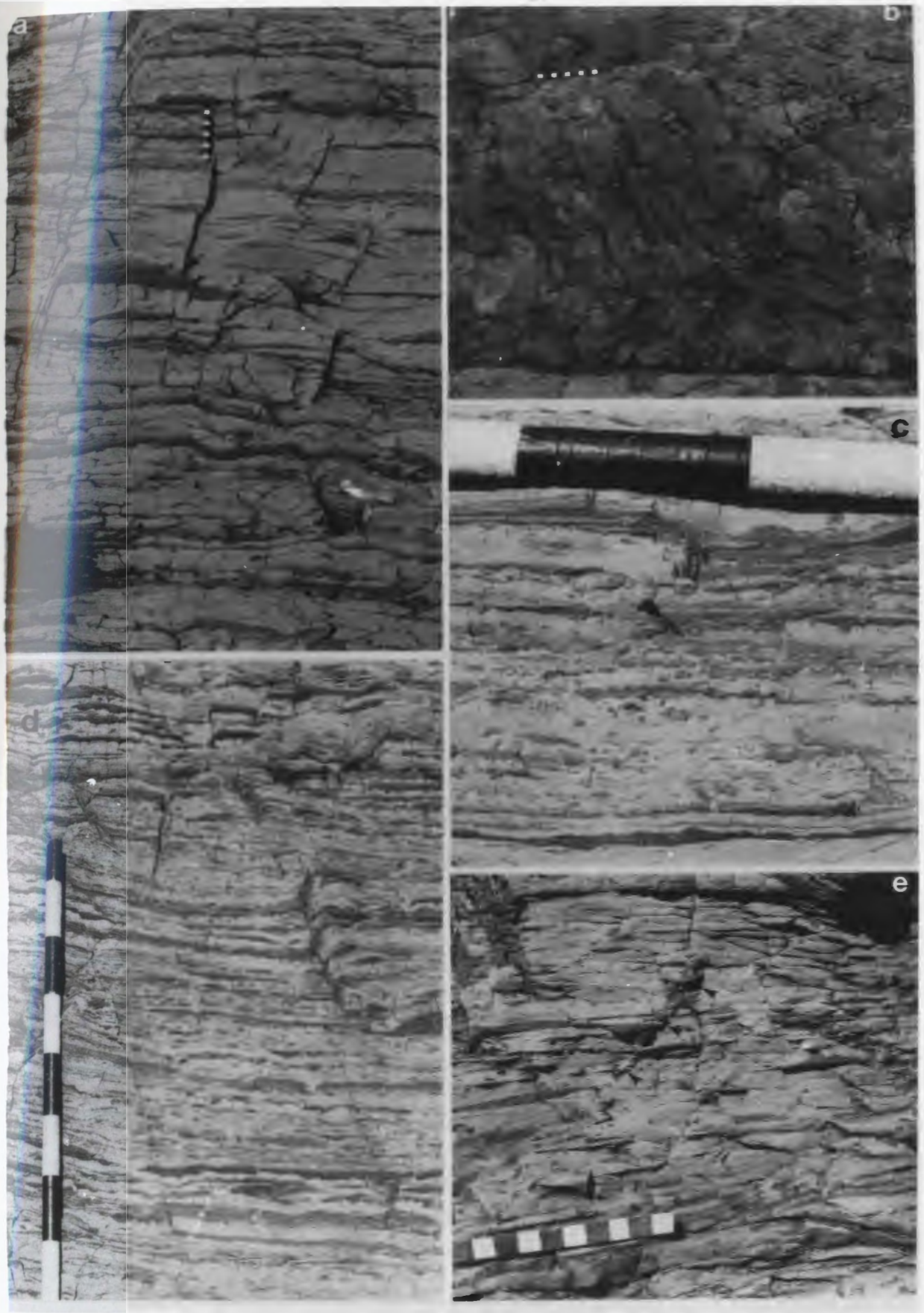
a
b
c
d
e

introduced to replace the term 'tidal bedding' (Wunderlich, 1970) which had obvious genetic connotations. Interlaminae of S0 and S2 beds resemble De Raaf et al.'s (1977) 'Lithotype M2'. The scale and pinch-and-swell nature of the sandstone laminae in their Lithotype M2 is particularly similar. Incipient-ripple lenses and lateral transitions from parallel laminae into cross-laminae, both features of S2 laminae, were attributed by De Raaf et al. (1977) to wave reworking during the late stages of deposition. A heterolithic facies described by Soegaard and Eriksson (1985) is also similar in that it includes form-discordant ripples with bundled upbuilding, draping laminae and other features that they attribute to waves. These wave-generated features are discussed by Boersma (1970), De Raaf et al. (1977), Allen (1981a), Harms et al. (1982) and others (see Figure 4.4).

The few examples of sole markings on these sandstone laminae indicate that the initial sand deposition was by unidirectional currents that were capable of scouring the underlying sediment surface. The lack of visible internal laminae in many of the sandstones reflects a homogeneous grain-size population and leaves little information about depositional processes. During the late stages of deposition or after deposition, the sand was reworked by waves, forming incipient ripples, small form-discordant ripples and sandstone lenses, climbing wave-ripple laminae and in some cases starved, low-amplitude wave ripples. The lack of current lineations or parting lineations may reflect a loss of upper-plane-bed parallel laminae during this late stage reworking.

The straight-crested ripples with high spacing-to-height ratios must be either rolling-grain ripples, postvortex ripples or early-formed vortex ripples. The internal structures of the S2 ripples are similar to those of two-dimensional vortex ripples (Harms et al., 1982). Therefore the low-amplitude ripples are considered vortex ripples that were in the early stages of development, formed in a thin layer of sediment.

The scale of bedding is indicative of either low-energy currents or low sediment supply. The latter is favored, as the nature of the bedding and the internal sedimentary

structures indicates frequent, episodic transport of sand by currents and frequent remolding of the sediment surface by waves.

4.5 VERY THIN SANDSTONE BEDS: S3

These beds consists of 1-10 cm-thick, brown-weathering, fine sandstone. Over large stratigraphic intervals S3 beds constitutes 20-40% of the strata (the rest being dominantly S1 and S2 beds), while thin stratigraphic intervals (a few tens of centimeters) may contain as much as 80% or more. The beds are generally continuous and fairly even in thickness.

Internal sedimentary structures are often well preserved in these sandstone beds. The beds are always sharp-based, but may have sharp (Plate 7a,b,d,e,f) or gradational (Plate 7c) upper surfaces. Grading characterizes roughly half of these beds, the rest appearing ungraded on the weathered surface. The grading is generally from fine sandstone to very fine sandstone, or from fine sandstone to siltstone; a small fraction of beds may grade up from medium sandstone. The following internal structures have been noted: (1) nongraded, apparently structureless, (2) graded but otherwise structureless, (3) ripple cross-laminated, including erosional-stoss and depositional-stoss climbing-ripple types (Plate 7b,f, 7f), the latter of which, in turn, includes those with symmetrical and asymmetrical profiles showing upwardly decreasing amplitude ('Type C' climbing ripples of Jopling and Walker (1968) (Plate 8c), (4) ripple form sets with asymmetrical profiles and form-concordancy (Plate 7a), and those with symmetrical profiles with high or low spacing-to-height ratios, (5) ripples with bidirectional bundled lenses, unidirectional cross-laminae opposed between adjacent crests and offshooting laminae (Plate 8d; Figure 4.5b), and (6) planar or undulatory parallel laminae. The following sequences of structures have been noted: (1) asymmetrical or symmetrical ripples overlain by draping laminae, (2) cross-

PLATE 7: S3 BEDS (FA 2)

a: S3 beds from GB-49.2B with sharp bases and sharp or gradational tops. Low-relief ripples in center of photo show variation in internal structure between crests (a feature of wave ripples). The crest on left is symmetrical, with wavy lamination, while the crest on the right appears slightly asymmetrical and is unidirectionally cross-laminated. Stratigraphic top is up. Scale is 15 cm long.

b: Wavy to stoss-preserved climbing ripples in S3 bed at FD-271.65. Stratigraphic top is up. Scale is 15 cm long.

c: The S3 bed below the scale has a sharp base (arrows) with large flute marks that are seen in cross-section. The top of the bed is gradational into the siltstone above, with draping/offshooting lamination cryptically preserved in siltstone at the top of the bed. this weathering pattern, which is shared by graded rhythmites, makes it difficult to define the top of the bed. Stratigraphic top is up. Scale is 10 cm long.

d: The reworked upper surface of this parallel laminated bed (GB-76.5B) locally displays symmetrical sharp-crested ripples. Note parallel lamination below the crest on the right side of photo. Stratigraphic top is up. Scale is 15 cm long.

e: Parallel to wavy laminated bed (FD-332.5) with upper surface that is locally remolded into a ripple geometry. The rippled upper surface of the overlying bed displays variability in crest size and shape. The crest in the top left corner is somewhat rounded, unidirectionally cross-laminated and has very low-angle cross-laminae, features associated with combined-flow ripples. Stratigraphic top is up. Scale is 10 cm long.

f: Stoss-preserved climbing wave-ripples lamination from S3 bed at FD-226.3 showing a high angle of climb (below scale) and symmetrical profiles. Stratigraphic top is up. Scale is 15 cm long.

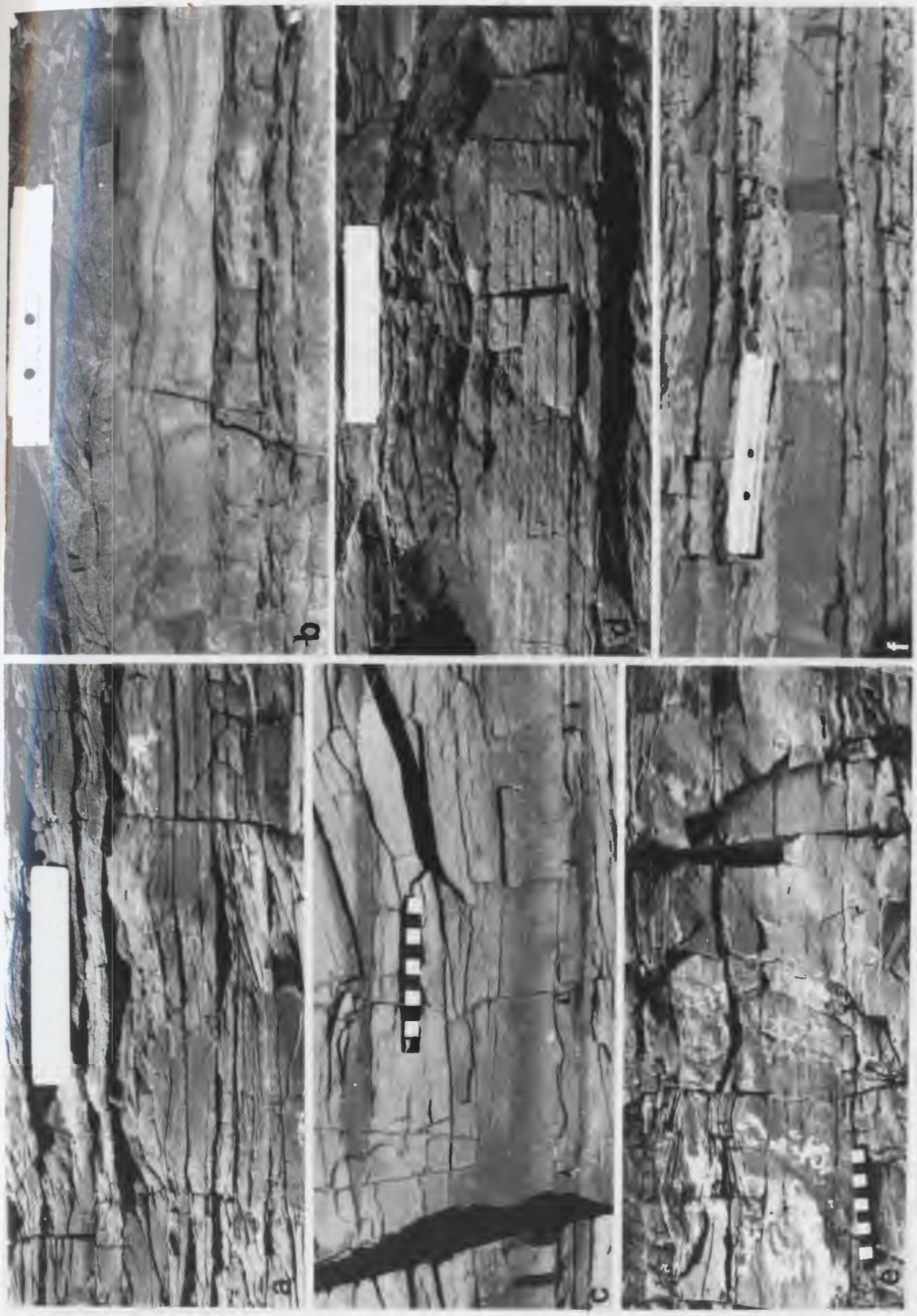
b
d
f
a
c
e

PLATE 8: S3 BEDS CONT'D (FA 2)

a: Symmetrical ripples at FD-75.3. Note differences in peakedness of adjacent crests. Stratigraphic top is up. Scale is in 10 cm divisions.

b: Fine sandstone bed (S3) at FD-274.2 with variation in size and shape of adjacent symmetrical crests along a ripple train. Stratigraphic top is up. Scale is 15 cm long.

c: Depositional-stoss climbing wave-ripple lamination in an S3 bed from Brunette Island (BrI-98.6). Note upward change from asymmetrical to more low-relief symmetrical ripple crests. Stratigraphic top is up. Scale is in cm.

d: Symmetrical form-discordant ripples in concretion from GB-137.7B with bundled upbuilding, scooped lower bounding surfaces, bidirectional bundled lenses and draping lamination. These are 'classic' features of wave-formed ripples as originally outlined by Boersma (1970). Stratigraphic top is up. Scale is 1 cm long.

e: Features preserved within this carbonate concretion include parallel lamination (top and bottom) and climbing-ripple cross-lamination separated by scooped lower bounding surfaces. Stratigraphic top is up. Scale is 15 cm long.

f: Low-relief, long wavelength, stoss-preserved climbing ripples with locally high angles of climb preserved within this carbonate concretion from GB. Stratigraphic top is up. Scale is 10 cm long.

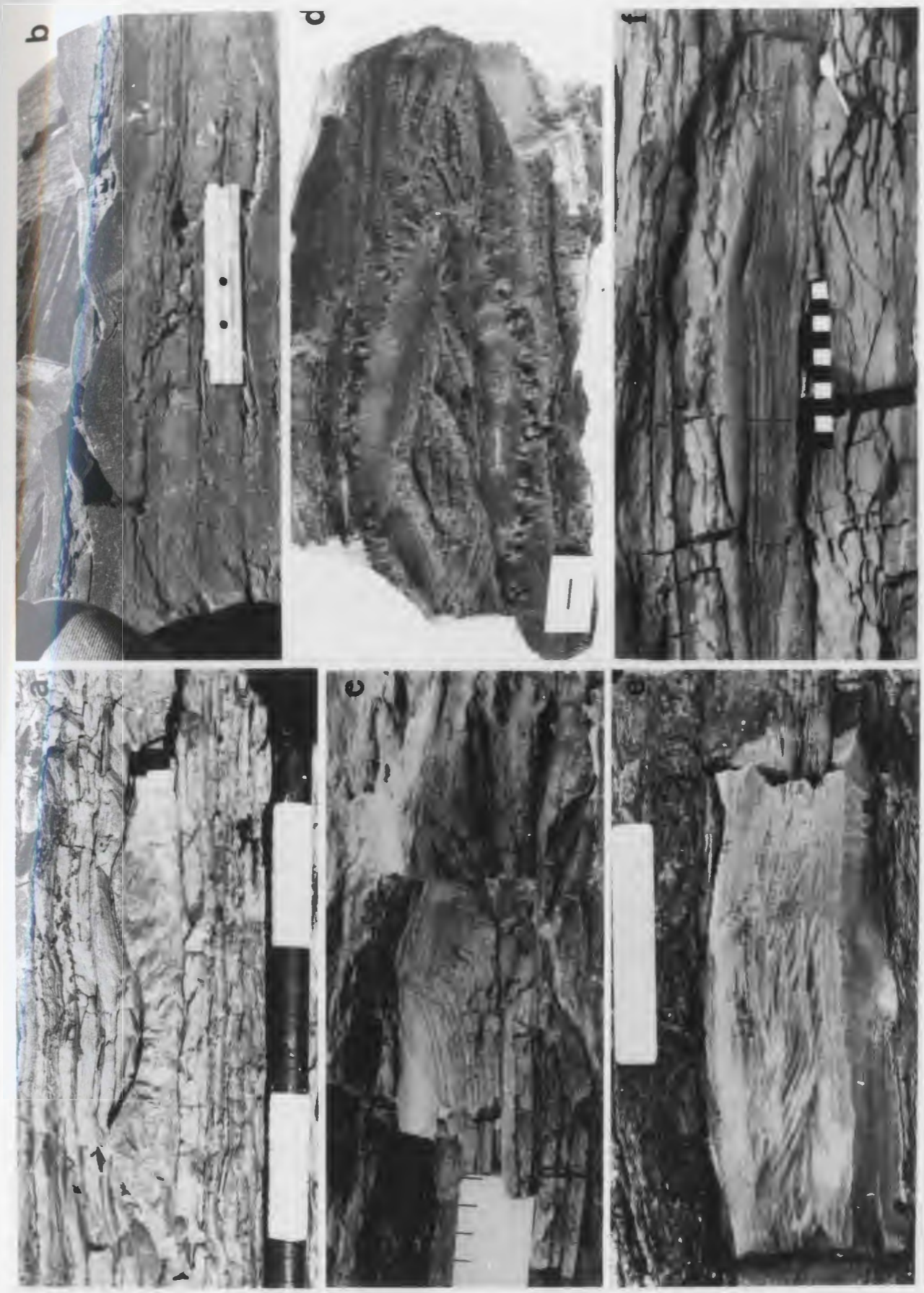
b
d
f
a
c
e

Figure 4.5:

a) Sketch of carbonate concretion from a rippled S3 bed at GB-156.9B. Note strong variation in size, shape and internal structure between adjacent crests.

(b) Sketch of rippled S3 bed at FD-298.75 showing form-discordance, unidirectional cross-lamination opposed between adjacent crests, and offshooting and draping lamination.

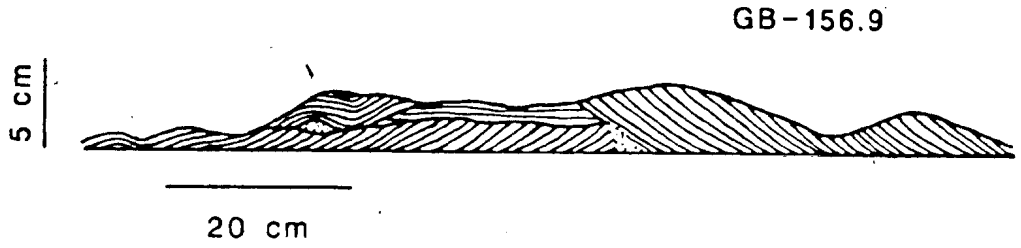
GB-156.9
5 cm
20 cm


FD-298.75
4 cm

laminae draped by laminae from adjacent cross-laminated set, and (3) planar or undulatory parallel laminae overlain by asymmetrical or symmetrical ripples (high or low spacing-to-height ratio) with or without draping laminae (Plate 7d,e). Parting lineation and current lineation is found associated with parallel lamination. Data on parting/current lineation orientations are given in Figure 4.2a (most of the data in this figure are from S3 beds; some data from S2 and S4 beds are also included).

Carbonate concretions, retaining precompactional thicknesses two to three times that of the rest of the bed, often preserve a wide variety of interesting sedimentary structures that are not visible in the portions of the bed not cemented by carbonate (see Figure 4.1). The following features have been noted from ripples in these concretions: (1) climbing sets of cross-laminae separated by irregular, often concave-up scour surfaces (Plate 8e), (2) stoss-preserved climbing-ripple laminae with symmetrical profiles (Plate 8f), and (3) form-discordant ripples that internally display bundled upbuilding, offshooting foresets, bidirectional bundled lenses and draping laminae (Figure 4.6; Plate 8d). In addition, some examples of both carbonate-cemented and non-carbonate-cemented ripples show strong variation in size, shape and internal structure of adjacent crests along ripple trains (Plate 7a,d, 8a,b; Figure 4.5a).

Lower bedding surfaces are well exposed and are covered by a wide variety of trace fossils and sole markings. The latter include flutes, grooves, prods, and current crescents. Flute marks vary from simple rounded and pointed forms to those with strongly curved and prominent 'beaks'. Although they may be found isolated on a surface, they are usually found in large numbers, as is generally the case with sole markings (Plate 9a). Different groove sets on the sole of a bed may vary in orientation, by as much as 50 degrees in extreme cases (Plate 9c). The various sole marks are well oriented with a consistent northeast-southwest trend (same as current lineations). The paleocurrent data from flute marks show a strong unimodal orientation toward the northeast (Figure 4.2d).

Figure 4.6: Line drawing of carbonate concretion from S3 bed at GB-137.7B. The ripples display such wave-diagnostic features as form-discordance, bundled upbuilding, offshooting forsets, bidirectional bundled lenses and draping lamination.

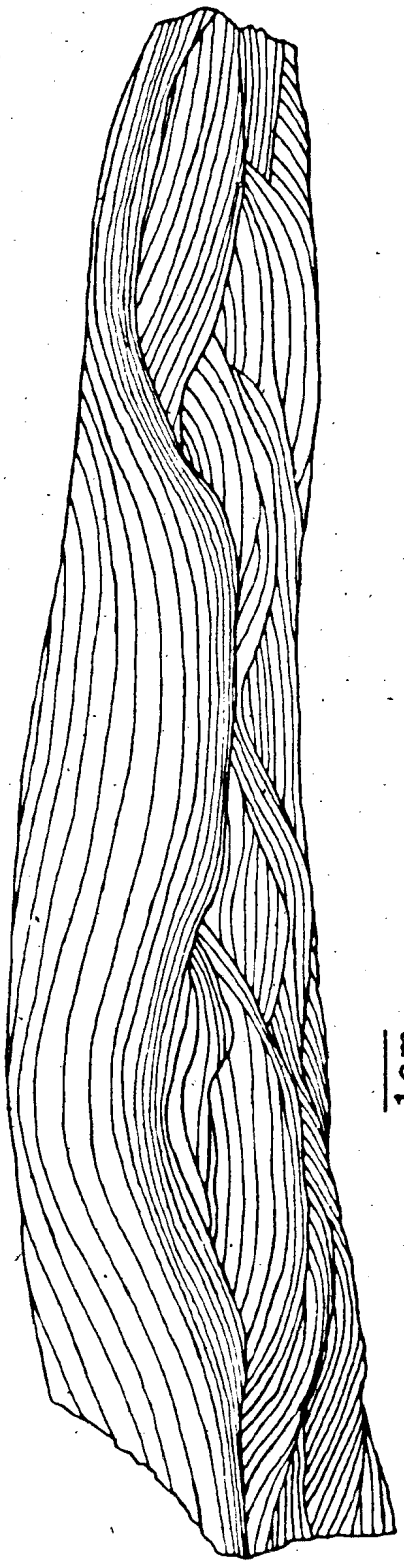
1cm

PLATE 9: S3 BEDS - SOLE MARKS (FA 2)

a: Multiple surfaces decorated with solemarks from fallen block at GB. Sole marks include grooves, flutes and prod marks. Scale (lower left) is 10 cm long.

b: Bulbous, irregular flute marks from the base of an S3 bed at GB. Groove marks are also present along sole at right side of photo. Flow was to upper right. Scale divisions are 10 cm.

c: Several sets of divergent and crossing grooves indicating paleoflow variation by as much as 50-60 degrees. Scale is in cm.

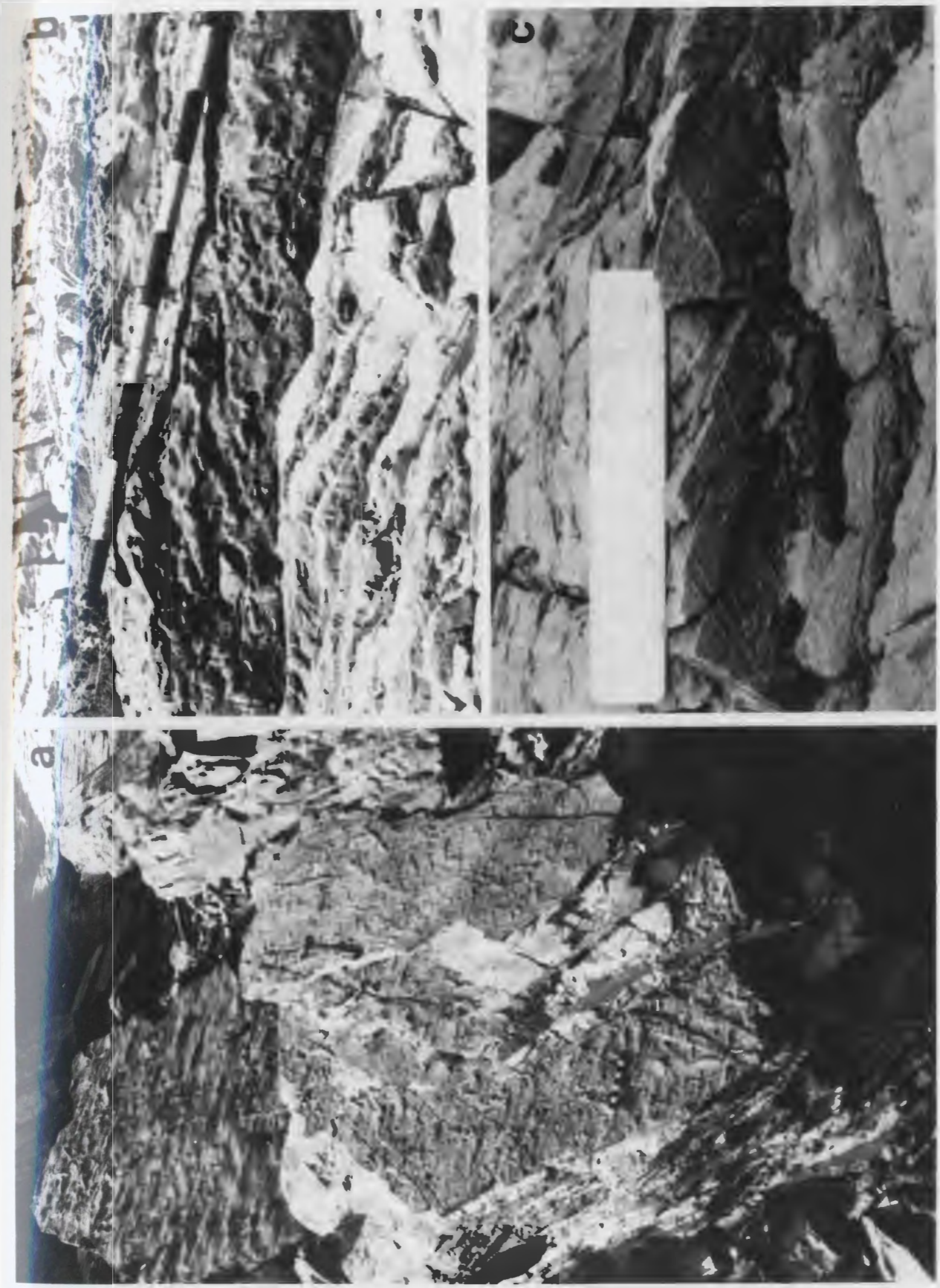
b
c
a

Upper bedding surfaces are also decorated with a wide variety of trace fossils and sedimentary structures. Ripples are the most common feature on these surfaces. By far the most common are ripples with large spacing-to-height ratios and straight to slightly sinuous, sometimes bifurcating crests (Plate 10d,e), and interference ripples with thin, widely spaced (at maximum spacing) crests (Plate 10c). One common type of ripple has sharp crests, slightly asymmetrical profile and high spacing-to-height ratios. The crests range from wavy with bifurcations to a nearly polygonal pattern (Plate 10f). The bedform migration directions can be deduced from the truncated stoss lamination (Plate 10c,f). The crests of asymmetrical ripples range from straight to linguoid. Many of the asymmetrical, unidirectionally cross-laminated ripples are highly three-dimensional and have rounded crests and very gently dipping lee surfaces (less than angle of repose) (Plate 10a,b).

Structures similar in character to wrinkle marks (Kinneya structures) are found along internal partings and at upper bedding surfaces of some sandstone beds.

4.5.1 Process Interpretation

The sharp lower surfaces covered with sole markings indicate that the currents transporting the sand were strong enough to scour the underlying siltstone. Prod and groove marks indicate that the current also carried tools that gouged and scraped the silty surface. It should be noted, given the discussion that will follow concerning the formation of various internal structures by waves, that most of these beds have either flat or only slightly wavy bases (not a characteristic of wave-formed beds; De Raaf et al., 1977). This, and the consistent unidirectional orientation of flute marks, indicates that for these beds the initial transport and deposition of sand was under the influence of unidirectional currents.

Most of the internal features of these beds — undulatory laminae, complex upbuilding of cross-lamination sets, etc. — are considered by various workers to be wave-

PLATE 10: S3 BEDS: WAVE/COMBINED-FLOW RIPPLES (FA 2)

a: Bedding-plane view of combined-flow ripples at FD-270 with strongly 3-dimensional geometries and rounded crests. Scale is 15 cm long.

b: Cross-sectional view of "a". An anomalously sharp and symmetrical crest in the center of the photo displays the low-angle (lower than angle-of-repose) of these cross-laminae. Scale is 15 cm long.

c: Combined-flow ripples with sinuous, slightly asymmetrical crests (FD-346.15). Eroded stoss laminae indicate flow from upper right to lower left. Slight interference pattern is indicated by subtle crests that are oriented roughly right to left. Scale is 15 cm long.

d: Combined-flow ripples from FD-271.5. Note sinuous, bifurcating crests. Eroded stoss-laminae indicate ripple migration towards the right. Scale is 10 cm long.

e: Extremely low-relief (<5 mm height), straight-crested wave ripples at FD-364.5. Note bifurcation of crest at top of photo. View of upper bedding surface. Scale divisions are 10 cm.

f: Close-up of "c" where the crests form a near-polygonal pattern. The eroded stoss laminae indicate migration towards the base of the photo. The origin of these kind of polygonal-crested ripples is enigmatic, forming either by pure oscillatory flow or combined-flow (J.B. Southard, pers. comm.). Scale is 10 cm long.

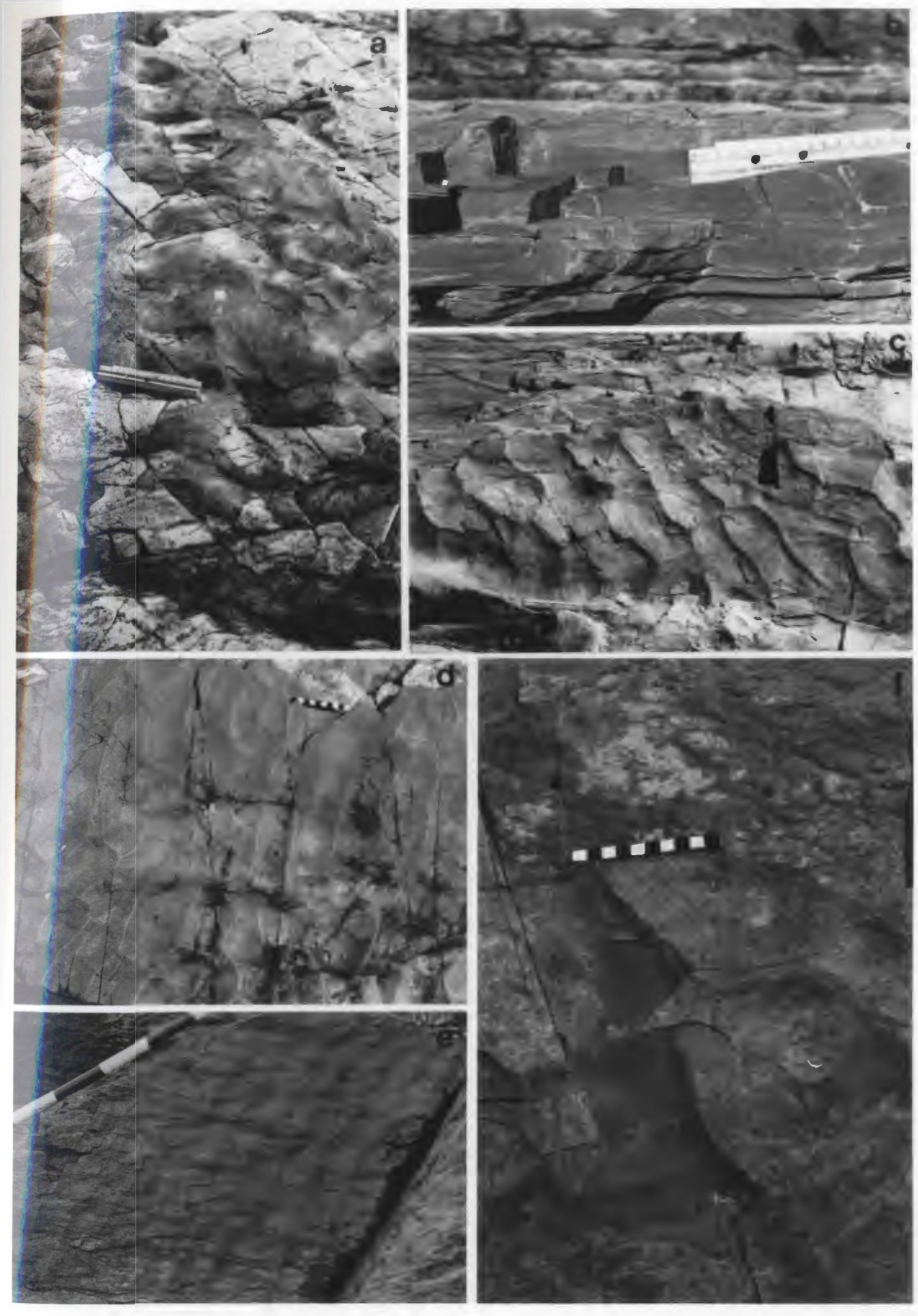
a
b
c
d
e
f

generated structures (Figure 4.4). In the S3 sandstones the most common of these features include bundled upbuilding, dissimilarity in internal structure and shape of adjacent sets, offshooting and draping foresets, late-stage draping laminae, and irregular, undulatory set boundaries. The complex upbuilding of sets of cross-laminae that characterize many of the S3 beds are diagnostic of two-dimensional vortex ripples (Harms et al., 1982). Climbing wave ripple laminae are very common, including those with upward decrease in amplitude like the current-generated 'Type C' climbing ripples (Jopling and Walker, 1968). The latter ripples are attributed to deposition from rapidly decelerating currents experiencing simultaneous (oscillatory) traction transport and suspension deposition. The strongly three-dimensional ripples with asymmetrical profiles and unidirectional cross-laminae are interpreted as combined-flow ripples based on their rounded crests and low-angle foresets (Harms, 1969; J. B. Southard, pers. comm.). Experimental data on combined-flow bedforms appears to be relatively meager. Work to date indicates that combined-flow ripples have characteristics of both unidirectional and oscillatory ripples, bearing more resemblance to one or the other depending on the relative importance of either process (Harms, 1969; Harms, et al., 1982). Combined-flow ripples are generally asymmetrical, but in comparison to current ripples, have more regular plan geometry, more rounded crests and lee faces that slope less than the static angle of repose (Harms, 1969). Very few ripples were noted that could not be readily attributed to either combined-flow or purely oscillatory processes. Even the small percentage of asymmetric, form-concordant ripples could have formed from wave motions (McKee, 1965; Boersma, 1970).

There are very few symmetrical ripples with small vertical form indices typical of fully developed vortex ripples, even though the internal structure of many S3 beds is one of intricate braiding of cross-lamination, typical of two-dimensional vortex ripples (Newton, 1968; see Figure 3-16, Harms et al., 1982). This can be explained by the fact that in most cases the upper portions of the sandstone beds are covered by late-stage laminae that drape these ripple forms, smoothing the topography of the small vortex ripples. Orbital (vortex)

ripples like these would have formed under conditions of short oscillatory motion, most likely "...in very shallow water under short-period waves. Long-period waves can generate similarly short orbital flow at the bottom in deeper water, but because of the [inverse] relationship [between mean velocity and period]..., ...the velocity will be reduced and threshold conditions are less likely to be reached" (Clifton and Dingler, 1984, p. 177).

Parallel laminae, where found at the base of S3 beds, are interpreted as having formed from strong unidirectional currents because of their association with current/parting lineations, and sole markings, such as well oriented flute marks. Flat to undulatory laminae above the base of the bed could also have formed by unidirectional currents, waves, or combined currents. Undulatory laminae are thought to be a feature of intense oscillatory flow (Allen, 1981a, p. 372; Harms et al., 1982).

In summary, the S3 sandstone beds were formed by a combination of waning unidirectional currents and waves. Sole markings indicate the influence of strong unidirectional currents during the initial stages of transport and deposition. The waning nature of the currents produced grading and vertical transitions from parallel laminae to combined-flow or oscillatory-flow ripples. In the late stages of deposition, waves reworked the sediment forming complex cross-laminae, offshooting and draping lamihae and other features diagnostic of oscillatory flow.

4.6 THIN TO MEDIUM SANDSTONE BEDS: S4

These S4 beds consist of grey-green to brown weathering, fine-grained sandstone. They display a remarkable range of internal structures. With few exceptions, these beds are normally graded. Their bases may be planar (Plate 11c,e) or highly irregular, showing truncation of underlying laminae or beds. These erosional irregularities include pot casts and gutter casts. The upper surfaces of these beds may be gradational into muddy siltstone

PLATE 11: S4 BEDS (FA 2)

a: The wavy to irregular lower surfaces (top is to right) and clearly erosional upper surfaces of these beds create lenticular and pinch-and-swell geometries (FD-241.5-242). The bed on the left is amalgamated. Scale is 15 cm long.

b: The upper portion of this bed at FD-318.7 is carbonate-cemented and displays complex cross-lamination passing upward into parallel lamination, which in turn pass upward into erosional-stoss climbing ripples. The parallel and ripple cross-laminae at the top of the bed may have been amalgamated to the lower division. If not, then the flow passed from the ripple field into the upper plane bed field and finally dropped back down into the ripple field during the final stages of sedimentation. Stratigraphic top is up. Scale is 15 cm long.

c: This complexly cross-laminated bed from 262.15 contains climbing stoss-preserving ripple lamination and smooth low-relief erosional surfaces. The rounded crests and low-angle cross-lamination indicate deposition from combined flows. Stratigraphic top is up. Scale is 15 cm long.

d: Polished slab of graded bed from FD with complexly cross-laminated lower division and a gradational top into muddy siltstone. Details of the stratification are slightly obscured by the fracture pattern and speckles of carbonate cement. Stratigraphic top is up. Scale is 1 cm.

e: Parallel laminated bed from FD-169.8 with relatively flat, though slightly fluted, base and a sharp upper surface. On the left side of the photo the bed is carbonate-cemented and the lamination stand out clearly. Stratigraphic top is up. Scale is 15 cm long.

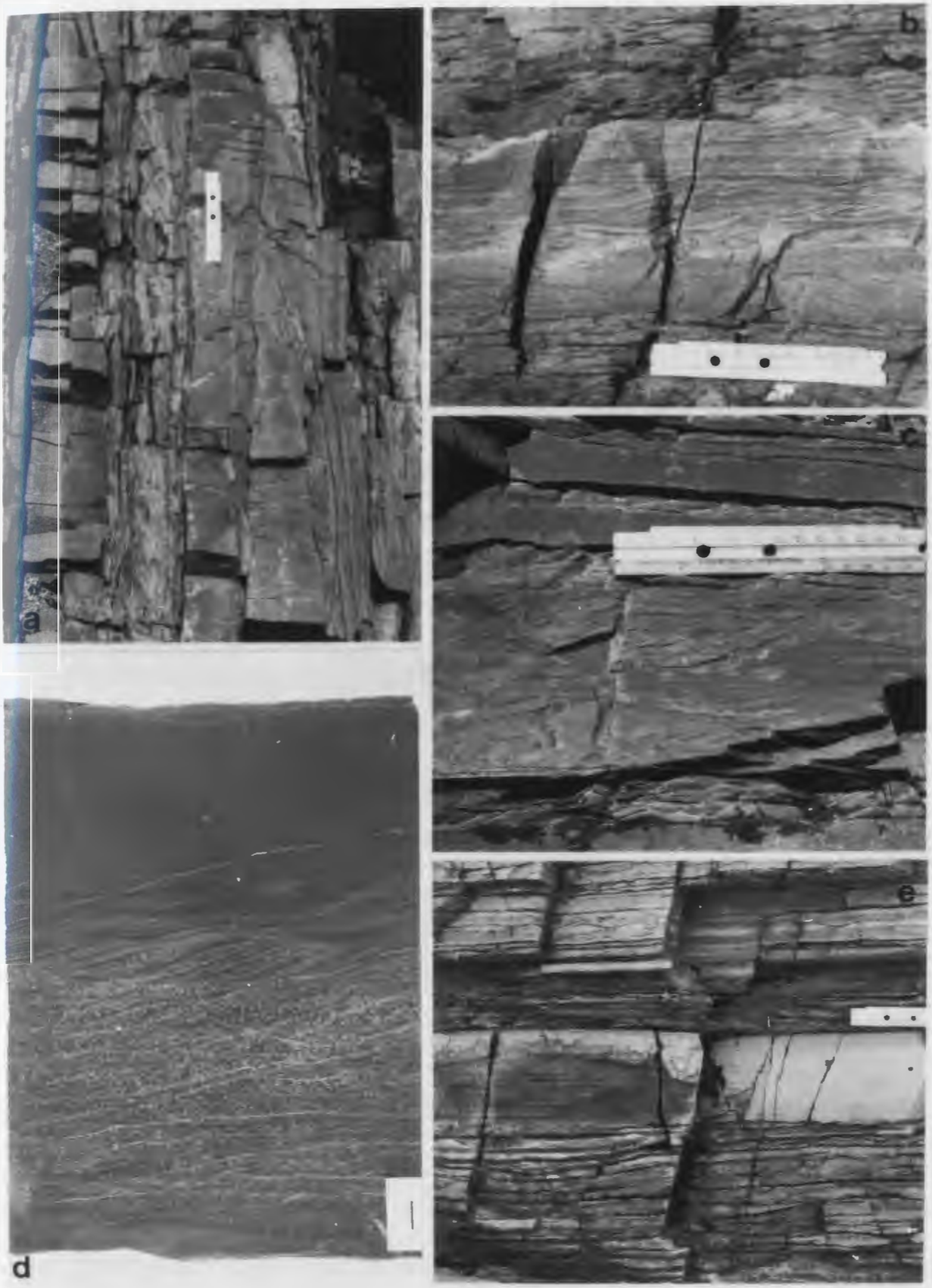
a
b
c
d
e

(Plate 11d), or erosional, with extreme cases showing local complete removal of the bed (Plate 11a). Internally, S4 beds range from apparently structureless to complexly laminated. They display parallel and wavy laminae (Plate 11e), complex upbuilding of cross-laminated sets separated by scooped bounding surfaces, and a wide variety of ripple-related laminae similar to those described for S3 beds (Plate 11b,c,d). Common vertical transitions include parallel laminae to complex cross-laminae and parallel laminae to form-concordant ripples, or form-discordant ripple form-sets, the latter showing draping and offshooting laminae.

Amalgamation of bedding is common, especially in the thicker beds. Each division of these amalgamated beds may show its own set of internal structures or sequence of structures, such as grading or parallel-laminated to ripple-laminated transitions. Vertical sequences like parallel laminae to ripple laminae are completely preserved only in the uppermost division. The lower layers show evidence of truncated structures and structure sequences.

The lower and upper surfaces of beds are often decorated with a variety of trace fossils and sedimentary structures. The beds display a suite of current- and tool-generated sole markings similar to those described for S3 beds. Ripple marks range from large asymmetrical forms with sinuous to linguoid crests, through straight-crested symmetrical forms, to interference types. Kinneya structures are also present on upper bedding planes. Postdepositional infaunal trace fossils are commonly absent from the lower parts of the thicker beds.

4.6.1 Process Interpretation

The processes associated with the deposition of the S4 beds are similar to those associated with S3 beds: the initial phase of deposition was dominated by unidirectional flow and the latter stages were dominated by combined flow or oscillatory flow. These

beds are different from S3 beds in that: (1) parallel laminae are more common and form thicker divisions, (2) the thicker beds more commonly have gradational tops with thick fine-grained caps, and (3) these beds are thicker and more commonly amalgamated. The preponderance of parallel laminae indicates relatively prolonged deposition from currents in the upper flow regime (whether unidirectional, oscillatory or combined). The greater thickness of these beds may also have contributed to the preservability of the parallel laminae, most common in the lower divisions of these beds, in that late-stage reworking by waves may have been confined to the uppermost part of the newly deposited sediment. S4 beds with thick fine-grained caps must have been deposited in a setting or at a time when postdepositional reworking by oscillatory currents was at a minimum. Amalgamation of beds indicates either a short time span between the deposition of successive sand beds or more vigorous erosion associated with the emplacement of these sands, by which a greater amount of intervening siltstone was eroded.

4.7 GRADED RHYTHMITE (GR) BEDS

Graded rhythmites in the CIF contain the following sequence of structures: (1) a basal division (not always present) of fine sandstone with a sharply defined erosional lower surface and a sharp or gradational upper surface (essentially identical to an S2 or S3 bed) overlain by (2) fine siltstone (>50%) with coarse siltstone/very fine sandstone laminae (S1 laminae) that become thinner, more widely spaced and finer upward, followed by (3) smooth-weathering fine siltstone with only a few (if any) very thin and widely spaced S1-type laminae (Figure 4.7; Plate 5c,d). The thicknesses of the upper divisions are approximately 3-10 cm. The upward increase in spacing of laminae is a general trend; there are some vertical variations of the spacing and coarseness/thickness of laminae. Individual laminae are remarkably planar and extensive, with very little variation in thickness.

The soles of the basal sandstone divisions have erosional markings (grooves, prods, flutes) and trace fossils, while the upper surface may be flat or rippled. Directly above the lower division, the laminae in the central division mimic the underlying surface, and then lose their topography upward.

4.7.1 Process Interpretation

The upper division of the CIF graded rhythmites contain no evidence of tractional processes, while the lower divisions (when present) may contain such evidence, in the form of upper-plane-bed parallel lamination and ripple cross-lamination. The initial phase of deposition of some GR beds was therefore preceded by some tractional transport, while the upper divisions may have been deposited solely from suspension. This shift, and the overall size grading, are strong evidence for deposition under decelerating flow. When taken in the context of the underlying and overlying divisions, the upwardly thinning and

Figure 4.7: Schematic diagram of graded rhythmite beds showing erosional lower surface (+/- sole marks), lower sandstone division (+/- traction structures), middle division with upward increase in spacing of fine sand laminae within siltstone, and upper siltstone division. Details provided in text.

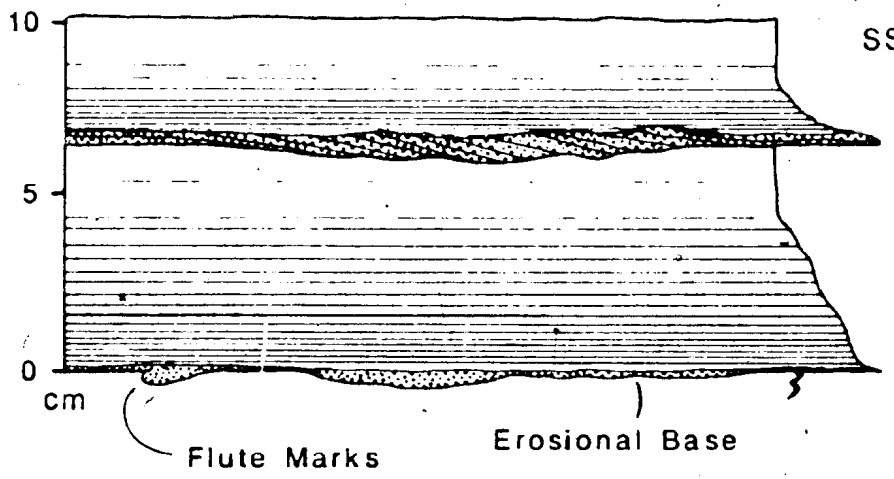

SSt w/ v. widely spaced, v. thin lam's

Ripple Cross-Laminations

SSt w/ cryptic lam's

Widely-Spaced Laminations

Closely-Spaced Laminations

Fine Sandstone Lower Division

fining laminae of the thick central division must also owe at least part of their character to decelerating flow conditions.

Graded rhythmites, described from both modern and ancient shallow marine facies, have been attributed to deposition from suspension clouds (Gadow and Reineck, 1969; Reineck and Singh, 1972; Dott and Bourgeois, 1982; Walzebuck, 1982). According to Reineck and Singh (1972), graded rhythmites are deposited from suspension during the waning stages of a storm. The settling of suspension clouds creates individual graded sand/silt laminae, which because of the weakness of the bottom currents are left unreworked as successive layers accumulate. The storm-generated rhythmites figured by Reineck and Singh (1972, Figure 2) are generally thicker and much less regular than those in GR Beds. Laminae produced by oscillatory flow are very irregular in general (De Raaf et al., 1977), while the laminae in these beds are planar, extensive, and of relatively even thickness.

Alternative explanations include storm-surge ebb currents, density currents, or either of these combined with oscillatory flow. It is unlikely that beds deposited from storm-surge ebb currents would differ greatly from those deposited from density currents. Ebb-surge currents on the Bering Shelf deposit beds that mimic Bouma turbidite sequences (Nelson, 1982). The role of oscillatory currents is difficult to evaluate. The laminae themselves show no evidence to suggest direct interaction of waves with the sediment, yet waves may have played an important part in maintaining sediment in suspension and regulating the rate of deposition from suspension.

4.8 CARBONATE-CEMENTED QUARTZITIC (Q) BEDS

These beds consist of medium- to very coarse-grained, white-weathering, carbonate-cemented, quartz arenitic sandstone beds (Plate 12a). Dark laminae, <1mm to

PLATE 12: Q-TYPE BEDS

a: These thin to medium Q-beds (arrows) include one anomalously thick bed at FD-86.4 (~20cm thick). Stratigraphic top is to upper left. Scale is 15 cm long.

b: Soft-sediment injections are illustrated in this close-up of FD-86.4. Note the 1 cm-wide vertical dike in center of photo. Thin sandstone sheets above the bed represent sills that spread out from these dikes. The sills tend to overlie depressions in the upper surface of this bed, further linking loss of sediment to injections above the bed. Stratigraphic top is up. Scale is 15 cm long.

c: Cross-laminated Q_b-type bed whose top surface was molded by waves into round-crested ripples (FD-225-226). Stratigraphic top is up. Scale is 15 cm long.

d: Irregularly-shaped wave-ripples are amalgamated to the top of this Q_b-type bed at FD-189.3. The amalgamation surface (arrow)is replaced laterally by a thin shale layer. In the lower part of the bed low-angle lamination pass upward into cross-lamination. A thin Q_a-type bed is located directly under the scale. Stratigraphic top is up. Scale is 10 cm long.

e: These symmetrical wave-ripples at FD-99.5 have rounded crests with variable heights (trough to crest). Note flat base to bed and small synaeresis cracks below crest on right. Stratigraphic top is up. Scale is 10 cm long.

f: Sharp-crested ripples (FD-260.1) with a thin division of grey fine sandstone above an ~2 cm-thick parallel laminated quartzitic division. In the center of the photo the quartzitic division has been completely eroded and a thin draping of fine sandstone covers the trough and the thin crest on the right. This bed formed as a graded bed that was reworked by waves into sharp-crested ripples. Stratigraphic top is up. Scale is 15 cm long.

g: This thin lenticular Q_a bed appears to be formed by the infilling of small, shallow scours. Stratigraphic top is up. Scale is 15 cm long.

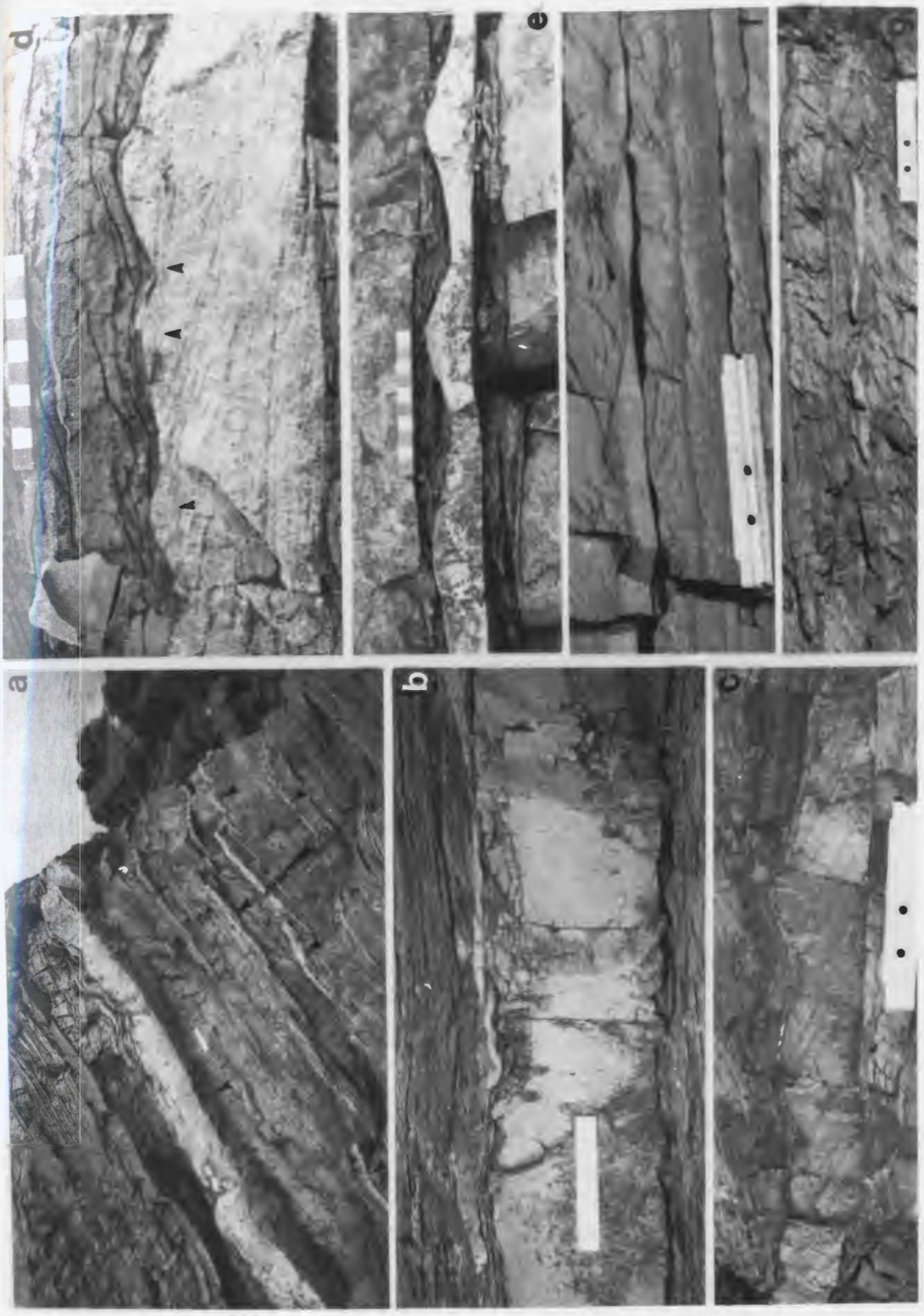
a
b
c
d
e
f

several millimeters thick (Plate 12d), are defined by, in addition to grain size variation and minor clay content, the concentration of chlorite patches that represent altered glauconite grains. These grains give the laminae a spotted appearance. On the fresh surface these grains are bright green.

S3 and S4 sandstone beds locally contain a thin basal division of this lithology, but these are not included in the following discussion. Beds that are dominantly (>50%) white, quartzitic sandstone but contain a thin graded top of gray sandstone (Plate 12f) will be included in this discussion. These beds can be divided into two types according to thickness; each is discussed below.

4.8.1 Laminae to Thin Beds: Q_a

Q-type beds less than 3 cm in thickness are defined as Q_a types. These beds typically pinch and swell, commonly to the point of being discontinuous over short distances. The majority of beds owe their discontinuity and thickness changes to infilling of shallow erosional scours (Plate 12g), while a small percentage are truncated from above. Thin, continuous laminae were also noted. Rare examples are slightly graded from coarse sandstone to medium/fine sandstone. Q_a beds are either devoid of internal sedimentary structures or are ripple cross-laminated. Ripple form sets range in character from small, starved, asymmetrical ripples to fairly continuous symmetrical ripples.

4.8.2 Thin to Medium Beds: Q_b

Q_b beds consist of conspicuous, thin to medium beds of white-weathering sandstone. These beds have both flat and irregular lower surfaces and gradational or sharp upper surfaces. Both lower and upper surfaces locally show evidence of erosion. The beds are usually extensive, but cases have been noted of both erosional truncation and

depositional pinch-out. Internally, these beds are structureless to slightly graded (coarse sandstone to medium/fine sandstone), parallel laminated or cross-laminated. Well developed symmetrical ripples (Plate 12c,e) and asymmetrical ripples were also noted (Plate 12d); these show significant changes in the size and geometry of adjacent crests (Plate 12c,d,e). Small gutter casts have been noted at the base of these beds, as well as small flame structures. One particularly thick sandstone bed (~20 cm) at FD-86.4 contains a transition from planar laminae to three-dimensional lenses. The upper part of this bed is irregular, and in places small vertical sandstone dikes, 1-2 cm wide, lead to sandstone lenses and sheets representing sills that spread out over a thin shale layer (Plate 12b). Some of the sandstone lenses above this bed show well developed cross-stratification and appear to be three-dimensional ripples that must have formed from reworking of these sills.

Cross-bedded units may contain a thin upper division of parallel laminae or small ripples. In some cases the upper surface of these cross-stratified beds appears to have been molded into ripples (Plate 12c). In Plate 12d an amalgamated bed is shown with a rippled upper layer; laterally these ripples separate from the underlying cross-bedded sandstone to form a distinct bed with an intervening thin shale bed.

4.8.3 Process Interpretation: Q Beds

Q beds are not just better sorted but also coarser grained than the beds with which they are interbedded, which means that they do not result solely from reworking and sorting of the available sediment, but rather from transport of sediment from adjacent areas. The depositional structures preserved in these beds record, for the most part, reworking of the sediment by waves.

Deposition of Q_a beds was often preceded or accompanied by erosion. Thin layers of quartzitic sand were spread out, dominantly by traction, to form thin beds and to fill in shallow, erosional scours. The sand was probably distributed by unidirectional currents

and then reworked by oscillatory currents into wave ripples — even the asymmetrical ripples have rounded crests and strong irregularities between crests. Starved ripples formed when the layer of sand undergoing traction transport was too thin to create a complete bedform. In these cases the current strength was either too low to transport enough sediment to the depositional site, or the amount of sediment available at the source was insufficient. The first scenario is more likely, given that Q_b beds can be found in close stratigraphic proximity.

Assuming an abundant source of sand, Qb beds formed under higher-energy conditions than Q_a, simply on the basis of bed thickness. The well sorted sand was transported by traction, forming parallel laminae and cross-laminae. Evidence for predepositional or syndepositional erosion of the substrate is found in some beds (gutter casts) and not in others (sharp, flat base). During the later stages of deposition or after the initial deposition, the sediment was reworked by oscillatory currents into large symmetrical two-dimensional and three-dimensional vortex ripples. Currents also scoured the upper surfaces of these beds, locally eroding through the entire thickness of the bed. Postdepositional features like flame structures and sand volcanoes formed as a result of postdepositional liquefaction.

4.9 THICK-BEDDED TO VERY-THICK-BEDDED FINE SANDSTONE BEDS: T

These beds consist of thick to very thick (up to 1.8 m), grey-green weathering sandstones that are dark gray to black on the fresh surface. These are exposed over a narrow stratigraphic range from FD-137.3 to FD-143.2 (Plate 28a,g) and at FD-168.2. In most cases these beds have amalgamation surfaces that break the beds up into divisions 10-50 cm thick. The lower and upper surfaces are commonly erosional, although not highly

irregular. The lower bedding surfaces truncate underlying bedding, and the upper surfaces cut down to different levels in the bed.

Most of these sandstone beds appear structureless. Two exceptions were noted: one in which the lower amalgamated division of one bed has horizontal laminae, and a second in which a lenticular, concave-up division at the top of one bed has cryptic cross-laminae.

4.9.1 Process Interpretation

In a fine-grained, thin-bedded sequence like the CIF, sandstone beds like these that are one to two orders of magnitude thicker than the surrounding beds are recording rare sedimentary environments or unusual conditions. Unfortunately there is a paucity of sedimentary structures, and to a large degree the weathering pattern has further concealed those structures that are present. It appears that the variation in thickness of these beds is primarily explained by infilling of an erosional depression. There is no evidence to indicate that these beds formed as lateral accretion deposits in a migrating channel (i.e., there are no thick cross-sets). These beds do contain amalgamation surfaces, indicating that deposition was in stages and that shale drapes may have separated the sandstone layers before erosion and deposition of sand, but the depositional processes remain enigmatic.

4.10 HUMMOCKY-CROSS-STRATIFIED BEDS: H

A summary of hummocky cross-stratification is given below. This is folowed by the description and process interpretation of H-Beds.

4.10.1 Summary/Process Interpretation: HCS

Hummocky cross-stratification (HCS) has received much attention from sedimentologists during the last ten years. The term was coined by Harms et al. (1975), but the structure was described earlier by Gilbert (1899), Campbell (1966) and Goldring and Bridges (1973). HCS has the following characteristics: (1) lower bounding surfaces are erosional and low-angle (<15°); (2) laminae are parallel or near-parallel to the lower surface; (3) laminae thicken laterally (usually into swales) within a set, with their dip diminishing upward; and (4) dip direction of laminae are scattered. In plan view, well preserved HCS beds show isolated, radially symmetrical mounds (hummocks) spaced 1-6 m apart (Duke, 1985). Beds may have prod and drag marks on their soles and wave ripples on their tops. Individual beds range from tens of centimeters to 5-6 m thick; most are 20-80 cm in thickness (Dott and Bourgeois, 1982). HCS is most commonly found in well sorted sediments of coarse silt to fine sand size; coarser grained exceptions exist (up to medium sand). According to Dott and Bourgeois (1982, p. 675) "The almost universal fine grain size of hummocky stratification must reflect efficient selective sorting of sand by suspension transport to the site of deposition".

Nearly all interpretations of HCS, including the early ones by Gilbert (1899), Campbell (1966) and Harms et al. (1975), emphasize the role of oscillatory currents. Purely unidirectional flows are generally ruled out due to the isotropic orientation of dipping laminae and the common association with wave ripples. Some workers (Harms et al., 1975; Dott and Bourgeois, 1982; Harms et al., 1982; Southard, 1984) interpret the

structure solely as a wave-generated bedform. Laboratory data from wave tanks and oscillatory flow ducts (Harms et al., 1982) show a distinct stability field for three-dimensional wave ripples between two-dimensional ripples and oscillatory-flow plane bed. These three-dimensional wave ripples look similar in plan to bed-surface geometries observed in HCS, and they become less steep and more rounded with increasing maximum orbital speed (Um) (Southard, 1984). Peak velocities would be greater than that necessary for the formation of regular, straight-crested wave ripples: 0.5 m/s or more (Harms et al., 1975). It is not known, however, whether such three-dimensional vortex ripples in regular oscillatory flow figure in the generation of HCS observed in the sedimentary record. Southard (pers. comm.) feels that many if not most styles of HCS are formed from large three-dimensional bedforms deposited under conditions of complex rather than regular oscillatory flow, of the kind that must be felt by the sediment bed under complex sea states during passage of large storms. Confirmation of this hypothesis by laboratory experiments or systematic observations in shelf settings is lacking.

Dott and Bourgeois (1982, p. 667) believe that "...Hummocky cross-stratification is the result of a combination of fallout and the molding of stationary hummocks and swales by flow induced by vigorous but waning wave oscillation as sand falls onto the smooth but undulating bed". They envision a zone of intense oscillatory flow near the bed where the HCS bedform is produced by deposition occurring near the boundary between the oscillatory lower rippled field and upper flat bed conditions (sheet flow).

The most widely held view is that HCS has a combined-flow origin (Allen and Pound, 1984; P. Allen, 1985; Greenwood, 1984; Greenwood and Sherman, 1986; Hunter and Clifton, 1982; Swift et al., 1983; Swift, 1984; Nottvedt and Kreisa, 1987). Swift et al. (1983) outline the hydraulic conditions responsible for bedforms on the Atlantic shelf that they call 'hummocky megaripples'. These bedforms are thought to form by combined flow in which there is an angular relationship between the unidirectional flow component and the wave-orbital component, or by multiple orientations of the latter. Allen (1985) argues on

theoretical grounds that given the observed wavelengths of HCS, an origin by progressive gravity waves is incompatible with the possible values of a/L under waves (a=amplitude of oscillations, L=wavelength of bedform), and suggests that a unidirectional component is necessary to explain the hummock spacing. This must be regarded speculatively, given the paucity of empirical data on complex oscillatory flows. If most HCS shows no strong preferred migration direction then this would argue strongly against combined flow with an appreciable unidirectional component.

Greenwood and Sherman (1986) provide the first verifiable, albeit limited (0.45 m x 0.30 m epoxy peels of box cores), description of HCS in recent sediments. Their data suggest that some HCS is a combined-flow bedform deposited under conditions close to those of upper plane bed. During deposition of their hummocky sands, oscillatory currents were dominant, with velocities greater than 1 m/s, while the unidirectional component was measured at 0.27 m/s. Deposition was triggered by sharp reductions in both unidirectional flow velocity (67%) and orbital velocity (19%); "...Since transport is proportional to the third power of the velocity, then rapid changes in sediment load accompany relatively small changes in orbital velocity" (Greenwood and Sherman, 1986, p. 40).

Walker and his students (Hamblin and Walker, 1979; Wright and Walker, 1981; Leckie and Walker, 1982; Walker, 1979,1982,1984) maintain that HCS beds are emplaced by turbidites. This is based on the fact that HCS beds have: (1) sharp lower surfaces without tractional structures, and (2) sole mark orientations that are consistent with stratigraphically adjacent turbidite sandstones. The sand is thought to be worked by waves during deposition from the turbidity current.

Laminae in HCS tend to conform to underlying scour surfaces, with individual laminae draping both swales and adjacent hummocks. An upward flattening of laminae within swales results from a general thickening of laminae towards the swale center, and the fact that the lowermost laminae in a swale may terminate against the margins tangentially (Hunter and Clifton, 1982, p. 132). Hunter and Clifton (1982) suggest that

these lamination styles indicate a combination of scour-and-drape and vertical growth of hummocks. Dott and Bourgeois (1982, p. 677), Bourgeois (1984), and Bourgeois and Smith (1984) consider HCS solely as a scour-and-drape structure. Brenchley (1985) and Brenchley and Newell (1982) describe examples in which laminae thicken over crests, and the general geometry indicates accretion instead of infilling of a hummocky surface. At a recent symposium (CSPG, 1984, Calgary) P. Allen postulated that HCS was polygenetic, with three types of lamination: (1) scour and drape, (2) vertically accreted or upbuilt and (3) tangential (laterally accreted from crests). It would appear from published accounts of HCS that many authors consider the first of these styles to be dominant. Observations by the author and J. Southard on the Late Precambrian Johnnie Formation in southeastern California indicate that in many cases laminae that appear to have formed from scour and drape can be shown to have been formed from migrating three-dimensional bedforms.

Hunter and Clifton (1982) and Dott and Bourgeois (1982) note that, in some cases, internal scour surfaces die out laterally into conformable, depositional, flat-lying laminae. Similar relationships have been noted by the author in sandstone beds from the Ordovician Beach Formation of Bell Island, Newfoundland and from numerous beds in the upper Proterozoic Johnnie and Wood Canyon Formations in Nevada and California. Such a relationship indicates that both erosion and deposition occurred simultaneously. This could be modelled as deposition from a stationary hummock that is increasing its amplitude under conditions of low to moderate aggradation rate, or from migration of a hummock under similar conditions.

Nottvedt and Kreisa (1987) suggest deposition from migrating bedforms, but they emphasize 'directional' aspects of HCS such as subtle downlaps and onlaps, and question the validity of the measurements and observations that support a truly three-dimensional geometry. Nottvedt and Kreisa believe that HCS is formed from an equilibrium bedform — a low-relief megaripple — whose migration creates a low-angle variety of trough cross-bedding that geologists call HCS. It seems likely that there is a complete spectrum from

purely oscillatory bedforms to purely unidirectional bedforms and that workers are approaching the study of these intermediate bedforms from different perspectives.

4.10.2 Description of H-Beds

These beds consist of medium beds of fine and very fine sandstone that are either hummocky (with meter-scale spacings) in their overall geometry, or display stratification similar to that described for hummocky cross-stratification (HCS), or both. About half of these beds are discontinuous across the outcrop exposure. In addition, many of those that are continuous change significantly in thickness or internal structure laterally. These beds may contain amalgamation surfaces, usually with the hummocky-cross-stratified sandstone truncating an underlying unit of structureless to parallel-laminated sandstone. The tops of H beds are marked by erosional truncation surfaces or by symmetrical ripples (Plate 14e). The lower surfaces are either very irregular or planar.

Convex-up hummocks and concave-up swales contain curved laminae that both dip, and intersect, at low angles (<20 degrees). Beds may be entirely composed of truncated swales without any hummocks, although many of the beds in this facies do display well defined hummocks (Plate 13b,c,d, 14b). At FD there are several discontinuous beds showing amalgamation with underlying sandstones. Well developed sandstone hummocks are spaced several meters apart. The hummocks are thickest above the deepest level of erosion into the underlying sandstone as seen in Figure 4.8, a sketch of FD-367.2 (Plate 13a,b). This bed displays: (1) complete erosion of the underlying bed under the main part of the hummock, (2) lenticularity of the hummocky-cross-stratified sandstone, (3) a relationship by which the sandstone hummocks are located above erosional depressions in the underlying sandstone bed, and (4) large symmetrical ripples on the upper surface. Many of these features are also displayed by FD-367.7, shown in Figure 4.9a (Plate 13d, 14b). This bed has symmetrical to slightly asymmetrical climbing ripples

PLATE 13: H-BEDS (FA 2)

a: A detailed sketch of this hummocky bed from FD-367.2 (stratigraphic top to left) is given in Figure 4.8. Note hummocky geometry next to notebook and erosional lower surface that locally defines a surface of amalgamation with an underlying sandstone bed. Notebook is 18.5 cm long.

b: Close-up view of "a" (stratigraphic top to left) showing hummocky internal structure, lower amalgamation surface (arrows) and symmetrical ripples on the upper surface near the top of the photo. Notebook is 18.5 cm long.

c: Completely isolated lenticular sandstone hummock with convex-up lamination at FD-367.2 (not on Figure 4.8). This bed (stratigraphic top to left) demonstrates complete erosional truncation of an underlying sandstone bed directly underneath a hummock. Notebook is 18.5 cm long.

d: Hummocky sandstone bed at FD-367.7 (stratigraphic top to right). Diagram of this bed is given in Figure 4.9. Bed pinches out at the top of photo and off photo at the bottom. Erosional lower surface truncates underlying sandstone bed (arrow). Symmetrical ripples cover top of bed in foreground. Scale is 15 cm long.

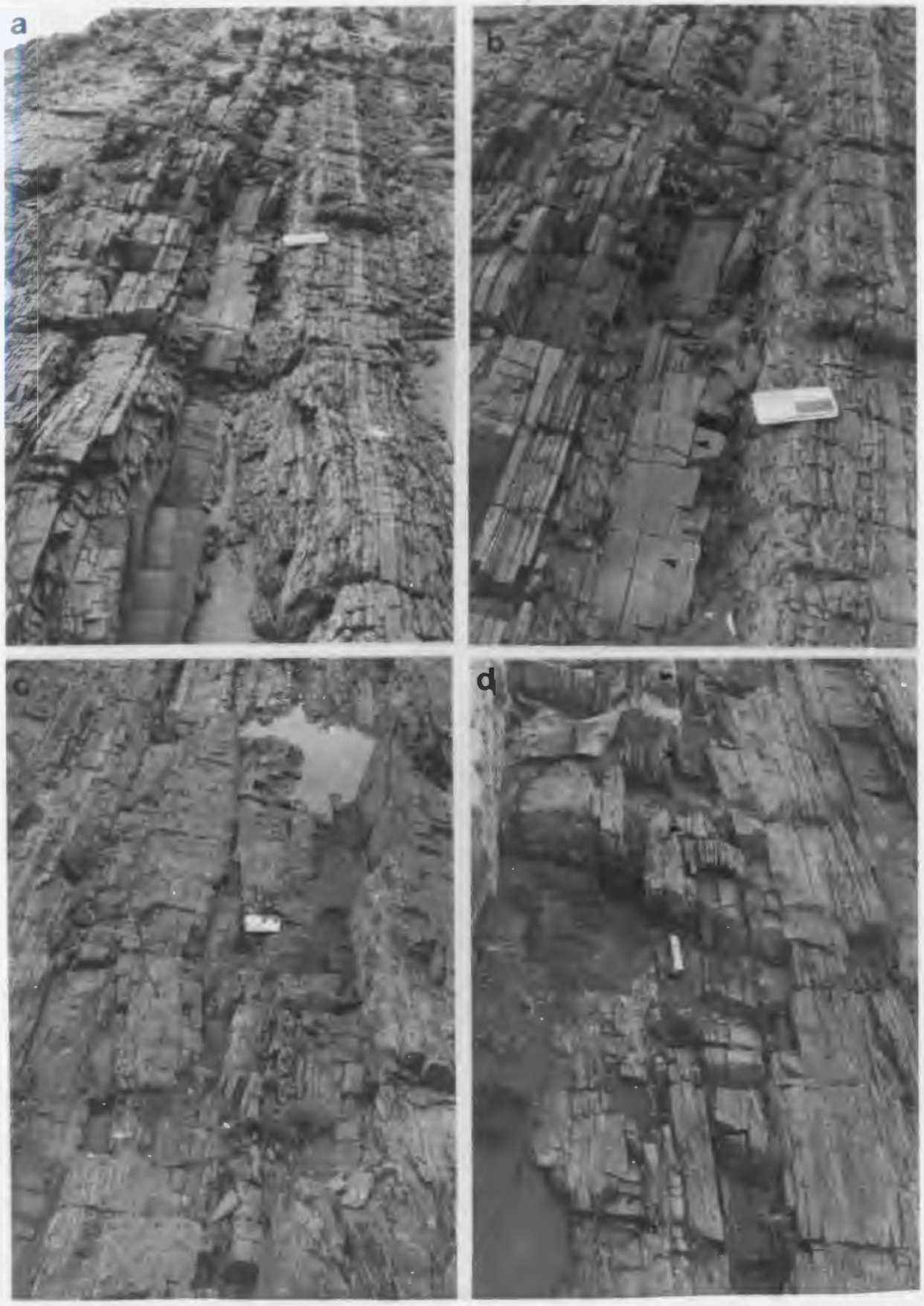
a
b
c
d

PLATE 14: H-BEDS CONT'D (FA 2)

a: Hummock with low-angle concave-up lamination at FD-367.2 (not on Figure 4.8). Note erosional lower amalgamation surface (arrow). Stratigraphic top is to upper right. Scale is 10 cm long.

b: Close-up of FD-367.7 showing convex-up lamination and low-angle internal scour surfaces. Stratigraphic top is up. Scale is 15 cm long.

c: Depositional(?) termination of an H-bed at FD-251.65. Base of bed essentially flat-lying. Stratigraphic top is up (bedding actually dipping near-vertical). Notebook is 18.5 cm long.

d: Close-up of FD-251.65 showing convex-up lamination that flatten out laterally across hummock. Stratigraphic top is up. Notebook is 18.5 cm long.

e: Symmetrical ripples at top of H-bed at FD-367.5. Nearly flat-lying laminae beginning to define hummock at right side of photo. Stratigraphic top is up. Scale is 10 cm long.

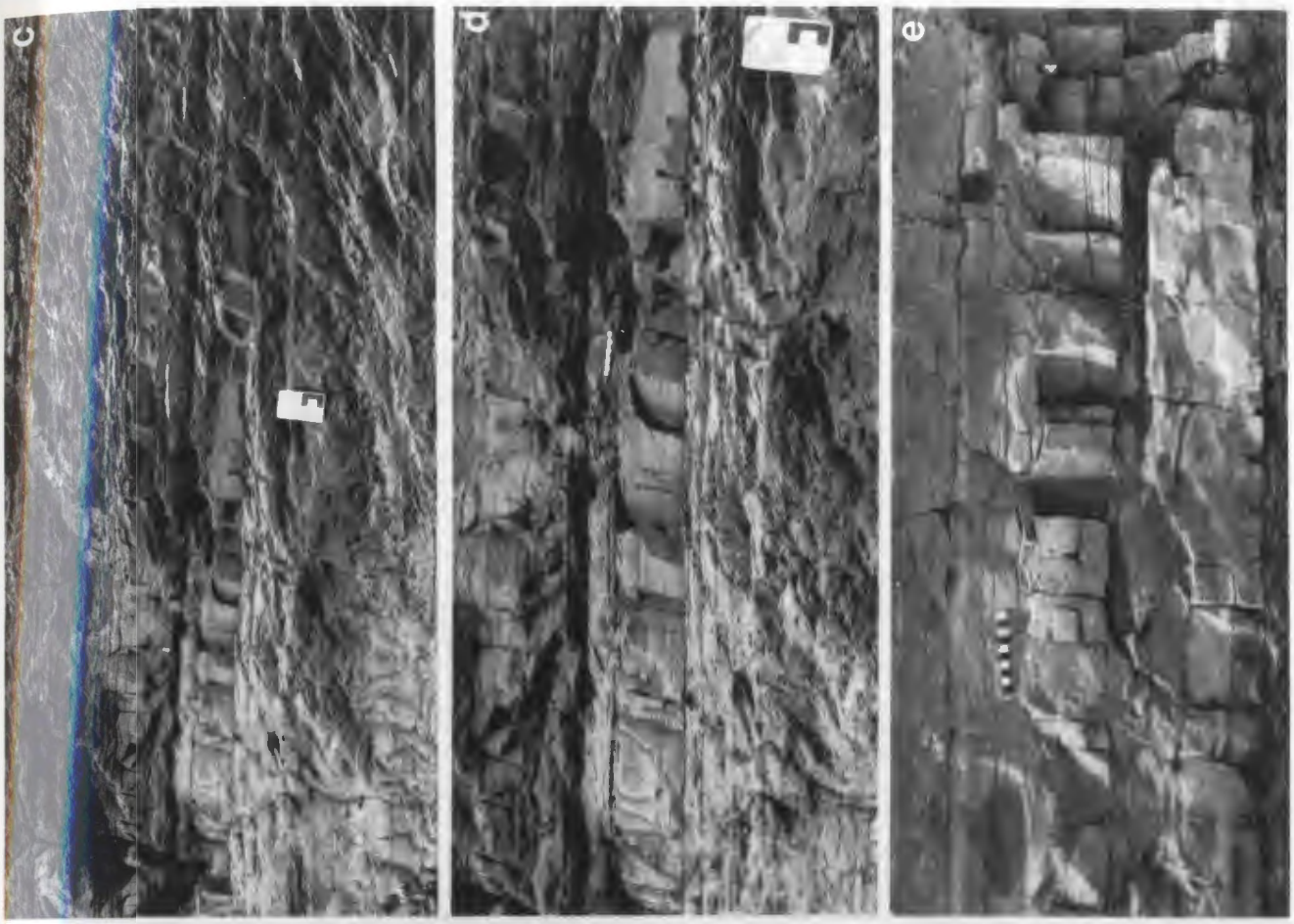
c
b
e

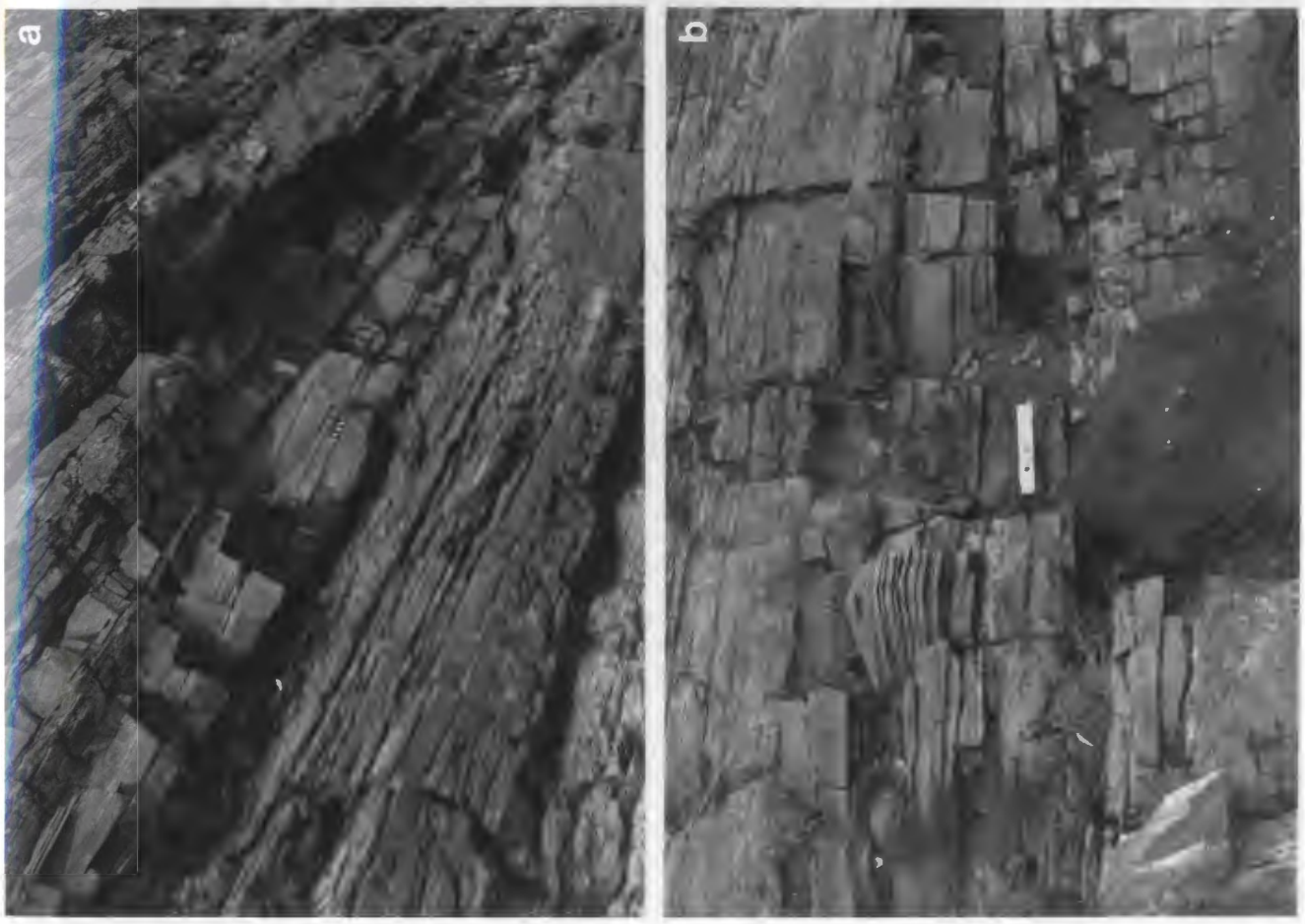
a
b

Figure 4.8: Sketch of H-Bed at 367.2. Full bed shown on top, and close-up of bed shown in two lower panels. See text for details.

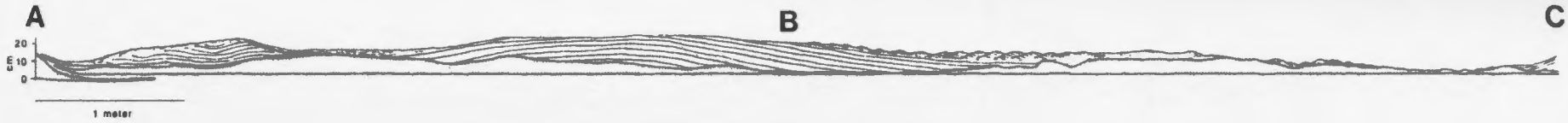
A
B
C
20
10
0
cm
1 meter

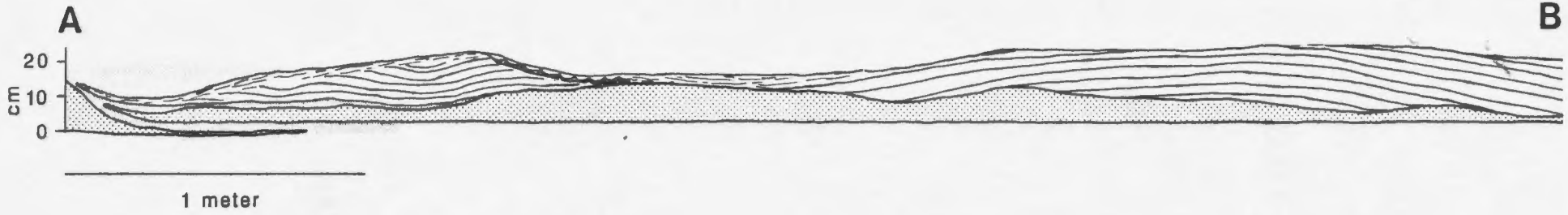
A
B
20
10
0
cm
1 meter

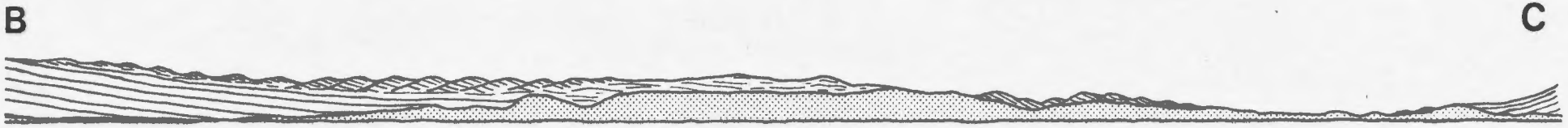
B
C

on the flanks of a hummock. Spillover lobes (see Seilacher, 1982) associated with unidirectionally cross-laminated symmetrical ripples were noted at the top of an H bed at FD-238.95 (Figure 4.9b). It is interesting to note that the lobes are spread out opposite to the direction of dip of the cross-laminae.

One discontinuous H bed at FD-251.65 has a planar base and no evidence of erosion at its upper surface (Plate 14c,d). In this case the bed consists of unidirectionally oriented very-low-angle cross-lamination. The bed pinches out in the same direction that the laminae dip, without indication of erosion of these laminae from above.

4.10.3 Process Interpretation of H-Beds

H-beds show most of the features normally associated with typical HCS, including wave-rippled tops. Spillover lobes, found at the top of FD-238.95, are also indicative of wave reworking. Planar-based beds indicate relatively little scouring of the underlying surface prior to deposition. H-beds with lower amalgamation surfaces have indications that as much as 10 cm of sand was eroded from the underlying layer (Figures. 4.9a, 4.8). These beds are thickest, with well developed hummocks, where much or all of the underlying layer is eroded. From Figures 4.9a and 4.8, one can see that the upward-doming lenses of sand must have had considerable relief above the sea bed. The curious position of the hummocks above the erosional depressions can be explained in a number of ways. Firstly, it is possible that the position of the hummocks over erosional depressions is entirely coincidental, and that with a statistically significant number of observations (a greater number of exposed examples), no correlation might exist. A second alternative is that the irregular erosional topography was sculpted by the same flow conditions that affected the overlying bedform, and that the shift from an erosional depression to a hummock of sand reflects a simple shift in the spatial position of hummocks and swales with time. The author has seen numerous examples of HCS in the rock record containing

Figure 4.9:

(A) Sketch of H-bed at FD-367.7. Note amalgamation surface and the development of the hummock over the erosional low.

(B) Sketch of H-bed at FD-238.95. Laminae in this bed dip at a low angle and contain subtle truncation surfaces. There are no well developed convex-up surfaces (>5 m lateral exposure) and the laminae have an apparent dip towards the northwest. Symmetrical ripples at top of this bed show similar apparent dip of cross-lamination. Spillover lobes associated with these ripples indicate movement of sand in a direction opposite to the underlying cross-lamination.

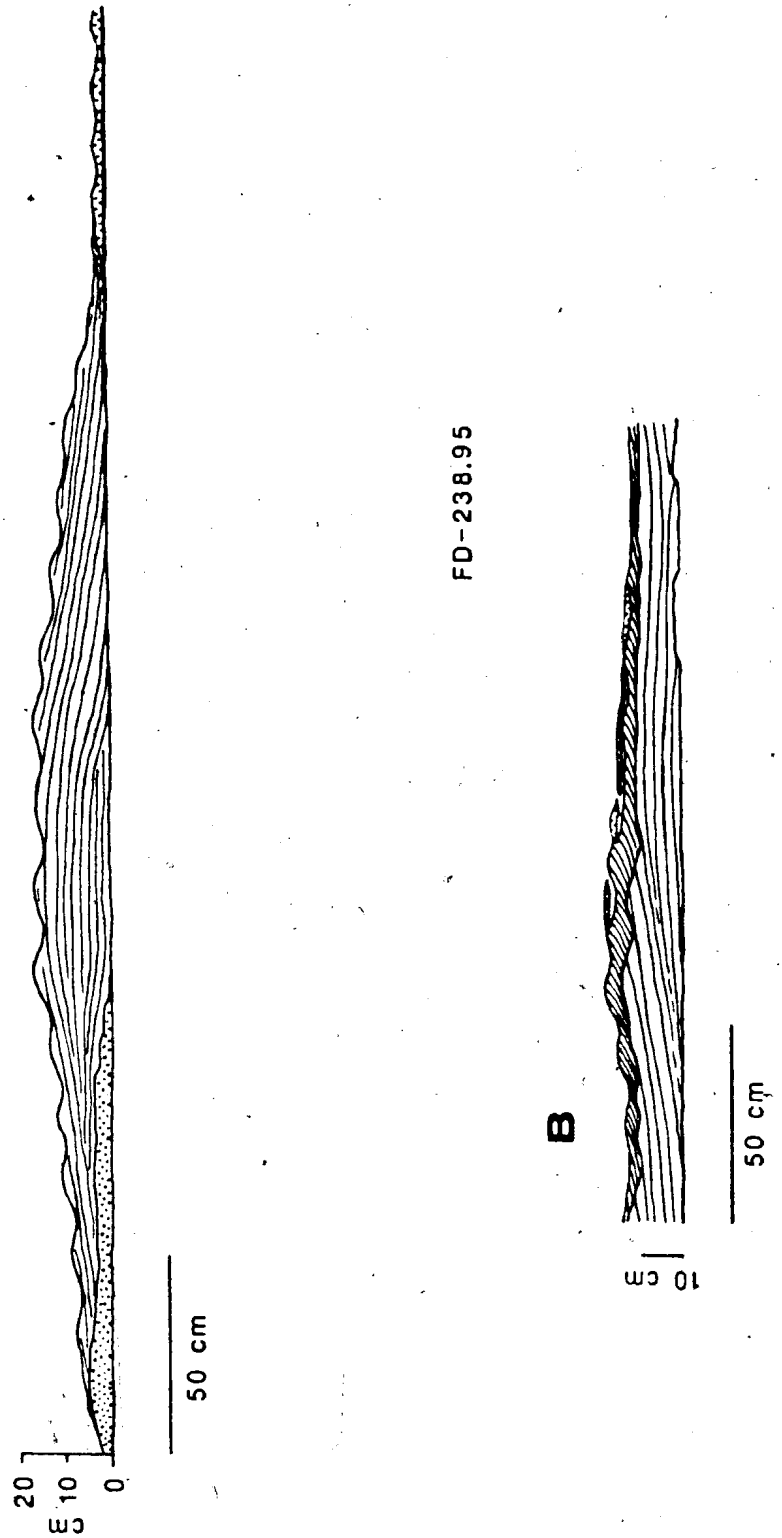
A
FD-367.7
20
10
0
cm
50 cm
B
FD-238.95
10 cm
50 cm

evidence for the shifting of hummocky bedforms with time and the vertical transitions from hummock to swales and vice versa. Reasons for a shift in bedform position with time would be numerous in both oscillatory and combined flow (e.g., shift of wind direction, change in orbital diameter or amplitude of oscillations during waning flow, variation in oscillatory asymmetry, shift in a unidirectional component due to Coriolis effects).

The discontinuous nature of most of these H beds is a reflection of the original depositional geometry of the bed, and not later erosion of the upper surface. The spacing of the bedform in the bed at FD-367.7 (Figure 4.9a) is on the order of 3-4 m, and thicknesses of this bed and the one at FD-367.2 (Figure 4.8) are approximately 15-20 cm. In summarizing the attributes of HCS, Walker (1982) suggests that typical spacings are 1-5 m, and typical heights, swale to hummock, are 20-40 cm. It is therefore apparent that these CIF beds, whose spacings are typical of most HCS (possibly even larger than average), have thicknesses that are smaller than the lowest suggested heights of these bedforms. Keeping in mind that the underlying substrate was not sand, but difficult-to-erode muddy siltstone, the discontinuity of the CIF beds is believed to result from deposition under conditions (long wave periods and large orbital diameters) that would have been capable of generating large, continuous HCS beds, but due to insufficient sediment supply, the construction of full-size equilibrium bedforms was not possible. By analogy with bedforms formed under unidirectional flow, these beds will be referred to as 'starved HCS'. The excellent preservation of hummocks and the lack of complete swales is not just unusual, but essentially the reverse of what is normally found in the rock record (Dott and Bourgeois, 1982). Little or no documentation exists for large-scale starved HCS features like these in the CIF. The closest analog would be the 'micro-hummocky lenses' of Dott and Bourgeois (1982; p. 678). These consist of small sandstone lenses in shale, with features 'suggestive' of HCS, which they also compare to starved ripples.

4.11 LOW-ANGLE CROSS-STRATIFIED SANDSTONE BEDS

The following description concerns one bed, exposed at FD-332.95 (Plate 15). This bed has, in two-dimensional cross section, a plateau-and-trough shape, with the bed thickness ranging from 0.4-17 cm. The 'plateaus' are very broad (several meters), with little surface relief (almost flat), while the troughs are much narrower, and are symmetrical in cross section. The symmetrical nature of the troughs on both northeast-southwest and northwest-southeast exposure faces indicates that these may take the shape of circular basins in three dimensions. The thickness of the bed in the troughs ranges from 0.4 to 4 cm. The troughs are spaced approximately 5 m apart. The widths of the troughs are 1.5 to 2 m. A detailed drawing of the salient features of this bed is given in Figure 4.10.

The internal structure of this bed is unique in that it contains very-low-angle laminae with a consistent dip towards the northeast (restored downdip direction of forsets is 059°). There are no internal truncation surfaces, and the laminae are remarkably uniform and quite planar (Plate 15d,e). Individual laminae, when traced from the base to the top of the bed across a hummock, extend for 2.6 meters horizontal distance, recording an apparent dip of 2.8°. True dip of the laminae, restored for dip of bedding, is 8°, much lower than angle of repose for sand in water — about 34 degrees (Pettijohn et al., 1973). The upper surface of this bed is generally flat to slightly undulating. The eastern limb of one trough is molded into large, irregular ripples (Plate 15c). Interestingly, small symmetrical ripples are found along a lamina for ~30 cm near the top of the bed (Plate 15e). In the axis of another trough the laminae terminate against a smooth, sharp, curved surface that is overlain by 1-2 cm of draping laminae, followed by small, straight-crested, symmetrical ripples whose crests parallel the long axis of the trough (Figure 4.10, Plate 15a,b). On the western limb the draping laminae parallel the underlying laminae, while on the eastern limb there is sharp discordance with the underlying laminae.

Figure 4.10: Low-angle cross-stratified bed at FD-332.95. Enlargement on left shows features in the swale. Enlargement on right show the extensive planar lamination. Further blow-up shows the presence of small wave ripples at the top of the bed and the upper reaches of one lamina.

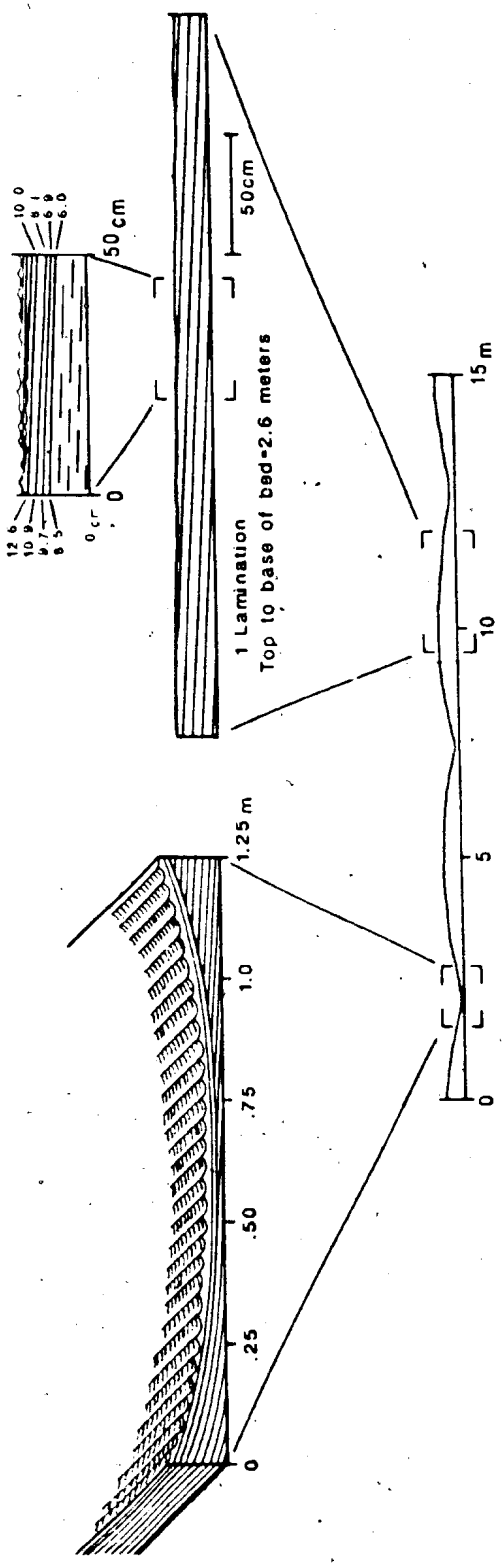
50cm
50 cm
1 Lamination
Top to base of bed=2.6 meters
15 m
10
5
0
1.25 m
1.0
.75
.50
.25
0

PLATE 15: LOW-ANGLE CROSS-STRATIFIED BED AT FD-332.95 (FIGURE 4.10)

a: Close-up of "b" showing draping lamination and symmetrical ripples as shown in Figure 4.10. Stratigraphic top is up. Scale is 10 cm long.

b: Upcurrent (western) limb of one swale. Note that the upper surface of in this bed is parallel to the internal lamination. Stratigraphic top is to upper left. Notebook is 18.5 cm long.

c: Broad shallow 'swale' with evidence for remolding of the upper surface of bed on the right (eastern) side of swale into large symmetrical ripples. Stratigraphic top is up. Notebook is 18.5 cm long.

d: The internal structure of this bed is one of low-angle cross-stratification that is remarkably planar and uniform. Stratigraphic top is up. Scale is 15 cm long.

e: Close-up of "d" demonstrates the planar nature of the laminae, even at the base of the bed where they do not appear to become asymptotic to the lower surface. Note symmetrical ripples on upper surface and small symmetrical ripples below scale along one lamina (see text and Figure 4.10). Stratigraphic top is up. Scale is 10 cm long.

C

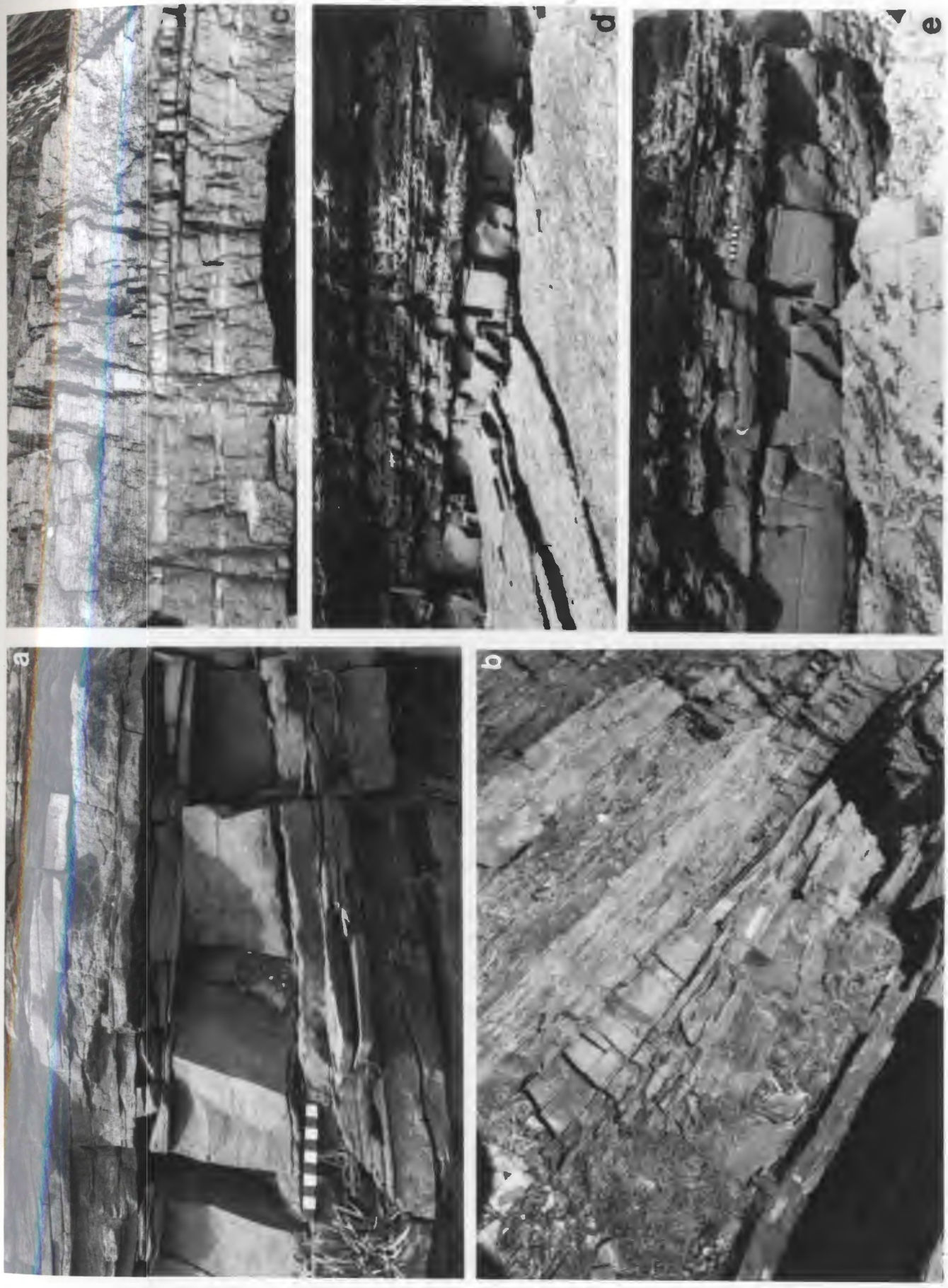
a
b
c
d
e

4.11.1 Process Interpretation

The laminae in FD-332.95, which (1) were deposited at an angle much lower that than angle of repose, (2) contain no internal truncations, and (3) are relatively planar, are most reminiscent of beach laminae formed from swash-backwash processes. The dip of the laminae in this bed is in the range reported for beach laminae, which are generally characterized by long lateral extent and even and regular thickness of laminae (Reineck and Singh, 1980, p. 107). Beach laminae usually contain planar internal truncation surfaces (see Thompson, 1937, Figure 2). Objections to a beach origin for these laminae, in addition to the lack of emergence features in the surrounding beds, include: (1) the overall bed geometry, which is similar in some respects to HCS, and (2) the clear evidence of erosion on 'downcurrent' sides of the troughs (downdip direction of laminae), and the conformable laminae on the upcurrent sides (roughly the same angle of dip as the laminae). These data suggest migration of a low-relief hummocky bedform under conditions of little or no aggradation.

The migrating bedform would likely have had a slightly higher amplitude, but postdepositional erosion of the ridges reduced the original topography. Wave ripples, formed mainly in the troughs, implicate oscillatory currents in the deposition of the underlying bed, and suggest that, as with 'typical' HCS, the upper surface layer of sand was reworked into ripples as the orbital velocity decreased during the latter stages of deposition. The small wave ripples on the upper part of the one lamina must have formed during a short break in deposition when the orbital velocity temporarily dropped into the ripple field. Later migration of the bedform buried the partly rippled slipface to preserve it as a lamina within the bed.

Nottvedt and Kreisa (1987) attribute HCS with asymmetry in both external geometry and internal structure (the dips of laminae are nonisotropic) to deposition from

migrating low-relief megaripples. The HCS beds that these authors describe also contain convex-up surfaces (preservation of stoss and lee sides), and were therefore formed by climbing bedforms (internal truncation surfaces dip upstream in the same manner as erosional-stoss climbing-ripples, but these climb at a higher angle than the stoss side of the bedform, preserving stoss laminae). The lack of internal truncation surfaces (form-concordance) in FD-332.95 is remarkable when one considers that beds with very-low-angle stratification — from wave-ripple laminae to HCS — are characterized by abundant internal truncation surfaces. 'Typical' HCS, as well as the most highly asymmetric forms described by Nottvedt and Kreisa (1987), contain low-angle truncation surfaces formed under strong oscillatory flow. In the case of FD-332.95, the lack of these scour-and-drape surfaces, the lack of convex-up (stoss) surfaces, and the planarity of the laminae is enigmatic. Some of this may be rationalized in terms of deposition under negligible aggradation rates. The preservation of the stoss sides of bedforms, whether they be climbing-ripples or HCS, is attributable to a high ratio of aggradation rate to migration rate. Migration of this hummocky bedform well past the time of deposition could explain the lack of stoss surfaces and internal truncations, assuming they were present initially. The planarity and regularity of the laminae are still particularly disturbing.

There is at present no agreement as to whether HCS is an oscillatory or a combined-flow structure, although the latter appears to have more support in the literature (see Section 4.10.1). One must question if FD-332.95, and for that matter the beds described by Nottvedt and Kreisa, might have been formed by asymmetrical oscillatory flow. Unidirectionally cross-laminated ripples (and climbing-ripple laminae) have been produced in flumes under asymmetrical oscillatory flow (Reineck, 1961; McKee, 1965) and are the most common types of small-scale oscillatory ripple structures in the rock record (Harms et al., 1982, p. 3-28). These smaller-scale structures are different in fundamental ways from FD-332.95, but the analogy is presented to indicate that purely oscillatory flow should not be ruled out.

4.12 THIN PEBBLE CONGLOMERATE (PC) BEDS

These beds consist of thin, lenticular, very coarse sandstone to pebble conglomerate, with varying proportions of finer-grained, well sorted sandstone. These coarse-grained sediments are found: (1) as thin laminae (minimum of 1-2 grains thick) to very thin beds within siltstone, (2) at the base of thick laminae/very thin graded beds, (3) along cross-laminae or gently undulating parting (amalgamation) surfaces within beds, (4) on the top surfaces of sandstone beds and (5) within small, lenticular, concave-up beds (Plate 16d). The conglomerates are dominated by quartz and volcanic clasts, with a small to moderate percentage of shale clasts or siltstone/mudstone intraclasts. These thin layers are highly discontinuous, but are generally extensive at any particular horizon at the outcrop scale.

There are several examples in which a thin layer of pebble- or granule-sized grains cover an upper bedding surface. At FD-34.9, sub-rounded quartz grains up to 4 cm in diameter overlie a thin, clean, coarse/very coarse sandstone bed. Plate 16e shows low-angle, cross-laminated, granule-bearing, coarse/very coarse sandstone that directly overlies a fine sandstone bed 1-2.5 cm thick at FD-342.05. Quartz granules are concentrated along foresets in this bed. The coarse sediment has a mounded top and thins rapidly. A few examples were noted in which isolated pebbles were floating within wave-ripple-laminated sandstone beds.

Small, thin lenses of conglomerate may contain remarkably coarse sediment. A pod of coarse/very coarse sandstone at FD-58.15 is less than 1 cm thick and only 6-7 cm long, yet contains a well rounded quartz clast nearly 2 cm in diameter on its upper surface.

PLATE 16: CONGLOMERATES (FA 2)

a: Bedding plane view of flat-pebble conglomerate at FD-162.8. Note grey siltstone clasts and darker phosphatic shale clasts. Scale is 15 cm long.

b: Cross-sectional view of pod of flat-pebble conglomerate at FD-158.7. Stratigraphic top is up. Scale is 10 cm long.

c: Slabbed surface of flat-pebble conglomerate from FD-158.7. Note irregular very thin clayey siltstone bed and similarity in color and texture to some clasts. Stratigraphic top is up. Scale is 1 cm long.

d: Discontinuous lamina of granule conglomerate with erosional lower surface at FD-341.3. Stratigraphic top is up. Scale is 10 cm long.

e: This lenticular granule-bearing coarse/very coarse sandstone at FD-342.05 directly overlies a thin fine sandstone bed. Note concentration of granules along low-angle cross-laminae. Stratigraphic top is up. Scale is 10 cm long.

f: Outcrop view of Pebbly mudstone at FD-48.45 . Note clast-rich lower division and thicker overlying division with scattered small clasts. Stratigraphic top is up. Scale is in cm.

g: In this polished slab of "f", the contact between the lower clast-bearing division and upper claystone division is very sharp (arrows). The three parts of the lower division are clearly visible: 'A' sandstone laminae (arrow at base of bed), 'B' laminated silt/clay with large clasts, and 'C' clast-rich silty mudstone. The lower division is normally graded in terms of maximum clast size and reverse-to-normally graded in terms of average grain size. Note flat to low-angle lamination within the clast-rich lower division that are defined, in part, by elongate shale clasts. Stratigraphic top is up. Scale is 1 cm long.


b
c
a
d
A
B
C
B
A
B

4.12.1 Process Interpretation

In a facies association dominated by siltstone and sandstone, the presence of coarser-grained sediments point to special conditions. In marine sequences, thin beds of these types are commonly interpreted as lag or condensation deposits. Brenner and Davies (1973) distinguish between 'swell lags' and 'storm lags'. Swell lags are formed in situ by repeated cycles of disruption and gravity settling of sediment that result from pressure gradients associated with high-amplitude ocean swells. Storm lags are gravels that are transported during storms through channels and laterally spread out into sheets. The almost complete lack of scattered coarse-grained sediment in the siltstones and sandstones with which these beds are interbedded clearly indicates lateral transport of this coarse-grained sediment. Transport was often by traction, as attested by granules/pebbles resting on low-angle cross-laminae. The association of pebbles with wave-ripple laminae indicates transport by strong oscillatory currents, probably associated with storms. When found at the tops of beds, pebble layers are diagnostic of storms (Levell, 1980b).

The extensive (albeit discontinuous) nature of many PC beds may have an analog in pebble layers described from a number of ancient sequences (Anderton, 1976; Brenner and Davies, 1973; Johnson, 1977; Levell, 1980a, 1980b; McCave, 1973). Well sorted sheetlike pebble beds are considered by McCave (1973) to be diagnostic of wave action.

Levell (1980a) presents a model for granule/pebble lags found at the top of sheet sandstones in Late Precambrian rocks from Finnmark, Norway. These lags are formed by winnowing of gravel-bearing sand, which implies conditions in which the rate of erosion exceeds the rate of deposition. Most of the lags described by Levell have evidence of transport — some are cross-bedded. The concentration of coarse-grained sediment is attributed to currents, waves/storms or a combination. Lags may form in situ by storm waves or in the scour pits of migrating megaripples under the influence of strong currents.

During storms these megaripples may be reworked, further winnowing and concentrating gravel-sized sediment.

The PC Beds, being significantly coarser grained than the lithologies with which they occur, were likely transported some distance by storm currents and then, in cases, reworked by waves. In many cases, these lags were deposited in depressions that were likely created by erosion just prior to their deposition. It is unlikely that these lags developed in the scour pits of migrating megaripples, given the internal structure and thinness of the sandstone beds with which they are interbedded.

4.13 FLAT PEBBLE CONGLOMERATE BEDS

Flat pebble conglomerates occur at several levels within the FD and SI outcrops. The bases of these beds are very sharp, and they rest almost exclusively on fine-grained beds. Their fabric is one of grain support, with a variable quantity of clean, coarse and very coarse sandstone matrix (Plate 16b,c).

Nearly all clasts are of two types: (1) black shale clasts that weather with a blue tint (revealing their phosphatic nature), and (2) gray to green siltstone to mudstone clasts. These clasts occur in subequal proportions. Brown-weathering sandstone clasts and white quartzite pebbles were also noted in beds at Sagona Island.

The thickness of the conglomeratic beds varies significantly over short distances. Over the length of an outcrop these beds are often discontinuous. These include thin lensoid beds (Plate 16b), with erosional concave-up lower surfaces, that range in length from a few centimeters to 70 cm. On a small scale, beds may have mounded upper surfaces, with local near-vertical imbrication in the upper parts of the bed. Flat-pebble conglomerate is also found in the lower parts of sandstone beds. At FD-161.1, the lowest centimeter of a 3 cm thick, parallel-laminated fine sandstone bed is conglomeratic. The

lower bedding surface is planar, and the conglomerate pinches out laterally, with the laminae in the overlying sandstone draping over the conglomeratic division.

Locally, conglomerate is complexly interbedded with thin siltstone/mudstone layers. Lenticularity of the different lithologies makes it difficult, in some slabs cut from large rock samples, to distinguish between thin siltstone layers and long siltstone clasts (Plate 16c).

Both the siltstone clasts and the phosphatic shale clasts show evidence of partial to complete replacement by amoeboid patches of neomorphic sparry calcite crystals up to 2.5 mm in diameter. The siltstone/mudstone clasts are replaced more often, and more thoroughly, in this way than the black shale clasts. The pseudospar is light colored, as is the sandy matrix, requiring more than cursory observation to determine the relative abundance of these two materials.

The phosphatic shale clasts are variable in shape. Many are near-spherical or bladed, but the dominant form is disc-shaped (Plate 16c). There is a general relationship between shape and size, with the larger grains being more disc-shaped and less spherical than the smaller grains. Most shale clasts are well rounded. Some have sharp edges — most common in disc-shaped examples — that indicate brittle fracture. Calcite- or quartz-filled tension gashes present in these clasts do not penetrate the surrounding matrix, indicating that these were present in the clast prior to deposition. The composition of these clasts ranges from homogeneous shale to laminated shale to shale with floating medium to coarse quartz sand grains to clasts that are nearly 50% sand grains and 50% mud. These clasts reach large proportions; the SI-61.3 bed contains one disc-shaped clast whose long and intermediate diameters are 22 cm and 12 cm, respectively.

The siltstone/mudstone clasts vary from gray (siltstone) to bright green (mudstone). These clasts are also elongate in cross section, but their three-dimensional geometries are difficult to discern on the weathered outcrop. Slabbed hand samples show that these clasts exhibit evidence of internal plastic deformation; this includes tapered and ragged edges,

angular bends, and indentation by other more competent clasts (e.g., black shale clasts) (Plate 16c). A minor percentage of clasts have sharp irregular edges indicative of brittle deformation. The color and texture of many clasts are identical to the underlying siltstone/mudstone. Some slab surfaces show the arrested disarticulation of parts of the substrate to form clasts.

The clasts in these beds define a fabric that is highly variable along strike. Clasts may be found at any angle to bedding, including vertical. The dominant fabric is one in which the tabular clasts have their long and intermediate axes parallel or subparallel to bedding. Most samples contain domains in which clasts are imbricated at an angle to bedding. Large domains with imbrication angles of 30 degrees from bedding are not unusual. Some small domains may exhibit nearly vertical imbrication.

4.13.1 Process Interpretation: Flat Pebble Conglomerate Beds

The sharp, primarily concave-up, lower surfaces indicate erosion of the underlying substrate prior to deposition. These lenticular beds record the conglomeratic infilling of shallow scours or channels. One might speculate that despite the lack of three-dimensional exposure the consistent thinness and limited extent of these beds as seen in two dimensions indicates that the scours were not very extensive, even along their long axis. FD-161.1, described above, is the one bed in which the lower bedding surface is demonstrably planar. This bed is difficult to interpret because deposition of the conglomerate may have been synchronous with the overlying sandstone, or may have preceded it by a short period. If the latter is true, then the conglomerate stood up in relief above the sea floor. Either way, the deposition was not preceded by erosion directly under the bed at that particular location. In another case, relief above the sea floor is indicated by the irregular, mounded upper surface, with local vertical packing. This resulted from deposition and reworking of a

small, conglomeratic, low-relief 'bar', possibly by waves (see discussion of fabrics below).

The siltstone/mudstone clasts were in various stages of consolidation at the time of erosion and deposition, showing evidence of both brittle and plastic deformation. Semilithified clasts were plastically deformed by interactions with surrounding, competent clasts. The lithologic similarity with the surrounding fine-grained beds and the rheologic behavior indicates that these siltstone/mudstone clasts are rip-ups of the underlying sediment surface. Similar squeezing and distortion of clasts are recorded in flat-pebble conglomerates described by Berg (1975).

The black phosphatic shale clasts show no indication of plastic deformation. Their well rounded, tabular shapes, quartz-filled tension gashes and sharp, broken edges indicate that these clasts represent long-reworked, lithified fragments of shale and sandy shale that deformed brittlely.

There are several published accounts of modern examples of vertically imbricated flat pebbles (Dionne, 1971; Sanderson and Donovan, 1974) and shells (Greensmith and Tucker, 1968, 1969; Sanderson and Donovan, 1974). Most ancient flat-pebble conglomerates have fabrics similar to these CIF examples — dominantly flat-lying and less well sorted than the modern examples (McKee, 1945; Roehl, 1967; Jansa and Fischbuch, 1974; Kazmierczal and Goldring, 1978; Chow, 1986).

Winnowing by currents is indicated by the quartzitic, mud-free matrix. This is also supported by the local development of imbrication, especially the small microdomains of near-vertical imbrication. Well sorted flat-pebble conglomerates with consistent vertical packing of clasts (see Roehl, 1967; Sanderson and Donovan, 1974) represent a more reworked state than these CIF examples, which are more poorly sorted and predominantly have bedding-parallel fabrics. The polymictic nature of the conglomerates and the 'exotic' nature of the shale clasts indicates at least modest transport of the shale clasts to their site of

deposition. The large size of the clasts in these beds and the fact that semilithified, fine-grained sediments were eroded prior to deposition implies high-energy current conditions.

4.14 PEBBLY MUDSTONE BED

The following discussion is based solely on one interval (primarily one bed) exposed at FD-48.45. Plate 16e,f should be referred to for the following description. This bed is well graded, with the grading defined on a number of different criteria. The bed is normally graded overall, with a distinct grain size break near the base that divides the bed into a lower clast-rich division and an upper fine-grained division. The lower division is a matrix-supported sand- and pebble-bearing silty mudstone of variable thickness (3-4 cm average). The upper division is a normally graded, green claystone with thin silt laminae at the base and widely scattered sand grains throughout. The thickness of this upper division is difficult to discern, because the top of the bed is difficult to define in the outcrop, but it is at least 10 cm and possibly as much as 20 cm. The contact between these divisions is defined by a sharp color contrast as well as by an obvious grain-size difference.

The lower clast-rich division is quite variable both laterally and vertically. It consists of subround to round, fine sand to pebble-sized clasts of various compositions supported by a matrix of green-grey clay and fine silt. This coarser fraction makes up approximately 25% of the lower division. The clasts are floating in the fine-grained matrix, yet along strike there is variability in the degree to which clasts are found in point contact.

The lower division can be subdivided into three parts. At the base is a discontinuous, and sometimes wispy, very fine sand lamina. The maximum thickness of this sand lamina is 3 mm. Even where this lamina is missing, the contrast is sharp between the pebbly lower division and the green mudstone that underlies this bed. Above this sand lamina is 5-8 mm of interlaminae of clayey siltstone and claystone with widely dispersed

large pebbles. The third part of this lower division is 2-3 cm of silty claystone with abundant, normally graded, sand to granule sized clasts. Ignoring the thin sand lamina at the base, the whole lower division can be considered normally graded in terms of maximum grain size (pebbles to granules to various grades of sand). The transition from the lower parts of this division to the graded clast-rich horizon makes the whole lower division inverse-to-normally graded in terms of average grain size.

In some places, elongate shale clasts and sand grains in the lower division are well aligned, forming horizontal or low-angle planar laminae that alternate with clast-poor silty mudstone laminae. The laminae may be difficult to define, but an estimate of thickness for the coarse laminae is 1-2 mm, and for the silty mudstone laminae, 1-3 mm.

The clasts include white to pink quartz grains and clasts of siltstone and dark shale. The latter are in most cases elongate and range compositionally from homogeneous shale to laminated shale to shale with floating sand/silt grains. These shale particles reach dimensions of 1.8 cm X 3 mm in cross section. Cross-sectional diameters of the more spherical quartz grains range up to 11 mm.

The upper division of this bed consists of 10-20 cm of claystone containing approximately 15% floating detritus. Most of this detritus is very fine sand, while a fraction consists of medium to coarse sand-sized quartz and sedimentary rock fragments and elongate black shale clasts (4 mm maximum length). The elongate clasts are predominantly oriented parallel to bedding. The initial 3-4 cm that immediately overlies the lower clast-rich division consists of light-colored claystone with wispy, irregular, thin silt laminae. These laminae die out rapidly above into siltstone with only rare, discontinuous silt laminae. Normal grading in this division may be defined on the percentage of silt and on the abundance (but not size) of floating coarse grains.

A centimeter below this bed is a thin (<2 mm) discontinous very fine sand lamina similar in character to the basal lamina in the bed above. The intervening green claystone contains widely dispersed clasts of similar composition to those described above. The

matrix is relatively homogeneous and the clasts, although less abundant than in the bed above, are remarkably large (up to 1.5 X 1.5 cm).

4.14.1 Process Interpretation: Pebbly mudstone bed

The bed described above is surprisingly complex. The variety of well preserved depositional fabrics in this bed indicates that the presence of matrix-supported clasts is not related in any way to postdepositional processes (e.g., inmixing by burrowing organisms). Pebbly mudstones are characteristically interpreted as debris flows (e.g., Hampton, 1972; Crowell, 1957 — although Crowell did not specifically use the phrase 'debris flow, he did talk about "viscous sluggish slumps" p. 1004). The matrix-supported fabric of this bed does indicate that at the time of deposition the flow had some degree of matrix strength. The clast density and number of clast contacts is greater than the more 'typical' pebbly mudstones described in the literature (Aksu, personal communication). In a few places along the length of exposure of the bed it appears that the density of clasts is significant enough to warrant the consideration of dispersive pressure as a support mechanism during transport. The style of lamination in the upper division seems too regular and organised for debris-flow deposition, yet sand is dispersed in the fine-grained matrix. These data suggest that the depositing flow was likely of intermediate character, involving a number of different support mechanisms that changed with time.

The inverse-to-normal grading in the lower, coarse-grained division is similar to that described by Aksu (1984) for inferred Quaternary debris flows in Baffin Bay. At the base of debris flows, a zone of strong shear is characterized by decreased strength and competence, making inverse grading likely at the base of debrites (Hampton, 1975). Stratification in debrites, with elongate grains parallel to flow, reflects laminar flow conditions (Fischer, 1971). The laminae in the normally graded part of the lower division of FD-48.45 could be attributed to sorting along shear planes at the base of a rigid plug

exhibiting discontinuous, downward growth during freezing of the flow (Hampton, 1975; Aksu, 1984). However, laminae in debris flows are typically quite crude, while in this facies they are on a very fine scale. The relatively high concentration of coarse grains and the presence of thin laminae may indicate that this bed was deposited by a debris flow with a lowered density and viscosity.

The character of the upper division suggests even more dilute flow with significantly less strength. The silt laminae that characterize the lower part of this upper division are similar to Stow and Shanmugam's (1980) T_4 and T_5 laminae described for fine-grained turbidites. The matrix-supported fabric is interpreted as a function of matrix strength. The presence of silt laminae and the high clay content of the matrix argues against a mass settling event. If this flow was uniformly turbulent and dilute, the coarse grains would have settled to the base of the flow. The flow associated with the upper division of the bed was probably a slightly diluted, partly turbulent debris flow. The dilution, and therefore the degree of turbulence, may have been more important at the base of this upper division, where the turbiditelike laminae are best developed.

The nature of the contact between the upper and lower divisions is a rapid gradation, showing no evidence of an erosional or depositional time break. If these divisions were not deposited by two temporally distinct flows, a mechanism would be required to generate two different density regimes within one flow (ie., a stratified flow). Perhaps the upper division represents a low-density cloud of sediment formed by the stripping of sediment off of the upper surface of the debris flow during transport. The shear associated with downslope movement of the debris through water would allow for erosion and mixing of sediment above the debris flow. In the experiments by Hampton (1972), debris flows with moderate water content (70-75%) formed denser clouds of suspended material than did flows with lower water content. The sediment, supplied by erosion of the snout, travelled backwards and mixed with the overlying water to form a cloud. In a natural setting, this dispersion, moving slower than the head of the debris flow,

would flow downslope over the top of the debris after it had come to rest. Depending on the quantity of sediment thrown into suspension, and the quantity of fluid inmixing, the resulting dispersion might be of variable character, but with turbulence a very likely attribute (Fisher, 1983). Whether a 'surface transformation' (Fisher, 1983) as described by Hampton (1972) could yield a slurry with any strength — the upper division does have medium/coarse sand-sized grains — has never been demonstrated.

Assuming that the lower division of FD-48.45 was transported predominantly as a debris flow, an attempt is made to calculate the strength of the flowing debris and the slope on which it came to rest. Two parameters of the flow must be estimated in order to perform these calculations: density of debris (for calculation of strength and slope) and thickness of bed at time of deposition (for calculation of slope). Modern subaerial debris flows have densities from 2.0-2.4 g/cm^3. Little is known about the densities of modern subaqueous debris flows, but an estimate of 2.0 g/cm^3 seems reasonable (Hiscott and James, 1985, use 2.2 g/cm^3 for subaqueous flows in the Cow Head Group). A value of 8 cm, which is twice the thickness of the lower clast-rich division, is used as an estimate of original bed thickness. This value seems reasonable given the mud/silt content, and agrees with estimates of compaction derived from carbonate concretions in the CIF. These estimates have been bracketed to cover a range of possible values. The upper and lower density ranges picked were 1.5 and 2.4 g cm^{-3} for density and 6 and 10 cm for bed thickness (1.5 and 2.5 times observed bed thickness). Debris strength can be calculated based on maximum clast size (D_{max}) using the formula

$$D_{max} = 8.8k/g(s-f)$$

where k is yield strength, s is density of the clast, f is density of the fluid matrix and g is the gravitational constant (Hampton, 1970). Using a D_{max} of 1.1 cm and a value of 2.65 (quartz) for s, strength values for fluid densities of 1.5, 2.0 and 2.4 g cm^{-3} are given in Table 4.1. These values were used in estimation of slope (Hampton, 1970) using the formula

f (g cm-1)	k (dynes cm-2)	T_c (cm)	sin θ	Slope (degrees)
1.5	140.9	6	.0479	2.746
		10	.0288	1.650
2.4	30.6	6	.0037	0.212
		10	.0022	0.122
2.0	79.7	8	.0102	0.584

TABLE 4.1: Debris strength and slope estimates for FD-48.45. Debris strength was calculated from maximum clast size Dmax using Hampton's (1970) formula Dmax=8.8k/g(s-f), where k=yield strength, s=density of clast, f=density of fluid matrix and g=gravity constant. The calculations are based on a measured value of D_{max} of 1.1 cm and a clast density (s) value of 2.65 (quartz). Three bracketing values of strength were calculated using fluid matrix densities (f) of 1.5, 2.0 and 2.4g cm-2. Slope estimates were calculated using Hampton's (1970) formula Tc=k/ysin θ, where T_c=critical thickness, y=unit weight of debris and θ=slope angle. Slope calculations are included for upper and lower bracketing values of fluid density and bed thickness.

$T_c = k/y \sin \theta$

where T_c is critical thickness, y is unit weight of debris and θ is slope angle. Table 4.1 contains the slope calculations using the upper and lower bracketing values of fluid density and bed thickness. The calculated minimum value of slope is 0.126 degrees, and the maximum is 2.746 degrees. Using the assumed values of T_c= 8 cm and f= 2.0 g cm^{-3}, the strength of the flowing debris is estimated at 79.65 dynes cm^{-2}, with deposition on a slope estimated at 0.584 degrees.

4.15 GUTTER AND POT CASTS

The term "gutter cast" has been used by various workers to refer to erosional structures that range from downward-bulging sole structures to isolated channels. The following discussion will refer almost exclusively to deep, narrow, erosional features which occur isolated or 'connected' by an overlying thin sandstone bed (e.g., Plate 17e). Pot casts (cylindrical pillars of sandstone) are also prominent features of F.A. 2.

The gutter casts of this facies association show variability in lithology and in geometry, as seen in cross section (Figure 4.11; Plate 17) and plan view (Figure 4.12; Plate 18). The gutter casts are dominantly composed of fine sandstone, and less commonly of white-weathering, well sorted fine to medium sandstone (Figure 4.11d; Plate 17e) and granule to pebble conglomerate (Figure 4.11k; Plate 17b). The latter consists of phosphatic shale clasts, green siltstone intraclasts and large quartz pebbles set in a well sorted medium to coarse sandstone. Cross sections perpendicular to the long axes of the gutter casts show the long axes of the clasts to be dominantly parallel to bedding, with a few cases showing local imbrication of the clasts at the sides of the structure. These conglomeratic beds also show weak normal grading. The sandstone gutter casts are most commonly either massive or planar-laminated. Oscillatory-flow-type laminae, including low-angle wavy, draping and

Figure 4.11: Schematic diagram of cross-sectional views of gutter casts. Labels "a" to "k" are referred to in text. Gutter cast "f" is unusual in that it has a lower projection that may link up with a sedimentary dike. The presence of current-generated markings rules out an 'injection' origin for the cast, but this association of features was noted in several beds.

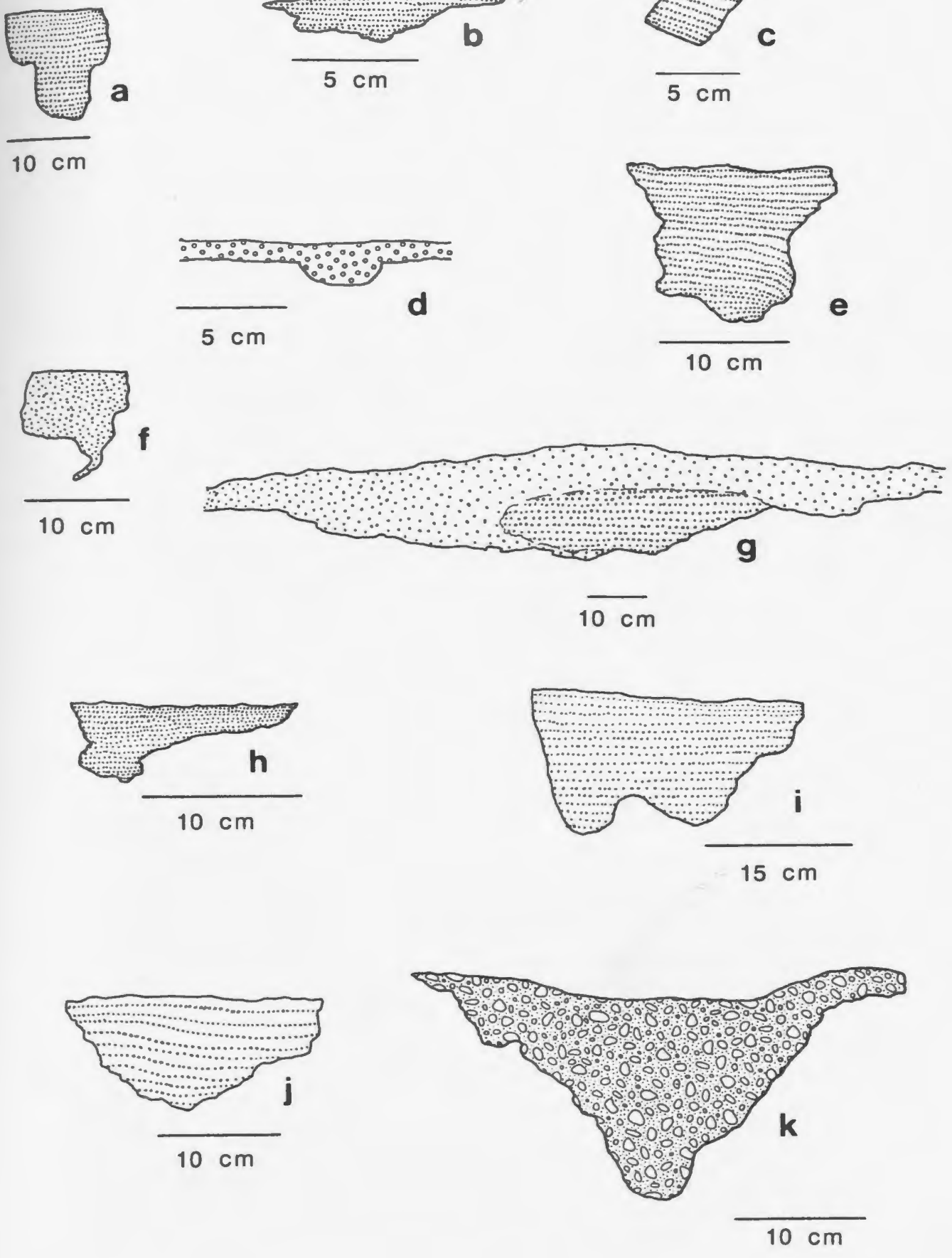
a
10 cm
b
5 cm
c
5 cm
d
5 cm
e
10 cm
f
10 cm
g
10 cm
h
10 cm
i
15 cm
j
10 cm
k
10 cm

Figure 4.12: Schematic diagram of plan views of gutter and pot casts. Labels "a" to "g" are referred to in text.

(f) The trend and plunge of the long axes of pot cast "A" and the mold left by the excavation of pot cast"B" is toward the left (roughly northeast). Pot cast "C" indicates a long-axis trend and plunge towards the right (southwest).

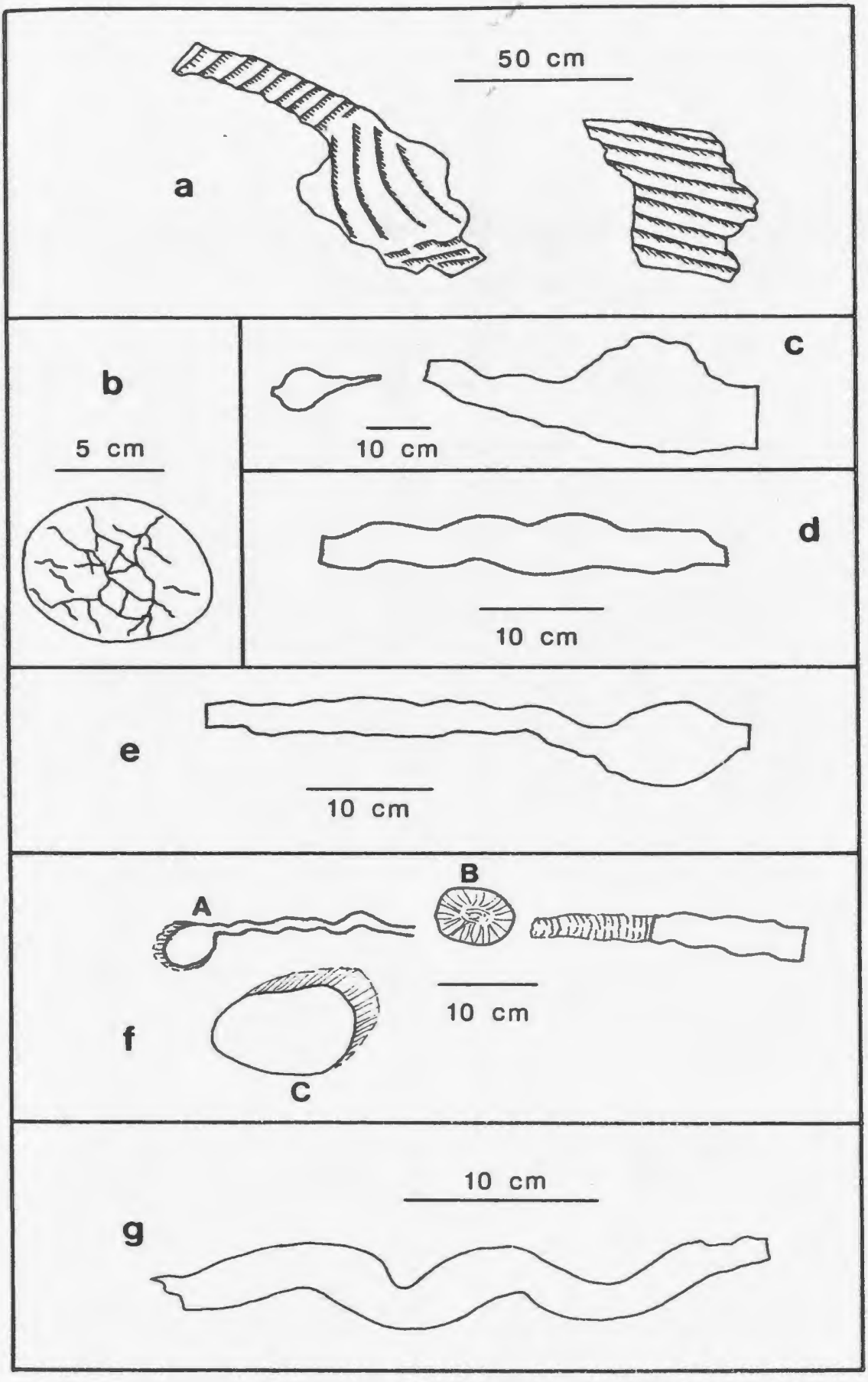
50 cm
a
b
5 cm
c
10 cm
d
10 cm
e
10 cm
A
B
f
C
10 cm
10 cm
g

PLATE 17: GUTTER CASTS (FA 2)

a: Flat-bottomed, steep-walled gutter cast. Bending of the gutter cast and overlying sandstone laminae is attributed to compaction. Note irregular injection feature (arrowed). Stratigraphic top is up. Black division on scale is 10 cm.

b: Irregular V-shaped conglomeratic gutter cast. Note large quartz clasts up to 1 cm across. Stratigraphic top is up. Scale is 2.5 cm wide.

c: The internal lamination of this hour-glass shaped gutter cast is slightly disturbed by compaction. The locally overhanging wall (on the left) is considered an original feature. Stratigraphic top is up. Black division on scale is 10 cm.

d: This gutter cast also has overhanging margins near the base of the structure. Note asymmetry and mild bending of laminae. Stratigraphic top is up. Divisions on scale are 10 cm.

e: Rounded symmetrical gutter cast at base of quartzarenitic sandstone. Stratigraphic top is up. Divisions on scale are in cm.

f: Bilobate gutter cast with steep wall on left and more gentle wall on right (base highlighted in ink). Stratigraphic top is up. Scale is 15 cm long.

g: Three dimensional view of steep-walled, U-shaped gutter cast. Note small trace fossils and spiraling (?) groove marks on the side. Stratigraphic top is to upper left. Scale is 2.5 cm wide.

h: Slightly-oblique cross-sectional view of large, wide gutter cast. The well-defined laminae (lower right) are within a partly-formed carbonate nodule. Stratigraphic top is up. Divisions on scale are 10 cm.

i: Close-up of "h" above showing parallel lamination (in nodule) that are overlain by climbing wave-ripple lamination. Stratigraphic top is up. Scale is 10 cm long.

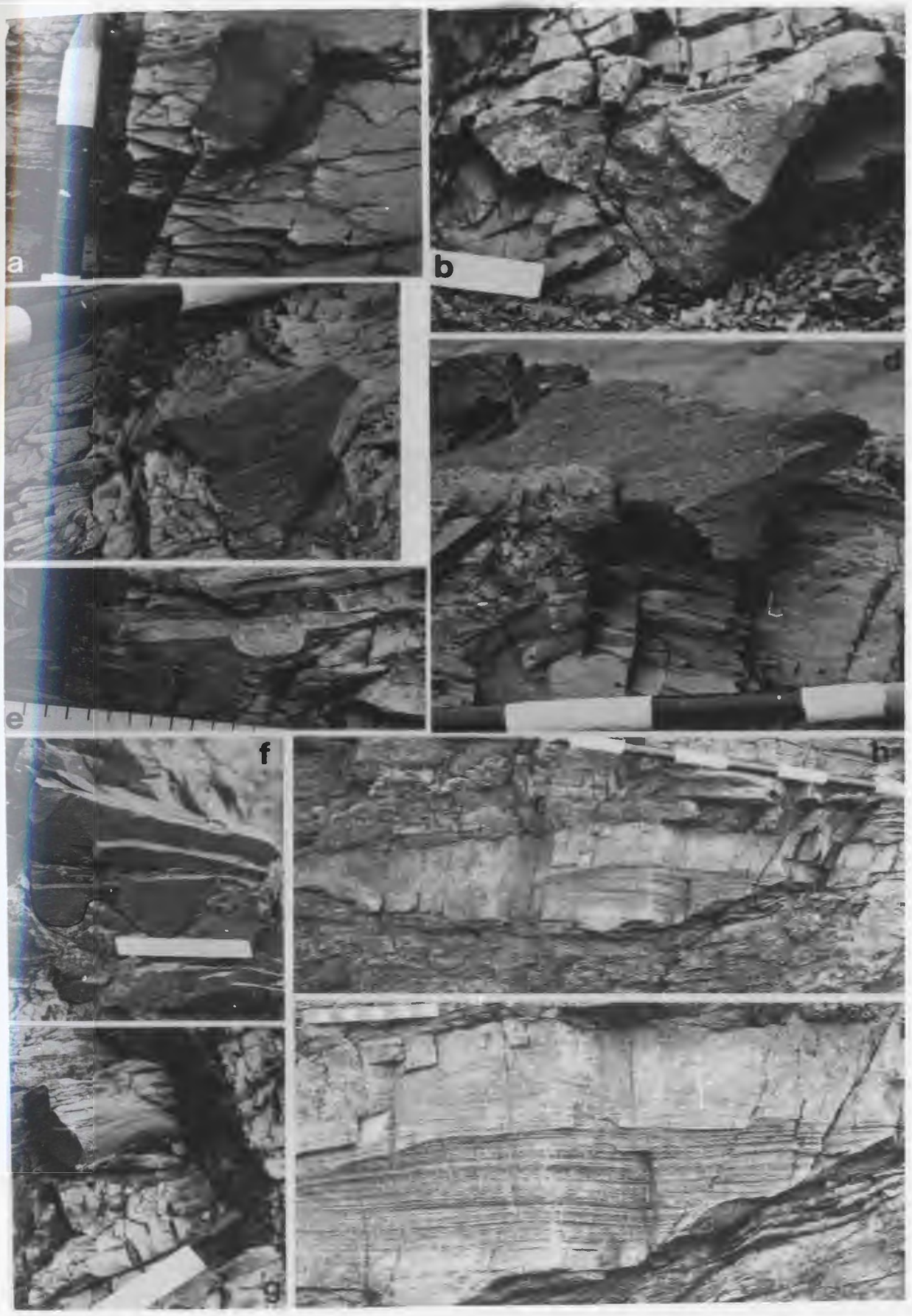
a
b
d
e
f
h
g

PLATE 18: GUTTER CASTS - PLAN AND SIDE VIEWS (FA 2)

a: Sinuous gutter cast. Bedding plane view. Scale is 10 cm long.

b: Oblique view of the side of an isolated gutter cast (no overlying sandstone bed) from GB. Stratigraphic top is to upper right with the maximum thickness of the gutter cast on the left. Note erosional termination of underlying sandstone bed. Post-depositional trace fossils are only found along the sole on the right, on upper portion of wall near the top of the gutter cast. The thickness normal to the top of the gutter to which these burrows are found is approximately 3.5-4 cm. Scale is in cm.

c: The geometry of this gutter cast is straight to slightly irregular in plan view. Note widening of gutter cast opposite scale. Divisions on scale are 10 cm.

d: This bedding plane view shows pinch-out of a gutter cast toward the northeast (background). Divisions on scale are 10 cm.

e: Bedding plane view of two gutter casts with wave-rippled upper surfaces. The gutter cast on the left has multiple sets of ripple crests. See Figure 4.12a and text for details. Divisions on scale are 10 cm.

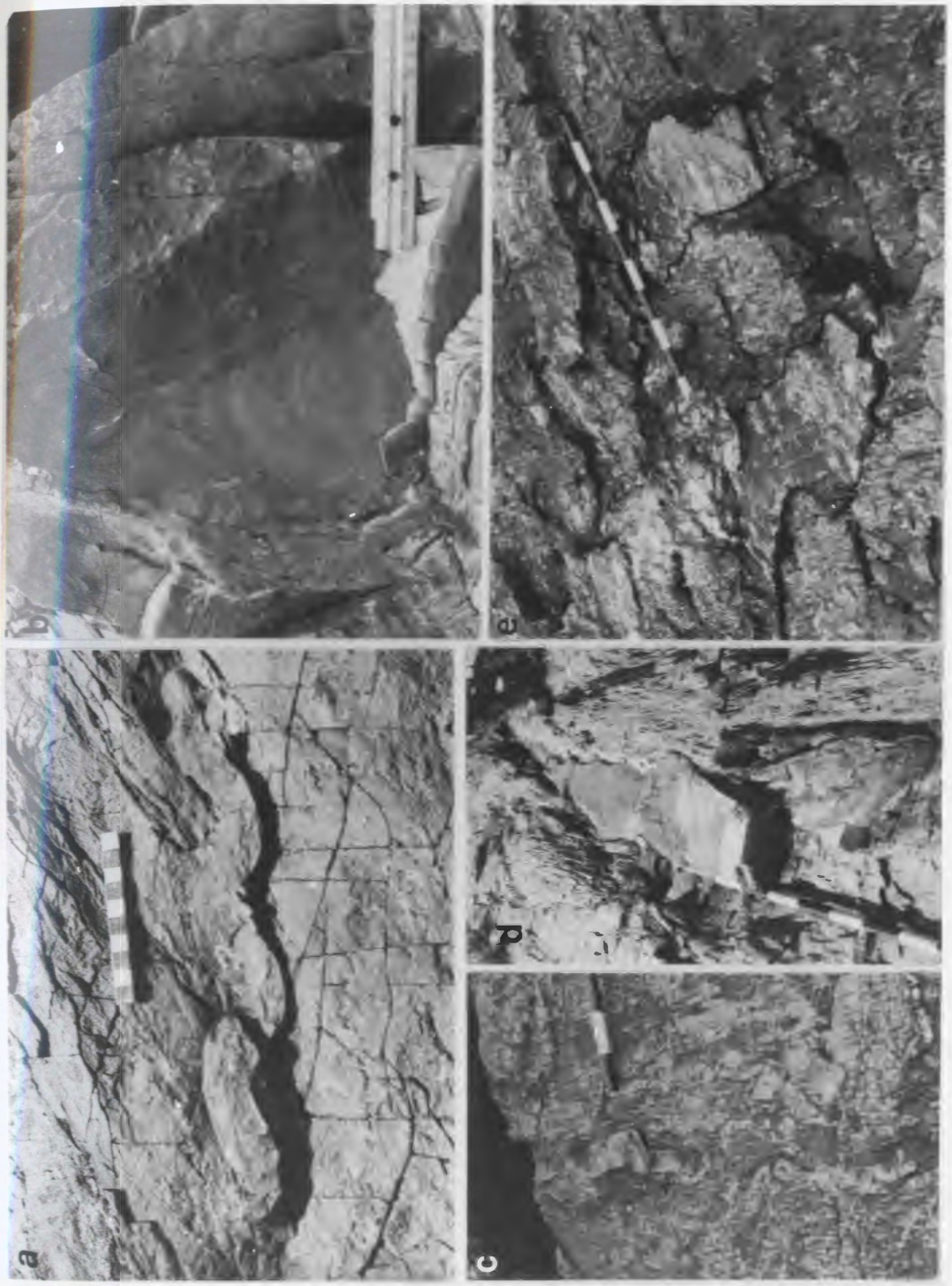
b
e
a
d
c

offshooting laminae and climbing symmetrical-ripple laminae, have also been noted in the upper portions of some beds. Subtle disconformities within the internal stratification of gutter casts were noted in only a few cases. Amalgamated gutter casts are also uncommon. Carbonate nodules are found within these beds (Figure 4.11g; Plate 17h,i), and in many cases the entire bed experienced early carbonate cementation.

The cross-sectional shapes of these gutter casts range from symmetrical (Figure 4.11a,d,k) to strongly asymmetrical (Figure 4.11h), and include U-shaped, bilobate (Figure 4.11i; Plate 17f), V-shaped (Figure 4.11k; Plate 17b), semicircular (Figure 4.11d; Plate 17e), flat-based forms (Figure 4.11c; Plate 17a) and wide, shallow forms (Figure 4.11g; Plate 17h,i). Extremely steep to overhanging walls are common (Figure 4.11c,e,f,h; Plate 17a,c,d). Compaction has altered the shape and internal stratification in some of these beds (Figure 4.11c,e,j; Plate 17a,c). Cross-sectional views that are parallel or nearly parallel to the long axes of these gutter casts are wide and shallow. The ratio of maximum width to maximum thickness (taken roughly normal to long axes of the gutter casts) for a small sample of isolated gutter casts (n=16) is 2.6, with ratios noted as low as 0.4. Average maximum width is 9.1 cm and average maximum thickness is 6.2 cm. The thicknesses are generally one or more orders of magnitude thicker than the sandstone beds with which they are intercalated.

Sole markings are common features along the sides and bases of these beds. The markings include groove marks, poorly developed prod and flute marks, and postdepositional trace fossils. Groove marks are generally parallel to subparallel to the long axes of the gutter casts and circular to downward-spiraling on pot casts. In the case of one sinuous gutter cast, grooves on the wall are parallel to the gutter between meanders and plunge obliquely downward along the 'inner' wall of the gutter at the meander bend (Plate 17g). Trace fossils on the walls of isolated gutter casts are found to a depth of only 3-4 cm below the paleosurface; deeper surfaces of the gutter cast are either smooth (Plate 18b) or bear current marks. The traces are generally small and show no evidence of fluting.

The plan-view shapes of the gutter casts vary from narrow (Figure 4.12d-g; Plate 18a and 19a,b) to wide (Figure 4.12a,c; Plate 18c,d,e) and straight (Plate 18c) to sinuous (Figure 4.12d,f,g; Plate 18a and 19b) to highly irregular. The long axes of 90 gutter casts measured at FD (Figure 4.13b) show a strong northeast-southwest orientation. Full three-dimensional views of several sinuous gutter casts show that their geometry is comparable to modern meandering rivers in that cross sections perpendicular to flow are strongly asymmetrical on the bends, with the steep to overhanging walls on the outside of the meander bend. Well defined sinuous gutter casts are thin, with widths less than a few centimeters. From the small number of observed sinuous gutter casts it appears that the thinner ones are also more sinuous. Numerous examples of bifurcating gutter casts were noted, as well as those that taper and pinch out along strike (Plate 18d). All of the bifurcating beds that were noted had their 'forks' opening toward the northeast, and nearly all of those that showed pinchout did so towards the northeast as well. The upper bedding surfaces of some gutter casts are covered with symmetrical ripple marks with high spacing-to-height ratios. The crests of these ripples are generally perpendicular to the trend of the gutter cast, but beds with multiple directions were noted. The crest orientations appear to be controlled by the plan-view geometry (Figure 4.12a; Plate 18e).

In some cases pot casts are closely associated with gutter casts. Gutter casts are seen originating from and leading into, then out of, pot casts (Figure 4.12c,e,f; Plate 19a,b). One interesting example is shown in Figure 4.12f (Plate 19b), where a slightly sinuous gutter cast leads into the mold of a pot cast, which leads to a thinner, more sinuous gutter cast and finally into a small pot cast. The pot casts in this facies association have a wide variety of shapes and sizes. Most are composed of sandstone without a basal lag, while others are conglomeratic. These pot casts commonly weather out as partially free-standing structures. They range from discs to rounded loaflike forms to tall pillars. They range from remarkably small (1 cm in diameter) to large (nearly 20 cm in diameter; Plate

PLATE 19: POT CASTS (FA 2)

a: Pot cast found along the length of a gutter cast. Bedding plane view. Scale is 10 cm long.

b: Bedding plane view in which northeast is to the left. The large pot cast to the left of the scale has its central-axis plunging roughly south. Above the scale, a small pot cast and an exhumed (larger) pothole are found along a gutter cast that is wider and slightly sinuous on the right and thinner and more sinuous on the left. The central-axis of the small pothole plunges toward the northeast and the shape of the exhumed pothole indicates a similar tilt. See Figure 4.12f and text for details. Scale is 10 cm long.

c: Bedding plane view of two pot casts. Pot cast at top of photo widens and spirals downward. Divisions on scale are 10 cm.

d: Oblique view of prominent-weathering pot cast with well-developed downward-spiraling shape. Scale in foreground is 10 cm long.

e: The shrinkage cracks on the upper surface of this pot cast are the only ones noted on any pot or gutter cast, or any beds with which they are intercalated. Scale is in cm.

f: Cross-sectional view of a downward-widening, asymmetric pot cast. Divisions on scale are 10 cm.

g: Oblique view of bowl-shaped pot cast. Concentric grooves are visible on sides. Scale is in cm.

h: Bedding plane view of very large pot cast exhibiting a slight tilt of the central axis toward upper right. Black division on scale is 10 cm.

i: Loaf-shaped, downward-widening pot cast with grooves on side. Stratigraphic top is up. White division on scale is 10 cm.

j: Sharp rectangular cross-sectional shape of this pot cast is unusual. The pot cast shows grading from laminated fine sandstone to massive to subtly-laminated very fine sandstone. Stratigraphic top is up. Width of scale is 9 cm.

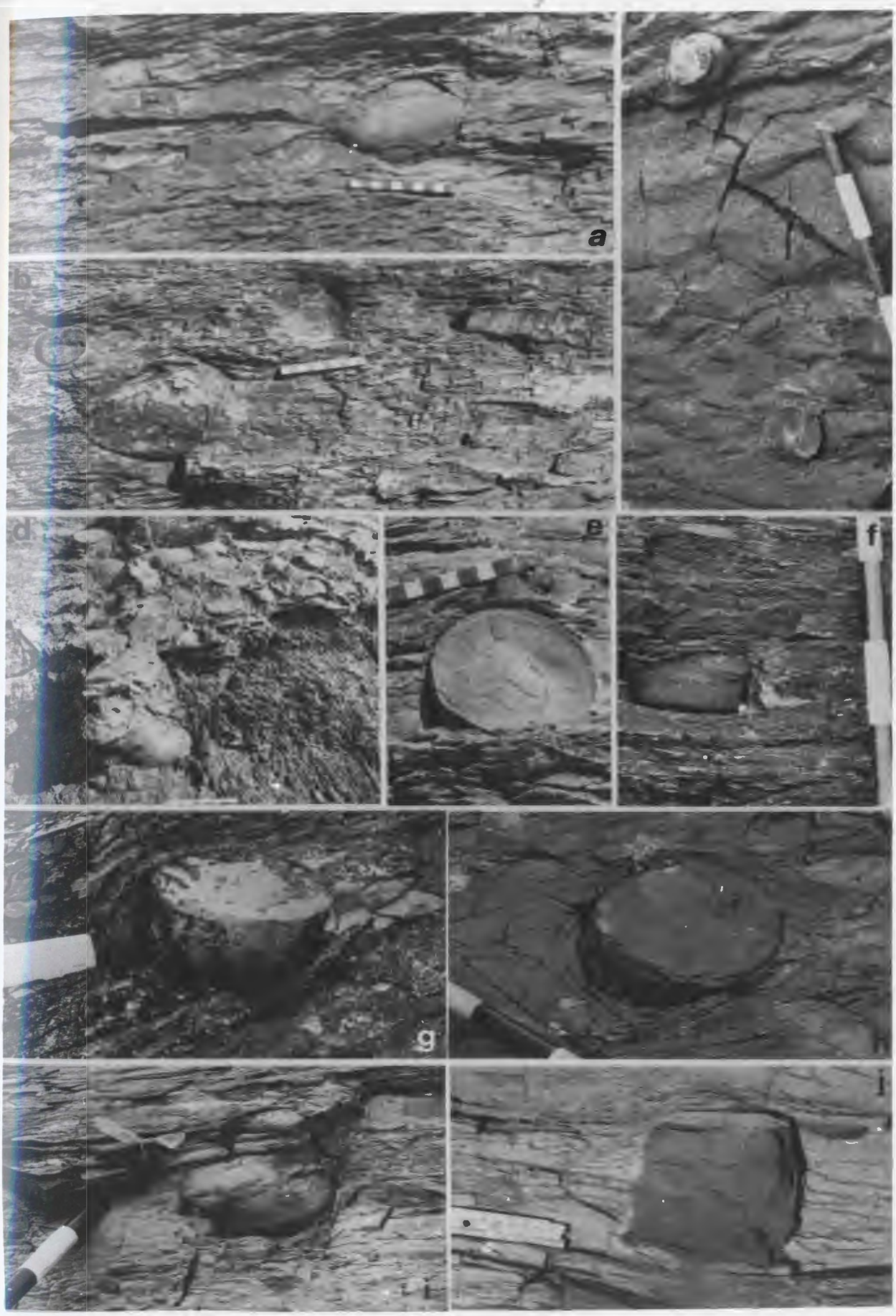
a
b
c
d
e
f
g
h
i

19i). Numerous examples were noted in which pot casts widened downward (Plate 19c,d,f,i), and a few well exposed examples had a snaillike or corkscrew shape (Plate 19c,d) similar to potholes found in bedrock along modern rivers. The bottoms of pot casts are commonly deepest around the outside, with a central erosional high: the form resembles the base of a wine bottle. Shrinkage cracks were noted at the top of one pot cast (Figure 4.12b; Plate 19e). The central axes of the pot casts are commonly tilted from the paleovertical (<30°) (Plate 19c,d,h,i); measurements of the direction in which these potholes tilt (given as the trend-direction in which the central axis plunges) is given in Figure 4.13a.

4.15.1 Process Interpretation

The term "gutter cast" was first used by Whitaker (1973) for downward-bulging sole structures and isolated channels in Llandoverian rocks in Norway. The gutter casts were interpreted to form from current erosion. Erosional structures of a variety of sizes and shapes have been described in the literature using a host of different names such as priels, furrows, Rinnen, Erosionrinnen, large groove casts, rills, cut-and-fill, scour-and-fill, and gouge channels (Table 4.2). The wide range of size, shape, lithology and internal stuctures of these erosional structures argue that their origin is polygenetic. This may be true for the gutter casts in F.A. 2.

Field observations are in agreement with Whitaker (1965,1973) that there is a continuum between isolated or "separated" gutter casts and those connected by an overlying bed that may be a small fraction of the thickness of the gutter cast to several times its thickness. It is reasonable to assume, as Whitaker suggested, that the control on this variation is one of sediment supply. Separated types are formed when there is insufficient sediment to form a complete bed, while the other types form under conditions of higher sediment supply.

Figure 4.13: Rose diagrams: (A) trend associated with direction of plunge of the central axis of pot casts (n=31), and (B) trend of long axes of gutter casts (n=90). Data from the lower 35 meters of the Fortune Dump section.

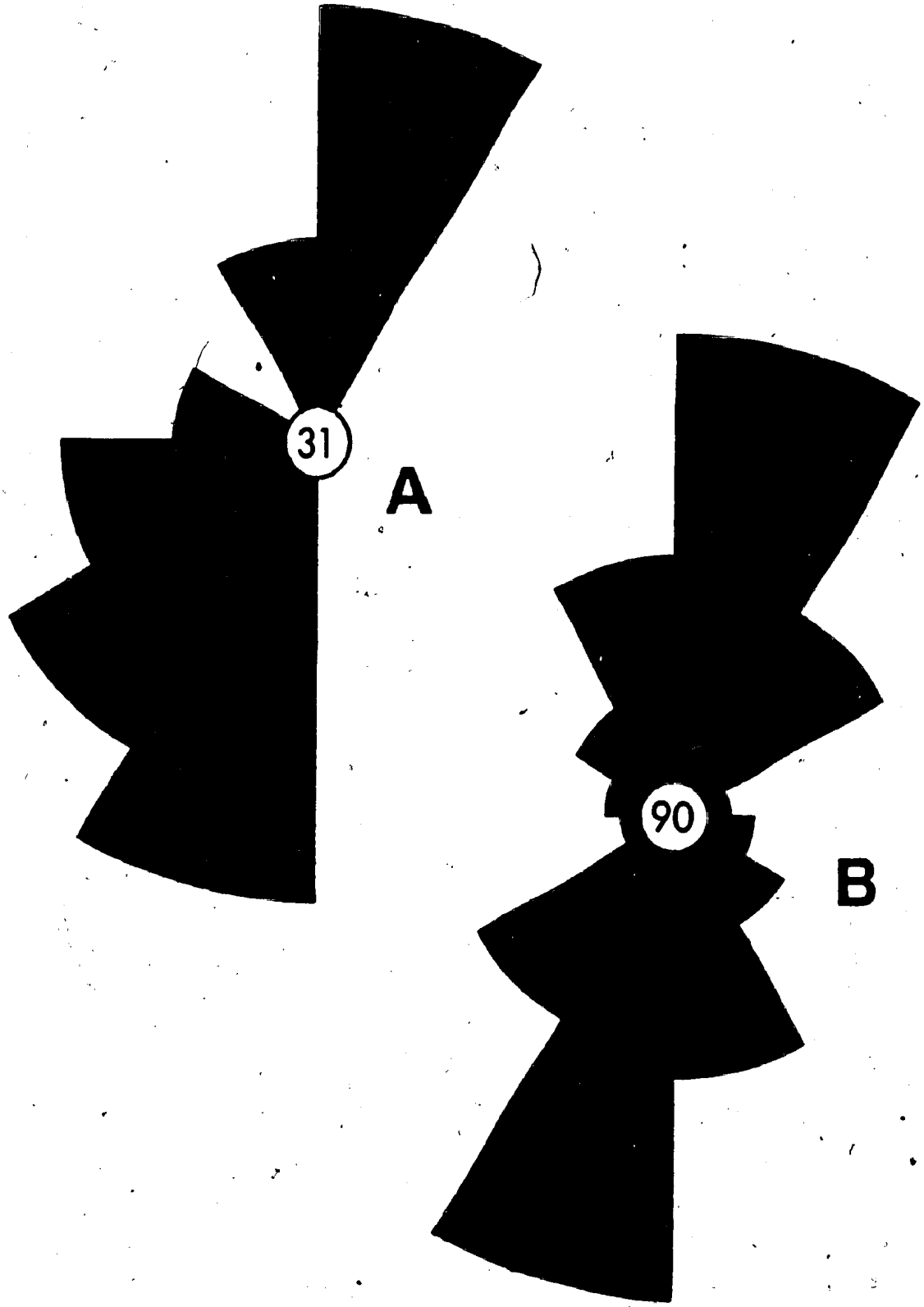
31
A
90
B

Table 4.2

AUTHOR	NAME OF STRUCTURE	DIMENSIONS	SHAPES	PLAN VIEW	ALIGNMENT	FILLINGS	SOLE MARKINGS	ADDITIONAL COMMENTS
Aigner and Futterer, 1978	Pot and gutter casts	W=0.20cm D=5.10cm	Symm to asymm U-shaped rarely V shaped	Few m long, one 2km long, no bifurcs or meanders	Parallel to coastline	LS. Structureless, occasionally lam's accumulations, ripples wet mud clast, shells, pebbles	Tool mark impacts parallel to gutter at slightly oblique scratches from shells	Sediment of base of gutter rests as a lag, stabilized, gut casts on one end, gradual thinning at other end
Allen, 1974	Small Channels	——	Variable W>C. Vert to overhanging walls	——	——		——	No description or interpretation
P. Allen, 1962	Elongate flute casts	W=0.5 2m, D=x1m	U- to V-shaped. Asymm at channel bends, terracing and undercutting upstream, shallow downstream	Straight and sinuous, usually L=1.5 12m	Para to PC of overlying current ripples and to sense of overlying SS textures, perp. to shore	SiSt, SS or granule grit, fascicular concave up shells and or fish debris	Groove and prod marks, set out preferred orientation of prods	Proximal half terminates at SS (rises sq or to full sand sheet). Flute sizes proportional to size of turbidites
Basset and Walton, 1960	Scour-Fill/Gouge Channels	W=1m D=0.5 m to W=2m D=1m	Flat based, vert walls rounded symm to asymm	Parallel sided or converging cuts like flute	Strong orientation	Grits, massive, parallel lam or cross lam	Small marks on tg marks	Structures eroded by turbidity currents
Berry, 1961	Longitudinal ripples	W1=1.5 7cm (4.2Ave) Amp=0.3 2cm (0.7 ave), R=3.5 18	Symm and asymm, curved to flat base, vert to overhanging walls	Regular and para, slow bifurcate	Para to grooves, perp to lave ripple crests	SS fill, then SaSt at base, para wr, may curve up at sides	Scts and grooves on base of troughs	Non marine, streamers of sand in low, parallel erosion of grooves
Bridges, 1972	Furrows	W= ~20 cm, D=7.8 cm	Symm to Asymm w undercut bank	Less than 2m exposed, sgn of termination	Oblique angle to paleoslope	V, low angle lams, cross surfs, concave up lams	Small grooves/prods up to 20° from long axis, downslopping ridges on steep banks	Cut by discrete helical flow, flood tide, currents, associ w storm wave activity
Broadhurst, 1968	Prods	——	——	——	——	50% calc base (shells/organics) SS above	——	Tidal environment
Daley, 1964	Runnel Casts	W=3.5 4cm, D=1.25 2cm	Deep U-shaped W/D=3.2, Shallow - W/D=12.1, Symm to asymm, Vertical to overhanging walls	Non-branching, de bute both ends, some steeper on one end, shallow and straight, most sinuous	53 readings, 85% are N15 33E, currents moved perpendicular to shoreline	Planar lams, some w fish debris at base washed in before tllamy or lag	Lineations from differential cementation, track fossils	These are sole markings or disconnected rods (cf Whitaker, 1965), cut by shore prep currents
Dineley, 1968	Linear structures	W=1-3m D=no value given	Semi-circular outline	Contin >8ft, linear slightly irreg, bifurc, sep by 15°	Trend varies 15° from pala current lineation	Same as overlying bed	——	Drag marks?
Friend, 1965	Long Welts Simple Irregular	W=5cm, relief=3cm, 10-15cm apart 5 cm deep to crest, 3cm relief	Flat crests More rounded in outline	Generally straight, bulb sinuous Sinuous, often branched join neighbors	Parallel to grooves and current crescents Parallel to grooves and current crescents	Coarsest of overlying muds/sands	——	Welsh cyclothems
Greensmith, 1965	Cut and fill structures Groove casts, Concentric GCs	Max D=8ft, smaller=D=1.3ft D=3m, Concentric GC's D=1-2", D=5"	Round to V-shape, symm-asymm, steep-sided Narrow	—— Sinuous, 2-3ft long	Para to ripple PC's, perp to ripple crests	Mud-fine SS w/ x-bedding Base of pebbly SS beds	—— ——	Delta top, delta lobe features Drag marks, Concentric forms current/drag marks
Greensmith et al., 1980	Gutter marks/Gutter casts	Max W=6.15 cm, D=20 cm	Narrow-deep to broad-shallow, symm lobate or asymm/overhanging walls to asymm w steep side/long axis	5m exposed, aligned partly sinuous, branching, no terminations	Well-oriented, perp to ripple crests	Graded massive, concave-up base ripple x-lam, scour surfs, fossil, pebble, driftwood lags	——	Overhanging walls, rapid filling after erosion, shallow subtidal, subaerial sand sheets
Kuenen, 1957	Gouge Channels	20-50 cm deep, 1.5-2 m wide	Symm to asymm, shallow to deep	Perfectly para, no terminations, L=12m min	Para to current deduced from other structs	Planar lam, fine grad clay-volcanic lam	Para grooves, drag and flute marks	Origin unclear
Martinson, 1965	Prods	Ave W=10-15 cm D=5-8 cm	——	——	Well-oriented, ripple PC's slightly diff	Casts on siltstone beds, no detail	——	Term 'Prod' is common German name
Neglegael, 1965	Scour-and-fill	Most <2m	Symm, approximates triangle w/ rounded lower corner	Base of sheet, join and divide, downstream isolated	Well-oriented, somwt spread of data	Conglomerate	——	Load casting not (rarely) more likely when W/D>2
Reinhalf, 1938	Groove ripples	W(wavelength)=3m, amp=70cm, max=12m, Larger ones shallower	Roughly symm	——	——	Cut into mud, filled w sand, no details	——	W/height normally 8.5-9, shallow ones up to 20, rides flat, cut by tides
Pleasman, 1961	Rinnen	W 2m D=0.5m	Rounded to slightly asymm	Straight channels at least 10m long	Long axis para to other current indications	Unbedded graded conglomeratic SS	——	——
Prentice, 1962	Large Groove Casts Basin Casts	Ligest W=4cm, D=2cm Deep W=20-30cm, W=8-15 cm Shallow 20x10-2 cm to 1.5 m dia	Nearly semi-circ to asymm Cast: central depression, mold of ones high, W=2C to hole W=2cm, D=1cm	Slightly sinuous, tadpole both ends Elongate to near circular	Roughly perp to shore Roughly perp to shore	Generally parallel laminated Ripple bedded SS, ridges/terraces on edge of cast cut at top level of sediment fill	Smooth or curved grooves variably oriented, generally para to long axis	Origin unclear - cut by plant debris? Inverted dome structures - cross between potholes and gutter casts
Richter, 1967	Erosion channels	Max W=2m, D=45cm, Min W=15, D=10cm	Rounded, symm to asymm	——	Para to current lineations, flutes + ripple PC	Cut in mud, filled w sand, one mud-fill	——	——
Schroder, 1965	Erosion rinnen	Widths on average m, D=1cm-1m	Rounded symm to asymm w steep walls	Similar to river system, smaller upstream	Fair orientation, some small ones at high angle	Massive cross lam or horiz lam SS, clay-pebble congl	Flutes, steep on flanks, shallow in center	Helical flow, similar to tidal creeks
Schuller, 1967	Rill	W=3-40cm, D=~2-3cm	Rounded, symm	——	——	Fine-grained LS, rest of bed absent	——	——
Schwarz, 1975	Tidal grooves	W=5-25cm, D=>10cm	X-sect irreg, often overstepped	Bifurcations form net like systems	——	Lime mudstone/calcarenite, intraclasts, shell debris, planar and x-bedding graded or massive	Flute grooves/prods, bottom and sides	Mud crack/ripples found on cut surf, some modified by combustion, tidal flat cut into cohesive beds
Tucker, 1968	Channels Longitudinal Groove Casts	3 m wide, 30 cm deep Up to 10 cm wide	Box-shaped or rounded Semicircular	Poorly exposed, at least 2 3m long ——	Both are para to ripple paleocurrents, perp. to shoreline	Coarse grnd, horiz lam, cmmoclst LS	—— ——	May be tg grooves/flutes, some certainly flutes, Groove structures no explanation
Van Eden, 1970	Longitudinal Ridge and Furrow	D=6cm, mutual dist. ~20 cm	Sharp, V-shaped x-sect	para for few sq m, crescent-shaped cast upcurrent	Mutually actional, local relief and vegetation	Casts on base of overlying SS, no detail	——	Veg leaves river overflow cuts gutters
Van Straaten, 1954	Longitudinal ripples	W=1.5-6cm, Amp=0.2-2cm, R=10-12	Symm w rounded crests and troughs	Remarkably straight crests, parallel for >10m	Para to tidal currents, perp to shore, perp to fossil ripples in adjacent sand patches	——	——	Weak and rare formed, modern tidal flat WL is steeply
Whitaker, 1973	Gutter casts	Ave W=8cm, D=4cm	Smooth, symm or asymm w/ vert to overhanging walls	Straight, parallel and widening	18-30° more easterly than groove orientation	Graded bioclastic LS, calc SiSt, convex up laminae, x-lams, horiz, concave up lams, along fossils para gutter	Traces (Chondrites), grooves, prods	Ripped tops PC up to 80° from gutter trend, x-sect of fill differs from gutter walls by 30-60°
Williams, 1881	Channel-fillings	W=3-8 or 9ft, D=6-18in	Rounded, symm	Extend for m-km of 100ft	Numerous examples are para to each other	Parallel lam SS, cc incl, wavy laminated	Fine grooves diagonally oriented	Helical flow, tg number in beach sh
Winchers, 1973	Rinnen	W=20-380cm, D=20-75cm	Symm or asymm triangular, U-shaped or box-shaped	Many are >40m long, few sinuous, change in x-sect	Oriented roughly offshore	1 example x-lam, pebble layers found where x-bedding dips	——	Width-depth ratio chart
Wood and Smith, 1957	Groove Cast	D=0.25 in., W=0.5-1 in (ave)	——	Parallel sided, rectilinear ridges, Lasts mm	Para to flutes/bounce casts vary by 30°, these cross-cut	Greywacke, same grn size as bed above	Minor ridges that vary along length	Cut by mudstone chips leaving ridges, Chips worn down and incorporated into SS
	Shooting Flow Cast	Up to 4 in. deep, 1 ft wide	——	Persistent for full length of outcrop	——	——	Minor longitudinal marks on surface	——
Worsely, 1971	Prods	——	——	——	Well oriented, para to transported body	Casts on base of siltstone beds, no detail	——	——

There are two main phases in the development of these gutter casts: erosion, followed by deposition. The timing between erosion and deposition not only may be difficult to ascertain but also may vary from bed to bed. Goldring and Aigner (1982) present criteria for recognizing time breaks between erosion and deposition. These criteria include: (1) fine-grained and banded (heterolithic interlamination) fills, (2) the history of colonization and/or trapping of organisms, and (3) evidence of predepositional bioturbation. Close examination did not reveal any fine-grained gutter casts, and there is no sign of predepositional colonization, borings or burrows. The burrows on the base of the gutter casts are considered postdepositional because: (1) they are not fluted, and (2) they extend only a limited, yet consistent, depth below the ancient sediment-water interface. A preliminary study of the sandstone beds in F.A. 2 by the author and G. Narbonne (data not included in thesis) indicates that the depth of burrowing by infauna during the deposition of the Lower CIF was ~3-4 cm. Sandstone beds greater than this thickness show no evidence of postdepositional burrowing. This is consistent with data from the gutter-cast beds. All of the above observations support a relatively short time between cutting and filling of the gutter cast beds in F.A. 2.

In some CIF beds steep side walls are obviously due to differential compaction (Figure 4.11c), while many clearly represent an original erosional geometry (Figure 4.11e,h). Goldring and Aigner (1982) consider sandstone gutter casts, especially with steep to overhanging margins, as early-filled structures. Overhanging walls must have been very common in the CIF potholes, because many if not most pot casts are tilted and/or widen downward. Even in quite cohesive sediments, however, such steep walls would not be expected to endure the combined influence of waves and sediment-laden currents for a prolonged length of time.

The process of fluvial pothole erosion was thoroughly covered by Alexander (1932), who studied the potholes found in bedrock in glaciated regions. His conclusion

that these were formed by the grinding action of tools (sand to boulder size) carried by stationary eddies replaced the longheld belief that they were formed by vertically plunging water (see review by Higgins, 1957). The characteristics of bedrock potholes are remarkably similar to the pot casts from F.A. 2, and are considered good analogues in terms of process. One major difference is that the CIF potholes were eroded into a semicohesive to cohesive substrate of clayey silt, and because of this, currents alone could form a pothole without the need of a large tool. The presence of delicate groove marks on the side of the CIF pot casts indicates that sand-sized sediment may have aided in the erosion of the pothole as an abrasive agent. Alexander (1932) demonstrated that the flow within potholes takes the form of a jet that enters at one side of the pothole and spirals downward along the outer wall to form a vortex, with flow returning upward through the center of the vortex. The axis of the vortex is not vertical, but forms a spiral. "The working end of this axis is obliquely directed and off center at the bottom of the tube, and this off-center position moves about the axis of the pothole as it is deepened. The spiral vortex acts as a sort of spiral tool and under favorable and constant conditions drills into the rock in 'corkscrew' fashion, thus giving rise to spiral fluting" (Alexander, 1932, p. 322). The pattern of grooves and the geometry of some pot casts in the CIF indicate a similar origin.

The occurrence of a spiraling or ropelike pattern of grooves on the soles of gutter casts has led to the suggestion that they are formed by helical flow of currents moving parallel to the long axes of the gutters (Williams, 1881; Schroder, 1965; Bridges, 1972; Whitaker, 1973). Other authors (Kuenen, 1957; Wood and Smith, 1957; Prentice, 1962; Aigner and Futerrer, 1978) describe parallel or near-parallel orientations of sole markings (grooves, prods, flutes) that also argue for unidirectional flow as the agent of erosion. On the other hand, Allen's (1962) 'elongate flute marks' have unoriented prod marks and Bloos's (1976) gutter casts have bidirectional prod marks, which raises the possibility of erosion by multidirectional and bidirectional currents. The longitudinal grooves of the CIF

gutter casts — and the one example with suggestions of a spiral pattern — argue for erosion by unidirectional flow.

Another indication of unidirectional flow is the observation that some gutter casts originate from potholes. Aigner and Futterer (1978) noted gutter casts in the field that had pot casts at one end and gradually died out at the other. They suggested that these potholes and gutters are produced by currents interacting with obstacles forming horseshoe hollows that were later developed into channels in a downstream direction. They simulated these conditions in the laboratory and created what they considered similar-looking potlike and channellike scours. In the few examples in the CIF in which a gutter cast is seen to originate from a pot cast, the pot cast was on the southwest end of the structure, which would support unidirectional flow toward the northeast. The origin of gutter casts outlined by Aigner and Futterer may be applicable to only a small percentage of CIF gutter casts. The main evidence against such an origin for most of these gutter casts is that (1) there are very few examples in which gutter casts are directly associated with potholes, (2) many gutters are very extensive and of remarkably uniform width for several meters, and (3) some gutter casts are wider than any of the observed potholes.

In Aigner and Futterer's experiments the hollows (potholes) that formed around obstacles became deeper on their upstream end and shallower on their downstream end, where they eventually graded directly into a gutter. The resulting 'tilt' of the hole (central axis plunging upstream) corroborated their field observations in which pot casts were similarly tilted with respect to the inferred (unidirectional) paleocurrents. If, as the work of Aigner and Futterer indicates, the 'tilts' of pot casts have paleocurrent significance, then the bimodal-bipolar data on pothole tilt for F.A. 2 (Figure 4.12a) would suggest the influence of bidirectional currents such as tides (the strong mode to the southwest would suggest more active flow to the northeast, as the experimental data suggest 'upcurrent' tilting). This means either: (1) flow was bidirectional, (2) both unidirectional and bidirectional currents were operating at different times, or (3) the polarity of the tilt of a pothole can vary under

unidirectional flow (i.e., central axes of adjacent potholes tilt upstream or downstream). The third possibility is preferred based on the lack of supporting evidence for bidirectional flow and the facts that: (1) the pinchouts and bifurcations of gutter casts are preferentially oriented toward the northeast, (2) those gutter casts that originate from pot casts suggest northeast flow, and (3) the sandstone beds with which these features are intercalated contain abundant evidence that the initial stages of deposition of these beds took place under northeast-directed unidirectional flow (see Chpt 4). The possibility that some or all of the pot and gutter casts were formed by oscillatory currents (waves) is considered unlikely given the features observed.

The differences in the plan-view geometry of CIF gutter casts may be related to flow parameters such as velocity, intermittency of flow, and patterns of water motion. Straight, well oriented forms suggest regularity in flow, possibly associated with longitudinal vortices (Williams, 1881). Sinuous gutter casts show numerous features, in addition to spiraling grooves, that suggest erosion by longitudinal vortices in a manner similar to modern rivers (see Bridges, 1972; Whitaker, 1973). It is likely that the narrow, sinuous gutters in the CIF formed from slower flows, and that wider, straight to highly irregular channels form from faster flows that would tend to cut through the meander bends.

As discussed above, the 'depositional' stage in the formation of the gutter casts appears to be one of rapid accumulation of sediment in freshly eroded scours. The massive and uniform parallel-laminated nature of most of the sandstone beds supports this interpretation. The ripples found on the top of several gutter casts are considered wave ripples on the basis of their symmetrical profile and their extremely large spacing-to-height ratios. These ripples and the oscillatory-flow-type ripple laminae in the upper portions of some gutter casts indicate that waves influenced the late stages of deposition of these gutter casts. The thickness of the gutter casts (generally 10-100 times thicker than the associated sandstone beds) and the evidence for rapid infilling of the gutters is compatible with

deposition under thick sediment flows that deposited sediment almost exclusively in the gutters.

In at least one example (Figure 4.12a), it appears that the erosional structure may not have been completely filled during the depositional stage, so that the lip and the shape of the scour affected the flow. The pattern of ripple-crest orientations in Figure 4.12a, with crests transverse to the gutter in its narrow portion and nearly parallel to the gutter in the widened portion, indicates that both directions of oscillatory flow may have operated simultaneously, as neither set of crests shows evidence of superposition or modification of the other. This variable orientation of ripples is best explained as a wall effect that is in part governed by the overall geometry of the scour.

In summary, the characteristics of the gutter and pot casts indicate that: (1) despite some ambiguous, and possibly contradicting, evidence, erosion is thought to have been caused by unidirectional (possibly reversing ?) flow; (2) the timing between erosion and sediment infilling was short, possibly only a few hours or less; (3) in at least a few cases, notably the small sinuous gutter casts, longitudinal helical flow is suggested; (4) potholes were formed by stationary eddies in a manner similar to that outlined for bedrock potholes, except with currents causing the erosion (with sand as an abrasive) instead of a large tool; and (5) gutters are well oriented in a southwest-northeast orientation (present-day coordinates), and related evidence suggests paleoflow toward the northeast.

4.16 DISORGANIZED BEDS

4.16.1 Disturbed Beds

These beds consist of slightly to moderately disturbed interbeds of siltstone (S0) and sandstone (S1, S2 and S3) (Plate 20). The deformed units are underlain and overlain by horizontal strata, but lack a well defined scar or slip surface (shear plane) and therefore have subtle boundaries. Internally these units contain planar laminae at angles to bedding, swirled and rolled laminae, and small recumbent folds. There are also planar-tabular clasts and partially detached layers with relatively sharp terminations of laminae. Disruptions are such that the various pieces of gently folded strata may either be visually reconstructed or generally placed in an undisturbed stratigraphic framework by the recognition of marker beds. Folds in the strata lack a consistent vergence.

Examples of these beds vary from poorly exposed strata like that at FD-392, where a thin zone of bedding is slightly undulose, to well exposed cases like FD-168.2, where over 80 m of excellent lateral exposure shows evidence of progressive deformation along the bed (Figure 4.14). The exposure at FD-168.2 has been divided into eastern and western sections (Figure 4.14). The fundamental feature of this exposure is a clearly defined lateral change from (a) well-bedded sandstone and siltstone layers with disturbed bedding (eastern section), to (b) a clast-rich siltstone bed (Raft-Bearing Bed — Section 4.16.3) (western section). An 8-10 m covered interval separates these sections. Marker horizons that stratigraphically overlie the raft-bearing siltstone bed in the western section can be traced across to the eastern section. The western section is described below in Section 4.16.3.

At the eastern limit of the eastern section only the slightest hint of bedding disruption can be detected. This disruption is stratigraphically equivalent to the top and central parts of the siltstone bed in the western outcrop. Thin beds are locally gently folded, resembling small ball-and-pillow structures. From east to west across this eastern section

PLATE 20: DISTURBED STRATA AT FD-168.2 9 (FA 2)

a: The slightly deformed zone is in strata beneath the hammer handle. Stratigraphic top up. Hammer is 38.5 cm long.

b: The disruption of bedding appears to be confined to a small area above the scale, with the laterally adjacent strata on the left side of the photo relatively undeformed. Stratigraphic top is up. Scale is 15 cm long.

c: Isolated synclinal forms of disrupted strata, as seen in this photo (arrow), are common along this horizon. Stratigraphic top is up. Scale is 15 cm long.

d: A more strongly-deformed portion of this horizon is shown beneath scale Stratigraphic top to upper left. Scale is 15 cm long.

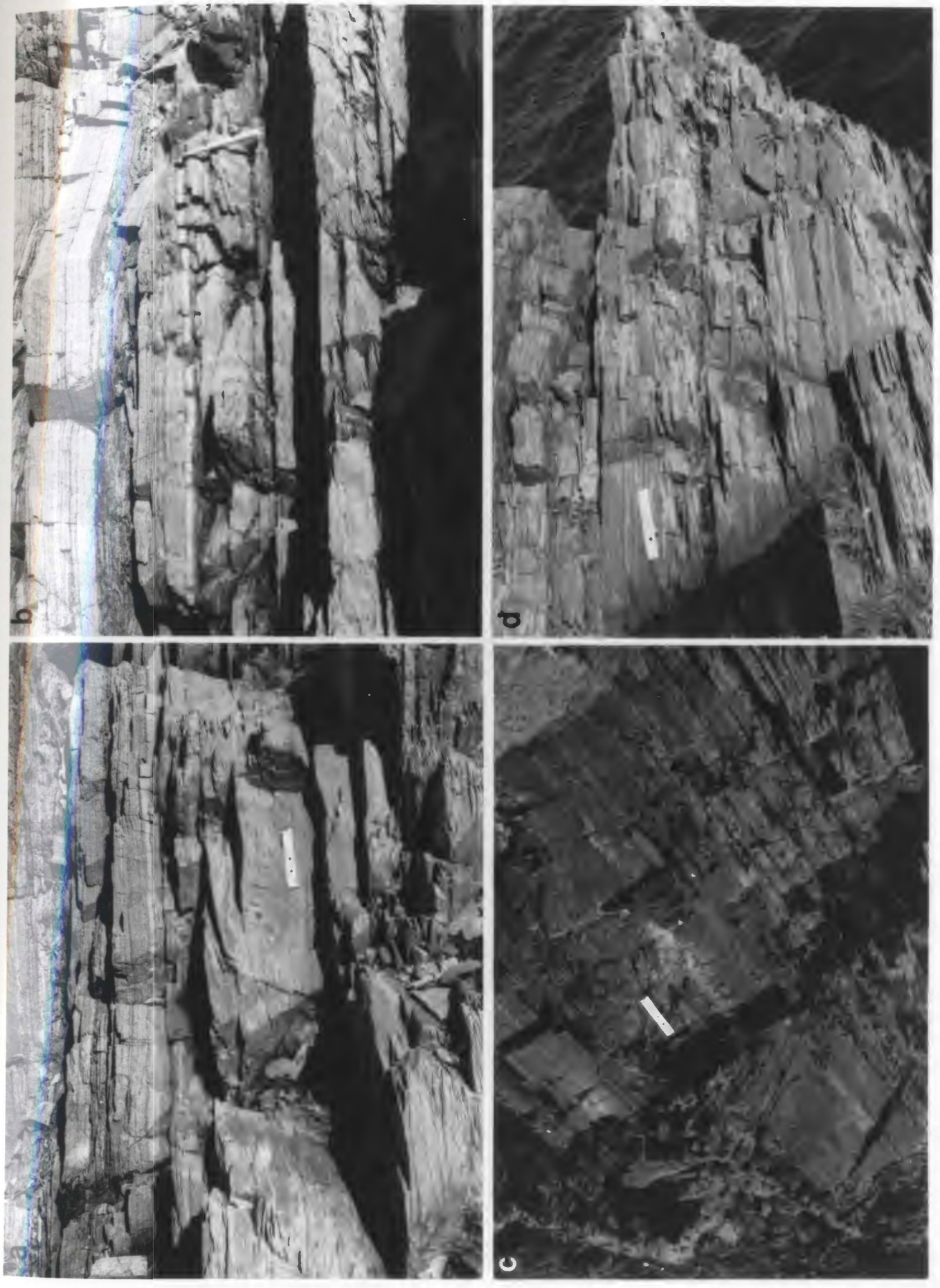
b
d
c

Figure 4.14: Sketch of outcrop at FD-168.2. The outcrop is divided into an 'Eastern Outcrop' of disturbed bedding and a 'Western Outcrop' with a raft-bearing bed. These two exposures are separated by a covered interval several meters wide. The exposure is otherwise continuous, with the exception of a covered interval of 1.8 m between B and B' in the Eastern Outcrop. The scale for each part of the outcrop is the same.

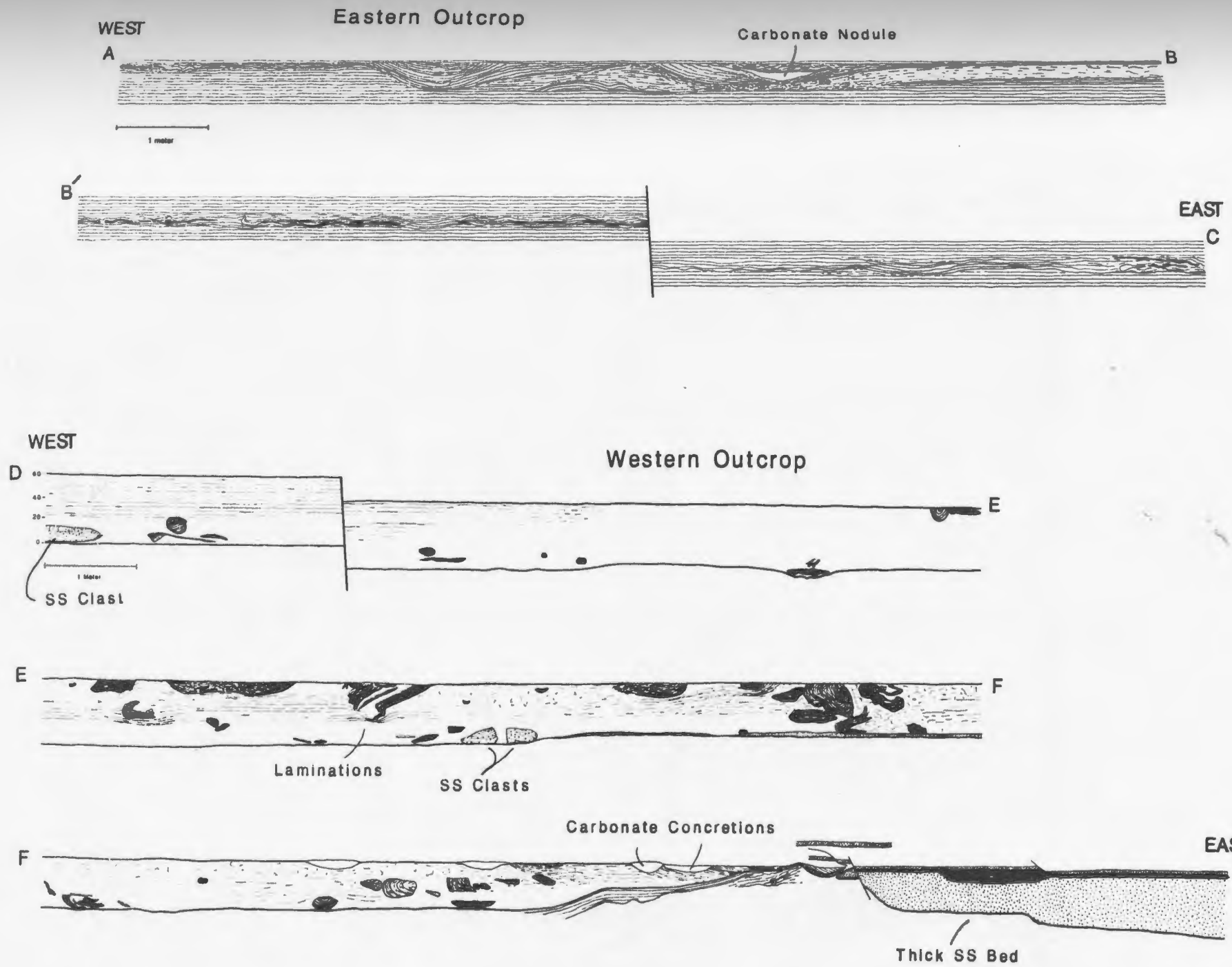
Eastern Outcrop
WEST
A
Carbonate Nodule
B
1 meter
B'
EAST
C
WEST
Western Outcrop
D
E
SS Clast
E
F
Laminations
SS Clasts
Carbonate Concretions
F
EAST
G
Thick SS Bed

there is a progressive increase in the intensity and depth of bedding disruption. Within this deformed zone, packages of strata are rolled and bent (Plate 20a) locally into widely spaced synformal structures (Plate 20d). At the westernmost part of this eastern section (Figure 4.14, A-B), a stratigraphic interval equivalent to the upper 25-30 cm of the correlative raft-bearing bed (Figure 4.14, D-G) is disrupted strata. It is more difficult to visually reconstruct original configurations of strata in this area.

There is little evidence to suggest significant lateral transport. There is no well defined basal shear plane within the exposure. The base of the deformed strata is locally better defined than elsewhere, but would be considered a shear zone, and not a shear plane.

4.16.1.1 Process Interpretation: Disturbed Beds

The deformation associated with these beds was largely plastic, as indicated by the folded, rolled and swirled laminae. The sediment was likely semiconsolidated at the time of deformation. Brittle deformation was minor.

The lack of a well defined scar or slip surface (shear plane) and the lack of consistent vergence to the folds suggest that significant downslope movement did not occur. In the western half of this eastern exposure (Figure 4.14, A-B) the base of the disturbed zone is better defined, and may represent a shear zone. This may mark a lateral transition from more or less in situ deformation to sliding, or downslope movement.

The semiconsolidated nature of these beds at the time of deformation, and the apparent lack of significant downslope motion, suggest that much of the disruption took place by loading, possibly associated with high pore pressures and partial liquefaction.

4.16.2 Unifite Beds

These beds are composed of graded to nongraded siltstone and silty mudstone characterized by a lack of obvious internal structure or very subtle fine lamination (Plate 21). The bases of these beds are very sharp, and the tops vary from gradational to very sharp. The lower parts of these beds are generally too fine grained to allow exposure of soles by preferential weathering. These beds range from 10-70 cm in thickness, averaging 36 cm at the FD exposure. These beds are called 'unifites', a descriptive term applied in the deep basins of the Mediterranean by Stanley (1981, p. 77) to "structureless or faintly laminated, often thick, mud layer[s] revealing a fining-upward trend".

These beds are normally tabular over the full extent of their outcrop exposure. At FD-27.3, however, there is an abrupt termination of a 35 cm thick siltstone bed. This bed is macroscopically homogeneous and devoid of 'rafts' or clasts of any kind. The bed is tabular in shape over most of the outcrop. At its eastern limit the bed dramatically pinches from its normal thickness of 35 cm to zero thickness over a distance of 1.4 meters (Plate 21a,b). The geometry of the bed over this interval is that of a channel margin with a horizontal upper surface and a gently curved, downcutting lower surface against which underlying sandstone and siltstone beds terminate. The exact geometry of this pinch-out is slightly obscured by weathering and cleavage effects.

Cut and polished slabs provide information about the internal sedimentary structures of these beds that cannot be gained from the outcrop due to the fine grain size and homogeneous texture of these beds. Slabs reveal beds ranging from (a) megascopically structureless, to (b) very slightly laminated, to (c) subtly graded and laminated, to (d) graded and laminated with current-generated structures. Figure 4.15 shows an end-member classification scheme for these unifite beds; a continuum of bed styles exists between the end members.

PLATE 21: UNIFITE BEDS (FA 2)

a: Channel-like margin (arrows) of macroscopically homogeneous unifite bed at FD-27.3. Stratigraphic top is up. Scale has 10 cm divisions.

b: Close-up of "a" showing termination (arrows) of surrounding, flat-lying beds. Stratigraphic top is up. Scale has 10 cm divisions.

c: Polished slab of Type 1A unifite from PM-100.2. Close examination reveals no visible size grading or lamination. Note the extremely sharp base and top and small pseudonodules detached from base of the bed. Stratigraphic top is up. Scale is 1 cm long.

d: Disorganized beds from FD-~72-76 with unifite bed (on right below white-weathering quartzitic bed) and raft-bearing bed (underneath notebook). These beds are considerably thicker than the surrounding thin beds of sandstone and siltstone. Stratigraphic top is to upper left. Notebook is 18.5 cm long.

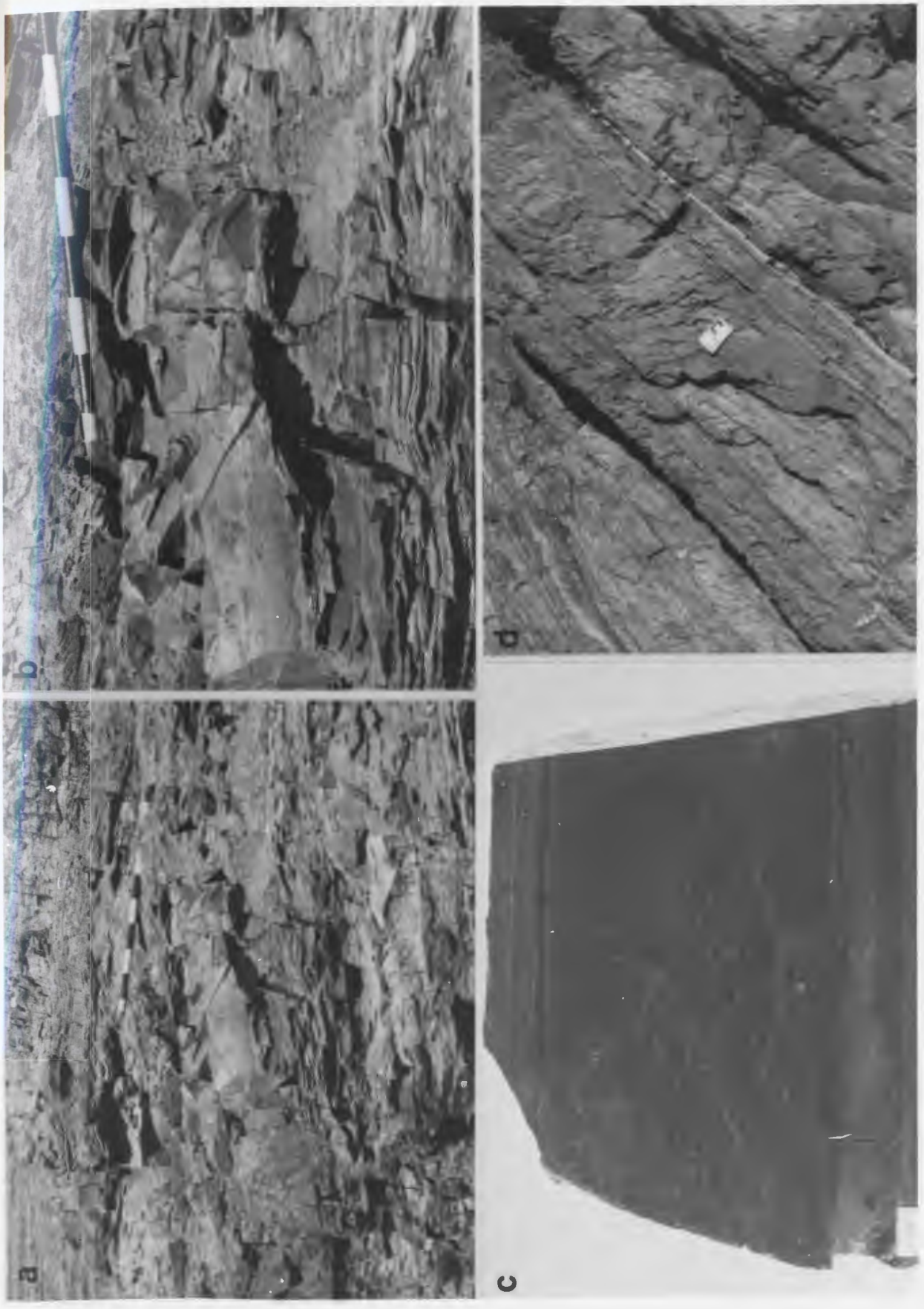
b
a
d
c

Figure 4.15: Unifite classification scheme and process interpretation. Dominant characteristics of the three unifite types are given on the right. These represent a continuum of bed types whose characteristics are thought to be a function of degree of water entrainment and the extent to which turbulence is a factor (represented on left). Turbidite divisions for Type 3 Unifites are those of Stow and Shanmugam (1980).

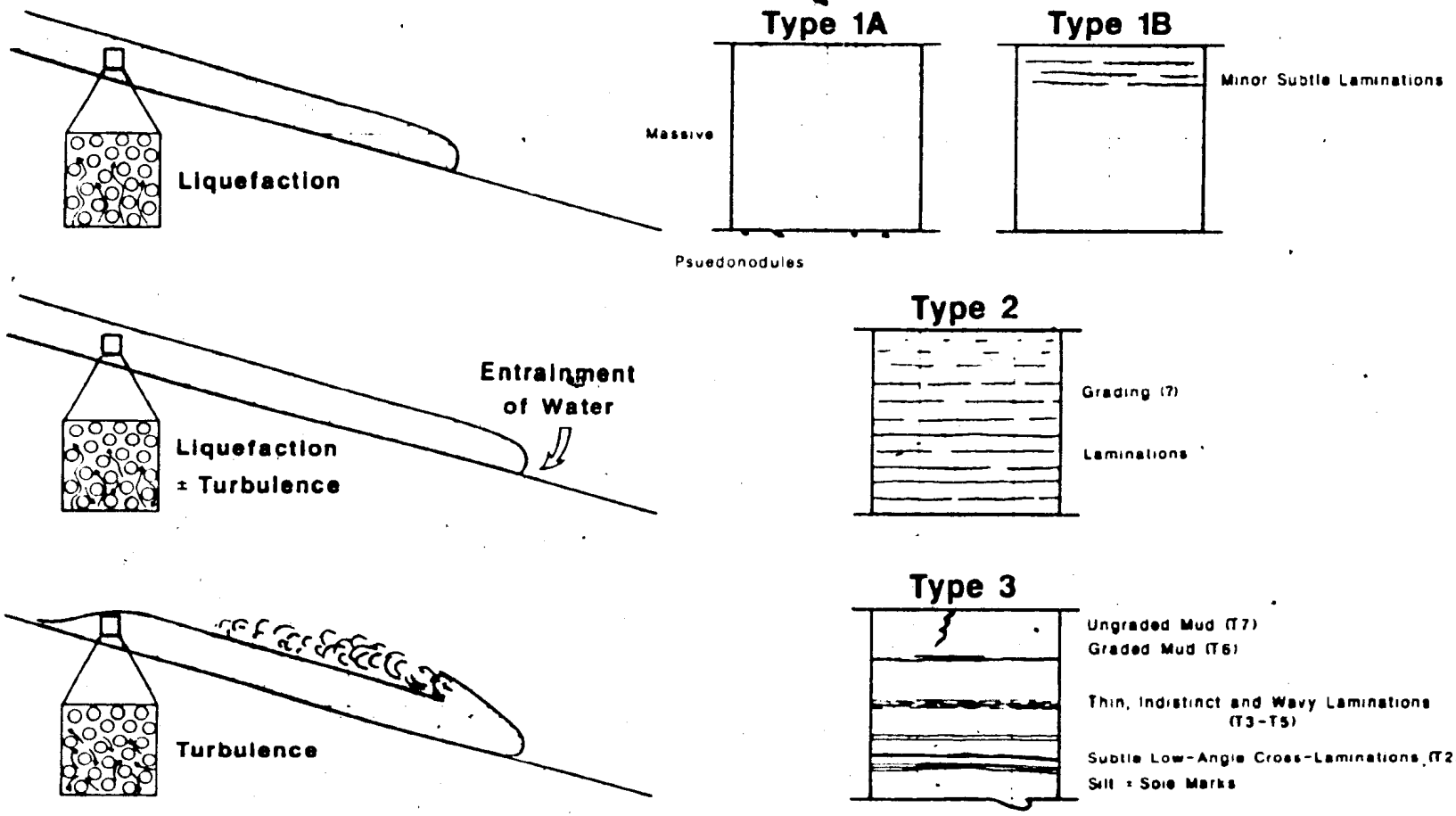
Liquefaction
Type 1A
Type 1B
Massive
Minor Subtle Laminations
Psuedonodules
Entrainment
of Water
Liquefaction
± Turbulence
Type 2
Grading (?)
Laminations
Turbulence
Type 3
Ungraded Mud (T7)
Graded Mud (T6)
Thin, Indistinct and Wavy Laminations
(T3-T5)
Subtle Low-Angle Cross-Laminations (T2)
Silt ± Sole Marks

Type 1 unifite beds are massive (1A) or very cryptically laminated (1B). Plate 21c shows a polished slab of a 14 cm thick, type 1A siltstone bed from PM-100.2. No grading or unambiguous lamination are visible. Throughout the bed are slightly elongate shale particles of coarse silt to very fine sand size. These particles appear to define a slight bedding-parallel fabric, and in the lower half of the bed, possible vague laminae by variation in their abundance. The base of this bed is sharply defined and displays flame and load structures. Small pseudonodules detached from the base of the bed are present in all stages of formation. The upper surface is remarkably sharp and planar.

PM-98.9 is another bed that appears structureless in the field — it contains only the slightest hint of lamination (Type 1B) on the slabbed surface. Where this bed is locally carbonate-cemented, however, it appears to contain very thin laminae.

Type 2 unifite beds contain subtle laminae but lack strong grading. Subtle grading, if present, consists of a slight increase in clay content at the top of the bed. Laminae, defined by subtle changes in grain size, are found near the base in some beds (e.g., FD-21.3) and near the top in others (FD-65.95). Very thin coarse silt laminae are locally visible in outcrop. As a rule, laminae are not detectable on the outcrop, but they are in slabs, where they may be quite subtle.

Type 3 unifites are characterized by distinct lamination and grading, both of which may or may not be detectable in outcrop. Groove marks, flute marks and small gutter casts have been noted on the base of two beds (FD-33.4, FD-51.4). Typical of these Type 3 beds is a 55 cm at FD-33.4 that contains a lower division of silty mudstone with indistinct and wispy silt laminae and a thick, light-green claystone cap. Large carbonate concretions formed within this upper mudstone unit.

Grading (clayey siltstone to claystone) is obvious in a slab of a bed at FD-27.3. This bed contains a variety of subtle internal structures. A 5 cm green clayey siltstone layer forms the base of the bed. The central part of the bed (~19 cm) is an interlayering of light

green silty mudstone with: (a) thick (up to 1 cm), distinct, regular to slightly irregular silt laminae, and (b) thin, streaked, indistinct silt laminae. The former are extensive but are neither planar nor uniform in thickness. These thicker laminae locally contain subtle low-angle cross-laminae. The upper 8-11 cm of the bed consists of light green claystone. The base of this claystone division is gradational from the silt-streaked mudstone below. The entire bed, including the claystone cap, contains black clay particles of fine sand to silt size. A fairly uniform concentration throughout the bed indicates that their abundance is not a function of grain size. The claystone cap contains a few large grains, the largest being a very coarse sand-sized, black, siltstone rock fragment.

A few exceptional examples of Type 3 unifites consist of relatively coarse-grained sediments with well preserved internal sedimentary structures. A 35 cm thick siltstone bed at FD-174.4 has a 2-7 cm thick graded layer at its base. Parallel-laminated medium sand in the lower few centimeters is overlain by a form set of small current ripples with variable crest height in fine sandstone. The overlying clayey siltstone is macroscopically devoid of structure except for grading to a claystone cap.

'Slurried beds' described by Hiscott and Middleton (1979, p. 317-318) are similar in thickness to the CIF unifite beds, and are similarly devoid of internal sedimentary structures. The beds described by Hiscott and Middleton are sandier and in some cases have characteristics in common with the raft-bearing beds (e.g., large rip-up clasts). The 'slurried beds' described by Burne (1970, p.221-226) are also similar to the CIF unifites, in that the lower division of these beds consists of clayey siltstone with a normally graded sand component overlain by a thick division of mudstone. The top of these beds contains radially arranged cross-laminae of fine sand or silt that are interpreted as sand volcanoes formed by eruption of water from the compacting deposit. The central parts of the beds described by Burne (1970) contain vertical tubes of lighter-colored sediment representing fluid-escape pillars. These beds also contain variable quantities of mudstone fragments.

4.16.2.1 Process Interpretation: Unifite Beds

Unifite beds were clearly deposited by single events. This conclusion is based on their: (1) anomalous thickness relative to the beds in surrounding strata, (2) relatively homogeneous grain size and texture, (3) normal grading (some beds), and (4) sequences of sedimentary structures (some beds). The thicknesses of these unifite beds are at least an order of magnitude greater than the average thickness of the beds with which they are found. Aside from reworking of sediment by burrowing organisms, of which there is no evidence in this case, there are no reasonable mechanisms by which one could generate these anomalously thick, very homogeneous, fine-grained beds except by resedimentation of unlithified sediment. The differences in internal structure between the various types of unifites argues for variation in depositional processes, which will be outlined below.

These CIF beds are closely similar to unifites described from the Mediterranean Sea by D. J. Stanley and others (Rupke and Stanley, 1974; Stanley, et al., 1980; Stanley, 1981; Stanley and Maldonado, 1981). Stanley's (1981, p. 79,81) idealized unifite sequence consists "...at the base, of graded, faintly laminated, silt and silty clay ..., and trends upward to more subtly or not graded, structureless and somewhat finer-grained mud...". Most of the unifites fall into one of two groups: (1) uniform, subtly graded muds, and (2) faintly laminated and graded muds. In comparison with published 'ideal' fine-grained turbidite sequences, Stanley associates the first group with Piper's (1978) E_2 and E_3 divisions and Stow and Shanmugam's (1980) T_6 and T_7 divisions. The faintly laminated beds are compared to the E_1 to E_2 and T_4 to T_6 divisions of these workers, respectively (Stanley, 1981, p. 79). When compared with the fine-grained turbidite models of Piper (1978) and Stow and Shanmugam (1980), the massive, nonlaminated Type 1 unifites (e.g., PM-100.2, see Plate 21c) would correspond with the E_3 and T_7 divisions of their idealized sequences, respectively.

The model for deposition of the CIF unifites (Figure 4.15) emphasizes the continuum of characteristics of these beds and relates them to a continuum of proposed processes. The primary controls on the presence or absence of features such as grading and lamination are: (1) concentration in the flow, and (2) the degree to which turbulence becomes an effective mechanism of grain support. In this model, concentration and level of turbulence are a function of the degree of entrainment of ambient fluid.

A turbidity-current model is considered inappropriate for Type 1 beds because of: (1) their sharp upper surfaces, (2) the lack of internal structure, especially lamination and grading, and (3) paleoenvironmental considerations. Instead, deposition from high-concentration liquefied flows (Lowe, 1976a) is advocated. Sediment concentration and grain size are primary controls on the character of the deposit from a liquefied flow. Deposition from liquefied flows can be described in terms of a hindered-settling model (Middleton and Southard, 1984, p. 4-18 to 4-21) in which the interfaces between clear water and the dispersion, and between the dispersion and the deposited sediment, converge, with the dispersion maintaining constant density throughout. In high-concentration flows with limited size range, there will be limited size segregation and therefore little or no grading (Middleton and Southard,1984, p. 89). High concentrations would certainly preclude any traction processes (Middleton and Hampton, 1973; Lowe, 1976a). Flows of this nature would be nonturbulent (Lowe, 1976a). Lower concentrations and a more variable grain size distribution would lead to turbulence and the development of grading, lamination and other internal sedimentary structures.

Terzaghi (1950, 1956) pioneered the work on spontaneous liquefaction and described natural occurrences in Holland and Norway. Liquefied flow results from gravity-induced movement of a liquefied sediment, or from liquefaction of a moving sediment slide (Lowe, 1976a, p. 289). Spontaneous liquefaction takes place in loosely packed or metastable sediment subjected to vibrations or other stresses (Seed, 1968). Attainment of a

stable configuration with closer packing and reduced pore volume requires the expulsion of water from the system. The active displacement of water creates high pore pressures that suspend and separate the grains, counteracting normal stress and allowing fluid behavior. Theoretically, liquefied flows will therefore flow on very gentle slopes, until the excess pore-fluid pressures dissipates.

Grain size is one of the major controlling factors determining (a) the length of time that a liquefied flow experiences high pore pressure, and therefore (b) the distance of flow. Using a velocity estimate of 1.7 m/s, derived from laboratory and field data for liquefied flows, Lowe (1976a) predicted that the distance of travel for a 1 m-thick flow of 0.0625 mm silt could be as great as 2.0 km. The influence of grain size is dramatically illustrated by his estimation of only a 19 m flow distance for very coarse sand (0.1 mm) under the same conditions.

Middleton (1969, 1970) calculates the time for pore pressure to dissipate within a liquefied flow using the equation:

$$T=dp/v \qquad \text{(eq. 1)}$$

where T is time, d is thickness, p is the fractional increase in porosity produced by liquefaction, and v is upward flow velocity of escaping pore fluid. For 0.1 mm sand, he gives estimates for p and v of 5 per cent and .01 cm/s, respectively. Based on grain size and compaction data from carbonate concretions in the CIF, a precompaction thickness of 75 centimeters (twice average bed thickness) is considered a reasonable estimate for the unifites of FA 2. The time for dissipation of excess pore pressure using these values would be approximately 375 seconds. Pore-fluid expulsion times are a direct function of permeability, which means that the addition of small clay-sized particles, which clog pore throats, will cause a marked increase in these times. Because the above estimate is valid for well sorted 0.1 mm sand, and the CIF unifites are mostly clayey siltstones, it follows that the expulsion of pore fluid in the unifites must have taken considerably longer than the time calculated above.

Van der Knaap and Eijpe (1968) make a similar attempt to calculate 'relaxation' time using the equation

$$T=4L^2/c\pi^2 \qquad \text{(eq. 2)}.$$

In this equation, the relaxation time T, is calculated from the sediment thickness L, and a relaxation coefficient c, calculated from various empirical data. Results are given for coarse and fine sand. Using the lower of the c values from the two runs on fine sand given in their Table 1, and a thickness of 75 centimeters, gives a relaxation time of 161.7 seconds. The permeability of the sediment was measured and used by Van der Knaap and Eijpe to calculate c. From their formulas it is clear that a linear relationship exists between permeability and relaxation time. If the permeability of the CIF unifites was an order of magnitude smaller than the well sorted fine sand used in their experiments (a reasonable assumption), then the relaxation time would increase an order of magnitude to 1617 seconds (~27 minutes).

Lowe (1976a) gives resedimentation rates (resedimentation time divided by bed thickness) for liquefied beds of uniform spheres (from Andersson, 1961). Assuming that the dissipation of pore pressure calculated in the above equations would result in deposition, Lowe's (1976a) resedimentation rates should be comparable with those given above. For grains of diameter 0.0125 mm, the resedimentation rate is 2.7 s/cm. This means a bed 100 cm thick would resediment 270 seconds after liquefaction. This value is very close to 287.2 derived from eq. 2. A similar thickness of 0.0625 mm silt would resediment in 1188 seconds (~20 minutes). The addition of a component of fine silt and clay in the CIF unifites would substantially increase this estimate of resedimentation time. Even the shorter times calculated for fine sand are considered by Morgenstern (1967) and Middleton (1970) to be large enough "...to permit acceleration of the liquefied sand mass down slope to velocities where turbulence and mixing with the overlying water might lead to the formation

of a turbidity current" (Middleton, 1970; p. 267). This would imply that, on theoretical grounds, the transformations envisioned for the CIF unifites (Figure 4.15) are feasible.

If the interpretation of Type 1 unifites as products of liquefied flows is correct, then these beds were deposited prior the onset of turbulence in the flows, because of either: (a) the early dissipation of excess pore pressures, or (b) a decrease in slope before a significant distance of flow. Either of these alternatives are plausible. The average slope on continental shelves is only 0° 07' (Morgenstern, 1967), but much higher slopes are found in certain nearshore environments (Terzaghi, 1956; Moore, 1961). Estimates of slope during the deposition of the lower part of member 2, based on the pebbly mudstone bed at FD-48.45, range from 0.126° to 2.746°, with 0.584° considered the most reliable estimate (see Section 4.14). The reductions in slope necessary to trigger deposition of the Type 1 liquefied flows might have been fairly small, and could be reasonably explained by local variations in shelf topography.

The graded and laminated Type 3 unifite beds are believed by the author to represent those liquefied flows that became turbulent (Figure 4.15), and transformed into turbidity currents. This transformation was likely accomplished by entrainment of water, causing reduction of density and viscosity and allowing Reynolds number to increase above values for onset of turbulence.

Structures found in beds like FD-27.3 compare favorably to those described for fine-grained turbidites (Piper, 1978; Stow and Shanmugam, 1980), and thick unifites described by Stanley and others (see Stanley, 1981). This bed is characterized by distinct grain-size breaks, but overall it can be said to exhibit distribution grading, considered a feature of low-density turbidity currents (Middleton, 1967). The thin, regular to irregular laminae found above the lower silt layer in this sample are comparable with Stow and Shanmugam's (1980) T_2 and T_3 laminae, even to the point of having subtle low-angle cross-laminae. Laminae of this type indicate that silt grains, deposited from suspension, were subsequently moved as traction load, possibly as low-amplitude climbing ripples.

Indistinct and wispy laminae in this bed would correspond to Stow and Shanmugams' T_4 and T_5 units. Laminae of this type are attributed by Stow and Bowen (1980) to sorting processes acting on silt grains and clay flocs in the viscous sublayer. The graded claystone cap simply represents suspension deposition of clay-sized particles from the dilute tail of the flow. The T_2 — T_5 laminae locally occur out of sequence. Factors responsible for these perturbations in sequence include fluctuations in flow velocity, and nature of the bed surface (i.e., cohesive or granular or rippled) (Stow and Shanmugam, 1980, p. 39).

Visual estimates of the clay content of Type 3 beds range up to 50% (claystone caps may constitute as much as 15% of the thickness of the bed). Depending on the sediment concentration in the flows, there is the potential for the depositing flows to have some degree of strength, assuming that at least some percentage of this clay was unflocculated. Whatever strength these flows may have had, it was not great enough to suppress turbulence — the well developed grading and silt/mud laminae clearly reflect turbulence during deposition.

Type 2 beds exhibit characteristics transitional between Type 1 and Type 3 beds. These beds are therefore interpreted as the deposits of flows that reached only an intermediate stage in the evolution of a liquefied flow (Type 1) to a fully turbulent flow (Type 3). The development of lamination and minor grading indicate that some size segregation occurred. Development of these features is again considered a byproduct of entrainment of water into a liquefied flow (Figure 4.15). Grain-support mechanisms in Type 2 flows probably included: (1) high pore fluid pressure and (2) minor turbulence.

4.16.3 Raft-Bearing Beds

Raft-bearing beds consist of siltstone, similar in character to the unifite beds, that contain clasts, or 'rafts', of thinly interbedded sandstone and siltstone of the same nature as the interbedded lithologies (S0, S1, S2 beds). These raft-bearing beds also display laminae

that are commonly swirled and deformed around clasts (Plate 23c,d). Bedding thickness varies from 16 to 110 cm, with an average of 45-50 cm. Where laminae are cryptic and rafts are particularly sparse, the distinction between these beds and unifite beds is sometimes difficult. In extreme cases, such as FD-67.3, the bed would be essentially indistinguishable from those in the unifite subfacies (Type 1 or 2) except for a few small rafts in the upper part of the bed. One must therefore assume that there is a continuum between these bed types.

Rafts are found in a variety of sizes, from a few centimeters across to large ones 60 X 20 cm in cross section. The rafts occur as contorted masses, angular fragments, and coherent slabs with relatively intact, gently folded to flat-lying bedding (Plate 22g,h, 23a,b). These rafts are found at many positions within a bed. Some beds, such as FD-88.2, have rafts concentrated in the lower third of the bed (Plate 22c), while others (e.g., FD-360.15) have rafts concentrated in the central and upper parts of the bed (Plate 23d). Slabbed surfaces of some of these rafts show features similar to the 'flow rolls' of Sorauf (1965), including basin-shaped curvature, local development of tight folds, and fault offset of laminae (Plate 22e). Redeposited carbonate nodules have also been noted in these beds.

Grading, where present, is defined by a thin layer at the base only, with the remainder of the bed macroscopically ungraded. An example is a 20 cm bed at FD-71.7 that has at its base a 1.6 cm parallel-laminated fine sandstone division with a sharp base and an indistinct top. At one point along the base, there is a thin (1cm thick), tapered pod of well sorted, coarse sand 26 cm long (Figure 4.16, Plate 22d). The lower laminae in the fine sandstone division terminate against the side of the pod, while the upper laminae drape over the pod. Another example of grading is found at FD-251.05, where a 40 cm siltstone bed with abundant rafts has a graded division 2 cm thick consisting of well sorted, coarse to fine sandstone, at its base.

Several raft-bearing beds show signs of incorporation by gravitational sinking of laminae/beds from above. For example, very thin fine sand beds that overlie a raft-bearing

PLATE 22: RAFT-BEARING BEDS (FA 2)

a: A 45 cm-thick bed at FD-223.6 (arrows at top and base) with rafts (including transported carbonate nodules) at all levels within the bed. Stratigraphic top to upper left. Notebook is 18.5 cm long.

b: Close-up of "a" shows downward loading of overlying sandstone bed and depression of laminae directly underneath the load feature. Stratigraphic top is up. Scale is 2.5 cm wide.

c: This one meter-thick raft-bearing bed at FD-88.2 has rafts confined to the lower 30 cm of the bed. Stratigraphic top to upper left. Notebook is 18.5 cm long.

d: Thin pod of well-sorted coarse sandstone and overlying fine sandstone laminae at the base of a 20 cm-thick bed at FD-71.7. Sketch is given in Figure 4.16. Stratigraphic top to up. Scale is 15 cm long.

e: Slabbed surface of raft from FD-276.75. Note tight fold on right and fault offset of laminae on the left. Width of photo is 21 cm.

f: Large raft at the top of a bed at Brunette Island (BI-38.4). Division on scale (lower left) is 10 cm. Stratigraphic top to up.

g: This bed at FD-360.15 has an extremely sharp base and large contorted rafts that are confined to the central and upper portions of the bed. Stratigraphic top to up. Scale is 15 cm long.

h: Same bed as "g" with large bowl-shaped raft. Stratigraphic top is to upper right. Scale (on left) is 2.5 cm wide.

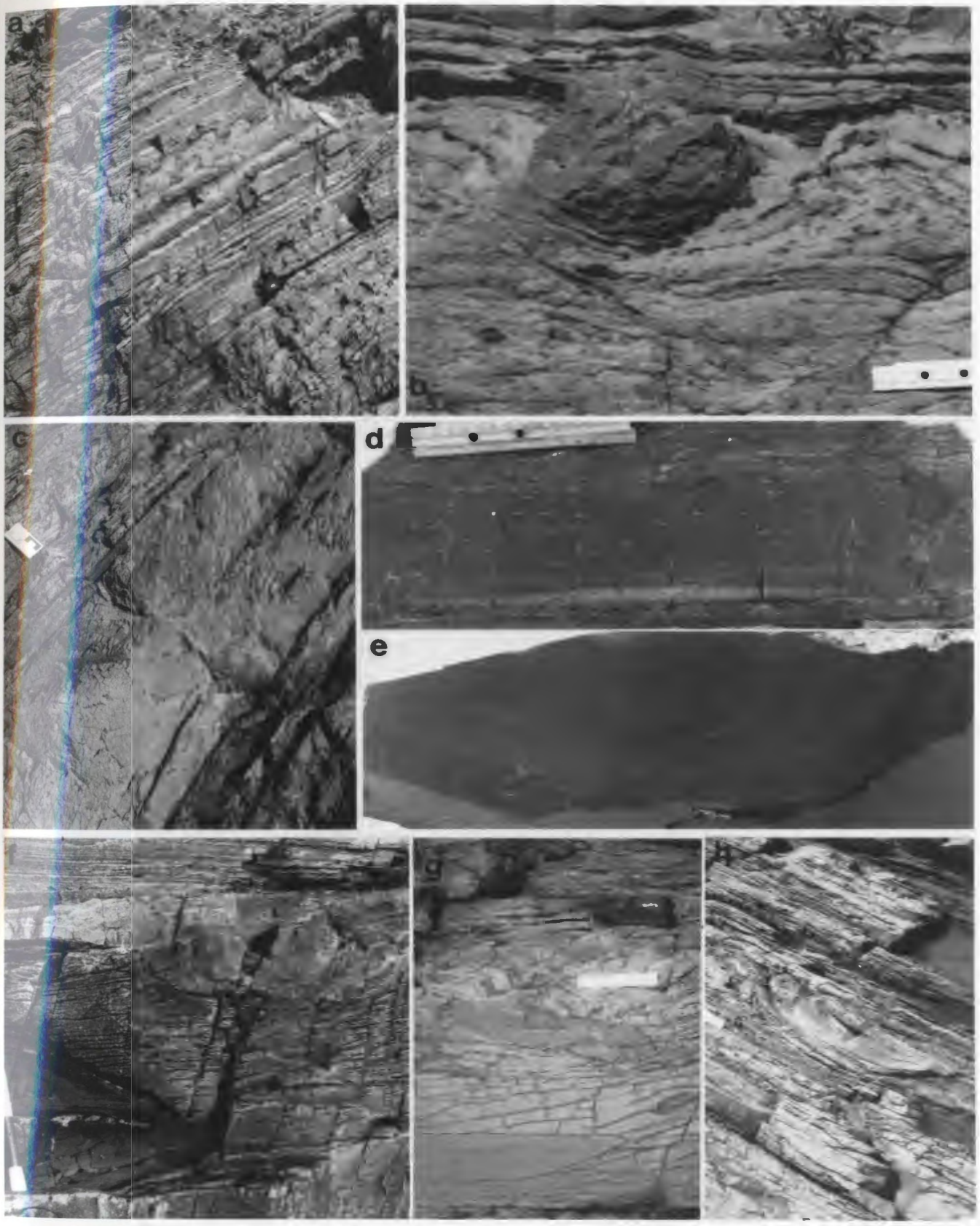
a
b
c
d
e
f
g
h

PLATE 23: RAFT-BEARING BEDS CONT'D (FA 2)

a: This photo of the bed at FD-168.2 (Figure 4.14) shows a large folded raft at the top of the bed and two rounded sandstone clasts on the right ("A" and "B"). See text for details. Stratigraphic top is up. Scale is in 10 cm divisions.

b: Close-up of top of large raft in "a". The laminae/very thin beds within the raft are sharply terminated at the top, including the carbonate nodule directly above the scale. Stratigraphic top is up. Scale is in cm.

c: This 65 cm-thick bed at FD-74.0 contains swirled laminae and rafts at all levels within the bed. Rounded corners of folded strata on seen on the right, while more angular clasts are found above scale. Stratigraphic top is up. Scale is 15 cm long.

d: This photo of FD-168.2 shows the well-developed lamination that characterize this bed. These laminae are bent over and under the rafts. Stratigraphic top is up. Scale is in cm.

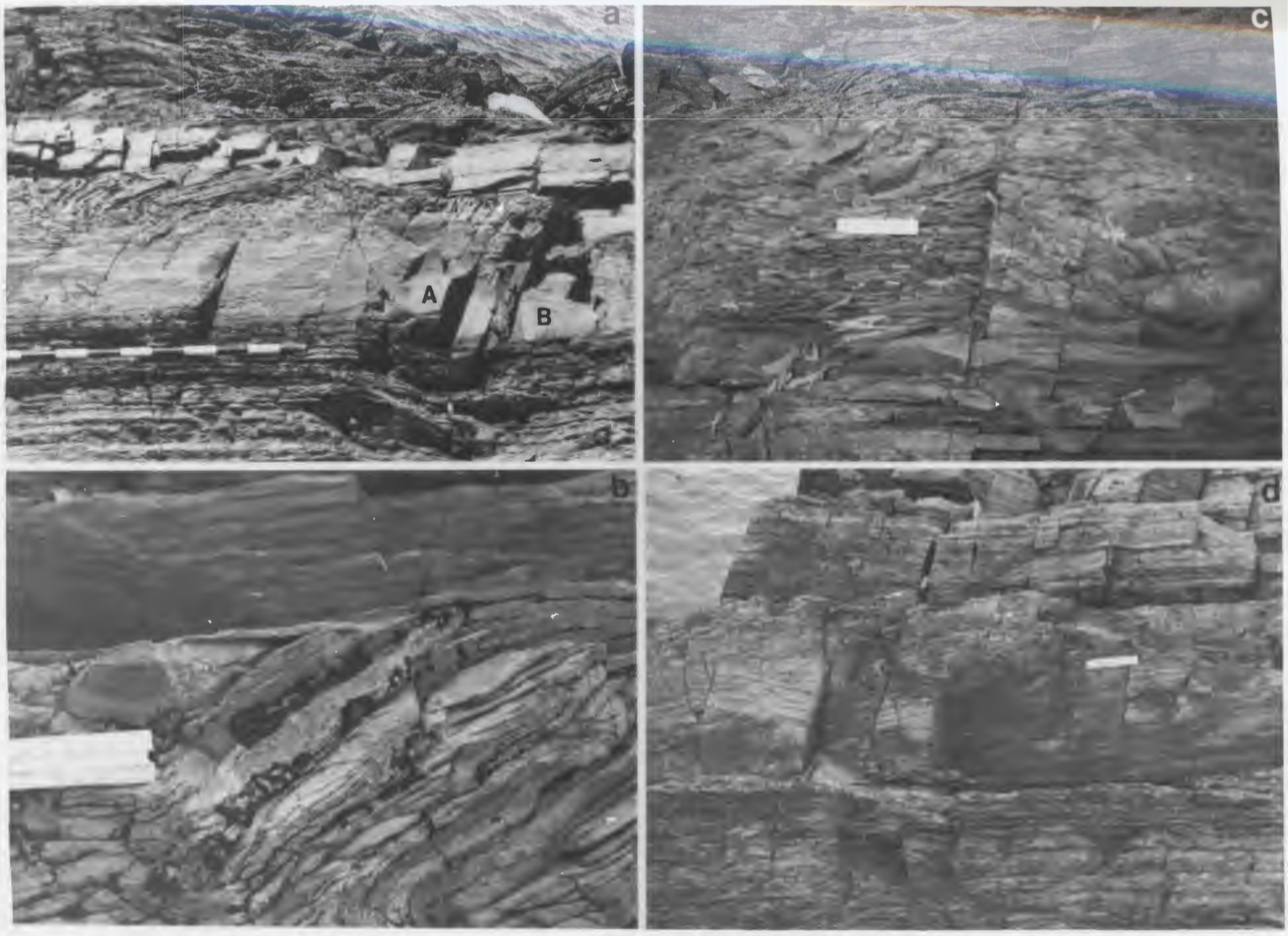
a
A
B
c
b
d

Figure 4.16: Sketch of 20-cm-thick raft-bearing bed at FD-71.7. Lower division of fine sandstone at the base contains wavy and climbing-ripple cross-lamination and pods of white-weathering coarse sandstone.

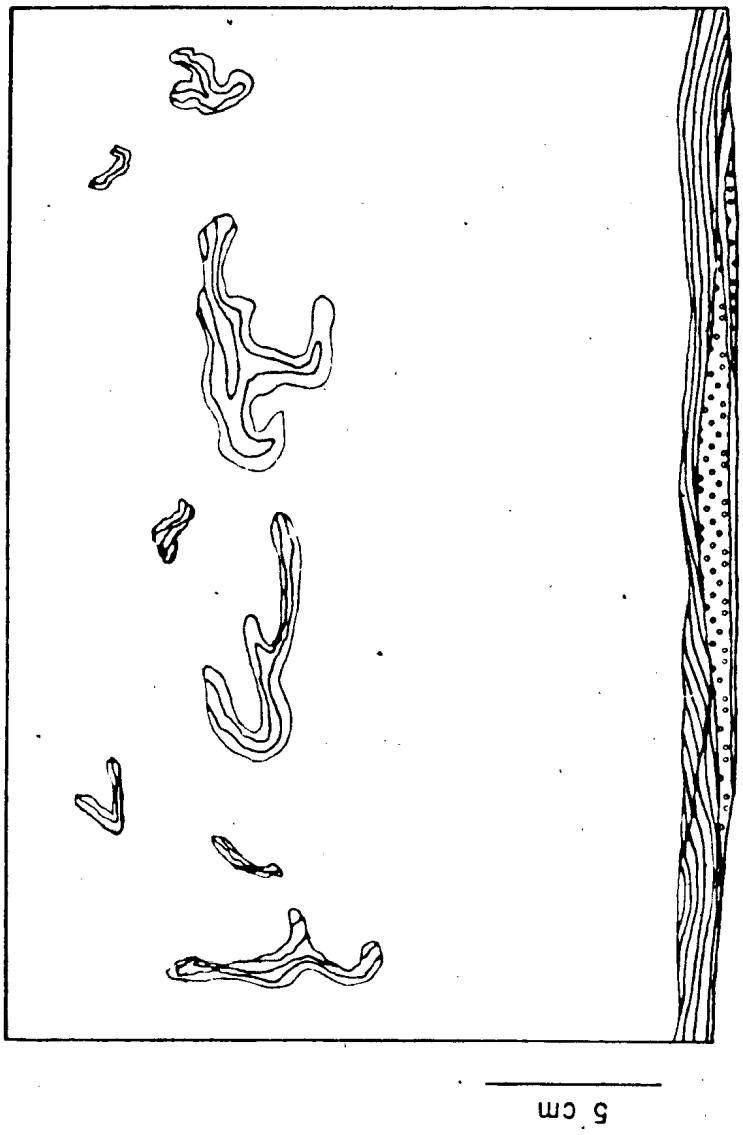

FD-71.7

5 cm

bed at FD-54.7 are in various states of disruption, and in various states of detachment and loading into the upper mudstone division of the underlying bed. This is the only example noted in which there are irregular patches of sandstone without sharp boundaries. At the top of FD-223.6, the overlying very thin bed of sandstone and siltstone is bent into a downward-oriented ball that has internally broken and distorted sand laminae (Plate 22a,b). The spacing of laminae shows a fourfold decrease directly under the ball and a bowing up of laminae on either side of the ball (Plate 22b).

Raft-bearing beds are generally tabular. FD-360.15, for example, may be traced for over 120 m without any change in thickness. In a few cases thickness and character of these raft-bearing beds change along their length. The best exposed example, FD-168.2, is described below.

As mentioned in the Section 4.16.1, the outcrop at FD-168.2 has been divided into an eastern section with disturbed bedding and a western section with a raft-bearing siltstone bed. A detailed drawing of this western section is given in Figure 4.14 (D-G). Most of this exposure consists of a 55-60 cm thick raft-bearing siltstone bed. Near the eastern end of this exposure the siltstone bed pinches out. The change in thickness across the outcrop (from west to east) is fairly gradual, becoming more dramatic over the last 3 m. At the point of termination, a massive, gray, fine sandstone bed cuts downsection toward the east. The top of this sandstone bed is planar, with the exception of a 10 cm deep, meter-long, siltstone-filled scour. This bed increases thickness rapidly, from 0 to 30-35 cm over a distance of 60 cm, maintains constant thickness for 1.5 m, then increases in thickness to 60 cm thick before the end of the outcrop.

Measurements were taken from a marker horizon several meters below this bed to: (1) the top of the siltstone bed at the far western end of the outcrop, and (2) the top of the disturbed zone on the far eastern end of the outcrop, where bedding is only mildly disrupted. The measurements were made ~80 m apart and were different by only 1 cm.

The siltstone bed at FD-168.2 is noteworthy in many ways. Firstly, the top of the bed is remarkably planar. The top of one large raft of interlaminated sandstone and siltstone shows evidence of sharp truncation where the upper bed surface cuts indiscriminately across the laminae at a high angle to the internal bedding of the raft (Plate 23b). Secondly, across most of the outcrop the bed contains laminae that are best developed in the central part of the bed (Plate 23a,d). The lower part of the bed is locally massive, while the upper part either has well defined laminae like the central part of the bed or, more commonly, a swirled, partly homogenized texture. In several examples, laminae in the central part of the bed, directly under large rafts, are curved downward and compressed (Plate 23a). Laminae are similarly bent over some rafts, but are slightly less deformed in these situations (Plate 23c). In one case, the central laminae are bowed up over a clast projecting upward from the massive lower part of the bed.

Restricted to the lower part of the bed are rounded, gray, faintly laminated sandstone clasts that are similar in color, grain size, and texture to the thick sandstone bed at the eastern end of the western outcrop (Figure 4.14; Plate 23a). The laminae in these clasts may be gently folded or planar. In either case, they terminate abruptly at the edges of the clasts.

Most contorted sandstone/siltstone rafts are found in the upper part of the bed. One raft consists of a fairly coherent bedded slab that, with slight reconstruction, samples a stratigraphic thickness of approximately 25 centimeters. Several fragments of carbonate concretions are present as clasts within this bed.

There are few good ancient analogs for these raft-bearing beds. The 'slurry sandstones' of Hiscott and Middleton (1979, p. 317) consist of "...fine to coarse sand dispersed in an abundant muddy matrix". Most of the beds are structureless, though a few have "...swirled internal structure, distorted fragments, convolute bedding and

pseudonodules...". These beds contain large slabs of shale and siltstone up to, and greater than, 1 m in length.

The 'rubble bedding' of Morris (1971, p. 415-418) consists of nonoriented, angular to rounded, unfolded to rolled-up blocks of sandstone or thinly bedded sandstone/shale set in mudstone of different character. The mudstone may be massive, folded and squeezed fissile shale, or seemingly uncontorted shale. The clasts, derived locally from adjacent strata, may be as large as 150 m or more across. The 'slurried bedding' described by Morris (1971, p. 418-419), was deposited by flows of friable sand that incorporated varying quantities of mud, both nonlithified and lithified.

The 'fragmented bedding' of Wood and Smith (1957, p. 172) consists of muddy siltstone, 0.3-0.6 m thick, with a thin graded layer at the base and tabular to strongly curved fragments of bedded sandstone and mudstone above. Sandy patches with indefinite boundaries were also noted. These patches are analogous to the sand patches described above for FD-57.4. Patches such as these were <u>not</u> noted in any other CIF beds.

The 'slurried beds' of Burne (1970, p. 221-226, see his Figure 8) consist of three units: (1) a graded layer of sand in muddy siltstone matrix with few shale clasts, (2) muddy siltstone with 'partially digested' and contorted fragments of mudstone and fluid-escape pillars, and (3) cross-laminated sand volcanoes. Some aspects of the CIF beds are analagous to features from his two lower units. His upper unit is not found in the CIF beds.

4.16.3.1 Process Interpretation: Raft-bearing Beds

Raft-bearing beds display a fairly wide range of characteristics that indicate deposition by a variety of processes. At one end of the spectrum are beds that would be unifites if not for the presence of a few scattered rafts. Other beds contain well developed lamination and large and abundant rafts. The presence of these clasts at all levels in these

beds, especially at the top, indicates that the sediment had strength. Strength is considered a property of debris flows. The sedimentary structures/fabrics of debris flows include: matrix support, random fabrics, variable clast size, variable matrix, rip-up clasts, rafts, inverse grading, and possible flow structures (Nardin et al. 1979). Many of these characteristics are typical of the raft-bearing beds.

In debris flow, strength and buoyancy effects, necessary for the support of large clasts, are provided by muddy matrix. Strength is divided into cohesive strength, from electrostatic attraction of clay minerals, and frictional strength, due to grain-to-grain contacts; according to Trask (1959) and Pierson (1981), frictional strength (due to grain-to-grain contacts) is significantly more important as a means of clast support than cohesive strength.

Particle support in debris flows may be derived from: (1) frictional resistance to settling, (2) matrix cohesion, (3) buoyancy, (4) elevated pore pressures, and (5) dispersive pressure (Pierson, 1981). Any combination of these mechanisms may have been important in the transport and deposition of the raft-bearing beds, with the exception of dispersive pressure. The strength of a fluid strongly influences the role of dispersive pressure in a flow. Once grains are dispersed in a matrix-rich slurry, matrix strength can support them, and dispersive pressure becomes less significant because grains are not free to collide as frequently or with significant momentum (Middleton and Hampton, 1973). The presence of clay in the matrix of the raft-bearing beds makes dispersive pressure an unlikely means of significant particle support .

The rafts in the CIF beds are clearly ripped-up pieces of previously deposited sediment. Early-formed carbonate nodules in the sediment were also eroded and carried in these flows. The rafts were in a semilithified state at the time of their erosion and deposition. Most rafts deformed plastically, if only at their edges. A few of these rafts may be load features like the examples of Sorauf (1965) (e.g., FD-223.6). Incorporation of younger, overlying sediment by postdepositional liquefaction and loading occurred in a

disorganized manner (FD-54.7) or as well defined load balls (FD-223.6). Wood and Smith (1957) and Hiscott and Middleton (1979) describe load balls and pseudonodules, respectively, from similar types of beds. The rarity of sand patches (as in FD-57.4) in raft-bearing beds indicates that the incorporation of completely unlithified sand was minimal. Other workers have described large, variably deformed rafts of eroded underlying or adjacent sediment from a wide variety of debris-flow deposits. These include 'slurry' deposits (Wood and Smith, 1957; Burne, 1970; Morris, 1971; Hiscott and Middleton, 1979), pebbly mudstones (Dott, 1963; Stanley, 1975; Alvarez et al., 1985; Hein, 1985), and clast-supported to matrix-supported conglomerates (Fisher, 1981). In debris flows, large clasts can be moved at low velocities on low gradients (Middleton and Hampton, 1973).

The dramatic manner in which the laminae at the top of FD-223.6 change spacings under, and next to, the large load ball (Plate 22b) indicates that the depression of laminae under this feature and other rafts was caused by early loading, with possible later exaggeration by compaction. Such postdepositional plastic behavior might explain why no beds display clasts that project above their top. Debris flows (or any hybrid flow that has enough strength to carry large clasts) can contain clasts that project above the top of the bed (Johnson, 1970). Many of the raft-bearing beds have rafts exclusively in their upper parts, often right at the top, but none that project above the top of the bed. One possibility is that the flows were not dense enough to support projecting clasts: the clasts were at best neutrally buoyant. A second alternative is that a small percentage of these clasts were projecting above the top of the bed at the time of deposition, and that these clasts either: (1) sank down into the underlying sediment shortly after deposition, (2) were erosively planed off, or (3) both. Evidence that clasts may have been projecting above the surface of some beds is found in a large raft at the top of FD-168.2. Strong depression of the laminae below this raft indicates gravitational sinking after deposition. Sharp termination of the bedding in this raft clearly demonstrates that strong erosional planation formed the flat upper bed

surface. These data suggest, but do not prove conclusively, that the clasts projected above the top of the bed after deposition.

The outcrop is not extensive enough to prove that these raft-bearing beds were deposited by channelized flows (the best exposure, FD-352, shows over 120 m of constant thickness). The field relationships at FD-168.2 indicate that at least some were deposited by channelized flows. Of the original sediment that must have been excavated to form the shallow channel at FD-168.2, only a small percentage can be accounted for by the rafts. The rest must have been carried downslope, either with the flow, or in part by processes acting prior to arrival of the flow (e.g., slumping). It is remarkable, then, that the stratigraphic position of the top of FD-168.2 is identical to the top of the corresponding slightly disturbed zone to the east. Assuming that before failure and movement of the sediment the sea floor was essentially planar on a large scale, then either the deposition of this bed resulted in no change in topography, or erosive processes subsequently acted on the new depositional surface to reestablish planarity. As stated above, the sharp, planar erosional top to this bed indicates that currents acted to greatly reduce topographic irregularities after deposition.

Flowing debris normally consists of a two-part system: the lower zone is characterized by high shear stress, in which flow is taking place, and the upper zone is a rigid plug that is being carried passively (Johnson, 1970). Deposition occurs by downward growth of the plug as the shear stress drops below the shear strength for progressively lower parts of the flow (Hampton, 1975). Rheological models for debris flow include 'cohesive' models (Coulomb-viscous and Bingham plastic models) and 'dispersive-pressure' models (Shultz, 1984; Lowe 1976b). The muddy nature of the CIF beds indicates that these beds were deposited by flows that exhibited dominantly cohesive-plastic behavior (Shultz, 1984: Type I flow).

Little is known about variations in rheological behavior within individual debris flows, due to the inherent problems involved with monitoring such flows in the field and in

the laboratory. Vertical variations in strength within a flow could be influenced by a number of factors, such as variations in density, viscosity, water content, pore-fluid pressure, texture, and others. The features in the bed at FD-168.2 (Figure 4.14) may be partly explained by rheological variation within the depositing flow. As described earlier, this bed may be very loosely divided into: (1) a lower, clast-bearing, locally massive layer, (2) a laminated, clast-poor, middle layer, and (3) an upper, raft-rich layer with swirled, partly homogenized laminae. The upper part of the FD-168.2 flow exhibited substantial strength, as evidenced by the large size of the clasts it maintained. The disruption of the laminae in this upper layer is most complete in zones where rafts are most abundant (see Figure 4.14). If the flow in this part of the flow was laminar, then the mixing and swirling of laminae was due to interactions among clasts.

The lower, nonlaminated part of the bed also contains scattered clasts, but most of the larger ones can be seen to be lying directly on the lower bed surface. The gray sandstone clasts are found only in this position within the bed (Figure 4.14). The similarity in color, grain size, etc. with the sand body shown in Figure 4.14 suggests that these clasts were derived from the upslope extension of that sand body, or from a similar sand body, when it was in a semilithified state (the clasts have bent laminae). The fact that these blocks were resting directly on the underlying substrate at the time of deposition indicates they were too heavy to be carried by the flow. The presence of other, less dense, rafts on the base of the bed indicates that, possibly as a result of liquefaction, elevated pore pressures or higher water content, the strength in this part of the flow may have dropped significantly in the late stages of deposition, though not completely because there are numerous clasts floating well above the base of this lower layer. Aksu's (1984) description of Quaternary submarine debrites includes those in which he feels the lower part of the flow exceeded the plastic limit and behaved as a liquid, while the upper part of the flow continued to deform plastically. Pierson (1981) and Hampton (1975) both mention liquefaction or fluid behavior in debris flows. Pierson (1981, p. 58) gives three mechanisms that could convert the

gravitational energy of a flow into particle lift: turbulence, dispersive pressure, and dilatancy. These factors would "enlarge the pore space between grains and break grain contacts, throwing more of the load weight on the fluid and effectively causing partial liquefaction of the debris mass" (ibid., p. 59).

Ignoring effects from dispersive pressure, a likely scenario for FD-168.2 is one in which the lower part of the flow experienced a decrease in shear strength to the point where it behaved partly like a liquid. This loss of strength might be attributable to (1) high shear stresses in this part of the flow and/or (2) an increase in water content in the lower layer by incorporation of water below the nose of the flow ('surface transition', Fisher, 1983). The heavier, less buoyant clasts could have then settled to the bottom, while others were maintained above the sea floor. The middle and upper parts of the bed might have been riding as a passive semirigid plug at the time. Coleman (1981) describes mudflows from the Mississippi Delta in which the method of transport involves movement of a rigid plug over and within a zone of liquefied mud. He notes for these flows that "the presence of partially disintegrated rafted blocks suggests laminar or plug flow rather than turbulent flow" (p.74).

An alternative scenario would see deposition of the bed completed without the flow exhibiting any liquid behavior, but with residual high pore pressure in the lower layer that facilitated partial, postdepositional liquefaction. The presence of thin, coarse, sometimes graded layers at the base of some of these beds supports a syn-transport reduction in strength at the base of some of these flows. In these cases, the lower parts of these flows may have become partly turbulent, permitting size grading.

If, at FD-168.2, the disturbed horizon and the raft-bearing bed were formed simultaneously, then this horizon would represent either: (1) the lateral development of a debris flow from an incipient slump, or (2) a difference in deformation style related to a difference in such factors as the local depositional slope, degree of liquefaction, or variation of lithification/sediment strength.

In summary, raft-bearing beds have features that indicate that the depositing flows: (1) had strength (large floating clasts), (2) deformed plastically in places (contorted intraclasts, internal fold and swirl structures, loaded laminae), and (3) were laterally associated with disturbed bedding (of slump origin). These features are best explained by subaqueous debris-flow mechanisms.

4.16.4 Chaotic/Deformed Horizons

Two examples of chaotic/deformed horizons from FD are discussed in detail below. Similar beds were also noted in FA 2 at Brunette Island. At FD-231.1, a horizon 1.7 m thick consists of a lower chaotic unit 30-50 cm thick and an upper siltstone unit 1.2-1.4 m thick (Figure 4.17). The upper siltstone unit contains no macroscopically recognizable laminae. The chaotic lower unit consists of a sandstone bed 0-19 cm thick overlain by large, variably oriented sandstone slabs within deformed interbeds of sandstone and siltstone. The lower sandstone bed displays rapid changes in thickness, mostly as a result of basal erosion (Plate 24c). The upper surface of this bed, however, is not planar. Some clasts at high angles to bedding appear to have pierced down into the sandstone bed and caused sharp reductions in thickness (Figure 4.17). Parts of the sandstone bed appear massive, while others display contorted laminae and ball-and-pillow structures, as well as irregularly shaped clasts and oblate spheroids of carbonate-cemented sandstone. One slab 10-12 cm thick, lying 15 cm above the lower sand bed, is oriented parallel to bedding, and appears to be an 'in-place' erosional remnant of a once more extensive sandstone bed (Plate 24c "a"). Very thin sandstone and siltstone beds that intervene between this 'upper sandstone bed' and the lower sandstone bed are only locally contorted. This upper sandstone bed has light-colored carbonate-cemented laminae in the lower 3-4 cm that are also present in most of the clearly detached large blocks. The variable position of these

Figure 4.17: Sketch of chaotic/deformed horizon. Note dramatic thickening of lower sandstone bed. Laminae in the sandstone clasts match up with upper sandstone bed (on right). Clasts are found in matrix of massive siltstone which forms a 1.2-1.4 m thick bed above. Divisions on scale are 10 cm. Stratigraphic top to upper left.

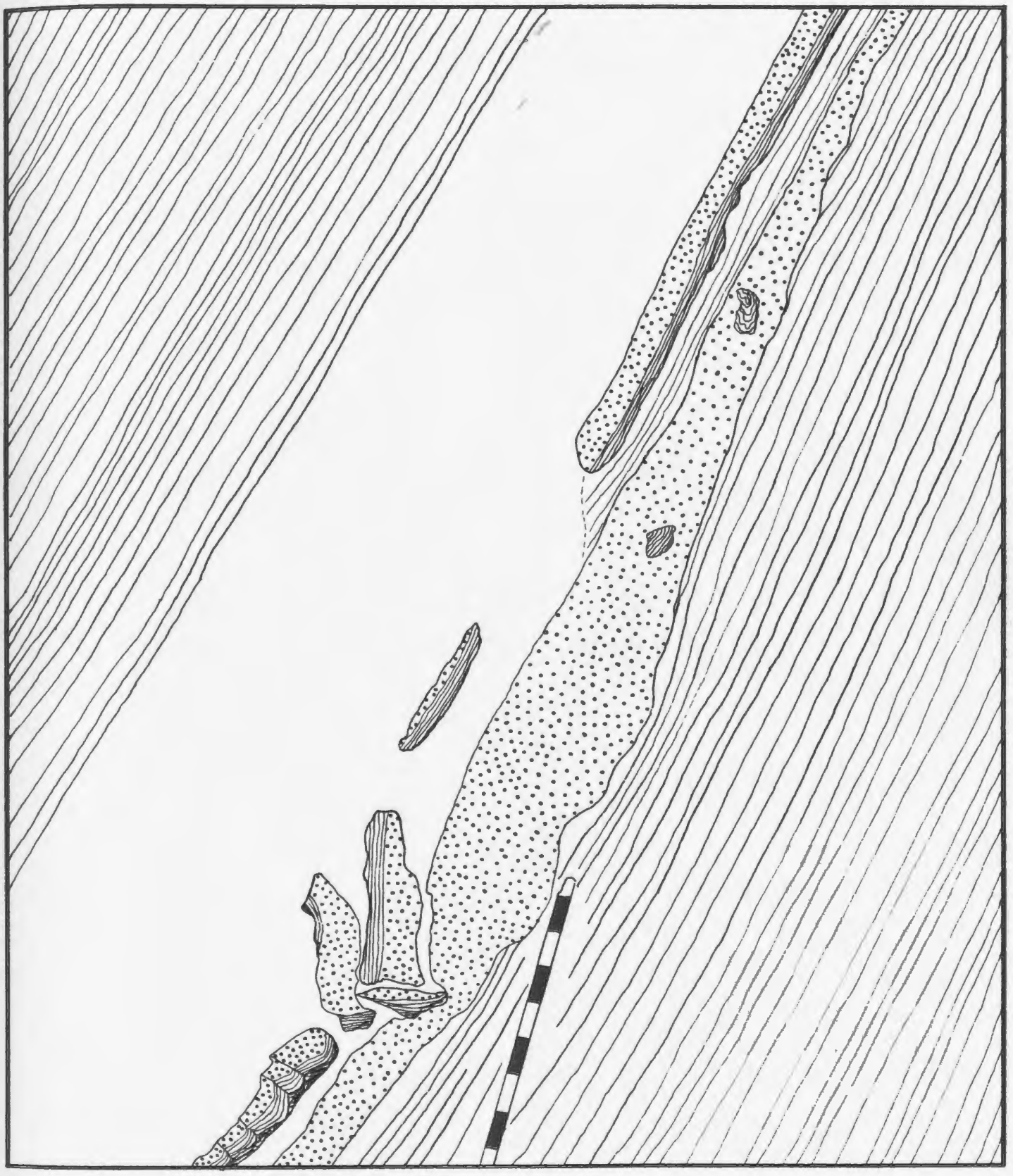

PLATE 24: CHAOTIC/DEFORMED HORIZONS

a: Buckled horizon at FD-346.2 showing large synformal structures to the left of the notebook and increased depth of disruption from top to bottom of photo. Stratigraphic top is to left. Notebook is 18.5 cm long.

b: Close-up of "a" showing hummocky cross-stratified sandstone bed that overlies the buckled surface. Stratigraphic top is up. Scale is 10 cm long.

c: A sketch of this slide horizon at FD-231.1 is given in Figure 4.17. Note thickening of lower sandstone bed, carbonate-cemented lower division of overlying sandstone bed ("a") and fragments of this upper sandstone bed in the lower left of the photo ("b"). The remaining strata in photo to left is structureless muddy siltstone. Stratigraphic top is to left. Divisions on scale are 10 cm.

d: Another view of FD-231.1 with large clasts of sandstone. Bedding is vertical with stratigraphic top to right. Divisions on scale are .10 cm.

e: Close-up of the lower part of "c" showing tabular clasts (outlined in ink) with rounded edges. The carbonate-cemented lower division of the 'upper' sandstone bed in "c" is seen in these clasts and the orientations indicate both lateral and rotational movements. Divisions on scale are 10 cm.

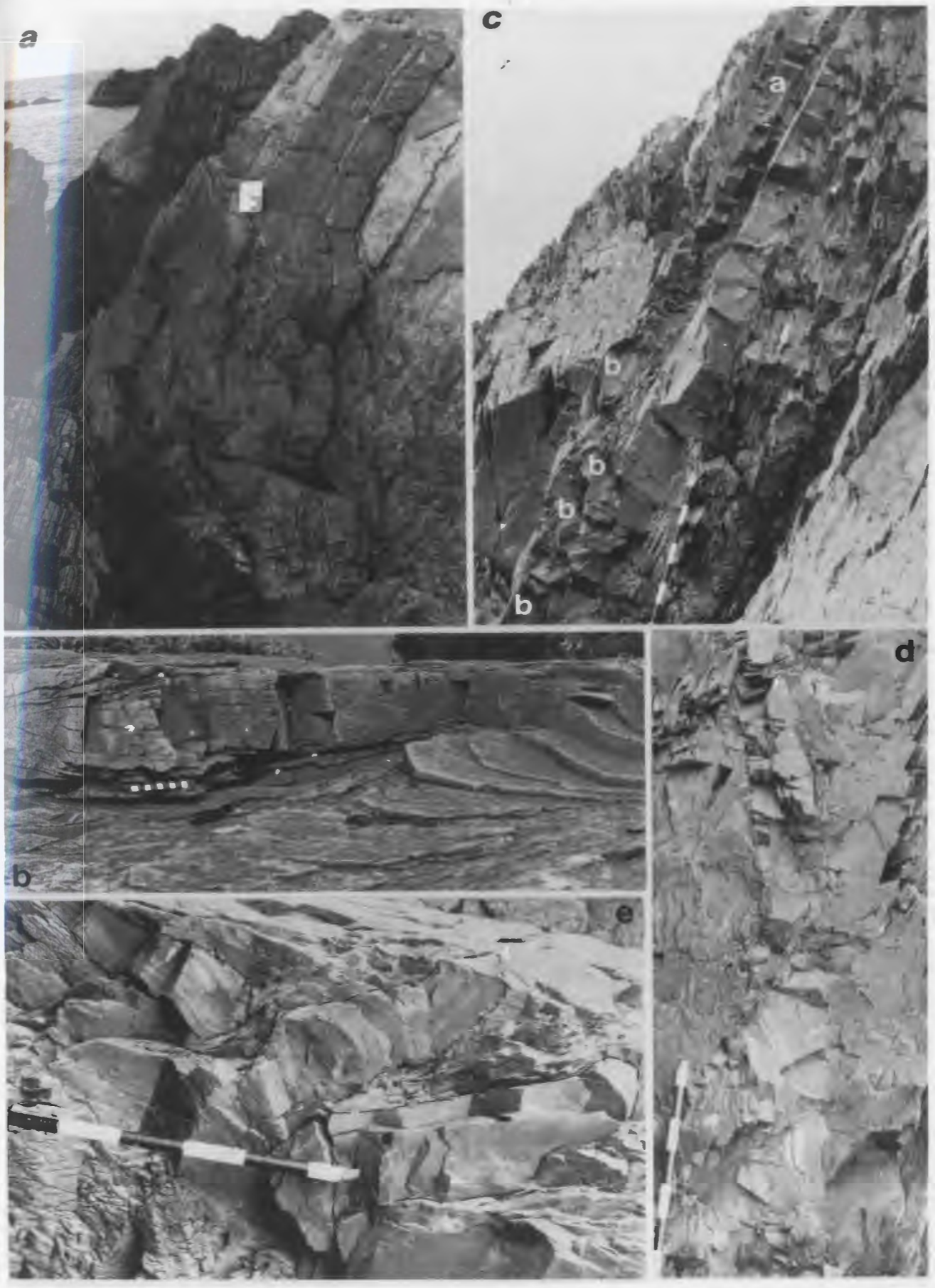
a
c
a
b
b
b
b
b
d
e

laminae in these blocks indicate that some clasts are upside down (Plate 24e). The largest of these blocks is 80 cm x 12 cm in cross section. The laminae within these blocks are flat-lying to moderately curved and either terminate sharply or are bent at the edge of the clasts. One large block pierces well into the lower sandstone bed, with a greater accumulation of sand against the block on its southern side than the northern side, where there is a 'shadow' of little sand (Figure 4.17). Laminated carbonate concretions are also present as clasts.

A second example of a chaotic/deformed horizon is at FD-346.2, where 35-40 cm of thin and very thin beds of sandstone and siltstone terminate against a westwardly downcutting shear zone/surface that is overlain first by folded strata and then by cross-stratified fine sand. The dislocation zone cuts stratigraphically down through the 35-40 cm of strata across a lateral distance of 2-3 m, then assumes an orientation parallel to bedding. To the west, the bedding-parallel surface is a well defined decollement. To the east, where this disturbance is at a high angle to bedding, the surface is not clearly defined, and is more akin to a shear zone (Plate 24a). In the western part of the outcrop the overlying strata are regularly folded into sharp anticlines and wide, gentle synclines, maintaining a fair continuity of bedding. The axes of these wide synclines are oriented N60E. To the east, the folded strata are quite irregular, and small individual synclines (~8 cm stratigraphic thickness) of folded strata are found surrounded, laterally and below, by churned siltstone. The small synclines in the eastern part of the section show broken edges, often in a stepwise fashion perpendicular to bedding. One of these small synclines has an axial orientation of N47E.

The fine sandstone that overlies these folded structures is up to 40 cm thick in the deep synclinal depressions, filling in the irregular surface with cross-laminae that indicate slipface migration towards the NW. In the eastern part of the outcrop, where the folded and partly homogenized strata define a thin zone of deformation, this sandstone bed is much thinner, 8-10 cm. In this eastern area, the sandstone contains extensive, low-angle laminae

that form widely spaced, low-relief, convex-up domal patterns (hummock-and-swale geometry) (Plate 24b). The laminae are locally separated by low-angle internal truncation surfaces, and the upper surface of the bed contains symmetrical-crested ripples. These features are diagnostic of hummocky cross-stratification (see Section 4.10.1).

4.16.4.1 Process Interpretation

The horizon at FD-231.1 records a number of different processes influenced by gravity. Sliding is recorded in the lower unit. A truncation surface is clearly visible at the termination of the upper sandstone bed, and distinctive laminae in the sandstone blocks indicate that these were derived from the upper sandstone bed Figure 4.17, and then rotated within the mass as it moved downslope. The clasts were only moderately deformed during transport. The lower sandstone bed contains evidence of fluid flow: swirled and contorted laminae, ball-and-pillow structures, and spheroids of sandstone.

The thick upper clayey siltstone unit has many of the attributes of the unifite beds (described below), including abnormal thickness, lack of internal structure (massive) and lack of well defined grading. The observations that (a) siltstone makes up much of the matrix of the clast-rich lower zone and (b) there is no distinct break between the lower unit and this upper siltstone unit, indicate that the two are genetically related. It is not readily apparent what sequence of events led to the deposition of this unit. If sliding (lower unit) triggered a muddy flow (upper unit), then one would expect the muddy unit to have been deposited downslope from the area of sliding. There are two possible explanations for the superposition of these units: (1) the thick muddy flow had sufficient density to exert enough shear stress on the sea floor to cause sliding under the flow, and also eroded and moved the sand blocks, or (2) the muddy flow was generated upslope from the slide, but at the same time, and the fine-grained flow moved over, and was deposited on top of, the slide. The first explanation is less appealing because a slump- or slide-generated flow

would likely be deposited primarily downslope from the slide deposit itself. Stanley (1982) describes deep-water welded flows with lower slump division and overlying sandy turbidite divisions that are similar to FD-231.1 in that the contact between the slump and the turbidite is gradational and pieces of the slump are found in the overlying turbidite. He reasons that there are two conditions needed to produce a welded couplet: (a) short transport distance between point of failure and site of deposition and (b) an environment that can accommodate and preserve these deposits. Stanley concludes that in the deep sea the only likely setting for these welded flows would be a channel with failure and sliding of a fan valley wall followed by an overriding turbidity current. In the case of FD-231.1, the exposure is not extensive enough to ascertain the geometry of this horizon. The great thickness of the upper siltstone division would argue for containment within a channel, and the channel geometry of some unifite beds in the CIF lends support to this possibility. Such a channel might not have been a permanent feature on the sea floor, but rather may have been a scar formed at the time of deformation by downslope transport of sediment during sliding.

The horizon at FD-346.2 records somewhat less intense deformation. The deformed sediment package moved along a fairly well defined surface/zone. From the limited exposure, it appears that the movement was towards the west or north. The sharp anticlines and wide synclines at the western part of the outcrop formed as an accommodation of stresses created by the sliding mass. The deformation was compressional, and the sediment responded plastically, but with some integrity. The sharp terminations to bedding in the small synclines in the eastern part of the section indicate that part of the deformation was brittle. The overall structure indicates that the layers essentially buckled, with the greatest amount of deformation occurring towards the west. The northeast trend of the synclines indicates maximum compressive stresses oriented roughly northwest, which is roughly the direction of erosional downcutting, and by inference the general direction of dip of the local slope.

A close temporal association of sand deposition with sliding is suggested by: (1) the lack of a fine-grained drape over the slumped surface (a clay drape would have been relatively easy to deposit and difficult to erode in the topographic (synclinal) depressions), and (2) the anomalous thickness of the sandstone bed (roughly 3-4 times the maximum thickness, and an order of magnitude thicker than the average thickness, of the surrounding sandstone beds).

The close association between hummocky cross-stratified sandstone and this slide feature may be significant for the interpretation of the bed. It should be noted that only a few scattered examples of HCS were found in the several hundred meters of FA 2 strata below this horizon. Hummocky bedforms are considered a storm-generated feature (see Section 4.10.1), formed, at least partially, under the influence of long-period oscillatory currents. Storm-generated waves have been considered as a factor in slope failures by many authors (Dott, 1963; Henkel, 1970; McGregor, 1981; Coleman, 1981; Prior and Coleman, 1982; Saxov, 1982; Koning, 1982). Henkel (1970) describes how changes in pressure associated with the passing of waves create cyclic shear stresses that remould the sediment as a result of decrease in strength and increase in pore pressure. These changes to the sediment result in failure and downslope movement.

The intimate association of HCS and the slide features at FD-346.2 suggests a link between stresses generated by major storms and initiation of mass movement. Such a link has never been documented in the rock record, probably because of the low probability of: (1) depositing sand directly on the surface of a slide; (2) generating unequivocal storm features in the sand bed, and (3) preserving the whole sequence. Most ancient slides are described from deep-water settings (e.g., slope), where deposition is well below the influence of waves.

4.16.5 Summary Process Interpretation of Disorganized Beds

There appears to be a genetic link between many of the disorganized beds described above. The evidence for these various links, the evidence for transitions between bed types and the processes associated with such transitions are reviewed below.

Liquefaction is likely to have been an important triggering mechanism in all of these beds because of the abundance of muddy siltstone in FA 2. Unifite and raft-bearing beds, as well as many of the thin interbeds associated with disturbed and slumped horizons, are composed of sediment of this grain size. Cohesionless fine sands and silts possessing a slight content of fines or organic matter are highly susceptible to liquefaction (Andresen and Bjerrum, 1967; Terzaghi and Peck, 1948; Keller, 1982). Silt-sized particles are particularly susceptible as they have no intergranular electrostatic attraction, but are also too light to shift into stable packing at the time of deposition (Andresen and Bjerrum, 1967).

Given the proper grain-size distribution, other factors that control susceptibility to liquefaction are: (1) vertical and lateral homogeneity, (2) degree of lithification, (3) pore-pressure conditions, and (4) rate of accumulation (Moore, 1961). The primary control is accumulation rate (Terzaghi, 1956; Middleton and Hampton, 1973; Hein and Gorsline, 1981), which in metastable sediments is faster than the rate of consolidation increase and pore-water reduction.

Earthquakes have been noted as a means of initiating liquefied flows (Andresen and Bjerrum, 1967) and slides (Morgenstern, 1967). Cyclic shear stress associated with storms has also been implicated as an 'initiation process' by numerous authors (see Section 4.16.4.1). The suite of features at FD-346.2 imply that storm-related forces may have been an important causative element in the formation of these beds.

Most workers indicate that liquefied flows can originate on very low slopes (<1 degree) (Moore, 1961; Morgenstern, 1967; Middleton and Southard, 1977; Prior and

Coleman, 1982). Depositional slope may generally have less effect than accumulation rates, and the associated rate of consolidation, on the formation of a wide variety of mass-movement structures. Morgenstern (1967) describes cases where highly consolidated sediment is stable at very high angles (over 30 degrees). On the other hand, sliding is common in areas of high accumulation rate, such as the Mississippi Delta, on slopes as low as 1 degree or less (Shepard, 1955; Terzaghi, 1956; Moore; 1961; Embley, 1982). No particular feature or bed type described above requires high slopes (i.e., debris flows may be common on slopes <1 degree — Hein and Gorsline, 1981). The primary controls in disposing the sediments of FA 2 to liquefaction and flow were probably grain-size distributions and depositional rates. Intermediate to high (1-5 degrees) slopes, if present, would have aided in the development of these gravity flows.

For many years authors have contemplated the continuum of processes associated with gravity flows (e.g., Dott, 1963; Middleton and Hampton, 1973; Shultz, 1984), but continue to use end-member classification schemes (e.g., Middleton and Southard, 1984). These end-member classifications are ingrained in our language and make it difficult to convey information without using them. Nevertheless, any number of support mechanisms may be active temporally and/or spatially (vertically or laterally) during the deposition of a single bed. The sequential development of flows of different character has been addressed by Fisher (1983), Middleton (1970), Shultz (1984) and others. Figure 4.18 summarizes what I believe to be the full range of possible transitions in transport mechanism. The paleoenvironmental interpretations of the various facies in FA 2 (Section 4.22) will, in part, determine the applicability of some of these process transitions. Based solely on the information from these beds, the evidence for certain transitions is more compelling than others. Liquefaction and/or sliding are thought to trigger all of the various mass movements and gravity flows (Figure 4.18).

Liquefaction has long been implicated in the generation of turbidites (Morgenstern, 1967; Middleton, 1970). The evidence for transitions from liquefied flows to turbidity

Figure 4.18: This diagram illustrates a wide variety of possible flow transitions for the disorganized beds of FA 2. Flow transitions are summarized with arrows in lower right. Some transitions are more likely than others based on facies characteristics (discussed later). Quadrilateral in lower left shows interpreted support mechanisms for the different bed types at the time of deposition.

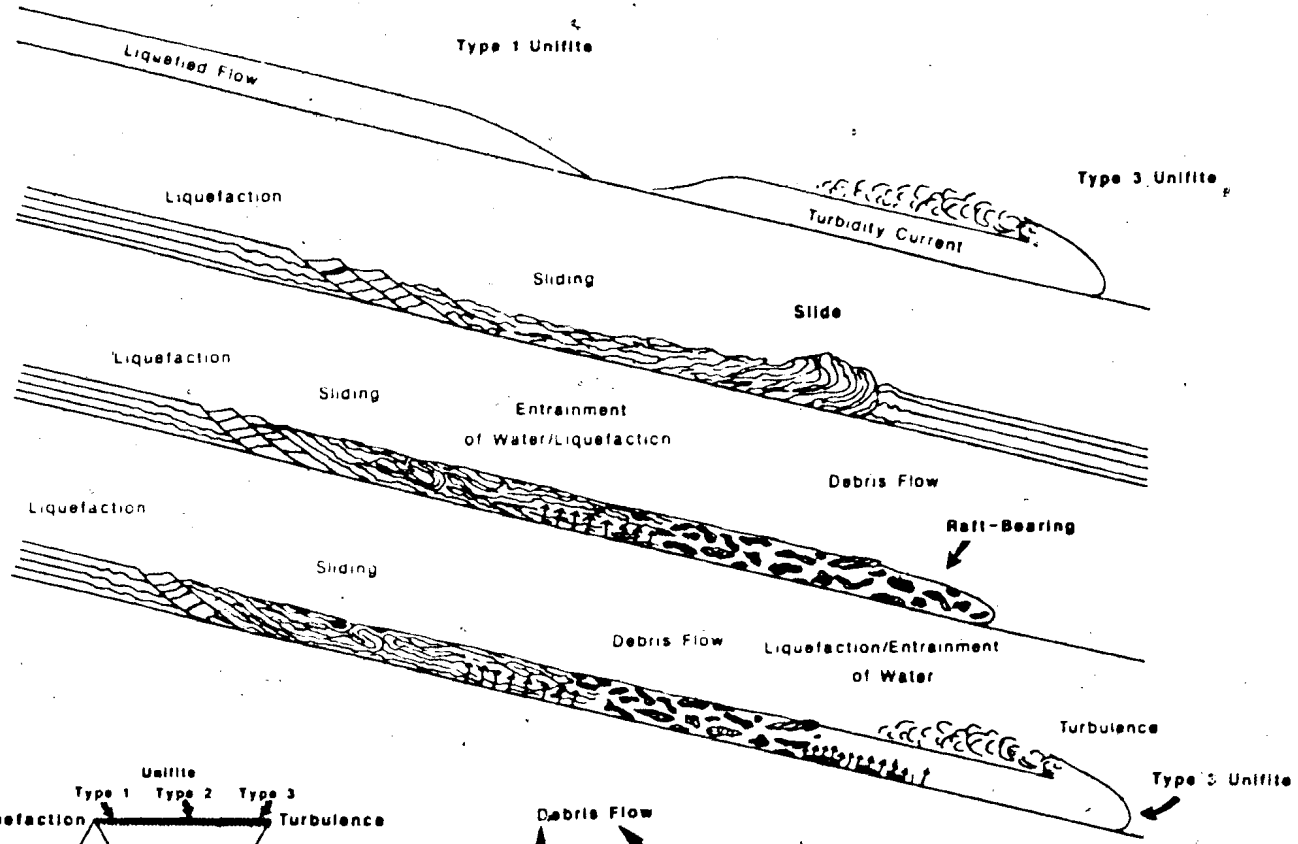

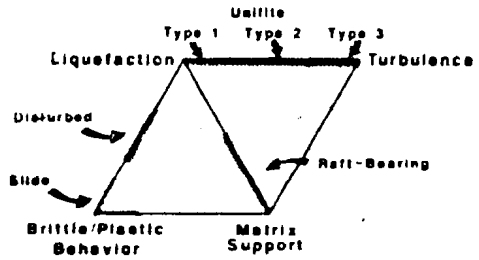

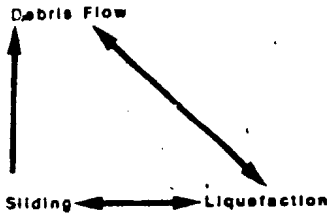

Liquefied Flow (Type 1) → Type 2 → Turbidity Current (Type 3)

currents (Unifites 1-3), given in Section 4.16.2.1, is based on a wide spectrum of unifite bed types. These bed types show features of both end-member flow types, as well as those of intermediate character (Type 2 Unifites), implying a lateral transition between these flow types. A transformation from a slide to a debris flow, or from a debris flow to a turbidity current, requires strength reduction at the time of failure, and for the latter case, requires sufficient acceleration of the mass downslope to reach velocities needed for turbulence (Morgenstern, 1967, p.206; Hampton, 1972). Cohesive strength, an attribute of flows with clay contents as low as 5% (Hampton, 1972; Rodine and Johnson, 1976), may be reduced during flow by dilation, entrainment of water, and an increase in pore pressure (Pierson, 1981). The association of structures at FD-168.2 strongly implies that the transition from sliding to debris flow was important in the deposition of many of these disorganized beds. There is no direct evidence to suggest that debris flows (leading to raft-bearing beds) may have transformed to turbidity currents (leading to unifite Type 3 beds). The fact that there are a few examples of raft-bearing beds with few, if any, laminae and rafts raises this possibility. The downslope transition of a debris flow to a turbulent flow would be accompanied by the settling of clasts through a progressively weaker slurry. This type of transition would leave clast-rich deposits upslope and clast-poor or clast-free deposits downslope (Shultz, 1985).

In addition to temporal changes in flow types, there is also the possibility that different bed types may have formed in different areas, from the same event or series of events, and subsequently interacted during downslope movement. As an example, one interpretation for the thick unifitelike cap to the slide bed at FD-231.1 is that it was deposited from a flow generated simultaneously upslope that later flowed over the slid strata.

In summary, the arguments outlined above, and those in the process interpretation sections for individual beds, have established: (1) a grain size distribution that favors susceptibility to liquefaction, (2) a likelihood that high sediment accumulation rates may

have played a role in creating underconsolidated sediments (metastable packing), important for liquefaction, (3) a gradation of bed types in the unifite subfacies that can be related to flows along a continuum between liquefied flows (Type 1) and turbidity currents (Type 3), (4) a possible link between incipient sliding (disturbed subfacies) and debris flow (raft-bearing subfacies) (e.g., FD-168.2), (5) the theoretical feasibility of proposed flow transitions (3 and 4), (6) a possible link between sliding and unifite deposition (e.g., FD-231.1), and (7) strong evidence to suggest that sliding was caused, at least in some instances, by storm-related processes.

4.17 GUTTER CAST FACIES (2.1)

The Gutter Cast Facies is dominantly composed of S0, S1 and S2 beds with moderate to abundant gutter casts (Plate 25a,b,e). The sandstone content, excluding gutter casts, varies roughly from 10-40%, with S3 beds making up a very minor percentage (<2%). Q beds make up about 5% of this facies. Where the gutter casts are most abundant, the bedding is thinner, with fewer Q beds. For instance, an 11 m interval from FD-24-35 contains no sandstone beds thicker than 2.5 cm, except for gutter casts. Unifite beds (Types 1 and 2) are prominent, forming 10-15 % of the facies. One or two raft-bearing beds have been noted in strata that are marginally considered to be this facies (thicker sandstone beds and few gutter casts). Ptygmatically folded sandstone dikes are surprisingly abundant (Plate 25b,c,d). Wave ripples are present on S2 beds, locally as starved forms. Wave ripples are also found at the top of wide gutter casts.

4.18 SANDSTONE—SILTSTONE FACIES (2.2)

This lithofacies forms most of Member 2 and contains the full range of bed types described above and a wide variety of sedimentary structures. Two subfacies are defined below based on the clustering of bed types and sedimentary structures.

4.18.1 Siltstone-Dominated Subfacies: 2.2A

Visual estimates of the total sandstone content of this subfacies (Plate 26d) range from 5-40% and average about 15-20%. A few thin zones, most notably FD-168.8-170.7, have abnormally high sandstone content (70-85%), primarily in the form of rippled, wavy, and lenticular S2 and S3 beds. For comparison with Subfacies 2.2B, the percentages of

PLATE 25: GUTTER CAST FACIES (FROM FD-20-30)

a: This photo shows the general appearance of this facies. Note thin sandstone beds, gutter casts (a few prominent ones are arrowed), and a few small carbonate nodules ("C"). Stratigraphic top is up. Divisions on scale are 10 cm.

b: This close-up of the upper right of "a" shows the scale and style of interbedding of S1 and S2 laminae (and a few S3 beds). Note large, ptygmatically folded sandstone dike on right. Stratigraphic top is up. Scale is 10 cm long.

c: Large, ptygmatically folded sandstone dike (above scale) cutting across S1 and S2 laminae. Stratigraphic top to upper left. Scale is 10 cm long.

d: Bedding plane view of "c". Note triangular-shaped sandstone body at intersection of three arms (arrows) of the dike. Scale is 10 cm long.

e: Close-up of bedding showing S1 and S2 laminae, unusual shaped gutter casts and numerous Skolithes annularis traces. Stratigraphic top is up. Scale is 2.5 cm wide.

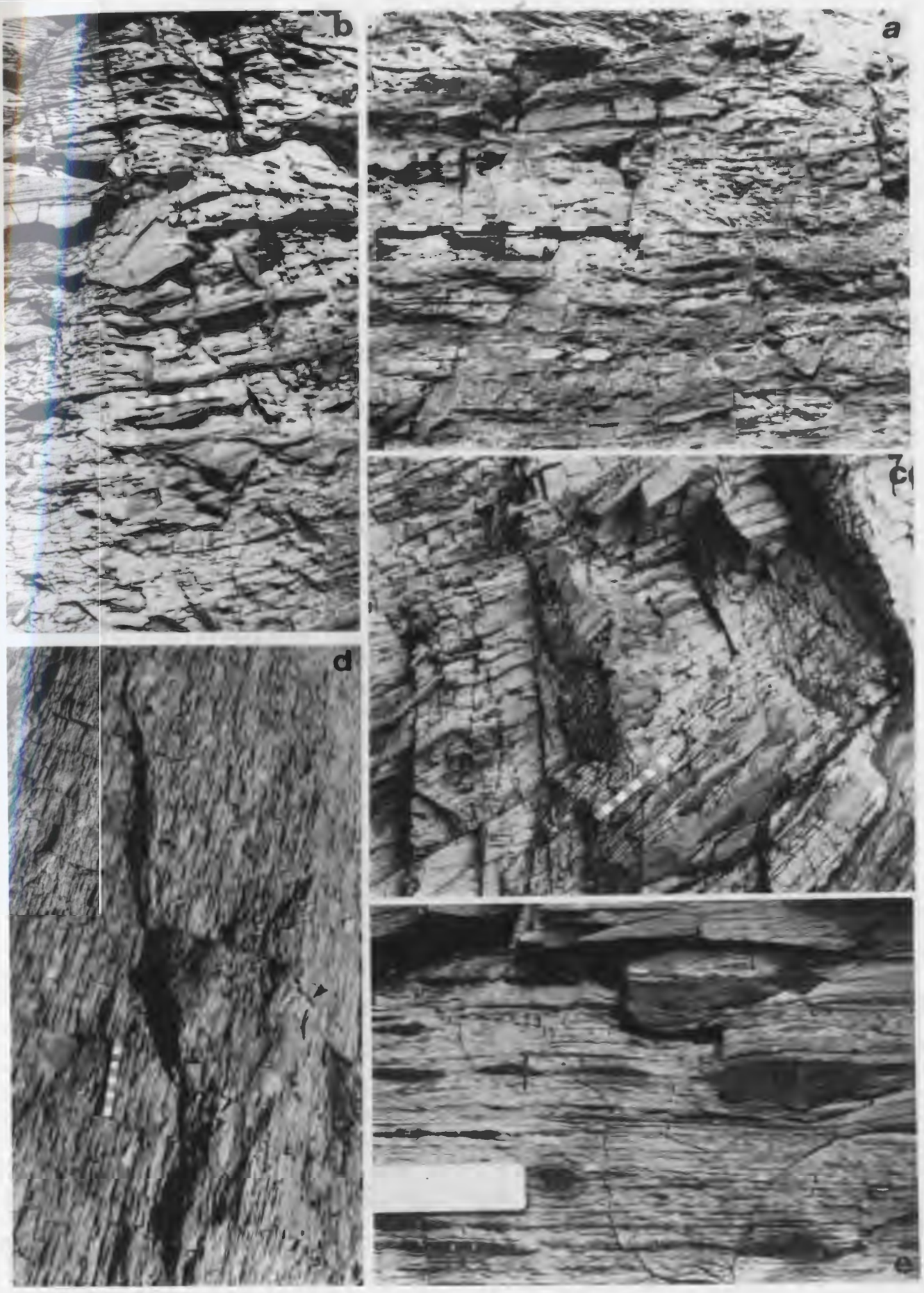
b
a
c
d
e

PLATE 26: FACIES ASSOCIATION 2

a: Fault separates Green Laminated SIltstone (Facies 2.4) from thick package of strata of the Red Siltstone Facies (FD-285-294) (lower left of photo). At the top of the photo is the thin package of Red Siltstone at FD-310.75-311.85. Stratigraphic top to upper left.

b: This strata (FD-347-350) of the Sandy Subfacies (2.1B) lies above the slide horizon at FD-346.2. These strata are in striking contrast with the very thin and thin beds below this level. Stratigraphic top is up. Notebook is 18.5 cm long.

c: The strata directly below the Red Medium-Thick Bedded Sandstone/Shale Facies (1.4) above FD-103.7 consists of sandstones and shales that have picked up a strong slaty cleavage (FD-99.8-FD-103.7). These are in sharp contact with the underlying sandstones and siltstones of the Gutter Cast Facies (2.1) (in the foreground). Stratigraphic top is up. Notebook is 18.5 cm long.

d: Typical exposure of Silty Subfacies (2.1A) at GB with moderate amount of sandstone (mostly S2 and S3 beds). Small portions of the thicker (S3) beds are exposed. Many of the thinner beds were disrupted by burrowers. Stratigraphic top is to left. Scale is 1 m long.

e: Sandy Subfacies (2.1B) at FD-68-72 with numerous S3 beds and an S4 bed in the foreground. Stratigraphic top is to upper left. Scale is 15 cm long.

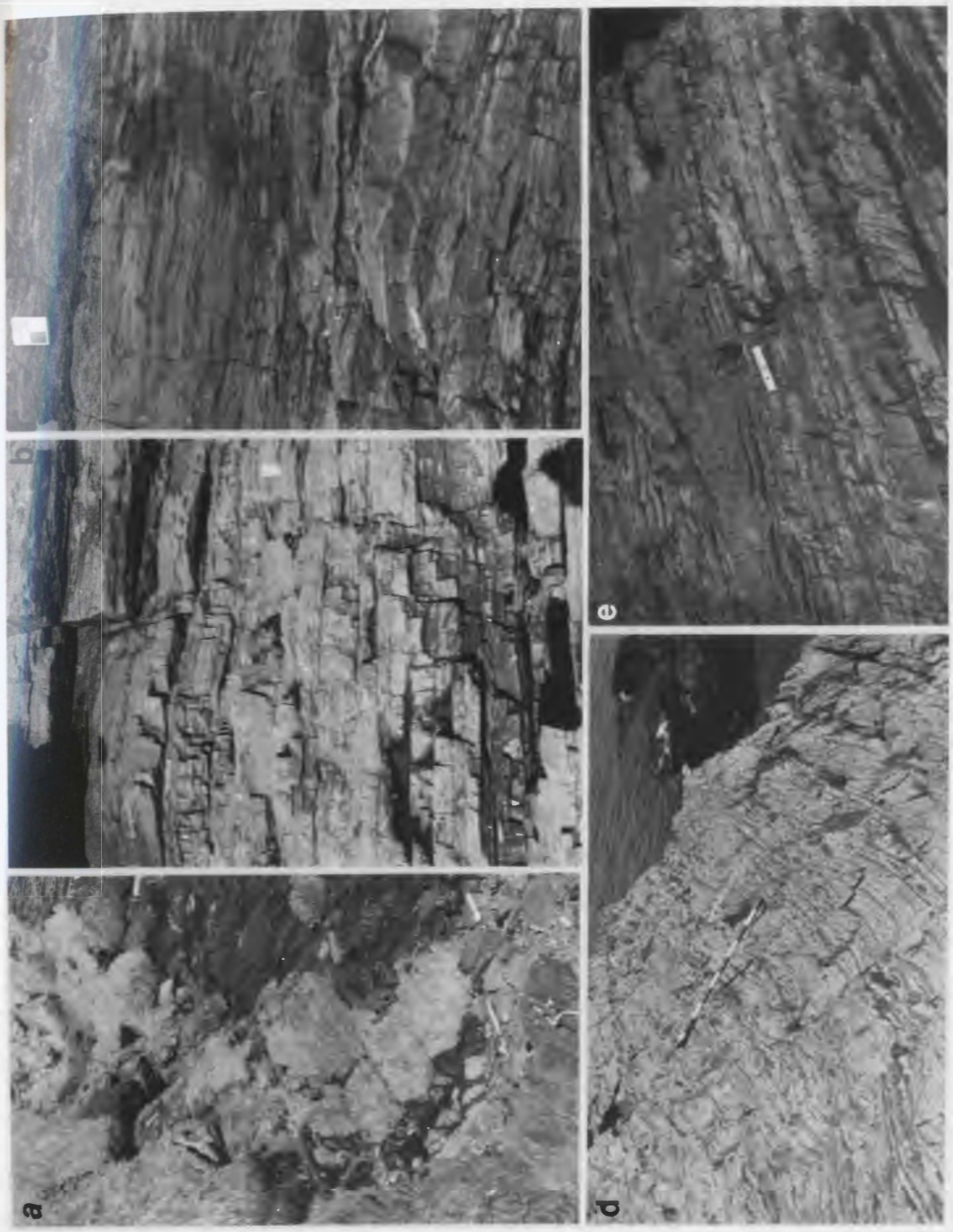
a
b
c
d

various bed types have been calculated for a 40-m interval of this subfacies (FD-155-195). In this interval 2.0% of the strata are Q beds, and significantly, only 2.75% are beds thicker than 3 cm. Two unifite/raft-bearing beds make up 2.5%.

In comparison to Subfacies 2.2B, the S3 and S4 beds in this subfacies are more continuous: there are very few pinch-outs and they less often exhibit pinch-and-swell geometries. This coincides with fewer erosional upper surfaces. Fewer beds in this subfacies display undulatory and draping laminae, form-discordant ripples, and complexly interwoven cross-laminae.

4.18.2 Sandstone—Dominated Subfacies: 2.2B

The Sandstone—Dominated Subfacies is characterized by a high percentage of sandstone beds that are greater than ~3 cm in thickness (H beds, S4 beds and thick S3 beds) (Plate 26b,e), and a distinct paucity of Q beds. Thickness percentages of these bed types were calculated for this subfacies over a 40-m interval from FD-225-265. The sandstone beds > ~3 cm thick comprise 19.7% of this interval, while 0.08% are Q beds. The highest percentage of these thicker sandstone beds at the FD locality is found from FD-345-350, where these beds make up 57.8% of the section. A lower limit of thicker sandstone beds (>3 cm) for this subfacies is arbitrarily placed at approximately 10-15%. Visual estimates of the total sandstone content of this subfacies, including H beds and S1-S4 beds, is commonly 40-60%, reaching 70% or more for thin stratigraphic intervals. Unifite and raft-bearing beds are present, but these are very widely spaced. For example, in the 40-m zone described above (FD-225-265), there are only three such beds, forming only 6% of that interval (including the abnormally thick bed at FD-231.1).

This subfacies is also characterized by the distinctive geometry, sedimentary structures, and textures of many of the S3 and S4 beds. In this subfacies there is a marked abundance of oscillatory-flow structures, i.e. draping and offshooting laminae, form-

discordant ripples, and symmetrical ripples. Even more striking visually is the percentage of beds with significant irregularities in thickness associated with erosional lower and upper surfaces, especially the latter. Complete pinch-out of S3 and S4 beds is not unusual.

4.19 RED SILTSTONE WITH VERY THIN SANDSTONES: FACIES 2.3

Facies 2.3 consists of red siltstone with thickly laminated to very thinly bedded, white to green, fine to medium sandstones (Plate 27c). This facies exhibits bedding styles that range from regular and slightly disrupted to wispy, blebby, and extremely discontinuous. Sandstone layers make up less than 30% of this facies. The sandstone laminae are found in packages up to 15 cm thick that contain as much as 50% sandstone. These alternate with siltstone-rich packages of subequal thickness that may contain as little as 2-5% sandstone. Sandstone beds are conspicuously bright green, in contrast to the surrounding red siltstone. Many sandstone laminae and sandstone-filled burrows have diffuse green halos. Isolated green spots occur within relatively homogeneous red siltstone, but are not abundant. There is a conspicuous absence of shrinkage cracks in this red-colored facies. Sole markings are rare in these thin sands, but flutes were noted on the base of one bed (FD-286.25).

The red siltstone is inhomogeneous in terms of grain size and structures. Subtle, thin layers of light red mudstone are interlayered with the siltstone and sandstone. The siltstone contains a small (<2%) but variable percentage of fine to medium grained quartz sand and detrital micas (muscovite and minor biotite). The coarse fraction of the siltstone is found as floating grains and as laminae that are a fraction of a millimeter (one or two grains) thick. Some layers have 20-25% coarse silt and very fine sand sized micas that impart a sparkling sheen to the rock under the proper lighting conditions.

PLATE 27: RED AND GREEN SILTY FACIES

a: Outcrop view (stratigraphic top to left) of Thinly Bedded Red Sandstone/Siltstone Facies (2.3) at FD-285-294 ("A" - between arrows) and at 310.75-311.85 (on far left of photo - not clearly discernable). The Green Laminated Siltstone Facies (2.4) at FD-295-310.75 ("B") is in center and foreground. The green rocks on far right are Facies 2.2. The trace of a thrust fault with just a few meters of throw runs from the lower right to upper left in photo.

b: Close-up of Green Laminated Siltstone Facies (2.4) from FD-305.45 showing white-weathering carbonate-cemented sandstone laminae and poorly developed carbonate nodule. Spacing of laminae inside and outside of the nodule indicate that it formed after considerable compaction. A small phosphatic nodule has been incorporated (?) into the carbonate nodule. Stratigraphic top is up. Scale is 10 cm long.

c: Thinly Bedded Red Sandstone/Siltstone Facies (2.3) (FD-310.75-311.85). Note white-weathering, carbonate-cemented sandstone laminae with sharp lower and upper surfaces. The irregular, slightly elongate vertical sandstone lenses (e.g., below scale) are cross-sectional views of Teichichnus rectus. Stratigraphic top is up. Scale is 15 cm long.

d: Close-up view of Green Siltstone Facies (2.4) from FD-303-304 with thick parallel and ripple cross-laminated carbonate-cemented sandstone laminae. Note Teichichnus rectus burrow to right of ruler. Stratigraphic top is up. Scale is in cm.

e: This close-up of the Green Siltstone Facies (2.4) (FD-296.8) shows a thick sandstone lamination with incipient ripple cross-laminae (lower left) and rounded pyrite nodule with orange iron-stain halo (center). Stratigraphic top is up. Scale is in cm.

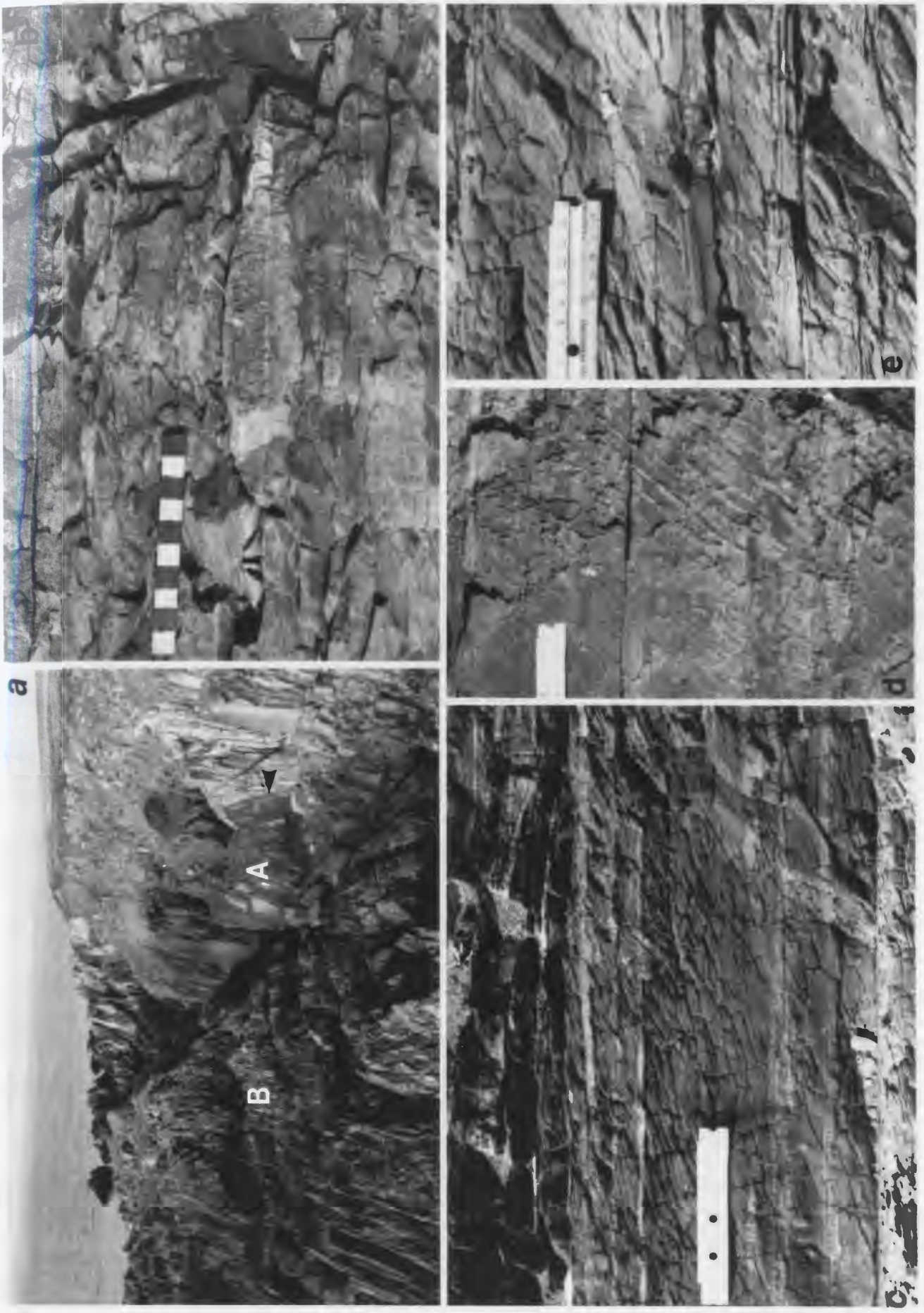
a
A
B
b
c
d
e

Ripples are the dominant sedimentary structure. Small starved current ripples are locally very common. Sand beds at the FD and PM localities display ripple bedding with complex internal structure. Irregular scour surfaces are present within these rippled beds, and extensive laminae often drape the ripple form sets. One particularly interesting concretionary sandstone bed at PM-15.6 shows starved form-concordant climbing ripples overlain by draping laminae with internal scour surfaces (Figure 4.19). Strongly bioturbated zones, tens of centimeters thick, alternate with zones characterized by moderately intact laminae/beds. Teichichnus sp. burrows are locally abundant.

4.19.1 Process Interpretation

The thickly laminated/very thinly bedded nature of the sandstone beds and the fine grain size of the background sediment indicate that the sediment was deposited under generally low-energy conditions. The abundance of small current ripples, and the lack of current lineations or large-scale bedforms indicates currents of low velocity. Starved ripples indicate that at times the supply of coarse-grained sediment was low. Discontinuous and disrupted bedding resulted, at least in part, from the action of burrowing organisms, as evidenced by a high concentration of burrow mottles and traces.

The millimeter-thick sandstone laminae in the siltstone may be attributable to winnowing and reworking. Thick laminae to very thin beds of sandstone with ripple lamination were deposited under lower-flow-regime conditions. The planar and wavy, horizontal and low-angle laminae in some sandstone beds indicate that at times oscillatory currents were reworking the sea floor. The bed at PM-15.6 (Figure 4.19) records initial unidirectional transport of sand in the lower flow regime (starved ripples), which was followed by deposition and reworking of sand by oscillatory currents (draping and complex cross-laminae).

Figure 4.19: This partially carbonate-cemented sandstone bed at PM-15.6 contains a form set of small isolated current ripple crests (enlargement) overlain by draping lamination with internal scour surfaces.

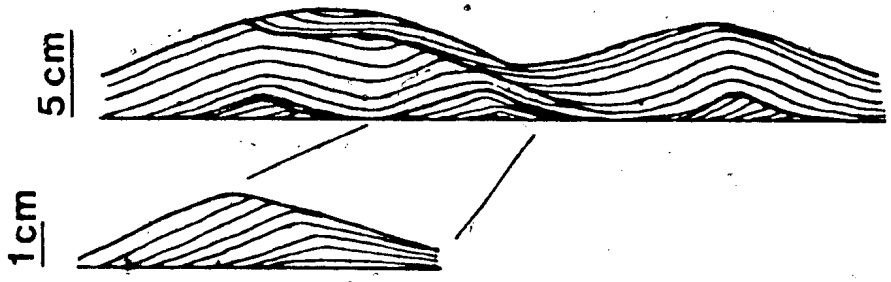
5cm
1cm

The green coloring of the sandstone beds is a diagenetic byproduct formed under reducing diagenetic conditions (see discussion in Section 3.2.1.1). Reducing fluids preferentially moved through these coarser, more permeable layers imparting a green color, while the less permeable muds retained their red color. These fluids affected the surrounding siltstone, as shown by the color halos. Isolated green spots are 'reduction spots' marking burrows or local accumulations of organic matter.

4.20 GREEN SILTSTONE WITH CARBONATE-CEMENTED VERY THIN SANDSTONE BEDS: FACIES 2.4

Facies 2.4 consists of green siltstone with very thin and thin fine sandstone beds, many of which are carbonate cemented. These beds do not weather prominently (Plate 27a), so bedding-plane and sole features are rarely observed, although a few groove and flute marks and Planolites montanas traces have been noted. Although ripples are common, they are difficult to measure due to lack of three-dimensional exposure. All noted cross-sectional views of ripples from this lithofacies at FD show a consistent foreset orientation, dipping roughly northeast. This lithofacies locally contains abundant Teichichnus sp. burrows (Plate 27e) and coarser-grained, very micaceous, thin sandstone beds.

This lithofacies generally contains less than 5% sandstone. The most sandstone-deficient exposures contain as little as 1-2% sandstone and no sandstone beds >1.5 cm thick for as much as 5 m of stratigraphic section. Despite the mostly structureless appearance of the siltstone, thin laminae (<2 mm) (comparable to S1 laminae Facies 2.1/2.2), are visible on some weathered surfaces (Plate 27b,d). These millimeter-thick laminae locally form graded rhythmite beds (see Section 4.7) with upward decrease in sandstone laminae thickness and an increase in their spacing. Nearly all of the sandstone

beds are uniformly carbonate-cemented. Carbonate concretions are found along some carbonate-cemented beds (Plate 27b), and more rarely along beds that are not carbonate-cemented. Sandstone beds display the following sedimentary structures: (1) parallel lamination, (2) ripple cross-lamination (Plate 27e), (3) parallel lamination overlain by current-ripple cross-lamination, (4) same as 3, but with a scoured upper surface filled in with draping laminae followed by more ripple cross-laminae, and (5) complex cross-lamination with internal scour surfaces and draping laminae.

Notable features of this lithofacies are pyritic and phosphatic nodules. Both types of nodule may also occur as single, isolated features or in trains along thin sandstone beds. The phosphatic nodules are dominantly elongated parallel to bedding, and average approximately 2-3 cm in length and 1 cm in thickness. Evidence for early formation of these features is given in Section 3.4. Additional evidence for early formation, noted in this lithofacies, include: (1) the preservation of delicate varvelike laminae of very fine sandstone and siltstone in the nodules, and (2) the incorporation of these phosphate nodules into larger carbonate concretions, which themselves contain evidence of development prior to significant compaction. One or two isolated examples appear to be at a slight angle to bedding.

Pyrite nodules are similar in size to the phosphate nodules, and while some are elongate in shape (roughly parallel to bedding), they tend to be more rounded. These weather with a dull gray metallic sheen or with light yellow to dark brown crusts and iron-stain halos (Plate 27e). On a fresh surface these nodules are gray and fine-grained, with a distinct radial fabric.

4.20.1 Process Interpretation: Facies 2.4

The fine-grained nature of this lithofacies and the thickness of the sandstone beds point towards a low-energy setting with infrequent deposition of sand during higher-energy

events. Sand transport direction is not known precisely, although it appears to have been roughly towards the northeast. The sand beds were deposited under upper-flow-regime (parallel lamination) and lower-flow-regime (ripple lamination) conditions. A few beds have parallel-laminated lower divisions and ripple-laminated upper divisions suggesting decelerating flow conditions during deposition. Sandstone beds with complex cross-laminae and scooped erosional lower bounding surfaces and draping laminae are diagnostic of deposition by oscillatory or combined currents (Boersma, 1970; De Raaf et al., 1977; Harms et al., 1982; Figure 4.4). The graded rhythmites are also interpreted as beds deposited from waning flows (see Section 4.7). The thin sandstone laminae, including those arranged in graded rhythmites, are enigmatic and contain no evidence diagnostic of deposition from oscillatory/combined flow or unidirectional currents.

Interstitial fluids, and possibly even the bottom waters, were reducing, as indicated by the presence of phosphatic nodules and pyrite balls (see Section 3.4.1). The green color also supports reducing diagenetic conditions (Figure 3.4). The paucity of burrows — only a few were noted — may also reflect low-oxygen conditions inhospitable to burrowing organisms. Calcite cementation of sand layers took place under the chemical conditions that stimulated precipitation of phosphate, namely high pH (see Section 3.4.1). These sand layers were preferentially cemented because their high permeability allowed movement of fluids during diagenesis.

4.21 LITHOFACIES DISTRIBUTION: FA 2

The Gutter Cast Facies (2.1) is present in the lower part of member 2. At FD, this facies forms much of the strata from FD-18.3 (the member 1/2 boundary) to FD-99.8 (in addition to Facies 2.2-Subfacies A). The strata most clearly distinct and recognizable as Facies 2.1 are from FD-22-35 and from FD-~80-99. This facies is also present at GB (GB-187-200B), but unfortunately much of the section at the base of member 2 is broken by faults at this locality. This facies is present at the same stratigraphic position — at the base of member 2, on the east side of the Burin Penisula at Lewins Cove in the interval LC-12-30B. This facies makes up ~14% of the strata of FA 2.

The Sandstone/Siltstone Facies (2.2) composes the bulk of member 2 (~80% of FA 2), and is found at FD, GB, LC, PM (Point May), BI (Brunette Island), and CI (Chapel Island). The two subfacies are intergradational and interstratified. Only a few packages of strata are clearly definable as Subfacies 2.2B; one 3.5 m-thick package is directly above the buckled horizon at FD-346.2. The association of this interval with the buckled horizon is intriguing because other sandstone-rich (although not necessarily thick-bedded) zones are found above a raft-bearing bed at FD-168.2 and a unifite bed at FD-92.6.

The red-colored Facies 2.3 (~2% of FA 2) forms two distinctive horizons within member 2: a thick one traceable between GB (GB-119.9-125.1B), FD (FD-285-294), and PM (PM-14.8-20.6), and a thinner, stratigraphically higher horizon, present at GB-141.5-142.4B and FD-310.75-311.85 only. The thick horizon at PM is the most sandy, FD is less sandy, and GB is the least sandy. The green, finely laminated siltstones of Facies 2.4 (~4% of FA 2) are found primarily between these two red horizons at GB (GB-125.1-141.5B.) and FD (FD-294-310.75); the outcrop shows an upward increase in sandstone content, and a short distance above the upper horizon of Facies 2.3 this facies grades rapidly into Facies 2.2. Teichichnus sp. burrows were noted in Facies 2.4 at FD a few meters directly above the lower horizon of Facies 2.3. Facies 2.4 is found at PM where it is

more sandy and more burrowed than at other localities. Facies 2.3 and 2.4 are both present on Brunette Island, and appear to also be present as far north as Chapel Island.

4.22 FA 2 PALEOENVIRONMENTAL INTERPRETATION: FLUVIAL-DOMINATED, STORM-INFLUENCED DELTA

4.22.1 Introduction

The exceptional preservation of sedimentary structures in many outcrops of FA 2 allows detailed description and process interpretation of various bed types (Chapter 4). This facies association is intriguing in that many of the features of Facies 2.2 (Sandstone/Siltstone Facies) and to a lesser degree Facies 2.1 (Gutter Cast Facies) — the volumetrically dominant facies — are typically associated with deep-water sedimentary sequences. These include: graded bedding with well developed flute marks and other sole markings, graded rhythmites, and a host of gravity-flow deposits including slides, liquefied flows, turbidites and debris flows (including pebbly mudstones). The close association with facies deposited in a shoreline setting (FA 1) makes this an unusual and challenging sequence to interpret, and leaves great potential for refining and expanding existing models for shelf sedimentation, particularly with reference to storm deposition.

Evidence given earlier in Chapter 4 indicates that the bulk of FA 2 was deposited in nearshore and inner-shelf settings (between the shoreline and storm wave base). This is based on the close association with facies deposited at the shoreline (with evidence of periodic exposure), the presence of HCS, and the abundance of wave ripples and wave-ripple laminae. The hydrodynamic regime in this setting is one of the most complex of any depositional environment because of the interaction of waves, tides, currents, fluvial input, and storms. The following section will deal first with 'evidence for waves and tides',

which is followed by 'evidence for storm sedimentation', particularly in relation to Facies 2.1 and 2.2. This will be followed by a section entitled: 'evidence for deltaic sedimentation', which will include paleoenvironmental discussion of all of the facies in FA 2 (2.1, 2.2, 2.3, and 2.4).

4.22.2 Evidence for Waves and Tides

In the lower part of member 2, the Gutter Cast Facies (2.1) and the Siltstone/Sandstone Facies (2.2) are transitional with facies from FA 1 that clearly suffered subaerial exposure at the time of deposition. This indicates a shallow subtidal origin, particularly for Facies 2.1. A very striking aspect of these facies is that, despite considerable thickness and excellent exposure, there is a complete lack of direct evidence for either beaches or tidal sand ridges, characteristic features of wave- and tide-influenced shorelines, respectively. There is, however, evidence throughout FA 2 for the influence of tides and waves.

The evidence for tides includes a bimodal-bipolar distribution of ripple paleocurrents from Facies 2.2 at FD (see Figure 4.2c). This paleocurrent information suggests that sand beds emplaced from the southwest were at times reworked by flood-tidal currents (the paleocurrent information from FA 1 — Figure 3.3 — indicates ebb-tidal asymmetry). Additional, albeit weak, circumstantial evidence for tidal influence is facies transitions with well developed muddy intertidal facies (Facies 1.1, 1.2) in the lower part of Member 2.

The evidence for waves includes abundant wave ripples and wave-ripple laminae, although most of these are associated with the storm deposits discussed below. The wave-ripple data from FD (Figure 4.2e) indicate a wide range of wave orientations, but the data from PM, CI, and GB (Figure 4.3) are compatible with a northeast-facing shoreline.

Despite this evidence for wave reworking, waves apparently did not have a strong and continuous influence on the sediments of FA 2.

Less is known about the character of the shoreline, and the influence of waves and tides, during the deposition of the upper part of member 2 than for the lower part, since shoreline facies (which best reflect these processes) are not exposed in the upper part of the section. There is, however, no evidence for major changes in the sedimentary regime in the upper part of member 2. Facies 2.2 dominates the upper part of member 2, and there is no obvious difference in appearance from its occurrences lower in the section.

4.22.3 Evidence For Storm Sedimentation

For some time now there has been a growing awareness of the episodic nature of sedimentary processes (see Dott, 1983). The role of storm events in carrying sand onto shelves and forming distinctive 'storm-generated' sedimentary structures and facies has come to light only over the last 20 years. Studies of the effects of storms on modern shelves by Ball et al. (1967), Hayes (1967), Perkins and Enos (1968), and Gadow and Reineck (1969) sparked interest in finding analogs in the rock record. The early 1970's saw a proliferation in the description of ancient storm facies (e.g., Ball, 1971; Goldring, 1971; Hobday and Reading, 1972; Reineck and Singh, 1972; Brenner and Davies, 1973; Goldring and Bridges, 1973; Ager 1974). Recent years have seen the refinement of facies models for tempestite deposition, with particular emphasis on HCS (the term 'tempestite' was coined by Gilbert Kelling for storm-generated sandstones; see Ager, 1974).

The evidence that storm processes played an important role in the deposition of Facies 2.1 and 2.2 comes from: (a) the S2-S4 sandstone beds and (b) additional beds/features. S2-S4 sandstone beds (Sections 4.4-4.6) were deposited from waning flows under conditions of combined unidirectional/oscillatory flow. The early stages of deposition were dominated by strong unidirectional flow and the late stages were

dominated by oscillatory flow. The upward transition from parallel laminae to combined-flow or wave-generated laminae, so common to the CIF beds, are a fundamental distinguishing feature of tempestite beds (De Raaf et al., 1977; Goldring and Bridges, 1973; Kreisa, 1981; Aigner, 1982, Seilacher, 1982; Brenchley, 1985; and many others). This forms the upper part of an idealized tempestite sequence proposed by Aigner (1982), based on observations on the Muschelkalk limestones of SW Germany. The full idealized sequence is similar to the Bouma sequence in all respects except that the Bouma T_c (and T_d?) division is replaced by wave ripples. Bouma-like sequences have been described from graded sand layers in the Bering Sea that are interpreted as tempestites by Nelson (1982).

The S2-S4 sandstones of FA 2 generally lack the lower "a" division that Aigner and Nelson describe. This is attributable to a relatively homogeneous source of sediment, lacking a coarse-grained component that would normally make up a graded lower division. The data from the CIF beds are consistent with models of storm deposition (e.g., Walker, 1984) in which sediment is entrained near the shoreline and moves offshore in high-velocity, bottom-hugging, sediment-laden flows, with deposition occurring under conditions of high wave swell (above storm wave base) that continues long after most or all of the bed is deposited.

There are many other aspects of these sandstone beds and also other features and bed types that are characteristic of storm deposition (e.g., pot and gutter casts, graded rhythmites, and flat-pebble conglomerates). Table 4.3 is a comparison of storm-generated features from ancient tempestites with those of Facies 2.1 and 2.2. The similarity is striking and clearly suggests a strong influence of storms during the deposition of F.A 2.

The paleocurrent information from sandstone beds in Facies 2.1 and 2.2 indicates well oriented flow to the northeast, which is parallel to the inferred motion of tidal currents from FA 1 (NE-SW bimodal/bipolar pattern). This implies that the tempestite flows were moving more or less perpendicular to the shoreline.

TABLE 4.3: STORM-GENERATED SEDIMENTARY FEATURES FROM FA 2

STORM-GENERATED SEDIMENTARY FEATURES	FA 2
Interbedded coarse (storm) and fine (fair-weather) beds	√
Sharp/scoured base — gradational top	√
Pot and gutter casts	√
Flat-pebble conglomerate	√
Lags	√
Thickening and thinning and lenticular beds	√
Reworked but autochthonous fauna	N.A.
Infiltration textures	N.A.
Escape burrows	√
Graded rhythmites	√
Wave-generated undulatory lamination	√
Vertical sequence: planar lamination to wave-generated lamination	√

* N.A.= Not Applicable

The mechanisms by which sediment is carried out onto the shelf are at present poorly understood. Discussions tend to center on three types of currents: wind-forced currents, storm-surge-ebb currents, and density currents (see discussion in Walker, 1984). Wind-forced currents are shore-parallel currents driven by shear stresses applied to the sea surface by the wind. Storm-surge-ebb currents are offshore-directed bottom currents that form in response to hydraulic heads associated with coastal setups during storms. Modern-day observations of these 'relaxation' flows indicate that they are strongly affected by the Coriolis Effect (except at low latitudes) and evolve into shore-parallel geostrophic flows. Turbidity currents are a special case of density current in which the excess density is supplied by dispersed sediment.

Turbidity currents flow downslope by gravity acting on the density difference between the dispersion and the surrounding sea water. Grain support comes primarily from turbulence generated by the flow, but on a high-energy shelf, waves would tend to agitate and mix bottom flows like a stirring rod. Grain support from turbulence generated by waves and other currents may be an important factor in nearshore settings, losing influence with greater depth and distance from shore. Whether or not this additional source of turbulence should invalidate unqualified use of the term 'turbidity current' for these flows may be debated, although it is important to recognize that, especially in proximal situations, these are in fact complex 'combined' currents.

Using a broad definition of the term 'turbidity current', there is considerable evidence for shelf turbidity currents (for reviews see Walker, 1984, and Brenchley, 1985). This includes evidence for storm sand transport more than 100 km offshore, and high velocities (>~1 m/s — see Section 4.10.1) at these great distances from shore. Many oceanographers doubt that storm surges would be capable of carrying sediment at these velocities for such distances.

Studies of the rock record suggest intervals from 400-15000 years between tempestites, with an average of 5000 years (see Walker, 1984, Table 2; data from Hamblin and Walker, 1979; Goldring and Langenstrassen, 1979; Brenchley et al., 1979; Aigner, 1982; Kreisa, 1981). It has been argued, using these data, that the events responsible for tempestites in the rock record may not have been recognized by oceanographers and that these events are considerably stronger than those studied today. The sandstones in FA 2 have many of the characteristics of turbidites, but there is no evidence to rule out strong storm-surge-ebb currents.

4.22.4 Theoretical interactive-flow model for deposition under oscillatory and unidirectional currents: application to S3/S4 Beds

From the above discussion, it is inferred that tempestites deposited above storm wave base, including the S3/S4 beds of this study, are affected initially by unidirectional flow and later by combined or oscillatory flow. The sedimentary structures, and sequences of sedimentary structures, in these beds can therefore be understood in terms of an interplay between unidirectional and oscillatory flow components. An interactive-flow model of deposition is presented in an attempt to explain a wide range of sedimentary structures and structure sequences in tempestites, which will be then applied to S3 and S4 beds. The model attempts to explain the style, thickness and sequence of stratification as a function of the initial oscillatory and unidirectional flow velocities and their relative rates of decrease.

In nature, both flow components may change in both direction and speed during storms (Swift et al., 1983). In order to accurately model tempestite deposition in nature these factors and others such as grain size would have to be addressed. This is a clearly unmanageable number of variables, and so for simplicity it will be assumed that the

unidirectional and oscillatory flow components have the same orientation and that the grain size does not vary significantly during deposition. At this point an "initial-velocity graph" can be constructed (Figure 4.20a) whose axes are the initial values of unidirectional velocity $(U_o)_0$ and oscillatory velocity $(U_u)_0$, the two components of flow. The initial conditions of any particular event can be represented by a single point on this graph. At high velocities the initial conditions are associated with conditions of upper-flow-regime plane bed, while at lower velocities ripple bedforms of various types are stable. The plane-bed field has been divided into an oscillatory-dominant, unidirectional-dominant and combined-flow field, the last of which has subequal influence of both unidirectional and oscillatory flow. When deposition occurs in the bedform field, the nature of the ripples at any particular time is a function of the relative strength of the unidirectional and oscillatory components.

For any particular flow, once the initial values of oscillatory and unidirectional velocity are plotted on Figure 4.20a as a point, the conditions of deposition with time can then be presented by a curve on this graph. In nature, the velocity of each component would decrease with time during the course of a storm event but not in a simple manner. As a simplification, only smooth curves will be considered. An infinite number of curves could be drawn from each point, each of which would result in a particular sequence of stratification.

For the sake of this discussion, predictive stratification sequences will be based on linear deceleration curves. With this in mind, a two-dimensional graph ("deceleration graph") whose axes are the rate of decrease of velocity of unidirectional $-dU_u/dt$ and oscillatory $-dU_o/dt$ flow is constructed (Figure 4.20b). For any initial condition on the initial-velocity graph, a deceleration history of both flow components can be represented on the deceleration graph. In the upper left portion of the deceleration graph, the unidirectional-flow component has a more rapid deceleration, while the oscillatory-flow component has a slower deceleration. In the lower right portion of the graph the oscillatory-

Figure 4.20: Theoretical interactive-flow model for deposition under combined oscillatory/unidirectional currents.

(A) "Initial-velocity graph" whose axes are initial unidirectional velocity $(U_u)_o$ and initial oscillatory velocity $(U_o)_o$. The initial conditions for any particular flow can be plotted as a point on this graph. The upper right-hand part of this graph, corresponding to high values of oscillatory and unidirectional velocities, is the upper-regime plane-bed field. This has been subdivided into oscillatory (OPB), unidirectional (UPB), and combined (CPB) plane-bed fields based on the dominant flow conditions.

(B) Assuming linear deceleration conditions, the time history of a flow can be represented by a single point on this "deceleration diagram" which plots the relative values of negative acceleration of unidirectional flow $-dU_u/dt$ and oscillatory flow $-dU_o/dt$ components.

(C) Generalized bedform stability fields for combined-flow conditions, assuming one uniform grain size, are given in the plot of unidirectional velocity U_u versus oscillatory U_o velocity. More comples graphs of this kind will be useful in the prediction of vertical stratification sequences (Figure 4.21).

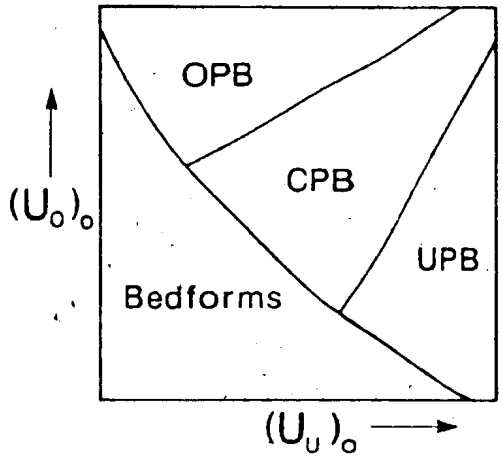
OPB
CPB
UPB
Bedforms
$(U_o)_o$
$(U_u)_o$

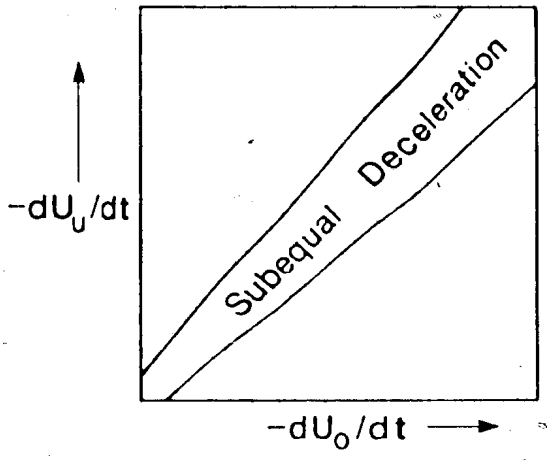
Subequal
Deceleration
$-dU_u/dt$
$-dU_o/dt$

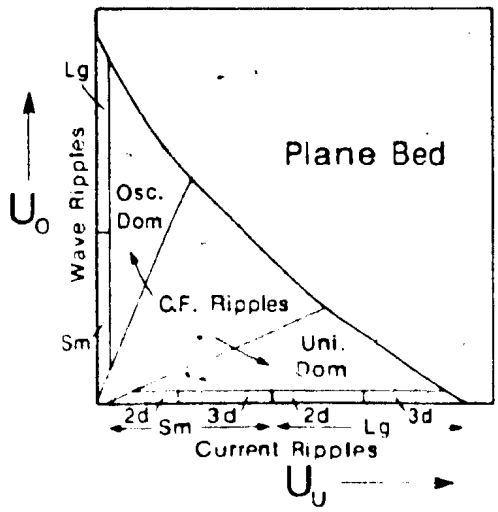
Lg
Wave Ripples
Plane Bed
Osc.
Dom
C.F. Ripples
Sm
Uni.
Dom
2d
Sm
3d
2d
Lg
3d
Current Ripples
U_o
U_u

flow component has a faster deceleration, while the unidirectional-flow component has a slower deceleration. In the central area the components decelerate similarly (Figure 4.20b).

Figure 4.21 illustrates how these graphs can be used to predict vertical stratification sequences. A point has been chosen on the initial-velocity graph in the plane-bed field where the unidirectional component is dominant. This is done to make this discussion relevant to the S3/S4 tempestites of the CIF, whose initial stages of deposition were dominated by unidirectional flow. Seven separate time-velocity histories are represented by the letters A-G on the deceleration graph in Figure 4.21. For each point a vertical stratification sequence is presented, flanked by a graphical representation of the change in velocity with time of each component. In order to standardize the predictive stratification sequences it is assumed that both the total thickness of deposited sediment and the rate of deposition are constant. Variations in the latter would primarily affect only the rate of climb of various bedforms.

The vertical stratification sequences presented in Figure 4.21 are determined by a combination of deductive reasoning, intuition, and educated guessing, due of the poor state of understanding of combined-flow bedforms and their response to varying flow conditions. The combined-flow stability fields given by Harms et al. (1982, Figure 2-18) can be used as a guide, or predictive tool, in determining stratification types under the various flow conditions (assuming equilibrium between the flow and the bed). Figure 4.20c is a generalized two-dimensional representation of these combined-flow bedform stability fields. There is, of course, some difficulty in comparing the predicted sequences with the rock record, one of which is distinguishing between different types of ripples, particularly the various types of combined-flow ripples. Ripples formed under complex oscillatory flow, which would not be represented in this model, are probably important components of tempestites, and these might be difficult to distinguish from other ripple types. An added problem in comparing the predicted features with those observed is the inability to distinguish between different types of plane-bed lamination (unidirectional-

Figure 4.21: Representative suite of vertical stratification sequences. A point has been chosen in the upper-plane-bed field of the "Initial conditions" diagram. Seven different deceleration histories (A-F) were chosen, each representing the change in velocity of both components with time. The velocity-time histories of each component are graphically represented next to the proposed vertical stratification sequences associated with each point. See text for details.

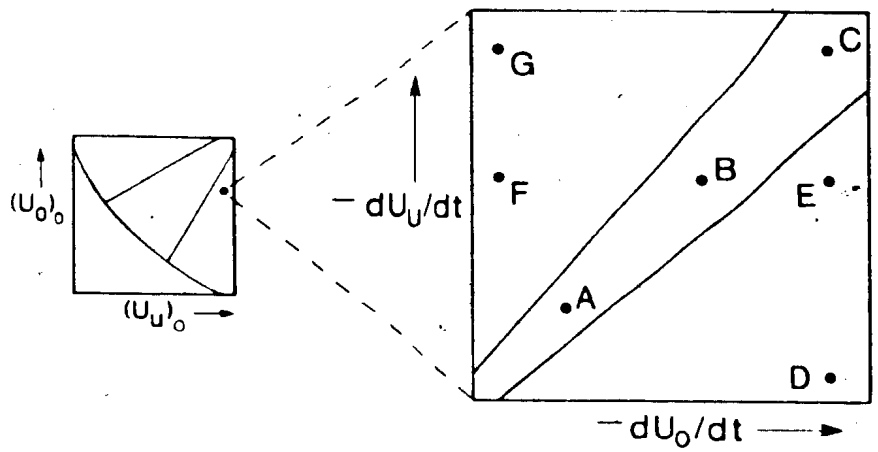
$(U_o)_o$
$(U_u)_o$
$-dU_u/dt$
$-dU_o/dt$
G
C
F
B
E
A
D

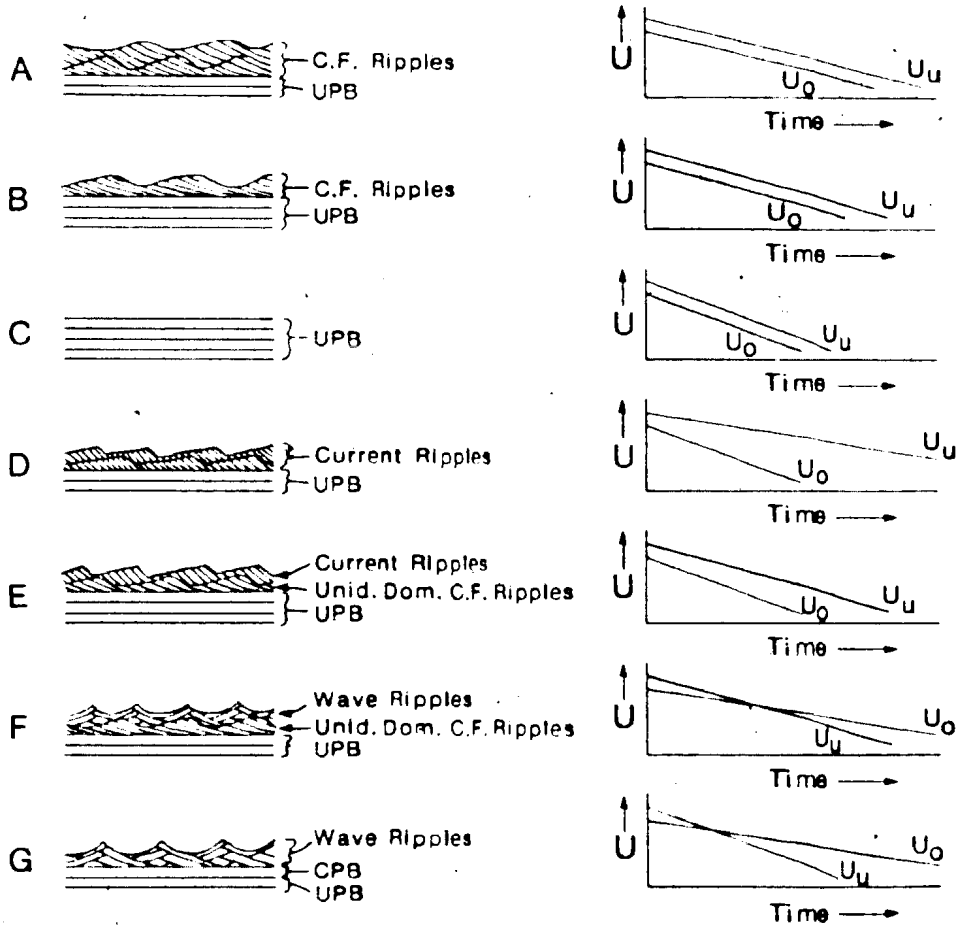
A
C.F. Ripples
UPB
B
C.F. Ripples
UPB
C
UPB
D
Current Ripples
UPB
E
Current Ripples
Unid. Dom. C.F. Ripples
UPB
F
Wave Ripples
Unid. Dom. C.F. Ripples
UPB
G
Wave Ripples
CPB
UPB
U
U_o
U_u
Time

dominant, oscillatory-dominant, or combined). Despite these formidable difficulties the model can be used to understand an individual vertical stratification sequence, or groups of sequences.

In the case of S3/S4 beds, it can be seen that under the initial conditions determined for these beds, namely combined flow with high initial unidirectional velocities, that some sets of deceleration curves are applicable, while others are not. For instance, the stratification sequences associated with examples C, D, and E in Figure 4.21 are not common in S3/S4 beds, and therefore the velocity-time histories associated with these examples are not applicable. The implication is that the S3/S4 flows did not decelerate at a rate faster than bedforms could form (example C), and that the influence of unidirectional currents did not generally outlast the effects of oscillatory currents (examples D and E).

It is possible using this model to focus on the bedforms that are found at the top of beds (bed tops are passively draped to a variable extent), especially as cross-sectional views are not available at some outcrops. It is obvious that, under the conditions outlined for this model, in most cases the velocity of one component of flow (b) will drop below a level which is negligible in its effect on bedform development (at or near threshold velocity for sand movement) before the other (a). As illustrated in the velocity-time diagram on Figure 4.22, there will therefore be a time gap between these components, designated $T_{a\text{-}b}$, where a is the longer-lasting component. If this time gap is less than the time necessary for the development of an equilibrium "a" bedform (T_{eq}), then the top of the bed will contain either parallel lamination or combined-flow ripples. If $T_{a\text{-}b}$ is greater than T_{eq}, then current or wave ripples will form at the top of the bed, depending on which component is "a", the longest lasting (Figure 4.22). Of course, wave or current ripples can form at the top of beds under wholly unidirectional or oscillatory flows, respectively, and therefore this applies only to combined-flow situations. The time gap $T_{a\text{-}b}$ would depend on the slope of each velocity curve and on the initial velocities of each component. For instance, in Figure 4.22, two separate points were chosen on the initial velocity graph (#1 and #2), and it is

Figure 4.22: Under the conditions of the theoretical interactive-flow model, the type of bedform found at the top of a bed is a function of which component of flow drops below threshold velocity for sediment movement first, and whether the time lag between the first and second component's deceleration below threshold velocity ($T_{a\text{-}b}$) is large enough to develop equilibrium bedforms (i.e., $>T_{eq}$). The box on the right demonstrates that if the time lag is greater than Teq, the bed will be topped with current or wave ripples depending on whether the unidirectional or oscillatory component is longer lasting. The speed at which the flow decelerates and the initial flow conditions are a factor. Points 1 and 2 have been chosen on the initial-conditions diagram. Similar deceleration curves, shown as similar points on the deceleration diagrams, are chosen for each. In "1" the time gap between components $T_{u\text{-}o}$ is $<T_{eq}$ and therefore the bed is topped with parallel laminae or combined flow ripples. In "2" the time gap is greater because of the initial disparity in the velocity of the components, and the time gap allows for the development of current ripples at the top of the bed.

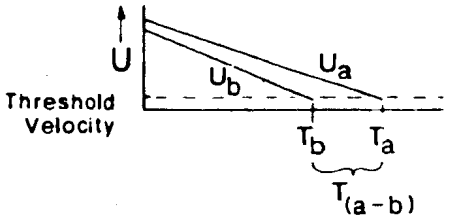

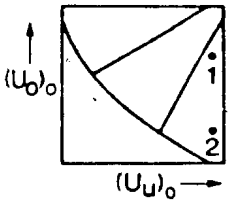

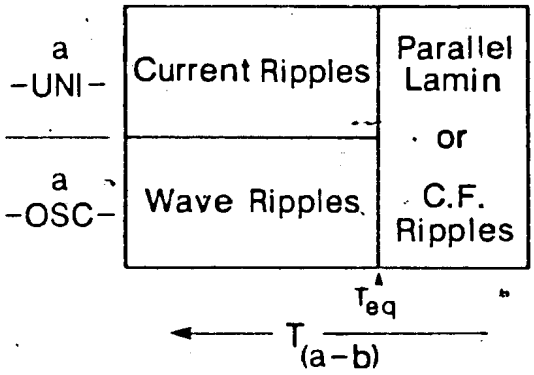

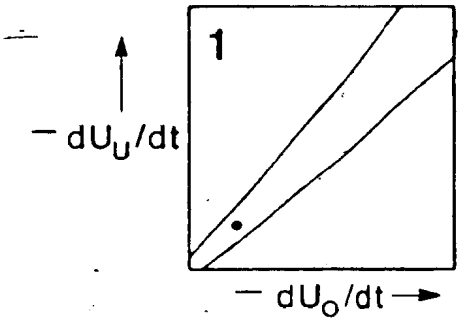

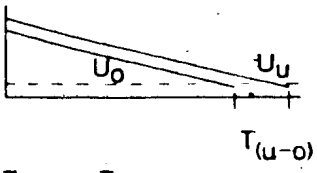

$T_{u-o} < T_{eq}$

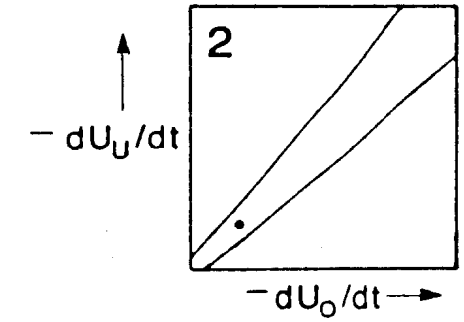

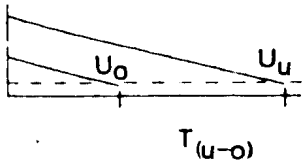

$T_{u-o} > T_{eq}$

shown that under similar conditions of deceleration (similar slopes on the velocity-time graphs), one of these (#2) will develop current ripples during the latter stages of deposition and the other will not.

If this diagram represents, at least in a general way, the main controls on vertical stratification sequences in tempestites, then it should be possible, considering the underlying assumptions, to recreate these conditions in a flume or tank. A program of experiments in a long-period combined-flow tank to generate a wide range of combined-flow stratification styles could aid greatly in the prediction of vertical stratification sequences by, among other things, constraining the stability fields of particular combined-flow bedforms. Work of this kind would also help in evaluating the feasibility of reconstructing the conditions outlined in this model within a flume or tank.

4.22.5 Tempestite Facies Model for CIF

Discussion of tempestites almost always concerns ancient or modern sandy shorelines. The model developed by Walker (1984) is a paradigm used by most geologists. In this model sand from the shoreface is carried offshore by turbidity currents and is deposited in the form of HCS above storm wave base and distal tempestites below storm wave base. An interesting aspect of this model is the hypothesis that part of the shoreface liquefies in response to intense cyclic wave loading, allowing for the rapid passage of large quantities of sediment into suspension.

At several horizons within the lower part of member 2 there are gradational transitions between intertidal and subtidal deposits. These indicate a shoreface dominated by fine-grained sediments, not sand. The Gutter Cast Facies (2.1) is found at these transitions both at the boundary between members 1 and 2 and the transition into Facies 1.4 at FD-103.7. This suggests that Facies 2.1 was deposited in the shallow subtidal zone and Facies 2.2 was deposited in deeper water. An interesting aspect of this reconstruction is a

seaward shift from very thin lenticular beds (dominantly S2) and abundant gutter casts to more continuous and thicker beds (S3/S4) without many gutter casts. Trends of proximality/distality for tempestites have been discussed by Brenchley et al. (1979), Aigner (1982), Aigner and Reineck (1982), Nelson (1982), and Brenchley (1985). Proximal to distal trends in these studies include both changes in bed thickness and sedimentary structures (Figure 4.23a). In these models, thick, often amalgamated, sandstone beds (SCS) dominate the nearshore and progressively thinner sandstone beds (HCS and distal tempestites) reflect increasing distality. A model for FA 2, given in Figure 4.23b, has a very different association of sedimentary structures and bed thicknesses. In this model the shallow subtidal is a zone of throughput with high-velocity, sediment-laden flows eroding deep narrow scours (gutter casts). Very little sand is deposited outside of these scours: most of the sediment bypasses the very shallow subtidal zone and is deposited in deeper water. As storm-generated flows move into deeper water they start to decelerate, resulting in less significant erosion of the sea floor and increased deposition, to form more continuous and regular beds (Subfacies 2.2A). At some distance from shore, bed thickness reaches a maximum (Subfacies 2.2B), and more distally bed thickness decreases. The distal tempestites, deposited below storm wave base, are represented by FA 3. Implicit in this model is the understanding that vertical bed-thickness distributions at any particular point along the shoreline must depend on the variation in intensity of the storms involved. And so, for instance, S4 beds are sporadically found throughout the section within otherwise thin-bedded strata, and S1-S3 beds are found within the thicker-bedded Subfacies 2.2B.

This model is based on observations solely from vertical lithofacies distributions. The weakest part of this model concerns the development of the thicker sandstone beds (including S4 and H-beds) of Subfacies 2.2B. The relationship of these beds to the shoreline cannot be demonstrated in the same manner as the thinner-bedded Facies 2.1 and Subfacies 2.2A, and these beds cannot be related to storm wave base (except to say they

Figure 4.23: Comparison of standard tempestite model versus proposed model for FA 2. Proximality trends in the standard model (A) include constantly decreasing bed thickness away from the shoreline with a shift from SCS sandstones to HCS sandstones to distal turbiditelike beds. The Model for FA 2 (B) shows a bed-thickness trend that first increases then decreases away from the shoreline. The proximal setting is one of bypass with erosion the dominant process (many gutter casts). Passing seaward, gutter casts die out and bed thickness increases. Rare HCS is formed in the thicker sandstone beds farther out on the shelf. Below storm wave base (SWB) distal tempestites are turbiditelike in character (FA 3).

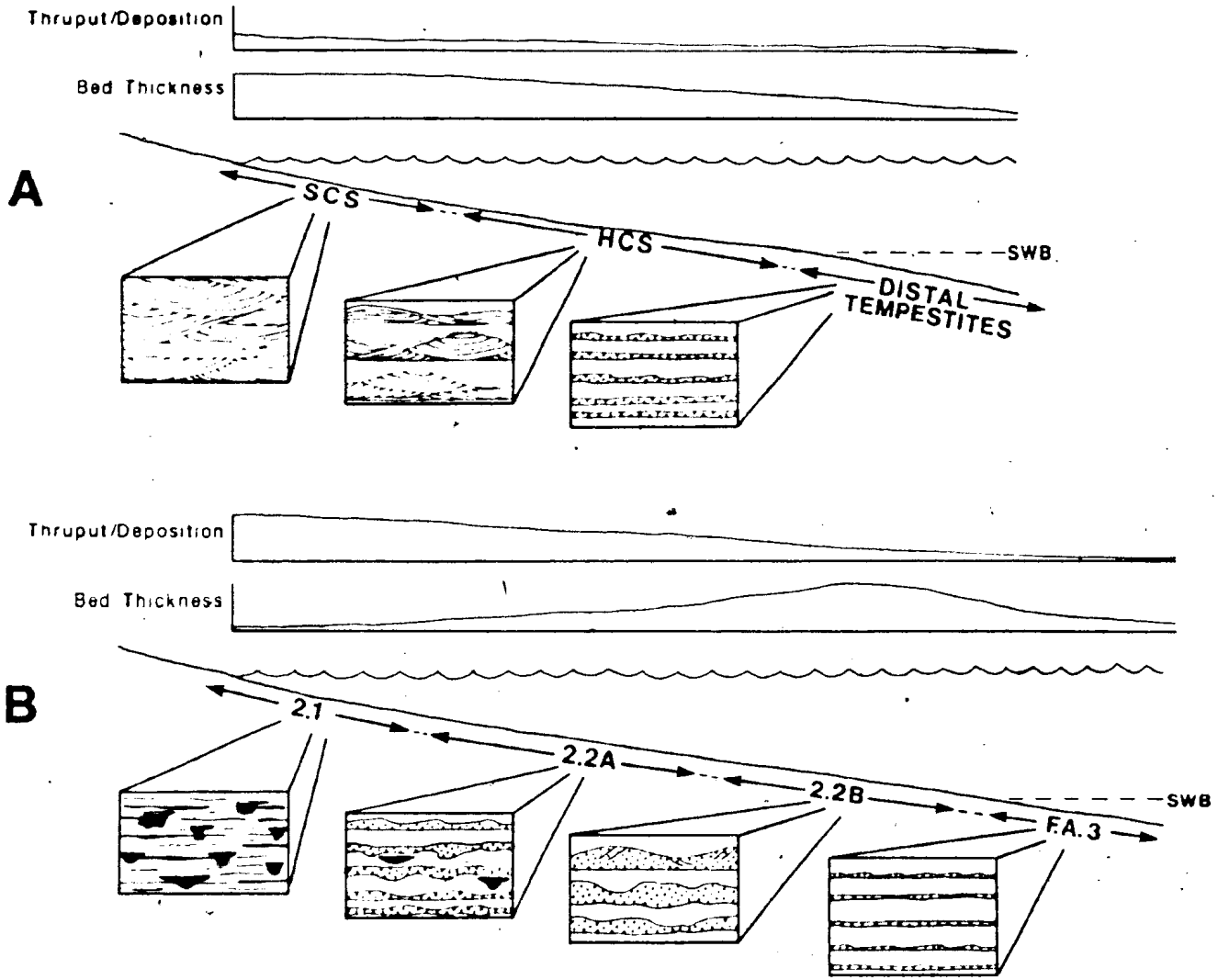
Thruput/Deposition
Bed Thickness
A
SCS
HCS
SWB
DISTAL
TEMPESTITES
Thruput/Deposition
Bed Thickness
B
2.1
2.2A
2.2B
SWB
F.A. 3

form above it) in the same way as FA 3. There is evidence to suggest that at least one stratigraphic occurrence of Subfacies 2.2B may be related to a temporal change in the depositional system. Approximately 3.5 meters of Subfacies 2.2B strata occurs immediately above a chaotic/deformed horizon at FD-346.2 (see Section 4.16.4). Strata above and below this package of Facies 2.2B contain widely spaced very thin to thin sandstone beds, while the strata in the package contain numerous thin to medium sandstone beds with highly erosional upper surfaces, amalgamation surfaces, and abundant wave ripples. The origin of this package and other sandstone-rich packages associated with disorganized beds will be discussed in more detail below. In the meantime it is important to note that not all occurrences of Subfacies 2.2B appear as dramatically within the section; in fact, most are highly gradational with Subfacies 2.2A. For this reason, there is no reason to suggest that major changes in shoreline processes are necessary to explain a slightly higher concentration and thickness of sandstone beds. Autocyclic changes associated with particular depositional systems (e.g., deltas) will be discussed below.

An important difference between the model proposed in Figure 4.23b and standard models for storm-influenced shorelines (Figure 4.23a) is the rarity of HCS beds. There are two possible reasons for this: (1) most beds in FA 2 are not thick enough to develop recognizable HCS, and (2) the conditions necessary to produce HCS were not met very often. The most common bed thicknesses of HCS are 20-80 cm, although they range from a few centimeters to well over 1 meter (Dott and Bourgeois, 1982). Very few data are available on bed thicknesses of HCS, but available data and observations by the author suggest that there are no natural size breaks of the kind known to characterize unidirectional bedforms, and therefore thin beds of HCS, if they had been abundant in the CIF, would have been recognized. It appears at this time that HCS requires the following: (1) long wave periods, (2) complex wave oscillations and (3) high velocities (See Section 4.10.1). One aspect of the depositional system of FA 2 that might have an effect on one or more of these factors is the concentration of fine-grained sediment. It is readily apparent that for

much of the time during the deposition of Facies 2.2 the substrate was fine-grained, and at some periods the water column may have had high levels of suspended sediment. Numerous authors (Nair, 1976; Augustinus, 1980; Wells and Coleman, 1981; McCave, 1985; Rine and Ginsburg, 1985), in the study of deltaic systems, have commented on the effects of high suspended-sediment concentrations on waves. These effects include: (1) attenuation of waves, and (2) drop in amplitude, and change to solitary wave shape (smaller, sharp-peaked crests with flat troughs that are at still water level) (Wells and Coleman, 1981). There is no way to know if, or how often, high sediment concentrations characterized the inner shelf during the deposition of Facies 2.2, but even partial attenuation of waves by such a process might have be an important factor in suppressing the formation of HCS.

4.22.6 Evidence for Deltaic Sedimentation

The dynamics of deltaic sedimentation, affecting both the morphology and overall character of the delta, are determined by the basin geometry, which in turn controls the interaction among waves, tides and sediment input. Waves and tides tend to rework sediment into well sorted sands in the form of beaches, shoals, and tidal sand ridges, while the mud tends to be carried offshore, and in the case of tide-dominated shorelines, to the tidal flats as well. Deltas affected by high tidal ranges tend to form in large funnel-shaped indentations in the shoreline and contain large subtidal shoreline-perpendicular sand ridges (e.g., Ganges-Brahmaputra and Ord Deltas). Deltas subjected to strong wave power tend to form beach-barrier shorelines (e.g., São Francisco and Senegal Deltas). Highly constructive deltas, dominated by fluvial processes, tend to form with lobate to bird-foot morphologies in enclosed or semi-enclosed basins (e.g., Mississippi and Po Deltas).

As mentioned in Section 9.22.2 there is no direct evidence for a beach facies in the lower part of Member 2, where foreshore/intertidal sediments are repeatedly exposed. One

possibility is that the lack of a beach facies is related to the abundance of siltstone in FA 2. Modern inner shelf settings with abundant fine-grained sediments are generally associated with large deltas, especially in areas of moderate to low wave and tidal influence. These deltas may have high rates of deposition of fine-grained sediments: e.g., Mississippi and Huanghe (Yellow River) Deltas. Muddy coasts are furthermore often characterized by high suspended-sediment concentrations (Wells and Coleman, 1981). As mentioned above in the discussion of HCS beds in FA 2 (Section 4.22.3), the effects of a muddy substrate and high suspended-sediment concentrations associated with deltas include significant attenuation of waves. The shape of deltas, which "...tend to be fronted by broad, gently sloping subaqueous profiles [may also cause] the waves [to] undergo significant refraction, shoaling and frictional attenuation as they approach the shoreline" (Elliot, 1978, p. 112). If the deposition of FA 2 was characterized by high depositional rates of fine-grained sediments, the influx of sediments would work to offset the destructive effects of tides and waves and explain the lack of beach or tidal-sand-ridge facies. If FA 2 was deposited within a deltaic setting with high suspended-sediment discharge, there should be evidence for high depositional rates. Such evidence is described below.

The most important aspect of FA 2 that calls for high sedimentation rate is the abundance of nearshore instability features. The process interpretations for the gravity-flow deposits of FA 2 (see Sections 4.14.1.2 and 4.14.5) emphasized the role of high sedimentation rate in generating conditions suitable for failure (high pore pressures and liquefaction) on the slopes typical of nearshore marine settings. According to Moore (1961), failure of metastable (underconsolidated) sediments is "...of greatest importance in specialized, near-shore neritic or estuarian [sic] environments" (p. 355-356), and is "normally found in the marine environment only off large rivers carrying predominantly fine-grained silt and clay-sized material" (p. 351).

Instability features from the Mississippi Delta have received considerable attention (Shepard, 1955; Terzaghi, 1956; Moore, 1961; Coleman and Garrison, 1977; Roberts,

1980; Embley, 1982; Prior and Coleman, 1982). Mass-movement features from the Mississippi Delta include collapse features, slides (bottleneck and rotational), mudflows (with gullies and overlapping lobes) and faults (Prior and Coleman, 1982). Active slope failures, including collapse structures and silt flows, have also been described recently from the Huanghe Delta (Prior et al., 1986). A variety of gravity-flow structures, including slides and debris flows, have been described from the delta front at the head of a fjord in British Columbia (Prior et al., 1984). It is readily apparent that a full range of gravity flows is possible in delta-front settings, and that the types of mass movements described for FA 2 are compatible with a deltaic origin. In fact a deltaic setting may be the only reasonable alternative, given the low slopes that are typical of most shallow shelf settings and the fact that on modern shelves gravity-flow features are found only in areas of high sediment input associated with deltas.

Additional evidence for high sedimentation rates of mud is the small number of amalgamated sandstone beds in FA 2 (some Q, S4, and H beds). Amalgamated tempestites would be expected under conditions where little sediment is deposited between storms or where successive storms are separated by short periods of time. There is no way of knowing the timing of storms during the deposition of the CIF, but it seems unlikely that, in a shallow subtidal setting, such a remarkable paucity of amalgamated beds could result without a high input of fine-grained sediment. Another piece of evidence to support high sediment accumulation rates is the abundance of sedimentary dikes in the shallow subtidal deposits of Facies 2.1. These dikes register the movement of water-laid sand experiencing elevated pore pressures. Rapid burial of water-laid sand by fine-grained sediments does not allow the slow release of water, and the high pore pressures that result eventually lead to the vertical injections of sand.

The evidence outlined above indicates that deposition of FA 2 took place in a nearshore setting characterized by high sedimentation rates, probably within or along the flanks of a delta. Due to limitations imposed primarily by lateral outcrop distribution a

detailed reconstruction of deltaic environments cannot be achieved. This is a serious limiting factor in the reevaluation or modification of existing models of deltaic deposition. The process interpretations of the various facies have allowed the paleobathymetric positioning of lithofacies and the reconstruction of depositional processes. Furthermore, the association of particular depositional processes, for instance storm processes and gravity-flow deposition, may prove important in expanding facies models of shelf sedimentation.

4.23 DEPOSITIONAL MODEL

The model for tempestite sedimentation developed for FA 2 (Figure 4.23b) is compatible with a deltaic model. Sandstone beds with the characteristics of turbidites have been described from a number of ancient deltaic deposits (McBride et al., 1975; De Raaf et al., 1965; Walker, 1969; Horowitz, 1966; Allen, 1960). Storm-generated sand beds with Bouma sequences have been described from the Yukon River Delta in Norton Sound, Alaska, a shallow embayment of the Bering Sea (Nelson, 1982; Howard and Nelson, 1982). The Yukon River Delta supplies sediment directly into the Bering Sea, where waves erode and suspend large volumes of sediment that are carried offshore during storms. The exact nature of the transport of the sediment is not known, although Nelson (1982) prefers a storm-surge-ebb origin.

4.23.1 Source of Sand

One fundamental question concerning deposition of tempestites in FA 2 is the source of the sand. As argued above, during deposition of the lower part of Member 1 there is no evidence for beaches. One possible source of sand may have been the tidal flats

(Facies 1.1/1.2) that flanked the inferred delta. Facies 1.1 contains abundant scours and erosional surfaces, indicating that sediment ~~was be~~ing actively removed from the tidal flat. It is difficult to imagine, however, that the quantity of sediment removed from this setting would be enough to form extensive sand beds over much of the shelf.

Another possible source of sandy sediment within fluvial-dominated delta settings is cheniers. Cheniers are found along coasts that flank large deltas; examples include the Guyana and Surinam coasts flanking the Amazon River (Augustinus, 1980; Brouwer 1953) and the Gulf Coast adjacent to the Mississippi River (Hoyt, 1969; Gould and McFarlan, 1959). These features form under conditions of low wave and tidal energy in areas with effective longshore currents and a variable supply of dominantly fine-grained sediments (Elliot, 1978). Cheniers form at times of low sedimentation rate when waves and currents can winnow the shoreline sediments to form sandy beaches. During times of high sedimentation rate there is progradation of mud flats. It has been demonstrated in Gulf Coast region that periods of progradation and reworking correspond with times of switching of the active delta (Gould and McFarlan, 1959). Because cheniers are a likely component in a fine-grained fluvial-dominated deltaic system such as envisioned for FA 2, these cannot be ruled out as a possible source of sand. Cheniers may be appealed to particularly in the case of the Q Beds, whereby these could act as a source of well sorted sand. It has already been pointed out that there is no direct evidence for the existence of beaches in the lower part of member 2, while the upper part of member 2, which is sandier than the lower part, does not have any preserved shoreline deposits. One could therefore postulate that cheniers formed during the deposition of the upper part of member 2 and that these acted as sand sources at this time. There is, however, a strong similarity in the character of the sandstone beds (i.e., color, grain size, sorting) between the upper and lower parts of member 2, arguing for a continuity of sediment source during the deposition of the entire member.

The most logical source of sand would be direct input from the fluvial distributaries. McBride et al. (1975, p. 504) have interpreted deltaic sandstone beds from Late Cretaceous rocks of northern Mexico as "...turbidity currents that were generated when sediment-laden flood water debouched from delta distributaries". The proximal beds have erosional bases, rare flute and groove casts, but no graded bedding. Beds they consider prodeltaic contain more abundant flute and groove marks and common Bouma T_b and T_c units.

The direct input of sand from distributaries may help explain a number of features of the tempestite model for FA 2 that are at odds with the standard models. One major difference between these models is the presence of an area dominated by erosion and throughput in the shallowest subtidal setting (Gutter Cast Facies) in the model for FA 2. One problem in understanding the development of this facies in its paleoenvironmental setting, in terms of the standard models of tempestite deposition, is that there is a limited space between the shoreline and the shallow subtidal zone in which sediment flows could attain sufficient momentum to create a zone of erosion and throughput. This enigma is solved by allowing for fast-moving sediment flows to be debouched from distributary channels into the shallow subtidal environment, where they erode the sea floor on entry into the marine setting and then spread out to deposit their load across the delta-front, prodelta and shelf environments. The limited exposure of shoreline deposits in member 2 make such speculation difficult to prove, especially since there are no preserved channel deposits that are unequivocally distributary in nature.

4.23.2 FA 2 Mass-Movement Deposits

4.23.2.1 Introduction

The study of subaqueous mass-movement features has primarily been focused on deep-sea fan and slope deposits, both Holocene and ancient. Holocene deltaic mass movements have received increasing attention, particularly those of the Mississippi Delta; however, these deltaic slides and gravity flows "...have rarely been observed in ancient counterparts" (Coleman, 1981, p. 84).

Hubert (1972) describes an example of synsedimentary slumps in Upper Cretaceous deltaic deposits from Wyoming. Large, elongate sandstone pillows in the shape of flattened cylinders formed in the outer delta platform/upper prodelta region with their long axes parallel to the shoreline. Hubert documents a downslope progression from vertically loaded pillows to inclined and overthrusted pillows to slump folds. This example is a suitable analog to the style of deformation envisioned for the disturbed facies described in this thesis, particularly the lateral changes in degree of deformation described for FD-168.2, and the model of proposed transformation from disturbed beds to raft-bearing beds. It is important to note that the rocks that Hubert described were deposited in a sandy, wave-dominated, highly destructive delta.

Klein et al. (1972) describe one of very few ancient deltaic deposits with abundant and diverse gravity-flow deposits. These include slump folds, pull-aparts, contortions, pebbly mudstones, slurry deposits with large clasts, and sandy grain-flow [?] deposits. These deposits are geographically and stratigraphically concentrated in what are thought to represent lower delta-front troughs, as described by Shepard (1955) and Shepard and Dill (1966). Klein et al. (1972) suggest downslope transitions from sliding/slumping (upper delta front) to grain flows/slurry flows to turbidity currents (lower delta front troughs).

Despite having more sandy facies, the gravity-flow deposits are similar in character and variety to those of the CIF.

Any model for the mass-movement deposits of FA 2 must explain (a) the abundance of unifite beds in the Gutter Cast Facies (2.1) and in strata transitional between this facies and the Sandstone/Siltstone Facies (2.2), (b) the lack of any disorganized beds in the shelf (below storm wave base) deposits of FA 3 (see Chapter 5), and (c) the presence of disturbed and raft-bearing Beds and chaotic/deformed horizons in Facies 2.2, particularly in association with sandy intervals that in cases are rich in S3/S4 beds. These points are addressed below.

4.23.2.2 Unifite Deposition: Upper Delta Front

In the deep-sea setting a variety of mass movements including slumps, slides and debris flows are found along the continental slope and in submarine fan environments, while unifites are found in basin plain depressions. Stanley and his coworkers (Rupke and Stanley, 1974; Stanley et al., 1980; Stanley, 1981; Stanley and Maldonado, 1981) have demonstrated convincingly that unifites deposited in these deep-water catchment basins represent "...end-products of a sediment gravity flow continuum..." (Stanley, 1981). In Stanley's model mud preferentially bypasses the slope as individual gravity flows that undergo a series of downslope transformations which end in deposition from low-density muddy turbidity currents. It is clear from the paleoenvironmental reconstruction of lithofacies for FA 2 that the unifite beds, which are volumetrically important in the Gutter Cast Facies (2.1) and in the more proximal parts of the Sandstone/Siltstone Facies (2.2), are not the residuals of a long, complex, flow-transformation sequence. Slumps, slides and debris flows are found only in the more distal deposits of Facies 2.2, a situation opposite to that which characterizes the deep-sea environments.

The unifite beds must have been formed from failure of sediments in the lower reaches of distributary channels/upper delta front or in adjacent mudflats (i.e., Wells et al., 1980). The intertidal deposits that are transitional with Facies 2.1 consist of heterolithic lithofacies of sandstone and shale (FA 1) and are not likely candidates as sediment sources for unifite beds. Lindsay et al. (1984) have emphasized the importance of sediment failures at the edge of fine-grained distributary mouth bars as an important process in transporting sediment onto the prodelta region of the Mississippi Delta. Shears, faults, blocky mudflows, gullies and bottleneck slides extend from the front of the distributary mouth bars out across the delta front (same as delta-front trough deposits described earlier by Shepard, 1955, and others).

One possibility for the origin of the CIF unifites, given their channelized nature, is that they were deposited in an upper-delta-front setting (see Roberts, 1980; Prior and Coleman, 1982) from liquefied flows or turbidity currents that were generated locally in the lower reaches of a distributary channel. These may have formed from failure of the local sea floor or muddy delta-front mouth bars. The well graded and stratified unifites (Type 3) may have been generated closer to shore (upstream?) to have allowed evolution into a turbidity current prior to deposition on the delta front. Excellent analogs for these silty flows are described by Prior et al. (1986) from the Huanghe (Yellow River) Delta. They describe 100-500 m wide, silt-flow gullies that form on slopes of 0.3-0.4° on the delta front. These gullies are up to 3-4 km long, but generally have a relief of only about 1 m. These gullies are filled with acoustically transparent sediments that lack internal structure or bedding and are thought to have been generated by liquefaction. Liquefaction of deltaic silts on slopes less than 1 degree has also been described from the Klamath River Delta (Field et al., 1982).

4.23.2.3 Chaotic/Deformed Horizons, Raft-Bearing Beds, Disturbed Horizons: Lower Delta-Front/Prodelta

In muddy deltas, such as the Mississippi Delta, the transition from the delta front to the prodelta (sometimes referred to as the prodelta platform), is marked by an increase in slope. The bulk of mass-movement features (slumps, slides and various gravity flows) in these deltas are found at and below this major break in slope in the lower delta front/upper prodelta area. It is clear from descriptions of these modern deposits that many of their characteristics are similar to those of the disorganized beds in FA 2. The delta-front debris flows described by Prior et al. (1984) as remolded pieces of the sea floor, derived from faulting and sliding on the upper delta front, are incorporated into water-rich sediments to form large lobes of block-bearing flows. These are likely analogs for the raft-bearing beds, which also contain blocks that were clearly derived from adjacent substrate. The chaotic/deformed horizons of FA 2 have analogs in the slides and slumps that are documented from modern deltaic settings. Coleman et al. (1974) describe rotational slumps associated with distributary-mouth bars of the Mississippi River.

4.23.2.4 Shelf Environment

If one can assume that the shelf deposits of FA 3 (described in Chapter 5) are reasonably representative of the shelf environment during deposition of FA 2 (FA 3 is gradational with, and found stratigraphically above, FA 2 in all outcrops), then the lack of gravity flows in this FA 3 indicates, as one would expect, that the transition from the prodelta to the shelf area was marked by a decrease in slope and consequently a reduction in the susceptibility of sediments to failure. An even more important factor in the reduced susceptibility of sediments on the shelf to failure would be the much lowered sedimentation rate in this environment.

4.23.2.5 Disorganized Beds and Sandstone-Rich Intervals

As mentioned earlier, in certain cases the sandstone content of strata directly above some disorganized beds is anomalously high. In these examples one is forced to consider a genetic link between the high sandstone content and the disorganized bed. Such cases include all disorganized bed types including chaotic/deformed horizons (FD-346.2), unifites (FD-92.6), raft-bearing and disturbed beds (FD-168.2). The most striking, and most important, example is at FD-346.2, in which HCS sandstones are found directly overlying a buckled surface, and in several meters of strata above this horizon. It was suggested in Section 4.16.4 that the features at FD-346.2 provide a link between storm processes and mass movements in FA 2. Such a link has been suggested for Holocene sediments but has never been observed directly or documented in the rock record.

Henkel (1970), studying the effects of Hurricane Camille in the Gulf of Mexico, provided a theoretical basis for understanding wave loading of submarine sediments. Henkel and others (Hampton et al., 1978; Coleman, 1981; Cita, et al., 1982; Lindsay et al., 1984; Kraft et al., 1985) have attributed failures on the Mississippi Delta, and elsewhere, to fluctuations in bottom pressure associated with large surface waves. Storm waves off of the Huanghe Delta reach heights of up to 7 m and are considered a probable cause for sediment failure on the delta (Prior et al., 1986, p. 94). According to Watkins and Kraft (1976), storm-induced sediment failure is plausible in water depths up to 150 m. If, as suggested, the sediments of Facies 2.1 and 2.2 were susceptible to failure because of the rapid deposition of silt, then any number of factors other than storms, such as earthquakes, could have also caused mass movements. Given the strong imprint that they had on the character of these facies, storms are likely to have been an important triggering mechanism.

The sandy zones above certain disorganized beds are up to 3-4 m thick, and were therefore obviously not deposited by single storms; in fact, these may represent several

thousands of years of deposition. Without data on depositional rates it is difficult to evaluate the time span associated with these sandy packages. It is difficult to explain the sudden appearance of sandstone above these mass-movement deposits by such factors as climatic changes or by shifting of deltaic distributaries. The shift of a delta distributary might cause an increase in the percentage of sandstone, but (a) there is no reason to expect this to initially cause a slump or gravity flow, and (b) the thickness of sandy section would likely be greater (there is less than a meter of sandy strata above FD-92.6). A more probable cause is believed to be a drop in relative sea level. Pressure forces associated with large storm waves increase in shallow water (Wiegel, 1964), so that a lowering of relative sea level would probably increase the probability of storm-induced failure. Such a lowering might also induce greater erosion at the shoreline and explain the increase in sandstone content.

4.23.2.6 Gravity Flows: Summary

Evidence would suggest that the CIF unifites were formed in very shallow water (upper delta front) on relatively low slopes. Disturbed horizons, slumps, slides and debris flows formed on higher slopes at the transition between the lower delta front and the prodelta, where gravity effects were more important. On the open shelf, characterized by low sedimentation rates and low slopes, sediment failure was not a factor. Storm effects have been both implicated in, and proven theoretically feasible as, causes of sediment failure. The association of a submarine slide and HCS at FD-346.2 strongly suggests that at least some mass movements in FA 2 were triggered by wave-loading effects. The association of certain mass-movement deposits and sandstone-rich horizons is difficult to reconcile. A rapid lowering of relative sea level may be the best hypothesis to explain this association.

In the sections on process interpretation for the raft-Bearing Beds (4.16.3.1) it was suggested, based on relationships at the top of FD-168.2, that currents actively eroded the sea floor in an attempt to reinstate planarity after deposition of this debris flow. It is interesting to note that slump horizons in the Cretaceous deltaic deposits described by Hubert (1972) also have beveled upper surfaces that were cut by currents prior to renewed deposition. The nature of these eroding currents is unknown, but it is intriguing to consider how much sediment may have been deposited and eroded without leaving any mark in the rock record.

4.23.3 Delta-Abandonment Deposits

Process Interpretations for Facies 2.3 and 2.4 (Sections 4.19.1 and 4.20.1, respectively) call for quiet-water sedimentation with low sand input. Facies 2.3 was deposited under oxygenated conditions that supported burrowing infauna. Facies 2.3 strata, particularly at PM, contain evidence for periodic wave reworking of sandstone laminae. The sediments of Facies 2.4 were not disturbed by infauna, and the evidence suggests that the interstitial fluids, and possibly even the bottom waters, were reducing during deposition.

Both Facies 2.3 and 2.4 are found in relatively thin, stratigraphically restricted packages over a wide area, making them excellent marker horizons (Figure 1.5). As mentioned in Section 1.5, the thick package of Facies 2.3 exposed at GB was used by Bengtson and Fletcher (1983) as the boundary between member 2 and member 3 (the member 2A/2B boundary of this report). This package is also present at FD and PM.

There is far too little information in these facies alone to allow delineation of depositional environments, but given the restricted stratigraphic range and the gradational relationship with the deltaic deposits of the Sandstone/Siltstone Facies (2.1), this facies is

thought to have formed during times of delta abandonment. According to Elliot (1978, p. 129), "In general, abandonment facies comprise thin but laterally persistent marker horizons composed of facies which reflect relatively slow rates of sedimentation".

The shift from the red siltstones of Facies 2.3 to the green siltstones of Facies 2.4, as seen at the PM, FD, and GB localities, records (a) a decrease in sandstone content, (b) a loss of wave-formed lamination, (c) a loss of burrows, and (d) a shift from oxidizing to more reducing conditions. These changes are all consistent with a shift toward increased water depth. Assuming a relatively constant subsidence rate, abandonment of a delta lobe would dramatically reduce the ratio between sedimentation rate and subsidence and would result in deepening. After abandonment the sand content of the sediments would decrease because of decreased sand supply and increased distality as deepening continued. The loss of wave-formed laminae imply a shift toward water depths below or near storm wave base. The shift from oxygenated conditions that supported an infaunal population (Facies 2.3) to reducing or partly reducing conditions that were inhospitable to organisms (Facies 2.4) is also consistent with increased water depth, assuming some degree of oxygen stratification, for which there is evidence in FA 1 and FA 4 (Chapter 6).

4.23.4 Channel Deposits

It is clear from the description and process interpretation of T-Beds (Section 4.9) that they represent channel-fill sandstones. The lack of cross-laminae in these T-Beds argues that these are not lateral-accretion deposits. The thinning- and fining-upward sequence from FD-137.3 to FD--154 (Plate 28a,g) commences with T-Beds and interbeds of green siltstone (S0) that are clearly subtidal in origin and are in sharp contact with the shrinkage-crack-bearing Facies 1.2. The upward transition into Facies 1.1/1.2 indicates that this is a shoaling-upward sequence. As a rough estimate of channel depth, the thickness of strata from the base of the first and thickest T-Bed (FD-137.3) to the point

PLATE 28: SHOALING CHANNEL SEQUENCE (FA 2)

a: Full shoaling channel sequence from thick sandstone beds to red and green, thin-bedded shales and sandstones. Stratigraphic top is to right. Field of view covers approximately 15 m of strata (~FD-137-152).

b: Well-aligned synaeresis cracks on top surface of bed at FD-151.85. Notebook is 18.5 cm long.

c: Current (?) ripples on bedding plane at FD-153.1 are overprinted with shrinkage cracks. The are large and semi-polygonal, indicating that they may be desiccation features. Scale is 15 cm long.

d: Large desiccation cracks at FD-152.8. Numerous generations of cracking are distinguishable, a criteria diagnostic of desiccation (Plummer and Gostin, 1981). Notebook is 18.5 cm long.

e: Red shale and sandstones from FD-146-147. Note shale chip conglomerate, erosional upper surfaces, wave ripples and abundant shrinkage cracks. Stratigraphic top is up. Scale is in centimeters.

f: Large, rounded phosphatic shale clasts and desiccation (?) cracks on bedding surface at FD-153.1. Scale is 15 cm long.

g: Close-up of base of shoaling channel sequence from the thick (1.8 m maximum thickness) sandstone bed at the base (FD-137.3) to the red shales and sandstones at FD-146-147. The lower sandstone bed is in erosional contact with red sandstone laminated/very thinly bedded shales of Facies 1.2. Stratigraphic top is to upper left. Photo covers approximately 13 m of strata. The same interval is shown from a different angle in "a".

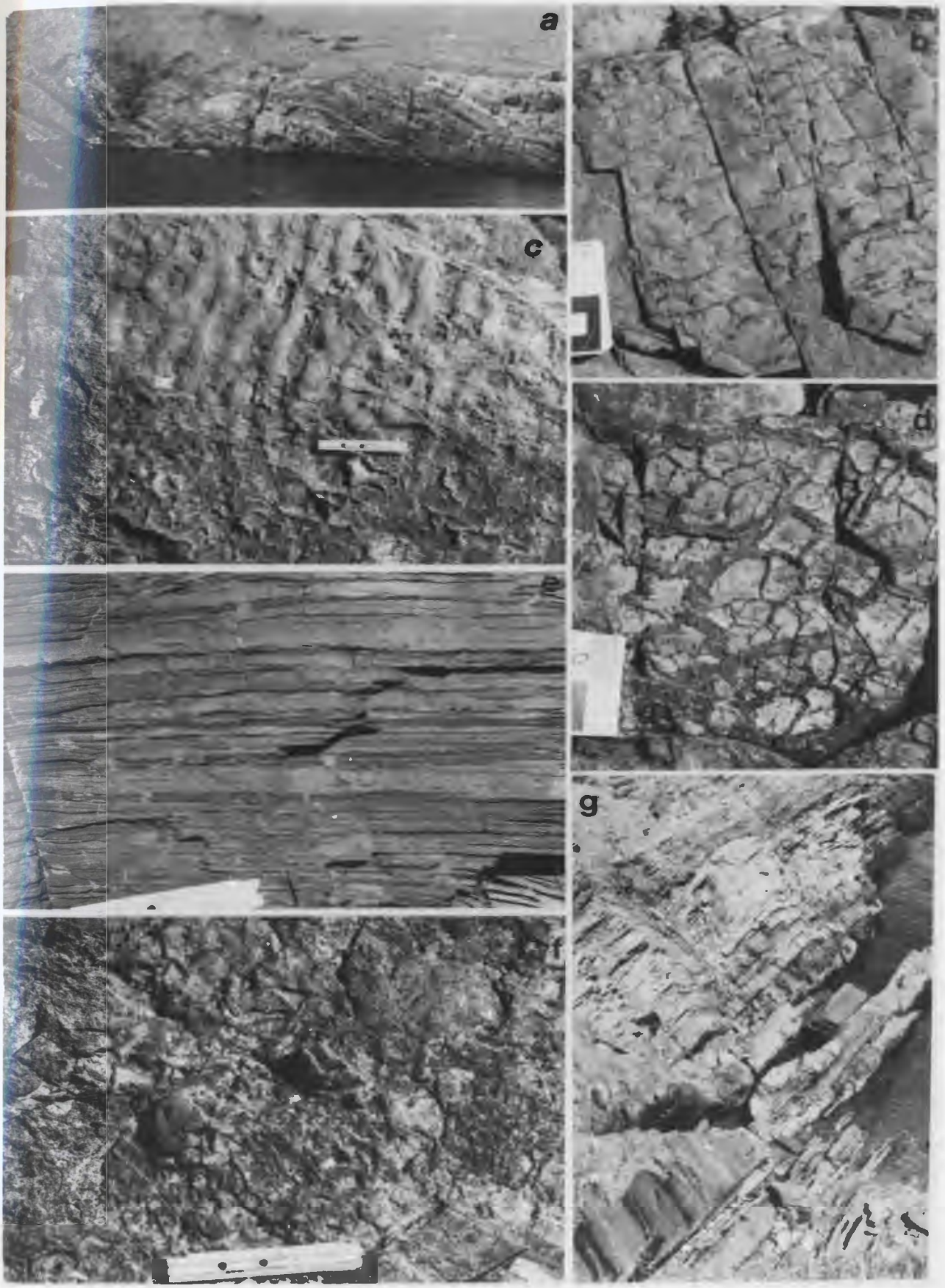
a
b
c
d
e
f
g

where the rocks take on a red tint and exhibit shrinkage cracks (FD-145), is 7.7 m. A single lenticular T-bed at FD-168.2 is within strata of the Sandstone/Siltstone Facies and has a thickness of only 60 cm. From the field relationships, the maximum depth of the infilled channel was not likely much greater than 60 cm (the full length of the bed is not exposed). There is no exposure where one can trace a channel sandstone from intertidal to subtidal deposits, but if these channels did extend across the shoreline into the subtidal zone, then one could expect a reduction in channel depth as the channel died out seaward.

It is not possible to deduce with certainty the nature of these channels. The thin-bedded, fine-grained strata in the shoaling sequence above FD-137.3 argue for channel abandonment and deposition of a local mud blanket. The strata may represent the infilling of an abandoned tidal channel or an estuarine channel. There is no evidence to suggest whether or not these channels were fed by a fluvial source.

Chapter 5

FACIES ASSOCIATION 3: LAMINATED SILTSTONE

5.1 INTRODUCTION

Facies Association 3 consists entirely of one facies (Facies 3.1), and constitutes all of member 3. The entirety of the following description is based on observations from the outcrop at Dantzic Cove.

5.2 LAMINATED SILTSTONE FACIES (3.1)

The Laminated Siltstone Facies consists of grey-green siltstone with fine laminae to thin beds of fine sandstone (Plate 29a). The weathering pattern is one of numerous, extensive bedding planes with variably spaced 'steps' (Plate 29b). The soles of beds are never exposed. The upper bedding planes display current ripples (Plate 29c,h), current lineations (Plate 29d,h), and a limited range and modest quantity of trace fossils (Plate 29g). Ripples are dominantly straight or sinuous crested with asymmetrical profiles. Rare linguoid ripples are present, as are ripples with more symmetrical form, the latter having very high spacing-to-height ratios (e.g., 30). Only unidirectionally oriented cross-laminae are observed within any of the ripples, even those with relatively symmetrical profile. Transitions from straight to sinuous to linguoid or interference ripples may be seen on a

PLATE 29: LAMINATED SILTSTONES (FA 3)

a: Close-up of lamination near the base of the DC section. The sandstone laminae are more abundant and less disrupted than those upsection. Note ripple cross-lamination preserved in concretions at top of photo (arrow). Stratigraphic top is up. Scale is 15 cm long.

b: Outcrop view of FA 3 showing abundant bedding planes, many of which display ripples and current lineations. Stratigraphic top is up. Height of outcrop face on right (arrowed) is approximately 40 cm.

c: Bedding plane view of straight- to sinuous-crested current ripples. Scale is 15 cm long.

d: Current-lineated surface at DC-85.0. The lineations show variations in orientation up to 40 degrees. Notebook is 18.5 cm long.

e: Carbonate nodule preserving precompactional thickness of very thin sandstone bed. Note ripple cross-lamination within the concretion and thin sandstone lamina that bows -up over the top of the concretion. Stratigraphic top is up. Scale is in centimeters.

f: Bedding plane view of septarian nodule. These form in nodular bodies by hardening of the exterior and dehydration and shrinking of the interior to form shrinkage cracks. Scale is 15 cm long.

g: Cross-sectional view of laminae disrupted by Teichichnus rectus burrows at DC-125. Stratigraphic top is up. Scale is in centimeters.

h: Sandstone bed at DC-82.9 with lower division of parallel laminated, current-lineated medium sandstone and upper division of current ripples. Paleocurrent direction for current lineations is shown by arrow. Note that crest-line orientations for the ripples form an acute angle to this direction indicating a clockwise shift in paleocurrent. Notebook is 18.5 cm long.

i: Partially carbonate-cemented sandstone bed at DC-138.4 in transition zone from FA 3 to FA 4. Thin sandstone laminae are locally bioturbated at base, but the thicker bed is undisturbed. Scour-and-fill structure above the bed has erosional upper and lower surfaces. Stratigraphic top is up. Scale is 15 cm long.

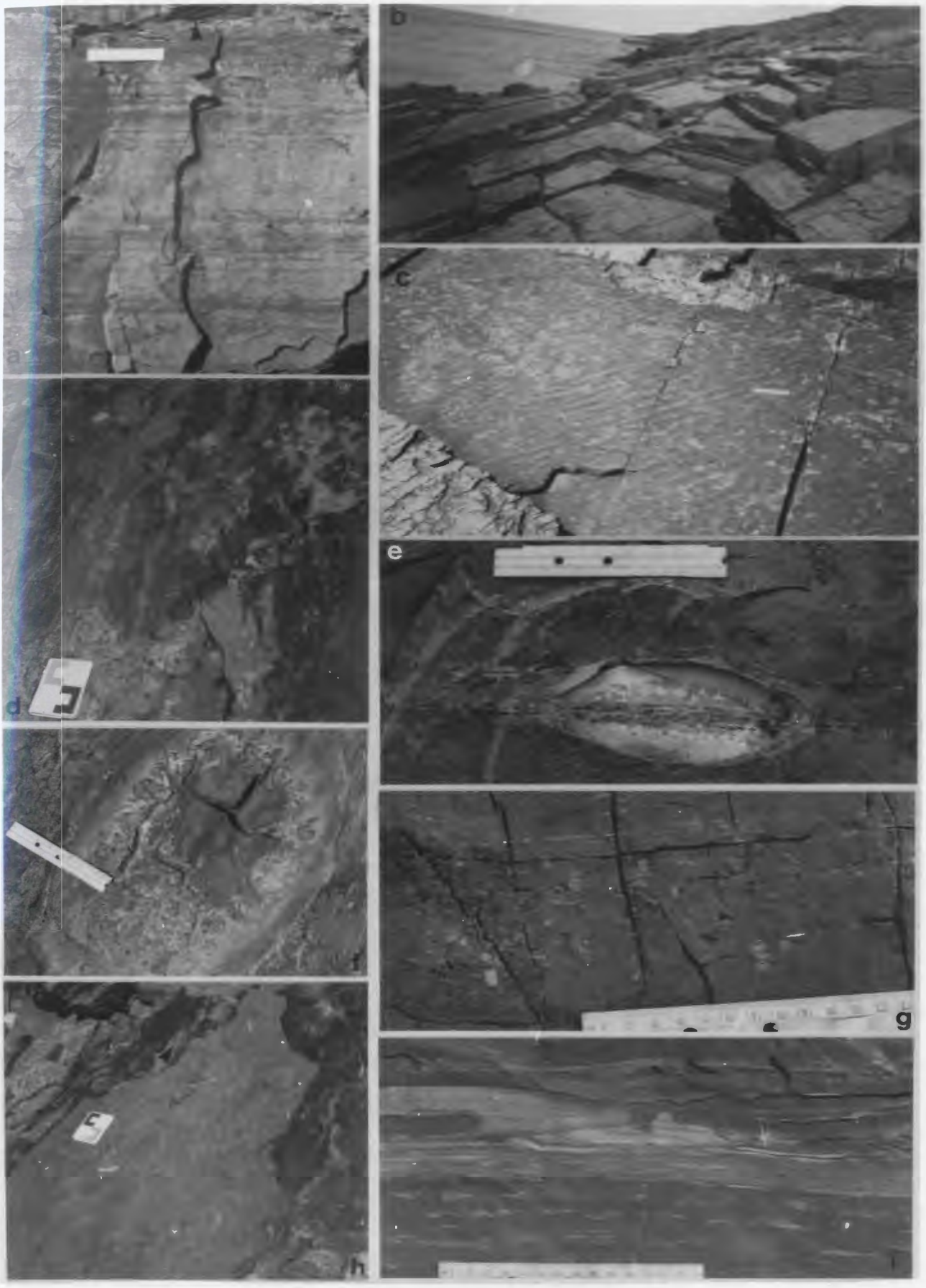
a
b
c
d
e
g
h
i

single bedding-plane exposure. Flat, wide crests are exhibited by some ripples, but it is difficult to tell if this is a primary feature or a function of weathering.

Carbonate concretions are prominent features in this facies (Plate 29e,f). These form bedding-parallel elongate nodules that are generally 2-3 times wider than they are thick, although parts of sand layers may also be carbonate cemented for a good part of their length and could therefore be considered as thin, tabular nodules. Nodules are concentrated along specific horizons, usually along sand beds. These concretions are early diagenetic features that record original thicknesses and preserve sedimentary and biogenic structures that were lost or altered during compaction elsewhere. The nodules may be structureless (and sand free) or contain such structures as bioturbated sand layers, structureless sand layers, parallel lamination, ripple lamination, and combinations thereof.

The sandstone beds are very extensive, but may be of variable thickness along strike (pinch and swell). These beds have sharp, erosional lower surfaces and moderately sharp upper surfaces, and are only locally visibly graded. Thick sandstone laminae locally have loads along their base, but otherwise have little internal structure.

Grain size and sedimentary structures are closely related in this facies (Figure 5.1). Medium sandstone (and some fine sandstone) laminae, from 1 mm (several grains thick) to >1 cm, form sheets of uniform thickness that nearly always contain current lineations and parting lineations. Very thin and thin fine sandstone beds contain ripple cross-laminae or a common motif of parallel laminae that are overlain by ripple cross-laminae. Fine sandstone beds locally display ripple form sets that are very thin — e.g., 2 mm under trough and 6 mm under crest (DC-86.6). At DC-103, a 2-3 cm-thick fine sandstone bed (6.5 cm thick where carbonate cemented) is fully composed of stacked sets of climbing-ripple cross-laminae. Very fine sandstone and coarse siltstone laminae, not much coarser than the background sediment, and ranging from a few mm to > 1 cm thick, are generally parallel laminated, yet do not contain current lineations or parting lineations. These laminae occur isolated and as upper divisions of ripple-cross-laminated fine sandstone beds. It can be

Figure 5.1: Summary of bed types and interpretations for beds of various grain sizes in Facies Association 3. Sedimentary structures and ranges of bed thickness are given. See text for further discussion.

Grain Size	Bed Thickness	Interpretation
Medium Sandstone		
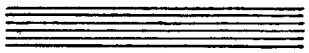	0.1cm - >1cm	Upper flow regime plane bed
Medium → Fine Sandstone		
	<1cm - 2cm	Upper flow regime plane bed to lower flow regime ripples
Fine Sandstone		
	0.5cm - 1.5cm	Lower flow regime ripples
	<1cm - 2cm	Upper flow regime plane bed to lower flow regime ripples
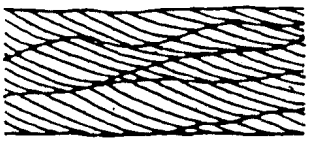	1.5cm - 3cm	Lower flow regime (climbing) ripples Rapid deceleration (high flux to bed)
V. Fine Sandstone		
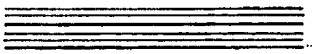	Few mm - >1cm	Lower flow regime plane bed

seen from the above description that there is no indication of a correlation between grain size and bed thickness.

Some graded beds contain lower, medium sandstone divisions with current lineations, and upper fine sandstone divisions with current ripples. In several examples where both current lineations and ripple crests are well exposed, the inferred paleocurrent directions show an upward clockwise rotation (Figure 5.2; Plate 29h).

Wrinkle marks (Kinneya structures), small ripplelike features, are found on bedding planes, sometimes directly on top of ripples. These locally maintain a consistent orientation across as much as 5 m or more of outcrop, and in one case are oriented nearly at right angles to the crest trend of the underlying ripples.

This lithofacies is characterized by stratigraphic variation in the abundance of certain sedimentary structures. Some stratigraphic intervals contain abundant parallel lamination with spectacular current lineations and parting lineations. Other intervals contain abundant ripples, while some intervals contain more evidence of biogenic reworking and fewer physical sedimentary structures and bedding-plane exposures. Paleocurrent data, given in Figure 5.3, include readings of current lineations, ripple migration directions and ripple-crest trends.

5.2.1 Process Interpretation

Data from this lithofacies indicate that sand was transported by unidirectional currents. This interpretation is based on (1) the consistent unimodal cross-laminae, and (2) the fact that most of the ripples are simple, form-concordant types without draping laminae or internal discordance. Well developed parting lineations and current lineations indicate upper-plane-bed conditions (Allen, 1964). The abundance of parting lineations in this lithofacies indicates that the sand layers were deposited by turbulent, high-velocity currents. For medium sand, the initiation of sediment movement occurs at a U_* value of

Figure 5.2: Summary of structures and process interpretation for inferred 'geostrophic flow' beds. Sedimentary structures of these beds are shown in lower right, with the orientation, with respect to North (N), of ripple paleocurrent and current lineations (C.L.) from a representative bed. Block diagrams 1-4 illustrate the inferred progressive shift in paleocurrent from offshore-directed to shore-parallel flow. It is important to note that this shift takes place temporally, at any given locality, so that the vertical development of structures reflects the same shift in paleoflow, represented here in spatial terms. Inferred bed phases for Stages 1-4 are outlined on the velocity-size graph. Velocity-size diagram is for flow depth of 20 m (modified from Rubin and McCulloch, 1980).

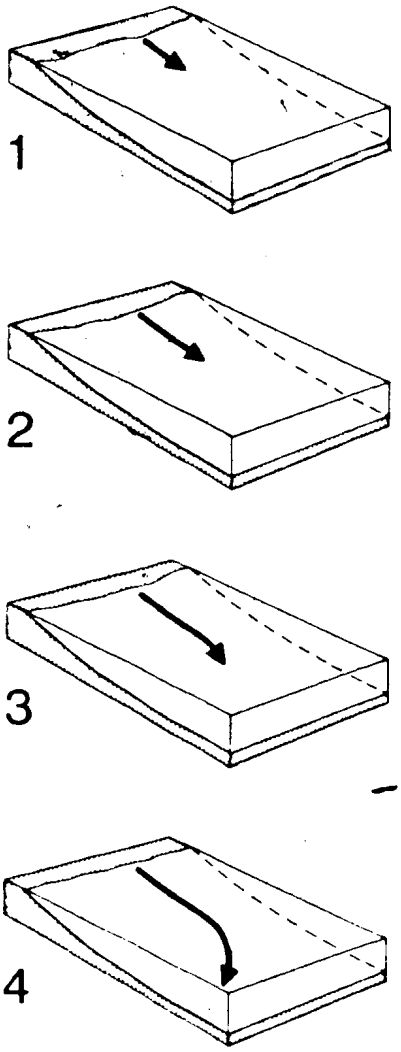
1
2
3
4

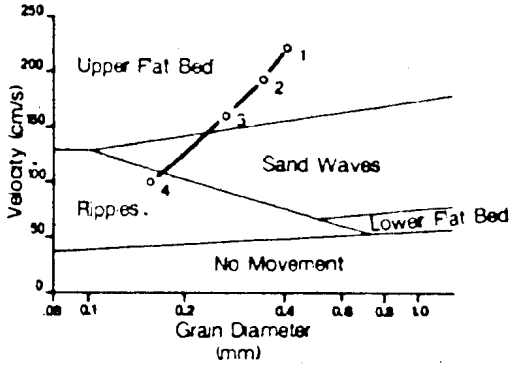
250
200
150
100
50
0
Velocity (cm/s)
Upper Flat Bed
Sand Waves
Ripples
Lower Flat Bed
No Movement
1
2
3
4
.08
0.1
0.2
0.4
0.6
0.8
1.0
Grain Diameter
(mm)

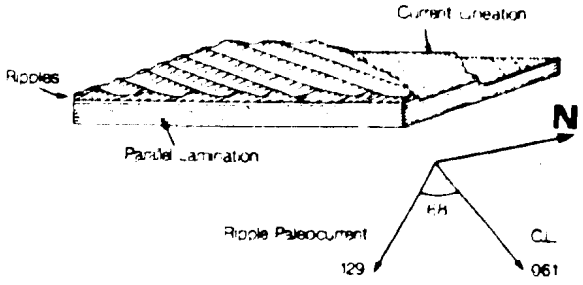
Current Direction
Ripples
Parallel Lamination
N
Ripple Paleocurrent
CL
129
061

Figure 5.3: Paleocurrent information from Facies Association 3. 'A' is ripple crest-trend data, 'B' is ripple paleocurrent data, and 'C' is orientation data on current/parting lineations.

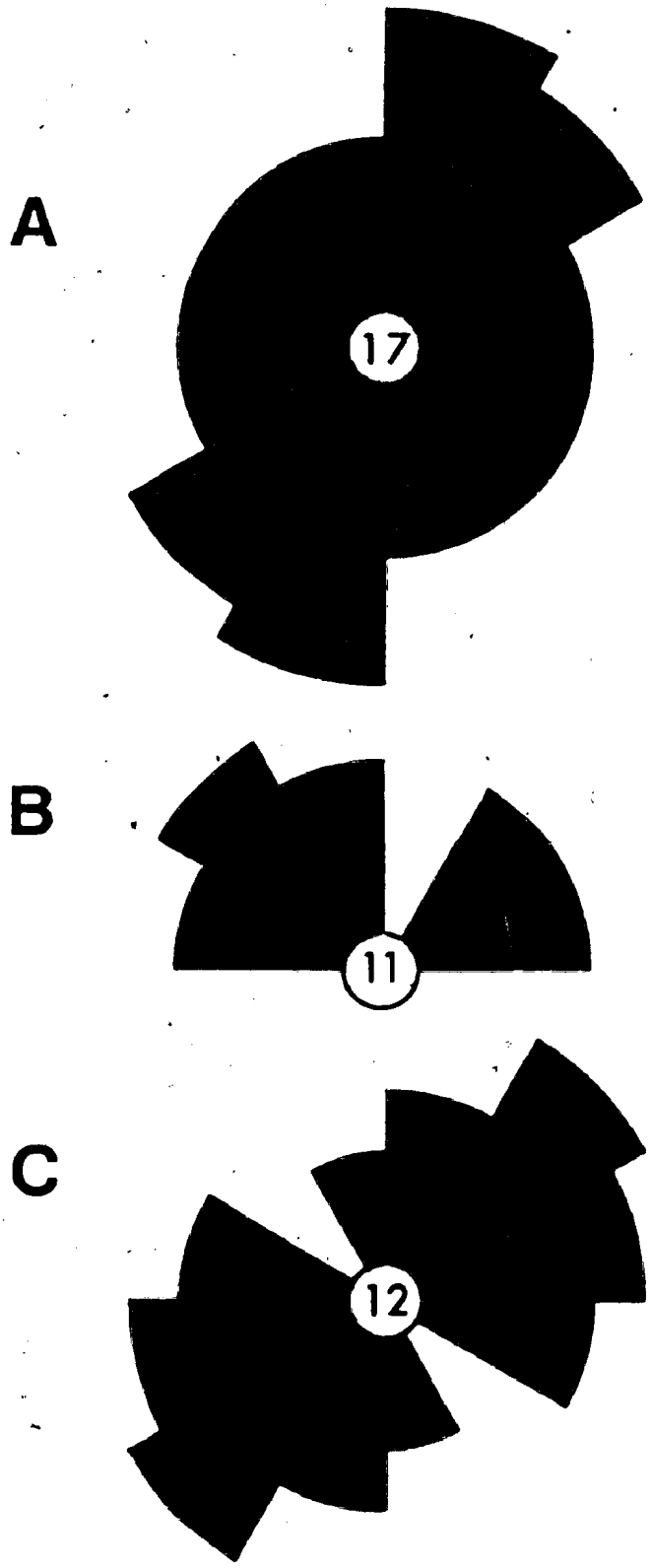
A
17
B
11
C
12

1.5 cm/sec (calculated from the Shields diagram; Blatt et al., 1980, p. 102). Available but limited data for the construction of size-velocity bed phase diagrams for large water depths suggest that upper-flow-regime conditions in medium sand indicate current velocities >100 cm/s (Rubin and McCulloch, 1980). Parallel-laminated very fine sandstone is interpreted as a lower-flow-regime structure. This is based on: (1) the lack of current lineations or parting lineations, (2) the presence of very thin mudstone/siltstone interlaminae, and (3) its common occurrence above ripple cross-laminae in graded (medium/fine to very fine) sandstone beds.

There is no direct evidence to suggest the direct influence of waves in the deposition of this lithofacies. Many of the ripples are straight-crested and asymmetrical; these could be interpreted as current ripples arrested during their initial stages of formation, before they reach equilibrium (Harms et al., 1982; p. 3-18). Thicker sandstone beds, such as DC-103 (3-4 cm), indicate that the flow was in the current-ripple field for nearly the full period of deposition.

Orientation data on parting lineations (Figure 5.3c) indicate that high-velocity currents were transporting sand in a northeast or southwest direction. Slower currents, responsible for lower-flow-regime bedforms (e.g., ripples), display a different pattern. Lateral variation in current strength is indicated by exposures displaying ripples that change from straight crested to linguoid, across the outcrop. The ripple-crest trends (Figure 5.3a) also indicate variability with a slight mode towards the northeast (flow to northwest or southeast), indicating that much of the ripple migration was at an angle to the direction given by current lineations. Ripple paleocurrent data indicates flow to all areas except the southwest, with a possible mode to the northwest (Figure 5.3b).

The common motif of parallel lamination overlain by ripple cross-laminae reflects a change from upper plane bed (parallel laminae) to lower-flow-regime ripple bed (ripples) conditions. Assuming constant depth, the ripples were formed at lower flow velocities than the underlying parallel laminae, and therefore the motif represents deposition from

decelerating currents. Thin current-lineated sandstone sheets without overlying ripple cross-laminae are difficult to interpret. It would appear that deposition went from upper flow regime plane bed to lower plane bed without the development of ripples. In Figure 5.2 there is a graph of grain size versus flow velocity showing bed phases in unidirectional flow for a flow depth of 20 m. This diagram shows a pinchout of the small-ripple field with increased sediment size. Given a grain size of medium sand (up to 0.5 mm), the range of velocities in which small ripples would be stable is not large. The flows that deposited these thin parallel-laminated beds may therefore have passed through the ripple field too quickly to allow for the development of ripples. Much of the time these flows would have been in the megaripple stability field, yet megaripple cross-stratification is also absent. There are several possible reasons why megaripples did not form. The most likely are: (1) the flows were much too thin to develop bedforms of this scale, and (2) megariples take a long time to equilibrate and were therefore unable to form in the time available. Similar explanations have been used to explain the absence of megaripple-scale cross-stratification in Bouma-type turbidites (Walker, 1965; J.R.L. Allen, 1984). The flows that deposited these parallel-laminated sandstones must have decelerated rapidly, particularly in the later stages of deposition when the flows passed through the small-ripple stability field.

Those parallel-laminated to ripple-cross-laminated beds that indicate an upward shift in paleocurrent are particularly intriguing. These beds are graded, and both the grading and the sedimentary structures indicate waning flow. The data indicate that the initial high-velocity flow was toward the northeast and that it shifted to southeast as the velocity decreased. One way to model these beds is as the deposits of flows whose direction is the outcome of a balance among (i) driving force, a combination of pressure gradient force, acting normal to the bottom isobars and thus directly offshore, and body force of gravity due to excess density, (ii) Coriolis force, acting normal to the current direction, and (iii) bottom friction force, acting opposite to the flow direction. In the early high-velocity sage of the current the dominant balance is between pressure gradient driving force and friction

force, and the flow direction is at a large angle to the shoreline; later, as the flow weakens by loss of suspended sediment, the dominant balance is between the driving force and Coriolis force, and the flow direction is almost parallel to the shore. Deflection due to Coriolis forces is to the right in the northern hemisphere, which is the case in these beds in Facies 3.1.

5.3 LITHOFACIES DISTRIBUTION/OUTCROP DESCRIPTION

This lithofacies is well exposed at Dantzic Cove (DC-0-~130), where the outcrop weathers in steps allowing for cross-sectional and upper bedding-plane exposures. At the northern end of this exposure, at the base of the section, the outcrop becomes faulted and the strike of bedding turns parallel to the coast. The minimum thickness of this lithofacies at DC is 130 m. At FD this lithofacies is exposed at the end of the exposure, where the strike of the beds become parallel to the coast and the section is badly faulted. This lithofacies is also present, but poorly exposed and badly faulted, at GB. A considerable thickness of this lithofacies is present on Chapel Island, where the gradual transition with FA 2 can be viewed, but the contact with FA 4 is not exposed.

At DC this lithofacies is confined to the lower ~130 m of the measured section (Figure 2.7). There is an upward decrease in sandstone percentage and an increase in the number of burrows noted within this interval. In the upper part of this interval bioturbation destroyed many of the internal structures, and may explain a paucity of bedding-plane exposures in this part of this section. Some stratigraphic intervals have an abundance of one or more particular structure(s). For instance, DC-80-90 contains abundant current-lineated parallel-laminated sandstone beds. Other intervals are dominated by ripples, carbonate concretions or other structures.

5.4 PALEOENVIRONMENTAL ANALYSIS FA 3: SUB-WAVE-BASE SHELF

The major conclusion to be drawn from the process interpretation section (5.2.1) is that the sandstone laminae of Facies 3.1 were deposited from waning currents below the influence of waves. Descriptions of sub-wave-base, storm-generated sandstones emphasize their similarity with turbidites (Hamblin and Walker, 1979; Brenchley et al., 1979; Walker, 1984; Brenchley, 1985). The Jurassic examples described by Hamblin and Walker (1979) (also see Walker, 1984) are graded beds, dominated by parallel and ripple lamination. Their beds commonly have parallel-laminated lower divisions and ripple-laminated upper divisions, which led the authors to suggest that these represent turbidite (T_{bc}) beds. The beds of Facies 3.1 have similar sedimentary sedimentary structures and are considered similarly to be distal tempestites. The gradational stratigraphic change from the proximal sandstones and siltstones of FA 2, containing evidence of wave activity, to this lithofacies indicates a gradual deepening. Tempestite proximality trends of bed thickness and sedimentary structures (e.g., Johnson, 1978; Aigner, 1982; Aigner and Reineck, 1982; Brenchley et al., 1979; Nelson, 1982) support this interpretation. The decrease in sandstone percentage and sandstone bed thickness in the transition from member 2-3 may have been due not only to the increased distality of the environment, but also to a decrease of sand input due to entrapment of terrigenous sediments during flooding of the shoreline with transgression (alluviation). The upward decrease in total sandstone percentage within member 3 indicates that even during the deposition of this member the factors that led to a decrease in sandstone content between Members 2 and 3 continued to operate. The lack of instability features, so common in FA 2, is also likely due to the shift to deeper water, where the effects of the deltaic environment — high sedimentation rates and high depositional slopes — are not a factor.

The strong northeast-southwest orientation of the current-lineation data must be taken in context with the stratigraphic gradation from Member 2 to Member 3 and the paleocurrent data from each facies association. The current lineations in FA 3 are parallel to the current lineations, and more importantly, the northeast-oriented flute marks, from FA 2. This indicates that high-velocity currents during the deposition of FA 3 were moving towards the northeast, as they had during the deposition of Member 2.

Aside from the current-lineation data, which represent transport directions associated with high-energy events, the data from ripples indicate a more scattered pattern, with much sediment transport occurring alongshore. Multidirectional paleocurrent patterns are considered by Benton and Gray (1981) to be diagnostic of outer-shelf deposits (their data were from current ripples). The ripple paleocurrent data are too sparse (n=13) to make a definitive statement concerning the dominant shelf processes. A few of the paleocurrents may be explained by geostrophic flow (toward the southeast), but paleocurrent data cover the all northern quadrants — especially the northwest — and therefore indicate a more diverse sediment dispersal pattern. Shelf currents moving parallel to the isobaths may be responsible for some rippling, but the data are too few to reach a firm conclusion concerning the pattern.

Chapter 6

LIMESTONE/MUDSTONE FACIES ASSOCIATION (4)

6.1 INTRODUCTION

Facies Association 4 consists of two lithofacies (Facies 4.1 and 4.2). Facies 4.1, volumetrically dominant, forms the bulk of member 4. Facies 4.1 is subdivided into two subfacies: 4.1A and 4.1B. The boundary between these subfacies is transitional.

6.2 RED, PURPLE AND GREEN MUDSTONE: FACIES 4.1

This facies consists of bioturbated purple, red, and green mudstones (Plate 30b), and is subdivided into two subfacies according to the abundance of sandstone laminae/beds and carbonate concretions, dominant colors, and other features. Color changes in this lithofacies may be sharp or gradational. Sharp color changes are not always parallel to bedding. Discontinuous red layers and irregularly shaped red spots are present within green mudstone, and vice versa. Red burrow mottles are present locally in green siltstone (e.g., DC-185.3).

PLATE 30: MUDSTONE FACIES (FA 4)

a: Contact between green mudstone (Facies 4.1) (lower part of photo) and grey mudstone (Facies 4.2) (upper part of photo) at Fortune North (FN-89-90). Note oxidation halos around pyritic nodules and steinkerns. Stratigraphic top is up. Scale is in centimeters.

b: Steep outcrop face with green bands in red mudstone (Facies 4.1) between LS 2 and LS 3 (DC-215-218). Stratigraphic top is up. Scale is in centimeters.

c: Pyritic steinkern of long, thin conical Orthothecid in Facies 4.2 (DC-~155). Scale is in centimeters.

d: Oblique view of green mudstone with carbonate concretions (DC-150). Note lack of bedding planes and irregular distribution of carbonate concretions, strikingly different features from FA 3. Scale is 15 cm long.

e: Bedding plane view of phosphatic nodules in purple mudstone at DC-182.4. Scale is 15 cm long.

f: Thin burrowed layers at DC-188.0. Note white calcite cement at top of some burrows. Stratigraphic top is up. Scale is in centimeters.

g: Rounded pyritic nodules in grey mudstone (Facies 4.2) from DC-169.0. Thick weathering rinds are light-colored (yellow). Oblique to bedding. Scale is in centimeters.

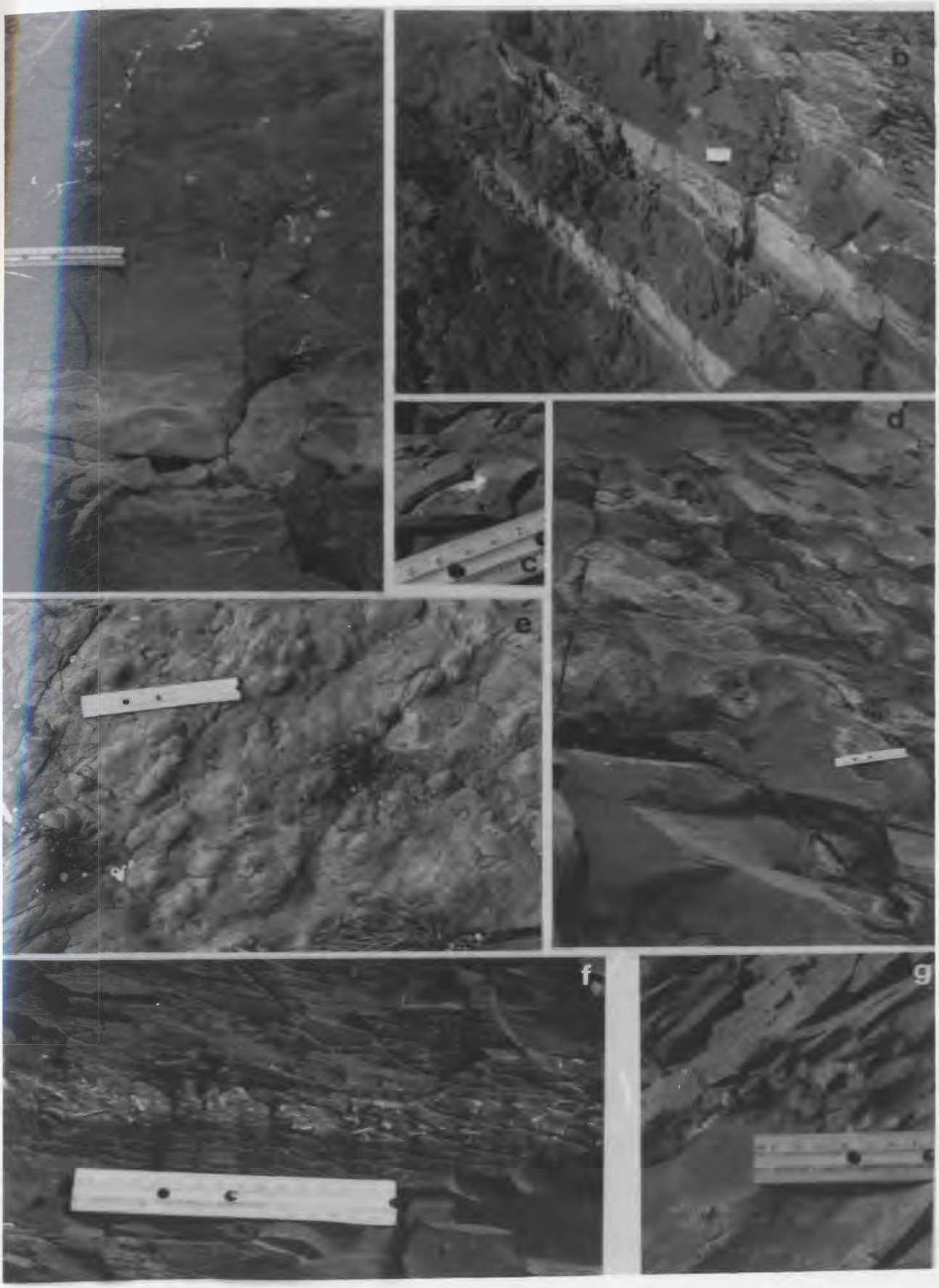
b
c
d
e
f
g

6.2.1 Subfacies 4.1A

This subfacies is characterized by a paucity of sandstone laminae/beds and a general lack of exposed bedding planes and sedimentary structures (e.g., ripples and current lineations). The color is dominantly green, but there are local red and purple horizons as well. Some weathered surfaces contain abundant, thin (<5 mm) Planolites sp. traces.

Carbonate nodules, a notable feature of this subfacies, range up to 30-35 cm in thickness, and are highly variable in length parallel to bedding, in extreme cases becoming relatively continuous carbonate beds. In comparison to nodules in other lithofacies in the CIF, and Subfacies 4.1B, the nodules in this subfacies do not preserve internal sedimentary structures, and do not appear to have their stratigraphic position controlled by bedding (Plate 30d). These nodules are elongate parallel to bedding, but are typically isolated, instead of forming in rows along bedding. The size and abundance of the carbonate nodules is greatest in the green mudstones, as opposed to the red and purple mudstones, which contain fewer and smaller nodules. Rare, thin sandstone laminae/very thin beds are commonly cemented by calcite, and are green when found in red or purple mudstone. Centimeter-scale phosphate and pyrite nodules are not common but are locally abundant (Plate 30e).

6.2.2 Subfacies 4.1B

This subfacies is similar to Subfacies 4.1A, but differs in the following ways: (1) it is dominated by red and purple mudstone; (2) it contains more thin laminae to thin beds of sandstone; and (3) it contains fewer and smaller calcite nodules. Widely spaced, discontinuous, carbonate-cemented sandstone laminae 0.5 mm thick are present, as well as

several 0.3-1 cm sandstone beds. The latter contain small current ripples, some of which are starved.

At DC, three carbonate-cemented sand beds greater than 2 cm thick (2.2-5.5 cm thick) were noted within this subfacies. These fine to medium sandstones contain parallel lamination, ripple cross-lamination and ripple form sets. Transition from parallel lamination to ripple cross-lamination is seen in one bed (DC-196).

A few thin burrowed calcareous siltstone beds are present at DC and FN. Two of these are present at DC (DC-188.0 and 188.12), with thicknesses of 2 cm and 1.5 cm, respectively (Plate 30f). These beds are green, but occur within red mudstone. Along most of the bed the lower contact of the green siltstone is sharp but disrupted, while the upper contact is gradational and also disrupted. Thin Planolites sp. traces 1-5 mm-wide are preserved as light pink/white lime mudstone within the noncalcareous green siltstone. A few burrows show incomplete geopetal lime mud filling and a minor quantity of occluding white calcite cement.

6.3 GRAY MUDSTONE: FACIES 4.2

Facies 4.2 consists of light to dark gray mudstones (Plate 30a) with abundant pyrite nodules and pyritic steinkerns (internal molds of small shelly fossils; Plate 30c), both of which are relatively rare in the green mudstones and absent in the red and purple mudstones of Facies 4.1. Small phosphate nodules (1-4 cm across) have been noted in this lithofacies, but they are not abundant. The pyrite nodules are centimeter-sized, irregularly shaped, and have prominent orange-weathering halos (Plate 30g). This lithofacies is generally devoid of coarse-grained detritus (a few sandstone laminae), obvious stratification, and calcite nodules. From stratigraphic intervals that contains gray mudstone (e.g., FN- 74-94 — see

Appendix D), it can be seen that calcite nodules make a sudden appearance in thin green intervals within thicker gray intervals.

6.4 PROCESS INTERPRETATION: FACIES 4.1 AND 4.2

Lithofacies 4.1 and 4.2 were deposited under low-energy conditions, possibly at a relatively low sedimentation rate. This conclusion is based on (1) the uniform, fine grain size, (2) scarcity of beds suggestive of higher-energy events, and (3) prominent bioturbation. Thin laminae to thin beds of sandstone were deposited by decelerating flows that experienced upper-flow-regime plane bed (parallel lamination) and lower-flow-regime ripple bed (ripple form sets and cross-laminae) conditions. Ripple cross-stratification resulted from unidirectional flow based on the form-concordant nature of the ripples and lack of features indicative of oscillatory or combined flow.

Although visible endichnial burrows are not common in any of the lithofacies in FA 4, bioturbation can be inferred from the lack of sedimentary structures and bedding planes, and from the high concentrations of well defined burrows exposed on some favorably weathered surfaces (other than bedding planes).

6.4.1 Comparison With Models For Oxygen-Deficient Basins

Rhoads and Morse (1971), working on sediments in the Gulf of California, developed a biofacies model for oxygen-deficient basins in which their three major biofacies are controlled by levels of dissolved oxygen (Figure 6.1). Anaerobic zones (less than 0.1 ml/l dissolved O2) are devoid of fauna. Dysaerobic areas (0.1-1.0 ml/l dissolved O2) are characterized by abundant, low-diversity, small-diameter, soft-bodied infauna. Aerobic settings contained a diverse calcareous fauna. There is recent disagreement on the

Figure 6.1: Biofacies model for oxygen-deficient basins. The three major biofacies are controlled by levels of dissolved oxygen. Modified from Rhoads and Morse (1971) and Thompson et al. (1985).

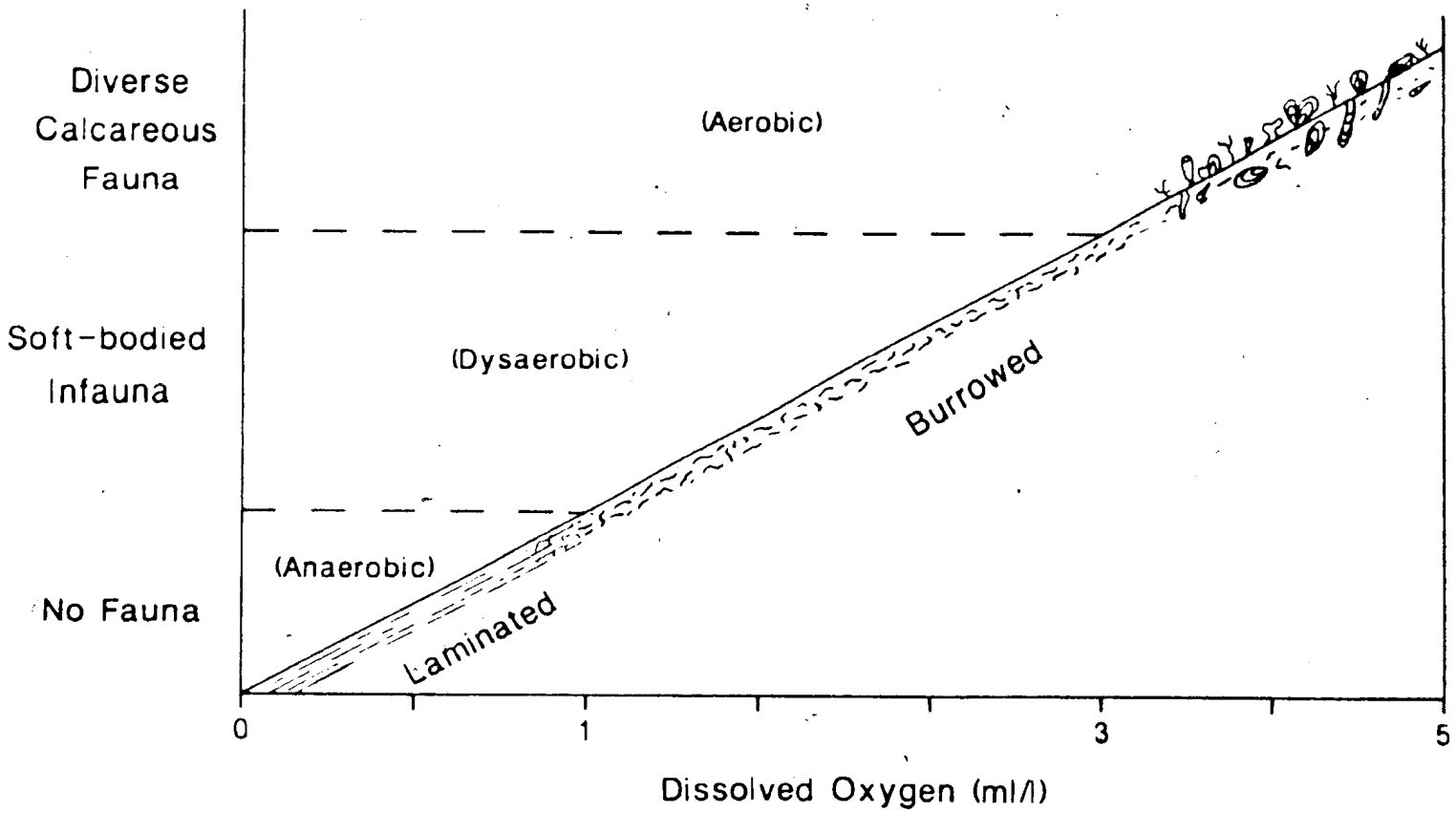
Diverse
Calcareous
Fauna
(Aerobic)
Soft-bodied
Infauna
(Dysaerobic)
Burrowed
(Anaerobic)
No Fauna
Laminated
0
1
3
5
Dissolved Oxygen (ml/l)

best values of dissolved oxygen for subdivision of these biofacies (see Thompson et al., 1985).

Byers (1977), and later others, have identified these biofacies in ancient rocks. Savdra et al. (1984) recently emphasized the problems involved in evaluating paleo-oxygen levels in ancient sediments. They encourage the use of multiple criteria, and that instead of making specific paleo-oxygen-level determinations, oxygen gradients should be used for ancient basins. The main parameters are: (1) sediment texture, including degree of burrowing, (2) burrow size, (3) paleontological data, (4) rock color, (5) presence of diagenetic minerals such as pyrite. These criteria will be applied to the lithofacies of FA 4.

The gray color of Facies 4.2 indicates higher organic content in these shales than those of Facies 4.1 (Figure 3.4). This higher organic content could have resulted from a number of factors. Facies 4.2 may have had higher initial concentrations of organics, but there is no evidence to substantiate this. A more probable explanation, given the lithofacies relationships (see discussion below) and the correlation between color, chemical precipitates (carbonate nodules, pyritic nodules/steinkerns), and organic structures, is that the final organic carbon content was a function of low Eh conditions in the upper sediment column, and possibly the bottom water, that favored the preservation of organics. For Facies 4.2 the degree of bioturbation and the small size of the preserved burrows are diagnostic of dysaerobic conditions (Byers 1977; Rhoads and Morse, 1971; Savrda et al., 1984; Savrda and Bottjer, 1986). According to Rhoads and Morse (1971), strong bioturbation in dysaerobic environments is related to the tolerance of mud-dwelling infauna to fairly high concentrations of H_2S.

The presence of pyrite and pyritic steinkerns in Facies 4.2 supports low-Eh diagenetic conditions. Pyrite is formed in low-oxygen conditions under more acidic conditions than that in which calcite is stable (Krumbein and Garrels, 1952) by the bacterial oxidation of organic matter through sulfate reduction and the consequent formation of H_2S

(Hallam, 1960; Berner, 1984; Raiswell and Berner, 1985). Moderate to high sediment accumulation rates allow for the burial of organics before elimination by aerobic oxidation.

Pyritic steinkerns are formed during early diagenesis in the upper few decimeters of sediment under low-Eh (dysaerobic) and low-pH conditions. Calcitic shelly fossils are dissolved and their molds filled with pyrite (Brett and Baird, 1986, Figure 11) before the elimination of the molds by compaction. Pyritic steinkerns are also diagnostic of moderate sedimentation rates (~1-10 cm/100 yrs) (Brett and Baird, 1986).

The conspicuous lack of early diagenetic carbonate nodules in Facies 4.2 supports lowered pH conditions. The precipitation of calcite nodules occurs under conditions of elevated pH, which in normal marine sediments would probably be created by the release of NH_3 during the breakdown of organic material (Berner, 1968). The lack of carbonate nodules in Facies 4.2 may be additional indirect evidence to suggest low-Eh conditions in which organic matter was not being oxidized to form NH_3.

It is not possible to determine the Eh conditions of the bottom waters during the deposition of Facies 4.2. The evidence, however, does suggest that at least the upper decimeters of the sediment column was reducing. Maynard (1982), in an analysis of Devonian-Carboniferous shales of the Appalachian basin, describes similar gray, pyrite-bearing shales that he attributes to deposition in settings in which bottom waters contain some oxygen, while the sediment column has lowered oxygen levels. Either partially oxidizing or fully reducing bottom waters would be consistent with the observations.

The green shales were deposited under slightly higher oxygen levels (Figure 3.4) in which enough organic matter was buried in the sediment to aid in the formation of abundant calcitic nodules. The diagenetic conditions were not sufficiently oxygen-depleted to generate pyrite nodules. The absence of shelly fossils or steinkerns from the green mudstones of Facies 4.1 can best be interpreted in terms of taphonomic controls (differential fossil preservation). The taphonomic explanation for the absence of calcareous fossils or pyritic steinkerns in the green muds of Facies 4.1 is that the factors contributing

to the solubility of these shelly fossils — primarily pH — were such that the shells dissolved, and because of the redox conditions of these muds (not in the pyrite stability field), the resulting shell molds were never filled. The molds were later eliminated by compaction, leaving no record that a calcareous fauna was ever present.

The red and purple mudstones of Facies 4.1 owe their color, the absence of pyrite nodules, and the paucity and small size of their carbonate nodules (carbonate nodules often form around nuclei of organic matter; Berner, 1968) to the early oxidative loss of organic matter under well oxygenated diagenetic conditions. The preservation of thin layers with calcareous shells indicates that the pH during early diagenesis was higher than that which characterized Facies 4.2 and the green shales of Facies 4.1. The presence of laminae and very thin sandstone beds in the red/purple-dominated Facies 4.1B may indicate that at least parts of this lithofacies may have escaped bioturbation, a situation consistent with the biofacies models described above (see Figure 6.1).

6.5 LIMESTONE FACIES

6.5.1 Introduction

At Dantzic Cove there are three continuous limestone beds (LS 1, 2, 3) within the mudstone/limestone facies association. There are also small discontinuous nodular horizons of lime mudstone. Only one of the three beds seen at Dantzic Cove is readily identifiable at the Fortune North (FN) and Radio Station outcrops. These latter outcrops also contain a large number of nodular horizons that are not present at Dantzic Cove.

At FN, one limestone bed is present within Facies Association 3 (Plate 31c), and is demonstrably a coalescence of calcareous nodules. The other limestone bed at FN is

PLATE 31: LIMESTONES 1 AND 2 (FA 4)

a: Extensive, white-weathering LS 1 at DC-135. Stratigraphic top is up. Notebook (left center) is 18.5 cm long.

b: LS 1 at DC -135. This close-up illustrates the nodular nature of the lower portion of this bed (directly above scale), which forms a more continuous band along strike. This nodular portion is probably diagenetic in origin. Various sized nodules are also evident in the mudstone below. Stratigraphic top is up. Scale is 15 cm long.

c: This limestone bed at Fortune North (FN-2.3) occurs within the laminated siltstones of Member 3. Note nodular masses at base. Hammer (center) is 30 cm in length.

d: This close-up of LS 2 clearly shows the contact (arrows) between the diagenetically precipitated 'underbed' (with irregular oxidation - reduction spots) and the overlying fossiliferous wackestone. The irregular, oncolite-bearing Fe/Mn hardground surface is seen at the top. Stratigraphic top is up. Scale is in centimeters.

e: LS 2 at DC-184.9. Carbonate nodule-bearing red mudstone is seen below and above the limestone bed. The limestone bed is 20 cm thick. Stratigraphic top is up.

f: Close-up of oncolites and ropy crust on this upper surface view of LS 2. Note onion-skin pattern of the oncolites. Scale is in centimeters.

g: Upper surface of LS 2. Note that within and overlying the oncolitic/encrusted surface is light-colored micritic limestone with a dendritic pattern that may represent burrow infillings. Notebook is 18.5 cm long.

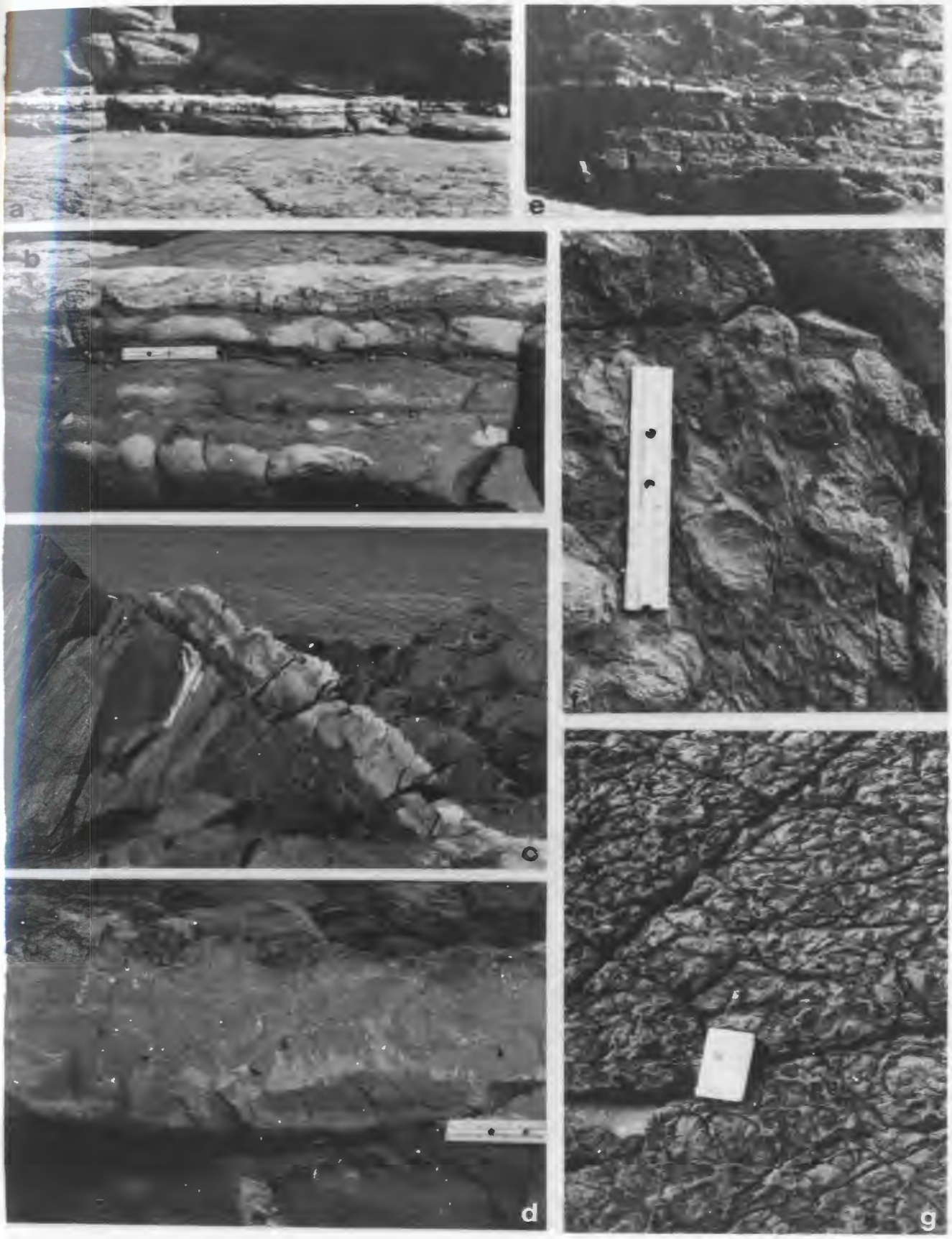
a
e
b
c
d
g

inaccessible. The following description therefore pertains only to the Dantzic Cove exposure.

6.5.2 Description

The limestone beds at DC illustrate an interesting stratigraphic progression of features. Each stratigraphically successive bed is both thicker and more complex in terms of internal structure. The three beds are 15, 24, and 60 cm thick, respectively. A sketch of each is given in Figure 6.2.

The lowermost bed (LS I) is a 15 cm thick, white, massive, micritic limestone that lacks any significant megascopic physical or biogenic structures (Plate 31a). The lower 6-8 cm consists of partially coalesced nodules. Above, and filling in between the nodules, is a 2-3 cm-thick layer of red shale (Plate 31b). The upper part of the bed is homogeneous white micritic limestone. The upper contact with the overlying grey-green siltstone is irregular but sharp.

This bed consists of microspar and pseudospar (Folk, 1965). Flat-lying, elongate, pseudospar crystals are locally present in a chloritic clay matrix. Possible burrow mottles are also present. A few specimens of the small leaf-like shelly fossil Sachtites have been found in this bed (Ed Landing, personal communication,1986).

The second major limestone bed (Plate 31e) is the first unit to contain abundant small shelly fossils. Some of the cone-shaped shells, mostly hyolithids, are remarkably large, with circular cross sections greater than 1 cm in diameter. The bed is dark red on the fresh surface, and averages approximately 24 cm in thickness. The lower 10 cm consists of structureless micrite with burrow mottles but no obvious shelly fossils. Above this unit is 10 cm of hyolithid-bearing wackestone with irregular packstone lenses. The contact between these layers is very sharp (Plate 31d), and the compositional contrast is enhanced

Figure 6.2: Sketch of limestone beds at Dantzic Cove (LS 1,2 and 3). The scale opposite LS 3 is the same for all three drawings. Descriptions of individual units are given in text.

LS 1

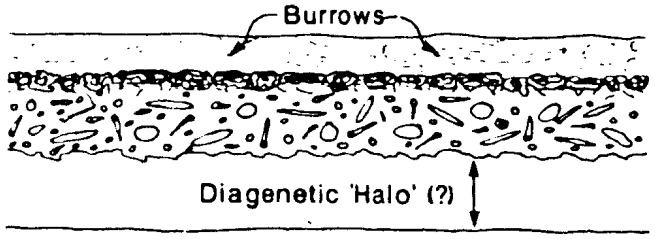

LS 2

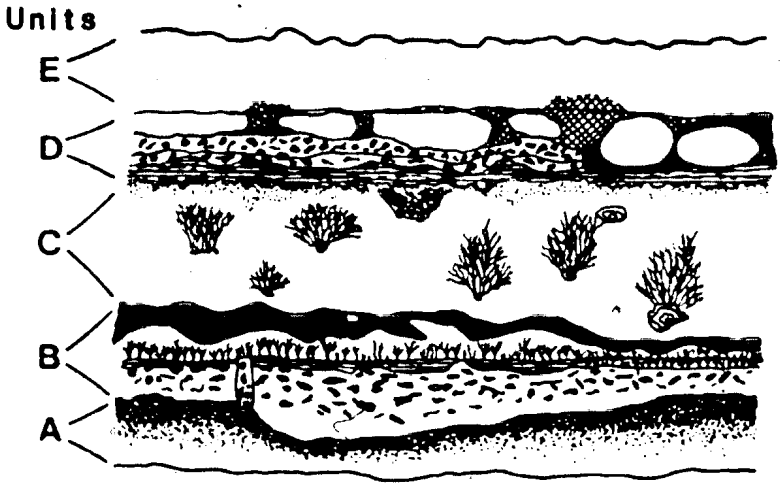

LS 3

Red Mudstone

Si/Mn Crust

Stromatolites

Shelly Fossils

Mudstone Clasts

Oncolite

Algae

Micritic Limestone

by a darker iron staining below the contact. This surface is irregular, displaying several centimeters or more of relief over very short distances.

Near the top of the bed there is a surface characterized by a black, irregular, ropelike, anastomosing crust of silicified and iron-manganese-mineralized shale (Plate 31f,g). Stringers of this crust also parallel the cleavage, penetrating a few centimeters downward into the limestone bed. The crust also surrounds low-relief, disc-shaped to irregular oncolites, 1-10 cm in diameter, that are scattered across this surface. The oncolites display an onion-skin concentric pattern of resistant red shale layers (Plate 31f). In many cases the outermost layer is a mineralized Si-Mn crust. Above this oncolitic surface is 4-5 cm of nodular micritic limestone in shale. It appears that the nodular fabric reflects a network of large burrows.

The third limestone unit (LS 3) is the only limestone bed at Dantzic Cove that can be traced to other outcrops. This bed crops out in Fortune Harbour and at the Radio Station locality. The thickness of this bed varies from 50-80 cm. The fauna consists of an Aldanella attleborensis assemblage that includes, among others, A. attleborensis, Lapworthella n. sp., Halkiera sp., and various helcionellids and orthothecids (see Bengtson and Fletcher, 1983). There is a wide variety of sedimentary structures and diagenetic features. The former include both constructional (depositional) and erosional features. The bed has been divided into 5 packages (Units A-E) that are shown in Figure 6.2 (see also Plate 32c).

At the base of the bed is a 3-8 cm pinkish-green unit (Unit A) that displays strong inverse grading (Plate 32b). The grains that make up this unit are not detrital, but discrete elongate crystals of calcite that occur with varying quantities of green siliciclastic mud matrix. The pseudospar calcite crystals grade upward from fine to coarse sand size, while decreasing in abundance. In the upper part of the unit these patches of clay matrix become interconnected, forming a background to a loose network of calcite grains that take on a vermiform texture. The calcite, and therefore the surrounding matrix, has a strong bedding-

PLATE 32: LIMESTONE 3 AT DC-220.1 (FA 4)

a: Slab of Units D and E etched by hydrochloric acid. Note thin curled-up mud lamina on base of tepee structure and the algal structures that grew vertically on this lamina (bottom center) and across the tepee floor. Irregular hardground surface is clearly visible (arrows). The central lighter band appears to be a mass of algae with abundant hyolithids and other shells. Stratigraphic top is up. Scale is 1 cm long.

b: Close-up of "b" showing Units A and B. Note upward increase in crystal size in Unit A. The displacive fabric is highlighted by dark-colored chloritic mudstone that weathers in positive relief. Irregular clasts of algal mat and mudstone are shown here in Unit B. A thick, red mudstone division separates this unit from Unit C. Stratigraphic top is up. Scale is 15 cm long.

c: View of large piece of float showing the full thickness of LS 3. A sketch of this photo is given in Figure 6.1. Stratigraphic top is up. Scale is 15 cm long.

d: The stromatolites of Unit D are cut by 'pillar' structures. The geometries illustrated in this photo include downward-tapering, upward-tapering and non-tapering. Many 'pillars' seem to extend down below the level of the stromatolitic lamination. The thin layer of laminae that covers all of these structures represents late-stage growth of the algal mat after cracking. Stratigraphic top is up. Scale is in centimeters.

e: Bedding plane view of 'pillar' structures in Unit D. Note polygonal shape of these cracks. These are interpreted as desiccation features. Scale is in centimeters.

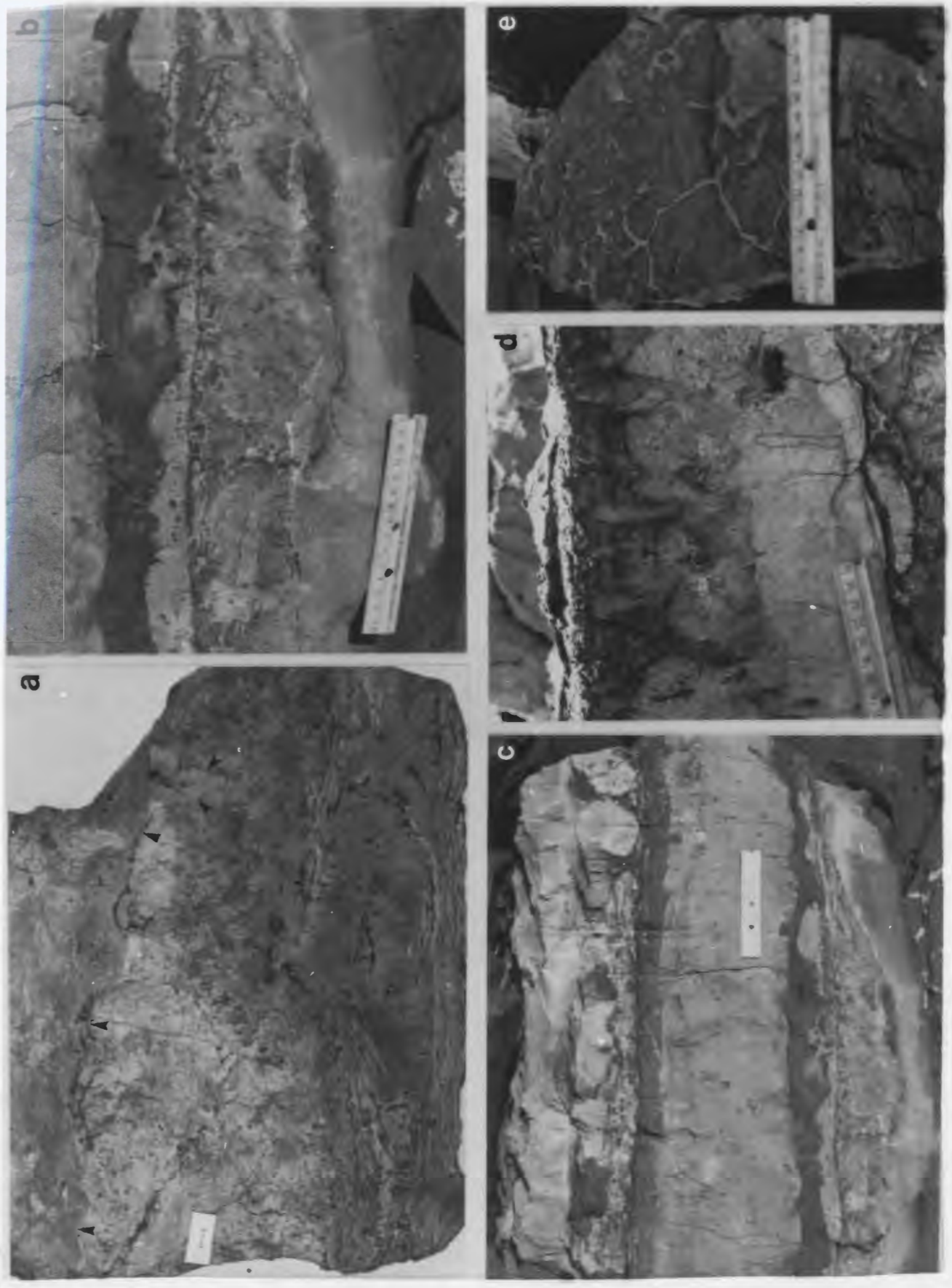
b
e
d
a
c

parallel fabric. Petrographic analysis indicates that the clay matrix contains chlorite and muscovite with grains of quartz, feldspar, and a very minor quantity of heavy minerals (e.g., zircon).

Unit B is a 7-15 cm stromatolite-bearing interval. The base of this unit is an irregular erosion surface that is either capped by a shale drape or amalgamated directly onto Unit A. The lower part of this unit is a chaotic zone containing angular to subrounded limestone intraclasts, oncolites, fragments of red mudstone (up to 1 cm in diameter), and well rounded blue/black-weathering phosphatic shale clasts (up to 2 cm in diameter) (Plate 32c).

Extensive planar stromatolite layers make up the upper part of this unit. These weather with relief due to the presence of red siliciclastic mudstone, much of which is silicified and/or manganese-impregnated. The top of the stromatolitic layers have relatively continuous, undisrupted laminae, while the lower parts are broken by irregularly spaced, variably shaped pillars of sediment of character similar to the underlying chaotic material (Plate 32d). These pillars extend below the level of the stromatolites into the chaotic material below, as outlined by subtle compositional or color variations. The pillars reach cross-sectional sizes of 42 mm in height and 17 mm in width. Rows of individual algae are also locally preserved within a micritic matrix (Figure 6.2).

Unit C of the bed is an 5-25 cm thick, massive, pink, variably fossiliferous micritic limestone (Plate 32c), locally containing finely disseminated siliciclastic silt particles. In thin section it is readily apparent that the micritic calcite has been a neomorphosed to a microspar texture. Over most of the outcrop Unit C is a sparse wackestone with a generally tabular geometry. The base of the unit is flat, and the upper surface has smooth, large-scale undulations. The unit is generally structureless except for 1-2 cm at the base and top of the unit, where there is local development of thin, dendritic structures interpreted to be Rivulariacean algae. These branching forms are normally 1-2 cm tall, but may be up to 5 cm in height. At the top of the bed these Rivulariacean algae are upwardly transitional into

the stromatolites of Unit D, which mantle the mounded topography of this unit. Widely dispersed at different levels within this portion of the unit are red and green shale clasts up to 1 cm across and oncolites up to 2.5 cm in diameter, from which similar algal forms project (Figure 6.2). Some of the oncolites and the shale clasts (green ones) have been silicified and Fe/Mn impregnated. In one example, an oncolite also contains authigenic barite crystals.

Unit D is similar to Unit B in that it contains conglomeratic material and stromatolitic layers. The unit is highly variable across the outcrop. The stromatolitic parts are more prominent than in unit B. Where the stromatolites are missing due to erosion, the resulting depressions are filled with mudstone clast and algal rip-ups.

'Pillars' of sediment, similar to those in Unit B, cut the stromatolites. These pillars either open downward, forming tapered rooflike structures, or widen and then narrow downward, forming elongate bulbous shapes (Plate 32d). Bedding-parallel views of these pillars reveal a distinct polygonal pattern (Plate 32e). Infilled sediment in some cases retains this pattern below the level of stromatolitic laminae.

Within the stromatolites are sheet-crack structures consisting of thin, elongate seams of white sparry calcite. The sparry calcite consists of fibrous marine cement and a late-stage (meteoric phreatic) blocky ferroan cement. Red-weathering algal structures, present along the base of these layers, represent some of the earliest known coelobiontic fauna. An important feature, noted within the stromatolites of this unit, is a tepee structure (Plate 32a). The scale of the tepee, up to ~50 cm long and 10 cm tall, and the overthrusted nature of the tepee roof is similar to some examples described by Asserto and Kendall (1977; see Figure 5). This tepee is filled with sparsely fossiliferous mudstone. Thin curled-up mud layers and dendritic algal structures are present on the base of the tepee in Plate 32a.

Within Unit D there are two examples showing the local development of mounded, lenticular pods of pink micritic limestone. These have flat bases that rest on stromatolitic

PLATE 33: LS 3: UNITS D AND E (FA 4)

a: Detail of Unit D with digitate and planar stromatolites in the lower portion of the photo and conglomerate above. The conglomerate contains oncolites, limestone and mudstone intraclasts, and large rounded volcanic clasts, one of which is seen in the center of the photo. Stratigraphic top is up. Scale is in centimeters.

b: Mud mound in Unit D. The base of this structure is flat and the top projects above the general level of the top of the bed. Stratigraphic top is up. Notebook is 18.5 cm long.

c: The small mud mound in Unit D in the center of this photograph is mantled on both sides by thick planar stromatolites that onlap and just barely cover the mound. Stratigraphic top is up. Scale is 15 cm long.

d: Siltstone-infilled depressions and rope-like crust on the top of LS 3, the crust appears to at least locally follow the pressure-solution cleavage. Scale is in centimeters.

e: Local shell hash accumulation (center) within micritic Unit E. Stratigraphic top is up. Scale is in centimeters.

f: Irregular masses of silicified shale are present sporadically throughout Unit E. This one contains thin bladed crystals of barite. Stratigraphic top is up. Scale is in centimeters.

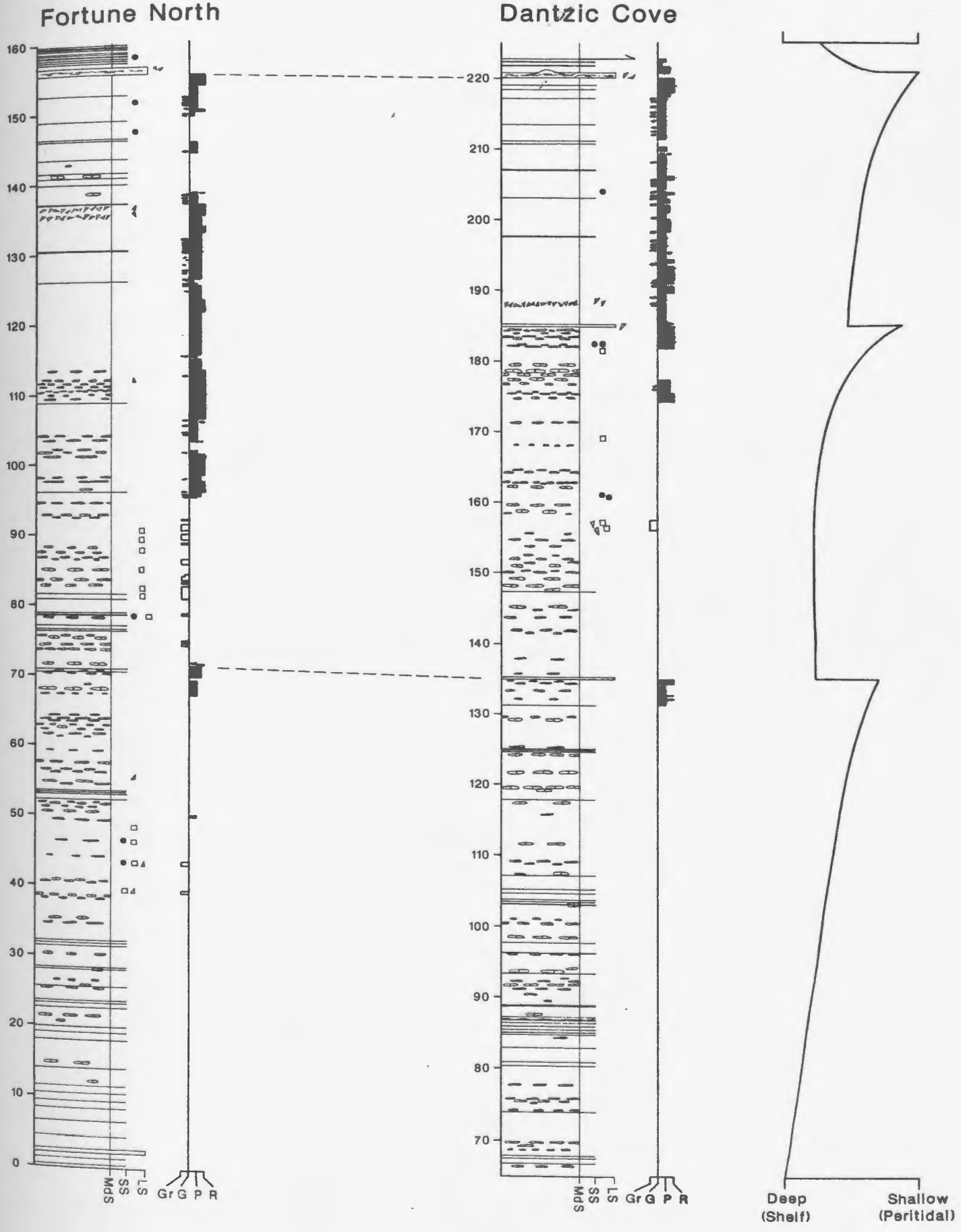
Fortune North
Dantzic Cove
160
150
140
130
120
110
100
90
80
70
60
50
40
30
20
10
0
220
210
200
190
180
170
160
150
140
130
120
110
100
90
80
70
Mds
SS
LS
Gr G P R
Deep
(Shelf)
Shallow
(Peritidal)

laminae, and domal tops, which are either confined within stromatolitic laminae (Plate 33c) or extend above into the overlying unit. One of these mud mounds is 2 m long at its base and 35 cm thick, extending 15-20 cm above the top of the bed (Plate 33d). In this case the upper parts of Unit D and E simply onlap or mantle this positive feature. The stromatolitic laminae are especially thick (10 cm) above the flanks of these mounds (Plate 33c).

The conglomeratic parts contain abundant red shale clasts; large limestone intraclasts (one well rounded example is 6.5 X 2 cm in cross-section); oncolites; well rounded quartz pebbles (up to 1.5 cm in diameter); a variety of shelly fossils, including abundant nested hyolithids; and well rounded volcanic clasts (Plate 33a).

Along most of the bed, the top of Unit D is covered with an irregular shale drape. Unit E consists of approximately 15 cm of pink/white bioclastic wackestone. There are pods of shell hash (Plate 33d) and several matrix-supported shell-rich layers, one of which contains a few small mudstone clasts. The lowermost shelly layer is a continuous, horizontal layer that abuts against the microtopography associated with the irregular upper surface of Unit D. Isolated large blocks of silicified and partly silicified shale, some containing elongate bladed crystals of barite, are found within Unit E. Locally, Unit E contains a denser population of dendritic algal structures and a higher concentration of shelly fossils. Plate 32a shows a sample with a thick intergrowth of dendritic algae within a matrix of wackestone. This sample contains two irregular surfaces (Plate 32a), each of which have deep indentations filled either with the overlying lithology or a lithology different in character from that which surrounds it. These depressions have sharp edges that truncate laminae and create overhangs along the wall. The very top of Unit E has siltstone-lined depressions with siltstone (Plate 33d) and red shale clasts, and local accumulations of shell debris.

6.5.3 Limestone Facies (4.3): Process Interpretation

6.5.3.1 LS 1

The texture of the first limestone bed (LS I), as seen in thin section (elongate pseudospar in clay matrix), indicates concretionary growth for all or most of the bed. The partially coalesced nodules in the lower part of the bed clearly support a diagenetic origin, at least for this part of the bed. The red color of the surrounding shale indicates that oxidizing conditions prevailed during early diagenesis (Figure 3.4).

6.5.3.2 LS 2

The red coloring of the second limestone bed (LS II) also indicates well oxygenated conditions. The lower, unfossiliferous, micritic part of the bed may have formed (1) by the deposition of lime mud — the structureless nature would be attributed to homogeneity of grain size or to reworking by burrowing organisms — or (2) as a diagenetic 'halo' below the overlying bed. In the first case, the irregular surface that separates the lower and upper parts of the bed would be interpreted as a submarine hardground surface, while the second alternative would have this contact represent a lower bedding plane from which a later, diagenetic layer grew downward (see Eder, 1982). Clear-cut evidence for hardground development (e.g., bored surfaces) is lacking. Well defined pseudospar textures, typical of concretionary growth (Coniglio, 1985), are also absent. Both models are equally plausible.

The fossiliferous wackestone of LS 2 contains no evidence of significant winnowing or current reworking, as the hyolithid shells are floating in a matrix of lime mud. Hyolithids are considered to be vagile epibionts of the phylum Mollusca (Raaben, 1969). The hyolithid shells are therefore interpreted as being at least approximately in situ.

because they neither settled from suspension nor required transport from an area of firm substrate. The oncolites near the top of LS 2 indicate rolling and growth of these structures under relatively high-energy conditions. The upper bedding surface with its oncolites and mineralized crust may represent an exposure surface. Unequivocal evidence for subaerial exposure of the sediments during deposition is, however, lacking.

6.5.3.3 LS 3

Process interpretations will be given for each unit in LS 3. Throughout the bed, siliciclastic (mudstone) and carbonate lithologies have been subjected to reactions with silica- and metal-bearing fluids. Layers and clasts of mudstone appear to have been particularly affected. All transitions exist, from red mudstone to dark green, silicified and manganese-impregnated mudstone. Carbonate was also affected, as seen in Plate 32a, in which a "front" of green coloring cuts across several layers in this sample. At the edge of this "front" the green color appears to be replacing the red coloration more preferentially in the wackestone matrix than in the algal structures. The green coloring that pervades part of this sample represents a manganiferous fluid front that moved though the upper part of the bed. The timing of this alteration and the precipitation of authigenic barite crystals at different levels throughout the bed is unknown.

The textures of Unit A indicate in situ, displacive precipitation of pseudospar crystals within an unlithified green mudstone matrix. Carbonate mobilized from the surrounding sediments and ambient sea water was precipitated as discrete crystals displacing the surrounding mud. Similar textures are described from concretionary calcite of the Cambro-Ordovician Cow Head Group in western Newfoundland by Coniglio (1985, see his plate 37F). Unit A grew downward from the base of LS 3, which may explain the downward-decreasing grain size. Similar diagenetic 'basal layers' have been described by Eder (1982), Meischner (1967), and others.

The lower conglomeratic part of Unit B represents deposition from high-energy currents. The irregular, and in places amalgamated, lower surface of this unit indicates that currents scoured the sediment bottom before deposition of the conglomeratic sediment. Semilithified carbonate sediment and red mudstone were eroded from the sea floor to form intraclasts. Pieces of cyanobacterial mat were also broken off and transported in a similar fashion. The well rounded nature of the phosphatic shale clasts indicate that these may represent previously reworked, well indurated detritus.

The planar stromatolites of Unit B are interpreted to represent the growth of cyanobacterial mats. Red mudstone laminae were deposited from suspension, due in part to the trapping action of the cyanobacteria. The pillars that cut this mat likely formed from shrinkage associated with periodic desiccation. This is based on the polygonal pattern exhibited by these features in Unit D, and a remarkable similarity in shape and scale to modern desiccation features in stromatolites (Shinn, 1972). Desiccation cracks in stromatolites from the Persian Gulf, described by Shinn (1972; Figure 1B,2), are similar to the CIF pillar structures, including a downward-opening geometry, presumably caused by later growth of the mat over the desiccation crack.

The sparse wackestone that characterizes most of Unit C is interpreted to represent an accumulation formed from the trapping and binding of algae. The energy conditions might have been higher than the fine grained lithology indicates, if algae acted to baffle currents and bind the sediment or if any submarine cementation occurred. A likely candidate for trapping and binding algae, at this time in earth history, would be Girvanella, and although the textures in this mudstone are suggestive of its presence, no calcified filaments are present. Poor preservation is to be expected, given the low preservation potential of Girvanella (Coniglio and James, 1985) and the neomorphosed nature of the limestone. The ability of algae to tolerate higher-energy conditions might explain the presence of large mudstone intraclasts and oncolites within the wackestone.

Processes operating during the deposition of Unit D were similar in kind to those associated with Unit B. Thick stromatolitic layers are considered to form from the growth of cyanobacterial mats. The polygonal pattern of "pillars" that break up the stromatolite are considered to be desiccation features.

The tepee structures are expansion structures (note overthrusting of roof in Plate 32a) that must have formed at, or very near, the sediment surface, as unreasonable forces would be needed to form a cavity of such height if the roof was overlain by a thick sediment cover. The upturned nature of thin mud and mat layers within (and at the base of) these tepee structures strongly suggest short-lived periods of subaerial exposure. These CIF examples are unusual in that the tepees formed entirely within stromatolitic layers. The tepees described by Asserto and Kendall (1977) are composed of vadose-cemented crusts of pelmicritic and intramicritic sediment that were subject to the following repeated sequence of processes: (1) desiccation forming fractures, (2) wetting, causing expansion of fractures, and (3) expansive crystallization of calcium carbonate in pores, joints, and fractures. Thermal expansion and moisture swelling are cited as additional factors in the expansion of these structures. The sharp termination of laminae at the edges of the roof indicates rigid behavior of the mat during deformation, and therefore early cementation. This early cementation expanded the rapidly lithified mat to form these structures. The upraised mat roofs of the unit D examples do not appear to have been subject to abrasion and reworking, so these structures correspond to Asserto and Kendall's (1977) "embryo" stage of tepee development.

The sheet-crack structures in Unit D also appear to be features of expansion, resulting from processes similar to those that created the tepee structures. These sheet cracks must be formed close to the surface without the weight of significant overburden. The expansion of the mat to form these structures may have resulted from wetting/drying and cementation, as described for the tepees, or from buoyant effects from the release of

gases given off by respiring or decaying cyanobacteria. The association of these structures with polygonal cracks favors the former explanation.

The two domal, micritic lenses in Unit D are interpreted as bioherms formed by the binding and trapping action of cyanobacteria. The bioherm interpretation is based on their overall geometry and the fact that, in one case, the pod is draped by stromatolitic laminae, and in the other, the pod stands well above the top of bed and is onlapped by younger strata (part of Unit D and all of Unit E).

Syndepositional erosion is also indicated for this unit by the presence of limestone intraclasts and red mudstone fragments. Strong currents would be required for this erosion and for the transport of the coarse-grained detritus found in unit D. An estimate of current velocity for initiation of transport of this coarse detritus using a Shields diagram would be inappropriate because these clasts are isolated in fine-grained limestone and would therefore have been moving across a relatively smooth surface.

Relatively quiet conditions prevailed again during the deposition of Unit E. The more fossiliferous parts of Unit E were of similar origin to the sparser wackestone, but recording greater winnowing under slightly higher-energy conditions. The presence of well preserved algae strongly suggests trapping of mud by algae. The irregular surfaces shown in Plate 32a represent synsedimentary cementation and the development of hardgrounds. The sharp truncation of layers and the development of overhangs in some small depressions suggest early lithification. These depressions are too large to be borings, and their overall geometry rules out positive identification of these features as burrows. The surface may therefore have resulted from: (1) the lithification of a burrowed surface, (2) scouring of a previously lithified surface, or (3) both. The shell-hash layers may be explained, in part, by gentle reworking of the sediment. Intraclasts and shell hash accumulations in depressions on the upper surface of Unit E indicate scouring and subsequent reworking of the sediment surface.

The various units (A-E) of LS 3 contain a wide variety of sedimentary and biogenic features that indicate marked temporal changes in current strength. Biogenic features such as algal stromatolites and bioherms would have acted to damp wave energy and bind and trap sediment. Higher-energy events, possibly storms, resulted in erosion of sediment, local breakup of algal mats, and deposition of coarse-grained siliciclastic detritus.

6.6 LITHOFACIES DISTRIBUTION AND OUTCROP DESCRIPTION

All of member 4 (Limestone/Mudstone Facies Association) is exposed both at Dantzic Cove and Fortune North (Figure 6.3). Red and green mudstones of Facies Association 4 are found as far north as Chapel Island (Figure 1.1), but these were not studied in detail. At DC, near the lower boundary of member 4, the upper 15-20 m of member 3 shows evidence of a rapid increase in the level of bioturbation of the sediment and a loss of prominent bedding planes and ripple marks. This zone also contains abundant carbonate nodules, as do the mudstones between LS1 and LS2. It is within the zone between the lower two limestone beds that a 1-2 m-thick band of Facies 4.2 mudstone contains abundant steinkerns of Orthothecids and Aldanella attleborensis. Facies 4.2 is much more abundant at the FN locality. The upper part of Member 4 is dominated by Subfacies M1B (DC-195 to DC-220 and FN-115-155), containing laminae/thin beds of fine sandstone.

Each stratigraphically successive limestone bed at DC displays an increase in both bed thickness and complexity and diversity of sedimentary structures. A second trend concerns the color of the mudstones. At DC, the first stratigraphic appearance of red strata is 5 meters below LS 1. The strata are green for the next 40 m and then become red directly below LS 2. Most of the mudstone above LS 2 is red. The overall trend for member 4 is an upward increase in red versus green mudstones.

There are a number of interesting differences between the exposures of FA 4 at FN and DC (Figure 6.3). Several marker horizons allow detailed correlation between these sections. The most obvious marker horizons include LS 3 and the red mudstones that underlie LS 1. Additionally, 5 cm and 6.5 cm thick, tan-weathering, fine sandstone beds at FN-130.35 and DC-197.65, respectively, may also correlate. One limestone bed at FN (FN-3.2), found well down into member 3, appears to have formed from a coalescence of carbonate nodules and is not traceable, as a distinct bed, to DC. Of the three limestone beds

Figure 6.3: Stratigraphic columns of DC and FN showing correlation between sections. Inferred relative sea level curve, given on the right, is based on facies characteristics including diagenetic, biogenic, and primary sedimentary structures. More detailed stratigraphic sections from these localities are given in Appendix D.

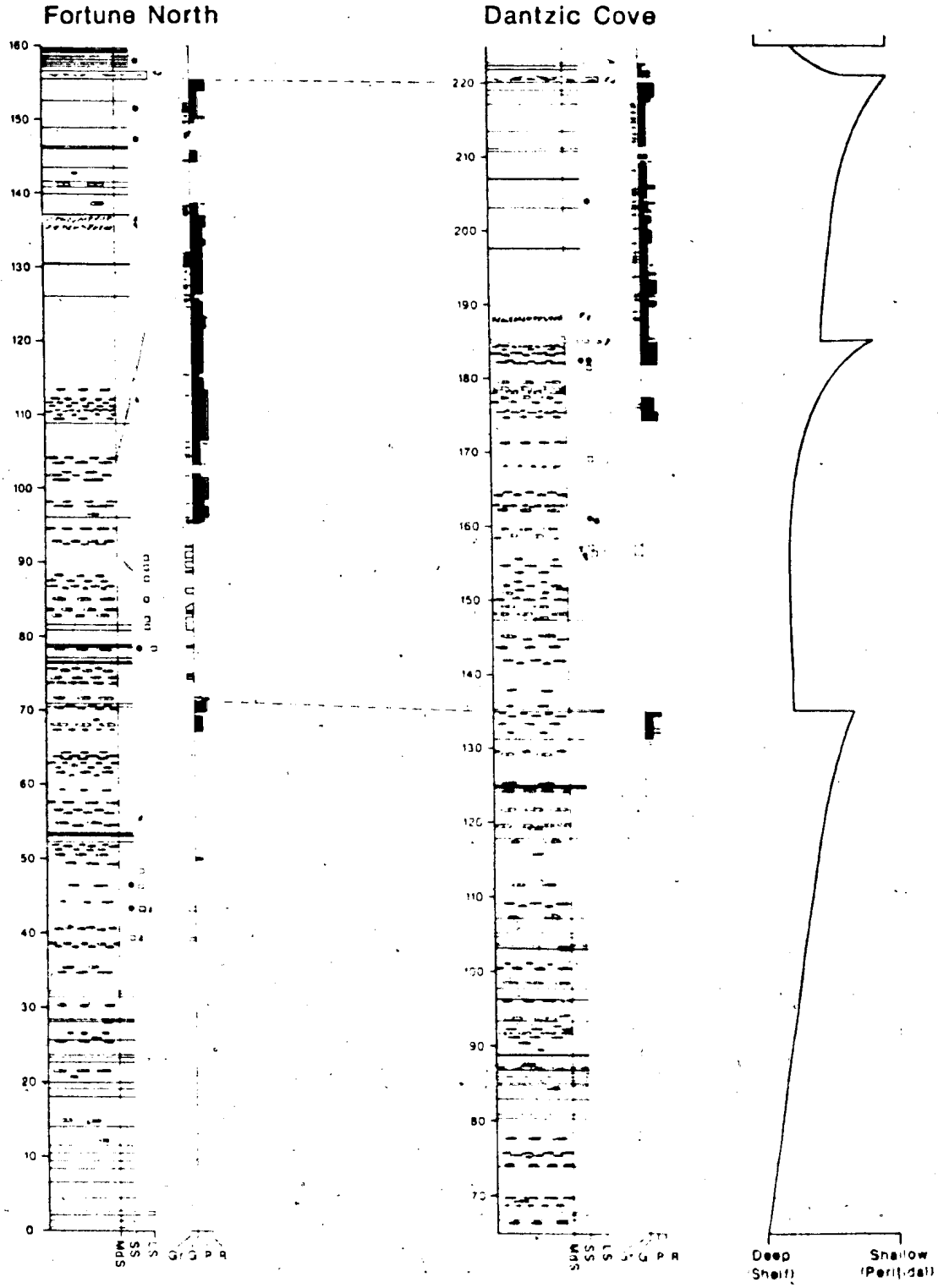
Fortune North
Dantzic Cove
Deep Shelf
Shallow (Peritidal)

at DC, only LS 3 is present at FN. The FN exposure does contain more steinkern-bearing gray mudstone (Facies 4.2). In both sections carbonate concretions are nearly absent in the top 30-50 m. At FN this zone contains some thick green colored intervals that are absent at DC.

6.7 PALEOENVIRONMENTAL INTERPRETATION FA 4: LOW ENERGY INNER SHELF AND PERITIDAL

The depositional environments designated for FA 3 and LS 3, which represent the stratigraphic limits of member 4, represent paleobathymetric limits for the deposition of this facies association. The paleoenvironmental interpretation for the Mudstone Facies (4.1 and 4.2) must incorporate a stratigraphic transition from the below-storm-wave-base deposits of FA 3, and intimate deposition with limestones that record very-shallow-water (peritidal) features (discussion below). These conditions alone point to the deposition of these fine-grained terrigenous sediments over a wide area of the inner shelf. The process interpretations for Facies 4.1 and 4.2 are consistent with deposition in an inner-shelf to shallow-subtidal setting.

The sedimentary structures and the inferred sedimentary processes (Section 6.5) indicate deposition of the Limestone Facies in peritidal settings. The features of LS 3 indicate deposition in a mosaic of shifting microenvironments. 'Micro-facies' included: (1) algal mats, (2) algally built (?) mud mounds, (3) low-energy, semirestricted (?) lime mudstone, (4) slightly higher-energy wackestone-packstones and (5) storm-sheet and channel coarse-grained debris. These constitute a small-scale facies mosaic that most likely formed, at least in part, in the intertidal zone (see James, 1984a). James (1984a; Figure 9) considers all of these features, and others (flat-pebble clasts and occasional burrows), all of which are present in LS 3, to be diagnostic of low-energy intertidal settings. Intertidal

conditions are also supported by the presence of tepee structures with relatively intact roofs. These would correspond in character to Asserto and Kendall's (1977) "embryonic" stage of development of these features that they consider diagnostic of lower Intertidal settings.

Intraformational debris in LS 3, including clasts of mudstone and limestone, was ripped up by storms or tides, or by small migrating tidal creeks or channels. Small channels also carried a significant fraction of quartzitic sand. The origin of the quartzitic sand may have been either fluvial or eolian Large volcanic clasts, rounded during fluvial transport, represent a thin scattering of clasts that was spread by streams flanking the tidal-flat region, possibly during river flood events.

As outlined in Section 6.5.3.2, LS 2 represents deposition in well oxygenated, moderate to high energy conditions (oncolitic debris). Subaerial exposure of the sediments during deposition cannot be demonstrated conclusively. The abundance of oncolites might suggest a very shallow subtidal setting in which fragments of algal mat, eroded from the intertidal area, were rolled around by tidal (?) currents. The lack of sedimentary and biogenic structures in LS 1 suggests deposition in a slightly deeper subtidal setting not colonized by algal mats or significant numbers of shelly fossils.

A full understanding of the sequence at DC rests, in part, on two important trends: (1) the progressive upward increase in bed thickness and complexity of the limestone beds and (2) the overall upward increase in red coloring of the mudstones, and the color variations below and above the limestone beds. The association of the red mudstones of this facies with the peritidal limestone beds confirms the strong relationship between color and relative water depth that is characteristic of much of the CIF. The overall upward increase in red coloring of the mudstone facies within member 4 parallels the progressively shallower water environments of deposition indicated by each successive limestone bed. The obvious conclusion to be drawn from this pattern is that member 4 represents a large-scale shallowing-upwards sequence, that records several smaller shallowing-upward

cycles, three of which are capped by limestone beds. Small shallowing-upward cycles restricted to the Mudstone Facies may be represented simply by green to red color changes without a limestone bed (e.g., FN-67-71.2). The gray mudstones of Facies 4.2 are found near the base of these shallowing cycles; they are never found in contact with red mudstone or the Limestone Facies. For this reason, Facies 4.2 is considered the deepest-water deposit of this facies association.

Comparison of the DC and FN sections (Figure 6.3) provides support for the paleobathymetric distribution of the lithofacies. There is no paleocurrent data from FA 4, but one could argue that given: (1) the general agreement of paleocurrent data among members 1-3, (2) the conformity of sedimentation represented by the transition from member 3 to member 4, and (3) the evidence for stable tectonics during the deposition of Members 2, 3 and 4, that significant changes in shoreline orientation with respect to that of the underlying sequence were unlikely. The paleocurrent data from FA's 1-3 indicate that locally the sediment-transport direction was towards the northeast and the shoreline was situated towards the southwest. The FN outcrop is presently located approximately 15 km northeast of DC, along a line roughly parallel to the regional fold axes. Assuming that there are no major structural offsets, FD should have a more distal assemblage of facies. If FN were more distal, and if the paleobathymetric interpretations given above are correct, one would expect greater abundance of Facies 4.2 and a lesser quantity of the Limestone Facies. This is, in fact, the case, as Figure 6.3 illustrates. Only one of the three limestone beds (LS 3) at DC can be traced to FN. The well developed exposure features in LS 3 indicate that it formed during the lowest stage of relative sea level for all of member 4, and would therefore be the most likely to have prograded into more offshore settings.

The observations are also consistent with ocean waters that were stratified in terms of dissolved oxygen during the deposition of this facies association. Facies 4.2, for instance, has a predictable vertical and lateral distribution, based on comparisons with ancient and modern dysaerobic shelf facies, and biofacies models (see Section 6.4.1) that

place dysaerobic facies in intermediate water depths between shallow nearshore aerobic facies and deep basinal anaerobic black shales (Figure 6.2).

6.7.1 Mixed Siliciclastic — Carbonate Systems: Model for FA 4

The depositional regime for FA 4 is one of a mixed shoreline with siliciclastic muds and minor thin limestones. It is well known that these sediments are normally mutually exclusive within modern environments as a consequence of the biogenic origin of most limestone: fine-grained siliciclastic sediments dilute carbonate sediments and negatively affect carbonate production by reducing the light available to organisms and by choking filter-feeding organisms.

Mixed siliciclastic and carbonate systems have recently been receiving attention at symposiums (McIlreath and Ginsburg, 1982; Doyle and Roberts, 1983) and in publications (Mount, 1984; Brett and Baird, 1985; Mack and James, 1986), but the general state of understanding lags behind many other facies systems. Mount (1984) describes the mixing of sediments in shelf settings. In his 'facies mixing model' the contacts between clastic and carbonate lithofacies are normally sharp due to rapid lateral changes or sharp boundaries between depositional environments. The sharply defined boundaries between Facies 4.1 and the Limestone Facies points to a clear-cut separation of carbonate and mudstone in the depositional setting.

Standard facies models for deposition on mixed carbonate-terrigenous shelves call for the deposition of land-derived sediment in nearshore environments and carbonate sediments in deeper-water subtidal settings (see McCave, 1969; Konopka and Dott, 1983; Mount, 1984; Gervirtman and Mount, 1986; Mack and James, 1986). This facies model is applicable to present-day settings like the Nicaraguan coast (Murray et al., 1983) and the Great Barrier Reef of Australia (Maxwell and Swinchatt, 1970). The trapping of terrigenous sediments in shoreline environments is modeled as a response to sea-level rises

(McCave, 1969; Maxwell and Swinchatt, 1970) that drown nearshore environments and result in the deposition of sand (see discussion of transgression/alluviation model by Brett and Baird, 1985).

Other mixed depositional systems include carbonate shelves with a deep-water shale facies in an outer shelf basin. In these examples storms periodically carry carbonates out into distal offshore basins where they form intercalations with shale (e.g, Kreisa, 1981; Kelling and Mullins, 1975). This is clearly not a reasonable analog for the lithofacies of FA 4, which were deposited along a shelf dominated by siliciclastic mudstone.

Marine cyclothems also contain both carbonate and terrigenous facies. Mid-continental cyclothems described by Heckel (1977) include two carbonate units; the lower units formed below effective wave base in an intermediate-depth offshore environment during marine transgression, and the upper units formed in nearshore to intermediate offshore environments during marine regression. During periods of eustatic sea-level lowering (upper unit) the width of the carbonate shelf increased, prograding into deeper offshore environments. At times of maximum regression the nearshore setting suffered an influx of detrital sediments, producing nearshore sand and shale facies. None of the depositional systems operative at any stage in the deposition of these cycles is directly analogous to that which characterized FA 4. The regressive limestones of these cyclothems are analogous in that they formed, in part, in a shallow subtidal to nearshore position and also formed during marine regression, but they are different in that they (1) contain different sedimentary structures, (2) were deposited in depositional environments that encompassed a far greater bathymetric area, and (3) produced a considerably thicker deposit (~3 m).

Shale-carbonate cycles of the Devonian Hamilton Group of New York State, interpreted by workers in terms of a transgression/alluviation model and recently reinterpreted by Brett and Baird (1985), provide an interesting comparison. The model is similar to that described for the mid-continent cyclothems, calling for deposition of

extensive limestone beds during marine regression. The richly fossiliferous limestone beds (wackestones, packstones and grainstones) contain abundant evidence to suggest storm deposition and constant reworking in shallow-shelf settings between fair-weather wave base and storm wave base. Fine-grained sediment was winnowed in these high-energy settings, then transported and deposited in a deep basinal setting. Relative sea level never dropped low enough for shoreline facies to be exposed in available outcrops (Brett, pers. comm., 1986), but even without a view of the shoreline facies, it is readily apparent that these rocks can at best provide only a partial analog for member 4. The Hamilton Group limestones formed during regressions, but are dissimilar in terms of depositional environment, sedimentary structures and composition. An interesting aspect of the Hamilton Group rocks which is analogous to the rocks of member 4 is color cycles associated with the limestone beds. The Hamilton limestones are underlain and overlain by shales that grade from medium gray to dark gray to black. Facies relationships indicate that the black shales are the deep-water facies, while the lighter-colored mudstones are the shallow-water facies. The distribution of red mudstones in FA 4 is analogous in that these light-colored mudstones appear below the first two limestone beds and are most abundant below LS3, the most shallow-water part of the sequence.

From the above review of mixed siliciclastic-carbonate systems it is apparent that there are generally two common types of mixed systems: (1) carbonate shelves that grade seaward into deep-water shale basins, and (2) shelves in which siliciclastic sediments are constrained, by a number of processes, to the shoreline and nearshore settings, allowing for the development of a carbonate facies in deeper clear-water shelf environment. Neither of these models is applicable to FA 4.

The model proposed by Button and Vos (1977) for some Lower Proterozoic deposits in South African is applicable, in some respects, to FA 4. Their model is similar in that the subtidal region consisted of fine terrigenous sediment (mudstone and shale), while carbonates were formed in the tidal-flat setting. The major difference between these models

is the presence of large, elongate bioherms — up to 10 m thick and 10 m wide — in the shallowest part of the subtidal. These may have their counterpart in the mud mounds and stromatolites of LS 3, but certainly not at the scale described by Button and Vos.

The above discussion indicates that appropriate ancient or modern analogs for FA 4 do not exist. A new depositional model has been constructed in which carbonate deposition takes place in the peritidal environment while siliciclastic muds are deposited across the rest of the shelf. At times of maximum regression, the limestone units may have prograded and extended their aerial distribution to form thin sheetlike units. The source of the siliciclastic mud is enigmatic. It may have come from a laterally adjacent deltaic source - probably significant distances along the shoreline, given the lack of evidence for local deltas. The shelf at this time was zoned in terms of levels of dissolved oxygen. An oxygen-minimum zone was developed (Facies 4.2) in slightly deeper areas. This may have expanded/contracted or shifted bathymetrically due to any number of factors (e.g., changes in relative sea level).

An important question that must be answered with respect to this model is: Why was the carbonate restricted to the peritidal setting ? There are two possible answers to this question: (1) the sedimentation rate was too high on the shelf to allow for full-scale carbonate production, and (2) the climate was unsuitable. FA 4 was certainly deposited under low-energy conditions during a period when little or no sand-sized (or coarser) sediment was being supplied to the basin. Muds are generally thought to have low sedimentation rates, but this is of course an oversimplification. It was argued earlier (Section 6.4) that the preservation of pyritic steinkerns indicates moderate sedimentation rates, but it is unknown if this rate was sufficient to stifle carbonate production. The alternative hypothesis would require deposition in a semiarid/moderate climatic belt. Clearly the production of carbonate in these beds was organically controlled, with the carbonate being formed essentially in situ within the narrow peritidal belt. In a more moderate climatic

belt this belt would be the only marine setting in which water temperatures would be sufficiently high to allow for thriving communities of carbonate-secreting organisms.

Is there any evidence to support the conclusion that deposition occurred in a moderate climatic belt? The paleomagnetic results published by Irving and Strong (1985) on Marystown Group rocks from the Burin Peninsula, with ages of 623-606 Ma, suggest a paleolatitude position of 35°. This is at the present-day latitudinal limits of carbonate production in the oceans (Wilson, 1975, p. 1). Further support for this argument lies in the lack of significant thicknesses of carbonate within any of the lower Paleozoic of the Avalon Newfoundland Zone, while other lower Paleozoic sequences contain significant quantities of carbonate strata, even other Pan-African areas (e.g., Morocco).

The stratigraphic boundaries between the Limestone Facies (4.3) and the Mudstone Facies (4.1) are very sharp and indicate little lateral mixing of these facies belts. Assuming that the controls on the position of the carbonate belt, as discussed above, are correct, then a problem is posed as to why and how the siliciclastic mud of the inner shelf was kept out of the intertidal area. Along carbonate shelves, the sediments that accumulate in the peritidal setting (fine-grained sediments in the case of low-energy shorelines) are derived from the subtidal carbonate 'factory' (James, 1984b). Mesotidal and macrotidal siliciclastic shorelines, modern and ancient, also tend to be areas of accumulation of fine-grained sediments; this is thought to result from the action of tidal currents (Van Straaten and Kuenen, 1958). With a large reservoir of siliciclastic mud in the subtidal zone during the deposition of FA 4, it would seem logical that this sediment would have been transported onto the tidal flat, given the standard sediment-dispersal patterns of carbonate and siliciclastic systems. There are some thin siliciclastic mudstone layers associated with LS3, but these are minor; algae (e.g., stromatolites and bioherms) were actively trapping and binding carbonate mud. Most explanations for why siliciclastic muds were not transported onto the tidal flat are at odds with the available data. For instance, one might appeal to a barrier to physically obstruct the transport of siliciclastic mud into the tidal-flat region, but

there is no evidence to suggest that barrier islands or any other sandy environments were part of the local depositional system. The possibility that siliciclastic mud was not transported onto the tidal flat because of weak or negligible tidal currents is dismissed because well developed tidal flats would not have developed in the absence of tidal processes. This problem remains an important, yet unexplained, part of this facies model.

Chapter 7

GREEN SANDSTONE/SILTSTONE FACIES ASSOCIATION (5)

7.1 INTRODUCTION

FA 5 composes the lower part of member 5. This facies association has been subdivided into two facies: 5.1 (~60% of FA 5) and 5.2 (~40% of FA 5). Exposure of this facies association is best at Dantzic Cove, and most of the description below pertains to this outcrop. Aside from some decent exposure at Fortune North, there are no other locations with reasonable access and exposure to view this facies association.

7.2 SANDY SILTSTONE FACIES: 5.1

This lithofacies has been subdivided into two subfacies based primarily on bed thickness and total percent of sandstone. The lithofacies is characterized by little variation in grain size, which accounts, in part, for the surprising lack of visible internal structures, the paucity of bedding planes, and the total lack of exposed soles. As a consequence, paleocurrent data are relatively sparse. Data for current lineations and ripples are given in Figure 7.1.

Figure 7.1: Paleocurrent information for F.A. 5 at DC. (A) Current lineations for Facies 5.1, (B) Ripple paleocurrents for Facies 5.1, (C) Current lineations for Facies 5.2, (D) Ripple crest-trend orientations for Facies 5.2.

A

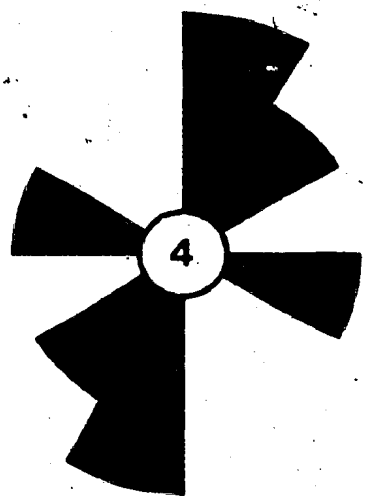

B

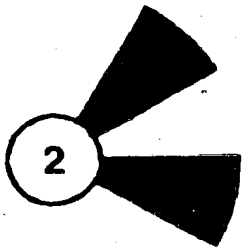

C

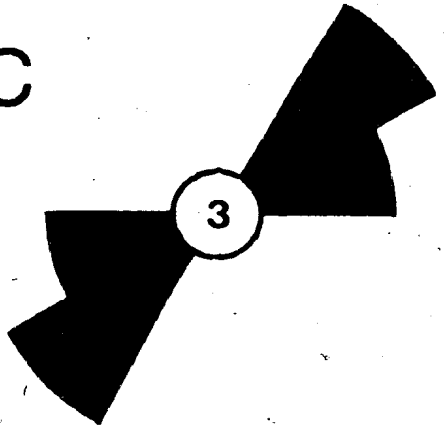

D

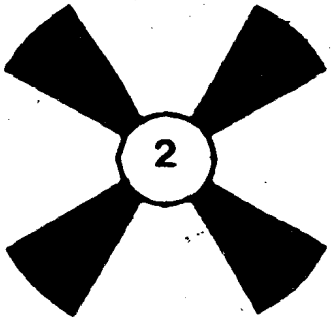

One feature common to this facies is rare, thin, concave-up, sandstone-filled scours, found both isolated (Plate 34d) and along the bases of sandstone beds (Plate 34c). These structures are generally 5 -15 times wider than they are thick (Table 7.1). In cross section they normally have smooth, symmetrical lower surfaces. They are invariably filled with a single set of cross-laminated, carbonate-cemented, white-weathering sandstone (Plate 34d). The upper surface may be disrupted (Plate 34c) in the same manner as the thin sandstone beds of this lithofacies, described below. One example was noted with an asymmetric, sharp, angular, lower surface (Plate 34d).

7.2.1 Subfacies 5.1A: Thickly Laminated Sandstone/Siltstone

This subfacies is composed of green-grey sandy micaceous siltstone with thick laminae to very thin beds of very fine- and fine-grained sandstone that weather dark gray to black, or, if carbonate cemented, weather white. Sandstone beds less than a centimeter thick often have a characteristic churned or disrupted appearance (Plate 34b). Disruption may be limited to the upper parts of these beds. Distinct burrows are also preserved, cross-cutting these sandstone beds.

Sandstone beds form approximately 15-25% of this subfacies on average. Thin beds of gray/white-weathering, carbonate-cemented sandstone, 4-6 cm thick, make up a small percentage. As noted earlier, the thickness of carbonate-cemented units represents original or precompactional thicknesses. These preserve delicate sedimentary and biogenic structures that are elsewhere obscured during compaction. The sandstone beds display sharp lower surfaces and indistinct or highly disrupted upper surfaces. The dominant internal structures are parallel lamination and ripple cross-lamination. Some beds display repeated alternations between these structures without any apparent trend in order of appearance. Many beds contain parallel laminae at their bases and ripple cross-laminae

PLATE 34: GREEN SANDSTONE/SILTSTONE FACIES ASSOCIATION (FA 5)

a: Thick parallel laminated bed from Facies 5.2 with upper convolute lamination. Stratigraphic top is up. Scale is 15 cm long.

b: Discontinuous carbonate-cemented laminae to thin beds of sandstone from FN. Some sandstone laminae show load and flame structures and little disruption, while others were strongly burrowed. Stratigraphic top is up. Scale is 15 cm long.

c: Small scour at base of carbonate-cemented sandstone from lower part of Member 5 at FN. Scour has one steep, sharp wall. Upper surface of bed was reworked by burrowing organisms. Stratigraphic top is up. Scale has 10 cm divisions.

d: Shallow scour-and-fill structure with cross-lamination, from lower part of Member 5 at FN.. Stratigraphic top is up. Scale has 10 cm divisions.

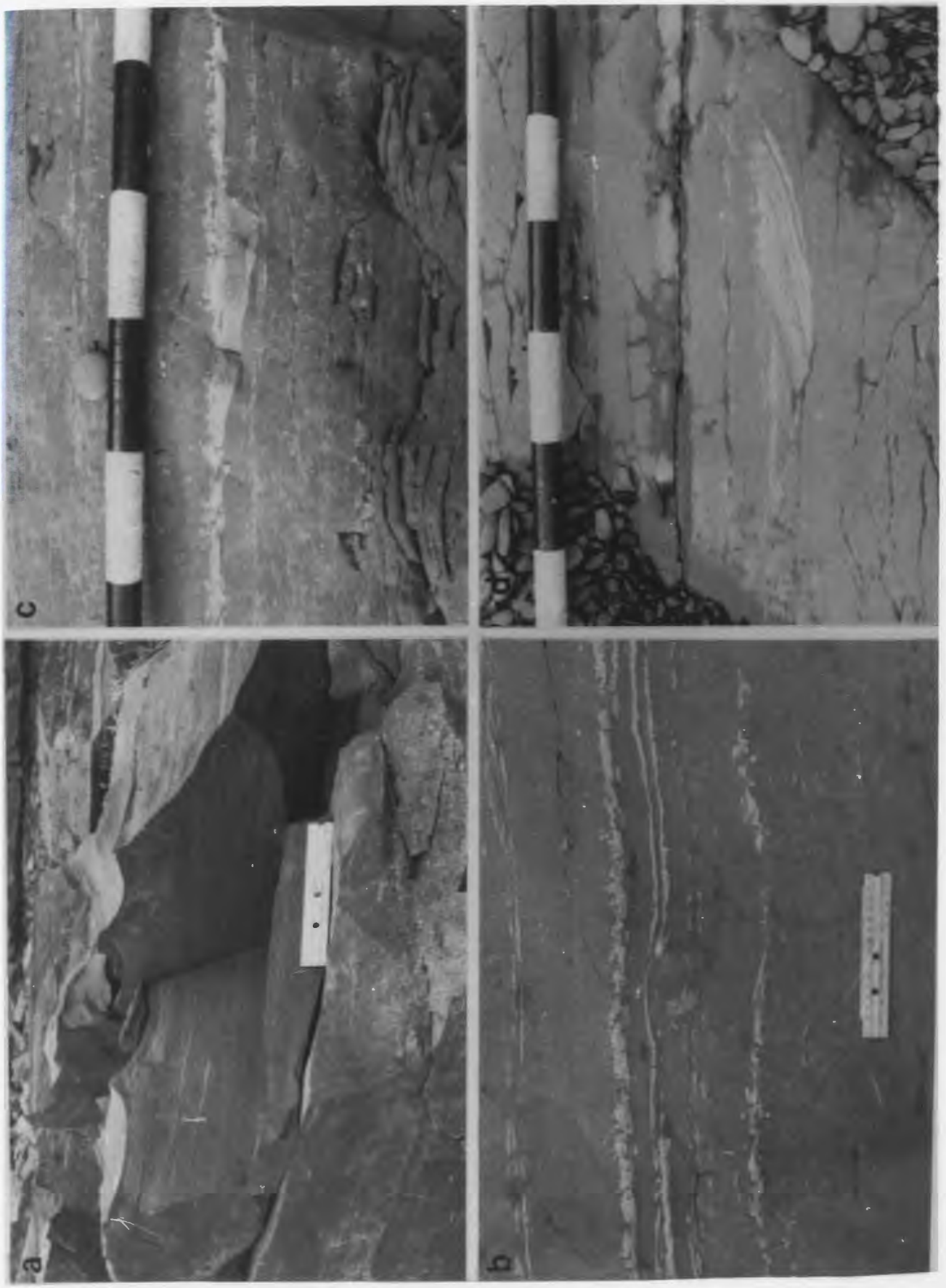
c
a
b

TABLE 7.1 SIZE DATA ON SCOUR-AND-FILL STRUCTURES (FA 5)

Width (cm)	Thickness (cm)	Width/Thickness
20	2	10
35	2.5	14
35	4.5	7.8
55	9	6.1

above, but a significant percentage also reveal the opposite sequence. Some of the parallel-laminated beds contain parting lineations.

7.2.2 Subfacies 5.1B: Very Thin and Thin Bedded Sandstone/Siltstone

Very thin and thin beds of black-weathering sandstone, 1-6 cm thick, make up 25-30% of this subfacies. The number of carbonate-cemented beds is less than in Subfacies 5.1A. The sandstone beds display sharp lower surfaces and indistinct or highly disrupted upper surfaces. These beds may show subtle distribution grading. The dominant internal sedimentary structures are parallel lamination and ripple lamination. Many of these dark sandstone beds are massive, even on a slabbed surface.

A representative stratigraphic section of this subfacies (DC-285.6-286.5) is presented in Figure 7.2. This small section represents one of the few parts of the weathered outcrop where structures are preserved in detail. Cut slabs from this part of the outcrop reveal the nonsandstone part of this subfacies to be a mixed lithology of red-tinted mudstone and gray siltstone. This can be separated into a sandy siltstone with discontinuous thin laminae of red mudstone and a second lithology in which mudstone generally composes 25-40% (up to 80% in cases). The former may be tens of centimeters thick, while the latter is found as 1-2 cm thick layers that often drape the black sandstone beds (Figure 7.2). Planolites and large other trace fossils are found at the top of many of the sandstone beds (Figure 7.2).

7.2.3 Process Interpretation: Facies 5.1

Sedimentary structures indicate upper-plane-bed traction deposition (parallel lamination with parting lineations) and lower-flow-regime ripple migration. Vertical variation in the sequence — and in cases multiple alternation — of these features indicates

Figure 7.2: Representative stratigraphic section of Facies 5.1 (Subfacies B) from DC-285.6-286.5. Details are extremely difficult to see on the weathered outcrop under less-than-ideal lighting conditions. See text for details.

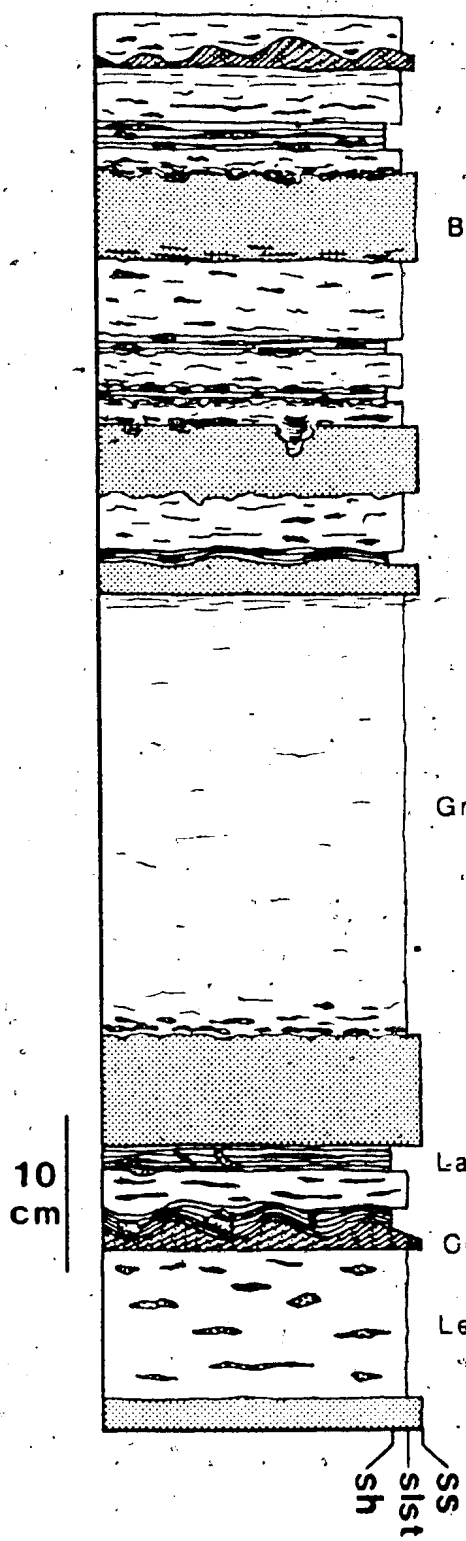
Black weathering sandstone beds
DC-285.6-286.5
Gray sandy siltstone
10 cm
Laminated shale with burrows
Current ripples
Lenticular sandstone laminations
sh
slst
ss

that there were temporal fluctuations in current strength during deposition. The deposition of sandstone, excluding the rare scour-and-fill structures, was apparently not preceded by erosion.

The churned and disrupted appearance of many of the thinner sandstone beds, and the upper surfaces of the thicker sandstone beds, is attributed to reworking by burrowing infauna. Distinct burrows are found cutting through or down into sandstone beds.

The lenticular sandstone structures are interpreted as shallow scour-and-fill features. The cross-laminated sandstone records infilling of sand into the scour by essentially unidirectional currents. In most examples there is no evidence to indicate that the substrate was cohesive prior to erosion (e.g., no wall overhangs). The scour in Plate 34c has one relatively steep wall, and may therefore have formed in semicohesive sediment.

The difference in the scale of bedding and the quantity of sandstone between the two subfacies may be attributed either to variable supply of sand-sized sediment to the depositional site, or variable competence and capacity of the currents. The fact that a higher percentage of thin sandstone beds in Subfacies 5.1B lack evidence of bioturbation indicates that sedimentation rate may have been higher than for Subfacies 5.1A.

In Subfacies 5.1B the red laminated mudstone can be attributed to suspension deposition. This is supported by the draping style: e.g., differential thickness over crests vs. troughs of ripples (Figure 7.2).

The data in Figure 7.1 are too sparse to make a definitive statement about paleoflow, although they do suggest that net sediment transport may have been directed toward present northeast and east.

7.3 THIN-MEDIUM BEDDED SANDY SILTSTONE: FACIES 5.2

This lithofacies is characterized by interbedding of green-grey sandy micaceous siltstone and thin to medium beds of gray very-fine-grained sandstone, some of which have greyish-white-weathering fine-grained sandstone divisions at their base. Thin layers of laminated mudstone are present, but because these are difficult to detect on weathered surfaces it is difficult to assess the volumetric importance of this lithology. There is little variation in grain size in this lithofacies, making it very difficult in places to see structures, or even the nature of bedding. Another byproduct of this low variability in grain size is a lack of exposure of soles. A few upper bedding surfaces are exposed and a limited number of biogenic and sedimentary structures are present. The overall weathering pattern precluded the collection of many paleocurrent readings; available data are given in Figure 7.1.

Figure 7.3 is a short detailed stratigraphic column from part of this lithofacies. This illustrates the graded — fine grained sandstone to sandy siltstone — nature of many beds. The bases of some beds contain poorly laminated fine sandstone with a sharp lower surface showing ball-and-pillow and flame structures. Some beds have angular shale chips, up to 3 cm in length, floating in the sandstone. Most shale chips have a bedding-parallel orientation.

Parallel lamination is by far the most abundant sedimentary structure in the sandstone beds. Beds up to 25 cm thick may be composed solely of parallel laminae. Associated with these parallel laminae are current lineations and parting lineations. There is a notable paucity of ripples and ripple cross-lamination in this lithofacies. The ripple form sets or ripple cross-laminae that were observed have asymmetric profiles and unidirectional cross-laminae.

Figure 7.3: Representative stratigraphic section of Facies 5.2 from DC-302.4-303.04. See text for details.

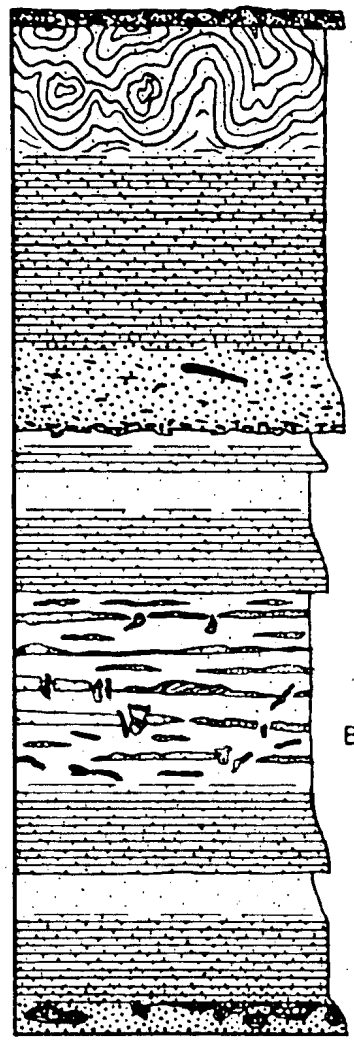

DC-302.4-303.04

Thin and very thin beds of fine-grained sandstone may dominate parts of this lithofacies. In these instances the sandstone is usually disrupted into irregular sandstone masses, many of which define indistinct and distinct burrows (Figure 7.3). In one example (Figure 7.3), convolute laminae cap a graded bed (Plate 34a). From their appearance, the contorted laminae were likely parallel laminated prior to deformation.

Also present are small, lenticular, cross-stratified scour fills of sandstone similar to those described for the Sandy Siltstone Facies (5.1). Two of these scours have dimensions of 15 cm (length) X 3 cm (depth) and 21 cm X 6 cm, with width to thickness ratios of 5 and 3.5, respectively.

7.3.1 Process Interpretation: Facies 5.2

The grading displayed by many of the thin to medium sandstone beds of this lithofacies indicates deposition by decelerating flows. The sharp lower surfaces of the fine sandstone layers and the presence in these beds of angular mud chips indicates erosion prior to deposition. The flame and ball-and-pillow structures at the base of these layers indicate rapid deposition of water-laden sand that was followed by liquefaction and loading.

The abundance of thick parallel-laminated beds with parting lineations requires sustained deposition under upper-flow-regime conditions. Those beds composed solely of parallel-laminated very fine sandstone do not show evidence of erosion prior to deposition. The scarcity of ripples and the thickness of parallel-laminated divisions indicate that the range of conditions under which the upper-plane-bed phase existed may have been quite large. This may be partly attributable to deposition from currents with high sediment concentration. During deposition with high suspended load, the transition from ripples to plane bed occurs at lower velocities, extending the plane-bed field (Blatt et al., 1980, p.

143). The ripple geometries and styles of ripple cross-laminae indicate deposition by currents, not waves.

In one bed, parallel laminae were deformed into convolute laminae. Rapid deposition of sediment of this grain size would have made it a likely candidate for liquefaction and subsequent soft-sediment deformation.

It is tempting to relate the sequences of structures found in these graded sandstone beds to the Bouma (1962) sequence. Where present, the fine sandstone division at the base, however, differs from the Bouma T_a division in that it is not strongly graded, and contains, in some cases, cryptic, horizontal laminae. In general, the weathering pattern of these beds is so poor as to make it difficult to evaluate contacts between divisions accurately. Despite this, the sequence of structures in these beds is best explained by deposition from decelerating sediment-laden turbulent flows, possibly from turbidity currents.

The sparse paleocurrent readings indicate possible northeast or southwest flow during deposition of the parallel-laminated beds. The ripple-crest trends are few and inconclusive.

The small lenticular sandstone beds are shallow scour-and-fill structures. The simple cross-laminated sandstone fill indicates that unidirectional currents transported sand into a scoured depression. The width-to-thickness ratios are much smaller than those in other lithofacies; i.e., these are deeper features. Given the low variability in grain size, and assuming a range of sediment characteristics (compaction, organic content, water content, packing) similar to Facies 5.1, then it may be concluded that the structures in this lithofacies formed by more intense scour and erosion, under higher-energy currents, than those in Facies 5.1.

7.4 LITHOFACIES DISTRIBUTION

The lowermost occurrence of the Green Sandstone Facies Association marks the base of Member 5. In the southwest Burin Peninsula region this is directly above LS 3 of Member 4. The most accessible and best exposed outcrop of this facies association is at Dantzic Cove. Strata of Subfacies 5.1A are also accessible in Fortune Harbour, where they are exposed stratigraphically just above LS3. The exposure at Dantzic Cove contains, stratigraphically, the following (nonrepeated) sequence of facies: Subfacies 5.1A, Subfacies 5.1B, and Facies 5.2. This is is then overlain stratigraphically by the Red SS Facies Association.

At Dantzic Cove and Fortune Harbour, Subfacies 5.1A immediately overlies LS 3, and is red colored for a few meters. Small sandstone-filled scours are present for a short stratigraphic interval above the base of Member 5, but are quickly lost upsection. Much of this subfacies is very poorly exposed. The exposure of Subfacies 5.1B is better at DC, but the weathering pattern is still poor. At DC, only in the upper 5-10 m of this subfacies, directly below the transition into Facies 5.2, are sandstone-filled scours observed. The upper transition into the Red SS Facies Association is also characterized by much weathering and, in places, poor exposure.

7.5 PALEOENVIRONMENTAL INTERPRETATION: STORM-DOMINATED SHELF BELOW STORM WAVE BASE

The sedimentological data for interpretation of depositional environment of this facies association are relatively sparse. Two aspects of this facies association are useful in assigning the deposition to environments below storm wave base: (1) the sandstone beds

do not show evidence of reworking by waves, and (2) there is upward transition into thick sandstone beds with HCS (Red SS Facies Association). The sequence of facies exposed at DC, both within this facies association and when taken in total with the overlying exposure of the Red Sandstone Facies Association, clearly define an upward-coarsening and upward-thickening sequence. The facies association is interpreted as the deposit of a prograding storm/wave-dominated system (full discussion to follow Paleoenvironmental Interpretation of FA 6: Section 8.6).

In many other prograding sequences in which the upper parts are dominated by the storm-generated structures HCS and SCS, as is the case at DC, the sandstone beds in the lower parts of the sequences are interpreted as distal-equivalents of HCS beds that are deposited below storm wave base. These distal beds are turbiditelike in character, containing whole or partial Bouma sequences (Hamblin and Walker, 1979; Leckie and Walker, 1982; Walker, 1984). Numerous authors have discussed proximality trends in tempestites (Brenchley et al., 1979; Aigner and Reineck, 1982; Nelson, 1982). Brenchley et al. (1979) correlate proximality with changes in (1) sandstone percentage, (2) grain size, (3) bed thickness, (4) bed frequency and (5) sedimentary structures. Higher values of 1-4 indicate more proximal conditions. With the exception of grain size, which is fairly consistent, these factors do increase upsection at DC. Consistency in grain size is this case probably a function of a consistent supply of relatively unchanging source material. Proximality is also reflected in the sedimentary structures found in the lower divisions of sandstone beds, with higher-energy structures dominating closer to shore. Although sedimentary features are hard to see in Facies 5.1, thin current-rippled beds are present, and it is evident that parallel lamination (upper flow regime) dominates Facies 5.2. This facies association compares well with the prograding sequence described by Hamblin and Walker (1979). Their more 'distal' facies (Facies A) contains thin beds with Bouma T_{bc} sequences and bioturbated tops, features similar to Facies 5.1. Their more proximal, thicker-bedded Facies B contains Bouma T_b, T_{bc} and T_c beds and small-scale coarsening-

upward sequences that they interpret as prograding storm-turbidite lobes. The weathering pattern of the exposure at DC is not good enough to document small-scale coarsening-upward cycles clearly, but a large-scale upward increase in bed thickness and prominence of parallel lamination was noted.

The bulk of this facies association was apparently deposited in an offshore setting below the influence of storm waves. Given the shallow-water conditions represented by LS 3 and the general lack of shallow-water sedimentary structures at the base of Member 5, it would appear that there was a very rapid deepening at the beginning of Member 5 deposition. The depositional system represented by this facies association and the Red Micaceous Sandstone Facies Association (6) was being established during the early stages of this deepening event. The small scour-and-fill structures, present a short distance above LS 3 in Subfacies 5.1A, were formed as deepening began, while still in shallow water. The stratigraphic appearance of similar scours in the upper exposure of Subfacies 5.1B and Facies 5.2 parallels the increase in various proximality criteria associated with the transition into Facies 5.2, and indicates shallowing.

Chapter 8

RED MICACEOUS SANDSTONE FACIES ASSOCIATION (6)

8.1 INTRODUCTION

The Red Micaceous Sandstone (RMS) Facies Association contains one facies, which has been subdivided into two subfacies. Conglomeratic beds, occurring within both subfacies, are described separately following the description of each subfacies. This facies association is well exposed at Dantzic Cove and at Sagona Island. Additional exposures include Fortune North, Radio Station (between Fortune and Grand Bank), Pieduck Point, and other minor localities along the southwest shore of the Burin Peninsula. This same facies is present in the Random Formation, and its distribution is given by Hiscott (1982) and Green and Williams (1974).

8.2 RED MICACEOUS SANDSTONE (RMS) FACIES (6.1)

This lithofacies is dominantly composed of fine, red, micaceous sandstone of relatively uniform grain size, composition and color. This uniformity makes it difficult to see internal sedimentary structures readily in less-than-ideal lighting conditions. The sandstone ranges in color from greenish-pink to pink to deep red. The red coloring is

derived from hematitic clays and cement. Variable concentrations of glauconite peloids are also present. This lithofacies, present in the overlying Random Formation, was described by Hiscott (1982). He documented braided, erosional gully systems from two surfaces at the Dantzic Cove exposure (Plate 37c). The floors of these channels are littered with mudstone and sandstone intraclasts and phosphatic shale clasts. The sandstone mounds that are left as erosional remnants have abundant pothole structures that are also filled with clasts (see Hiscott, 1982, Figure 9D).

The dominant bedding style of this lithofacies is one of parallel subhorizontal stratification separated by low-angle truncation surfaces. This stratification, and the presence of isolated beds that in three-dimensional exposures exhibit mounded topography, support the conclusion by Hiscott (1982) that this lithofacies contains amalgamated hummocky cross-stratification.

8.2.1 Thin to Thick Bedded Subfacies: 6.1A

Although Hiscott (1982) did not describe individual, nonamalgamated HCS beds from the RMS facies of the Random Formation, they are present in the CIF (Plate 35e). This subfacies contains hummocky beds of red micaceous sandstone that, at their thinnest, vary in thickness from ~10 cm in the swales to ~20 cm in the hummocks. Spacing of the hummocks ranges from 0.8 to 1.2 m. The sandstone beds of this subfacies are locally deformed into large ball-and-pillow structures a meter or more across.

In this subfacies layers of shaly siltstone drape hummocky surfaces. These show greater thickness over swales than over hummocks. Sandstone beds are irregular in thickness (Plate 35h) and often pinch out. A bed at DC-329.4 ranges from 0-65 cm across 13 m of outcrop; a line drawing of the geometry of the bed and the internal stratification is given in Figure 8.1. The style of stratification and the overall geometry of this particular bed is not typical of HCS. The spacing of hummocks in HCS beds has been given as 1-5

PLATE 35: RED MICACEOUS SANDSTONE FACIES ASSOCIATION (FA 6)

a: Transition zone between FA 5 and FA 6 at Dantzic Cove (DC-~310-325). Thin to medium sandstone beds are separated by burrowed siltstone. Sandstones are primarily parallel laminated, although rare HCS beds have been noted. Stratigraphic up is to upper right.

b: Bioturbated siltstone in the transition zone. Trace fossils include Teichichnus rectus, Planolites beverlyensis, and Planolites montanus. Scale is in centimeters.

c: Thick and medium beds of red micaceous sandstone at DC-400.2-402.7 with low-angle truncation surfaces. Stratigraphic top is toward upper left. Notebook is 18.5 cm long.

d: Low-relief wave (vortex) ripples on top of an HCS bed. A second set of ripples is superimposed at a high angle to the dominant set forming a 'ladder-back' configuration. Paired vertical burrows, Planolites beverlyensis and Paleophycus tubularis traces are prominent. Scale is in centimeters.

e: Well-exposed 3-dimensional view of HCS bed at DC-402.7. Hummocks are spaced several meters apart. Stratigraphic top is toward upper right. Notebook is 18.5 cm long.

f: Peculiar mottled fabric in bed from Subfacies 6.1A at DC-330. The dark and light mottles are subequal in proportion in this particular bed. Stratigraphic top is up. Notebook is 18.5 cm long.

g: Top surface view of hummocky bed in "e" showing well-developed current lineations. These features, rarely seen in this facies association, help confirm the notion that HCS is formed at or near the transition to upper plane bed. Scale is 15 cm long.

h: Medium to thick beds of red micaceous sandstone of Subfacies 6.1A. Note hummocky and swaly topography, mottled fabrics, and abundant bedding planes associated with thin siltstone partings. Stratigraphic top is toward upper right. Notebook is 18.5 cm long.

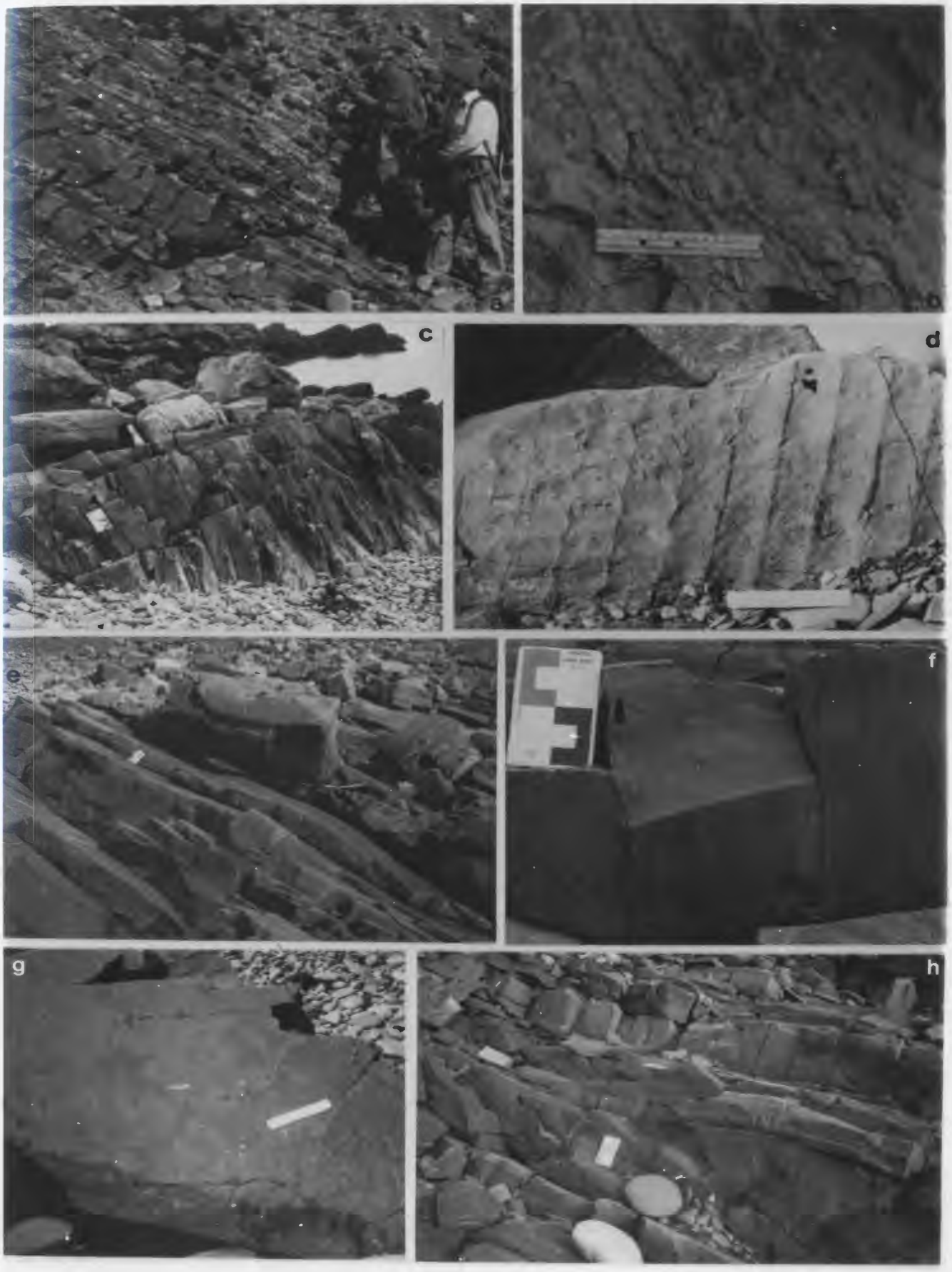
a
b
c
d
e
f
g
h

Figure 8.1: Outcrop drawing of Facies 6.1A showing irregular bed thicknesses and hummocky bedding surfaces. The lowest bed in the upper panel, DC-329.4, ranges from 0-65 cm across 13 m of outcrop. This bed is illustrated with the internal truncation surfaces drawn in (middle and lower panel); the lower panel is drawn with vertical exaggeration to emphasize the lateral variation in the position of internal truncation surfaces. The bed is dominantly planar laminated. The size and overall geometry of this particular bed is not typical of HCS.

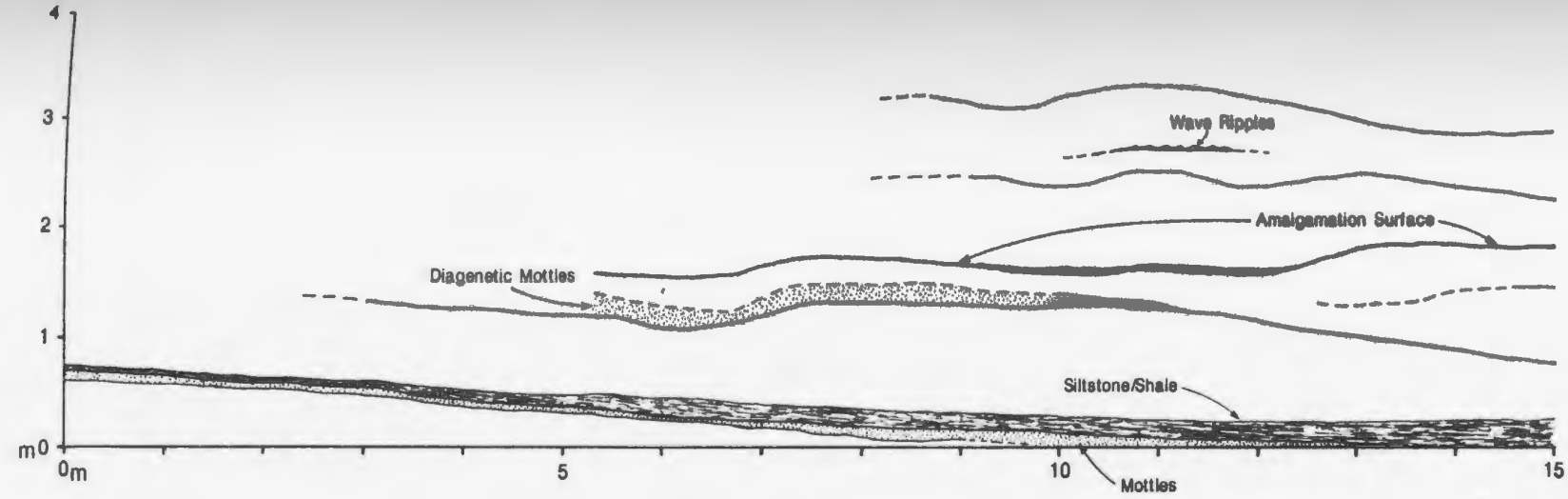
4
3
2
1
m0
0m
5
10
15
Wave Ripples
Amalgamation Surface
Diagenetic Mottles
Siltstone/Shale
Mottles


1
0.5
m0
0m
5
10
15

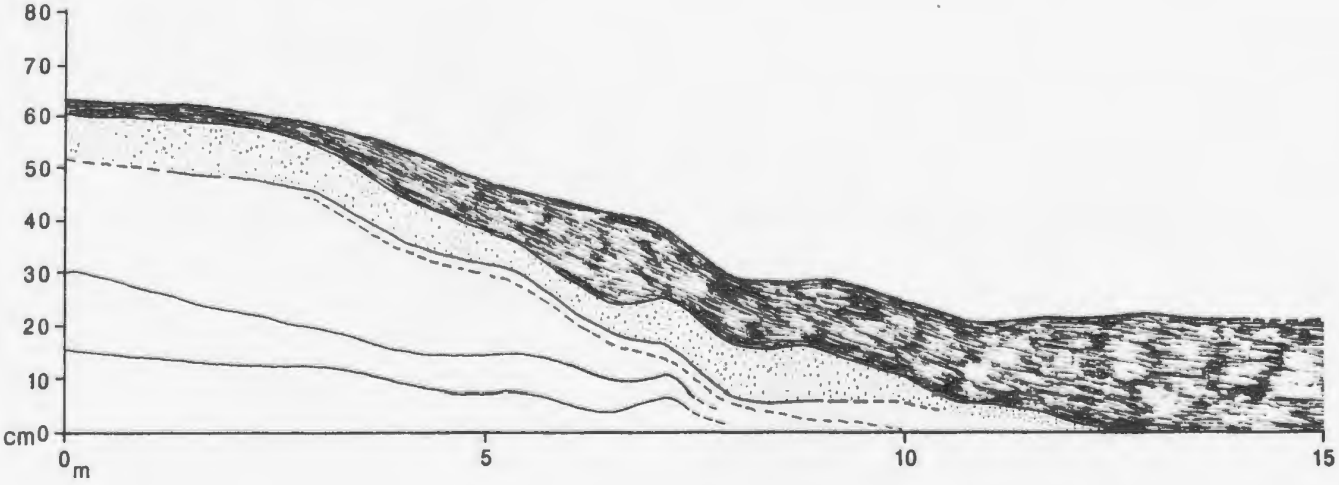
80
70
60
50
40
30
20
10
cm0
0m
5
10
15

m by Campbell (1966), Hamblin and Walker (1979) and Leckie and Walker (1982), and as 'one to a few meters' by Bourgeois and Smith (1984), Dott and Bourgeois (1982), Harms et al. (1975) and Harms et al. (1982). Possibly the largest reported spacing, 1-10 m, is given by Gilbert (1899). This value is anomalously large compared to those reported from numerous recent studies, and may therefore be suspect. The distance from crest to trough of the sandstone bed in Figure 8.1 is at least 13 m — the spacing measurements given above are crest-to-crest distances. If one were to imagine a semblance of symmetry to this structure the wavelength would be on the order of 20 m or more.

Bedding planes in this subfacies are locally covered with shale-chip conglomerates (Plate 36e). These are composed of thin, red shale clasts that are generally only a fraction of a millimeter thick. The long axes of these chips range from a few millimeters to ~10 cm. Blue-weathering phosphatic shale chips are found in thin layers and lenses, along internal truncation surfaces and floating within sandstone beds (Plate 36d). Additional bedding-plane features include ripples and burrow marks. Two surfaces at DC display ripples. At DC-329.4 there are poorly preserved ripples with a wavelength of 5 cm and a crestline trend of 001 degrees. On top of this surface there are also simple Planolites traces. A complex suite of features is exposed on an undulatory surface at DC-331.9 (Plate 35d). Ladderback ripples with two sets of ripples with straight crests and high spacing-to-height ratios are oriented nearly at right angles, with crestlines of 172 degrees and 066 degrees.

Traces present on the DC-331.9 surface include Planolites beverlyensis, Paleophycus tubularis, and Diplocraterion sp.. The latter are vertical burrows represented by pairs of circular raised ridges of sand, 3-5 mm wide (Plate 35d).

Two scales of stratification have been identified in the sandstones of this subfacies. Two types of first-order stratification are distinguished; the first (1A) is a subtle lamination defined by the relative abundance and spacing of second-order laminae and diagenetic mottles; the second (1B) is defined by sharp-based, white-weathering, 0.5-2 cm laminae/beds that appear to be associated in places with the low-angle truncation surfaces

PLATE 36: CONGLOMERATE BEDS (FA 6)

a: Interlamination of granule/pebble conglomerate and red micaceous sandstone in zone at DC-351.1-351.85. Much of the conglomerate forms parallel laminae which may have been deposited in upper flow-regime plane-bed conditions. Conglomerate also fills wide, shallow scours. Large mudclasts are found in the conglomerate at top of photo. Scale is 15 cm long.

b: Granule/pebble conglomerate and red micaceous sandstone in same zone as "a". Some conglomerate forms low-angle planar lamination. Beds directly above scale have abundant mudstone intraclasts that generally have a bedding-parallel fabric. Stratigraphic top is up. Scale is 15 cm long.

c: Symmetrical ripples in pebble bed. The dramatic change in the shape and size of adjacent crests is typical of wave-formed structures. Stratigraphic top is up. Notebook is 18.5 cm long.

d: Diffuse laminae of phosphatic shale chips in thick sandstone bed of Subfacies 6.1B. Stratigraphic top is up. Scale is 15 cm long.

e: Bedding plane view of red mudstone intraclasts in red micaceous sandstone (Facies 6.1). Scale is 15 cm long.

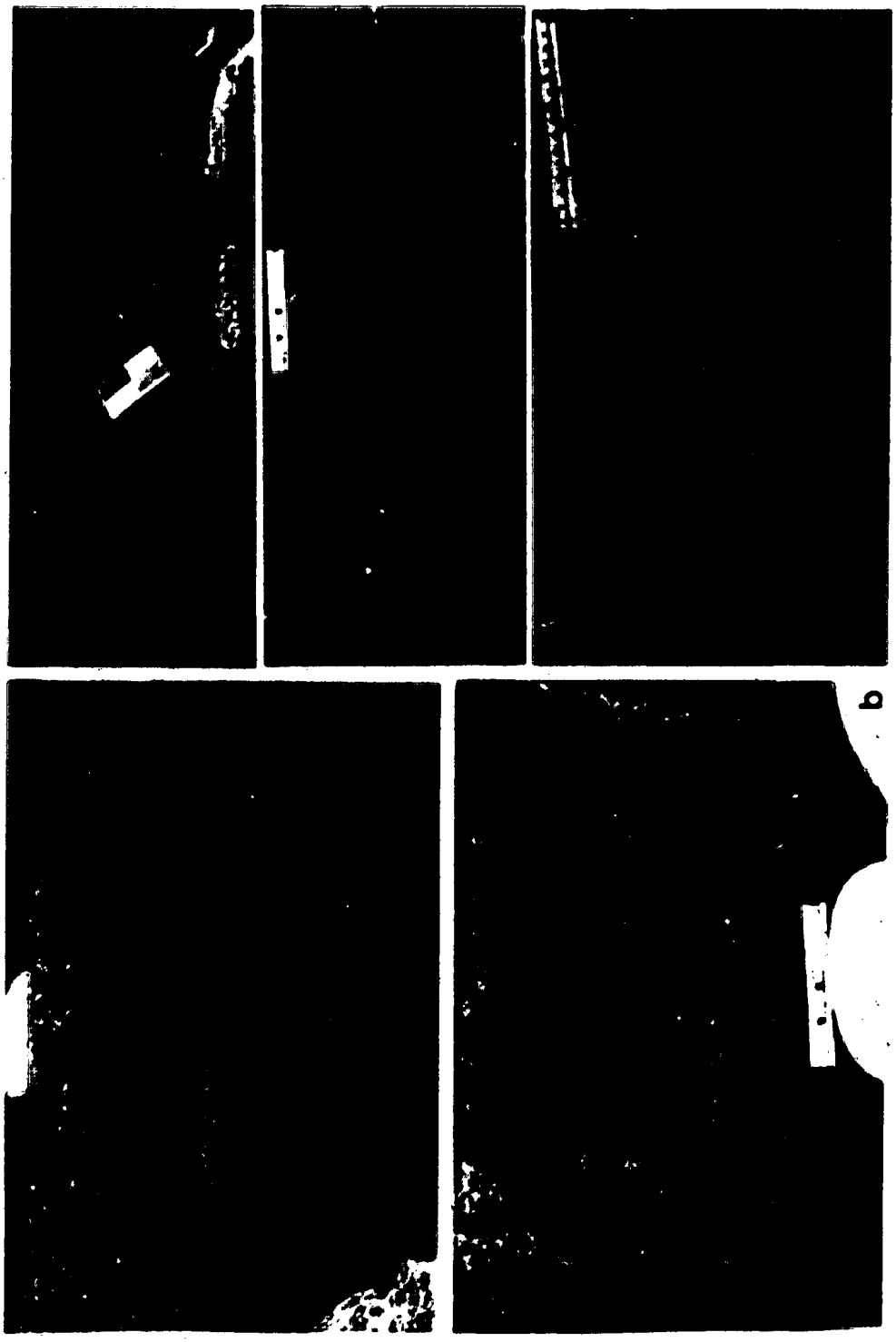
b

described above. The latter was described by Hiscott (1982, see Figure 8) as "widely spaced coarse laminae". The second order of stratification is defined by closely spaced, red clay laminae a fraction of a millimeter thick and spaced <1mm-3mm apart.

The appearance of all of these laminae is strongly tied to a peculiar mottled fabric (Plate 35f). Mottling is defined by the relative abundance and spotty development of white, carbonate-cemented fine sandstone and red, hematite-stained, clay-rich sandstone. In those beds that have >~60% carbonate-cemented sandstone, mottles are defined by clay-rich blotches. In these examples, the second-order laminae are not always present. If present, the laminae stand out against the light-colored background and are overprinted by the red mottles, which are similar in color (slightly lighter red) and composition. Interestingly, many mottles end abruptly against these laminae. Individual beds may contain parallel, first-order laminae (and mottles) at their base and only mottles above, or vice versa.

In samples dominated by red, clay-rich sandstone, mottles are defined by blotches of carbonate-cemented sand, and second-order laminae are difficult to see. Widely spaced, white laminae (1B), where present, are set against a background of darker, iron-rich sands. These laminae are rich in carbonate cement and show only a few red mottles.

8.2.2 Massive subfacies: 6.1B

This subfacies weathers smoothly, with fewer pronounced bedding planes, due to uniformity in grain size (Plate 37b). Thin siltstone layers are widely spaced, marking the breaks between 1-2 m sandstone beds. Despite its relatively massive nature the rock is characterized by well defined parallel laminae that are separated by low-angle truncation surfaces. These truncation surfaces locally take the form of isolated, wide, shallow scours that are filled with gently curved, low-angle (less than angle of repose) stratification. The scale and geometry of the scours and the stratification are similar to swaly cross-stratification, first formally described by Leckie and Walker (1982). The sandstone beds of

PLATE 37: FA 6: CIF/RANDOM FORMATION

a: Very-thick sandstone bed from Subfacies 6.1B at Dantzic Cove that passes from parallel lamination (base of photo and below) to low-relief swaly stratification. Stratigraphic top is up. Notebook is 18.5 cm long.

b: Thick and very-thickly bedded Subfacies 6.1B (DC-~345-350). The outcrop weathers with few bedding planes. The homogeneous sandstones fracture concoidaliy. Bedding dips to left. Stratigraphic top is to the left.

c: Dendritic gully system in RMS Facies of the Random Formation, as seen looking down on upper bedding plane. These gullies are filled with phosphatic shale chip conglomerate and sandstone intraclasts. One meter staff (center) for scale.

d: Trough cross-stratified bed of red micaceous sandstone stratigraphically directly below the first occurrence of white quartzarenite, typical of the Random Formation. This is the only trough cross-bedding noted in Facies 6.1. Stratigraphic top is up. Notebook is 18.5 cm long.

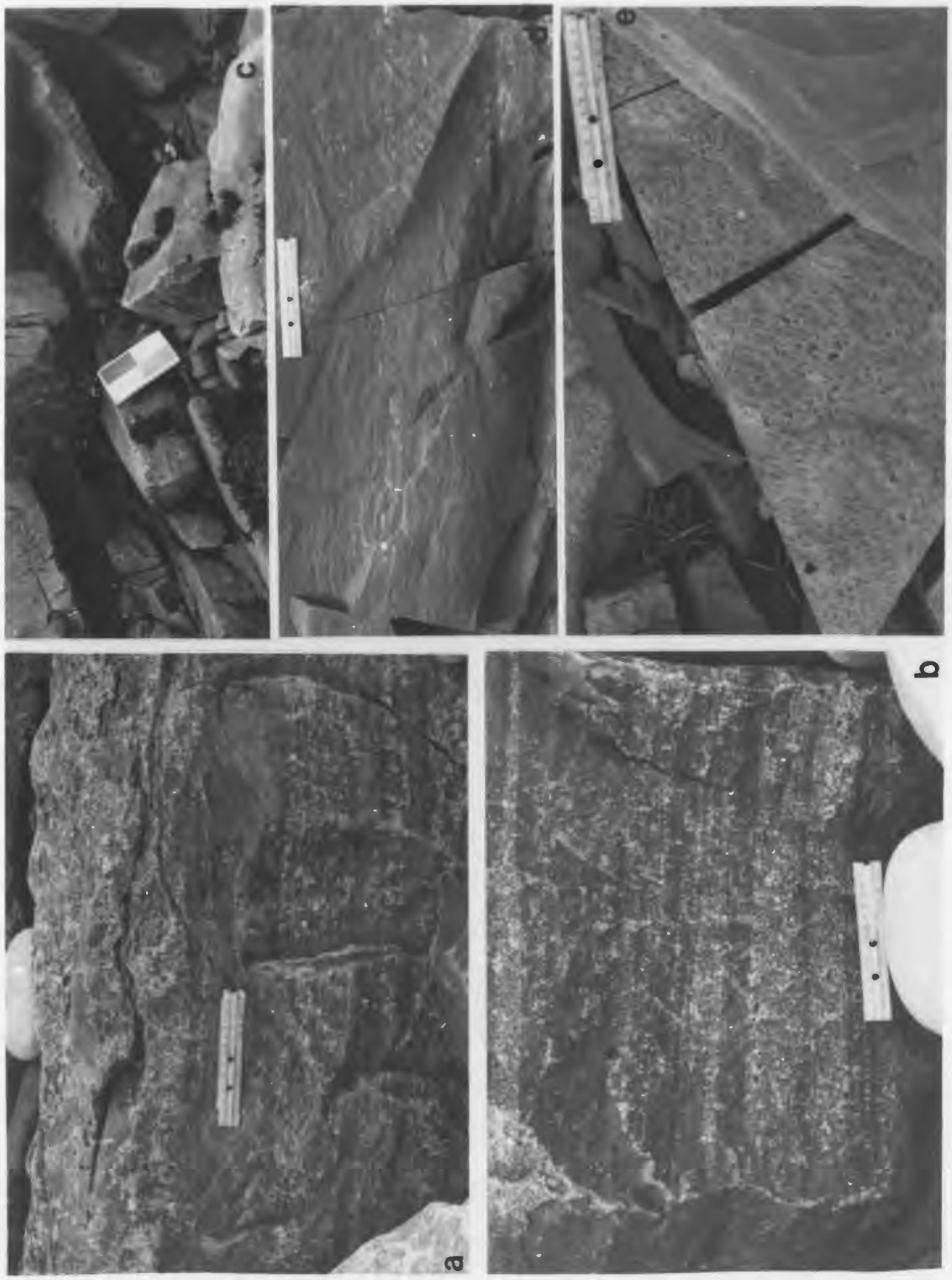
c
d
e
a
b

this subfacies commonly have parallel to gently undulating laminae in their lower half, while the upper part is dominated by long-wavelength swaly cross-stratification (Plate 37a). The top surfaces of many of these beds are swaly on a very broad scale — several meters wavelength. Phosphatic shale-chip layers are also found in this subfacies, commonly floating within sandstone.

8.2.3 Process Interpretation: Facies 6.1 (RMS)

Hiscott (1982) interpreted sandstone beds from this same facies of the overlying Random Formation as 'amalgamated HCS' (Bourgeois, 1980; Dott and Bourgeois, 1982; Wright and Walker, 1981), a bedding style that Leckie and Walker (1982) call 'swaly cross-stratification' (SCS). Although there does not appear to be agreement on the use of these terms (Walker et al., 1983; Dott and Bourgeois, 1982; Pound, 1984), they are apparently synonymous for bedding dominated by isolated or superimposed concave-up, shallow scours or swales within low-angle, flat-lying laminae. The very local development of convex-up surfaces within SCS beds indicates a genetic link with HCS (Leckie and Walker, 1982; McCrory and Walker, 1986; Walker, 1982); this is implied by those who use the term 'amalgamated HCS'. This bedding style results from the amalgamation of HCS beds by the preferential loss of the topographic highs (hummocks) and draping mudstones during erosion (Bourgeois, 1980; Dott and Bourgeois, 1982; implied by Leckie and Walker, 1982; McCrory and Walker, 1986). Not all SCS may be formed by this process, however. Instead, isolated circular hollows may be scoured into parallel laminated sand, and later filled, without the formation of hummocks (Brenchley, 1985). This conclusion is drawn from cases in which the lowermost draping lamination in a swale laterally becomes a depositionally concordant lamina at the edge of the structure as the lamination spills out over undisturbed parallel-laminated sand (Brenchley, 1985; Leckie and Walker, 1982; McCrory and Walker, 1986). The term 'swaly cross-stratification' is

preferred by the author, and will be used in this thesis because of its utility in the field, and because it is nongenetic.

The stratification in Subfacies 6.1A, dominated by planar lamination and HCS, may represent deposition very near the HCS/upper-plane-bed boundary. During those times when the velocity dropped below upper plane bed, HCS formed. The siltstone/mudstone interbeds, representing fair-weather suspension deposition, accumulated to greater thickness in topographic lows. Wave-rippled surfaces that cap some HCS beds later played host to burrowing organisms. These ripples are vortex-type wave ripples that formed during the waning stages of HCS deposition when flow decreased in intensity from that which produced the hummocky cross-stratification below. Red mud-chip clasts are intraformational rip-ups that reflect the high-energy conditions prevailing during deposition of this subfacies. Blue shale chips were carried in suspension and deposited primarily along bedding or truncation surfaces, but also within continuous sandstone laminae.

The origin of the bed in Figure 8.1 is enigmatic. Deposition from a hummocky bedform is ruled out in this case, as the geometry and internal structure of this bed do not conform to published accounts of HCS. It has been argued that the wavelength of HCS is roughly equal to the bottom orbital diameter (Duke, 1984; Duke and Leckie, 1984); for the bed in Figure 8.1, this would indicate unrealistically large orbital diameters. This geometry could not have resulted from erosion of a thick HCS bed with 'average' hummock spacing, because the laminae extend the full length of the bed, roughly paralleling the upper bounding surface. Rapid thinning of HCS beds has been noted by other workers (see Dott and Bourgeois, 1982, Figure 2B, and McCrory and Walker, 1986, Figure 3), but with strong discordance between the laminae and the bounding surfaces. The pattern in Figure 8.1 indicates a relative continuity, with slight changes, of topographic relief during deposition. The origin of this structure remains problematic, since modern and ancient analogs are lacking.

Differences between Subfacies 6.1A and 6.1B may result from two factors: (1) a different degree of amalgamation of HCS beds and (2) variation in original thickness and structure of beds. In Subfacies 6.1A a number of the beds are not amalgamated, retaining their original hummocky geometry (Plate 35e.h). The same is also the case for Subfacies 6.1B, except that the spacings of the hummocks are much greater and the amplitude proportionately lower, so that these surfaces are more difficult to detect. It is often difficult, given the uniformity of grain size, to determine the exact nature of the internal stratification and the presence of amalgamation surfaces. Amalgamation of sandstone beds is easier to see in 6.1A because of the grain-size contrast due to the greater abundance of siltstone, while the degree of amalgamation of beds in 6.1B is more difficult to detect. Despite this, careful observations indicate that Subfacies 6.1B consists of 1-2 m distinct or only partially amalgamated sandstone beds. The thinness of the siltstone interbeds indicates either short periods of time between deposition of successive sands beds or incomplete erosion of thicker silt beds, or a combination of both.

A major difference between the sandstones of Subfacies 6.1B and the structure SCS, as described by other authors, is the dominance of low-angle, subparallel and undulatory laminae and only a moderate percentage of recognizably isolated swales. SCS typically contains as much as 90% mutually truncating swales (Walker, 1982), while in Subfacies 6.1B individual beds contain a lot of long-wavelength, low-amplitude swaly stratification without isolated swales. The transition from a lower, parallel-laminated division to an upper, swaly-stratified division was generated as the thick flows dropped from the upper-plane-bed field (lower part of bed) to a hummocky-bedform field (upper part). As there is no evidence to indicate that these beds are amalgamated, the standard interpretation for swaly cross-stratification as 'amalgamated HCS' does not apply to these beds. A reasonable alternative is that the SCS in these beds formed under conditions in

which the rate of migration of hummocks and swales was great enough, in comparison to the aggradation rate, to result in the preservation of swales, but not the hummocks.

Mudstone intraclasts and phosphatic shale clasts, noted along truncation surfaces by Hiscott (1982) in the Random Formation and by the author in the CIF, suggest: (1) periodic high-energy conditions, (2) erosion of penecontemporaneous mudstone layers and (3) availability of phosphatic shale chips. Dott and Bourgeois (1982) describe pebbles and intraformational clasts from all different levels of stratification of amalgamated HCS beds (p. 666). The red coloration in the RMS Facies may have resulted from low organic content, high Eh diagenetic conditions, or both (See discussion in Chapter 3.A).

8.3 GRANULE CONGLOMERATE (GC) BEDS

Granule conglomerate beds occur in both 6.1A and 6.1B Subfacies near the transition from the CIF to the Random Formation. These conglomerate beds consist of a grain-supported mixture of pink and white quartz, and gray to black sedimentary rock fragments of shale, siltstone and fine sandstone in a quartzitic sandy matrix. Quartz grains are generally well rounded and reach pebble size (d_{max} = 9 mm). Sedimentary rock fragments of a variety of shapes and sizes account for approximately 10% of the grains. The larger fragments, with long axes of tens of centimeters, tend to be more tabular.

The conglomerate is present as beds 2-10 cm thick that cover low-angle erosional surfaces and broad, shallow scours. At DC-341.5, beds of this conglomerate are interbedded with green very fine to fine sandstone that is identical in appearance and composition to the matrix of the conglomerate. Both the conglomerate and the sandstone are dominated by parallel lamination, with minor very-low-angle cross-lamination. Elongate shale and fine sandstone fragments within these sandstone beds have long axes up to several tens of centimeters long.

The conglomerate also forms a large, symmetrical-crested, rippled bedform at DC-406.1. The bed is fairly uniform in thickness for most of its length, measuring an average of 14 cm under the crests and 10 cm under the troughs. Thickness is more variable at the termination of the outcrop (Plate 36c). Wavelength of the ripples varies from 32 to 45 cm, with an average of 42 cm. Too little is exposed of the bed to determine the bedding-plane geometry of the crests, but the trend of the crests is fairly consistent at 040 degrees. Across most of the outcrop the cross-laminae dip northwest, but at the western part of the outcrop, near the low tide mark, the laminae dip to the southeast. The reversal takes place sharply between two adjacent crests.

8.3.1 Process Interpretation: GC Beds

The concave-up lower surfaces, the overall lenticular geometry of some beds, and the lithologies of the rock fragments indicate that the depositional surface was scoured by currents eroding fine-grained, semilithified sediments and transporting, mixing and redepositing the newly formed rip-up clasts with granule-sized detrital sediments. The local origin of most of the clasts is supported by the lithologic similarity with the surrounding beds. Also, the large size and shape of some of the rip-up clasts indicate relatively short transport, and presumably a short time between the erosion of the underlying sediment and deposition over the scoured surface. The black shale clasts were not derived locally, and must therefore have been transported from an adjacent environment. Parallel-laminated sand and conglomerate is interpreted as an oscillatory upper-plane-bed structure based on its interbedding with thick parallel-laminated and swaly-cross-stratified sandstones. The orbital velocities must have been high to create plane-bed conditions in this coarse-grained sediment. These would most likely be in the same range as those associated with HCS — ~1 m/s or more.

Reworking and winnowing of the sediment is indicated by the lack of mud matrix. High-energy conditions would have been required to erode semicohesive sediment and transport granule- to pebble-sized clasts. The shear velocity U_* required to initiate movement of the larger quartz pebbles in this facies would be approximately 30 cm/s (assuming that the source sediment was well sorted so that the Shields diagram applies in approximation).

The large rippled bed at DC-406.1 indicates reworking by oscillatory currents (waves). The grain size of this bed is too large for these to be current ripples (see Harms et al., 1982, Figure 2-5). The change in foreset orientation (see De Raaf et al., 1977), grain size and geometry (symmetrical crests) indicates that these are vortex ripples formed under oscillatory flow conditions. In oscillatory flow, increasing grain size parallels a growth in the stability field of vortex ripples at the expense of the plane-bed field, at values of higher U_m (Harms et al., 1982, Figure 2-18c; Plot of ΔU vs. U_m). Based on this, and grain-size considerations, the maximum orbital velocity U_m must have been quite high during the deposition of this bed. Similar paleoflow conditions would have created planar lamination in sand-sized sediment.

8.4 LITHOFACIES DISTRIBUTION: FA 6

F.A. 6 is well exposed at a number of localities along the Burin Peninsula and on Sagona Island. This facies association is not exposed on Chapel or Brunette Islands. The best exposure is at the DC exposure, but it is also exposed further south at Pieduck Point. To the northeast, a thick section is exposed just northwest of the inlet in the Town of Fortune (FN exposure). More exposure is found between the towns of Grand Bank and Fortune at the Radio Station outcrop and in less continuous exposures along the shore to the southeast.

8.5 PALEOENVIRONMENTAL INTERPRETATION FA 6: STORM/WAVE-DOMINATED INNER SHELF AND SHOREFACE

8.5.1 Introduction

The following discussion will be concerned first with defining the paleoenvironments of FA 6. The second part of this discussion will center on the vertical lithofacies distributions at DC and the implications for an overall depositional model and time history for FA 6.

8.5.2 Paleoenvironments

SCS and HCS, the two dominant sedimentary structures of Facies RMS, are generally accepted as storm-generated structures, which limits deposition to water depths above storm wave base. HCS has recently been documented from modern surf zones (Greenwood, 1984; Greenwood and Sherman, 1986). The preservation potential of HCS

in this setting would understandably be low. The general consensus among sedimentologists is that the preservation of HCS in the rock record (i.e., Facies 6.1A) indicates deposition below fair-weather wave base (~10 m. water depth). This is based on the presence of mudstone/siltstone interbeds, which would not likely be deposited in the shoreface setting, and the general lack of angle-of-repose cross-bedding (Walker, 1982, 1984). The great thickness of the sandstone beds in Subfacies 6.1B indicates a very proximal position relative to the sand source. The red coloration of the rock supports a shallow-water interpretation.

Facies RMS is therefore considered a storm-influenced offshore (Subfacies 6.1A) and shoreface (Subfacies 6.1B) deposit. A shoreface interpretation for Subfacies 6.1B is supported by the fact that SCS-bearing facies are commonly transitional into beach facies (Bourgeois, 1980; Dott and Bourgeois, 1982; Hamblin and Walker, 1979; Leckie and Walker,1982; McCrory and Walker, 1986). None of Facies RMS is considered to be of beach origin. The characteristics of beach lamination include: (1) low angle of dip of laminae and set contacts, (2) mostly erosional set contacts and (3) laminae that lie parallel to set contacts or onlap with slight divergence (Duncan, 1964, p. 194; Harms et al., 1982, see Figure 7.5; Komar, 1976, p. 370-375; Thompson, 1937, Figure 2). The strongly curved lower bounding surfaces, locally preserved hummocky and swaly surfaces, bioturbated siltstone interbeds and other features distinguish Facies RMS from beach-formed facies. Inverse grading of laminae, formed during backwash on the shoreface (Clifton, 1969), has not been noted in the red sandstones of the CIF or Random Formation. A beach origin is further discounted because of the high percentage of mica flakes, which according to Dott and Bourgeois (1982, p. 664) "...help distinguish hummocky from swash-zone laminae, which are purged of such grains by surf agitation".

Hiscott (1982), in a discussion of the RMS facies of the Random Formation, described dendritic erosional gullies whose floors are littered with a conglomerate of mudstone and shale clasts. These gullies were considered by Hiscott as lower-shoreface

rip-current channels cut into consolidated sands by relaxation currents during storms. New observations on these gully surfaces add some insight into depositional processes. In addition to shale and mudstone clasts, large rip-up clasts of sandstone (up to 15 cm across) were noted on gully floors. These strengthen the conclusion that the sand was at least consolidated or perhaps semilithified during erosion of the gullies. The shale and mudstone clasts that cover the gully surface locally exhibit vertical stacking. These clasts also line the bases of potholes, where they commonly are preferentially concentrated up against one side of the pothole. These data indicate that prior to final deposition in these channels (and potholes), shale chips and intraclasts were winnowed and reworked. Another interesting observation is that aside from the prominent parallelism of the gullies, oriented at ~045°, a secondary erosional pattern cuts across the outcrop at ~145°. Many of the potholes cut into the sandstone ridges are elongated parallel to this secondary direction. The flows that cut the prominent channels record the transport of sand, as well as mudstone and sandstone intraclasts and shale chips, into deeper water. The secondary channel pattern may represent modification of the sea floor by shore-parallel currents.

The description and interpretation of Facies RMS (given above) clearly indicates a shallow-water, storm-dominated system. Within this depositional system, Hiscott's (1982) interpretation of these gullies as storm-surge-current channels is most reasonable. The secondary erosional pattern points toward slope-parallel flow. The exact nature of this flow is enigmatic. Conglomerates in the hummocky-bedded Upper Cretaceous Cape Sebastian Sandstone have been interpreted by Bourgeois (1980) as winnowed sediment swept offshore by storm surges. She did not describe gully systems like those in the Random Formation. Dekay (1981) describes shoreface troughs from a modern barrier beach off the coast of Rhode Island. He reports that these troughs, formed in sands with planar lamination and possible HCS, are lined with coarse sand and gravel. Dekay considers the coarse-grained sediment to be a basal storm deposit exposed through erosional windows in the sand. The grain size of the storm layer prevented further erosion of the bottom,

resulting in a consistent lower limit to the channels. Its possible that the Random examples represent an analogous situation, but the presence of conglomerate in potholes on interchannel ridges indicates that some coarse-grained sediment was carried well up into the flow by vigorous currents. The features described by Dekay are dendritic lower-shoreface structures, and may present, in a general way, an analog for those in the Random Formation.

8.5.3 Conglomerate Beds

Conglomeratic sediments have been described from storm- and wave-influenced nearshore and shelf facies in modern settings (Channon and Hamilton, 1976; Clifton et al., 1971; Clifton, 1973; Flemming and Stride, 1967; Gillie, 1979; Yorath et al., 1979) and in ancient sequences (Anderton, 1976; Berg, 1975; Brenner and Davies, 1973; Clifton, 1981; Johnson, 1977; Levell, 1980a, 1980b; McCave, 1973). Conglomerates are often associated with HCS/SCS (Bourgeois, 1980; Dott and Bourgeois, 1982; Hiscott, 1982; Leckie and Walker, 1982; Leithold and Bourgeois, 1984; Wright and Walker, 1981). Hiscott (1982) noted granule conglomerate resting on internal truncation surfaces of amalgamated HCS beds in the Random Formation. The have been noted in the CIF as well (Photos G8-11).

Large, coarse grained, symmetrical gravel ripples are commonly associated with HCS (Leckie and Duke, 1984; Wright and Walker, 1981), SCS (Leckie and Walker, 1982; Unit 10B) and trough cross-bedded sandstones in the rock record (Leithold and Bourgeois, 1984). When found in conjunction with HCS/SCS these features are typically interpreted as storm-generated deposits emplaced by relaxation/turbidity currents. According to Leithold and Bourgeois (1984), gravel ripples from the Miocene of southwest Oregon represent river-mouth bars that were reworked by storm waves. Table 8.1 is a list of characteristics of literature examples of modern, large gravel ripples, formed, in part, from storm/wave activity. The gravel dunes of Facies GC are smaller than many of these ancient

TABLE 8.1: GRAVEL RIPPLES: PUBLISHED DATA ON AGE AND SIZE

AUTHOR	AGE	AMPLITUDE (cm)	WAVELENGTH (cm)
Yorath et al. (1979)	Modern	15-30	30-100
Clifton et al. (1971)	Modern	15-20	30-60
Channon and Hamilton (1976)	Modern	~30	100-200
Flemming and Stride (1967)	Modern	20-25 15	125 (Deep) 110 (Shallow)
Gillie (1979)	Modern	10-15	70-130
Leithold and Bourgeois (1984)	Miocene	10	100
Wright and Walker (1981)	Cretaceous	8 (max)	100 (average)
Leckie and Walker (1982)	Cretaceous	10-15	~100

examples. Leckie and Duke (1984) consider heights of 10-15 cm and wavelengths of 70-130 cm as typical of most ancient gravel dunes. The grain size and bedform height of the Facies GC beds are similar to the gravel waves described by Wright and Walker (1981), but the wavelengths are much smaller (42 cm vs. 1 m).

The gravel ripples described by Clifton et al. (1971) are found off steep beaches in high-energy nearshore settings. Gillie (1979) described modern storm-generated symmetrical bedforms of sandy gravel off the coast of New Zealand from approximately 18 m water depth (from Wright and Walker, 1981). Yorath et al. (1979) describe modern gravel waves from the shelf off the west coast of British Columbia from water depths of 80-105 m. The grain size of their storm-generated beds indicate minimum (threshold) orbital velocities of 30 cm/s for initiation of sediment movement. Near-bottom orbital diameters of 1.6 m are suggested by the ripple spacings (Yorath, et al., 1979). Gravel ripples in the North Sea have been attributed to reworking by winter storms (Flemming and Stride, 1967).

Data on recent and ancient examples of symmetrical, wave-rippled conglomeratic beds support the interpretation made for the Facies RMS sandstone beds; i.e, deposition took place in storm- and wave-influenced nearshore and shelf settings. The association of the granule conglomerate with small-scale erosional surfaces and larger gully systems, both in shallow-water facies, indicates that these coarse-grained sediments were derived from the shoreline, and were periodically carried out to sea during high-energy events.

8.5.4 Dantzic Cove

The bulk of the interpretation of this facies association is based on the exposures of the CIF and the Random Fm at Dantzic Cove. At DC the upper ~30-50 m of the CIF comprise a shoaling-upward sequence. Three distinct, albeit gradational, zones are described, in ascending order: transitional, lower and upper (Figure 8.2).

Figure 8.2: Stratigraphic column from the upper part of member 5 at Dantzic Cove showing the distribution of FA 5 and 6 and subdivision into transition, lower and upper zones (see text). Enlargements on right show representative features from each zone. The average bed thickness and the abundance of HCS, SCS, burrows, siltstone and conglomerate are diagrammatically plotted alongside the column on the left.

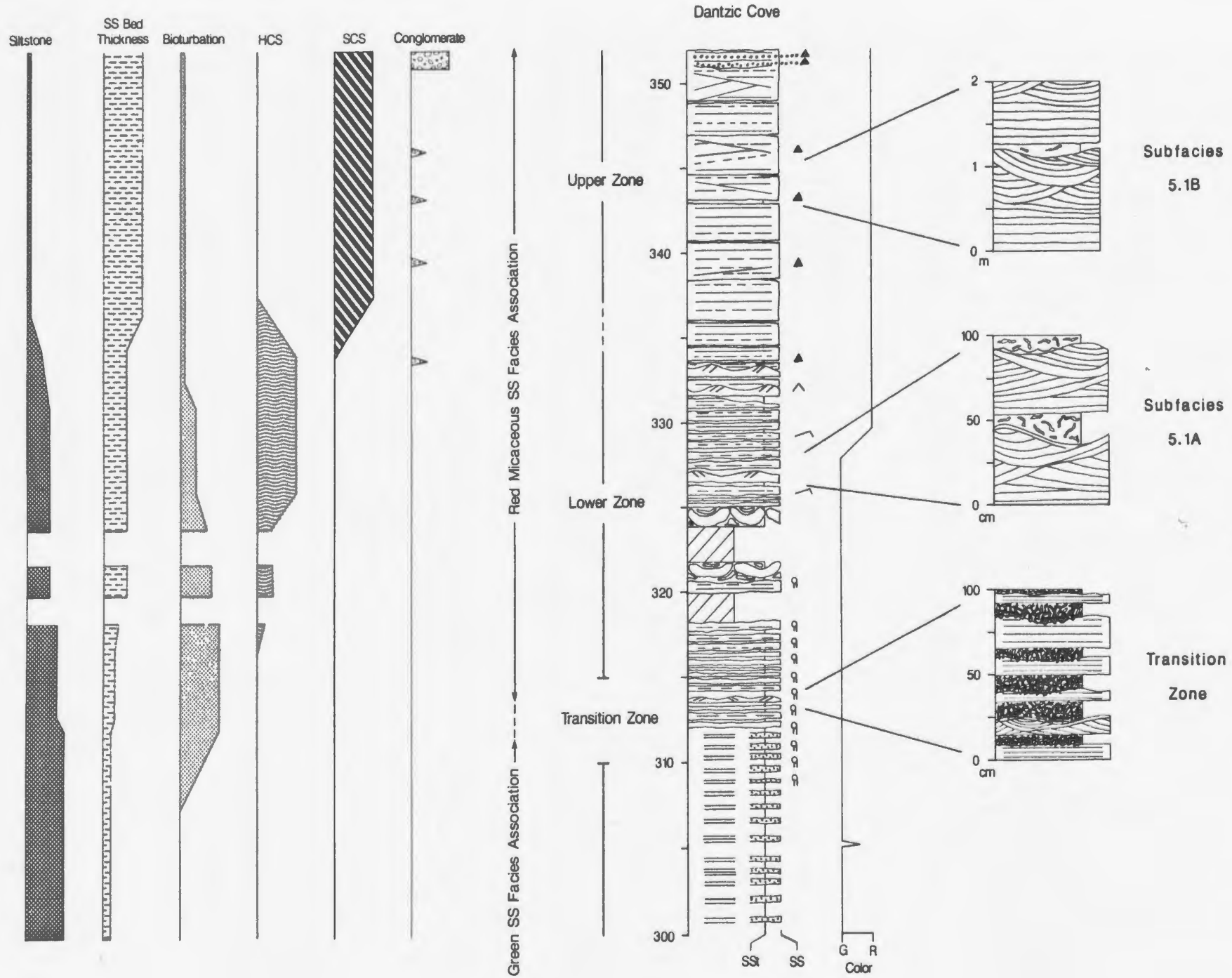
Siltstone
SS Bed Thickness
Bioturbation
HCS
SCS
Conglomerate
Dantzic Cove
Red Micaceous SS Facies Association
Green SS Facies Association
Upper Zone
Lower Zone
Transition Zone
350
340
330
320
310
300
SSt
SS
G
R
Color
2
1
0
m
100
50
0
cm
Subfacies 5.1B
Subfacies 5.1A
Transition Zone

The transition zone between Facies Association 5 (Green Sandstone/Siltstone FA) and this facies association (Plate 35a) occurs within the interval DC-~310-319.4. The exposure of Facies 5.2 shows a rapid increase in the degree of burrowing directly below this transition zone. The rock is composed of green-weathering, thin to medium bedded sandstone and brown-to-white weathering siltstone. The upper parts of the sandstones and all of the interbedded siltstones display intertwining networks of burrows (Plate 35b), a texture known as Fossitexturata figurativa (Schafer, 1956, p. 212). These burrows are carbonate cemented, and as a result the siltstones have a crumbly weathered texture. Despite the local difficulty in determining internal structures, it is readily apparent that this interval consists of parallel-laminated, and a few hummocky-cross-stratified, sandstone beds that show an upward increase in sandstone bed thickness and an upward decrease in thickness of bioturbated siltstone interbeds.

The lower zone, from DC-319.4-335.9, consists of Subfacies 6.1A displaying an upward increase in sandstone bed thickness and percent sandstone. Hummocky surfaces, silty interbeds, trace fossils and wave ripple marks were all observed within this interval. The lower part of this interval has large (>1 m across) ball-and-pillow structures. Ball-and-pillow structures of similar size have been noted in the same subfacies on the shoreline between Fortune and Grand Bank at the RS locality (Appendix B).

The upper section, DC-335.9-351.1, consists of Subfacies 6.1B with very few thin siltstone layers. Most beds are 1-2 m thick, with parallel laminae and SCS. Red shale clasts from 0.1-9 cm in length are found locally on exposed surfaces within parallel laminae. The first conglomeratic beds, occurring at DC-351.1, are thin, lenticular beds with erosional lower surfaces that are interbedded with thin to medium beds of parallel-laminated red sandstone (Facies 6.1B). The lower 10 m of the Random Formation is a complex mixture of well preserved HCS beds; recessive siltstones/shales; thin to medium beds and scour-and-fill structures of clean, white-weathering, fine to coarse sandstone; and conglomeratic

beds forming small scour fills, wide (several meters) channel fills and wave-rippled bedforms.

8.5.5 Paleoenvironmental Summary: Dantzic Cove

The vertical lithofacies transitions at Dantzic Cove indicate a progradational or shoaling-upward sequence, based on the upward coarsening and thickening of sandstones, changes in sedimentary structures, and upward loss of fine-grained interbeds and burrows.

Progradational storm-dominated lithofacies have been described by Chan and Dott (1986), Hamblin and Walker (1979), Handford (1986), Leckie and Walker (1982) and McCrory and Walker (1986). The transgressive sequences described by Bourgeois (1980) and Dott and Bourgeois (1982) are inverted analogs of the progradational sequences described by these other authors. In progradational sequences, swaly cross-stratification, if present, is always found above HCS, and often below a beach facies (Chan and Dott, 1986; Leckie and Walker, 1982; McCrory and Walker, 1986; Walker, 1982). This led Leckie and Walker (1982) to suggest that SCS was deposited above fair-weather wave base. Dott and Bourgeois (1982) state that this style of bedding, their HHH type, is deposited in very proximal, shallow waters, but these same authors (Dott and Bourgeois, 1982) maintain that the setting need not be above fair-weather wave base, but simply in shallow water, in a setting in which storms are frequent enough to erode sediment deposited during fair-weather conditions.

The upward trends in storm-dominated progradational sequences include: (1) an increase in average grain size, (2) an increase in sandstone bed thickness, (3) a decrease in percentage and thickness of bioturbated siltstone/shale interbeds, and (4) an increase in quantity of conglomerate. The exposure of FA 5 at DC shows all of these trends (Figure 8.2). These vertical trends reflect increasingly vigorous wave energy, and, consequently, harsher conditions for epifaunal and infaunal organisms. In a full, idealized, prograding,

storm-influenced sequence these trends are represented, from base to top, by: (1) tempestites deposited below storm wave base (SWB), to (2) interbedded HCS and bioturbated siltstones deposited between SWB and FWWB (fair-weather wave base), to (3) SCS deposited on the upper shoreface (predominantly above FWWB), to (4) planar, low-angle laminated beach sandstones with conglomerates and some high-angle cross-strata. In Upper Jurassic rocks of Alberta (Hamblin and Walker, 1979) coal horizons have been found to directly overlie SCS (McCrory and Walker, 1986).

Comparison of the DC stratigraphic sequence with published accounts of prograding storm-influenced shorelines indicates that at DC, the Green and Red Facies Associations represent, from base to top, deposition: (1) below storm wave base (SWB) (Green SS FA 5), (2) at or near SWB (transition zone), (3) between SWB and FWWB (Subfacies 6.1A) and (4) at or near FWWB (Subfacies 6.1B). Beach or other shoreline deposits are not represented at DC.

The change in color from green to red is concomitant with the shift from deeper to shallower water facies. This is a common feature of all of the facies associations of the CIF, and probably reflects original differences in organic content (see Section 3.2.1.1). Two factors might have established differences in the initial concentration of organics: (1) hydraulic sorting of fine-grained organic matter during transport and deposition in distal settings (Green SS FA), and (2) mechanical destruction of organic matter by waves in energetic shoreface settings (Red SS FA). Alternatively, the color trends might simply reflect differences in Eh during diagenesis, with the shallower-water settings having higher levels of dissolved oxygen.

The above discussion clearly indicates a nearshore, shallow-water setting for the deposition of the very thickly bedded sandstones of Subfacies 6.1B. These beds are 1-2 m thick; precompactional thicknesses may have been slightly larger than that observed in outcrop. This presents the following problem: how are laminated beds of this thickness deposited in a shallow-water setting? Depositing flows must have moved far enough to

have established and maintained upper-flow-regime conditions for a long period of time, but thickness and facies characteristics suggest deposition close to shore. It was precisely this problem which led Walker (1984) to revise his earlier facies model (Walker, 1979) that called for the erosion of a sandy shoreface by return currents and transport of sediment seaward by turbidity currents. In his new model, large volumes of sediment are put directly into suspension by liquefaction induced by cyclic wave loading of rapidly deposited fine sand. Liquefaction followed by downslope flow is more reasonable than grain-by-grain erosion of large volumes of sand by a storm-surge-ebb current, acceleration of the resulting flow to upper-flow-regime conditions, and then deposition of the sand, all within a very limited distance between the shoreline and the shoreface. It should be noted that this model is hypothetical, as it has not been observed in the modern.

On a regional scale, channelization or large-scale localization of the sand supply must be considered as an explanation for the extremely large volumes of sand represented by the Red Sandstone Facies Association. Several questions may be raised: (1) how laterally extensive are the deposits with HCS/SCS?, (2) what was the shoreline configuration? and (3) what was the influence of fluvial input? If the 2-m-thick beds of Subfacies 6.1B are sheetlike, then the volume of sediment is staggering for a nearshore setting. Although there is no direct evidence to support large-scale channelization near the shoreline, there is lateral variation in the distribution of this facies association. These red sandstones are much more abundant on Sagona Island than on the Burin Peninsula, and the distribution within the Random Formation shows much greater thickness in Fortune Bay than in other regions. The answer to some of the above questions can be addressed only after a discussion of facies trends in the Random Formation.

In the Random Formation, the association of amalgamated HCS, an indicator of wave-dominated settings (Dott and Bourgeois, 1982, p. 664), and trough cross-bedded quartz arenites (Facies 1 of Hiscott, 1982), deposited in an inferred macrotidal setting (Hiscott, 1982, p. 2038), presents what seems to be a paradox in terms of a

paleoenvironmental reconstruction. Dott and Bourgeois (1982) state that the "mere preservation of hummocky stratification or another wave-formed feature implies wave dominance, because other, more frequently acting vigorous processes, such as unidirectional tidal or rip currents would tend to destroy wave-formed features" (p. 679). For the Random Fm, one must conclude that the intimate association of facies reflecting such disparate paleoenvironmental conditions points to large changes — spatial or temporal (or both) — in depositional regime. Hiscott (1982) has chosen to assume that these facies represent laterally adjacent environments. A second alternative would call for allogenic processes, such as a change in sea level, to cause a change in the depositional setting. This alternative might imply the presence of subtle disconformities above and below thick packages of strata of particular facies.

The stratigraphic sections of the Random Fm at Deer Harbour (Trinity Bay, south of Random Island) and Dantzic Cove both contain one package (~12 and ~35 m, respectively) of red micaceous sandstones, although at DC there are certainly more of these sandstones (in the CIF) below the contact with the Random Formation. There is one example, directly below the first thick quartzite beds of the Random Formation at DC, in which red micaceous sandstone forms a thick trough-cross-stratified bed (Plate 37d). Trough cross-bedding is common in the Random Formation in the tidally influenced quartz arenites, so this red cross-stratified bed could represent a short time interval when micaceous sand was reworked and transported by tidal currents, or other currents not generated by waves. Aside from this example, there is in fact very little crossover of lithology and sedimentary structure and almost no interbedding of these lithologies on a small scale. If both of these lithologies — the fine, micaceous sandstone and the medium to coarse quartz arenite — existed along the same shoreline, and their respective depositional environments were subjected to lateral migration, one might expect more small-scale interbedding, especially at the upper and lower contacts.

If one chooses to reject the 'stratigraphic break' hypothesis, then one must construct an unusual facies model to account for the strange mix of lithologies and features. Hiscott's (1982) Figures 12 and 14 present a block diagram and facies map showing possible distributions of facies for the Random Formation at DC. These show the red sandstones forming in the shoreface and the cross-bedded quartz arenites forming in the deeper subtidal zone. From what is known about wave-dominated coastlines and their facies patterns, this reconstruction is highly unlikely. HCS and SCS sands should be laterally traceable into sheetlike sandstone beds that represent the more distal extensions of these storm beds (see Walker 1984 for review). In published accounts of recent and ancient tidal shorelines, well sorted sandstone beds with the characteristics of those described for the Random Fm are generally found in shallow subtidal settings (e.g., Evans, 1965; Driese et al., 1981; De Raaf and Boersma, 1971), a paleobathymetric position similar to that of SCS/HCS beds. It is therefore more likely that laterally along the Random shoreline there were parts dominated by storms and others dominated by tides. Juxtaposition of tide- and wave-dominated subenvironments is documented by Johnson (1975) from an ancient deltaic sequence. Johnson compares his late Precambrian sequence with that of the Niger delta (Allen, 1965; Weber, 1971). Allen (1965) describes wave-dominated beaches and tide-dominated mangrove swamps, both of which occupy the subaerial part (delta top) of the Niger delta. This illustrates that vastly different processes can characterize adjacent environments or microenvironments. Despite high tidal-current velocities in the mangrove swamps and channel mouth, the tidal range across most of the delta is less than 2 m, with a maximum of 2.8 m at the eastern edge (Allen, 1965, p. 554). It is more difficult to reconcile macrotidal facies with beaches and SCS/HCS facies, as must be done for the upper CIF and Random Formation.

If one considers the vertical lithofacies sequence that includes the upper CIF and full Random Formation at Dantzic Cove, then with the exception of the lower 10 m of

quartzites at the base of the Random Formation, a sharp line can be drawn at the ~55 m mark of the Random Fm (Hiscott, 1982, Figure 3b) to completely separate red sandstones from quartzitic facies. The implication is that through time the influence of storms, important in the upper CIF, was lost relative to tides, which dominate deposition in the Random Formation. The lower 10 m of the Random then represents a transition interval in which tidal processes were beginning to dominate some microenvironments. It would be a mistake to characterize the whole of the RF as a macrotidal sequence. The macrotidal interpretation is based on the characteristics and lateral distribution of the thick herringbone-cross-bedded quartzites (the upper part of the formation at DC) and other facies which are best developed in other outcrops outside of the Burin Peninsula. The upper CIF and RF may document a steady shift from wave and storm-dominance (upper CIF) to mixed or alternating wave/storm and tide influence (lower RF) to strong tidal dominance (upper RF).

Modern shorelines contain important clues to reconciling the close stratigraphic association of wave/storm-dominated and tide-dominated facies in the lower part of the Random Formation. Macrotidal conditions are locally established on wide, flat shelves, especially along shorelines embayed by estuaries. High tidal ranges, like those necessary to form a deposit like the quartzitic facies of the Random Formation, are produced in these embayments by funneling effects, particularly when the the tides and the shape of the basin produce a resonance effect (e.g., Bay of Fundy). Hiscott's (1982) paleogeographic reconstruction of the Random Formation shoreline shows an embayment opening toward the southwest. It is also important to realize that repeated relative sea-level fluctuations probably occurred during the deposition of the entire Late Precambrian-Lower Cambrian sedimentary sequence (Rencontre, Chapel Island and Random Formations) (this study and Smith and Hiscott, 1984). Could changes in relative sea level, when combined with a distinctive paleogeography, combine to produce the stratigraphic sequence preserved in the rock record?

The study by Terwindt (1981) on the mesotidal basins of the North Sea demonstrates that in an area affected by both tides and waves the lithology and sedimentary structures of particular environments are strongly dependent on the relative magnitude and temporal changes in these processes. Swift and Thorne (1986) consider sediment input rate, relative sea level and mean annual fluid power expenditure to be the main controls on shelf sedimentation. Macrotidal conditions, in which sediment input is low in comparison to fluid power (fluid power is high in macrotidal shorelines, as compared to storm/wave-dominated shelves, because of the frequency of high-energy events — once or twice daily as opposed to once or twice a year), are characterized by considerable winnowing and reworking of sediment and bypassing of fines. Amos and Zaitlin (1985) demonstrate an interdependence of tidal range and lithofacies characteristics in the Bay of Fundy. They show that the primary control on the tidal range in this large embayment is sea level. Basins like the Bay of Fundy have a geometry that, when combined with the proper relative sea level, can experience high tidal ranges. During times of low sea level the conditions in the Bay of Fundy are either microtidal or mesotidal, and silts and clays are more common. Periods of higher sea level are associated with larger tidal ranges and a higher percentage of sand (Amos and Zaitlin, 1985). By way of analogy with the Bay of Fundy, the red micaceous sandstones in the lower RF could have formed during times when the position of relative sea level favored a lower tidal range and wave- and storm-dominance, and the quartz arenites that dominate the upper RF could have formed during times when sea level position caused resonance effects in the basin and increased the tidal range. The influence of shelf width on tidal range and sediment character is emphasized by Richards (1986), who describes a similar shift from wave/storm dominance to tidal dominance in the Lower Triassic of France, which he attributes to tidal amplification during transgression. The transition from wave/storm domination (upper CIF) to tidal domination (upper RF) may be linked to the general rise in sea level and onlap (towards the northeast) during the

deposition of the Random Formation (Anderson, 1981), which created a wider shelf area with amplified tides in flooded river-mouth estuaries.

Chapter 9

DEPOSITIONAL HISTORY OF THE CHAPEL ISLAND FORMATION

9.1 INTRODUCTION

This study fills a major gap in the understanding of the Late Precambrian — Cambrian sedimentary history of the Newfoundland Avalon Zone. The sedimentology and depositional history have been established for the units underlying and overlying the CIF, the Rencontre (Smith and Hiscott, 1984) and Random (Anderson, 1981; Hiscott, 1982) formations, respectively. The Avalonian sedimentary strata of this age record a shift from tectonically active fault-bounded basins (Rencontre Formation) to a tectonically stable platform (Random Formation). The early tectonic regime of the North American Avalon Zone was either extensional or transtensional (strike-slip movement) (Nance and Socci, 1987; Rast and Skehan, 1987) with the latter preferred on sedimentologic grounds (Smith and Hiscott, 1984). This chapter is aimed at describing the depositional history of the CIF and completing the history of the Late Precambrian — Cambrian transition.

The depositional history of the CIF has been divided into three phases. These are shown in Figure 9.1 with a curve representing the inferred position of relative sea level during each phase. The first phase covers the transition from the underlying Rencontre Formation and the deposition of members 1, 2, and part of 3. The second phase includes the deposition of the upper part of member 3 and all of member 4. The third phase concerns the deposition of member 5 (FA 5 and 6) and the transition into the overlying Random

Figure 9.1: Generalized stratigraphic section for Chapel Island Formation showing inferred relative sea level curve. The three phases of CIF history outlined in this study are given next to the curve.

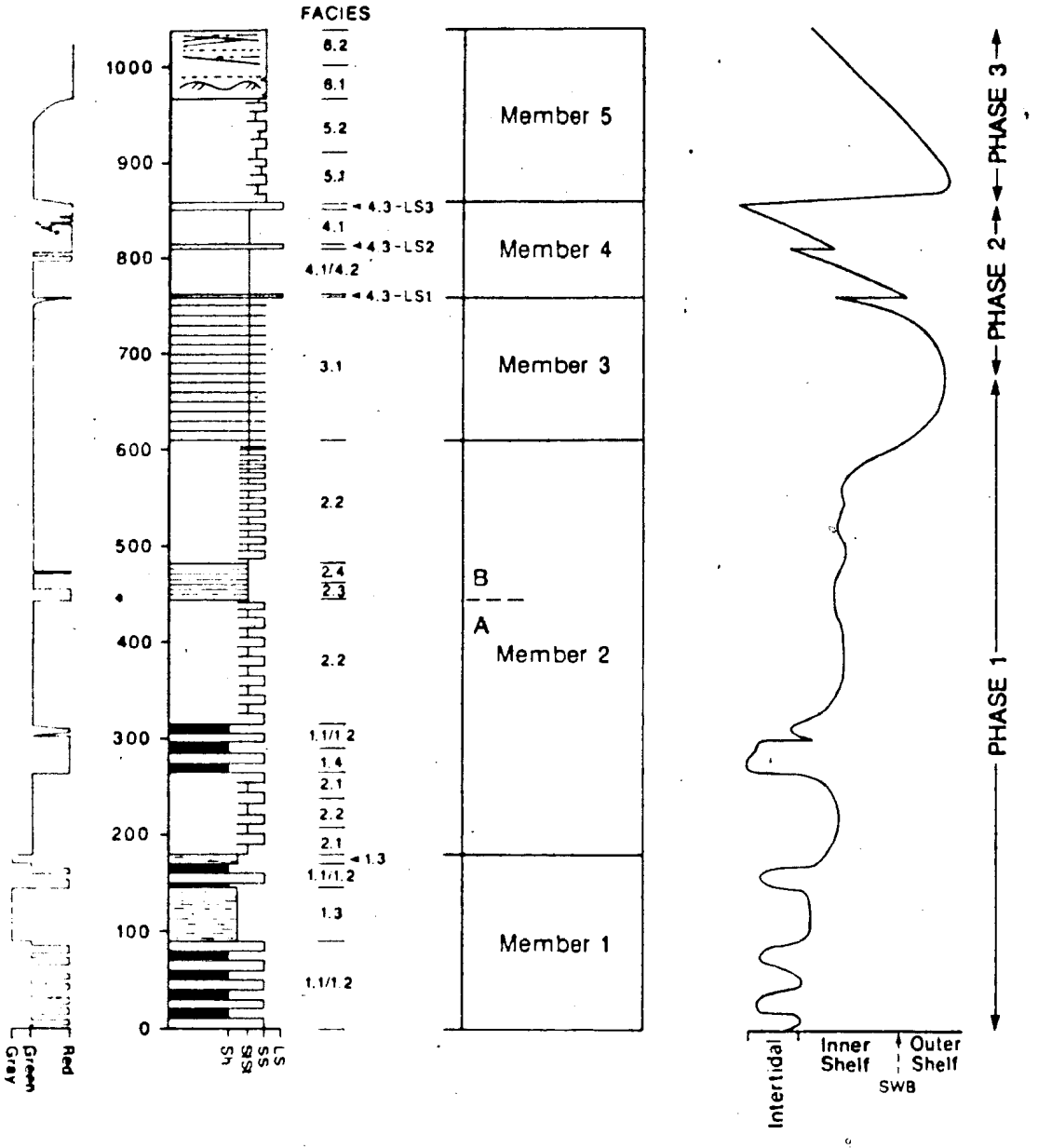
FACIES
1000
900
800
700
600
500
400
300
200
100
0
6.2
6.1
5.2
5.1
4.3-LS3
4.1
4.3-LS2
4.1/4.2
4.3-LS1
3.1
2.2
2.4
2.3
2.2
1.1/1.2
1.4
2.1
2.2
2.1
1.3
1.1/1.2
1.3
1.1/1.2
Member 5
Member 4
Member 3
B
A
Member 2
Member 1
Gray
Green
Red
Sh
SSh
SSs
Ls
Intertidal
Inner Shelf
Outer Shelf
SWB
PHASE 1
PHASE 2
PHASE 3

Formation. Generalized paleoenvironmental interpretations of these phases are given in Figure 9.2.

9.2 PHASE 1: RISE IN RELATIVE SEA LEVEL

It has been established that the Early Cambrian was a time of eustatic sea-level rise (Brasier, 1980; Mathews and Cowie, 1979; Vail et al, 1977), and that this transgression is recorded in the Newfoundland Avalon Zone, especially with regard to the deposition of the areally extensive Random Formation (Anderson, 1981; Hiscott, 1982; Smith and Hiscott, 1984). Anderson (1981, p. 825) considered the stratigraphic transition from the Rencontre Formation to the CIF to represent the initial stage of the global Cambrian transgression. Given the complex history of changes in relative sea level evident in both the Rencontre Formation (Smith and Hiscott, 1984) and the CIF (this study) it seems unlikely that the influence of eustatic sea-level rise can be filtered out of the complexity of basin tectonics and changing depositional systems so as to clearly identify the initial stage of the Cambrian transgression in Newfoundland. However, the regional onlap displayed by the Random Formation and other quartzites of this age throughout the world does suggest deposition during a eustatic rise.

9.2.1 Rencontre Fm — Member 1

The depositional history of the Rencontre Formation, as outlined by Smith and Hiscott (1984), was complex, with several periods of uplift and subsequent relative sea-level rise and onlap. Deposition took place in a northeast-southwest trending fault-bounded basin in a variety of nonmarine environments and in tidally influenced marginal-marine settings. Much of the sedimentation is thought to have been associated with fan deltas.

Figure 9.2: Paleoenvironmental reconstructions for the three phases of deposition of the CIF. No scale is given or implied. A and B are detailed views of the study area; C shows view from northeast Avalon. Arrows point north.

(A) Phase 1 diagram shows a deltaic system with fringing tidal flats developed in an area of moderate relief. Deep-water silts represent FA 3. Lower conglomerates and sands are the deposits of the Rencontre Formation, deposited in a fault-bounded basin.

(B) Phase 2 is a time of lowered relief with deposition on a low energy muddy shelf with a peritidal carbonate facies mosaic. The shelf at this time is thought to be oxygen stratified forming a belt of aerobic mud on the innermost shelf and dysaerobic mud in deeper water.

(C) Phase 3 diagram portrays a 180° reversal of the shoreline in relation to Phases 1 and 2. CIF deposits include shoreface (Facies 6.1b), offshore (Facies 6.1a) and outer shelf (FA 5). Large quantities of sediment are thought to have been shed from a sediment source to the northeast at this time (uplifted area in the foreground). The conglomerates and sandstones of the Signal Hill Group are considered possible proximal equivalents.

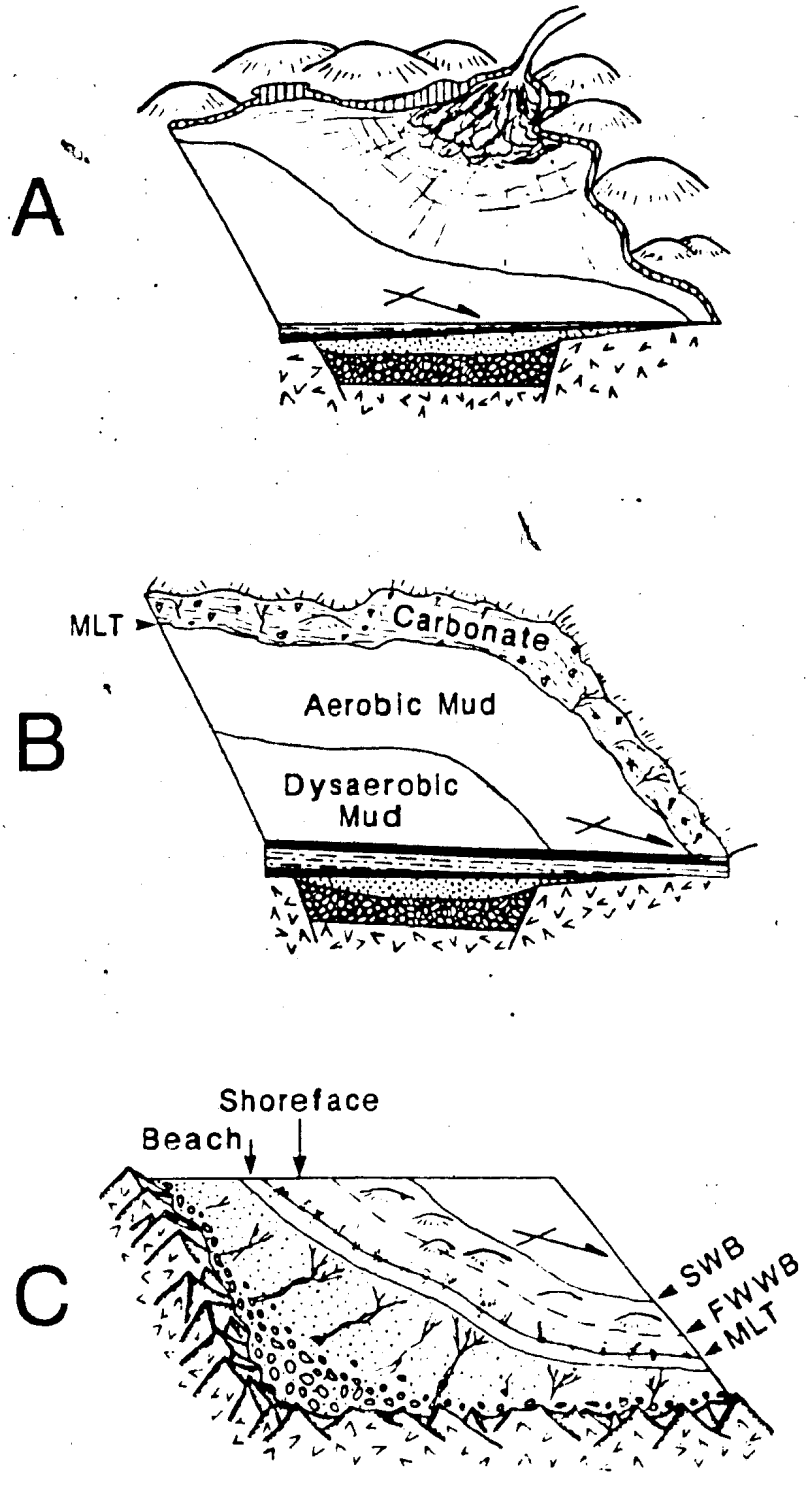
A
B
MLT
Carbonate
Aerobic Mud
Dysaerobic
Mud
C
Shoreface
Beach
SWB
FWWB
MLT

The stratigraphic sequence Rencontre Fm — member 1 — member 2 is clearly a transgressive sequence recording a rise in relative sea level (Figure 9.1). The first part of this transgression corresponds to the last phase of deposition of the Rencontre Fm, as outlined by Smith and Hiscott (1984; their Phase 5). They document transgression, widespread marine onlap, and "...the establishment of a broad zone of uniform peritidal sedimentation" (Smith and Hiscott,1984, p. 1388) at this time. This transgression followed an earlier period of uplift, and must therefore be understood in terms of a shift toward gradual tectonic subsidence and a denudation of the hinterlands associated with more stable tectonically conditions. The lower part of member 1, composed of the red and green tidal-flat deposits of Facies 1.1 and 1.2, represents a continuation of the conditions in place during the closing stages of Rencontre deposition. Suggested paleoenvironments for Facies 1.1 and 1.2 are shallow subtidal zone/lower tidal flats and middle to upper tidal flats, respectively. Facies 1.3 is thought to have been deposited in quiet, nearshore, semirestricted environments.

According to Smith and Hiscott (1984), sediment source areas shifted considerably during deposition of the Rencontre Formation. Their paleocurrent data for the last stage of Rencontre deposition (in Fortune Bay area, including Brunette and Chapel Islands) were "complicated", with modes toward the east and southeast. The paleocurrent data from exposures of member 1 of the CIF on the Burin Peninsula (primarily GB) display a clear NE-SW bimodal-bipolar pattern, which has been interpreted (see Section 3.6) as a record of strong tidal currents, with ebb-tidal asymmetry, in a sea whose shoreline was locally oriented NW-SE, and which opened toward the northeast.

The upper part of member 1, dominated by Facies 1.3, is sandwiched between the tidally influenced shoreline deposits of Facies 1.1 and 1.2 and the fluvial-dominated deltaic deposits of member 2. The upper part of member 1 records deposition either prior to, or during, the establishment of a large, fine-grained, deltaic system. If Facies 1.3 was associated with either a developing or fully developed deltaic system, then a plausible

paleoenvironment, based on facies characteristics and vertical lithofacies transitions, would be a semirestricted delta-top bay. The Mississippi River Delta, which has received considerable attention over the years (early "classic" studies include: Trowbridge, 1930; Russell and Russell, 1939; Fisk, 1952; Fisk et al., 1954; Scruton, 1960; Coleman and Gagliano, 1964; Kolb and Van Lopik, 1966; Frazier, 1967), is a reasonable analog because the interdistributary deposits consist of dark varvelike interlaminae of silt/fine sand and clays and the distributary channels are fixed for long periods of time, allowing for the accumulation of thick interdistributary deposits (Kolb and Van Lopik, 1966). The Mississippi Delta also has a delta plain which is open seaward into the delta front, allowing waves to mildly rework the sediments of the interdistributary bays — it would be necessary to invoke a similar situation to explain the erosional surfaces present in Facies 1.3.

If one accepts a deltaic origin for the upper part of member 1, then the delta must have had characteristics midway between those of the modern tidally dominated Colorado Delta in the northern Gulf of California, which has large, extensive tidal flats (Meckel, 1975; also see discussion of Klang and Ord Deltas in Coleman, 1981), and those of a fluvially dominated delta such as that of the modern Mississippi River (Elliot, 1978) with thick interdistributary bay deposits. If one rejects a deltaic hypothesis for the upper part of member 1, then the deltaic system represented by member 2 must have developed in a relatively short time period, and the deposits of Facies 1.3 might then represent a semienclosed basin of unknown extent, spatially adjacent to, and intertonguing with, well developed tidal flats.

9.2.2 Member 2-3

Member 2 and the bulk of member 3 record continued transgression. The highly variable nearshore and inner-shelf deltaic deposits of member 2 (FA 1 and 2) pass upward into the outer-shelf (below storm wave base) laminated siltstones of member 3 (FA 3).

Stratigraphic intervals of red beds (Facies 1.1, 1.2, 1.4) in the lower part of member 2 clearly indicate that this transgression was accompanied by small-scale fluctuations in relative sea level. The great thickness of member 2, with facies reflecting a limited range of paleobathymetric settings (shoreline to inner shelf), suggests that the deltaic system existed for a considerable length of time with a reasonable balance between the rate of subsidence, position of eustatic sea level, and volume of sediment input.

Although it is not possible to prove with certainty the cause of much of the variability within FA 2, most or all of it could be modelled in terms of autogenic changes in the deltaic system. In other words, vertical and lateral lithofacies changes could be a record of the response of segments of the shoreline to shifting distributaries and shoreline environments. Such is certainly the case with the upward-fining and -thinning sequence at FD-137.3, in which shoaling resulted from infilling of a tidal channel. The shallowing represented by red-bed horizons in the lower part of member 2 could have resulted from shoreline progradation onto the inner shelf during a period of high sediment influx. Furthermore, the very thinly bedded siltstones of Facies 2.3 and 2.4, which formed a fine-grained blanket on a portion of the delta, is thought to have resulted from sediment starvation at a time of shifting of the delta distributary to another part of the shoreline (delta abandonment). The stratigraphic occurrences of Subfacies 2.2A and 2.2B could also have been controlled by autogenic processes (see Section 4.22). Spatial variation in sediment input is supported by the thick (1-2 m thick) slumped sandstone horizons on Brunette Island in the lower part of member 2. These imply that this locality experienced higher rates of sedimentation than equivalent localities on the Burin Peninsula.

The paleocurrent information for FA 2 is remarkably consistent both stratigraphically and between outcrops. Figure 4.2 contains paleocurrent data for FA 2 from numerous localities on the Burin Peninsula and within Fortune Bay. The paleocurrents indicate that the shoreline was oriented northwest-southeast with storm-generated flows moving offshore toward the northeast. The only paleocurrent data for FA 3

comes from DC, and these data indicate that the distal tempestites of FA 3 were being emplaced from the same direction as the proximal tempestites of FA 2. The widespread distribution and uniformity of character of member 3 throughout Fortune Bay and on both east and west sides of the Burin Peninsula strongly suggest that either a basinwide increase in subsidence or a eustatic sea-level rise was responsible for this Phase 1 transgression, particularly in the later stages.

9.3 PHASE 2: FALL IN RELATIVE SEA LEVEL, LOW SEDIMENT SUPPLY

Phase 2, from the middle of member 3 to the top of member 4, is interpreted as a thick shoaling sequence on which are superimposed smaller-scale fluctuations in relative sea level (Figure 9.1). Depositional environments shift dramatically during Phase 2 from outer shelf (FA 3) to subaerially exposed peritidal limestones (Facies 4.3). Despite reasonable outcrop exposure, there is almost no paleocurrent data from FA 4. The paleocurrent data from FA's 1-3 suggest that no major paleogeographic changes occurred during the course of Phase 1. The distribution of lithofacies between DC and FN, particularly the Grey Mudstone Facies (4.2) and the Limestone Facies (4.3), is consistent with a shoreline to the southwest, as it was during Phase 1. This indicates, in light of a lack of evidence for tectonic adjustments in members 3 and 4, that the paleogeography during Phase 2 did not change significantly from that inherited at the end of Phase 1.

The 'member 4' nearshore and inner shelf was clearly very different from that which characterized members 1 and 2. Member 4 records quiet-water sedimentation along a low-energy, tectonically inactive coast. The percentage of sandstone and coarser sediment in member 4 is negligible in comparison to members 1-3. The highlands that supplied the vast quantities of sandy sediment for the Rencontre and the lower CIF must have been denuded, so that the hinterland was one of low relief during the deposition of member 4.

The presence of the Red, Purple and Green Mudstone Facies (4.1) on Chapel Island, roughly 100 km away from Dantzic Cove (present-day geography), indicates that similar conditions prevailed over a fairly large geographic area.

The model for deposition of member 4 calls for restricted deposition of the Limestone Facies (4.3) in peritidal environments. At times of maximum regression the limestone facies prograded seaward, but locally extensive sheets such as LS 3 formed only during the lowest and most persistent low stands. LS 3 is found at the RS, FN and DC outcrops with little or no variation in thickness while LS 1 and 2 are found only at DC. It should be noted that Bengtson and Fletcher (1983) interpreted the first of a series of limestone beds at Duck Point, on the east side of the Burin Peninsula, as LS 3. Whereas the stratigraphic relationship between this exposure and those on the west side of the Burin peninsula and elsewhere are complex and unresolved, E. Landing (pers. comm.) regards the lowest limestone bed at Duck Point to be part of the Bonavista Formation, based on paleontological and lithostratigraphic evidence. The Bonavista Formation would appear to be resting directly on top of member 3 of the CIF in this area. The missing strata, members 4 and 5 of the CIF and the entire Random Formation, were either (a) removed by erosion, or (b) never deposited because the area was a local high. Both explanations are difficult to defend on sedimentological and stratigraphic grounds, and only further work will resolve this issue. Little can therefore be said about the eastward extent of the CIF limestones, and member 4 in general.

The northern extent of member 4 is only slightly better understood. The exposure of member 4 on Chapel Island is incomplete, but of sufficient thickness that, given the lack of limestone beds at this locality, doubt is cast on the presence of the limestone facies in the northern part of Fortune Bay. The degree of exposure needed to delineate basin margins and lithofacies distributions in the northern part of Fortune Bay during Phase 2 is lacking.

9.4 PHASE 3: RAPID DEEPENING FOLLOWED BY SHALLOWING

The deposits of member 4 are followed stratigraphically by a thick coarsening-upward sequence (member 5) that represents sediment deposited on a prograding wave- and storm-dominated shelf. The strata at the base of member 5 — a few meters of purple mudstones followed by many tens of meters of the thinly laminated to thinly bedded sandstones and siltstones of Facies 5.1 — are poorly exposed (DC), faulted and inaccessible (FN and RS). The sandstone beds of Facies 5.1 are considered to be distal tempestites deposited far below storm wave base. The strata immediately above the intertidal-supratidal deposits of LS3 must therefore have been deposited during a period of rapid deepening, the actual rate of deepening being open to some speculation because of the inability to date these rocks on a fine scale.

Strata of the Thin to Medium Bedded Sandy Siltstone Facies (5.2), whose stratigraphic distribution is confined to the middle of member 5, are thought to have been deposited below, and at the transition to, storm wave base. The red micaceous sandstones of F.A. 6, at the top of member 5, represent deposition under conditions of considerable sediment influx and strong storm and wave influence. The thickness and wide distribution of this sandstone requires the uplift and emergence of a highland area to act as a new supply of sandy sediment. This source must have been distant from the southeast Burin Peninsula exposures to account for the lack of proximal fluvial/alluvial deposits in member 5.

To the northeast, on the Avalon Peninsula, the Signal Hill Group (Figure 1.2) contains a record of prograding fluvial and alluvial plain deposits. Might these be the proximal equivalents of the shelf facies found in member 5? As described in Section 1.3.2, during latest Precambrian time deposition on the Avalon Peninsula was being controlled by a rising mountain front situated toward the northeast. Prior to the deposition of the Random Formation, the sedimentary basin in that area appears to record a depositional history

separate from that of the Fortune Bay basin. The combined effects of continued uplift in the northeast and eustatic sea-level rise resulted in deposition of the Random Formation as a continuous unit across these previously separate basins. Is the early development of the extensive 'Random' basin recorded in the sudden deepening at the beginning of Phase 3?

The lateral and vertical distributions of lithofacies and the available paleocurrent data suggest that deposition of the Rencontre Formation and Phases 1 and 2 of the CIF occurred in a northeast-southwest trending basin. Paleocurrent data from the Rencontre Formation showed deposition directed into and along the axis of this trough. Data from Phases 1 and 2 of the CIF indicate a similar basin geometry, but one in which deposition was directed toward the northeast over a wide area of Fortune Bay. The paleocurrent information from FA's 5 and 6 is unfortunately quite sparse. Paleocurrents and other data from the Random Formation can be brought to bear on questions of paleogeography. The Random Formation is in gradational contact with the CIF in Fortune Bay, but elsewhere — to the east and north — it rests disconformably on older units. This led Anderson (1981) to conclude that sedimentation was centered in Fortune Bay and that marine transgression and onlap occurred toward the northeast. This is supported by the lack of Random lithologies in Conception Bay, where lower Cambrian strata lie directly on the faulted and folded Precambrian Conception Group (e.g., Bacon Cove). Paleocurrent data from cross-beds in the Random Formation are quite variable between localities but, combined with lateral lithofacies distributions, are consistent with a shoreline situated to the northeast (Hiscott, 1982). This conclusion is reasonable but somewhat unsatisfying considering that there is no control on paleogeography to the south, where there is no outcrop, and to the west, where the Avalon Zone is in fault contact with the Gander Zone.

It does appear, however, that within Fortune Bay a major reorientation of the shoreline occurred at the beginning of Phase 3, with a near reversal of onshore-offshore direction from southwest-northeast to northeast-southwest. The proposed uplift at the beginning of Phase 3 must have played an important part in this reorientation. The details

of this tectonic activity are not known, but the land area toward the southwest must have suffered increased subsidence and a breaching and transgression by the sea from that direction. The sudden deepening at the base of Phase 3 supports this interpretation. It should be emphasized that the geomorphologic regime in place at the end of Phase 2 would have been as ideal as any to carry out such a reorganization. At the end of phase 2 the highlands were substantially diminished, with sedimentation occurring along a low-energy, low-relief shoreline. Simply on grounds of lowered relief, it would have been easier to have major changes in shoreline position and orientation at this time.

Deepening, and the subsequent marine regression of Phase 3 (Figure 9.1), which resulted, at least in part, in the progradation of a thick clastic wedge of sediment (member 5), may possibly, therefore, have been linked to uplift and high sediment input from the highlands to the northeast, on the Avalon Peninsula. This prograding clastic wedge dramatically increased the shelf width and set up the conditions necessary for marine onlap and the high tidal ranges recorded by the Random Formation. The northeastern-directed onlap is considered a response to eustatic sea-level rise. Considerable discussion (Section 8.5) has been given to the stratigraphic relationships at the transition from the upper CIF to the Random Formation in terms of the sedimentology and the inferred marine processes. Hiscott (1982) provides a facies analysis of the Random Formation, which was deposited on a wide, tectonically stable platform, primarily under macrotidal conditions.

9.5 DISCUSSION

In the preceding section, the depositional history of the CIF has been divided into three phases, the details of which are far more complex than previously thought. The northeasterly directed paleocurrent data from Phase 1 help define a paleogeography undetected by previous workers, and the shift to a shoreline situated toward the northeast

(beginning of Phase 3), a paleogeography inherited by the Random Formation, appears to reflect a very important tectonic event. A similar 180-degree change in orientation occurs between the Random and Bonavista Formations, the latter of which was deposited during transgression and onlap directed toward the southwest (Anderson, 1981).

The depositional history of the CIF raises some interesting questions concerning the tectonic history of the Avalon Zone. The CIF is a very thick sequence (c.1000 m) which, particularly during member 2, was deposited under conditions of high subsidence rates (high sedimentation rate yet a thick section with little paleobathymetric variation). The record of the Rencontre, Chapel Island, and Random Formations indicates that the Fortune Bay basin was clearly expanding at this time. Basin expansion and high subsidence rates are generally considered features of extensional tectonic regimes. Similar conditions could, however, be associated with strike-slip tectonics, as Smith and Hiscott (1984) suggest. This begs the question of whether the Fortune Bay area was a local basin or a shoreline caught up in a continental-scale rifting event similar to that described for the ancient North American continent (Bond and Kominz, 1984). As discussed in Section 1.3.4, in the view of O'Brien et al. (1983, p. 195) "The controlling features of the Proterozoic evolution of the Avalon Zone are a series of linear intracratonic troughs and small ocean basins that formed during thinning and separation of the crust by ductile spreading, rupture, and delamination". Given the dramatic shifts in shoreline orientation (1) during deposition the Rencontre Formation, (2) at the beginning of Phase 3 (this study) of the CIF, and (3) prior to the deposition of the Bonavista Formation, a small-basin model is clearly suggested. The margins of this basin were established for the Rencontre Formation (Smith and Hiscott, 1984), but are poorly known for the Chapel Island Formation

9.6 AVALONIAN STRATA IN NEW BRUNSWICK

Correlations have been made between Avalon rocks and Pan-African rocks in Morocco and elsewhere (Hughes, 1972; O'Brien et al., 1983; King and O'Brien, in press). Detailed correlation over such distances is expectedly much more difficult than it is elsewhere in the Canadian Avalon Zone.

The author briefly visited outcrops of CIF equivalents in New Brunswick during September of 1986. The strata in New Brunswick have some striking similarities and some significant differences. The CIF equivalent, the Ratcliffe Brook Formation, rests unconformably on the volcanics, sandstones, and conglomerates of the Precambrian Cold Brook Formation. The Ratcliffe Brook Formation is overlain by white-weathering quartzites of the Glen Falls Formation which are approximately correlative with the Random Formation. The Glen Falls is much thinner and contains less shale than the Random Formation, but is of similar age and lithology.

There are some sandstone-laminated red mudstones in the lower Ratcliffe Brook Formation that bear some resemblance to facies in the lower CIF, but the most striking similarity is between the strata at the top of each formation (below the quartzitic formations). The strata at the top of the Ratcliffe Brook Formation are identical to FA 6 of this study in lithology, bedding characteristics, and sedimentary structures. They consist of meter-thick, planar laminated, red, micaceous sandstones with low-angle truncation surfaces and associated pebble conglomerate lenses and wave-rippled pebble beds. This remarkable similarity suggests that similar shoreline conditions existed in both areas prior to the deposition of the quartzitic units, which are well known as being regionally, and even globally, extensive. It would be interesting to examine outcrops from other Avalonian outcrops in North America, or their equivalents in Europe or Africa, to see if a similar facies association precedes the quartzitic units in these areas as well. It is certainly not

found in this position on the ancient North American platform, at least not in the northern Appalachians (e.g., Myrow, 1983).

There are no limestone units in the Ratcliffe Brook Formation, so the shelly-fossil record is quite minimal. The trace-fossil record from the New Brunswick outcrop is sparse in comparison to the CIF, but general correlations can be made with the trace fossils that are present.

Chapter 10

SUMMARY

Measurement of stratigraphic sections has allowed the delineation of member boundaries and member thicknesses and the correction of errors in the lithostratigraphy of the CIF, and has provided a framework for the accurate tabulation of biostratigraphic information, most importantly the ranges of shelly fossils and trace fossils. Lithostratigraphic and biostratigraphic work, the latter undertaken as a series of joint projects with various workers, has provided the basis for the presentation of the CIF as a boundary stratotype for the Precambrian — Cambrian boundary at a meeting of the Precambrian — Cambrian Boundary Working Group scheduled for August of 1987.

Measured sections, in association with numerous slabbed and polished hand samples, have served as a primary data base for facies analyses and the reconstruction of depositional history. The main conclusions of these analyses are given below.

Facies Association 1 consists of four lithofacies; Red and Green Sandstone/Shale Facies (1.1), Shaly Facies (1.2), Gray to Black Shale Facies (1.3), and Medium-Thick Bedded Sandstone/Shale (1.4). The first two facies dominate the lower part of member 1 and represent lower tidal flat/shallow subtidal and middle/upper tidal flat settings, respectively. Bedding characteristics, sedimentary structures and paleocurrent data indicate that tidal currents were the main agents of transport and deposition and that these

environments may have exhibited an ebb-tidal asymmetry. Facies 1.3 was deposited in semirestricted shoreline environments of uncertain affinity. Partially enclosed shoreline embayments, including interdistributary bay environments, are considered probable settings for this facies.

Facies Association 2 consists of four lithofacies: Gutter Cast Facies (2.1), Sandstone/Siltstone Facies (2.2), Thinly Bedded Red Siltstone/Shale Facies (2.3), and Green Laminated Siltstone Facies (2.4). The first two facies are considered upper delta front and lower delta front/prodelta environments, respectively. Facies 2.3 and 2.4 are delta abandonment facies, and as such, form laterally extensive marker horizons within the central part of member 2.

Storm processes left a strong imprint on Facies 1.1 and 1,2. S2-S4 Beds record deposition under the influence of combined flows with unidirectional currents dominating the early phase of deposition and combined flow or oscillatory currents dominating the later stages of deposition. An interacti e-flow model has been presented to explain storm-generated vertical stratification sequences under combined flow conditions as a function of initial velocities and time-velocity histories of each component of flow (unidirectional and oscillatory). This model is applicable to a small group of vertical stratification sequences and will be useful as a guide to the reconstruction of bed configurations through time, only after considerable experimental work has been done to constrain bedform stability fields under combined-flow conditions.

Flat-pebble conglomerates formed under storm conditions from the erosion and transport of rounded shale clasts and the penecontemporaneous rip-up of semiconsolidated silty bottom sediments. H Beds are hummocky cross-stratified sandstones that are also storm-generated. These beds are commonly amalgamated with underlying sandstones and are often lenticular. The H beds are considered starved forms whose discontinuity is due to a level of available sediment that was insufficient to create a complete bedform. A low-angle cross-stratified bed was described and interpreted in terms of deposition from a low-

relief hummocky bedform in which bedform migration far exceeded aggradation rate. Gutter casts and pot casts, generally considered storm features, are spectacularly exposed in the CIF. Pot casts represent the infilling of variably shaped circular to slightly oval depressions formed by the erosion of the substrate by spiralling eddies or whirlpools. Gutter casts are polygenetic features that form by the infilling of elongate scours. In some, but not all, cases the flow appears to have been helical. Both pot casts and gutter casts were formed under high-energy relaxation currents associated with storm events.

Based in part on the vertical distribution of lithofacies within member 2, a model for tempestite deposition has been proposed in which tempestite proximality trends differ greatly from the standard models presented for sandy shorelines in which bed thickness is greatest nearshore and decreases seaward. In the model devised for the CIF, the shallow subtidal area consists of S1 beds and discontinuous S2 beds in association with numerous pot and gutter casts — the Gutter Cast Facies. This is transitional into deeper-water deposits characterized by more continuous S2-S4 beds and H-beds of the Siltstone/Sandstone Facies. Finally, in the outer-shelf (FA 3) region sandstone laminae are deposited below the influence of storm waves. The most proximal setting is an area of throughput, with the gutter casts recording erosion of the underlying substrate by strong seaward-flowing relaxation currents. In deeper water the throughput/deposition ratio decreases and thicker, more extensive beds are deposited. In the outer-shelf area distal tempestites are very thin because most of the sediment is deposited above storm wave base. From the shoreline toward the outer shelf, tempestite bed thicknesses first increase then decrease, with a maximum somewhere between fair-weather wave base and storm wave base.

The abundance and wide variety of marine slides and gravity flows in Facies 1.1 and 1.2 earmarks these shallow-water deposits as deltaic in origin. These mass-movement deposits demand unusually high sedimentation rates, necessary for such failures on the low slopes typical of the shelf environment. The siliceous nature of the fine-grained sediments

of the CIF allows slabbing and detailed examination and interpretation of siltstone/mudstone gravity-flow deposits. Support mechanisms in these gravity flows changed both spatially and temporally, and many deposits register conditions that would make them intermediate in character between the end members of the commonly accepted four-part classification scheme (liquefied flow, turbidity current, debris flow, grain flow). For instance, the thin pebbly mudstone bed described in detail in Section 4.14 was deposited from a flow intermediate in character between a debris flow and a turbidity current. Unifite beds record all transitions from liquefied flows to turbidity currents. Raft-bearing beds are thought to have been emplaced by debris flows, although these beds appear to grade into turbidites. Disturbed horizons form from in situ loading. Chaotic horizons are submarine slumps and slides, many of which probably formed as a result of failure induced by storm-wave loading.

Facies Association 3 consists of only one lithofacies, the Laminated Siltstone Facies (3.1). Sandstone beds in this facies represent distal tempestites deposited by waning flows on the outer shelf below storm wave base. Parallel-laminated sandstone beds with current lineations and parting lineations imply upper-flow-regime conditions, and for those beds that lack overlying current ripples, very rapid current deceleration is implied. Beds are commonly parallel laminated at their base and ripple cross-laminated above. Data from some of these beds indicate a clockwise shift of paleocurrents during deposition. These beds have been modeled as deposits of geostrophic flows in which sediment-laden storm currents are deflected by the Coriolis effect. One tentative conclusion to be drawn from this is that deposition took place in the Northern Hemisphere. This model may be applicable to other sequences containing similar beds as a paleogeographic tool useful in determining whether deposition occurred in the Northern or Southern Hemisphere.

Facies Association 4 consists of three lithofacies: Red, Purple and Green Mudstone Facies (4.1), Grey Mudstone Facies (4.2), and Limestone Facies (4.3). A facies model based on the lithologic characteristics, sedimentary and biogenic structures, and lateral and

vertical lithofacies distributions of these facies calls for deposition along a low-energy muddy shelf in which the ocean was oxygen-stratified and limestone deposition was restricted to the peritidal zone. Biofacies models for modern oxygen-deficient basins are used here to reconstruct paleo-oceanographic conditions. Facies 4.2 was deposited in the inner shelf under dysaerobic conditions. Facies 1.1 was deposited in the shallow subtidal under moderate (green mudstone) to high (red mudstone) oxygen levels.

The peritidal limestones, which form the cap of large-scale shallowing cycles, were deposited during times of maximum regression. It is unknown whether these formed a facies belt at all times during the deposition of member 4 or if the limestones formed only at times of low sea level, when they would have prograded seaward to form thin, extensive sheets. The limestone beds contain a wide variety of interesting structures, most of which are generally considered good indicators of tidal-flat deposition: algally built mud mounds, extensive stromatolites, oncolites, tepee and sheet-crack structures, desiccation cracks, and rip-up clasts. The carbonate sediments are thought to be locally derived (autochthonous), primarily by the action of cyanobacteria.

A new but problematic facies model has been developed for this facies association. The restriction of limestones to the shoreline is thought to be paleolatitudinally controlled: estimates for the CIF place the field area at 30°-35° latitude. The well developed tidal-flat facies imply effective tidal currents, yet siliciclastic mud from the subtidal region does not appear to have been transported onto the tidal flats. This remains an unexplained part of this facies model.

Facies Association 5 consists of two lithofacies: Sandy Siltstone Facies (5.1) and the Thin/Medium Bedded Sandy Siltstone Facies (5.2). The sandstone beds in these facies are dominantly parallel laminated and represent tempestites deposited below storm wave base. This facies association forms the base of a coarsening- and fining-upward sequence that characterizes member 5.

Facies Association 6 consists of one facies, the Red Micaceous Sandstone Facies (6.1), which has been subdivided into two subfacies: Thin to Thick Bedded Subfacies (6.1A) and Massive Subfacies (6.1B), which were deposited along a storm-dominated shoreline in offshore and shoreface environments, respectively. Subfacies 6.1A contains planar-laminated and hummocky-cross-stratified sandstones and thin burrowed siltstone beds. The massive-bedded Subfacies 6.1B is planar laminated and swaly cross-stratified. The vertical transition at Dantzic Cove from FA 5 to Subfacies 6.1A to 6.1B is a shoaling (progradational) sequence and is similar in many respects to published accounts of ancient storm-dominated shoreline sequences. Large, wave-formed, two-dimensional gravel ripples and phosphatic shale chip conglomerates were formed when coarse-grained detritus was eroded from the shoreline, swept out onto the shelf, and reworked during storm events.

At the contact between the CIF and the Random Formation, the close stratigraphic proximity and minor interbedding of wave- and storm-dominated nearshore deposits from FA 6 with quartzarenitic sandstones of tidal origin from the Random Formation appears to be a paradox in terms of paleoenvironmental reconstruction. The vertical lithofacies changes are explained by a temporal shift from a storm- and wave-dominated shoreline to a tide-dominated shoreline, resulting from a relative sea-level rise. Interbeds of the two lithologies in the lower Random Formation formed during a transitional period when tidal range was changing in response to an interaction between the paleogeography and rising relative sea-level.

This study fills a gap in our understanding of the Late Precambrian — Early Cambrian sedimentary history of the Newfoundland Avalon Zone. The CIF is important as a transitional sequence recording a shift from tectonically active fault-bounded basins (Rencontre Formation) to a tectonically stable platform (Random Formation). The sedimentary history of the CIF has been broken down into three phases.

The first phase covers the Rencontre Formation and members 1, 2, and part of 3 of the CIF. This phase records sea-level rise with a shift from the terrestrial and marginal marine redbeds of the Rencontre Formation to the laminated siltstones of FA 3, which were deposited in the outer shelf. Several periods of basin expansion and rise in relative sea level were documented from the Rencontre Formation by Smith and Hiscott (1984). The lower CIF represents a more extensive and more fundamental increase in relative sea level during which deposition initially took place in tidal-flat and shallow subtidal environments and then passed through a prolonged stage of deposition in deltaic environments before passing into the shelf setting. Throughout the field area, paleocurrents are clearly oriented toward the northeast during this phase, implying the existence of a land area toward the southwest.

Phase 2, which is represented by strata from lower member 3 to the top of member 4, is interpreted as a period of drop in relative sea-level and low sediment input. This phase produced a thick shoaling-up sequence, representing environments from outer shelf (FA 3) to subaerially exposed peritidal limestones (Facies 4.3), and contains evidence for smaller-scale fluctuations in relative sea-level. The paleogeography during Phase 2 appears to have remained essentially similar to that inherited at the end of Phase 1. The establishment of an extensive, low-energy, tectonically inactive coast during Phase 2 resulted in part from the long period of tectonic inactivity represented by the upper Rencontre Formation and lower CIF, during which the hinterlands were progressively denuded.

Phase 3, represented by member 5 (FA 5 and 6) and its transition into the Random Formation, is a period of rapid deepening followed by shallowing. During this phase a thick coarsening- and shoaling-upward sequence was deposited in a prograding wave- and storm-dominated depositional system. At the beginning of Phase 3 a deepening is recorded, in which environments shift from peritidal (LS 3) to below-storm-wave-base sandstone beds (Facies 5.1). Shoaling is recorded by an upward increase in tempestite bed thickness

and a shift from distal parallel-laminated sandstones of FA 5, to the thicker-bedded HCS and SCS beds of FA 6.

Phase 3 is a period of considerable sediment influx and strong storm and wave influence. The shift from the quiet low-energy shoreline of Phase 2, to the high-energy shelf of FA 6, in which sand is in abundant supply, requires the uplift and emergence of a highland area to act as a new supply of sandy sediment. The lack of proximal fluvial/alluvial deposits in the lower part of member 5 implies that the uplift must have been distant from the southeast Burin Peninsula, probably to the northeast of the field area in the Avalon Peninsula, where such uplift has been documented and fluvial/alluvial sediments dominate the stratigraphic column (Signal Hill Group). The available paleocurrent data and lithofacies trends in the overlying formations (Random and Bonavista Formations) is most consistent with a major reorientation of the shoreline at the beginning of Phase 3, with a near reversal of shoreline position from the southwest to the northeast.

The land area that lay toward the southwest of Fortune Bay during deposition of Phases 1 and 2 must have subsided, allowing breaching and transgression by the sea from that direction. The low relief of this land area at the end of member 2 time would have aided this shift.

At the end of Phase 3, following the progradation of the thick clastic wedge of member 5, a major transgression and onlap was recorded by the Random Formation. This onlap is considered a response to a eustatic sea-level rise. The thick prograded clastic wedge (member 5) increased the shelf width, which in combination with the subsequent eustatic sea-level rise, allowed the establishment of macrotidal conditions and the deposition of extensive quartzarenitic sandstones.

REFERENCES

Ager, D.V., 1974, Storm deposits in the Jurassic of the Moroccan High Atlas: Paloegeography, Paleoclimatology, Paleoecology, v. 15, p. 83-93.

Aigner, T., 1982, Calcareous tempestites: Storm dominated stratification in Upper Muschelkalk Limestones (Middle Trias, SW Germany), in Einsele, G. and Seilacher, A., eds., Cyclic and Event Stratification: Springer-Verlag, Berlin, p. 180-198.

Aigner, T. and Futerrer, E., 1978, Kolk-Topfe und -Rinnen (pot and gutter casts) im Muschelkalk - Anzeger fur Wattemeer?: N. Jb. Geol. Palaont. Abh., v. 156, p. 285-304.

Aigner, T. and Reineck, H-E., 1982, Proximality trends in modern storm sands from the Helgoland Bight (North Sea) and their implications for basin analysis: Senckenbergiana Marit., v. 14, p. 185-215.

Aksu, A.E., 1984, Subaqueous debris flow deposits in Baffin Bay: Geo-Marine Letters, v. 4, p. 83-90.

Alexander, H.S., 1932, Pothole Erosion: Journal of Geology, v. 40, p. 305-337.

Allen, J.R.L., 1960, The Mam Tor sandstones: a turbidite facies of the Namurian Deltas of Derbyshire, England: Journal of Sedimentary Petrology, v. 30, no. 2, p. 193-208.

Allen, J.R.L., 1964, Primary current lineation in the Lower Old Red Sandstone (Devonian), Anglo-Welsh Basin: Sedimentology, v. 3, p. 89-108.

Allen, J.R.L., 1965, The sedimentation and palaeogeography of the Old Red Sandstone of Anglesey, North Wales: Proceedings Yorkshire Geol Society, v. 35, p. 139-185.

Allen, J.R.L., 1974, Sedimentology of the Old Red Sandstone (Siluro-Devonian) in the Clee Hills Area , Shropshire, England: Sedimentary Geology, v. 12, p. 73-167.

Allen, J.R.L., 1979, A model for the interpretation of wave ripple-marks using their wavelength, textural composition, and shape: Journal Geological Society of London, v. 136, p. 673-682.

Allen, J.R.L., 1984, Sedimentary structures: their character and physical basis: Developments in Sedimentology no. 30, Parts 1 and 2, Elsevier, Amsterdam, 1258 p.

Allen, P., 1962, The Hastings Beds Deltas: Recent Progress and Easter Field Meeting Report, Proceedings of the Geologists Association, v. 73, p. 219-243.

Allen, P., 1981a, Wave-generated structures in the Devonian lacustrine sediments of SE Shetland, and ancient wave conditions: Sedimentology, v. 28, p. 369-379.

Allen, P., 1981b, Some guidelines in reconstructing ancient sea conditions from wave ripple marks: Marine Geology, v. 43, p. M59-M67.

Allen, P., 1984, Reconstruction of ancient sea conditions with an example from the Swiss molasse: Marine Geology, v. 60, p. 455-473.

Allen, P., 1985, Hummocky cross-stratification is not produced purely under progressive gravity waves: Nature, v. 313, p. 562-564.

Allen, P.A. and Pound, C.J., 1984, Constraints on the paleohydraulic significance of hummocky bedding: Sedimentology of Shelf Sands and Sandstones - Canadian Society of Petroleum Geologists Research Symposium Program with Abstracts, p. 22.

Alvarez, W., Colacicchi, R., and Montanari, A., 1985, Synsedimentary slides and bedding formation in Apennine pelagic limestones: Journal of Sedimentary Petrology, v. 55, no. 5, p. 720-723.

Amos, C.L. and Zaitlin, B.A., 1985, The effect of changes in tidal range on a sublittoral macrotidal sequence, Bay of Fundy, Canada: Geo-Marine Letters, v. 4, p. 161-169.

Anderson, M.M., 1975, Saint Pierre and Miquelon, in Fairbridge, R.W., ed., The Encyclopedia of World Regional Geology, Part 1, Encyclopedia of Earth Sciences, v. 8: Dowden, Hutchinson and Ross Inc., Strousburgh, Pennsylvania, p. 443-447.

Anderson, M.M., 1978, Ediacaran fauna, in Lapedes, D.N., ed., Yearbook of Science and Technology: McGraw-Hill, New York, p. 146-149.

Anderson, M.M., 1981, The Random Formation of Southeast Newfoundland: a discussion aimed at establishing its age and relationship to bounding formations: American Journal of Science, V. 281, p. 807-830.

Anderson, M.M., Bruckner, W.D., King, A.F., and Maker, J.B., 1975, The late Proterozoic 'H.D. Lilly Unconformity' at Red Head, northeastern Avalon Peninsula, Newfoundland: American Journal Science, 275, p. 1012-1027.

Anderson, M.M. and Conway Morris, S., 1982, A review, with descriptions of four unusual forms, of the soft-bodied fauna of the Conception and St John's Groups (late Precambrian), Avalon Peninsula, Newfoundland: Third North American Paleontological Convention, Proceedings I, p. 1-8.

Anderson, M.M. and Misra, S.B., 1968, Fossils found in the Precambrian Conception Group of Southeastern Newfoundland: Nature, v. 220, p. 680-681.

Andersson, K.E.B., 1961, Sedimentation and ideal fluidization: Svensk Kem. Tidskr., v. 73, p. 334-345.

Andresen, A. and Bjerum, L., 1967, Slides in subaqueous slopes in loose sand and silt, in Richards, A.F., ed., Marine Geotechnique: Univ. Illinois Press, Chicago, p. 221-239.

Anderton, R., 1976, Tidal shelf sedimentation: an example from the Scottish Dalradian: Sedimentology, v. 23, p. 429-458.

Asserto, R.L.A.M. and Kendall, C.G.St.C., 1977, Nature, origin and classification of peritidal tepee structures and related breccias: Sedimentology, v. 24, p. 153-210.

Augustinus, P.G.E.F., 1980, Actual development of the chenier coast of Suriname (South America): Sedimentary Geology, v. 26, p. 91-113.

Bagnold, R.A., 1946, Motion of waves in shallow water: Proceedings of the Royal Society, Ser. A, v. 147, p. 1-15.

Ball, S.M., 1971, The Westphalia Limestone of the northern midcontinent: A possible ancient storm deposit: Journal of Sedimentary Petrology, v. 41, no. 1, p. 217-232.

Ball, M.M., Shinn, E.A., and Stockman, K.W., 1967, The geologic effect of hurricane Donna in South Florida: Journal of Geology, v. 75, p. 583-597.

Basset, D.A. and Walton, E.K., 1960, The Hell's Mouth grits: Cambrian Greywackes in St. Tudwal's Peninsula, North Wales: Geological Society of London Quart., v. 116, p. 85-110.

Baturin, G.N., 1982, Phosphorites on the sea floor: Origin, composition and distribution: Developments in Sedimentology no. 33, Elsevier, The Netherlands, 343 p.

Bengtson, S. and Fletcher, T.P., 1983, The oldest sequence of skeletal fossils in the Lower Cambrian of southeastern Newfoundland: Canadian Journal of Earth Sciences, v. 20, p. 526-536.

Benton, M.J. and Gray, D.I., 1981, Lower Silurian distal shelf storm-induced turbidites in the Welsh Borders: sediments, tool marks and trace fossils: Journal Geological Society of London, v. 138, p. 675-694.

Benus, P. and Landing, E., 1984, Depositional environments and biofacies of the Bonavista Formation (Early Cambrian [Tommotian-Lower Atdabanian]), Eastern Newfoundland: Geological Association of America, Northeastern Section, Abstract with Programs, v. 16, no. 1, p. 3.

Berg, R.R., 1975, Depositional environment of Upper Cretaceous Sussex Sandstone, House Creek Field, Wyoming: American Association of Petroleum Geologists Bulletin, v. 59, no. 11, p. 2099-2110.

Berry, F.G., 1961, Longitudinal Ripples in the Upper Tunbridge Wells Delta, Kent, and their Probable Mode of Origin: Proc. Geological Association, v. 72, pt. 1, p. 33-39.

Berner, R.H., 1968, Calcium carbonate concretions formed by the decomposition of organic matter: Science, v. 159, p. 195-197.

Berner, R.H., 1984, Sedimentary pyrite, an update: Geochem. et Cosmochim Acta, v. 48, p. 605-615.

Blatt, H., Middleton, G.V., and Murray, R., 1980, Origin of sedimentary rocks: Prentice-Hall, Englewood Cliffs, New Jersey, 782 p.

Bloos, G., 1976, Untersuchungen uber Bau und Entstehung der feinkornigen Sandsteine des Schwarzen Jura alpha (Hettangium und tiefstes Sinemurium) im schwabischen Sedimentationsbereich: Arb. Inst. Geol. Paleontology University Stuttgart, N.F., v. 71, p. 1-296.

Boersma, J.R., 1970, Distinguishing features of wave-ripple cross-stratification and morphology: Unpublished Ph.D. Thesis, University of Utrecht, 65 p.

Bond, G.C. and Kominz, M.A., 1984, Construction of tectonic subsidence curves for the early Paleozoic miogeocline, southern Canadian Rocky Mountains: Implications for subsidence mechanisms, age of breakup, and crustal thinning: Geological Society of America Bulletin, v. 95, p. 155-173.

Boothroyd, J.C. and Hubbard, D.K., 1975, Genesis of bedforms in mesotidal estuaries, in Cronin, L.E., ed., Estuarine Research: Geology and Engineering, Vol. 2, Academic Press, New York, p. 217-234.

Bouma, A.H., 1962, Sedimentology of some flysch deposits: A graphic approach to facies interpretation: Elsevier, Amsterdam, 168 p.

Bourgeois, J., 1980, A transgressive shelf sequence exhibiting hummocky stratification: the Cape Sebastian Sandstone (Upper Cretaceous), southwest Oregon: Journal of Sedimentary Petrology, v. 50, p. 681-702.

Bourgeois, J. and Smith, J.D., 1984, Paleohydraulic significance of hummocky stratification: Sedimentology of Shelf Sands and Sandstones - Canadian Society of Petroleum Geologists Research Symposium Program with Abstracts, p. 65.

Bourgeois, J., 1984, Hummocks - Do they grow?: American Association of Petroleum Geologists Bulletin, (Abstract), v. 67, p. 428.

Brasier, M.D., 1980, The Lower Cambrian transgression and glauconite-phosphate facies in western Europe: Journal of the Geological Society, v. 137, p. 695-703.

Brenchley, P.J., 1985, Storm influenced sandstone beds: Modern Geology, v. 9, p. 369-396.

Brenchley, P.J. and Newell, G., 1982, Storm influenced inner-shelf sand lobes in the Caradoc (Ordovician) of Shropshire, England: Journal of Sedimentary Petrology, v. 52, p. 1257-1269.

Brenchley, P.J., Newell, G., and Stanistreet, I.G., 1979, A storm surge origin for sandstone beds in an epicontinental platform sequence, Ordovician, Norway: Sedimentary Geology, v. 22, p. 185-217.

Brenner, R.L. and Davies, D.K., 1973, Storm-generated coquinoid sandstone: Genesis of high-energy marine sediments from the Upper Jurassic of Wyoming and Montana: Geological Society of America Bulletin, v. 84, p. 1685-1698.

Brett, C.E. and Baird, G.C., 1985, Mixing of siliciclastic and carbonate sediments in shallow shelf environments: Geology, v.13, p. 324-327.

Brett, C.E. and Baird, G.C., 1986, Comparitive taphonomy: a key to paleoenvironmental interpretation based on fossil preservation: Palaios, v. 1, no. 3, p. 207-227.

Bridges, P.H., 1972, The significance of toolmarks on a Silurian erosional furrow: Geological Magazine, v. 109, no. 5, p. 405-410.

Broadhurst, F.M., 1968, Large scale ripples in Silurian limestones: Lethaia, v. 1, p. 28-38.

Bromley R.G., 1967, Marine phosphorites as depth indicators: Marine Geology, v. 5, p. 503-509.

Brouwer, A., 1953, Rhythmic depositional features of the east Surinam coastal plain: Geol. Mijnbouw, v. 15, p. 226-236.

Burne, R.V., 1970, The origin and significance of sand volcanoes in the Bude Formation (Cornwall): Sedimentology, v. 15, p. 211-228.

Burst, J.F., 1965, Subaqueously formed shrinkage cracks in clay: Journal of Sedimentary Petrology, v. 35, p. 348-353.

Bushinski, G.I., 1964, On shallow water origin of phosphorite sediments, in van Straaten, L.M.J.U., ed:, Deltaic and shallow marine deposits: Elsevier Publishing Co., p. 62-70.

Butler, A.J. and Greene, B.A., 1976, Silica resources of Newfoundland: Mineral Development Division, Newfoundland Dept. Mines and Energy, Report 76-2, 68 p.

Button, A. and Vos, R.G., 1977, Subtidal and intertidal clastic and carbonate sedimentation in a macrotidal environment: and example from the Lower Proterozoic of South Africa: Sedimentary Geology, v. 18, p. 175-200.

Byers, C.W., 1977, Biofacies patterns in euxinic basins: a general model, in Cook, H. E. and Enos, P., eds., Deep-water carbonate environments: Society Econ. Paleontologists and Mineralogists, Spec. Pub., no. 25, Tulsa, Oklahoma, p. 5-17.

Campbell, C.V., 1966, Truncated wave-ripple laminae: Journal of Sedimentary Petrology, v. 36, p. 825-828.

Chan, M.A. and Dott, R.H., 1986, Depositional facies and progradational sequences in Eocene wave-dominated deltaic complexes, southwestern Oregon: American Association of Petroleum Geologists Bulletin, v. 70, no. 4, p. 415-429.

Channon, R.D. and Hamilton, D., 1976, Wave and tidal current sorting of shelf sediments of England: Sedimentology, v. 23, p. 17-42.

Chow, N., 1986, Sedimentology and diagenesis of middle and upper Cambrian platform carbonates and siliciclastics, Port au Port Peninsula, Western Newfoundland: Unpublished Ph.D. thesis, Memorial University, St. John's, Newfoundland, 458 p.

Christie, R.L., 1978, Sedimentary phosphate deposits — an interim review: Geological Survey of Canada, Paper 78-20, 9 p.

Cita, M.B., Maccagni, A., and Pirovano, G., 1982, Tsunami as triggering mechanism of homogenites recorded in areas of the eastern Mediterranean characterized by the "cobblestone topography", in Saxov, S. and Nieuwenhuis, J.K., eds., Marine slides and other mass movements, Nato Conference Series 4, Marine Sciences, v. 6: Plenum Press, New York, p. 233-260.

Clifton, H.E., 1969, Beach lamination: nature and origin: Marine Geology, v. 7, p. 553-559.

Clifton, H.E., 1973, Pebble segregation and bed lenticularity in wave-reworked versus alluvial gravel: Sedimentology, v. 20, p. 173-187.

Clifton, H.E., 1981, Progradational sequences in Miocene shoreline deposits, southeastern Caliente Range, California: Journal of Sedimentary Petrology, v. 51, no. 1, p. 165-184.

Clifton, H.E. and Dingler, J.R., 1984, Wave-formed structures and paleoenvironmental reconstruction: Marine Geology, v. 60, p. 165-198.

Clifton, H.E., Hunter, R.E., and Phillips, R.L., 1971, Depositional structures in the non-barred high-energy nearshore: Journal of Sedimentary Petrology, v. 41, no. 3, p. 651-670.

Coleman, J.M., 1981, Deltas: Processes of deposition and models for exploration: Burgess Publishing Company, 124 p.

Coleman, J.M. and Gagliano, S.M., 1964, Cyclic sedimentation in the Mississippi River deltaic plain: Gulf Coast Association Geol. Socs. Trans., v. 14, p. 67-80.

Coleman, J.M. and Garrison, L.E., 1977, Geological aspects of marine slope stability, northwestern Gulf of Mexico: Marine Geotechnology, v. 2, p. 9-44.

Coleman, J.M, Suhayda, J.N., Whelan, T., and Wright, L.D., 1974, Mass movement of Mississippi River delta sediments: Transactions Gulf Coast Association of Geological Societies, v. 24, p. 49-68.

Coniglio, M., 1985, Origin and diagenesis of fine-grained slope sediments: Cow Head Group (Cambro-Ordovician), western Newfoundland: Ph.D. thesis, Memorial University, St. John's, Newfoundland, 684 p.

Coniglio, M. and James, N.P., 1986, Calcified algae as sediment contributors to Early Paleozoic limestones: evidence from deep-water sediments of the Cow Head Group, Western Newfoundland: Journal of Sedimentary Petrology, v. 55, no. 5, p. 746-754.

Cook, P.J. and McIlhinny M.W., 1979, A reevaluation of the spatial and temporal distribution of sedimentary phosphate deposits in the light of plate tectonics: Economic Geology, v. 74, p. 315-330.

Cook, P.J. and Shergold, J.H., 1984, Phosphorous, phosphorites and skeletal evolution at the Precambrian-Cambrian boundary: Nature, v. 308, p. 231-236.

Cowie, J.W., 1985, Continuing work on the Precambrian-Cambrian boundary: Episodes, v. 8, p. 93-98.

Crimes, T.P. and Anderson, M.M., 1985, Trace fossils from late Precambrian — Early Cambrian strata of southeastern Newfoundland (Canada): temporal and environmental implications: Journal of Paleontology, v. 59, p. 310-343.

Crowell, J.C., 1957, Origin of pebbly mudstones: Geological Society of America Bulletin, v. 68, p. 993-1009.

Dale, N.C., 1927, Precambrian and Paleozoic geology of Fortune Bay, Newfoundland: Geological Society of America Bulletin, v. 38, p. 411-430.

Daley, B., 1968, Sedimentary structures from a non-marine horizon in the Bembridge marls (Oligocene) of the Isle of Wight, Hampshire, England: Journal of Sedimentary Petrology, v. 38, p. 114-127.

Dallmeyer, R.D., 1980, Geochronology report — Current Research: Newfoundland Department of Mines and Energy, Mineral Development Division Report 80-1.

Dallmeyer, R.D., Hussey, E.M., O'Brien, S.J., and O'Driscoll, C.F., 1983, Chronology of tectonothermal activity in the western Avalon Zone of the Newfoundland Appalachians: Canadian Journal of Earth Sciences, v. 20, p. 355-363.

De Jong, J.D., 1965, Quaternary sedimentation in the Netherlands, in Wright, H.E. and Frey, D.G., eds., International Studies of the Quaternary: Geological Society Society of America Spec. Paper 84, p. 95-124.

Dekay, L.E., 1981, Morphodynamics of an undernourished barrier beach, East Beach, Rhode Island: Unpublished M.Sc. Thesis, University of Rhode Island, Kingston, Rhode Island.

De La Rue, E.A., 1951, Recheches geologiques et minieres aux Iles Saint-Pierre et Miquelon: Office De La Recherche Scientifique Outre-Mer, 20, reu Monsieur, Paris, 75 p.

De Raaf, J.F.M. and Boersma, J.R., 1971, Tidal deposits and their sedimentary structures: Geol. en Mijnb., v. 50, p. 479-504.

De Raaf, J.F.M., Boersma, J.R., and Gelder, A. Van, 1977, Wave-generated structures and sequences from a shallow marine succession, Lower Carboniferous, County Cork, Ireland: Sedimentology, v. 4, p. 1-52.

De Raaf, J.F.M., Reading. H.G., and Walker, R.G., 1965, Cyclic sedimentation in the Lower Westphalian of Devon, England: Sedimentology, v. 4, p. 1-52.

Dineley, D.L., 1960, The Old Red Sandstone of Eastern Ekmanfjorden, Vestspitsbergen, Geological Magazine, v. 97, p. 18-32.

Dingler, J.R., 1974, Wave-formed ripples in nearshore sands: Thesis, Univ. Calif. at San Diego, Calif., 136p.

Dingler, J.R. and Inman, D.L., 1977, Wave-formed ripples in nearshore sands: Proc. 15th Conf. on Coastal Engineering, Honolulu, Hawaii, p. 2109-2126.

Dionne, J.C., 1971, Vertical packing of flat stones: Canadian Journal of Earth Sciences, v. 8, 1585-1591.

Donovan, R.N. and Foster, R.J., 1972, Subaqueous shrinkage cracks from the Caithness Flagstone Series (Middle Devonian) of Northeast Scotland: Journal of Sedimentary Petrology, v. 42, p. 309-317.

Dott, R.H., Jr., 1963, Dynamics of subaqueous gravity depositional processes: American Association of Petroleum Geologists, v. 47, p. 104-128.

Dott, R.H., Jr., 1983, 1982 SEPM Presidential Address: Episodic sedimentation — How normal is average? How rare is rare? Does it matter?: Journal of Sedimentary Petrology, v. 53, no. 1, p. 5-23.

Dott, R.H., Jr. and Bourgeois, J., 1982, Hummocky stratification: Significance of its variable bedding sequences: Geological Society of America Bulletin, v. 93, p. 663-680.

Doyle, L.J. and Roberts, H.H., 1983, (conveners), American Association of Sedimentologists and Society of Economic Paleontologists and Mineralogists Conference: Carbonate to Clastic Facies Change 1: American Association of Petroleum Geologists Bulletin, v. 67, p. 404.

Downing, R.A. and Squirrell, H.C., 1965, On the red and green beds in the Upper Coal Measures of the eastern part of the South Wales Coalfield: Bulletin Geological Survey Great Britain, no. 23, p. 45-56.

Driese, S.G., Byers C.W., and Dott, R.H., Jr., 1981, Tidal deposition in the basal Upper Cambrian Mt. Simon Formation in Wisconson: Journal of Sedimentary Petrology, v. 51, no. 2, p. 367-381.

Duke, W.L., 1984, Paleohydraulic analysis of hummocky cross-stratified sands indicates equivalence with wave-formed flat bed: American Association of Petroleum Geologists Bulletin (Abstract with meeting), v. 68, no. 4, p. 472.

Duke, W.L., 1985, Hummocky cross-stratification, tropical hurricanes, and intense winter storms: Sedimentology, v. 32, p. 167-194.

Duke, W. and Leckie, D., 1984, Origin of hummocky cross stratification; Part 2. Paleohydraulic analysis indicates formation by orbital ripples within the wave-formed flat-bed field: Sedimentology of Shelf Sand and Sandstones — Research Symposium of Canadian Society of Petroleum Geologists, p. 32.

Duncan, J.R., 1964, The effects of water table and tide cycle on swash-bachwash sediment distribution and beach profile development: Marine Geology, v. 2, p. 186-194.

Eder, W., 1982, Diagenetic redistribution of carbonate, a process in forming limestone-marl alternations (Devonian and Carboniferous, Reheinisches Schiefergebirge, W. Germany), in Einsele, G. and Seilacher, A., eds., Cyclic and Event Stratification: Springer-Verlag, Berlin, p. 98-112.

Elliott, T., 1978, Deltas, in Reading, H.G., ed., Sedimentary Environments and Facies: Elsevier, New York, p. 97-142.

Embley, R.W., 1982, Anatomy of some Atlantic margin sediment slides and some comments on ages and mechanisms, in Saxov, S. and Nieuwenhuis, J.K., eds., Marine Slides and Other Mass Movements: Plenum Press, New York and London, p. 189-213.

Eriksson, K.A., 1977, Tidal deposits from the Archaean Moodies Group, Barberton Mountain Land, South Africa: Sedimentary Geology, v. 18, p. 257-281.

Evans, G., 1965, Intertidal flat sediments and their environments of deposition in the Wash: Quart. Journal Geological Society of London, v. 121, p. 209-245.

Field, M.E., Gardner, J.V., Jennings, A.E., and Edwards, B.D., 1982, Earthquake-induced sediment failures on a 0.75° slope, Klamath River delta: Geology, v. 10, p. 542-546.

Fischer, R.V., 1971, Features of coarse-grained, high-concentration fluids and their deposits: Journal of Sedimentary Petrology, v. 41, p. 916-927.

Fisher, R.V., 1983, Flow transformations in sediment gravity flows: Geology, v. 11, p. 273-274.

Fisk, H.N., 1952, Geological investigation of the Atchafalaya Basin and the problem of Mississippi River diversion: U.S. Army Corps of Engineers, Mississippi River Commission, Vicksburg, Mississippi, 145 p.

Fisk, H.N., McFarlan, E., Jr., Kolb, C.R., and Wilber, L.J., Jr., 1954, Sedimentary framework of the modern Mississippi delta: Journal of Sedimentary Petrology, v. 24, p. 76-99.

Flemming, N.C. and Stride, A.H., 1967, Basal sand and gravel patches with separate indications of tidal current and storm-wave paths, near Plymouth: Journal Marine Biol. Association U.K., v. 47, p. 433-444.

Fletcher, T.P., 1972, Geology and Lower to Middle Cambrian trilobite faunas of the southwest Avalon, Newfoundland: Unpublished Ph.D. thesis, Cambridge University, Cambridge, England, 530 p.

Folk, R.L., 1965, Some aspects of recrystallization in ancient limestones, in Pray, L.C. and Murray, R.C., eds., Dolomitization and limestone diagenesis: Society of Economic Paleontologists and Mineralogists, Special Publication no. 13, p. 14-48.

Frazier, D.E., 1967, Recent deltaic deposits of the Mississippi River: their development and chronology: Gulf Coast Association Geological Socs. Trans., v. 17, p. 287-315.

Friend, P.F., 1966, Clay fractions and colours of some Devonian red beds in the Catskill Mountains, U.S.A.: Quart. Journal Geological Society of London, v. 122, p. 273-292.

Froelich, P.N., Bender, M.L., Luedtke, N.A., Heath, G.R., and DeVries, T., 1982, The marine phosphorous cycle, in Berner, R.A., ed., Geochemical Cycles of Nutrient Elements: American Journal Science, v. 282, no. 4, p. 474-511.

Gadow, S. and Reineck, H.E., 1969, Ablandiger Sandstransporten bei Sturmfluten: Senckenbergiana Maritima, v. 1, p. 63-78.

Gevirtzman, D.A. and Mount, J.F., 1986, Paleoenvironments of an earliest Cambrian (Tommotian) shelly fauna in the Southeastern Great Basin, U.S.A.: Journal of Sedimentary Petrology, v. 56, no. 3, p. 412-421.

Gilbert, G.K., 1899, Ripple-marks and cross-bedding: Geological Society of America Bulletin, v. 10, p. 135-140.

Gillie, R.D., 1979, Sand and gravel deposits of the coast and inner shelf, East Coast, Northland Peninsula, New Zealand: Ph.D. thesis, University of Canterbury, Christchurch, New Zealand.

Goldring, R., 1971,Shallow-water sedimentation as illustrated in the Upper Devonian Baggy Beds: Memoir Geological Society of London, 5, 80 p.

Goldring, R. and Aigner,T., 1982, Scour and Fill: The significance of event separation, in Einsele, G. and Seilacher, A., eds., Cyclic and Event Stratification: Springer-Verlag, Berlin, p. 354-362.

Goldring, R. and Bridges, P., 1973, Sublittoral sheet sandstones: Journal of Sedimentary Petrology, v. 43, p. 736-747.

Goldring, R. and Langenstrassen, F., 1979, Open-shelf and near-shore clastic facies in the Devonian: Spec. Papers Palaeontology, v. 23, p. 81-97.

Goodwin, P.W. and Anderson, E.J., 1974, Associated physical and biogenic structures in environmental subdivision of a Cambrian tidal sandbody: Journal of Geology, v. 82, p. 779-794.

Gould, H.R. and McFarlan, E., 1959, Geological history of the chenier plain, southwestern Louisiana: Trans. Gulf-Coast Association Geological Socs., v. 9, p. 261-270.

Greene, B.A., 1975, Harbour Breton Map area, in Fleming, J.M., ed., Report of Activities for 1974: Newfoundland Dept. Mines and Energy, Mineral Development Division, Report 75-1, 133 p.

Greene, B.A. and O'Driscoll, C.F., 1976, Gaultois map area, in Greene, B.A., ed., Report of Activities for 1975: Department of Mines and Energy, Mineral Development Division, Report 76-1, p. 56-63.

Greene, B.A. and Williams, H., 1974, New fossil localities and the base of the Cambrian in southeastern Newfoundland: Canadian Journal of Earth Sciences, v. 11, p. 319-323.

Greensmith, J.T., 1965, Calciferous sandstone series sedimentation at the Eastern end of the Midland Valley of Scotland: Journal of Sedimentary Petrology, v. 35, p. 223-242.

Greensmith, J.T., Rawson, P.F., and Shalaby, S.E., 1980, An association of minor fining-upward cycles and aligned gutter marks in the Middle Lias (Lower Jurassic) of the Yorkshire coast: Proceedings of the Yorkshire Geological Society, v. 42, pt. 4, no. 29, p. 525-538.

Greensmith, J.T. and Tucker, E.V., 1968, Imbricate structures in Essex offshore shell banks: Nature, v. 220, p. 1115-1116.

Greensmith, J.T. and Tucker, E.V., 1969, The origin of Holocene shell deposits in the chenier plain facies of Essex (Great Britain): Marine Geology, v. 7, p. 403-425.

Greenwood, B., 1984, Hummocky cross-stratification: shelf or surf: Sedimentology of Shelf Sand and Sandstones — Research Symposium of Canadian Society of Petroleum Geologists, p. 39.

Greenwood, B. and Sherman, D.J., 1986, Hummocky cross-stratification in the surf zone: flow parameters and bedding genesis: Sedimentology, v. 33, p. 33-45.

Hallam, A., 1960, A sedimentary and faunal study of the Blue Lias of Dorset and Glamorgan: Phil. Trans. of the Royal Society, v. 243, Series B, p. 1-44.

Hamblin, A. and Walker, R.G., 1979, Storm-dominated shallow marine deposits: the Fernie-Kootenay (Jurassic) transition, southern Rocky Mountains: Canadian Journal of Earth Sciences, v. 16, p. 1673-1690.

Hampton, M.A., 1970, Subaqueous debris flow and generation of turbidity currents, Unpublished Ph.D. thesis, Stanford University, Stanford, California.

Hampton, M.A., 1972, The role of subaqueous debris flow in generating turbidity currents: Journal of Sedimentary Petrology, v. 42, no. 2, p. 775-793.

Hampton, M.A., 1975, Competence of fine-grained debris flows: Journal of Sedimentary Petrology, v. 45, p. 834-844.

Hampton, M.A., Bouma, A.H., Sangrey, D.A., Carlson, P.R., Molnia, B.M., and Clukey, E.C., 1978, Quantitative study of slope instability in the Gulf of Alaska: Proc. Offshore Technology Conf., Houston, Texas, Paper 3314, p. 2307-2318.

Handford, C.R., 1986, Facies and bedding sequences in shelf-storm-deposited carbonates — Fayetteville Shale and Pitkin Limestone (Mississippian), Arkansas: Journal of Sedimentary Petrology, v. 56, no. 1, p. 123-137.

Harms, J.C., 1969, Hydraulic significance of some sand ripples: Geological Society of America Bulletin, v. 80, p. 363-396.

Harms, J.C., Southard, J.B., Spearing, D.R., and Walker, R.G., 1975, Depositional environments as interpreted from primary sedimentary structures and stratification sequences: Society Econ. Paleontologists and Mineralogists, Short Course Notes No. 2, 161 p.

Harms, J.C., Southard, J.B., and Walker, R.G., 1982, Structures and sequences in clastic rocks: Society of Economic Paleontologists and Mineralogists, Short Course Notes No. 9, 249 p.

Hawarth, R.T. and Lefort, J.P., 1979, Geophysical evidence for the extent of the Avalon zone in Atlantic Canada: Canadian Journal of Earth Sciences, v. 16, no. 3, p. 552-567.

Hayes, M.O., 1967, Hurricanes as geologic agents, South Texas Coast: American Association of Petroleum Geologists, v. 51, p. 937-956.

Heckel, P.H., 1977, Origin of phosphatic black shale facies in Pennsylvanian cyclothems of mid-continent North America: American Association of Petroleum Geologists Bulletin, v. 61, no. 7, p. 1045-1068.

Hein, F.J., 1985, Fine-grained slope and basin deposits, California continental borderland: facies, depositional mechanisms and geotechnical properties: Marine Geology, v. 67, p. 237-262.

Hein, F.J. and Gorsline, D.S., 1981, Geotechnical aspects of fine-grained mass flow deposits: California Continental Borderlands: Geo-Marine Letters, v. 1, p. 1-5.

Henkel, D.J., 1970, The role of waves in causing submarine landslides: Geotechnique, v. 20, p. 75-80.

Hentz, T.F., 1985, Early Jurassic sedimentation of a rift-valley lake: Culpeper basin, northern Virginia: Geological Society of America Bulletin, v. 96, p. 92-107.

Hesse, R., 1975, Turbiditic and non-turbiditic mudstones of Cretaceous flysch section of the East Alps and other basins: Sedimentology, v. 22, p. 387-416.

Higgins, C.G., 1957, Origin of Potholes in Glaciated Regions: Journal of Glaciology, v. 4, p. 11-12.

Hiscott, R., 1982, Tidal Deposits of the Lower Cambrian Random Formation, eastern Newfoundland: facies and paleoenvironments: Canadian Journal of Earth Sciences, v. 19, no. 10, p. 2028-2042.

Hiscott, R. and James, N.P., 1985, Carbonate debris flows, Cow Head Group, western Newfoundland: Journal of Sedimentary Petrology, v. 55, no. 5, p. 735-745.

Hiscott, R. and Middleton, G.V., 1979, Depositional mechanics of thick-bedded sandstones at the base of a submarine slope, Tourelle Formation (Lower Ordovician), Quebec, Canada, in Doyle, L.J. and Pilkey, O.H., eds., Geology of Continental Slopes: Society of Econ. Paleontologists and Mineralogists Special Publication 27, Tulsa, Oklahoma, p. 307-326.

Hobday, D.K. and Reading, H., 1972, Fair weather versus storm processes in shallow marine sand bar sequences in the late Precambrian of Finmark, north Norway: Journal of Sedimentary Petrology, v. 42, p. 318-324.

Horowitz, D.H., 1966, Evidence for deltaic origin of an Upper Ordovician sequence in the central Appalachians, in, Shirley, M.L., ed., Deltas: Houston Geological Society, p. 159-169.

Houbolt, J.J.C., 1968, Recent sediments in southern bight of the North Sea: Geol. en Mijnbouw., v. 47, p. 245-273.

Howard, J.D. and Nelson, C.H., 1982, Sedimentary structures on a delta-influenced shallow shelf, Norton Sound, Alaska, in Nelson, C.H. and Nio, S.D., eds., The Northeastern Bering Shelf: New Perspectives of Epicontinental Shelf Processes and Depositional Processes: Geologie en Mijnbouw, v. 61, p. 29-36.

Howell, B.F., 1920, The Middle Cambrian beds at Manuels, Newfoundland, and their relations: American Philosophical Society, v. 51, no. 1330.

Hoyt, J.H., 1969, Chenier versus barrier: genetic and stratigraphic distinction: American Association of Petroleum Geologists Bulletin, v. 53, p. 299-306.

Hubert, J.F., 1972, Shallow-water prodelta flysch-like sequence in the upper Cretaceous deltaic rocks, Wyoming, and the problem of the origin of graded sandstones, in Proceedings, 24th International Geological Congress, Montreal, Section 6, Stratigraphy and Sedimentology: Geological Survey of Canada, Ottawa, p. 107-114.

Hubert, J.F. and Reed, A.A., 1978, Red-bed diagenesis in the East Berlin Formation, Newark Group, Connecticut Valley: Journal of Sedimentary Petrology, v. 48, no. 1, p. 175-184.

Hughes, C.J., 1970, The late Precambrian Avalonian orogeny in Avalon, southeast Newfoundland: American Journal of Science, v. 269, p. 183-190.

Hughes, C.J., 1972, Geology of the Avalon Peninsula, Newfoundland; and its possible correspondence with Morocco: Notes et Mem. du Serv. Geol. du Maroc, v. 236, p. 265-275.

Hughes, C.J., 1976, Volcanogenic cherts in the late Precambrian Conception Group, Avalon Peninsula, Newfoundland: Canadian Journal of Earth Sciences, v. 13, no. 4, p. 512-519.

Hunter, R.E. and Clifton, H.E., 1982, Cyclic deposits and hummocky cross-stratification of probable storm origin in Upper Cretaceous rocks of Cape Sebastian area, southwestern Oregon: Journal of Sedimentary Petrology, v. 52, p. 127-144.

Hutchinson, R.D., 1953, Geology of the Harbour Grace Map-area, Newfoundland: Canadian Geological Survey Memoir, v. 275, 43 p.

Hutchinson, R.D., 1962, Cambrian stratigraphy and trilobite faunas of southeastern Newfoundland: Geological Survey of Canada, Bulletin 88, 156 p.

Ingram, R.L., 1954, Terminology for the thickness of stratification and parting units in sedimentary rocks: Geological Society of America Bulletin, v. 65, p. 937-938.

Inman, D.L., 1957, Wave generated ripples in nearshore sands: U.S. Army Corps of Engineers, Beach Erosion Board, Technical Memo, 100.

Irving, E. and Strong, D.F., 1985, Paleomagnetism of rocks from Burin Peninsula, Newfoundland: hypothesis of Late Paleozoic displacement of Acadia criticized: Journal of Geophysical Research, v. 90, no B2, p. 1949-1962.

James, N.P., 1984a, Shallowing-upward sequences in carbonates, in Walker, R.G., ed., Facies Models: Geoscience Canada, Reprint Series 1, p. 213-228.

James, N.P., 1984b, Introduction to carbonate facies models, in Walker, R.G., ed., Facies Models: Geoscience Canada, Reprint Series 1, p. 209-211.

Jansa, L.F. and Fischbuch, N.R., 1974, Evolution of a Middle and Upper Devonian sequence from a clastic coastal plain - deltaic complex into overlying carbonate reef complexes and banks, Sturgeon - Mitsue area, Alberta: Geological Survey of Canada Bulletin, no. 234, 205 p.

Jenness, S.E., 1963, Terra Nova and Bonavista map-areas, Newfoundland: Geological Survey of Canada, Memoir 327, 184 p.

Jessen, W., 1932, Uber rezente und fossile Organismenpflaster: Palaont. Z., v. 14, p. 67-77.

Johnson, A.M., 1970, Physical Processes in Geology: Freeman, Cooper and Co., San Francisco, 577 p.

Johnson, H.D., 1975, Tide- and wave-dominated inshore and shoreline sequences from the late Precambrian, Finmark, North Norway: Sedimentology, v. 22, p. 45-74.

Johnson, H.D., 1977, Sedimentation and water escape structures in some late Precambrian shallow marine sandstones from Finmark, North Norway: Sedimentology, v. 24, p. 389-411.

Johnson, H.D., 1978, Shallow siliciclastic seas, in Reading, H. G., ed., Sedimentary environments and facies: Elsevier, New York, p. 207-258.

Johnson, K.G. and Friedman, G.M., 1969, The Tully clastic correlatives (Upper Devonian) of New York State: a model for recognition of alluvial, dune (?), nearshore (bar and lagoon), and offshore sedimentary environments in a tectonic delta complex: Journal of Sedimentary Petrology, v. 39, no. 2, p. 451-485.

Jopling, A.V. and Walker, R.G., 1968, Morphology and origin of ripple-drift cross-lamination, with examples from the Pleistocene of Massachusetts: Journal of Sedimentary Petrology, v. 38, p. 971-984.

Jungst, H., 1934, Geological significance of synaeresis: Geologische Rundschau, v. 25, p. 321-325.

Kazakov, A.V., 1937, The phosphorite facies and the genesis of phosphorites, in E.V. Britske, ed., Geological Investigations of Agricultural Ores, U.S.S.R.: 17th International Geological Congr. (U.S.S.R.), p. 95-113.

Kazmierczak, J. and Goldring, R., 1978, Subtidal flat-pebble conglomerate from the Upper Devonian of Poland: a multiprovenant high-energy product: Geological Magazine, v. 115, p. 359-366.

Keller, G.H., 1982, Organic matter and the geotechnical properties of submarine sediments: Geomarine Letters, v. 2, p. 191-198.

Kelling, G. and Mullins, P.R., 1975, Graded limestones and limestone — quartzite couplets: possible storm-deposits from the Moroccan Carboniferous: Sedimentary Geology, v. 13, p. 161-190.

Kennedy, W.Q., 1964, The structural differentiation of Africa in the Pan-African (± 500 Ma) tectonic episode: Res. Inst. Afr. Geol. Univ. Leeds, 8th Annual Report, p. 48-49.

Kidder, D.L., 1985, Petrology and origin of phosphate nodules from the midcontinent Pennsylvanian epicontinental sea: Journal of Sedimentary Petrology, v. 55, no. 6, p. 809-816.

King, A.F., 1980, The birth of the Caledonides: late Precambrian rocks of the Avalon Peninsula, Newfoundland, and their correlatives in the Appalachian Orogen, in Wones, D.R., ed., The Caledenides in the U.S.A.: Department of Geological Sciences, Virginia Polytechnic Institute and State University, Blacksburg, VA, Memoir 2, p. 3-8.

King, A.F. and Anderson, M.M., 1982, Bacon Cove unconformity and tillite, in King, A.F., ed., The Caledonide Orogen: Guidebook for Avalon and Meguma Zones: IGCP Project 27, Nato Advanced Study Institute Atlantic Canada, Stop 0-11, p. 58-60.

King, A.F., Brueckner, W.D., Anderson, M.M., and Fletcher, T.P., 1974, Late Precambrian and Cambrian sedimentary sequences of eastern Newfoundland: Guidebook for excursion B-6, Geological Association of Canada Annual Meeting, St. John's, Newfoundland, 59p.

King, A.F. and O'Brien, S.J., in press, Elements Pan-Africans des Appalaches de Terre Neuve et leurs Equivalents au Maroc: Notes et Memoires du Service Geologique du Maroc.

Klein, G. deV., 1967, Paleocurrent analysis in relation to modern marine sediment dispersal patterns: American Association of Petroleum Geologists, v. 51, p. 366-382.

Klein, G. deV., 1970a, Tidal origin of a Precambrian quartzite - the Lower Fine-grained Quartzite (Dalradian) of Scotland: Journal of Sedimentary Petrology, v. 40, p. 973-985.

Klein, G. deV., 1970b, Depositional and dispersal dynamics of intertidal sand bars: Journal of Sedimentary Petrology, v. 40, p. 1095-1127.

Klein, G. deV., 1971, A sedimentary model for determining paleotidal range: Geological Society of America Bulletin, v. 83, p. 2585-2592.

Klein, G. deV., 1977a, Clastic tidal facies: Continuing Education Publishing Company, Champaign, Illinois, 149 p.

Klein, G. deV., 1977b, Tidal circulation model for deposition of clastic sediments in epeiric and mioclinal shelf seas: Sedimentary Geology, v. 18, p. 1-12.

Klein, G. DeV., De Melo, U., and Favera, J.C.D., 1972, Subaqueous gravity processes on the front of Cretaceous deltas, Reconcavo Basin, Brazil: Geological Society of America Bulletin, v. 83, p. 1469-1492.

Kolb, C.R. and Van Lopik, J.R., 1966, Depositional environments of the Mississippi River Deltaic plain - southeastern Louisiana, in Deltas in their Geological Framework: Houston Geological Society, p. 17-61.

Komar, P.D., 1976, Beach processes and sedimentation: Prentice-Hall, Englewood Cliffs, New Jersey, p. 429.

Koning, H.L., 1982, On an explanation of marine flow slides in sand, in Saxov, S. and Nieuwenhuis, J.K., eds., Marine Slides and Other Mass Movements: Plenum Press, New York and London, p. 83-94.

Konopka, E.H. and Dott, R.H., Jr., 1983, Sandstone-Carbonate repetitive alternations: Butterfield Peaks Formation (Middle Pennsylvanian), Oquirrh Group, Central Utah: (Abstract) American Association of Petroleum Geologists Bulletin, v. 67, no. 3, p. 497.

Kraft, L.M., Helfrich, S.C., Suhayda, J.N., and Marin, J.E., 1985, Soil response to ocean waves: Marine Geotechnology, v. 6, p. 173-203.

Kreisa, R.D., 1981, Storm-generated sedimentary structures in subtidal marine facies with examples from Middle and Upper Ordovician of southwestern Virginia: Journal of Sedimentary Petrology, v. 51, p. 823-848.

Krogh, T.E., Strong, D.F., and Papezik, V., 1983, Precise U-Pb ages of zircons from volcanic and plutonic units in the Avalon Peninsula: Geological Society of America, Northeastern Section, Abstracts with Programs, 15, p. 135.

Krumbein, W.C. and Garrels, R.M., 1952, Origin and Classification of Chemical Sediments in Terms of pH and Oxidation-Reduction Potentials: Journal of Geology, v. 60, no. 1, p. 1-33.

Kuenen, P.H., 1957, Sole markings of graded graywacke beds: Journal of Geology, v. 65, no. 3, 231-258.Landing, E. and Benus, P., 1984, Lithofacies of the Smith Point (Lower Cambrian, Eastern Newfoundland) and the lowest occurrence of trolobites: Geological Association of America, Northeastern Section, Abstract with Programs, v. 16, no. 1, p. 45.

Leckie, D. and Duke, W., 1984, Origin of hummocky cross stratification; Part 1. Straight-crested, symmetrical gravel dunes; The coarse-grained equivalent of HCS: Sedimentology of Shelf Sand and Sandstones — Research Symposium of Canadian Society of Petroleum Geology, p. 51.

Leckie, D.A. and Walker, R.G., 1982, Storm- and tide-dominated shorelines in Cretaceous Moosebar—Lower Gates interval — outcrop equivalents of Deep Basin gas trap in western Canada: American Association of Petroleum Geologists Bulletin, v. 66, no. 2, p. 138-157.

Leithold, A.L. and Bourgeois, J., 1984, Characteristics of coarse-grained sequences deposited in nearshore, wave-dominated environments - examples from the Miocene of south-west Oregon: Sedimentology, v. 31, p. 749-775.

Levell, B.K., 1980a, A late Precambrian tidal shelf deposit, the Lower Sandfjord Formation, North Norway: Sedimentology, v. 27, p. 539-557.

Levell, B.K., 1980b, Evidence for currents associated with waves in Late Precambrian shelf deposits from Finmark, North Norway: Sedimentology, v. 27, p. 153-166.

Lilly, H.D., 1966, Late Precambrian and Appalachian tectonics in the light of submarine exploration of the Great Bank of Newfoundland in the Gulf of St. Lawrence: preliminary views: American Journal of Science, v. 264, p. 569-574.

Lindsay, J.E., Prior, D.B., and Coleman, J.M., 1984, Distributary-mouth bar development and role of submarine landslides in delta growth, South Pass, Mississippi Delta: American Association of Petroleum Geologists, v. 68, no. 11, p. 1732-1743.

Lowe, D.R., 1976a, Subaqueous liquefied and fluidized sediment flows and their deposits: Sedimentology, v. 23, p. 285-308.

Lowe, D.R., 1976b, Grain flow and grain flow deposits: Journal of Sedimentary Petrology, v. 46, no. 1, p. 188-199.

Mack, W.G. and James, W.C., 1986, Cyclic sedimentation in the mixed siliciclastic-carbonate Abo-Hueco Transition Zone (Lower Permian), southwestern New Mexico: Journal of Sedimentary Petrology, v. 56, no. 5, p. 635-647.

Martinson, A., 1965, Aspects of a Middle Cambrian thanatotope on Oland: Geologiska Foreningens i Stockholm Forhandlingar, v. 87, p. 181-230.

Matthews, S.C. and Cowie, J.W., 1979, Early Cambrian transgression: Journal of the Geological Society of London, v. 136, p. 133-135.

Maxwell, G.H. and Swinchatt, J.P., 1970, Great Barrier Reef: regional variation in a terrigenous-carbonate province: Geological Society of America Bulletin, v. 81, p. 691-724.

Maynard, J.B., 1982, Extension of Berner's "new geochemical classification of sedimentary environments" to ancient sediments: Journal of Sedimentary Petrology, v. 52, no. 4, p. 1325-1331.

Mazzullo, S.J., 1978, Early Ordovician tidal flat sedimentation, Western Margin of Proto-Atlantic Ocean: Journal of Sedimentary Petrology, v. 48, no. 1, p. 49-62.

McBride, E.F., 1974, Significance of color in red, green, purple, olive, brown and gray beds of Difunta Group, northeastern Mexico: Journal of Sedimentary Petrology, v. 44, p. 760-773.

McBride, E.F., Weidie, A.E., and Wolleben, J.A., 1975, Deltaic and associated deposits of Difunta Group (Late Cretaceous to Palaeocene), Parras and La Popa Basins, northeastern Mexico, in Broussard, M.L., ed., Deltas: Models for Exploration, Houston Geological Society, Houston, P. 485-522.

McCartney, W.D., 1967, Whitbourne Map-area, Newfoundland: Canadian Geological Survey Memoir, v. 341, 135 p.

McCave, I.N., 1969, Correlation using a sedimentological model of part of the Hamilton Group (Middle Devonian), New York State: American Journal of Science, v. 267, p. 567-591.

McCave, I.N., 1973, The sedimentology of a transgression: Portland Point and Cooksburg Members (Middle Devonian), New York State: Journal of Sedimentary Petrology, v. 43, no. 2, p. 484-504.

McCave, I.N., 1985, Recent shelf clastic sediments, in Brenchley, P.J. and Williams, B.P.J., eds., Sedimentology: recent developments and applied aspects: Blackwell Scientific Publications, England, p. 49-65.

McCrory, V.L. and Walker, R.G., 1986, A storm and tidally-influenced prograding shoreline — Upper Cretaceous Milk River Formation of Southern Alberta, Canada: Sedimentology, v. 33, p. 47-60.

McCullough, W.F., 1984, Commercial sand-gauge card: Distributed by W.F. McCullough, 3101 Eldridge ct., Beltsville, Maryland, U.S.A., 20705.

McGregor, B.A., 1981, Smooth seaward-dipping horizons — an important factor in sea-floor stability: Marine Geology, v. 39, p. M89-98.

McIlreath, I. and Ginsburg, R.N., 1982, (conveners), Symposium 27: mixed deposition of carbonate and siliciclastic sediments: International Association Sedimentologists, Abstract Papers, Eleventh International Congress Sedimentology, p. 109-113.

McKee, E.D., 1945, Cambrian history of the Grand Canyon region: Carnagie Inst. Wash. Publ., pt. 1, 230 p.

McKee, E.D., 1965, Experiments on ripple lamination, in Middleton, G.V., ed., Primary sedimentary structures and their hydrodynamic interpretation: Society of Economic Paleontologists and Mineralogists, Special Publication 12, p. 66-83.

McPherson, J.G., 1980, Genesis of variegated redbeds in the fluvial Aztec Siltstone (Late Devonian), Southern Victoria Land, Antarctica: Sedimentary Geology, v. 27, p. 119-142.

Meckel, L.D., 1975, Holocene Sand Bodies in the Colorado Delta Area, Northern Gulf of California, in Broussard, M.L., ed., Deltas: Models for Exploration: Houston Geological Society, Houston, Texas, p. 239-265.

Meischner, K.D., 1967, Palokogische Untersuchungen an gebankten Kalken — Ein Diskussions- Beitrag: Geologiska Foreningens i Stockholm Forhandlingar, v. 89, p. 465-469.

Middleton, G.V., 1967, Experiments on density and turbidity currents, III. Deposition of sediment: Canadian Journal of Earth Sciences, v. 4, p. 475-505.

Middleton, G.V., 1969, Grain flows and other mass movements down slopes, in Stanley, D. J., ed., The New Concepts of Continental Margin Sedimentation: American Geol. Institute, Short Course Lecture Notes, p. GM-B-1 to GM-B-14,

Middleton, G.V., 1970, Experimental studies related to problems of flysch sedimentation, in Lajoie, J., ed., Flysch Sedimentology in North America: Geological Association of Canada, Special Paper Number 7, p. 253-272.

Middleton, G.V. and Hampton, M.A., 1973, Sediment Gravity Flows: Mechanics of Flow and Deposition, in Turbidites and Deep Water Sedimentation: Society of Economic Paleontologists and Mineralogists, Pacific Section, Short Course Notes, p. 1-38.

Middleton, G.V. and Southard, J.B., 1977, Mechanics of sediment movement: Society of Economic Paleontologists and Mineralogists, Short Course 3, 246 p.

Middleton, G.V. and Southard, J.B., 1984, Mechanics of sediment movement: Society of Economic Paleontologists and Mineralogists, Short Course 3, 2nd edition, 262 p.

Miller, M.C. and Komar, P.D., 1980, Oscillation sand ripples generated by laboratory apparatus: Journal of Sedimentary Petrology, v. 50, p. 173-182.

Misra, S.B., 1969, Late Precambrian (?) fossils from southeastern Newfoundland: Geological Society of America Bulletin, v. 80, p. 2133-2140.

Moore, D.G., 1961, Submarine slumps: Journal of Sedimentary Petrology, v. 31, no. 3, p. 343-357.

Morganstern, R.N., 1967, Submarine slumping and the initiation of turbidity currents, in Richards, A. F., ed., Marine Geotechnique: Chicago Univ. Illinois Press. p. 189-220.

Morris, R.C., 1971, Classification and interpretation of disturbed bedding types in Jackfork Flysch rocks (Upper Mississippian), Ouachita Mountains, Arkansas: Journal of Sedimentary Petrology, v. 41, no. 2, p. 410-424.

Mount, J.F., 1984, Mixing of siliciclastic and carbonate sediments in shallow shelf environments: Geology, v. 12, p. 432-435.

Murray, S.P., Roberts, H.H., and Young, M.H., 1983, Control of terrigenous-carbonate facies transitions by Baroclinic coastal currents: Abstract, American Association of Petroleum Geologists Bulletin, v. 67, p. 522-523.

Myrow, P.M., 1983, A paleoenvironmental analysis of the Cheshire Formation, west central Vermont: Unpublished M.Sc. thesis, University of Vermont, Burlington, Vermont, 177 p.

Myrow, P.M., 1985, Shelf sedimentation across Precambrian-Cambrian boundary: Chapel Island Formation, Southeastern Newfoundland: Abstract, American associaiton of Petroleum Geologists Bulletin, v. 69, no. 2, p. 291.

Nagtegaal, P.J.C., 1966, Scour and Fill Structures From a Fluvial Piedmont Environment: Geologie En Mijnbouw, v. 45, p. 342-354.

Nair, R.R., 1976, Unique mud banks, Kerala, Southwest India: American Association of Petroleum Geologists Bulletin, v. 60, p. 616-621.

Nance, R.D. and Socci, A.D., 1987, Late Precambrian arc-platform transitions in the Avalon Terrane of the northern Appalachians: Geological Society of America, Northeastern Section, Abstract with Programs, v. 19, no. 1, p. 32.

Narbonne, G.M., Myrow, P., Landing, E., and Anderson, M.M., 1987, A candidate stratotype for the Precambrian-Cambrian boundary, Fortune Head, Burin Peninsula, Southeastern Newfoundland: Canadian Journal of Earth Sciences, Manuscript submitted February 13, 1987.

Nardin, T.R., Hein, F.J., Gorsline, D.S., and Edwards, B.D., 1979, A review of mass movement processes, sediment and acoustic characteristics, and contrasts in slope and base-of-slope systems versus canyon-fan-basin floor systems, in Doyle, L.J. and Pilkey, O.H., eds., Geology of Continental Slopes: Society of Economic Paleontologists and Mineralogists, Special Pub. 27, p. 61-73.

Nelson, C.H., 1982, Modern shallow-water graded sand layers from storm surges, Bering shelf: a mimic of Bouma sequences and turbidite systems: Journal of Sedimentary Petrology, v. 52, no. 2, p. 537-545.

Newton, R.S., 1968, Internal structure of wave-formed ripples in the nearshore zone: Sedimentology, v. 11, p. 275-292.

Niehoff, R., 1958, Die Primar Sedimentstrukturen Inbesondere die Schragschichtung im Koblenzquarzit am Mittlerhein: Geol. Rundschau, v. 47, p. 252-371.

Norrman, J.O., 1964, Lake Vatern: Investigations on shore and bottom morphology: Geograf. Ann., v. 46, 238p.

Nottvedt, A. and Kreisa, R.D., 1987, Model for the combined-flow origin of hummocky cross-stratification: Geology, v. 15, p. 357-361.

O'Brien, S.J., Strong, P.G., and Evans, J.L., 1977, The geology of the Grand Bank (1 M/4) and Lamaline (1 L/13) map areas, Burin Peninsula, Newfoundland: Mineral Development Division, Department of Mines and Energy, Government of Newfoundland and Labrador, Report 77-7, 16 p.

O'Brien, S.J., Strong, D.F., Strong, P., Taylor, S., and Wilton, D., 1976, Geology of the Marystown - St. Lawrence area: Newfoundland Dept. of Mines and Energy, Mineral Development Division, Report 76-1, p. 64-70.

O'Brien, S.J. and Taylor, S.W., 1983, Geology of the Baine Harbour (1 M/7) and Point Enragee (1 M/6) map areas, Burin Peninsula Newfoundland: Mineral Development Division, Department of Mines and Energy, Government of Newfoundland and Laborador, Report 83-5, 70 p.

O'Brien, S.J., Wardle, R.J., and King, A.F., 1983, The Avalon Zone: A Pan-African terrane in the Appalachian Orogen of Canada: Geological Journal, v. 18, p. 195-222.

Papezik, V.S., 1970, Petrochemistry of volcanic rocks of the Harbour Main Group, Avalon Peninsula, Newfoundland: Candian Journal of Earth Sciences, v. 7, no. 6, p. 1485-1498.

Perkins, R.D. and Enos, P., 1968, Hurricane Betsy in the Florida-Bahama area: Geological effects and comparison with Hurricane Donna: Journal of Sedimentary Petrology, v. 76, p. 710-717.

Pettijohn, F.J., 1949, Sedimentary rocks: Harper and Bros., New York, 526 p.

Pettijohn, F.J., 1975, Sedimentary rocks: Harper and Row, Company, New York, 628 p.

Pettijohn, F.J., Potter, P.E., and Siever, R., 1973, Sand and sandstones: Springer-Verlag, New York, Heidelberg, Berlin, 618 p.

Picard, M.D., 1965, Iron oxide and fine-grained rocks of Red Peak and Crow Mountain Sandstone Members, Chugwater (Triassic) Formation, Wyoming: Journal of Sedimentary Petrology, v. 35, p. 464-479.

Picard, M.D. and High, L.R., 1969, Some sedimentary structures resulting from flash floods, in Jensen, M.L., ed., Guidebook of Northern Utah: Bulletin Utah Geological Mineral. Survey, v. 82, p. 175-190.

Pickering, K.T., 1983, Small scale syn-sedimentary faults in the Upper Jurassic 'Boulder Beds': Scottish Journal Geology, v. 2, p. 169-181.

Pierson, T.C., 1981, Dominant particle support mechanisms in debris flows at Mt. Thomas, New Zealand, and implications for flow mobility: Sedimentology, v. 28, p. 49-60.

Piper, D.J.W., 1972, Turbidite origin of some laminated mudstones: Geological Magazine, v. 109, p. 115-126.

Piper, D.J.W., 1978, Turbiditic muds and silts on deep-sea fans and abyssal plains, in Stanley, D.J. and Kelling, G., eds., Sedimentation in Submarine Canyon, Fans and Trenches: Dowden, Hutchinson and Ross, Stroudsburg, PA, p. 163-176.

Plessman, W., 1961, Stromungsmärken in klastischen Sedimenten und ihre geologische Auswertung: Geol. Jarbuch, v. 78, p. 503-566.

Plummer, P.S. and Gostin, V.A., 1981, Shrinkage cracks: Desiccation or synaeresis?: Journal of Sedimentary Petrology, v. 51, no. 4, p.1147-1156.

Postma, H., 1967, Sediment transport and sedimentation in the estuarine environment, in Lauff, G.H., ed., Estuaries: American Association for the Advancement of Science, Spec. Pub. 83, Washington, D.C., p. 158-179.

Potter, D.B., 1949, Geology of the Fortune - Grand Bank area, Burin Peninsula, Newfoundland, Canada: Unpublished M.Sc. thesis, Brown University.

Potter, P.E., 1963, Late Paleozoic sandstones of the Illinois Basin: Illinois State Geological Survey Report of Investigations, no. 217, 92 p.

Potter, P.E., Maynard, J.B., and Pryor, W.A., 1980, Sedimentology of Shale: Springer-Verlag, New York, 306 p.

Pound, C.J., 1984, HCS: Problems, perspectives and misunderstandings: Sedimentology of Shelf Sand and Sandstones — Research Symposium of Canadian Society of Petroleum Geology, p. 59.

Prentice, J.E., 1962, Some sedimentary structures from a Weald Clay Sandstone at Warnham Brickworks, Horsham, Sussex: Proceedings Geological Association, v. 73, p. 171-185.

Prior, D.B., Bornhold, B.D., and Johns, M.W., 1984, Depositional characteristics of a submarine debris flow: Journal of Geology, v. 92, p. 707-727.

Prior, D.B. and Coleman, J.M., 1982, Active slides and flows in underconsolidated marine sediments on the slopes of the Mississippi delta, in Saxov, S. and Nieuwenhuis, J.K., eds., Marine slides and other mass movements, Nato Conference Series 4, Marine Sciences, v. 6: Plenum Press, New York, p. 21-49.

Prior, D.B., Yang, Z.-S., Bornhold, B.D., Keller, G.H., Lu, N.Z., Wiseman, W.J., Jr., Wright, L.D., and Zhang, J., 1986, Active slope failure, sediment collapse, and silt flows on the modern subaqueous Huanghe (Yellow River) Delta: Geomarine Letters, v. 6, p. 85-95.

Raaben, M.E. (ed.), 1969, The Tommotian Stage and the Cambrian lower boundary problem (translation published in 1981): New Delhi, Amerind, 359 p.

Raiswell, R. and Berner, R.G., 1985, Pyrite formation in euxinic and semi-euxinic sediments: American Journal of Science, v. 285, p. 710-724.

Rast, N., O'Brien, B.H., and Wardle, R.J., 1976, Relationships between Precambrian and Lower Palaeozoic Rocks of the "Avalon Platform' in New Brunswick, the Northeast Appalachians and the British Isles: Tectonophysics, v. 30, p. 315-338.

Rast, N. and Skehan, S.J., 1987, Late Proterozoic geologic setting of the Boston basin: Geological Association of America, Northeastern Section, Abstract with Programs, v. 19, no. 1, p. 53.

Redfield, H.E., 1958, The influence of the continental shelf on the tides of the Atlantic Coast of the United States: Journal Marine Research, v. 17, p. 432-448.

Reineck, H-E., 1961, Sedimentbewegung an kleinrippeln im watt: Senckenbergiana Lethaea, v. 42, p. 51-61.

Reineck, H-E., 1963, Sedimentgefuge im Bereich der sudlichen Nordsee: Abhandl. Senckenbergische Naturforsch. Gesell., v. 505, 138 p.

Reineck, H-E., 1967, Layered sediments of tidal flats, beaches and shelf bottoms of the North Sea, in G.H., Lauff, ed., Estuaries: American Association for the Advancement of Science, Spec. Pub. 83, Washington, D.C., p. 191-206.

Reineck, H-E., 1975, German North Sea tidal flats, in Ginsburg, R.N., ed., Tidal Deposits: Springer-Verlag, New York, p. 5-12.

Reineck, H.E. and Singh, I.B., 1972, Genesis of laminated sand and graded rhythmites in storm-sand layers of shelf mud: Sedimentology, v. 18, p. 123-128.

Reineck, H-E and Singh, I.B., 1973, Depositional sedimentary environments — with reference to terrigenous clastics: Springer-Verlag, Berlin, 439 p.

Reineck, H-E. and Singh, I.B., 1980, Depositional sedimentary environments: Springer-Verlag, New York, 549 p.

Reineck, H-E. and Wunderlich, F., 1967, Zeitmessungen an Gezeitenschichten: Nat. Mus., v. 97, p. 193-197.

Reineck, H-E. and Wunderlich, F., 1968, Classification and origin of flaser and lenticular bedding: Sedimentology, v. 2, p. 99-104.

Rhoads, D. C. and Morse, J. W., 1971, Evolutionary and ecologic significance of oxygen-deficient marine basins: Lethaia, v. 4, p. 413-428.

Rich, J.L., 1951, Three critical environments of deposition and criteria for recognition of rock deposited in each of them: Geological Society of America Bulletin, v. 62, p. 1-20.

Richards, M.T., 1986, Arrangement of wave- and tide-dominated shelf sequences in the Lower Triassic, France: Changes in shelf hydraulic regime due to variation in shelf width: Geological Society of America, Abstracts with Programs, v. 18, no. 6, p. 730.

Richter, D., 1967, Sedimentology and Facies of the Meadfoot Beds (Lower Devonian) in South-east Devon (England): Geologische Rundschau, v. 56, p. 543-561.

Rine, J.M. and Ginsburg, R.N., 1985, Depositional facies of a mud shoreface in Suriname, South America - a mud analogue to sandy, shallow-marine deposits: Journal of Sedimentary Petrology, v. 55, no. 5, p. 633-652.

Roberts, H.H., 1980, Sediment characteristics of Mississippi River delta-front mudflow deposits, in Transactions Gulf Coast Association Geological Societies: v. 30, p. 485-496.

Rodine, J.D. and Johnson, A.M., 1976, The ability of debris, heavily freighted with coarse clastic materials, to flow on gentle slopes: Sedimentology, v.23, p. 213-234.

Roehl, P.O., 1967, Stony Mountain (Ordovician) and Interlake (Silurian) facies analogs of recent low-energy marine and subaerial carbonates, Bahamas: American Association of Petroleum Geologists, v. 51, no. 10, p. 1979-2023.

Rubin, D.M. and McCulloch, D.S., 1980, Single and superimposed bedforms: a synthesis of San Francisco Bay and flume observations: Sedimentary Geology, v. 26, p. 207-231.

Rupke, N.A. and Stanley, D.J., 1974, Distinctive properties of turbiditic and hemipelagic mud layers in the Algero-Balearic Basin, Western Mediterranean Sea: Smithsonian Contributions to the Earth Sciences, Washington, v. 13, 40p.

Russell, J.R. and Russell, R.D., 1939, Mississippi River Delta sedimentation, in Recent Marine sediments: American Association of Petroleum Geologists Bulletin, v. 14, p. 153-177.

Rust, I.C., 1977, Evidence of shallow marine and tidal sedimentation in the Ordovician Graafwater Formation, Cape Province, South Africa: Sedimentary Geology, v. 18, p. 123-133.

Sanderson, D. and Donovan, R. N., 1974, The vertical packing of shells and stones on some recent beaches: Journal of Sedimentary Petrology, v. 44, no. 3, p. 680-688.

Savrda, C.E. and Bottjer, D.J., 1986, Trace-fossil model for reconstruction of paleo-oxygenation in bottom waters: Geology, v. 14, p. 3-6.

Savrda, C.E. and Bottjer, D.J., and Gorsline, D.S., 1984, Towards development of comprehensive euxinic biofacies model: evidence from Santa Monica, San Pedro, and Santa Barbara Basins, California Borderland: American Association of Petroleum Geologists Bulletin, v. 68, p. 1179-1192.

Saxov, S. 1982, Marine slides — some introductory remarks, in Saxov, S. and Nieuwenhuis, J.K., eds., Marine Slides and Other Mass Movements: Plenum Press, New York and London, p. 1-7.

Schafer, W., 1956, Wirkungen der Benthos-organismen auf der jungen Schichtverband: Senckenbergiana Lethaea, b. 37, p. 183-263.

Schenk, P.E., 1971, Southeastern Atlantic Canada, northwestern Africa, and continental drift: Canadian Journal of Earth Sciences, v. 8, p. 1218-1251.

Schroder, V.L., 1965, Zur Sedimentologie des Mittleren Buntsandsteins: Geol. Jahrbuch, v. 82, p. 655-704.

Schuller, M., 1967, Petrographie und Feinstratigraphie des Unteren Muschelkakes in Sudniedersachsen und Nordhessen: Sedimentary Geology, v. 1, no. 4, p. 353-401.

Schwarz, H.-U., 1975, Sedimentary structures and facies analysis of shallow marine carbonates: Contributions to Sedimentology, v. 3, p. 1-100.

Scruton, P.C., 1960, Delta building and deltaic sequence, in Recent sediments, northwest Gulf of Mexico: American Association of Petroleum Geologists Bulletin, p. 82-102.

Seed, H.B., 1968, Landslides during earthquakes due to soil liquefaction: American Society Civil Engineering Journal, Soil Mech. Foundations Div., v. 94, no. SM5, p. 1053-1122.

Seilacher, A., 1982, Distinctive Features of Sandy Tempestites, in Einsele, G. and Seilacher, A., eds., Cyclic and Event Stratification: Springer-Verlag, Berlin, p. 333-349.

Shepard, F.P., 1955, Delta front valleys bordering the Mississippi distributaries: Geological Society of America Bulletin, v. 66, p. 1489-1498.

Shepard, F.P. and Dill, R.F., 1966, Submarine canyons and other sea valleys: Rand McNally, Chicago, 391 p.

Shinn, E.A., 1972, Worm and algal-built stromatolites in the Persian Gulf: Journal of Sedimentary Petrology, v. 42, no. 4, p. 837-840.

Shultz, A.W., 1984, Subaerial debris-flow deposition in the upper Paleozoic Cutler Formation, western Colorado: Journal of Sedimentary Petrology, v. 54, no. 3, p. 759-772.

Singh, I.B., 1969, Primary sedimentary structures in Precambrian quartzites of Telemark, southern Norway, and their significance: Norsk Geologisk Tidsskrift, v. 49, p. 1-31.

Sleath, J.F.A., 1976, On rolling-grain ripples: Journal Hydraul. Res., v. 14, p. 69-81.

Smith, S.A. and Hiscott, R. N., 1983, Latest Precambrian to Early Cambrian basin evolution, Fortune Bay, Newfoundland: fault-bounded basin to platform: Canadian Journal Earth Sciences, v. 21, p. 1379-1392.

Sorauf, J.E., 1965, Flow rolls of upper Devonian rocks of south-central New York State: Journal of Sedimentary Petrology, v. 35, no. 3, p. 553-563.

Southard, J.B., 1984, Laboratory studies of oscillatory-flow bed configurations and their bearing on stratification in shallow-marine sands: Sedimentology of Shelf Sands and Sandstones - Canadian Society of Petroleum Geologists Research Symposium Program with Abstracts, p. 65.

Stanley, D.J., 1975, Submarine canyon and slope sedimentation (Gres D'Annot) in the French Maritime Alps: Ninth International Congress of Sedimentology, Nice, 131 p.

Stanley, D.J., 1981, Unifites: structureless muds of gravity-flow origin in Mediterranean basins: Geo-Marine Letters, v. 1, p. 77-83.

Stanley, D.J., 1982, Welded slump-graded sand couplets: evidence for slide generated turbidity currents: Geo-marine letters, v. 2, p. 149-155.

Stanley, D.J. and Maldonado, A., 1981, Depositional models for fine-grained sediments in the western Hellenic Trench, Eastern Mediterranean: Sedimentology, v. 28, p. 273-290.

Stanley, D.J., Rehault, J.P., and Stuckenrath, R., 1980, Turbid-layer bypassing model: The Corsican Trough, Northwestern Mediterranean: Marine Geology, v. 37, p. 19-40.

Stow, D.A.V. and Bowen, A.J., 1980, A physical model for the transport and sorting of fine-grained sediments by turbidity currents: Sedimentology, v. 27, p. 31-46.

Stow, D.A.V. and Shanmugam, G., 1980, Sequence of structures in fine-grained turbidites: comparison of recent deep-sea and ancient flysch sediments: Sedimentary Geology, v. 25, p. 23-42.

Strong, D.F., 1979, Proterozoic tectonics of Northwestern Gondwanaland: New evidence from Eastern Newfoundland: Tectonophysics, v. 54, p. 81-101.

Strong, D.F., O'Brien, S.J., and O'Driscoll, C.F., 1980, Stratigraphy and volcanology of the Western Avalon Zone of Newfoundland-from Proterozoic oceanic crust to Carboniferous ignimbrites: Geological Association of Canada Field Trip Guidebook, Trip 2, 20 p.

Strong, D.F., O'Brien, S.J., Taylor, S.W., Strong, P.G., and Wilton, D.H., 1978a, Geology of the Marystown and St. Lawrence Map areas: Newfoundland Dept. of Mines and Energy, Mineral Development Division, Report 77-8, 81 p.

Strong, D.F., O'Brien, S.J., Taylor, S.W., Strong, P.G., and Wilton, D.H., 1978b, Aborted Proterozoic rifting in eastern Newfoundland: Canadian Journal Earth Sciences, v. 15, p. 117-131.

Strong, P.G., 1976, Geology of the Lawn area, Southeast Newfoundland: Unpublished Honours Thesis, Memorial University of Newfoundland, 68 p.

Swett, K., Klein, G. DeV., and Smit, D.E., 1971, A Cambrian tidal sand body - the Eriboll Sandstone of Northwest Scotland: an ancient-recent analog: Journal Geology, v. 79, p.400-415.

Swift, D.J.P., 1984, What are the fluid and sediment dynamics of modern shelves and their implications for the rock record?: Sedimentology of Shelf Sand and Sandstones — Research Symposium of Canadian Society of Petroleum Geology, p. 67.

Swift, D.J.P., Figueiredo, A.G., Freeland, G.L., and Oertal, G.F., 1983, Hummocky cross-stratification and megaripples: a geological double standard?: Journal of Sedimentary Petrology, v. 53, p. 1295-1317.

Swift, D.J.P. and Thorne, J., 1986, Role of tidal currents in shelf sedimentation: Geological Society of America, Abstracts w/ Programs, v. 18, no. 6, p. 767.

Tankard, A.J. and Hobday, D.K., 1977, Tide-dominated back-barrier sedimentation, Early Ordovician Cape Basin, Cape Peninsula, South Africa: Sedimentary Geology, v. 18, p. 135-159.

Taylor, S.W., 1976, Geology of the Marystown map sheet (E/2), Burin Peninsula, Newfoundland: Unpublished M.Sc. thesis, Memorial University, St. John's, Newfoundland, Canada.

Terwindt, J.H.J., 1981, Origin and sequences of sedimentary stuctures in inshore mesotidal deposits of the North Sea, in Nio, S.D., Shuttenhelm, P.T.E., and van Weering, T., eds., Holocene Marine Sedimentation in the North Sea Basin: International Association of Sedimentologists Special Publication no. 5, p. 4-26.

Terzaghi, K., 1950, Mechanisms of landslides: Harvard University Department of Engineering Publication 488, Soil Mechanics Series 36, 40 p.

Terzaghi, K., 1956, Varieties of submarine slope failures: Proceedings 8th Texas Soil Mech. Foundation Engineering, 41p.

Terzaghi, K. and Peck, R.B., 1948, Soil Mechanics in Engineering Practice: John Wiley and Sons, New York, 566 p.

Thompson, A.M., 1970, Geochemistry of color genesis in red-bed sequence, Juniata and Bald Eagle Formations, Pennsylvania: Journal of Sedimentary Petrology, v. 40, p. 599-615.

Thompson J.B., Mullins, H.T., Newton, C.R., and VerCoutere, T.L., 1985, Alternative biofacies model for dysaerobic communities: Lethaia, v. 18, p. 167-179.

Thompson, W.O., 1937, Original structures of beaches, bars, and dunes: Geological Society of America Bulletin, v.48, p. 192-219.

Tomlinson, C.W., 1916, The origin of red beds: American Journal of Science, v. 42, p. 153-179.

Trask, P.D., 1959, Effects of grain size on strength of mixtures of clay, sand and water: Geological Society of America Bull, v. 70, p. 569-580.

Trowbridge, A.C., 1930, Building of Mississippi Delta: American Association of Petroleum Geologists Bulletin, v. 14, p. 867-901.

Tucker, M.E., 1969, Crinoidal Turbidites from the Devonian of Cornwall and their paleogeographic significance: Sedimentology, 13, p. 263-280.

Twenhofel, W.H., 1947, The Silurian strata of eastern Newfoundland with some data relating to physiography and Wisconsin glaciation of Newfoundland: American Journal of Science, v. 245, p. 65-122.

Vail, P.R., Mitchum, R.M., Jr., and Thompson, S., 1977, Seismic stratigraphy and global changes in sea level. Part 3: Relative changes in sea level from coastal onlap. Part 4: Global cycles of relative changes of sea level, in Payton, C.E., ed., Seismic stratigraphy — Applications to Hydrocarbon Exploration: American Association of Petroleum Geologists, Memoir 26, p. 63-98.

Van Eden, J.G., 1970, A reconnaissance of deltaic environment in the Middle Eocene of the south-central Pyenees, Spain: Geologie en Mijnbouw, v. 49, no. 2, p. 145-157.

Van Houton, F.B., 1973, Origin of red beds - a review: 1961-1972: Earth Planetary Science Annual Review, v. 1, p. 39-61.

Van der Knaap, W. and Eijpe, R., 1968, Some experiments on the genesis of turbidity currents, Sedimentology, v. 11, p.115-124.

Van der Lingen, G.J., 1969, The turbidite problem: New Zealand Journal Geology and Geophysics, v. 12, p. 7-50.

Van Straaten, L.M.J.U., 1950, Environments of formation and facies of the Wadden Sea sediments: Koninkl. Ned. Aardrijkskde Genoot., v. 64, p. 94-108.

Van Straaten, L.M.J.U., 1953a, Megaripples in the Dutch Wadden Sea and in the Basin of Arecachon (France): Geol. Mijnbouw, v. 15, p. 1-11.

Van Straaten, L.M.J.U., 1953b, Rhythmic pattern on Dutch North Sea beaches: Geol. Mijnbouw, v. 15, p. 31-43.

Van Straaten, L.M.J.U., 1954a, Composition and structure of Recent marine sediments in the Netherlands: Leidse Geol. Mededel., v. 19, p. 1-110.

Van Straaten, L.M.J.U., 1954b, Sedimentology of Recent tidal flat deposits and the psammites du Condroz (Devonian): Geol. Mijnbouw, v. 16, p. 25-47.

Van Straaten, L.M.J.U., 1959, Minor structures of some recent littoral and neritic sediments: Geol. Mijnbouw, v. 21, p. 197-216.

Van Straaten, L.M.J.U. and Kuenen, Ph.H., 1958, Tidal action as a cause of clay accumulation: Journal of Sedimentary Petrology, v. 28, p. 406-413.

Veeh, H.H., Burnett, W.C., and Soutar, A., 1973, Contemporary phosphorites on the continental margin of Peru: Science, v. 181, p. 844-845.

Von Brunn, V. and Hobday, D.K., 1976, Early Precambrian tidal sedimentation in the Pongola Supergroup of South Africa: Journal of Sedimentary Petrology, v. 46, p. 670-679.

Vos, R.G. and Eriksson, K.A., 1977, An embayment model for tidal and wave swash deposits occurring within a fluvially dominated Middle Proterozoic sequence in South Africa: Sedimentary Geology, v. 18, p. 161-173.

Walcott, C.D., 1900, Lower Cambrian terrane in the Atlantic province: Proceedings of the Washington Academy of Sciences, v. 1, p. 301-339.

Walker, R.G., 1965, The origin and significance of the internal sedimentary structures of turbidites: Proceedings Yorkshire Geological Society, v. 35, p. 1-32.

Walker, R.G., 1969, The juxtaposition of turbidite and shallow-water sediments — study of a regressive sequence in the Pennsylvanian of North Devon, England: Journal of Geology, v. 77, no. 2, p. 125-143.

Walker, R.G., 1979, Shallow marine sands, in Walker, R.G., ed., Facies Models: Geoscience Canada, Reprint Series 1, p. 75-89.

Walker, R.G., 1982, Hummocky and swaley cross stratification, in Walker, R.G., ed., Excursion 21A., Clastic units of the Front Ranges, Foothills and Plains in the area between Field, B.C., and Drumheller, Alberta: International Association of Sedimentologists, Field Excursion Guidebook, 11th International Congress, Hamilton, Ontario, p. 22-30.

Walker, R.G., 1984, Shelf and shallow marine sands, in Walker, R.G., ed., Facies Models: Geoscience Canada, Reprint Series 1, p. 141-170.

Walker, R.G., Duke, W.L., and Leckie, D.A., 1983, Hummocky stratification: Significance of its variable bedding sequences: Discussion and reply: Geological Society of America Bulletin, v. 94, p. 1245-1251.

Walker, T.R., 1967, Formation of red beds in modern and ancient deserts: Geological Society of America Bulletin: v. 78, p. 353-368.

Walker, T.R., 1974, Formation of red beds in moist tropical climates: a hypothesis: Geological Society of America Bulletin, v. 85, p. 633-638.

Walthier, T.N., 1948, Geology of the Grand Bank quadrangle, Burin Peninsula, Newfoundland: Unpublished Field Report, Geological Survey of Newfoundland, File 1L/14 (11), 24 p.

Walzebuck, J.P., 1982, Bedding types of the Toarcian black shales in NW Greece, in Einsele, G. and Seilacher, A., eds., Cyclic and event stratification: Springer-Verlag, New York, p. 512-525.

Waples, D.W., 1982, Phosphate-rich sedimentary rocks: Significance for organic facies and petroleum exploration: Journal of Geochemical Exploration, v. 16, p. 135-160.

Watkins, D.J. and Kraft, L.M., 1976, Stability of continental shelf and slope off Louisiana and Texas — geotechnical aspects, in Bouma, A.H., Moore, G.T. and Coleman, H.M., eds., Beyond the Shelf Break: American Association of Petroleum Geologists Short Course, New Orleans, II, BI-B34.

Weber, K.J., 1971, Sedimentological aspects of oil fields in the Niger Delta: Geol. en Mijnbouw, v. 50, p. 559-576.

Wells, J.T. and Coleman, J.M., 1981, Physical processes and fine-grained sediment dynamics, Coast of Surinam, South America: Journal of Sedimentary Petrology, v. 51, no. 4, p. 1053-1068.

Wells, J.T., Prior, D.B., and Coleman, J.M., 1980, Flowslides in muds on extremely low angle tidal flats, northeastern South America: Geology, v. 8, p. 272-275.

Whitaker, J.H. McD., 1965, Primary sedimentary structures from the Silurian and Lower Devonian of the Oslo region, Norway: Nature, v. 207, no. 4998, p. 709-711.

Whitaker, J.H. McD., 1973, 'Gutter Casts', A new name for scour-and-fill structures; with examples from the Llandoverian of Ringerike and Malmoya, Southern Norway: Norsk Geologisk Tidsskrift, v. 53, p. 403-417.

White, D.E., 1939, Geology and molybdenite deposits of the Rencontre East area, Fortune Bay, Newfoundland: unpublished Ph. D. thesis, Princeton University, 118 p.

White, W.A., 1961, Colloid phenomena in sedimentation of argillaceous rocks: Journal of Sedimentary Petrology, v. 31, no. 4, p. 560-570.

Widmer, K., 1950, The geology of the Hermitage Bay area, Newfoundland: Unpublished Ph.D. thesis, Princeton University, Princeton, New Jersey.

Wiegel, R.L., 1964, Oceanograhic Engineering: Prentice Hall, Englewood Cliffs, New Jersey, U.S.A.

Williams, G.L., Fyffe, L.R., Wardle, R.J., Colman-Sadd, S.P., and Boehner, R.C., 1985, Lexicon of Canadian Stratigraphy, Volume 6, Atlantic Region: Canadian Society Petroleum Geologists, Calgary, Canada, 572 p.

Williams, H., 1971, Geology of the Belleoram map-area, Newfoundland (1M/11): Canada Geological Survey Paper 70-65, 59 p.

Williams, H., 1979, Appalachian Orogen in Canada: Canadian Journal Earth Sciences, v. 16, no. 3, p. 792-807.

Williams, H. and Hatcher, R.D., 1983, Appalachian suspect terraines: Geological Society of America, Memoir 158, p. 33-53.

Williams, H., Kennedy, M.K., and Neale, E.R.W., 1974, The northeastward termination of the Appalachian orogen, in Nairn, A.E.M. and Stehli, R.G., eds., The Ocean Basins and Margins, Vol. 2: Planum Press, New York, p. 79-123.

Williams, H.S., 1881, Channel-fillings in Upper Devonian Shales, American Journal of Science, v. 121, p. 318-320.

Wilson, J.L., 1975, Carbonate facies in geologic history: Springer-Verlag, New York, Heidelberg, Berlin, 471 p.

Wincierz, J., 1973, Kustensedimente und Ichnofauna aus dem oberen Hettangium von Mackendorf (Niedersachsen): N. Jb. Geol. Palaont. Abh., v. 144, no. 1, p. 104-141.

Wood, A. and Smith, A.J., 1957, The sedimentation and sedimentary history of the Aberystwyth grits (Upper Llandoverian): Geological Society of London Quart., v. 114, p. 163-190.

Worsley, D., 1971, Faunal Anticipation in the Lower Llandovery of the Oslo region, Norway: Norsk Geol. Tidsskrift, v. 51, p. 161-167.

Wright, M.E. and Walker, R.G., 1981, Cardium Formation (U. Cretaceous) at Seebe, Alberta — Storm-transported sandstones and conglomerates in shallow marine depositional environments below fair-weather wave base: Canadian Journal Earth Sciences, v. 18, p. 795-809.

Wunderlich, F., 1970, Genesis and development of the "Nellenkopfenschichten" (Lower Emsian, Rheinian Devonian) at locus typicus in comparison with modern coastal environments of the German Bay: Journal of Sedimentary Petrology, v. 40, p. 102-130.

Yorath, C.J., Bornhold, B.D., and Thompson, R.E., 1979, Oscillation ripples on the northeast Pacific continental shelf: Marine Geology, v. 31, p. 45-58.

Zicker, E,L., Berger, K.C., and Hasler, A.D., 1956, Phosphorous release from bog lake muds: Limnology and Oceanography,.v. 1, p. 296-303.

Appendix A

LOCATIONS OF MEASURED STRATIGRAPHIC SECTIONS

Figure A1: Location of measured stratigraphic sections in northern Fortune Bay: Chapel Island, Sagona Island, and Brunette Island.

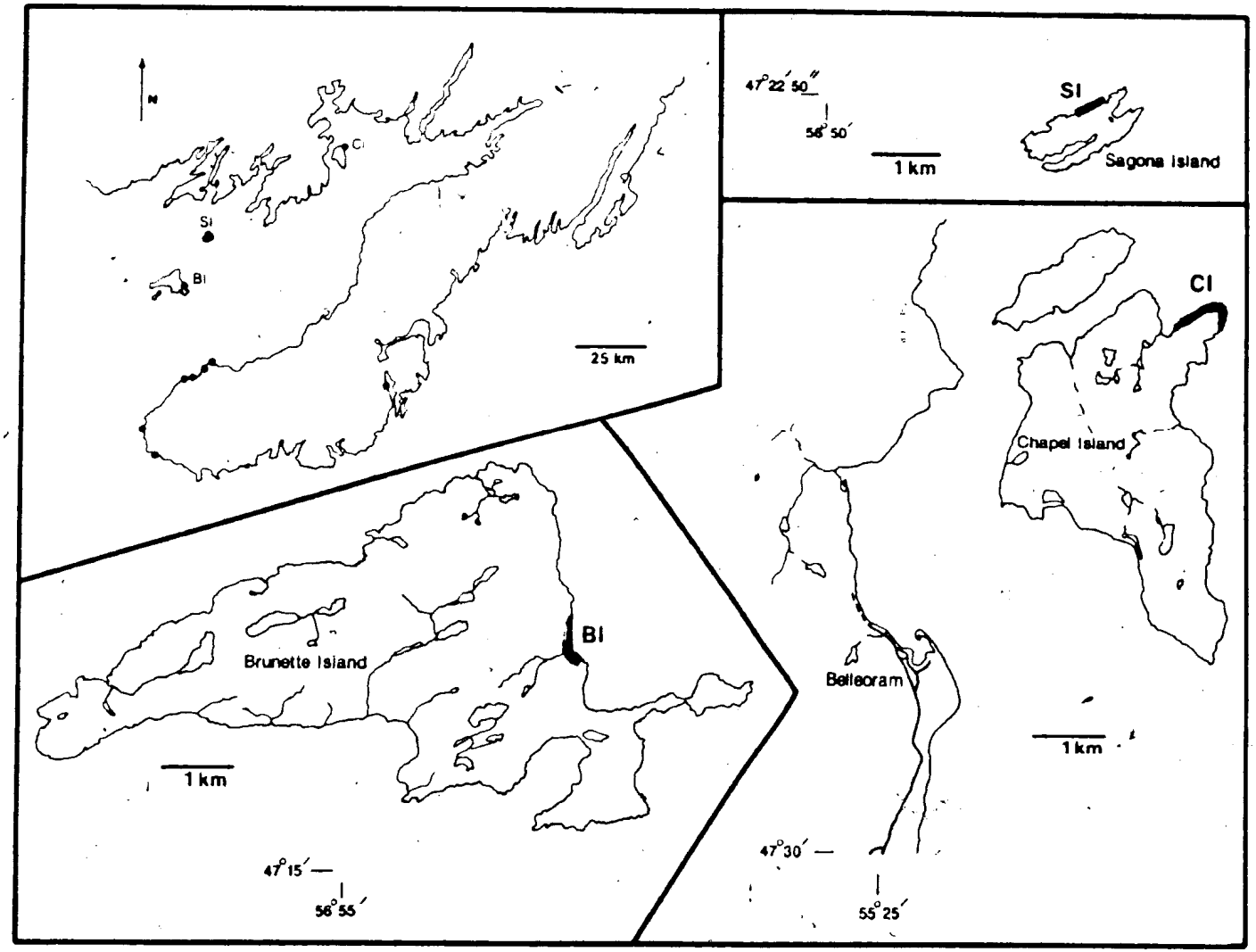
N
SI
BI
25 km
47°22'50"
56°50'
1 km
SI
Sagona Island
CI
Chapel Island
Belleoram
1 km
BI
Brunette Island
1 km
47°15'
56°55'
47°30'
55°25'

Figure A2: Location of measured stratigraphic sections in the Grand Bank – Fortune region: Grand Bank Head, Radio Station, Fortune North and Fortune Dump (Fortune Head).

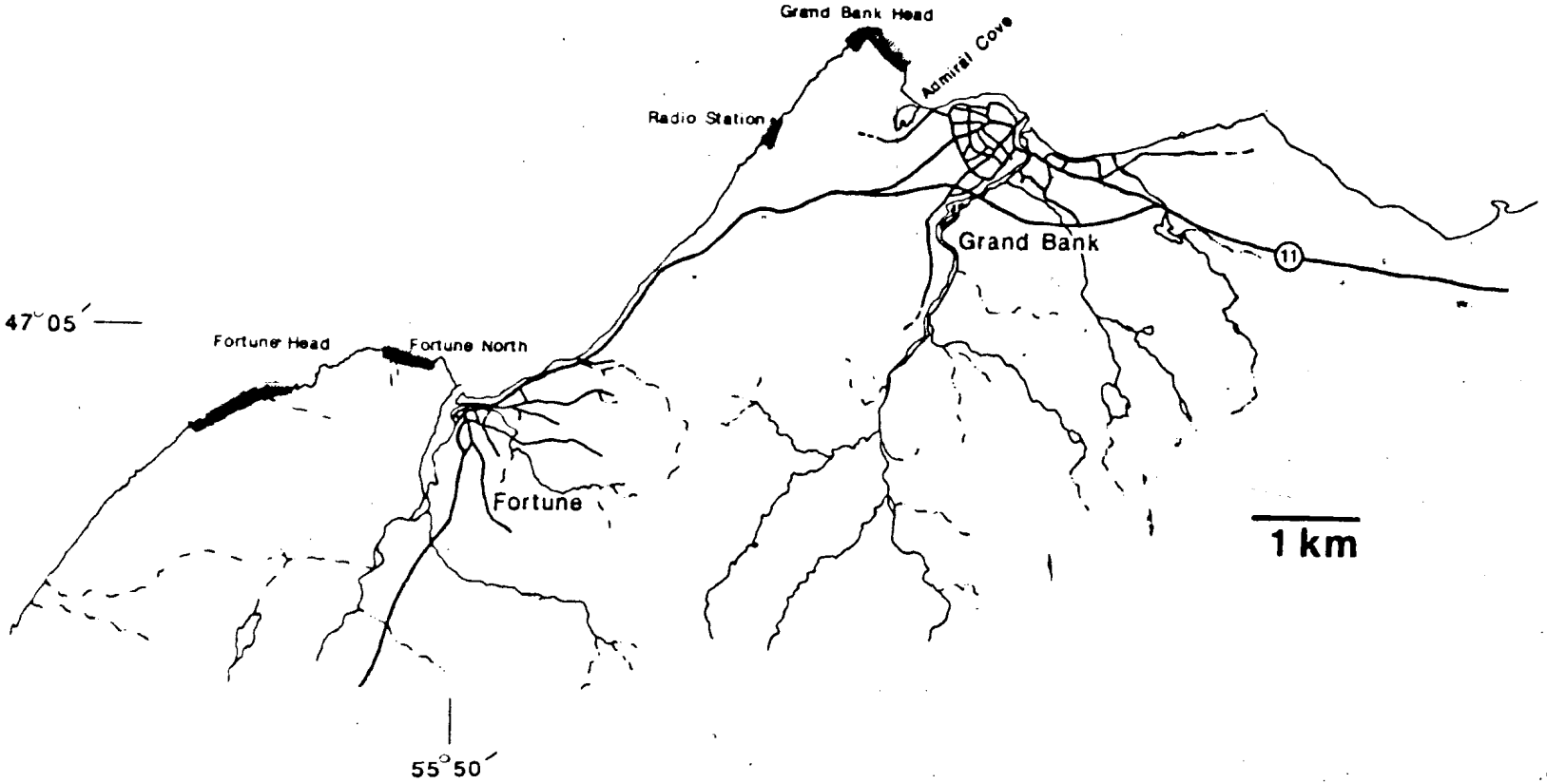
Grand Bank Head
Admiral Cove
Radio Station
Grand Bank
11
47°05′
Fortune Head
Fortune North
Fortune
1 km
55°50′

Figure A3: Location of measured stratigraphic sections on the southwest part of the Burin Peninsula: Dantzic Cove and Point May.

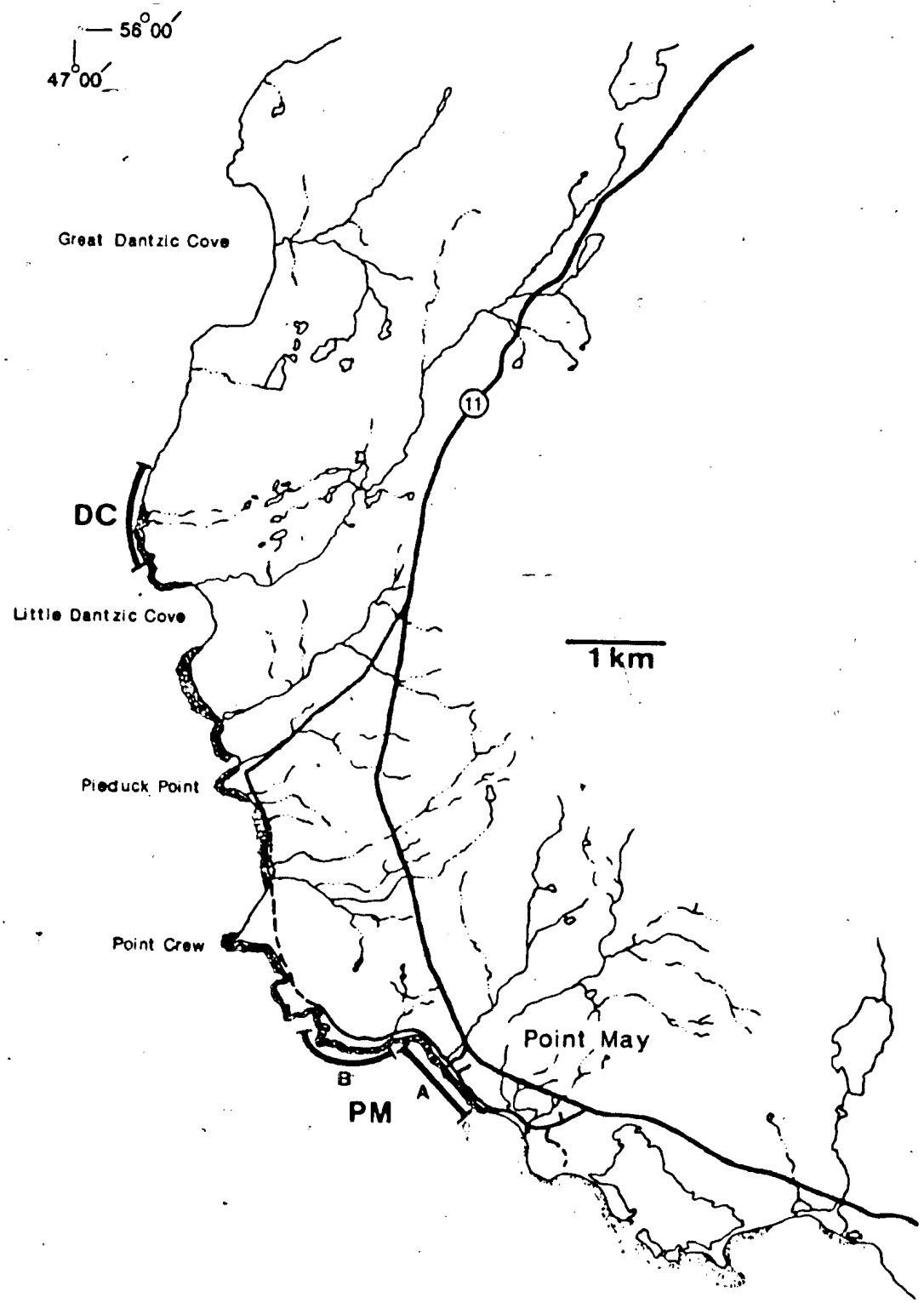
56°00'
47°00'
Great Dantzic Cove
11
DC
Little Dantzic Cove
1 km
Pieduck Point
Point Crew
Point May
B
A
PM

Figure A4: Location of measured stratigraphic section at Lewin's Cove.

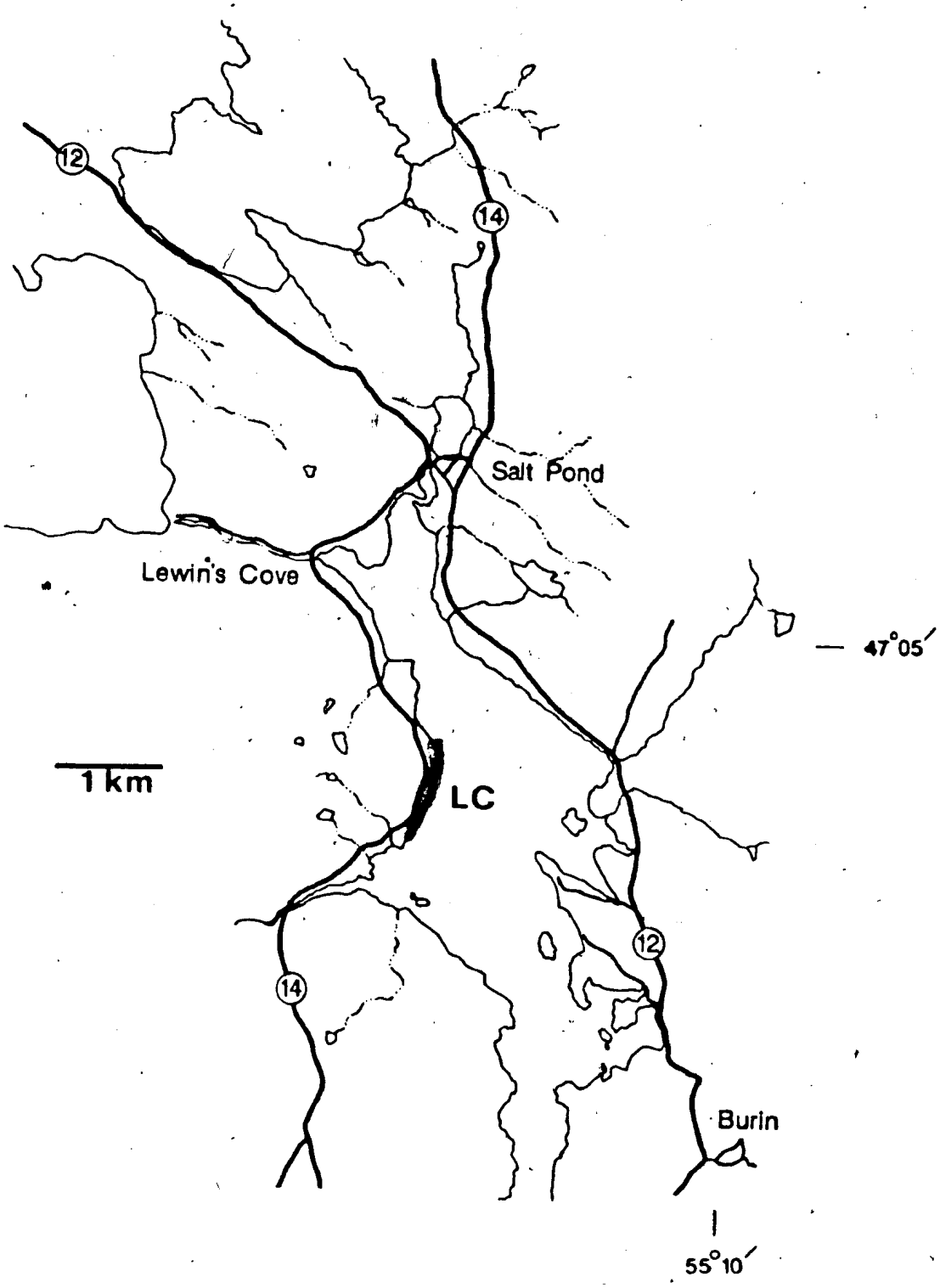
12
14
Salt Pond
Lewin's Cove
47°05′
1 km
LC
14
12
Burin
55°10′

Appendix B

MEASURED SECTIONS: CI, LC, BI, PM, RS, AND SI

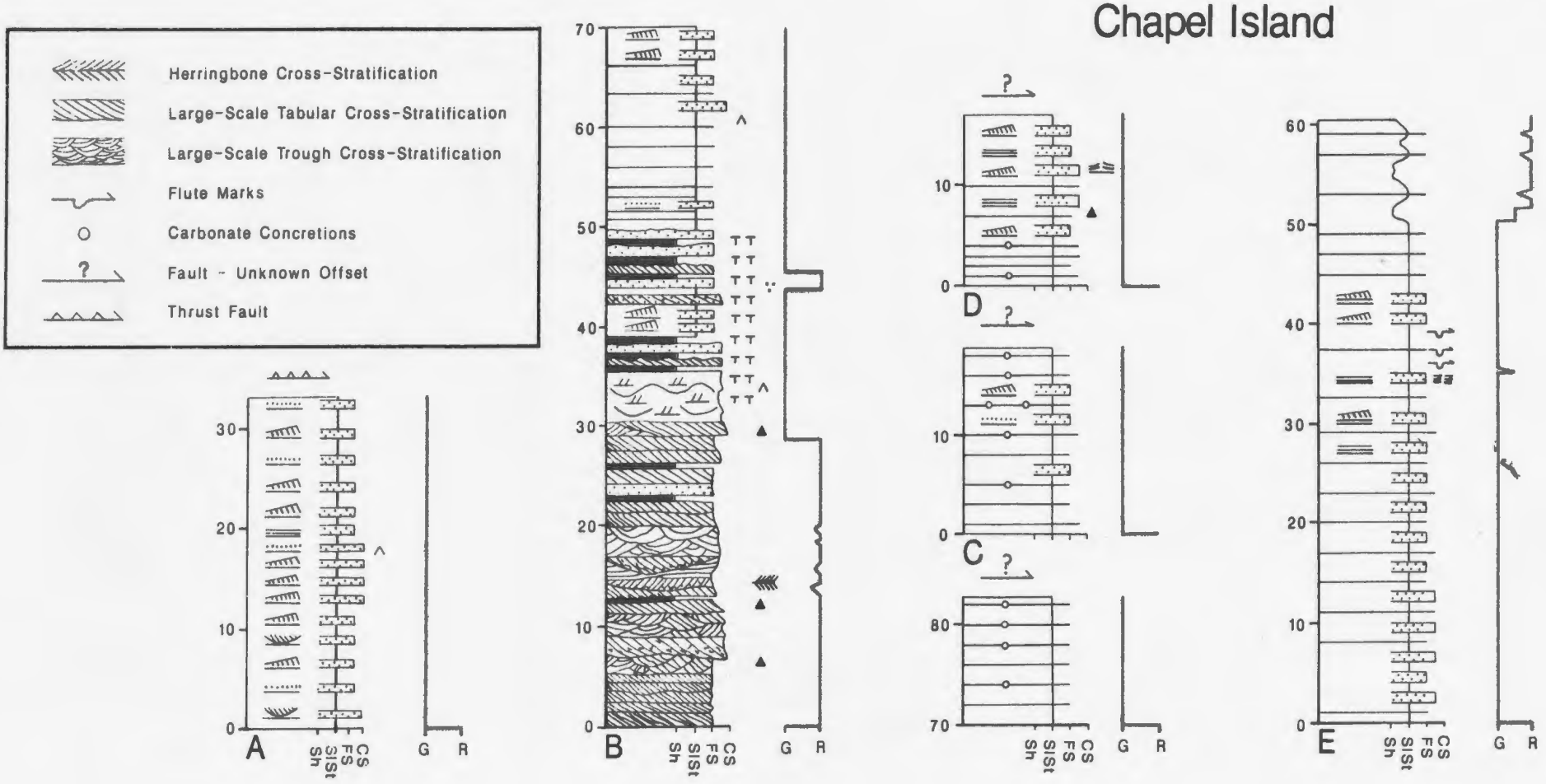
Chapel Island
Herringbone Cross-Stratification
Large-Scale Tabular Cross-Stratification
Large-Scale Trough Cross-Stratification
Flute Marks
Carbonate Concretions
Fault - Unknown Offset
Thrust Fault
A
B
C
D
E
CS
FS
SISt
Sh
G
R

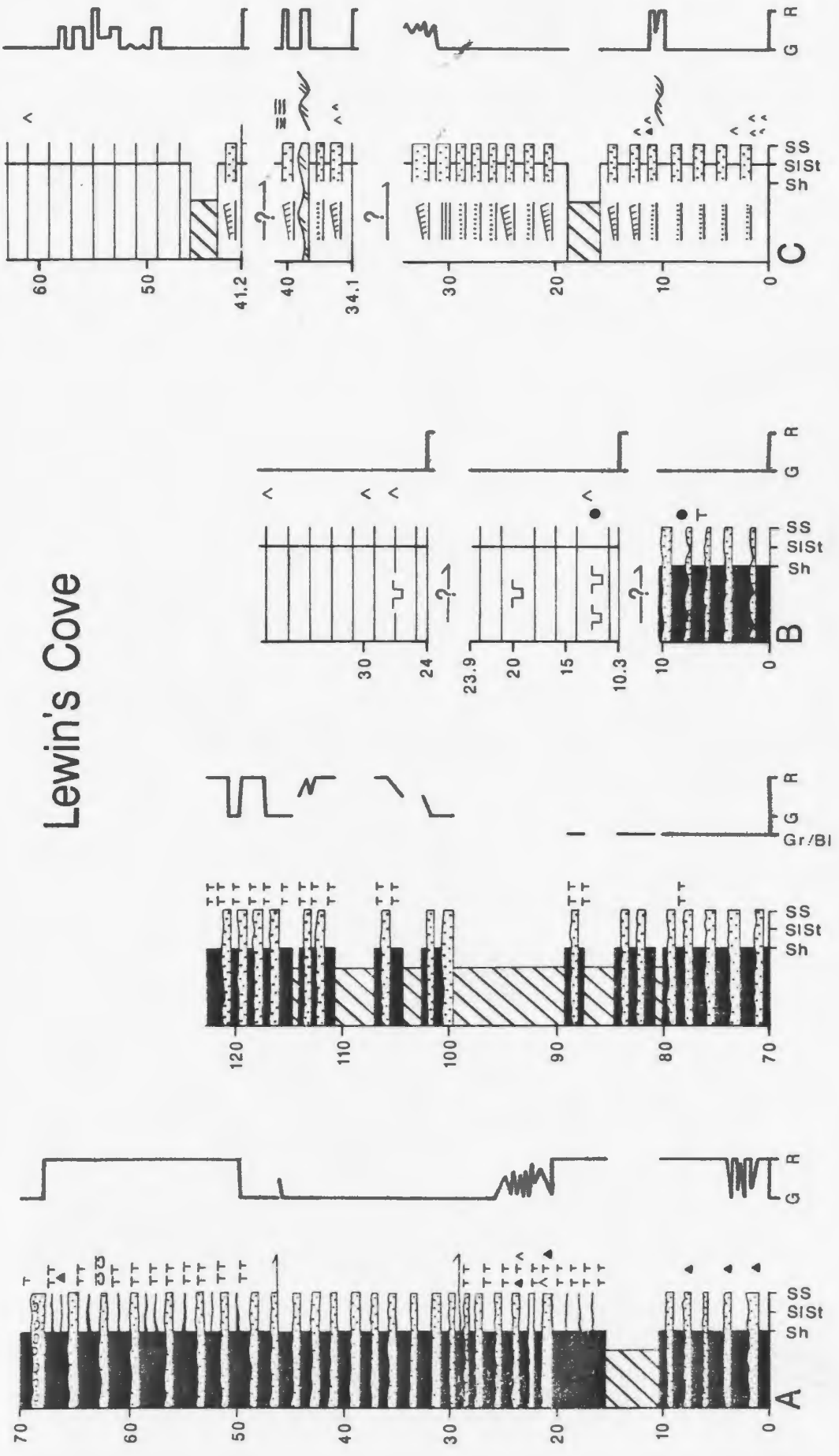
Lewin's Cove
A
B
C
SS
SISt
Sh
G
R
Gr/Bl
70
60
50
40
30
20
10
0
120
110
100
90
80
24
23.9
15
10.3
41.2
34.1

Brunette Island

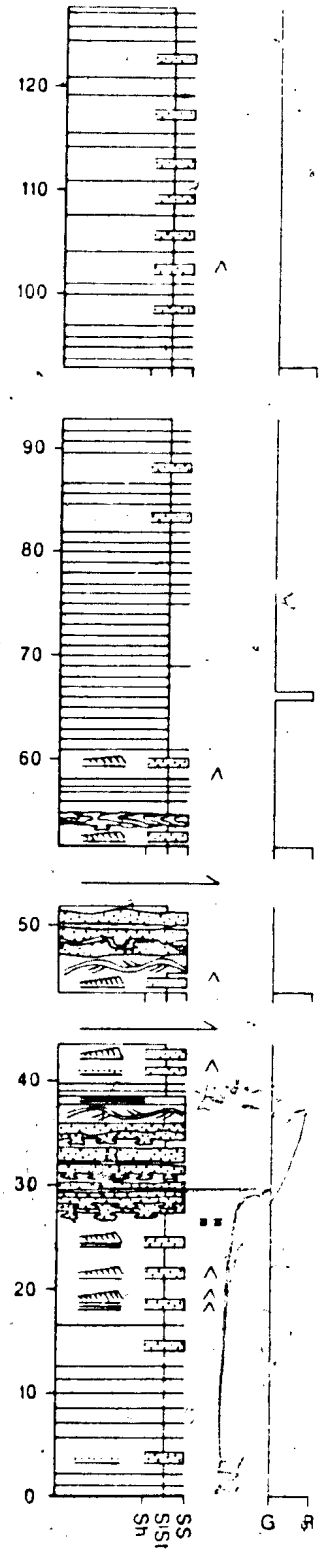

Point May

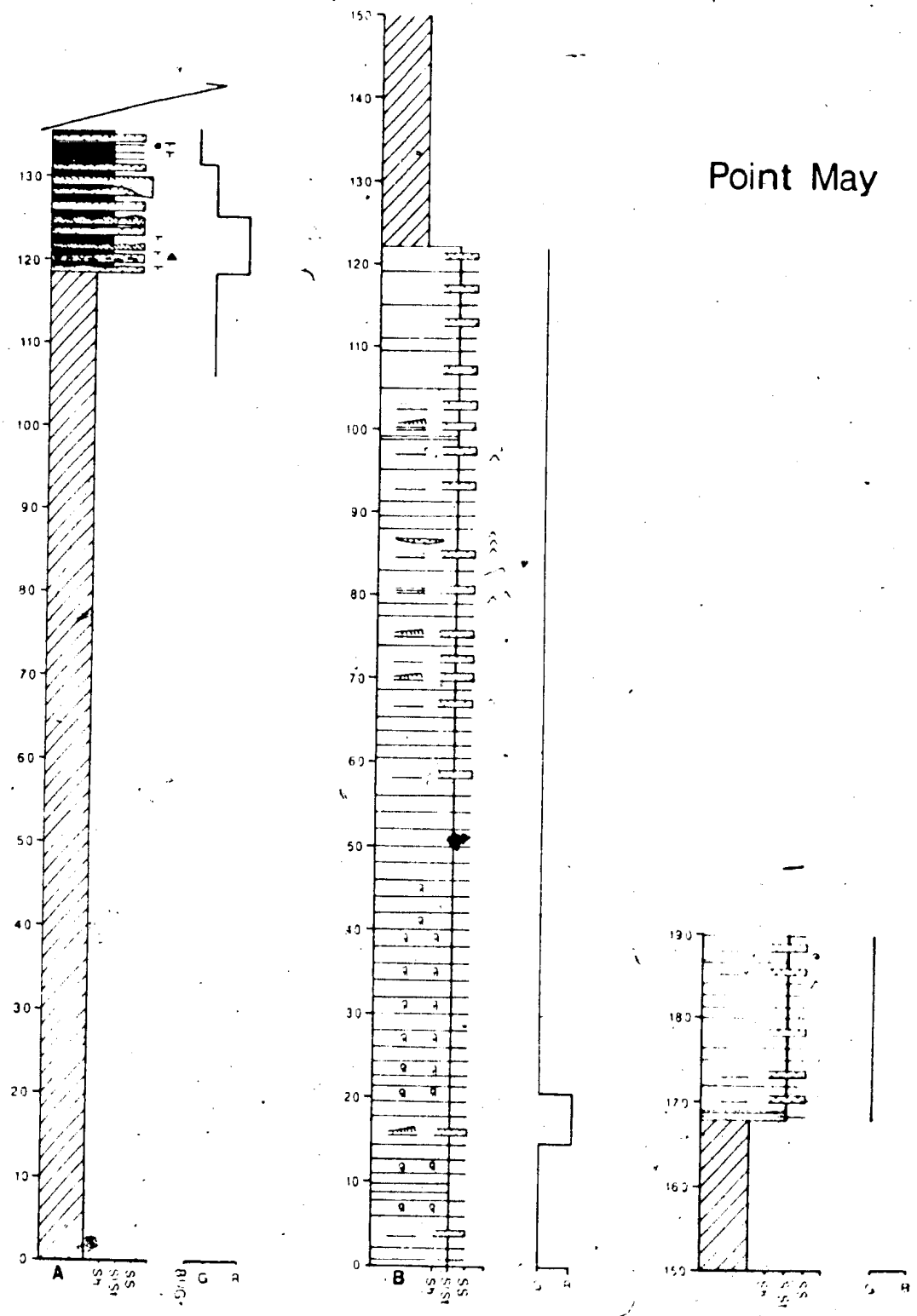

Radio Station

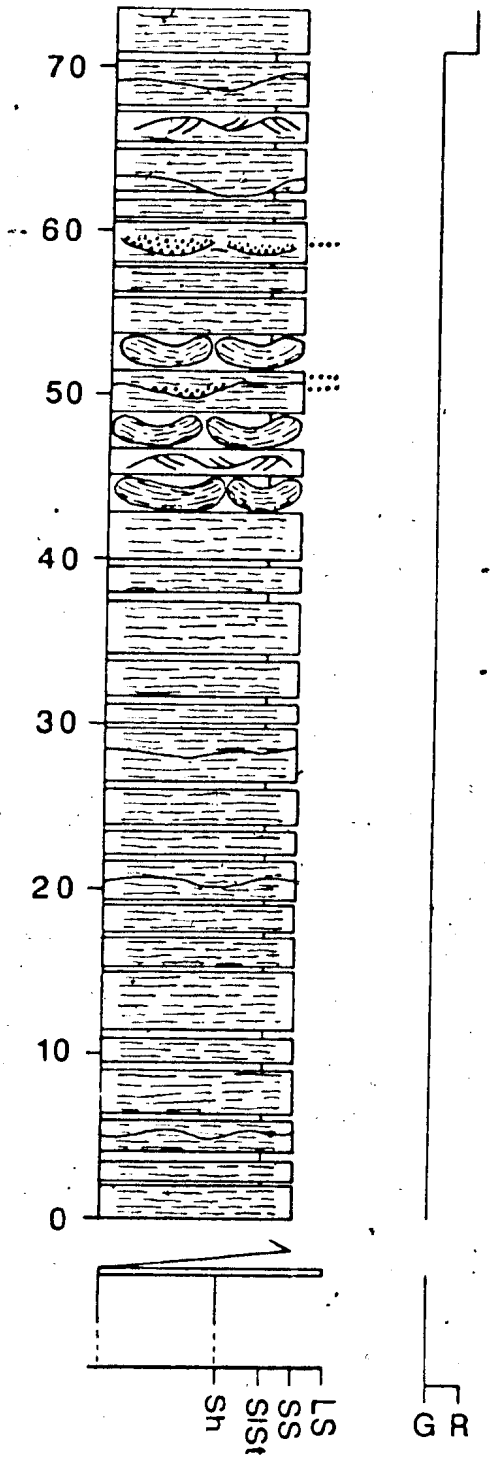

Sagona Island

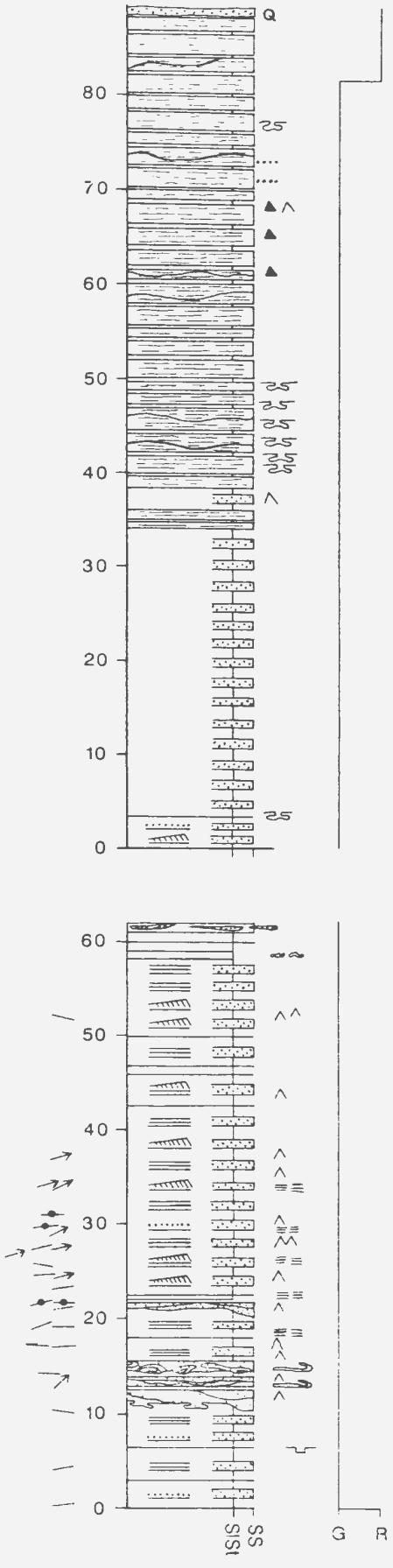

Appendix C

DETAILED MEASURED SECTION FOR FORTUNE DUMP

Figure C.1: Legend for Detailed Measured Section at Fortune Dump

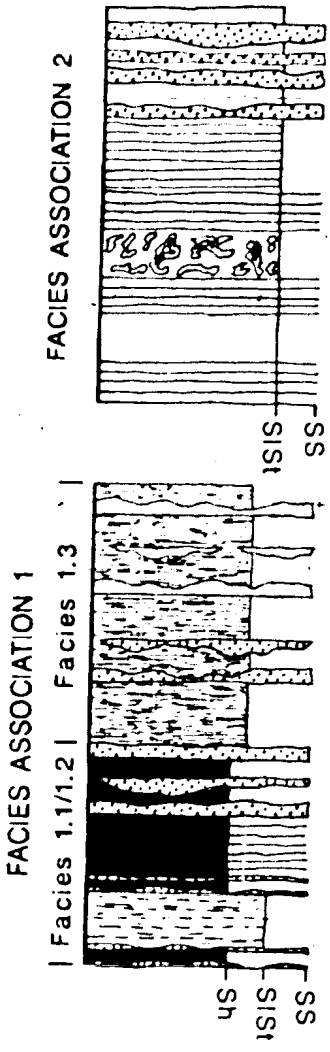

Medium to Thick Beds of Sandstone

Sandstone laminated Siltstone

Raft-Bearing Bed

Unifite Bed

Thin and V. Thin Beds of Sandstone

Detail Obscured by Weathering

Thin to Medium Beds of Sandstone/Quartzarenite

Thin to Medium Sandstone Beds

Laminae to Thin Beds of Sandstone

Laminated Siltstones

Legend

- Wave Ripples
- Cross-laminations
- HCS
- Q — Quartzarenitic Sandstones
- Gutter and Pot Casts
- Injection Structures
- Mudstone Clasts
- Shrinkage Cracks
- Phosphatic Shale Nodules
- Pyrite Nodules
- Carbonate Nodules

FORTUNE DUMP

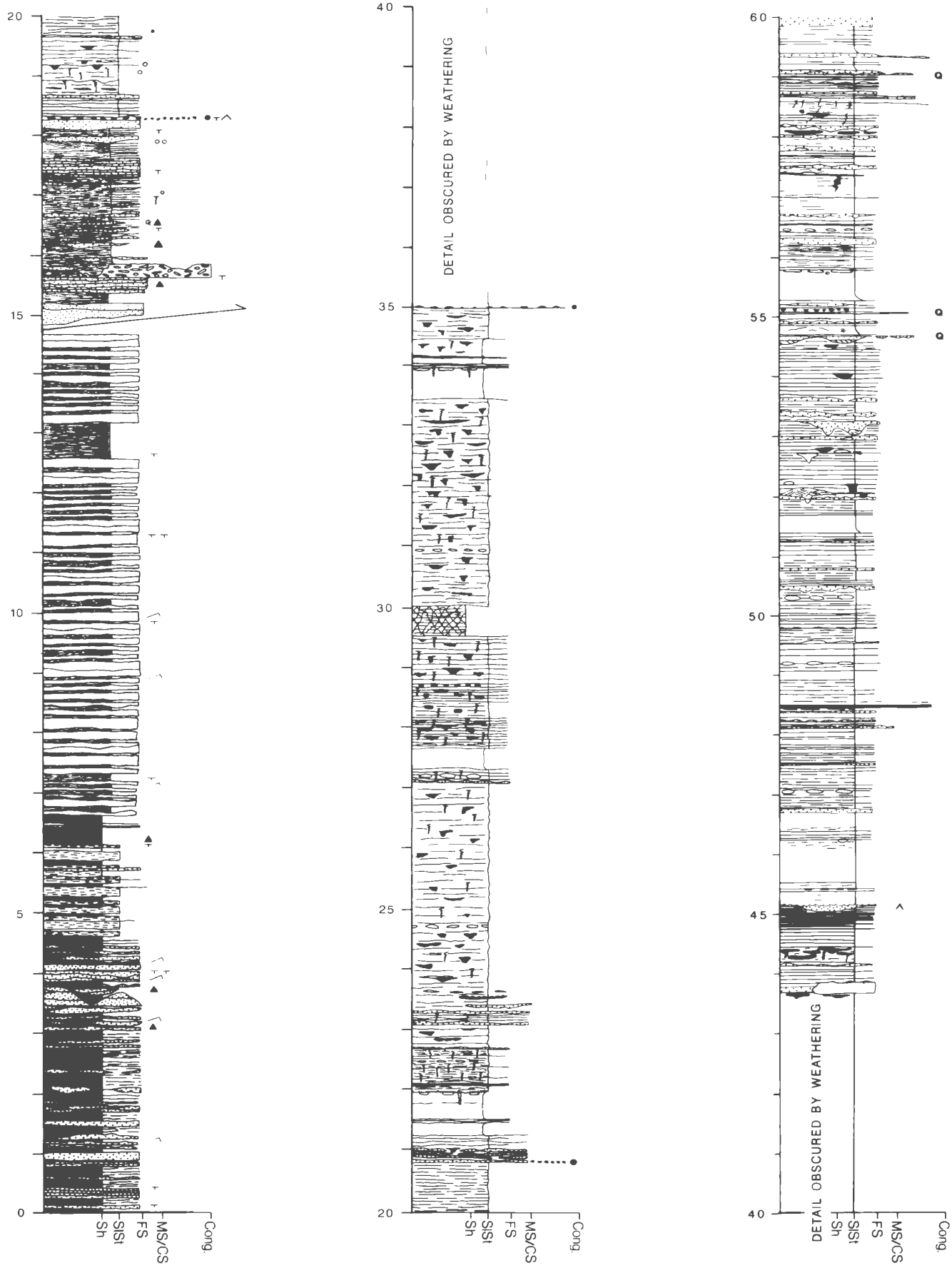

FORTUNE DUMP (CONT'D)

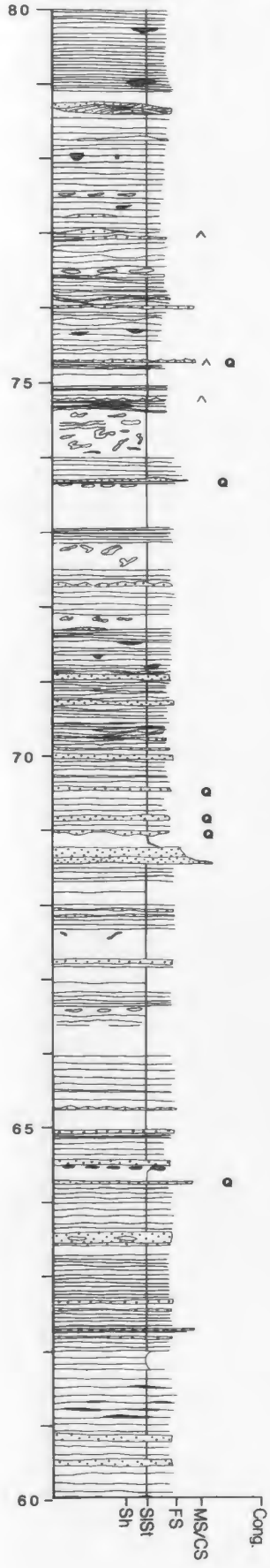

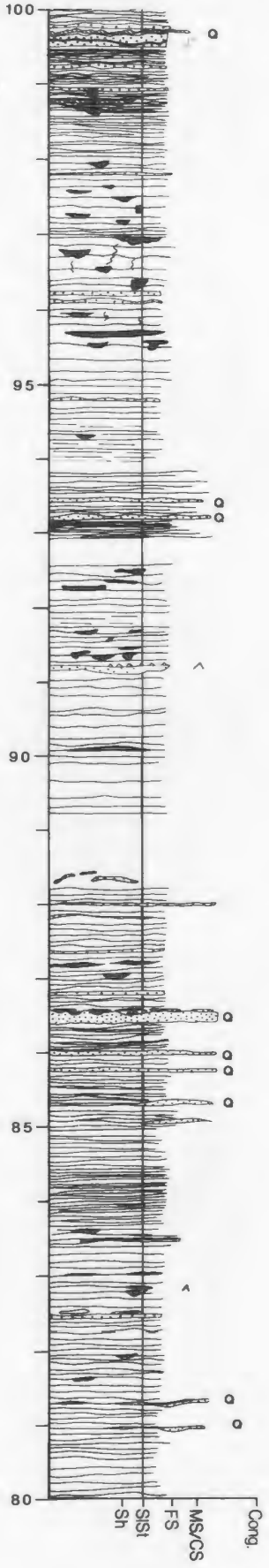

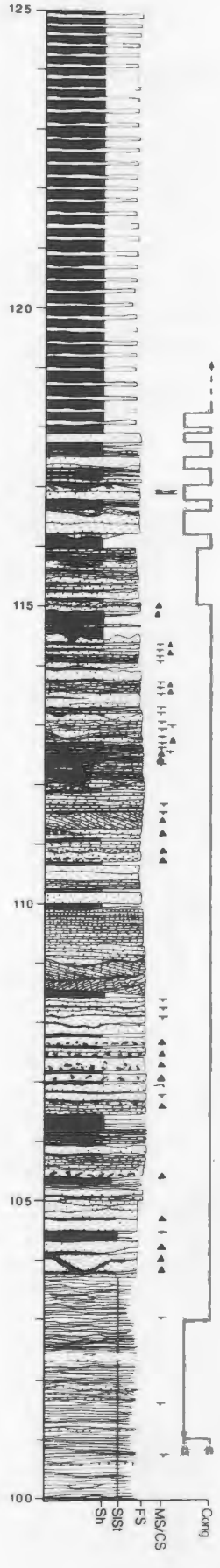

FORTUNE DUMP (CONT'D)

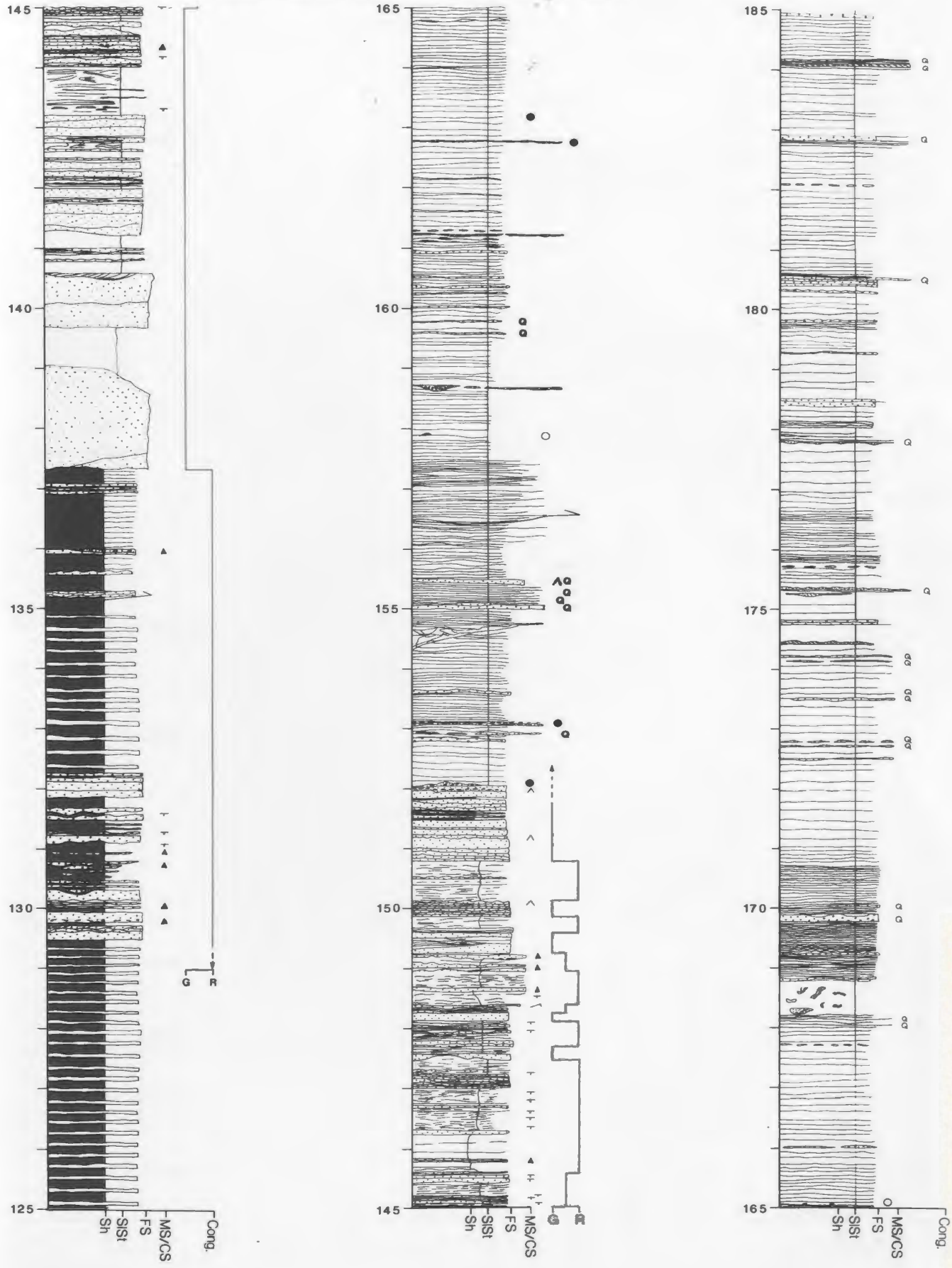

FORTUNE DUMP (CONT'D)

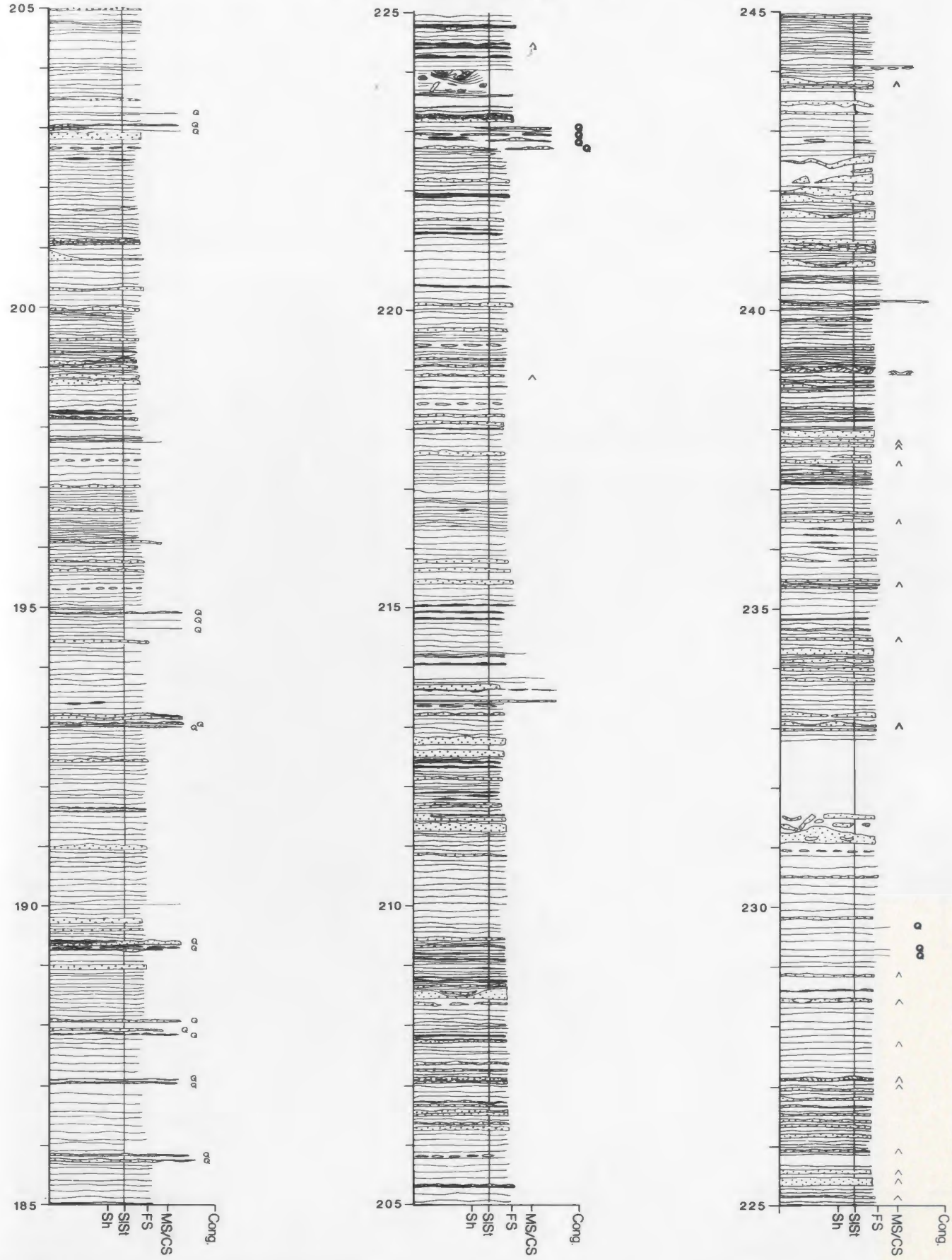

FORTUNE DUMP (CONT'D)

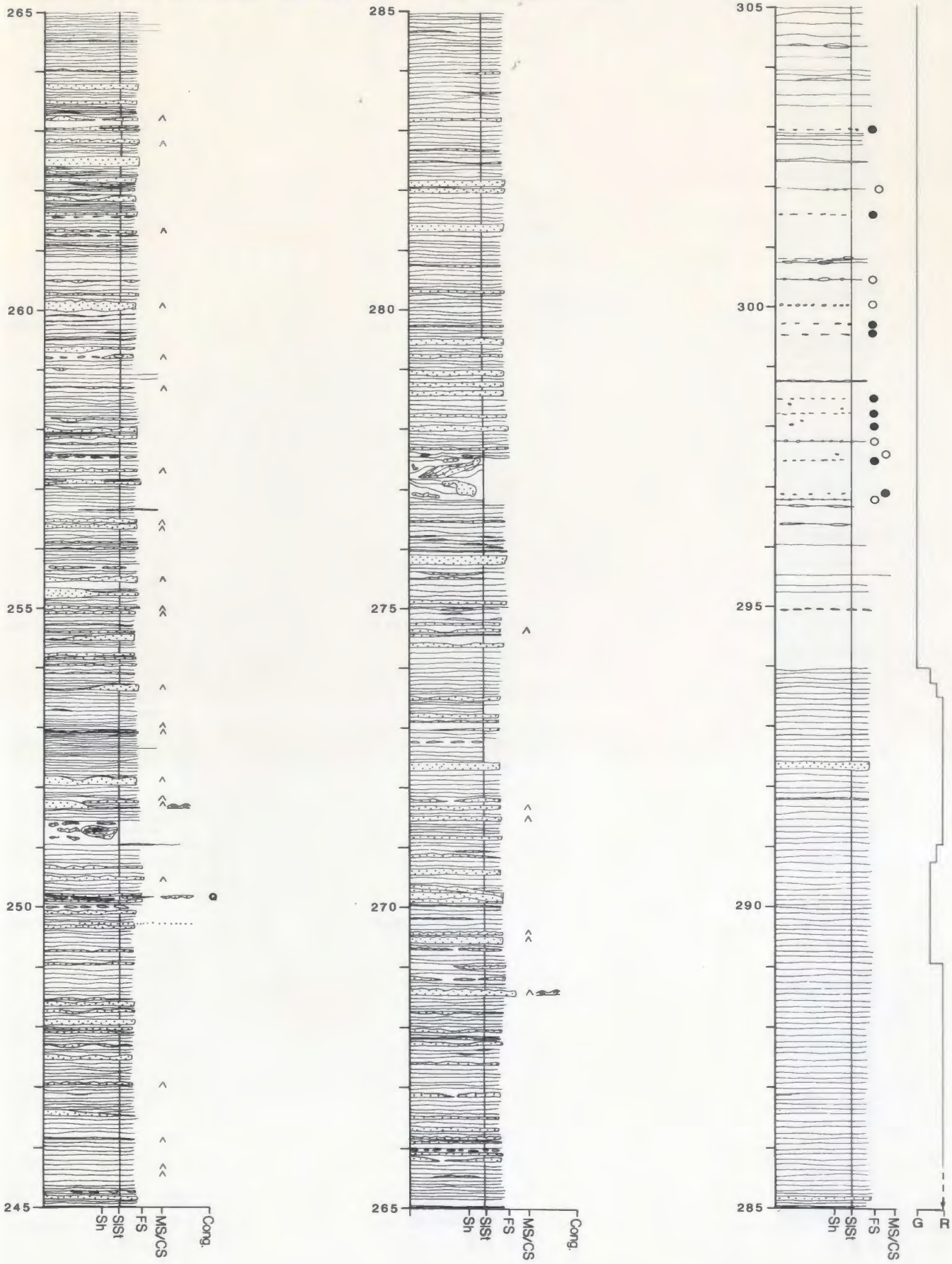

FORTUNE DUMP (CONT'D)

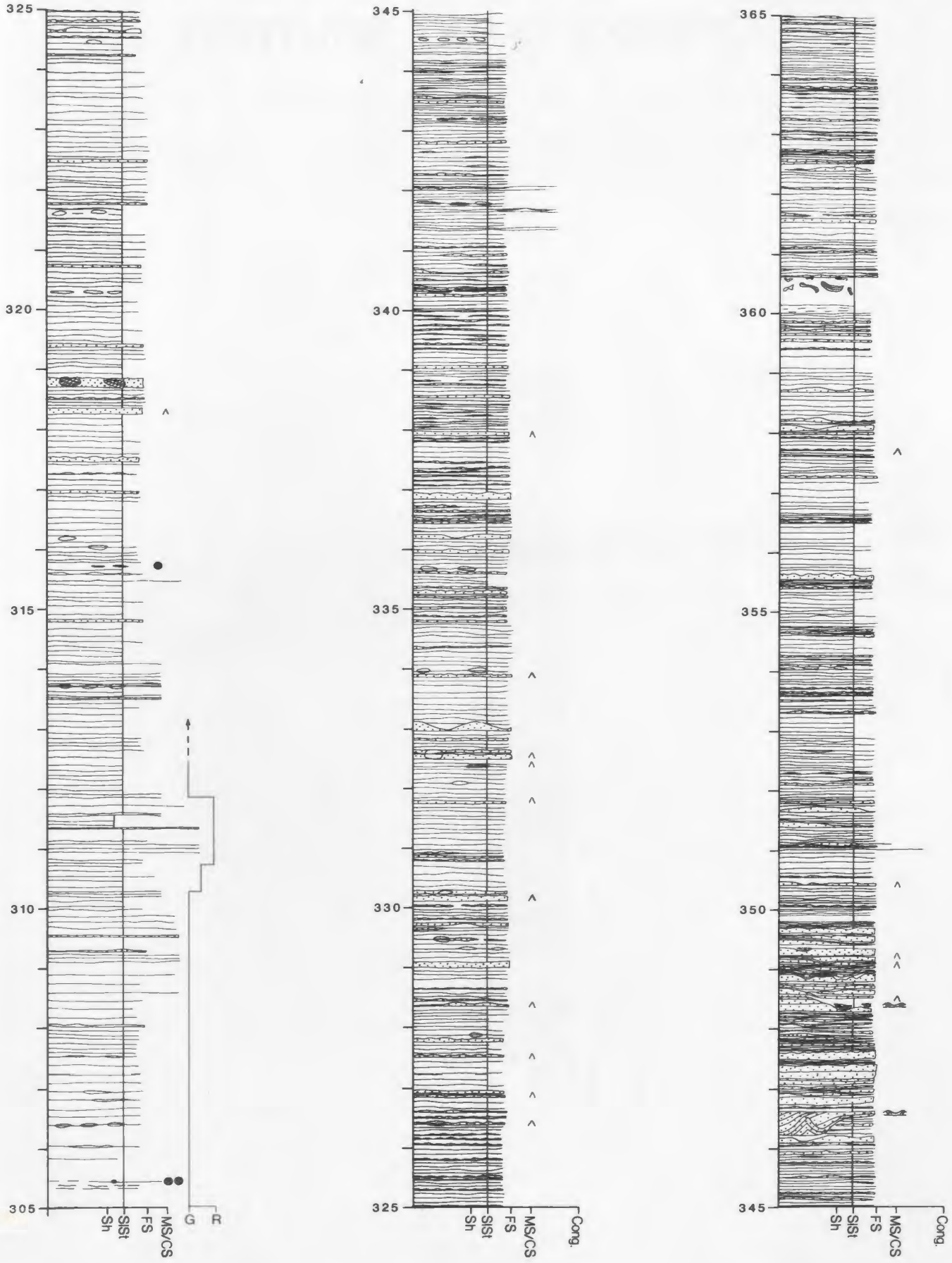

FORTUNE DUMP (CONT'D)

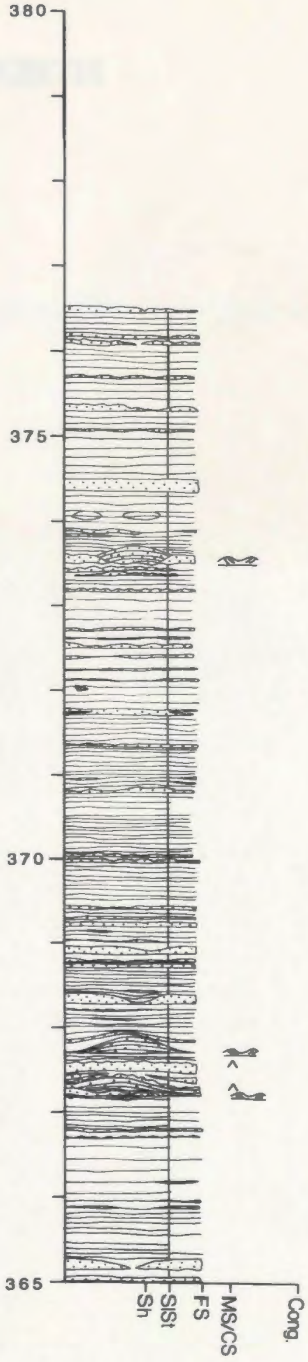

Appendix D

DETAILED MEASURED SECTIONS FOR

DANTZIC COVE

AND

FORTUNE NORTH

Figure D.1: Legend for detail measured sections from Dantzic Cove and Fortune North

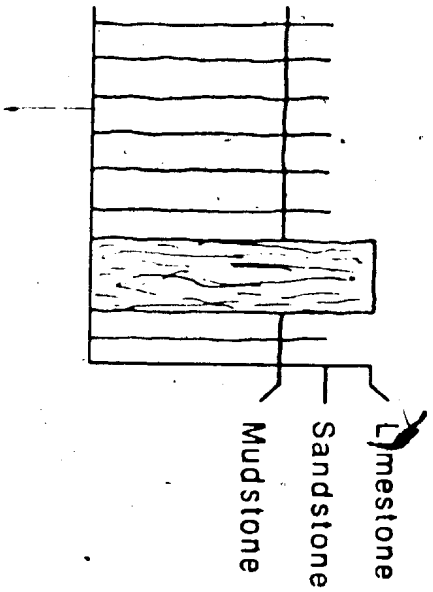

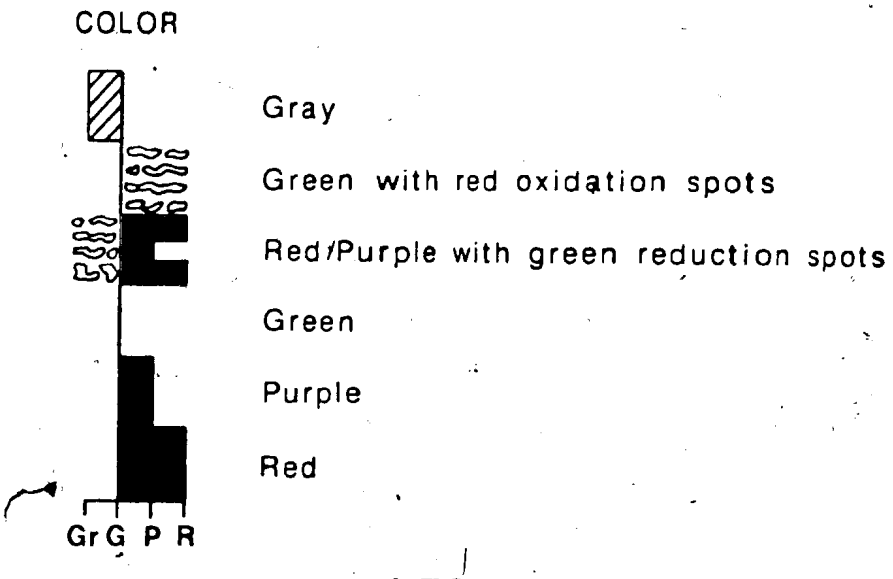

LEGEND

Carbonate mud mound

Mudstone clasts

Stromatolites

Oncolites

Shelly fossils/Steinkerns

Phosphate nodules

Carbonate nodules

Pyrite nodules

Figure D.2: Detailed Measured Section for Dantzic Cove.

DANTZIC COVE

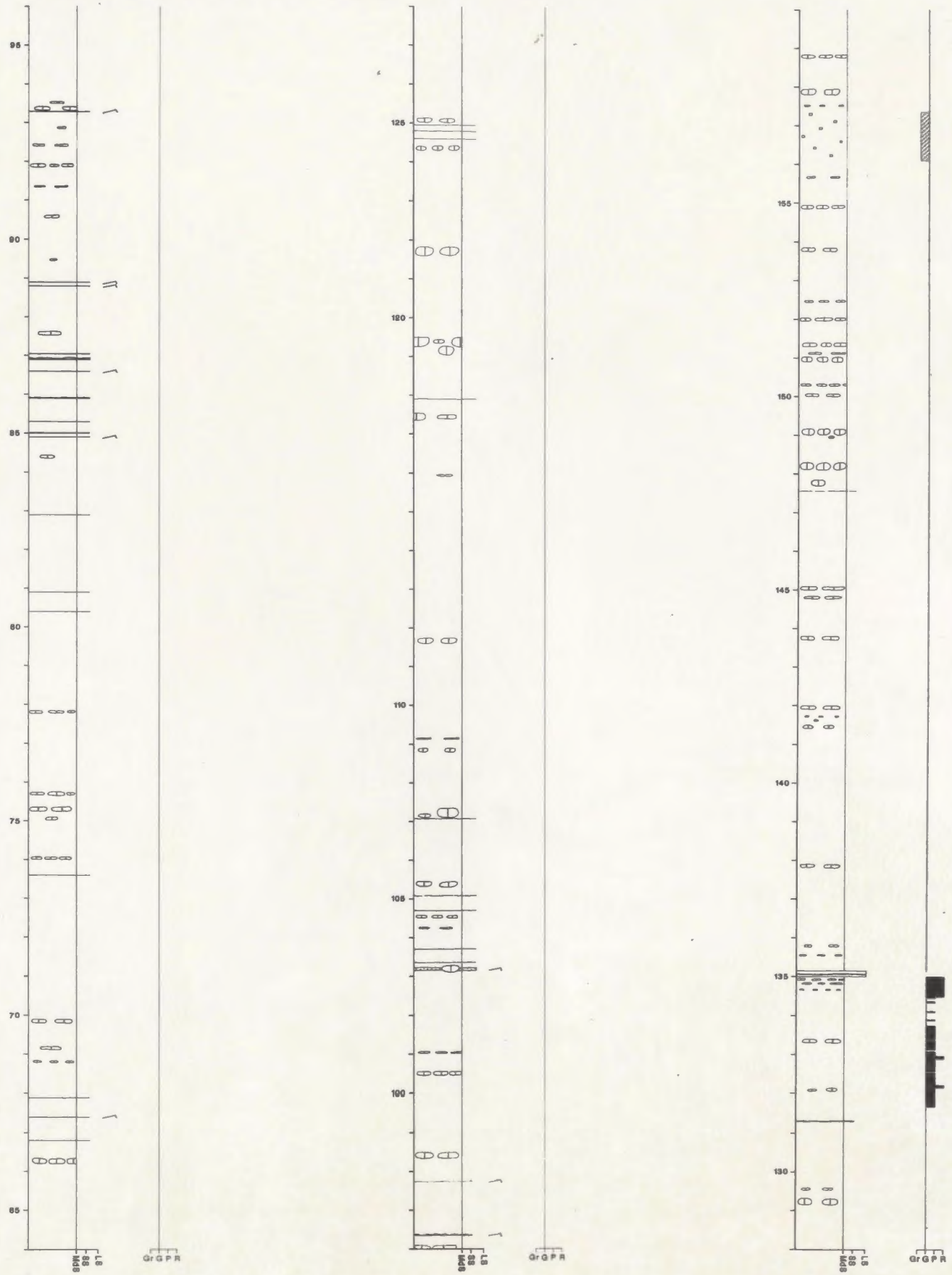

DANTZIC COVE (CONT'D)

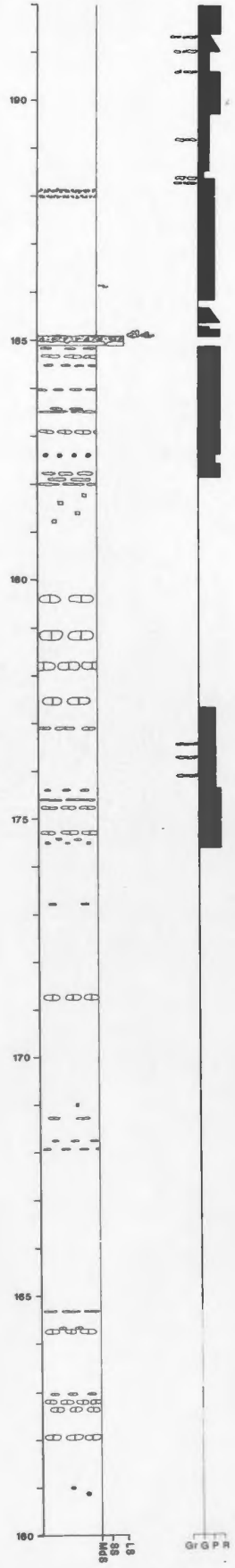

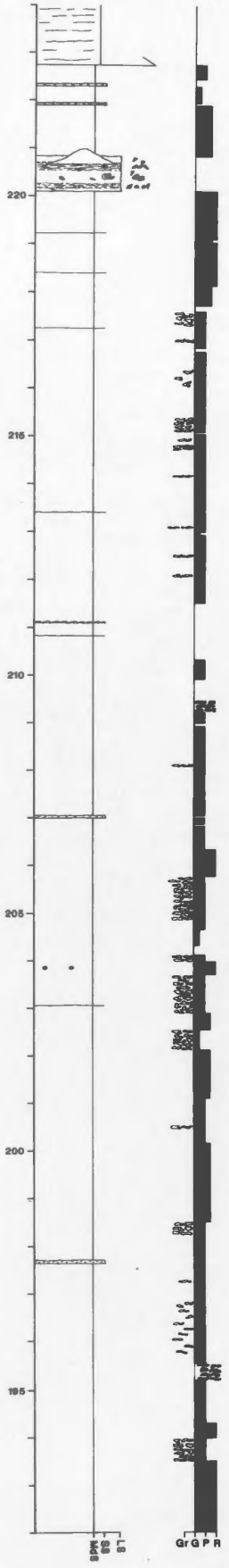

Figure D.3: Detailed Measured Section for Fortune North

FORTUNE NORTH